The role of the aryl hydrocarbon receptor interacting protein (AIP) in pituitary tumorigenesis:

A proteomic approach for explaining the clinical behaviour of *AIP* mutation-associated pituitary adenomas

Thesis presented by:

Laura Cristina Hernández Ramírez, MD

As a requirement to obtain the degree of:

Doctor of Philosophy

Under the supervision of:

Prof Márta Korbonits, MD, PhD

Prof Fulvio D'Acquisto, PhD

Centre for Endocrinology
William Harvey Research Institute
Barts and The London School of Medicine
Queen Mary University of London

London, UK. 21st August, 2015

Abstract

A subset of familial and sporadic pituitary adenomas is due to germline mutations in the aryl hydrocarbon receptor interacting protein gene (*AIP*). A systematic follow-up of cases and families with *AIP* mutation (*AIP*mut)-associated pituitary adenomas is lacking. The product of this novel tumour suppressor gene is a ubiquitously expressed co-chaperone of the heat shock proteins HSPA8 and HSP90, but besides of pituitary adenomas, there is no clear association of *AIP*muts to other neoplasms. The molecular processes leading to pituitary tumorigenesis in the presence of *AIP*muts and the mechanism for tissue-specific tumour suppressor function are unclear.

This research work describes the clinical features of *AIP*mut positive familial and sporadic pituitary adenomas in a large international cohort of patients, aiming to increase the knowledge about this condition and focusing on the screening-led detection of pituitary adenomas. To define the repertoire of interactions of AIP in the pituitary gland and to determine which interactions are lost by AIP mutants, a proteomic screening for molecular partners of AIP in a pituitary cell line was conducted. The stability of a panel of missense AIP mutant proteins and the mechanism of protein degradation were evaluated in half-life studies, and the relationship between protein stability and phenotype was analysed.

A number of novel features of *AIP*mut positive pituitary disease were identified, drawing attention to the high percentage of positive clinical screening of the apparently unaffected *AIP*mut carriers. The AIP tumour suppressor function is apparently mediated by its interaction with molecular chaperones, perhaps modifying their affinity for specific client proteins. AIP could exert an additional anti-tumorigenic action by regulating cytoskeletal organisation. AIP is processed via ubiquitination and proteasomal degradation, probably mediated by the FBXO3-containing SKP1-CUL1-F-BOX protein complex E3 ubiquitin-ligase. Enhanced proteasomal degradation conferred shorter half-life to most of the AIP mutants tested, with implications for the clinical presentation.

Table of contents

List of figures

List of tables

List of abbreviations

2H	Two-hybrid assay
3PAs	Three P Association (pituitary adenoma and phaeochromocytoma/paraganglioma)
α-GSU	Glycoprotein hormone subunit alpha
AC	Adenylyl cyclase
AC-MS	Affinity capture (pull-down)-mass spectrometry
ACTB	Actin, cytoplasmic 1
ACTH	Adrenocorticotropic hormone
AGO	Argonaute proteins
AGO1	Argonaute RISC catalytic component 1
AHO	Albright's hereditary osteodystrophy
AHR	Aryl hydrocarbon receptor
AIP	Aryl hydrocarbon receptor interacting protein
AIP	Aryl hydrocarbon receptor interacting protein gene
AIPL1	Aryl hydrocarbon receptor-interacting protein like 1
*AIP*mut	Mutation in the aryl hydrocarbon receptor interacting protein gene
AKT1	V-akt murine thymoma viral oncogene homolog 1
AKT2	V-akt murine thymoma viral oncogene homolog 2
AP-1	Activating protein 1
ARA9	AHR-activated 9 protein
ARHGEF6	Rac/Cdc42 guanine nucleotide exchange factor 6 gene
ARNT	Aryl hydrocarbon receptor nuclear translocator
ATF6	Activating transcription factor 6
ATP	Adenosine triphosphate
ATP5I	ATP synthase subunit e, mitochondrial
ATP5A1	ATP synthase subunit alpha, mitochondrial
ATP5D	ATP synthase subunit delta, mitochondrial
ATPase	Adenosine triphosphatase
BA	Biochemical activity
BAG1	BCL2-associated athanogene gene
BIRC5	Baculoviral IAP repeat-containing protein 5
BMI1	BMI1 proto-oncogene, polycomb ring finger gene
BMP2	Bone morphogenetic protein 2
BMP4	Bone morphogenetic protein 4
BMP4	Bone morphogenetic protein 4 gene
bp	Base pairs
BRAF	B-Raf proto-oncogene, serine/threonine kinase gene
BRCA1	Breast cancer 1, early onset gene
BRCA2	Breast cancer 2, early onset gene
C-terminal	Carboxyl-terminal

C4A	Complement C4-A
C16orf13	UPF0585 protein C16orf13
cAMP	Cyclic adenosine monophosphate
CBR1	Carbonyl reductase (NADPH) 1
CCDC120	Coiled-coil domain containing protein 120
CCNA1	Cyclin A1 gene
CCNA2	Cyclin A2 gene
CCNB1	Cyclin B1 gene
CCNB2	Cyclin B2 gene
CCND1	Cyclin D1
CCND1	Cyclin D1 gene
CCNE1	Cyclin E1 gene
CD40LG	CD40 ligand gene
CDC37	Hsp90 co-chaperone cell division cycle 37
CDK	Cyclin-dependent kinase
CDK9	Cyclin-dependent kinase 9
CDKI	Cyclin-dependent kinase inhibitor
CDKN1A	Cyclin-dependent kinase inhibitor 1A gene
CDKN1B	Cyclin-dependent kinase inhibitor 1B
CDKN1B	Cyclin-dependent kinase inhibitor 1B gene
CDKN2A	Cyclin-dependent kinase inhibitor 2A gene
CDKN2B	Cyclin-dependent kinase inhibitor 2B gene
CDKN2C	Cyclin-dependent kinase inhibitor 2C
CDKN2C	Cyclin-dependent kinase inhibitor 2C gene
CDS	Coding deoxyribonucleic acid sequence
CgA	Chromogranin A
cGMP	Cyclic guanosine monophosphate
CHIP	E3 ubiquitin-protein ligase carboxy terminus of Hsp70-interacting protein
CHX	Cycloheximide
Ck	Cytokeratin
CLEC7A	C-type lectin domain family 7, member A
CMA	Chaperone-mediated autophagy
CN	Cystic nephroma
CNC	Carney complex
CO-F	Co-fractionation
Co-loc	Co-localisation
Co-IP	Co-immunoprecipitation
COPS5	COP9 signalosome subunit 5 gene
CpG island	C-phosphate-G island
CRE	cAMP response element
CREB1	cAMP responsive element binding protein 1 gene

CRH	Corticotropin-releasing hormone
CRL	Cullin-really interesting new gene E3 ubiquitin-ligases
CRIP1	Cysteine-rich protein 1
CSNK2A1	Casein kinase 2, alpha 1 polypeptide
CTNNB1	Beta-catenin
DA	Dopamine agonists
DAPI	4',6-diamidino-2-phenylindole
DAPK1	Death-associated protein kinase 1 gene
ddH_2O	Double-distilled water
DSTN	Destrin (actin depolymerizing factor)
DICER1	Dicer1 ribonuclease type III
DICER1	Dicer1 ribonuclease type III gene
DKC1	Dyskeratosis congenita 1 dyskerin gene
DMEM	Dulbecco´s Eagle Modified Medium
DMSO	Dimethyl sulfoxide
DNA	Deoxyribonucleic acid
DNAAF2	Protein kintoun
dNTP	Deoxynucleotide
DRD2	Dopamine receptor D2 gene
DROSHA	Drosha ribonuclease type III
dsRNAs	Double stranded RNAs
DTT	Dihidrothreitol
DUBs	Deubiquitinating enzymes
DVL	Dishevelled segment polarity protein 1
E2F1	E2F transcription factor 1 gene
EBNA3	Epstein-Barr virus-encoded nuclear protein 3
EBV	Epstein-Barr virus
EEF1G	Eukaryotic translation elongation factor 1 gamma
EGLN1	Egl-9 family hypoxia-inducible factor 1 gene
EGF	Epidermal growth factor
EGFR	Epidermal growth factor receptor
EGFR	Epidermal growth factor receptor gene
EIF2G	Eukaryotic translation initiation factor 2 subunit 3
EMT	Epithelial-mesenchymal transition
ER	Endoplasmic reticulum
ERAD	ER-associated protein degradation
ERMS	Botryoid-type embryonal rhabdomyosarcoma
ESI	Electrospray ionisation
ESR1	Oestrogen receptor
ESRP1	Epithelial splicing regulatory protein 1
ExAC	Exome Aggregation Consortium

FANCD2	Fanconi anaemia complementation group D2
FBS	Foetal bovine serum
FBXO3	F-box protein 3
FD	Fibrous dysplasia
FDR	False discovery rate
FGF2	Fibroblast growth factor 2 (basic) gene
FGF8	Fibroblast growth factor 8
FGF23	Fibroblast growth factor 23
FGFR1	Fibroblast growth factor receptor 1 gene
FGFR2	Fibroblast growth factor receptor 2 gene
FGFR4	Fibroblast growth factor receptor 4
FGFR4	Fibroblast growth factor receptor 4 gene
FH	Fumarate hydratase gene
FIPA	Familial isolated pituitary adenoma
FKBP	FK506-binding protein
FKBP37.7	FK506-binding protein 37.7
FOLR1	Folate receptor 1 gene
FOS	FBJ murine osteosarcoma viral oncogene homolog gene
FOSB	FBJ murine osteosarcoma viral oncogene homolog B gene
FOXL2	Forkhead box protein L2
FSH	Follicle-stimulating hormone
G protein	Guanine nucleotide-binding protein
GADD45B	Growth arrest and DNA-damage-inducible beta gene
GADD45G	Growth arrest and DNA-damage-inducible gamma gene
GATA2	Endothelial transcription factor GATA-2
GDIB	Rab GDP dissociation inhibitor beta
gDNA	Genomic DNA
GDP	Guanosine diphosphate
GOF	Gain-of-function
GPR101	G protein-coupled receptor 101 gene
GTP	Guanosine triphosphate
GTPase	Guanosine triphosphate hydrolase
GH	Growth hormone
GHR	Growth hormone receptor gene
GHRH	Growth hormone-releasing hormone
GHRH	Growth hormone-releasing hormone gene
GHRHR	Growth hormone-releasing hormone receptor
GHRHR	Growth hormone-releasing hormone receptor gene
$G\alpha_o$	G protein subunit alpha o (“other”)
$G\alpha_{12}$	G protein subunit alpha-12
Gi	Inhibitory G protein

$G\alpha_{i1}$	Inhibitory G protein subunit alpha-1
$G\alpha_{i2}$	Inhibitory G protein subunit alpha-2
$G\alpha_{i3}$	Inhibitory G protein subunit alpha-3
$G\alpha_{q}$	G protein q (phospholipase C activating) subunit alpha
GIST	Gastrointestinal stromal tumour
GLI1	Zinc finger protein GLI 1
GLI3	Zinc finger protein GLI 3
GNA13	Guanine nucleotide-binding protein subunit alpha 13
GNAI2	Guanine nucleotide binding protein alpha inhibiting 2 gene
GNAQ	Guanine nucleotide-binding protein G(q) subunit alpha
GNAS1	GNAS complex locus (referring to the CDS for GNAS1 protein)
GnRH	Gonadotropin-releasing hormone
GPCR	G protein coupled receptor
GRB2	Growth factor receptor-bound protein 2
Gs	Stimulatory G protein
Gsα	Stimulatory G protein subunit alpha
Gsβ	Stimulatory G protein subunit beta
Gsγ	Stimulatory G protein subunit gamma
GST	Glutathione-S-transferase
GSTA1	Glutathione S-transferase A1
GSTM1	Glutathione S-transferase Mu 1
GSTM2	Glutathione S-transferase Mu 2
GSTP1	Glutathione S-transferase P
H&E	Haematoxylin-eosin
HA	Human influenza hemagglutinin
HDAC2	Histone deacetylase 2 gene
HECT	Homology to E6AP C-terminus
HMGA1	High mobility group AT-hook 1 gene
HMGA2	High mobility group AT-hook 2 gene
HESX1	Homeobox expressed in embryonic stem cells 1
HIF	Hypoxia-inducible factor
HIF1α	Hypoxia-inducible factor 1, alpha subunit (basic helix-loop-helix transcription factor)
HIF1β	Hypoxia-inducible factor 1, beta subunit (basic helix-loop-helix transcription factor)
HIF2α	Hypoxia-inducible factor 2, alpha subunit
HIF2A	Hypoxia-inducible factor 2, alpha subunit gene
HIF2β	Hypoxia-inducible factor 2, beta subunit
HIF3α	Hypoxia-inducible factor 3, alpha subunit
HOXA9	Homeobox A9 gene
HRAS	Harvey rat sarcoma viral oncogene homolog gene
HSPA5	78 kDa glucose-regulated protein
HSPA8	Heat shock cognate 71 kDa protein

HSPA9	Stress-70 protein, mitochondrial
HSP90A	Heat shock protein 90 alpha
HSP90AA1	Heat shock protein 90 alpha gene
HSP90B	Heat shock protein 90 beta
HSP90AB1	Heat shock protein 90 beta gene
hTERT	Human telomerase reverse transcriptase
IAA	Iodoacetamide
ICA	Internal carotid artery
IDH1	Isocitrate dehydrogenase 1 (NADP+), soluble gene
IFS	Isolated familial somatotropinoma
IGF-1	Insulin-like growth factor 1
IGF-2	Insulin-like growth factor 2
IGFBP-2	Insulin-like growth factor binding protein 2
IHC	Immunohistochemistry
IKBKG	NF-kappa-B essential modulator
IKZF1	IKAROS family zinc finger 1 gene
IPTG	Isopropyl-β-thiogalactoside
IRE1	Inositol-requiring gene 1
IRF7	Interferon regulatory factor 7
iRNA	Interference RNA
ISG15	Interferon-induced 15 kDa protein
ISL1	Insulin gene enhancer protein-1
JUN	Jun protooncogene
JUND	JunD protooncogene
KD	Knockdown
kDa	Kilodaltons
KHSRP	Far upstream element-binding protein 2 ()
KIF1B	Kinesin family member 1B gene
KDM4D	Lysine-specific demethylase 4D
KO	Knockout
LAMB	Lentigines, atrial myxomas and blue nevi
LAMP1	Lysosome-associated membrane glycoprotein 1
LANCL1	LanC-like protein 1
LAPTM4B	Lysosomal protein transmembrane 4 beta gene
LC	Lymphoblastoid cells
LCCSCT	Large-cell calcifying Sertoli cell tumours
Let-7	Let-7 microRNA precursor
LH	Luteinising hormone
LHX3	LIM/homeobox protein 3
LHX4	LIM/homeobox protein 4
LOF	Loss-of-function

LOH	Loss of heterozygosity
MAF	Minor allele frequency
MAGEA3	Melanoma antigen family A3 gene
MAPK	Mitogen-activated protein kinase
MAS	McCune-Albright syndrome
MAX	MYC associated factor X gene
MEG3	Maternally expressed 3 (non-protein coding) gene
MEM	Minimum essential medium
MEN1	Multiple endocrine neoplasia type 1
MEN1	Multiple endocrine neoplasia type 1 gene
MEN4	Multiple endocrine neoplasia type 4
MERTK	MER proto-oncogene, tyrosine kinase gene
MES	2-(N-Morpholino)ethanesulfonic acid (MES)
MGMT	O-6-methylguanine-DNA methyltransferase
min	Minute(s)
miRNAs	MicroRNAs
MLL	Mixed lineage leukaemia protein
MLPA	Multiplex ligation-dependent probe amplification
MRI	Magnetic resonance images
mRNA	Messenger RNA
MS	Mass spectrometry
MSHR	Melanocyte-stimulating hormone receptor
MT-CYB	Mitochondrially encoded cytochrome b gene
mtDNA	Mitochondrial DNA
MT-ND1	Mitochondrially encoded NADH dehydrogenase 1 gene
MT-ND2	Mitochondrially encoded NADH dehydrogenase 2 gene
MT-ND3	Mitochondrially encoded NADH dehydrogenase 3 gene
MT-ND4	Mitochondrially encoded NADH dehydrogenase 4 gene
MT-ND5	Mitochondrially encoded NADH dehydrogenase 5 gene
MT-RNR2	Mitochondrially encoded 16S RNA gene
MT-TM	Mitochondrially encoded tRNA methionine gene
MT-TI	Mitochondrially encoded tRNA isoleucine gene
MT-TL2	Mitochondrially encoded tRNA leucine 2 (CUN) gene
MT-TV	Mitochondrially encoded tRNA valine gene
MT-TW	Mitochondrially encoded tRNA tryptophan gene
MYC	V-myc avian myelocytomatosis viral oncogene homolog gene
m/z	Mass-to-charge ratio
N-terminal	Amino-terminal
NADSYN1	Glutamine-dependent NAD(+) synthetase
NAME	Nevi, atrial myxomas and ephelides
NEAA	Non-essential amino acids

NEDD8	Neural precursor cell expressed developmentally down-regulated protein 8
NEFL	Neurofilament, light polypeptide
NESP55	Neuroendocrine secretory protein 55 isoform NESP55
NEUROD1	Neuronal differentiation 1
NF1	Neurofibromin 1 gene
NFκB	Nuclear factor kappa B
NFPA	Non-functioning pituitary adenoma
NHLBI EVS	National Heart, Lung, and Blood Institute Exome Variant Server
NKX3-1	Homeobox protein Nkx-3.1
NLS	Nuclear localization signal
NMD	Nonsense-mediated mRNA decay
NME1	Nucleoside diphosphate kinase 1
NOTCH2	Neurogenic locus notch homolog protein 2
NOTCH3	Neurogenic locus notch homolog protein 3
NR3C1	Nuclear receptor subfamily 3, group C, member 1 (glucocorticoid receptor) gene
NR3C2	Mineralocorticoid receptor
OGTT	Oral glucose tolerance test
ODC1	Ornithine decarboxylase 1 gene
ORF	Open reading frame
P	*P* value
PAGE	Polyacrylamide gel electrophoresis
PAP	Pituitary adenoma predisposition
PAX6	Paired box protein Pax-6
PBS	Phosphate buffered saline
PCA	Protein-fragment complementation assay
PCR	Polymerase chain reaction
PDE2A	cGMP-dependent 3',5'-cyclic phosphodiesterase 2A
PDE4A	cAMP-specific 3',5'-cyclic phosphodiesterase 4A
PERK	PKR-like ER kinase
PHD	Prolyl-hydroxylase
PHPT	Primary hyperparathyroidism
PIK3CA	Phosphatidylinositol-4, 5-bisphosphate 3-kinase catalytic subunit alpha gene
PIT1	Pituitary-specific positive transcription factor 1
PITX1	Pituitary homeobox 1
PITX2	Pituitary homeobox 2
PKA	Protein kinase A
PL-MS	Proximity label-mass spectrometry
PLAGL1	Pleiomorphic adenoma gene-like 1 gene
POU3F4	POU domain, class 3, transcription factor 4
PP	Precocious puberty
PPB	Pleuropulmonary blastoma

PPARA	Peroxisome proliferator-activated receptor alpha
PPARG	Peroxisome proliferator-activated receptor gamma
PPIase	Peptidylprolyl *cis*-trans isomerase
PPNAD	Primary pigmented nodular adrenal dysplasia
PPP6R2	Serine/threonine-protein phosphatase 6 regulatory subunit 2
PRKACA	Protein kinase A catalytic subunit alpha
PRKACA	Protein kinase A catalytic subunit alpha gene
PRKAR1A	Protein kinase A regulatory type I subunit alpha
PRKAR1A	Protein kinase A regulatory type I subunit alpha gene
PRKCD	Protein kinase C delta gene
PRL	Prolactin
PROP1	Homeobox protein prophet of Pit-1
ptd-FGFR4	Pituitary tumour-derived fibroblast growth factor receptor 4
PTEN	Phosphatase and tensin homolog gene
PTGES3	Prostaglandin E synthase 3
PTH	Parathyroid hormone
PTHrp	Parathyroid hormone-related protein
PTN	Pleiotrophin gene
PTTG1	Pituitary tumour-transforming 1 gene
PTTG1IP	Pituitary tumour-transforming 1 interacting protein gene
qMS	Quantitative mass spectrometry
RARS	Arginyl-tRNA synthetase
RB1	Retinoblastoma 1 gene
RBMX	RNA binding motif protein, X-linked gene
RBR	RING-between-RING
RC	Reconstituted complex
RET	Rearranged during transfection tyrosine-kinase receptor
RET	Rearranged during transfection protooncogene
RHBDD3	Rhomboid domain containing 3 gene
RING	Really interesting new gene
RISC	RNA-induced silencing complex
RNA	Ribonucleic acid
RNase	Ribonuclease
RPA2	Replication protein A 32 kDa
RPS12	40S ribosomal protein S12
RPS14	40S ribosomal protein S14
RPS20	40S ribosomal protein S20
RPS21	40S ribosomal protein S21
RPS28	40S ribosomal protein S28
rRNA	Ribosomal RNA
RT	Room temperature

SCF	SKP1-CUL1-F-BOX protein complex
SDH	Succinate dehydrogenase
SDHA	SDH complex subunit A, flavoprotein (Fp)
SDHA	SDH complex, subunit A, flavoprotein (Fp) gene
SDHAF2	SDH complex assembly factor 2
SDHAF2	SDH complex assembly factor 2 gene
SDHB	SDH complex, subunit B, iron sulphur (Ip)
SDHB	SDH complex, subunit B, iron sulphur (Ip) gene
SDHC	SDH complex, subunit C, integral membrane protein, 15k Da
SDHC	SDH complex, subunit C, integral membrane protein, 15k Da gene
SDHD	SDH complex, subunit D, integral membrane protein
SDHD	SDH complex, subunit D, integral membrane protein gene
SDHx	Subunits A, B, C and D of the SDH mitochondrial complex II genes
SDS	Sodium dodecyl sulfate
sec	Second(s)
SF1	Steroidogenic factor 1
SHC1	Src homology 2 domain containing transforming protein 1 gene
SHH	Sonic hedgehog
SILAC	Stable isotope labelling by amino acids in cell culture
siRNAs	Small interfering RNAs
SIX6	Homeobox protein SIX6
SKP1	S-phase kinase-associated protein 1
SMAD2	SMAD family member 2
SMAD3	SMAD family member 3
SMARCA4	SWI/SNF related, matrix associated, actin dependent regulator of chromatin, subfamily a, member 4 gene
SNP	Single nucleotide polymorphism
SOD1	Superoxide dismutase 1, soluble
SOS1/2	Son of sevenless homologs 1/2 (Drosophila)
SOX2	SRY (sex determining region Y)-box
SOX5	SRY (sex determining region Y)-box gene
SRF	C-fos serum response element-binding transcription factor gene
SS	Somatostatin
SSA	Somatostatin analogue(s)
SSTR	Somatostatin receptor
SSTR2	Somatostatin receptor 2 gene
STI1	Stress-induced phosphoprotein 1
SUGT1	Suppressor of G2 allele of SKP1 homolog
SUMO	Small ubiquitin-like modifier
TAE	Tris-Acetate EDTA
TAP	Tandem affinity purification

TBX19	T-box 19
TCDD	2, 3, 7, 8-tetrachloro-*p*-dioxin
TCEP	Tris(2-carboxyethyl)phosphine hydrochloride
TCTP	Translationally-controlled tumour protein
TE	Trypsin-EDTA
TEAB	Triethylammonium bicarbonate
TEV	Tobacco etch virus
TGF-β	Transforming growth factor beta
THRB	Thyroid hormone receptor beta
THRB	Thyroid hormone receptor beta gene
TMEM127	Transmembrane protein 127 gene
TMT	Tandem mass tagging, tandem mass tags
TNNI3K	TNNI3 interacting kinase
TOMM20	Mitochondrial import receptor subunit TOM20 homolog
TP53	Tumour protein p53
TP53	Tumour protein p53 gene
TPD52	Tumour protein D52 gene
TPR	Tetratricopeptide repeat
TRH	Thyrotropin-releasing hormone
tRNA	Transfer RNA
TSH	Thyroid stimulating hormone
TUBB	Tubulin beta chain
TUBB2A	Tubulin, beta-2A chain
TUBB4B	Tubulin, beta-4B chain
UBA1	Ubiquitin-like modifier-activating enzyme 1
UBA6	Ubiquitin-like modifier-activating enzyme 6
UBC	Polyubiquitin C
UPR	Unfolded protein response
UPS	Ubiquitin-proteasome system
UQ	Ubiquinone
USP8	Ubiquitin specific peptidase 8 gene
USP19	Ubiquitin specific peptidase 19
UTR	Untranslated region
VAPA	VAMP (vesicle-associated membrane protein)-associated protein A, 33 kDa
VDR	Vitamin D receptor
VHL	Von Hippel-Lindau tumour suppressor, E3 ubiquitin protein ligase gene
WB	Western blot
WEE1	WEE1 G2 checkpoint kinase gene
WIF1	WNT inhibitory factor 1 gene
WISP2	WNT1-inducible signalling pathway protein 2
WNT	Wingless-type MMTV integration site family protein

WNT	Wingless-type MMTV integration site family gene
WNT4	Protein Wnt-4
WNT5A	Protein Wnt-5a
WT	Wild type
X-Gal	5-bromo-4-chloro-3-indolyl-beta-D-galacto-pyranoside
X-LAG	X-linked acrogigantism
XAP2	X-associated protein 2
XLαs	Protein GNAS isoform XLas

Acknowledgements

I would like to acknowledge the support of my funding bodies, the National Council of Science and Technology (CONACYT) and the Secretariat of Public Education (SEP) from Mexico, as well as the Barts and The London Charity. The financial support from these sponsors was fundamental for the accomplishment of my research goals.

A PhD degree is awarded to one person at a time, but scientific research cannot be understood in any other way than as the product of collective work. Therefore, I must refer here to the people who made my way through the last four years much smoother. For giving me the opportunity of being part of her research group, for her advises and criticisms, but, overall, for guiding my work while respecting my own initiatives and recognising my little successes, I am extremely grateful to Márta Korbonits. Her enormous contribution on the construction of my career will be unforgettable. I would also like to thank the great friends who started the adventure with me and stayed long enough to see the happy conclusion, Ida Pernicova and Daniela Aflorei. I am also infinitely grateful to other marvellous friends and colleagues I had the opportunity to work with during these years, in “order of appearance”: Sayka Barry, Federico Martucci, Giampaolo Trivellin, Judit Dénes, Craig Stiles, Maria Hérincs, Plamena Gabrovska, Serban Radian, Sharon Ajodha, Karen Young, Francesco Ferraù, Donato Iacovazzo, Márton Doleschall, Francisca Caimari and Mary Dang, as well as the rest of the Centre for Endocrinology staff. For making clear to me that the way is more important than the goal, thanks to all of you. I would also like to express my gratitude to Ashley Grossman for his support, as well as to Fulvio D’Acquisto, Chrisostomos Prodromou, Marc Morgan and Steven Lynham, for their invaluable help in different stages of my experimental work.

To my two great mentors and friends, who helped me starting an “affair” with science and who encouraged me to pursue a career in scientific research, no matter how difficult it seemed to be, Rafael Argüello and Moisés Mercado. Thank you for teaching me than being successful in life means helping others to make their dreams true.

To my fabulous and indefatigable friends, whose long-lasting fraternal love has filled every moment of my life, Yaneth Molina, Alicia San Juan and Karla Lam. Thanks for keeping my insanity within “socially acceptable” levels.

Fruits cannot come from trees with no solid roots. Infinite thanks to the roots of my life, my family Héctor Hernández, Patricia Ramírez and Patricia Hernández, for the unconditional support, love and patience you have offered me since I can recall.

Last but not least, for believing in me and for always being at my side, demonstrating that love is a dimension beyond space and time, thanks Christian Silva. Definitely, freedom is more delightful when it is shared with someone else!

Justification

Pituitary adenomas are common tumours originated in the adenohypophysis.[1] Even though these neoplasms are almost always histologically benign, they can cause considerable morbidity due to excessive hormonal secretion, and/or compression and local invasion of important surrounding structures.[2]

Most of the pituitary adenomas occur sporadically, and only around 4-5% of the cases are estimated to occur in a familial setting, either isolated or as part of endocrine tumour syndromes.[3] However, the proportion of pituitary adenomas that could potentially be inherited may be higher,[4] and this is especially true for some subsets of patients. For example, genetic forms of pituitary adenomas (both hereditary and non-hereditary) are more common within young patients;[5] in fact, up to 20% of the children with a hormone-secreting pituitary adenoma have a germline mutation in a known predisposing gene.[6;7]

Despite their relative rarity, familial pituitary tumours represent a very important group of conditions with a heterogeneous genetic background and a widely variable phenotype within affected families. A better understanding of the causative genes and the pathogenic mechanisms of this particular group of tumours is needed to improve the diagnosis and management of these patients, leading to a better prognosis.

Familial isolated pituitary adenoma (FIPA) is defined as the occurrence of pituitary adenomas in two or more members of the same family, in the absence of other clinical features. Around 20% of the cases of FIPA are due to mutations in the aryl-hydrocarbon receptor interacting protein gene (*AIP*).[8-11] Germline *AIP* mutations (*AIP*muts) also play an important role in a subset of sporadically diagnosed[7;12;13] pituitary adenomas and in somatotropinomas resistant to the treatment with somatostatin analogues (SSA).[14] In general, pituitary adenomas associated with *AIP*muts tend to arise at a young age, and to be large, aggressive, and relatively resistant to the treatment with SSA. However, the phenotype is variable and the clinical picture remains incompletely described, due to the rarity of these cases. This research work describes in detail the characteristic clinical features of *AIP*mut positive FIPA and sporadic pituitary adenomas in a large cohort of patients, which should be useful to increase the knowledge about this condition and to guide the genetic screening of these groups of patients. A successful outcome of genetic testing for disease-causative genes is the possibility of detecting the condition in a subclinical stage; therefore, information about the clinical screening and follow-up of *AIP*mut positive unaffected carriers and the prospective diagnosis of pituitary adenomas in these individuals is also provided.

A tumour suppressor function of *AIP* is supported by *in vitro* and *in vivo* models of pituitary tumorigenesis, and an abnormal or deficient protein is supposed to account for the phenotype of

pituitary adenomas. Nevertheless, while individuals with *AIP*muts develop only pituitary adenomas, AIP is a ubiquitously expressed protein and the reason for its tissue-specific tumorigenic effect is currently unknown. AIP has multiple interacting partners,[15] but none of them is known to exert a pituitary-specific function; therefore, the exact molecular mechanism for the development of pituitary adenomas in *AIP*mut positive individuals remains unveiled. In addition, AIP expression in somatotropinomas is a marker of responsiveness to the treatment with SSA in somatotropinomas;[16;17] therefore, AIP seems to also play a role in acromegaly not related to *AIP*muts. A better understanding of the molecular basis of *AIP*mut-related pituitary adenomas could lead to the implementation of disease-specific protocols of treatment, with an expectedly better clinical outcome. Also, a detailed description of the molecular pathways in which AIP is involved could reveal potential drug targets for acromegaly treatment. In addition, the protein stability of missense AIP mutants has been studied, as a means to determine the effect of clinically relevant *AIP*muts on the protein structure and function.

In summary, this research work is expected to increase the knowledge about the clinical features of *AIP*mut-related FIPA and sporadic pituitary adenomas, to provide guidance for *AIP*mut screening in patients and for the follow-up of apparently unaffected *AIP*mut positive carriers, to elucidate the molecular partners of AIP in the pituitary gland and to explain the pathogenic mechanism of missense *AIP*muts. This work should also provide evidence about the effect of missense *AIP*muts on protein stability, which could be a good method to determine pathogenicity.

General aims

- To confirm and extend the description of the genotype and phenotype of patients with *AIP*mut-related familial and *simplex* pituitary adenomas in a large cohort of pituitary adenoma patients, providing a comparison with *AIP*mut negative cases, and to perform a systematic follow-up of families to identify and characterise *AIP*mut positive carriers.

- To identify the molecular partners of *AIP* in the pituitary gland using a proteomic approach and to analyse the potential role of *AIP* in the pathways that drive pituitary tumorigenesis.

- To analyse the mechanism and speed of protein turnover of wild type (WT) AIP and AIP missense variants, and to correlate the protein half-life with the phenotype, using protein stability as an indicator of loss-of-function (LOF).

Chapter 1: General overview

The pituitary gland

Functional Macroscopic and Microscopic Anatomy

The pituitary gland coordinates the function and structural integrity of multiple endocrine glands, such as the thyroid, adrenals and gonads. Pituitary hormones also exert effects on other target tissues, including the cartilage and breast.[18] The term *pituitary* is derived from the Greek *ptuo* and the Latin *pituita,* 'phlegm', which refers to its nasopharyngeal origin.[18] The pituitary is located within the *sella turcica*, a recess of the sphenoid bone in the middle cranial fossa, above the sphenoid sinus,[19] and it is covered by the *diaphragma sella*e, a dural recess separating it from the suprasellar cistern (located superiorly), which is traversed by the pituitary stalk, a structure connecting the gland with the hypothalamic median eminence.[18;19] The optic chiasm is located anteriorly to the pituitary stalk (infundibulum).[20] Lateral to the pituitary gland are the cavernous sinuses, containing the internal carotid arteries, sympathetic fibres and the cranial nerves III, IV, V (ophthalmic and maxillary branches) and VI.[19] Anteriorly, the pituitary is flanked by the *tuberculum sellae* (the anterior part of the *sella turcica*) and the anterior clinoid processes, and posteriorly, by the *dorsum sellae* with the posterior clinoid processes.[21] An adult pituitary gland weights 400-900 mg and measures 13 mm transversally, 6-9 mm vertically and 9 mm anteroposteriorly,[18] though a physiological increase in size occurs during puberty and pregnancy.[22]

The pituitary gland is composed of an anterior lobe (adenohypophysis), comprising two thirds of the total volume of the gland, and a posterior lobe (neurohypophysis).[21] The anterior lobe is subdivided in three components, *pars distalis* (*pars glandularis*), *pars intermedia* and *pars tuberalis* (*pars infundibularis*), being the first the biggest one (80% of the volume of the adenohypophysis) and the responsible for the secretion of adenohypophysial hormones.[19;20] The *pars intermedia* is located between the *pars distalis* and the posterior pituitary, and corresponds to the intermediate lobe found in other species, though it is vestigial in humans.[19] The *pars tuberalis* extends upwards, surrounding the infundibular stalk.

The anterior pituitary is an endocrine tissue, composed of nests or cords of cuboidal cells, surrounded by venous sinusoids with a fenestrate epithelium, which collects the secretory products of the gland.[19] The classical histopathological description classified the cells of the anterior pituitary in three groups, according to their appearance in haematoxylin-eosin (H&E)-stained specimens: chromophobes, acidophils and basophils.[21] The use of immunohistochemistry (IHC) techniques allowed a more detailed classification, based on the secretory products of the cells, and currently, five different hormone-producing cell lineages are distinguished in the anterior pituitary.[21] Fifty percent of the cells are somatotrophs (producing somatotrophin or growth hormone [GH]), 10-30% are lactotrophs (producing prolactin [PRL]), 15-20% correspond to corticotrophs (producing adrenocorticotropic hormone [ACTH]), 10-15%

are gonadotrophs (producing luteinising [LH] and follicle-stimulating [FSH] hormones), and the less abundant cells are thyrotrophs (producing thyroid stimulating hormone [TSH], representing only 3-5% of all the cells).[22] Some cells do not stain with the antibodies to any of the anterior pituitary hormones, but they show secretory granules under electron microscopy; these cells are usually chromophobes.[21]

The anterior pituitary is frequently divided in three morphological areas, with different cellular composition: two lateral wings and a median wedge. Most of the somatotrophs are located in the lateral wings, but they also occupy a narrow posterolateral area, and they can be found scattered in the median wedge.[23] Lactotrophs are evenly scattered on the *pars distalis*, but they predominate in the posterolateral rim of the lateral wings.[23] Corticotrophs cluster in the central wedge, but they are also scattered in the lateral wings. Gonadotrophs can be found evenly distributed in the *pars distalis* and they are the main component of the *pars tuberalis*.[20] Thyrotrophs are mainly located in the anterior median wedge, with a few of them extending to the lateral wings and the pars tuberalis.[20;23]

The endocrine cells in the anterior pituitary are surrounded by non-endocrine, agranular cells known as folliculostellate cells, comprising 5-10% of the total pituitary cells.[20] Folliculostellate cells comprise an immunophenotypically heterogeneous population, playing an important role in controlling the behaviour of the surrounding cells, by the formation of a complex tridimensional network involved in the integration of the pituitary autocrine and paracrine loops, and as scavengers engulfing degenerated cells.[24;25] These star-shaped cells stain positive for S100 protein and/or glial fibrillary acidic protein, suggesting an astrocyte- or microglia-like origin,[26] but they can also express interleukin-6 and the major histocompatibility complex antigen type II (dendritic cell immunophenotype) and/or keratin (epithelial-like cells),[24] as well as other growth factors and cytokines, such as leukaemia inhibitory factor, basic fibroblastic growth factor, vascular endothelial cell growth factor and follistatin.[25] Other non-endocrine cells in the anterior pituitary are the granule-free, follicular cells[27] and large epithelial cells with strong cytoplasmic positivity for mitochondrial protein and cytochrome oxidase, corresponding to oncocytes.[28] The *pars intermedia* is not structurally distinct in the human pituitary, and the proopiomelanocortin-producing cells, supposedly originated from this area, are found scattered throughout the *pars distalis.*[29]

The posterior pituitary comprises the *pars nervosa*, the infundibular stalk, the hypothalamic median eminence and a structure at the base of the hypothalamus denominated tuber cinereum.[20] The *pars nervosa* is an extension of the ventral diencephalon (the embryological structure that forms the hypothalamus), formed by axons projecting from hypothalamic magnocellular neurons from the supraoptic and paraventricular nuclei, that secrete oxytocin and arginine-vassopressin,[30] surrounded by pituicytes.[21]

The function of the anterior pituitary is regulated by the secretion of multiple hormones and factors produced mainly by neurons located in the medial hypothalamus.[20] The medial eminence, containing axons from the periventricular, paraventricular and arcuate nuclei, is the principal structure linking the function of the hypothalamus and the pituitary gland.[20] This structure lies outside the blood-brain barrier, allowing the release of hypophysiotropic hormones and factors into a specialised hypophysial portal system, which irrigates the *pars distalis* with venous blood through the long portal veins.[19;20] The portal capillary plexus in the median eminence is irrigated by the superior hypophysial artery, a branch of the internal carotid. The *pars distalis* also receives venous blood from the posterior pituitary through the short portal vessels.[19] Other hypophysiotropic factors are not transported by the portal system, but released locally by axons originated from other structures of the central nervous system.[20]

The feedback regulation of the hypothalamus by peripheral humoral factors seems to occur via transcytosis through glial and endothelial cells in the blood-brain barrier, permeable capillaries that reach the cerebrospinal fluid and through bidirectional fenestrated capillaries.[20] The main factors involved in the hypothalamic-pituitary crosstalk are the neurohypophysial hormones (arginine-vasopressin and oxytocin) and the hypophysiotropic hormones, including: corticotropin-releasing hormone (CRH), cortistatin, ghrelin, gonadotropin-releasing hormone (GnRH), GH-releasing hormone (GHRH), somatostatin (SS), thyrotropin-releasing hormone (TRH) and urocortin.[20;31-33] Additionally, the anterior pituitary synthesises non-classical peptides, growth factors, cytokines, binding proteins and neurotransmitters, important for the autocrine/paracrine control of its own hormonal secretion and for the control of growth and cell proliferation under specific physiological conditions.[19]

The venous drainage from the anterior pituitary is carried out by the adenohypophysial veins, and the posterior pituitary is drained by the adenohypophysial veins. Both systems anastomose forming the confluent pituitary veins and end at the cavernous sinus. The posterior pituitary is irrigated by branches of the inferior hypophysial arteries.[19]

Embryology

The human hypothalamus-pituitary axis is established by the 20 weeks of gestation.[21] The anterior pituitary derives from the Rathke's pouch, an evagination of the oral ectoderm at the level of the oropharynx, evident by the third week of gestation.[34] During development, the anterior pituitary remains in close contact with the primordium of the ventral hypothalamus (the ventral diencephalon, derived from neuroectoderm); this relationship is critical for the differentiation of the pituitary endocrine cells.[35]

Most of the knowledge about pituitary embryogenesis proceeds from studies in murine models, but these data can be extrapolated to the human embryo. The earliest transcription factor implicated in the development of the pituitary primordium is homeobox expressed in embryonic stem cells 1 (HESX1).[34] Other early transcription factors expressed by the primordium include

pituitary homeobox (PITX) 1 and 2, transcription factor SOX-2 (SOX2), LIM/homeobox protein Lhx (LHX) 3 and 4, homeobox protein SIX6 (SIX6), beta-catenin (CTNNB1), zinc finger protein GLI (GLI) 1 and 3 and neurogenic locus notch homolog protein (NOTCH) 2 and 3.[35] Sequential phases of signalling events are implicated in the terminal differentiation of the pituitary cells. First, the bone morphogenetic protein (BMP) 4 signal (together with protein Wnt-5a [WNT5A] and fibroblast growth factor [FGF] 8), arising from the ventral diencephalon, induces organ commitment in the anterior pituitary.[36] Then, BMP2 expression appears in a region of oral ectoderm in which sonic hedgehog (SHH), which is initially uniformly expressed, selectively disappears. This ventral BMP2 signal and the dorsal FGF8 expression create opposing activity gradients, inducing overlapping patterns of specific transcription factors, favouring cell lineage specification. The main dorsally-expressed transcription factors are homeobox protein Nkx-3.1 (NKX3-1), SIX3, paired box protein Pax-6 (PAX6), and homeobox protein prophet of Pit-1 (PROP1).

Before the appearance of the ventral cells, pituitary-specific positive transcription factor 1 (POU1F1, also known as PIT1) leads to somatotroph, lactotroph, and thyrotroph development, while the steroidogenic factor 1 (SF1) is selectively expressed in the gonadotrophs. Attenuation of the BMP2 signal leads to terminal ventral cell differentiation, which is dependent on the transcription factors insulin gene enhancer protein-1 (ISL1), POU domain, class 3, transcription factor 4 (POU3F4), forkhead box protein L2 (FOXL2) and endothelial transcription factor GATA-2 (GATA2). The ventral to dorsal gradient induces GATA2 in the developing gonadotrophs and thyrotrophs, and in the gonadotrophs, this transcription factor stops PIT1 expression, favouring the appearance of SF1, FOXL2 and ISL1.[34] The absence of GATA2 dorsally is critical for differentiation of PIT1-positive cells to somatotrophs and lactotrophs. Protein Wnt-4 (WNT4) expression is needed for the expansion of the ventral pituitary cell types, and PAX6 attenuates the ventral signals directing thyrotroph and gonadotroph cell lineages.[34;36] Once these differentiation events are completed, the gonadotrophs, thyrotrophs, somatotrophs, and lactotrophs display a ventral-to-dorsal location, respectively.[36] However, the adequate morphogenesis and differentiation of the pituitary primordium is not completely explained by these gradients, and it depends also on the relationship between cellular responsiveness and concentration/time of exposure of individual opposing extracellular factors.[35]

The posterior lobe derives from the neural crest as an evagination of the floor of the third ventricle, and its sides fuse to form the neural stalk, while its superior portion forms a recess in the floor of the third ventricle, the median eminence.[21] The primordium of the posterior lobe migrates downward and is encapsulated together with the ascending cells of the Rathke's pouch; its development is completed by the end of the first trimester and by then vasopressin and oxytocin can already be detected in the tissue.[37]

Pituitary adenomas

Definition

Pituitary adenomas (ICD 8272/0) are common, benign tumours from epithelial origin, arising from and composed of adenohypophysial cells,[38-40] that can express and secrete hormones autonomously or behave functionally silent.[18] As specified by the World Health Organisation 2004 histological classification of pituitary tumours, primary tumours from a non-adenohypophysial origin, as well as metastatic lesions can also affect the pituitary gland.[39]

Pituitary adenomas are classically defined as monoclonal tumours, caused by *de novo* somatic mutations in a single cell.[41-43] Nevertheless, more than one abnormal clone can exist in a pituitary adenoma, either synchronically or asynchronically, with the potential of producing oligoclonal or polyclonal proliferation.[44] Although it is improbable that hypothalamic products, such as hypophysiotropic hormones or growth factors could initiate pituitary transformation, they could certainly facilitate the proliferation of a cell already containing a tumorigenic mutation.[45] The intrapituitary microenvironment could also contribute to pituitary adenoma development through dysregulated growth factor signalling, angiogenic stimuli such as hypoxia and the presence of progenitor mesenchymal cells.[46-48]

Even though pituitary adenomas are considered as benign tumours, their behaviour is highly variable, ranging from slowly growing intrasellar masses to rapidly growing tumours with macroscopically evident extrasellar extension and invasion.[38;40] In fact, around 30 to 45% of pituitary adenomas invade the cavernous or sphenoid sinus, and some of them display features or aggressiveness.[49] The clinical presentation of pituitary adenomas is also variable, including signs and symptoms derived from local compression (visual impairment, headache, intracranial hypertension, damage to cranial nerves) and/or clinical syndromes derived from hypersecretion of one or more pituitary hormones (acromegaly, gigantism, amenorrhoea-galactorrhoea, Cushing's disease and hyperthyroidism).[38] However, many tumours remain subclinical and are only detected incidentally (pituitary incidentalomas), either during imaging studies performed for other reasons, or as autopsy findings.[50] Pituitary carcinomas (ICD 8272/3), defined as tumours of adenohypophysial cells displaying distant metastases, are extremely rare.[39;39]

Clinical and histopathological classifications

Different classifications can be applied to pituitary adenomas. Clinically, they can be divided in hormonally active or functioning adenomas and non-functioning pituitary adenomas (NFPAs), the former representing approximately two thirds of the clinically diagnosed pituitary adenomas.[51] Based on their size, pituitary adenomas can be defined as microadenomas, measuring <10 mm in their largest diameter, or macroadenomas, with maximum diameter ≥10 mm.[38] Tumours with a maximum diameter ≥40 mm are considered giant adenomas.[39]

Classification systems based on image studies are important for the preoperatory evaluation of pituitary adenomas. Hardy's classification (based on radiographic images) divides pituitary adenomas in four grades, according to their size and local extension: grade I: microadenomas, minimally alter the appearance of the sella; grade II: macroadenomas, enlarge the sella or exhibit suprasellar extension, but no destruction of bony structures; grade III: invasive adenomas, locally erode the sella and show suprasellar outgrowth; grade IV: strongly invasive adenomas, destroying adjacent bony structures, with suprasellar outgrowth and invasion of bone, hypothalamus and cavernous sinus.[52] Modified versions of Hardy's classification are also frequently used.

Knosp's classification takes into consideration the degree of invasion of the cavernous sinus in magnetic resonance images (MRI): grade 0, no cavernous sinus involvement; grade 1, tumour surpassing the medial tangent (between the medial aspects of the intra and supracavernous internal carotid artery [ICA]), but not the intercarotid line (between the cross-sectional centres of the intra and supracavernous ICA); grade 2, extension beyond the intercarotid line, not surpassing the tangent on the lateral aspects of the intra and supracavernous ICA; grade 3A, tumour extension lateral to the lateral tangent of the intra and supracavernous ICA into the superior cavernous sinus compartment; grade 3B, tumour extension lateral to the lateral tangent of the intra and supracavernous ICA into the inferior cavernous sinus compartment; grade 4, total encasement of the intracavernous carotid artery.[53;54]

According to their degree of invasiveness, pituitary adenomas are classified as intrapituitary (confined within the gland), intrasellar (confined to the sella turcica, with no erosion of bony structures), diffuse (large and expansive, fill the sella turcica without bone erosion), or invasive (erode the sella, spread into neighbouring tissues).[38] Pituitary adenomas can display expansive growth (for example, suprasellar extension), when an interface is conserved between the tumour and the surrounding tissues, or invasive growth, when there is involvement of other tissues (dura, bone, nerves, vessels, etc.).[39;55] However, microscopic invasion, found in 35-46%[56;57] of the cases, is not considered a feature of aggressiveness.[39]

The World Health Organisation 2004 classification divides pituitary adenomas into the categories of typical adenomas, atypical adenomas and pituitary carcinomas, but the more detailed histological subclassification of these tumours is based on their IHC profile, considering also the cell lineage of origin and the main transcription factors expressed in each case,[39] as summarised in Table 1. Besides this classification, most of the pituitary adenomas are positive for synaptophysin, and in a lower degree, to chromogranin A (CgA) and/or low molecular weight keratins, such as cytokeratin (Ck).[39]

Table 1. Clinicopathological classification of pituitary adenomas[39;47;58-61]

Transcription factors (cell lineage)	Cell of origin	Tumour type and variants*	Frequency (% of total)†	IHC profile	Usual clinical presentation	Invasive (% of total)†
PIT1 family (GH-PRL-TSH)						
	Lactotroph	*Lactotroph adenoma (prolactinoma)*				
PIT1, ER, GH repressor		Densely granulated lactotroph adenoma	0.3	PRL, Golgi pattern	Hypogonadism and/or galactorrhoea	50
PIT1, ER, GH repressor		Sparsely granulated lactotroph adenoma	8.9	PRL diffuse cytoplasmic, α-GSU		NA
PIT1, ER		Acidophil stem cell adenoma		PRL, GH, fibrous bodies	Hypogonadism and acromegaly	NA
	Somatotroph	*Somatotroph adenoma (somatotropinoma)*				
PIT1		Densely granulated somatotroph adenoma	9.2	GH, α-GSU, Ck, CgA	Acromegaly, very rarely silent	52
PIT1		Sparsely granulated somatotroph adenoma	6.3	GH, fibrous bodies, α-GSU, Ck, CgA	Acromegaly or gigantism, very rarely silent	NA
PIT1, ER, GH repressor		Mixed GH and PRL (bicellular)	5.2	GH, PRL, α-GSU, β-TSH	Hypogonadism and acromegaly	31
PIT1, ER		Mammosomatotroph adenoma	1.1	GH, PRL, α-GSU, β-TSH	Acromegaly or gigantism	NA
PIT1, TEF, GATA-2	**Thyrotroph**	Thyrotroph adenoma (thyrotropinoma)	1.5	β-TSH, α-GSU	Hyperthyroidism	100
PIT1, ER, TEF, GATA-2	**PIT1 positive cells**	Plurihormonal adenoma	NA	GH, PRL, β-TSH, α-GSU	Variable	52
ACTH family						
	Corticotroph	*Corticotroph adenoma (corticotropinoma)*				
TBX19		Densely granulated corticotroph adenoma	7.2	ACTH, β-endorphin, β-LPH, Ck, CgA	Cushing's disease, Nelson's syndrome or silent (silent corticotropinoma type 1)	NA
TBX19		Sparsely granulated corticotroph adenoma	7.9	ACTH, β-endorphin, β-LPH, Ck, CgA	Cushing's disease, Nelson's syndrome or silent (silent corticotropinoma type 2)	NA
TBX19		Crooke cell adenoma	0.03	ACTH, β-endorphin, β-LPH, Ck, CgA	Silent, possibly Cushing's disease	85
Gonadotroph family						
SF-1, ER, GATA-2	**Gonadotroph**	Gonadotroph adenoma (gonadotropinoma)	25.2	β-FSH, β-LH, α-GSU, CgA	Silent or pituitary failure/mass effect. Rarely, gonadal hyperfunction	95
SF-1		Null-cell adenoma	19.8	CgA, negative for hormones, or scattered cells positive for β-FSH, β-LH, β-TSH or α-GSU	Silent or pituitary failure/mass effect	42

Transcription factors (cell lineage)	Cell of origin	Tumour type and variants*	Frequency (% of total)†	IHC profile	Usual clinical presentation	Invasive (% of total)†
SF-1		Null-cell adenoma, oncocytic variant (oncocytoma)	5.8	CgA, negative for hormones, or scattered cells positive for β-FSH, β-LH, β-TSH or α-GSU	Silent or pituitary failure/mass effect	NA
Unclassified adenomas						
Unknown	**PIT1 negative cells?**	Unusual plurihormonal adenoma	1.3	GH, PRL and TSH, usually together. Occasionally, FSH and LH, rarely ACTH	Silent or pituitary failure/mass effect (silent adenoma subtype 3), often acromegaly and/or hyperprolactinaemia	60

NA: not available. α-GSU: glycoprotein hormone subunit alpha.
* Names in parentheses are commonly used in the literature, and for practical reasons, they will be used in this text.
† As presented in [59]

It is important to keep in mind that tumours of any pituitary cell origin can also behave clinically as NFPAs, being the cell type only determined after IHC analysis. However, regardless of their clinical presentation with no hormonal excess, most of them express one or more anterior pituitary hormones with IHC analysis, and they are therefore termed silent adenomas. This presentation is apparently due to the production of hormones with no biological activity, or maybe due to a defect in the secretion mechanism. A small number of NFPAs, termed as null cell adenomas, are immunonegative for all the adenohypophysial hormones, though they are considered of gonadotroph origin, as most of them express LH and/or FSH messenger RNA (mRNA).[47;62] Finally, oncocytic tumours display a unique pattern characterised by a remarkable abundance of mitochondria (up to 50%), obscuring other organelles.[38] In around two thirds of the oncocytic pituitary adenomas, the phenotype is explained by somatic mutations in the mitochondrial DNA (mtDNA), affecting members of the respiratory complexes I and III, mtDNA promoters, and mitochondrial ribosomal RNA (rRNA) and transfer RNA (tRNA): *MT-CYB, MT-ND1, MT-ND2, MT-ND3, MT-ND4, MT-ND5,* H (heavy)-strand promoter PH1*,* L (light)-strand promoter PL*, MT-RNR2, MT-TL2, MT-TM, MT-TI, MT-TW* and *MT-TV* genes.[63;64]

Morphological features suggestive of an aggressive behaviour can be found in some pituitary adenomas, including invasive growth, elevated mitotic index, Ki-67 labelling index ≥3% and extensive nuclear staining for TP53 by IHC. Tumours with these characteristics, in the absence of metastases, are termed atypical pituitary adenomas (ICD 8272/1),[39] accounting for 2.7-15% of all the pituitary tumours.[55] Aggressive pituitary adenomas are tumours with atypical histological features, plus an aggressive clinical behaviour (reduced response to treatment, rapid growth and recurrence). Pituitary carcinomas (0.2% of all the operated pituitary tumours) may also exhibit features of aggressiveness and/or signs of malignancy (cellular/nuclear pleomorphism, nuclear hyperchromatism, increased nuclear/cytoplasmic ratio, mitotic figures, foci of necrosis, and invasive spread) but these features are not universal, and the diagnosis of pituitary carcinoma is only established in the presence of craniospinal or systemic metastases.[38;39] A recently proposed clinicopathological classification of pituitary adenomas takes into consideration the tumour size, IHC, invasiveness and proliferation, making it useful for prognosis. It divides the pituitary adenomas in five grades: 1a, non-invasive tumour; 1b, non-invasive and proliferative tumour; 2a, invasive tumour; 2b, invasive and proliferative tumour; and 3, metastatic tumour.[65]

Epidemiology

Considered the most common lesions affecting the sellar region, pituitary adenomas account for approximately 10-15% of all the intracranial tumours, based on surgical series, and 3-24% based on unselected autopsies,[38] representing the third most common intracranial tumour type, after meningiomas and gliomas[40]. Pituitary adenomas are common, but defining their exact prevalence among the general population is not easy, due to their variable clinical features and the high proportion of cases with no clinical manifestations. A metaanalysis reported a prevalence of pituitary adenomas of 14.4% in autopsy studies and 22.5% in radiological studies,

resulting in an overall estimated prevalence of 16.7%.[1] Clinically-relevant adenomas diagnosed due to symptoms are significantly less common, but recent data show a higher prevalence than previously suspected. When considering data from population based studies, the prevalence of pituitary adenomas varies between 1:1471 and 1:1064.[66-70]

The frequency of pituitary adenomas increases with age: while more than 30% of the people in the sixth decade of life carry an undiagnosed tumour, only 3.5-8.5% of all the pituitary adenomas are detected before the age of 20 years, and they are extremely rare before the age of 9 years.[71;72] The frequency of prolactinomas peaks between the second and fifth decades of life, and NFPAs usually present between the fourth and eighth decades of life, while the rest of the pituitary adenoma types do not have a specific distribution among age groups.[73] Prolactinomas are the most common pituitary adenomas (39%), followed by NFPAs, somatotropinomas and adrenocorticotropinomas, while thyrotropinomas are infrequent.[73] Before the age of 50, pituitary adenomas are more frequent in females, but they are more common in males during the sixth decade of life.[74] Prolactinomas, adrenocorticotropinomas and thyrotropinomas are more common in females, while NFPAs and somatotropinomas are more common in males; however, in older age groups, the differences in gender distribution are lost, except for NFPAs.[73]

Most pituitary adenomas present as sporadic tumours, but it has classically been considered that 4-5% of all the pituitary adenoma cases occur in a family setting, either isolated or as part of an endocrine tumour syndrome.[3] In a recent survey-based study conducted in a tertiary hospital centre, 7% of the pituitary patients referred a family history of pituitary adenomas.[75] Nevertheless, a registry-based study demonstrated that first degree relatives of pituitary adenoma patients have a relative risk of 2.8 of carrying themselves a pituitary adenoma[4] and, therefore, the frequency of familial cases could be underestimated. The proportion of inherited cases is higher among young patients; indeed, up to 20% of the children with a hormone-secreting pituitary adenoma have a germline mutation in a known predisposing gene.[6;7]

Genetic causes of pituitary adenomas

It is usually accepted that most of the pituitary adenomas arise as a result of multiple somatic mutations, but in some cases they are due to mosaic mutations (very rarely) or germline mutations. Pituitary adenomas due to germline mutations are considered potentially inheritable even in the absence of a second case in the same family, due to the possibility of transmitting the mutated predisposing gene from one to the next generation. The main genetic causes of pituitary adenomas are summarised in Figure 1.

Somatic alterations

The current evidence suggests that multiple somatic genetic mutations and/or epimutations conferring growth advantage to a single somatic pituitary cell give rise to clonal expansion and,

eventually, to a pituitary adenoma.[42] Alterations in the expression (by diverse mechanisms) of various genes involved in cell cycle and apoptosis regulation, as well as growth factors and their receptors, are common findings in pituitary adenomas.[2] However, it is not clear whether these alterations represent primary tumorigenic events, or if they occur as a consequence of other molecular abnormalities,[2;47] although the inactivation or overexpression of various cell cycle regulators is sufficient for the development of pituitary tumours in murine models.[47;76] This environment of genomic instability facilitates the accumulation of multiple mutations, but those affecting classical tumour suppressor genes (e.g. *TP53, RB1*) or oncogenes (e.g. *BRAF, HRAS, MYC*), which are generic findings in cancer, are rarely implicated in the pathogenesis of pituitary adenomas (and in other endocrine tumours), being found only in cases of atypical adenomas and pituitary carcinomas.[2;77-79] The best known genes involved in pituitary tumorigenesis are listed in Table 2.

***GNAS1* mutations: the *gsp* oncogene**

Signalling pathways involving the accumulation of intracellular cyclic adenosine monophosphate (cAMP) play crucial roles in multiple endocrine tissues, as many hormone receptors are, indeed, heptahelical transmembrane G protein coupled receptors (GPCRs). The production of cAMP by adenylyl cyclase (AC) is regulated by heterotrimeric guanine nucleotide-binding proteins (G proteins) conformed by three different subunits, α, β and γ. When the associated GPCR is inactive, stimulatory G protein subunit alpha (Gsα) is found in complex with Gsβ and γ, and bound to guanosine diphosphate (GDP).[80] After GPCR activation following ligand binding, Gsα dissociates from the other Gs subunits and exchanges GDP for guanosine triphosphate (GTP), with subsequent activation of effector proteins, such as ACs.[80;81] Due to its intrinsic GTP hydrolase (GTPase) activity, Gsα can deactivate itself by hydrolysing GTP to GDP, preventing the continued activation of the downstream signalling pathway.[82]

The *GNAS1* gene complex, located at 20q13.32, displays a complicated genomic imprinting, generating multiple alternative products from the paternal and maternal alleles, driven by the activation of alternative promoters (four sense and one antisense), differently imprinted.[83;84] The ubiquitously expressed Gsα subunit of Gs protein is the best known product codified by *GNAS1.* Gsα is transcribed from the exons 1-13 of *GNAS1*, originating four alternatively spliced products (two long, Gsα-1 and -2, and two short, Gsα-3 and -4), that might have variable biological roles.[85] Exons 2-13 are common to the other *GNAS1* products, NESP55 and XLαs. The expression of Gsα directed by an alternative promoter located just upstream the exon 1 is biallellic; however, *GNAS1* is imprinted in a promoter-specific fashion.[86] An alternative promoter located ~49kb upstream of exon 1 is methylated on the paternal allele, so the gene expression depends on the maternal allele.[83;84] This promoter drives the expression of the human homologue of the bovine neuroendocrine secretory granule protein gene, NESP55, which has a unique exon 1 at this region and shares the exons 2-13 with Gsα and XLαs.[83]

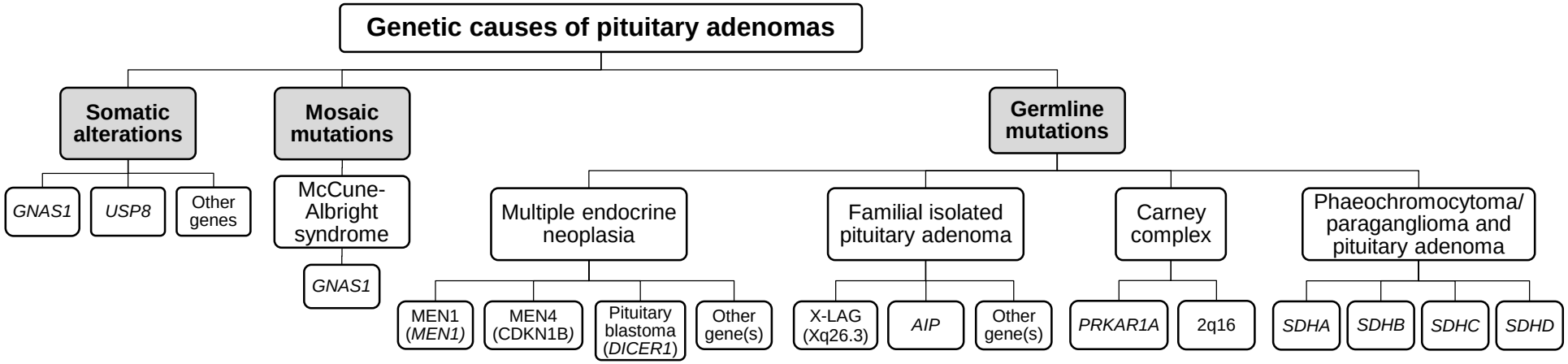

Figure 1. Genetic causes of pituitary adenomas.[8;87-95] Multiple somatic mutations and abnormalities in the expression of tumour suppressor genes/oncogenes are present in the vast majority of the pituitary adenomas, but they could theoretically coexist with germline mutations. The most common somatic mutations in pituitary adenomas are mutation in the *USP8* gene in corticotropinomas and the *gsp* oncogene (mutation in *GNAS1* codons 201 or 227) in somatotropinomas. The McCune-Albright syndrome (MAS) is a rare clinical entity, comprising the only known cause of mosaic genetic mutations causing pituitary disease. Seven clinical syndromes of inherited adenohypophysial tumours are currently known: multiple endocrine neoplasia (MEN) type 1 and type 4, the syndrome of pituitary blastoma due to *DICER1* mutations, FIPA including X-linked acrogigantism (X-LAG) and *AIP* mutation (*AIP*mut)-associated FIPA, Carney complex (CNC, due to mutations in the *PRKAR1A* gene or to still unknown genetic alterations in the 2q16 region) and the syndrome of pituitary adenoma and phaeochromocytoma/paraganglioma (3PAs). See details in text.

Table 2: Main genes involved in the pathogenesis of sporadic pituitary adenomas (modified from [2])

Gene name (other names)	Location (Chr)	Function	Molecular abnormality in pituitary adenomas	References
Tumour suppressor genes				
*AIP**	11q13.2	Co-chaperone, regulator of cAMP pathway	Decreased expression in invasive somatotropinomas	16;96
BMP4	14q22.2	Regulator of cell differentiation/proliferation in the anterior pituitary	Increased expression in prolactinomas	97
CDKN1A ($p21^{CIP1}$)	6p21.2	Cell cycle regulator (G1)	Decreased expression in NFPAs, increased in functioning adenomas (especially somatotropinomas)	98
*CDKN1B ($p27^{KIP1}$)**	12p13.1	Cell cycle regulator (G0/G1). Involved in cell migration, proliferation, neuronal differentiation, apoptosis. Tumour suppressor or oncogene	Decreased expression, especially in recurrent adenomas	99-107
CDKN2A ($p16^{INK4}$)	9p21.3	Cell cycle regulator (G1 and G2)	Decreased expression mostly by promoter methylation, mainly in NFPAs	108-116
CDKN2B ($p15^{INK4B}$)	9p21.3	Cell cycle regulator (G1)	Decreased expression partly by promoter methylation, homozygous deletion	113;114
CDKN2C ($p18^{INK4C}$)	1p32.3		Decreased expression mostly by promoter methylation	116-118
DAPK1	9q21.33	Positive mediator of programmed cell death induced by γ-interferon	Decreased expression either by promoter methylation or by homozygous deletion of the promoter CpG island	119
DKC1	Xq28	Pseudouridine synthase, rRNA modifier and telomerase regulator	LOF somatic mutation in one NFPA	120
GADD45B (GADD45-β)	19p13.3	Regulator of growth and apoptosis	Decreased expression in gonadotropinomas	121
GADD45G (GADD45-γ)	9q22.2		Decreased expression mainly due to promoter methylation in NFPAs, somatotropinomas and prolactinomas	122;123
MEG3	14q32.3	Long non-coding RNA, induces apoptosis, inhibits cell proliferation	Decreased expression in NFPAs	122;124-128
*MEN1**	11q13.1	Transcriptional regulator	LOF somatic mutations/deletions, reduced expression	129-133
PLAGL1 (ZAC1)	6q24.2	Transcription factor, role in pituitary development, differentiation, maturation and tumorigenesis	Decreased expression in NFPAs	134;135
RB1 (pRB)	13q14.2	Regulator of entry into cell division	Decreased expression partly due to promoter methylation in aggressive pituitary adenomas	113;114;136
RHBDD3 (PTAG)	22q12.2	Pro-apoptotic mediator	Decreased expression partly due to promoter methylation	137
SMARCA4 (Brg1)	19p13.2	Helicase and ATPase activities. Regulator of gene transcription by altering chromatin structure	Decreased expression, altered subcellular localisation in corticotropinomas	138
SSTR2	17q25.1	Heptahelical transmembrane GPCR for SS	Decreased expression in resistant somatotropinomas	139
THRB (TRβ)	3p24.2	Nuclear receptor for thyroid hormone	LOF somatic mutation and alternatively spliced variant in thyrotropinomas	140;141
TP53 (P53)	17p13.1	Trans-activator, negatively regulates cell division by controlling the expression of genes required for this process	LOF somatic mutations in atypical corticotropinoma and prolactinoma, post-radiotherapy aggressive corticotropinoma, pituitary carcinoma	142-145
WIF1	12q14.3	Inhibitor of WNT proteins	Decreased expression by promoter methylation	146

Gene name (other names)	Location (Chr)	Function	Molecular abnormality in pituitary adenomas	References
Oncogenes				
AKT1	14q32.33	Regulator of cell metabolism, proliferation, survival, growth and angiogenesis	Increased expression, especially in NFPAs	107
AKT2	19q13.2			
BMI1 (BMI-1)	10p12.2	Component of the polycomb repressive complex 1 (involved in the transcriptional repression of various genes)	Increased expression, genetic amplification	147-149
CCNA1 (cyclin A1)	13q13.3	Cell cycle regulation (G1/S and G2/M)	Increased expression, especially in recurrent adenomas	105;150
CCNB1 (cyclin B1)	5q13.2	Involved in G2-M transition	Increased expression	150;151
CCNB2 (cyclin B2)	15q22.2		Increased expression, correlating with HMGA1 and HMGA2	152
CCND1 (cyclin D1)	11q13.3	Promotes progression through the G1-S phase of the cell cycle	Increased expression, allelic imbalance in aggressive NFPAs and somatotropinomas	146;150;153-155
CCNE1 (cyclin E1)	19q12		Increased expression mainly in corticotropinomas	150;154
CREB1 (CREB)	2q33.3	Phosphorylation-dependent transcriptional activator of CREs	Constitutive activation by phosphorylation in somatotropinomas	156
EGFR	7p11.2	Transmembrane tyrosine kinase receptor for EGF	Increased expression in corticotropinomas, less importantly in other pituitary adenoma subtypes	157;158
FGFR1	8p11.23-p11.22	Transmembrane tyrosine kinase receptor for FGFs	Increased expression especially in NFPAs, decreased mRNA expression in thyrotropinomas	159
FGFR2	10q26.13		Decreased expression by promoter methylation	160
FGFR4	5q35.2		Increased expression of a N-terminally truncated cytoplasmic isoform (ptd-FGFR4) by alternative transcription initiation	161
FOLR1 (FR)	11q13.4	Mediator of transport of 5-methyltetrahydrofolate into the cells	Increased expression in NFPAs, decreased in prolactinomas and somatotropinomas	162
GNAI2 (Gi2α)	3p21.31	Adenylate cyclase and Ca^{++} influx inhibitor	GOF somatic mutations in NFPAs and one corticotropinoma	163;164
GNAS (GNAS1)	20q13.32	Stimulatory Gsα, AC activator	GOF somatic mutations, loss of imprinting, increased expression in some somatotropinomas	95;163-170
HDAC2	6q21	Histone deacetylase	Decreased expression in corticotropinomas	138
HMGA1	6p21.31	Various biological functions. Key role in growth and development	Overexpression	152
HMGA2	12q14.3	Various biological functions. Key role in growth and development	Amplification and overexpression in prolactinomas and NFPAs	171;172
HRAS (Ras)	11p15.5	GDP/GTP binding protein, regulator of cell division in response to growth factor stimulation	GOF somatic mutations in pituitary carcinomas	173-176
IKZF1	7p12.2	DNA-binding protein with crucial functions in the hematopoietic system and in the development of the immune system	Dominant-negative truncated isoform (Ik6)	177
LAPTM4B	613296	Required for lysosome homeostasis, acidification and function	Increased expression in NFPAs and corticotropinomas	117

Gene name (other names)	Location (Chr)	Function	Molecular abnormality in pituitary adenomas	References
MAGEA3	Xq28	Unknown function, but may play a role in embryonal development and tumour transformation or progression	Increased expression by promoter hypomethylation and histone acetylation in association with FGFR2 down-regulation	178
MERTK (CMP-tk)	2q13	Tyrosine kinase receptor, transduces signals from the extracellular matrix into the cytoplasm, several ligands	Increased expression in corticotropinomas, decreased in prolactinomas	162
ODC1 (ODC)	2p25.1	Catalyses decarboxylation of ornithine into putrescine	Increased expression in somatotropinomas, decreased in corticotropinomas	
PIK3CA	3q26.32	Catalytic subunit of phosphatidylinositol 3-kinase (coordinates cell proliferation, survival, migration, vesicle trafficking, degranulation)	GOF somatic mutations (invasive corticotropinoma, prolactinoma, plurihormonal adenomas and NFPAs) and genetic amplification	176
PRKACA (PKCα)	17q24.2	Kinase involved in growth factor- and hormone-mediated transmembrane signalling and cell proliferation	Increased expression, GOF somatic mutations in invasive NFPAs	179
PTTG1 (PTTG, securin)	5q33.3	Cell cycle regulation and cell senescence	Increased expression, especially in corticotropinomas	117;159;180;181
PTTG1IP (PBF)	21q22.3	Facilitator of nuclear translocation of PTTG1, potentiates transcriptional activation of FGF2 by PTTG1	Increased expression, especially in NFPAs	159
Other genes				
BAG1	9p13.3	Co-chaperone, regulator of HSP70/HSPA8 and PPP1R15A	Increased expression in somatotropinomas, prolactinomas, NFPAs	117
COPS5 (JAB1)	8q13.1	Probable protease subunit of the COP9 signalosome complex (involved in various cellular and developmental processes)	Increased expression in pituitary carcinomas	106
DRD2 (D2R)	11q23.2	Heptahelical transmembrane GPCR for dopamine	Decreased expression in resistant prolactinomas	182
FGF2 (bFGF)	4q27-28	Regulator of angiogenesis, cell survival, division and differentiation	Increased expression, decreased mRNA in thyrotropinomas	159
GHR	5p13-p12	Heptahelical transmembrane GPCR for GH	LOF somatic mutations in somatotropinomas	183
GHRH	20q11.23	Secretagogue for GH	Increased expression in somatotropinomas	184
GHRHR	7p14.3	Heptahelical transmembrane GPCR for GHRH	Truncated (alternatively spliced) in somatotropinomas	185
NR3C1 (GR, GCR)	5q31.3	Nuclear receptor for glucocorticoids	LOF somatic mutation and LOH in corticotropinomas	186;187
MT-CYB	MT (non-nuclear)	Component of the ubiquinol-cytochrome c reductase complex (complex III), a respiratory chain that generates an electrochemical potential coupled to ATP synthesis	LOF mutations in oncocytic pituitary adenomas	64
MT-ND1		Core subunits of the mitochondrial membrane respiratory chain NADH dehydrogenase (complex I). This complex transfers electrons from NADH to the respiratory chain. The immediate electron acceptor seems to be ubiquinone		63;64
MT-ND2				63
MT-ND3				63
MT-ND4				63;64
MT-ND5				63;64

Gene name (other names)	Location (Chr)	Function	Molecular abnormality in pituitary adenomas	References
H-strand promoter PH1		Predominant promoter of the mtDNA H-strand		[63]
L-strand promoter PL		Predominant promoter of the mtDNA L-strand		[63]
MT-RNR2		Mitochondrially encoded 16S rRNA		[64]
MT-TL2		Mitochondrially encoded tRNA leucine 2 (CUN)		[64]
MT-TM		Mitochondrially encoded tRNA methionine		[64]
MT-TI		Mitochondrially encoded tRNA isoleucine		[63]
MT-TW		Mitochondrially encoded tRNA tryptophan		[63]
MT-TV		Mitochondrially encoded tRNA valine		[64]
PITX2	4q25	Transcription factor, involved in the WNT/DVL/ CTNNB1 pathway	Increased expression in NFPAs	[188]
POU1F1 (PIT1)	3p11.2	Transcription factor, regulator of differentiation, expansion and survival of different pituitary cell types	Increased expression in somatotropinomas, prolactinomas and thyrotropinomas	[189]
USP8 (UBPY)	15q21.2	Deubiquitinase for EGFR	GOF somatic mutations in corticotropinomas	[94;190]

ATP: adenosine triphosphate; ATPase: adenosine triphosphatase; CpG island: C-phosphate-G (CpG) island; CREs: cAMP response elements; EGF: epidermal growth factor; EGFR: epidermal growth factor receptor; EGFR: epidermal growth factor receptor; GHRHR: GHRH receptor; GOF: gain-of-function; LOH: loss of heterozygosity; ptd-FGFR4: pituitary tumour-derived FGFR4.
* Germline mutations in these genes are associated to familial pituitary adenomas.

NESP55 is a protein expressed in secretory granules of neuroendocrine cells, expressed mainly in adrenal medulla, pituitary, and brain).[83] Loss of NESP55 expression is humans is not associated with an obvious phenotype.[85] There is another promoter ~35kb upstream the *GNAS1* exon 1 that, opposite to the NESP55 promoter, is methylated on the maternal allele.[86] This region contains three exons specific for the amino-terminal end of the protein XLαs: the XLαs exon 1 and two more alternative exons (known as A20 and A21) that are included (both or only A20) in only a small proportion of XLαs transcripts.[85;86] These three exons are spliced into alternative mRNA species and their expression is paternally-derived.[86] XLαs expression is limited to neuroendocrine tissues and it is apparently not activated by the same type of receptors that activate Gsα.[85] A fourth alternative promoter is located 2.5 kb upstream the Gsα exon 1, controlling the expression of an alternative first exon (exon A/B), that splices onto exon 2.[85;191] This promoter is methylated exclusively on the maternal allele[85] and its mRNA encodes a truncated form of Gsα.[191] Finally, a maternally methylated (paternally expressed) region ~3 kb upstream the XLαs exon 1 contains a promoter controlling the expression of multiple antisense transcripts that include the NESP55 exon and uses multiple splice sites.[84]

GNAS1 mutations associated to pituitary adenomas are always located at the codons 201 or 227, both of them within the exon 8.[192] These sites seem to be essential for the GTPase activity of Gsα, and LOF mutations at these locations produce a constitutively active Gsα subunit, the so called *gsp* oncogene.[95;193] Therefore, although the mutation effect is GTPase *inactivation*, these mutations are usually referred as *activating*, as the final functional consequence is constitutive activation of the cAMP signalling pathway.

Heterozygous somatic *GNAS1* mutations play a prominent role in the pathogenesis of somatotropinomas, where they are present in 4.4-59% of the cases.[194-201] Somatotropinomas harbouring a *GNAS1* mutation tend to be smaller,[198;202] to respond better to the treatment with SSA, and to be more often densely granulated somatotropinomas according to some,[203] but not all studies.[204] These mutations are also present in other types of pituitary adenomas (corticotropinomas and NFPAs),[164;205] though with a lower frequency, as well as in thyroid tumours,[206;207] ovarian and testicular stromal Leydig cell tumours,[208] in phaeochromocytomas (PHAEOs), paragangliomas (PGLs) and parathyroid adenomas in patients with multiple endocrine tumours,[207] and in multiple types of malignant neoplasms (renal clear cell carcinoma, pancreatic adenocarcinoma, hepatocellular carcinoma, and colorectal adenocarcinoma).[209] Mosaic *GNAS1* mutations at the codon 201 are the cause of the McCune-Albright syndrome (MAS).[210] In somatotropinomas, *GNAS1* mutations are almost always found in the maternal allele because Gsα is normally monoallelically expressed from the maternal allele in the pituitary.[168;211] However, the imprinting pattern is sometimes relaxed both in *GNAS1* mutation positive and negative tumours, suggesting a role for the biallelic expression of the protein in pituitary tumorigenesis.[168]

On the other hand, *GNAS1* mutations resulting in LOF of Gsα and, therefore, reduced or non-existent AC activity, are known as *inactivating* mutations.[212] Germline inactivating *GNAS1* mutations produce a variety of inherited syndromes mainly characterised by hormone resistance, short stature and/or calcium and phosphate imbalance, including cases with the clinical picture of Albright's hereditary osteodystrophia: pseudohypoparathyroidism (PHP) type Ia and Ic, pseudo-pseudohypoparathyroidism and progressive osseous heteroplasia.[209] Deletions in neighbouring genes, affecting the methylation pattern of *GNAS1* are the cause of PHP type Ib.[212] The specific phenotype present in a patient is given by the parent-of-origin of the mutated allele, due to the genetic imprinting present in *GNAS1*.

The *FGFR4* gene

The fibroblast growth factor receptor (FGFR) signalling pathway is disrupted in multiple types of cancer, by diverse mechanisms (somatic mutations, gene amplifications, autocrine ligand production). Paracrine signalling through FGFR1 to 4 and other tyrosine-kinase receptors in tumoral tissues can act as an additional mitogenic signal, amplifying the initial oncogenic stimuli, and a pro-survival effect depending on FGFR activation has been linked to chemotherapy resistance.[213] An N-terminally truncated isoform of FGFR4 with cytoplasmic localisation (in contrast with its normal membranous localisation), named pituitary tumour-derived (ptd)-FGFR4, is specifically expressed in pituitary adenomas.[214] The targeted expression of ptd-FGFR4 in a murine model induces prolactinomas.[161] In human pituitary adenomas, the expression of ptd-FGFR4 correlates with Ki-67, a proliferation marker.[215]

In addition, the *FGFR4* gene rs351855 single nucleotide polymorphism (SNP) c.1162G>A, (p.G388R), with a MAF of 0.3 in three different databases,[216-218] is a predictor of progression and poor prognosis in a variety of human neoplasms.[219] This polymorphism increases the receptor stability, producing sustained receptor activation *in vitro.*[220] A role for rs351855 as a facilitator of somatotroph cell tumorigenesis has been recently proposed.[221]

Regulation of gene expression by miRNAs

Small, non-coding molecules of RNA, known as microRNAs (miRNAs), act as posttranscriptional repressors of genetic expression through mRNA cleavage or translational repression.[222] Sequences codifying miRNAs are located throughout the whole genome and most of them comprise independent transcriptional units, though a minority of them are part of introns in genes, and around one third of the human genes are apparently targets for miRNA regulation.[222;223] Initially transcribed as pri-miRNAs that undergo different cleavage steps, mature single-stranded miRNAs are incorporated in the RNA-induced silencing complex (RISC) and, in the presence of extensive complementarity between the miRNA and the target sequence, the RISC cleaves the mRNA, while if there is incomplete complementarity, it represses the mRNA translation.[222]

Given their regulatory functions, in the setting of human neoplasms miRNAs can have either oncogenic or tumour suppressor activity, and the expression of multiple miRNAs has been found to be altered in different types of cancer, making them potential targets for diagnostic and therapeutic strategies.[224] Although multiple authors have addressed the miRNA expression profile in different types of pituitary adenomas and its impact on the clinical behaviour (reviewed in[225]), the most recent studies have focused on the regulatory effect of miRNAs on specific genes with a known role in pituitary tumorigenesis, and the most relevant results are summarised in Table 3.

Table 3: miRNAs regulating genes implicated in pituitary tumorigenesis (modified from[225])

miRNA(s)	Affected gene(s)	Target gene(s) function	Molecular abnormality in pituitary adenomas	References
miR-15a and miR-16-1	*RARS*	Arginyl-tRNA synthetase	Reduced expression in somatotropinomas and prolactinomas	226
Let-7	*HMGA2*	See Table 2	Increased expression in adenomas (all types) with low HMGA2 levels	227
miR-20a, miR-128a, miR-516-3p, miR-93 and miR-155	*WEE1*	Tyrosine-kinase specific for cyclin B1-complexed CDK1. Acts as a negative regulator of entry into mitosis (G2 to M transition)	Increased expression of miR-20a, miR128a and miR-516-3p in NFPAs and of miR-93 and miR-155 in somatotropinomas and NFPAs	228
miR-107	*AIP*	See Table 2	Increased expression in somatotropinomas and NFPAs	229
miR-15, miR-16, miR26a, miR196a2 and Let-7a	*HMGA1 and HMGA2*	See Table 2	Reduced expression in somatotropinomas, prolactinomas and NFPAs	230
miR34b, miR-326, miR374b, miR-432, miR-548c-3p, miR-570, miR-603, miR-633 and miR-320	*HMGA1, HMGA2* and *E2F1*	*HMGA1* and *2*: see table 2. *E2F1*: trancription factor,regulator of cell cycle and the action of tumour suppressor proteins	Increased expression of miR-320 and reduced expression of the rest of the studied miRNAs in somatotropinomas	231
miR-26b, miR-26a, miR-212, miR-107, miR-103, miR125b, miR-141, miR-144, miR-164, miR-145, miR-143, miR-15b, miR-16, miR-186, let-7b, let-7a3, miR-128	*PTEN* and *BMI1*	*PTEN:* lipid and protein phosphatase, tumour suppressor, modulator of cell cycle progression and cell survival. *BMI1:* component of a polycomb group multiprotein PRC1-like complex, transcriptional regulator of many genes throughout development	Increased expression of miR-26b, miR-26a, miR-212, miR-107 and miR-103, reduced expression of the rest of the studied miRNAs in somatotropinomas	149
miR-26a	*PRKCD*	Serine/threonine kinase involved in cell proliferation, apoptosis, and cell cycle regulation	Increased expression in corticotropinomas	232
miR-23b and miR-130b	*HMGA2* and *CCNA2*	*HMGA2:* see table 2. *CCNA2:* cyclin, promoter of cell cycle progression (G1/S and G2/M)	Reduced expression in somatotropinomas and NFPAs	233
miR-132, miR15a and miR-16	*SOX5*	Transcription factor, regulator of embryonic development and cell fate, and of cell proliferation, migration and invasion in neoplasms	Reduced expression in invasive pituitary adenomas	234
miR-34a	*AIP*	See Table 2	Increased expression in somatotropinomas with low *AIP* levels, inversely correlated with response to SSA	235

McCUNE-ALBRIGHT SYNDROME

Definition and general description

Originally described in the 1930s (first by McCune[236] and then by Albright[237]) as the triad of polyostotic fibrous dysplasia (FD), dermal *café-au-lait* spots and precocious puberty (PP), MAS is a complex genetic syndrome (OMIM #174800) encompassing also other diseases due to endocrine hyperfunction. In accordance with its current definition, the diagnosis of MAS is established in the presence of bone FD (monostotic or polyostotic) together with at least one manifestation of endocrine hyperfunction and/or *café-au-lait* spots. Therefore, the original clinical triad is known as *classic* MAS, while the presence of only one or two manifestations is known as *non-classic* MAS. *Café-au-lait* spots are the commonest component of the syndrome (53-95% of patients),[238] but they are frequently disregarded. In the largest series, composed of 113 European patients with clinical diagnosis of MAS, the classic triad was present in only 24% of patients, one third had two components of the triad and the rest had only one (usually PP).[239] MAS is extremely infrequent (prevalence around $1{:}10^5$-$1{:}10^6$ in the general population), but FD (especially the monostotic variant) is much more common.[240] Albeit there is a gender imbalance, with a predominance of female patients[239] the reason for this is unknown.

Genetics and pathophysiology

MAS is caused by mutations in the *GNAS1* gene[210] occurring at the postzygotic (i.e. somatic) level; therefore, there is no vertical transmission of the mutations and the clinical manifestations are widely variable, due to differential affection among body tissues (MAS patients are *somatic mosaics* for *GNAS1* mutations).[210;241] Theoretically, severe MAS cases are related to a mutational event at an early developmental stage,[193] and in agreement with this hypothesis, in MAS patients with involvement of several tissues, the same *GNAS1* mutation is found in all the tissues analysed.[239] Somatic mosaicism is, apparently, a *sine qua non* condition of MAS: cells bearing the mutation can only survive if they are interspersed with normal cells in the affected tissues,[241] as it has been proved for FD lesions.[242] *GNAS1* mutations causing MAS are never inherited, as they are apparently embryonically lethal.[193;241]

Gsα constitutive activation at multiple tissues is the accepted pathogenic basis of MAS, whereas there is not a clear contribution of the other *GNAS1* products to the clinical features.[210] However, Gsα is generally biallelically expressed, as has been shown for human foetal tissues[243] and lymphocytes,[86] in contrast with the tissue-specificity of clinical manifestations in MAS. It has been proposed that tissue-specific genomic imprinting in some organs could explain the pattern of MAS clinical features, depending on the origin of the allele bearing the *GNAS1* mutation.[244] This hypothesis is supported by the variable phenotypic expression of Albright hereditary osteodystrophy (AHO), a disease caused by inactivating *GNAS1* mutations, depending on the origin of the mutated allele. While maternal inheritance leads to AHO associated with pseudohypoparathyroidism, hypocalcaemia, hyperphosphataemia and multihormone resistance, paternal inheritance of the mutation results in AHO with

pseusopseudohypoparathyroidism, with no other clinical abnormalities.[245] The imprinting model should predict that Gsα is primarily expressed from the maternal allele (with imprinting of the paternal allele) in the specific hormone target tissues, explaining the absence of hormone resistance when the paternal allele is mutated.[85] This hypothesis has been proven in the murine renal cortex (a target for parathyroid hormone [PTH]), where Gsα expression is primarily from the maternal allele,[246] but not in the foetal renal cortex, where Gsα is biallelically expressed.[247] It is possible that Gsα imprinting exists only in fully mature renal tubules.[244]

In humans, tissue-specific imprinting has been demonstrated in the pituitary, where Gsα is exclusively expressed from the maternal allele.[168] Somatotropinomas (both those with and without *GNAS1* mutations) often show a relaxation of Gsα monoallelic expression, but retain the normal imprinting of NESP55 and XLαs, implying a possible role for loss of Gsα imprinting in somatotroph cell tumorigenesis.[168] In *GNAS1* mutation positive somatotropinomas, both sporadic and MAS-related, mutations almost always affect the maternal allele, in agreement with the pituitary-specific imprinting of this gene.[211] In thyroid and gonads, the expression of Gsα is mainly dependent on the maternal allele, but the paternal contribution is not negligible, indicating that genetic imprinting is not necessarily an all-or-nothing phenomenon.[248] Therefore, acromegaly occurs only in those MAS patients with an affected maternal allele, but there is no apparent relationship between the origin of the mutated allele and the rest of the MAS components,[211] each individual showing a particular distribution of abnormal cells in the affected tissues.

GNAS1 mutations in MAS patients always occur at codon 201 and usually result in the substitution of an R residue for an H or a C,[210;239] or, infrequently, by an S,[249] G[250] or L,[85] but mutations at the position 227 have never been found as MAS-causative.[85] The sensitivity for detection of *GNAS1* mutations in MAS patients is variable and tissue-dependent. For example, Lumbroso *et al* detected *GNAS1* mutations in 43% of 113 patients with clinical diagnosis of MAS, but when the samples were obtained from at least one known affected tissue, the percentage of positive samples rose to 90%.[239] While *GNAS1* mutations were detected in testis, thyroid muscle and endometrium in 100% of the samples analysed, the screening was positive in only 21 and 27% of peripheral blood lymphocytes and skin samples, respectively.[239] Despite the use of highly sensitive screening methods,[249] some samples (around 10%) are negative for *GNAS1* mutations.[239] Mutated cells might be confined to specific areas of the affected tissues, so it is advisable to screen pathological regions localised by histological studies.[239] Considering the limitations for the genetic analysis, MAS diagnosis is established based on clinical grounds. Nevertheless, detection of *GNAS1* mutations is especially important in those cases with partial or atypical presentation.[239]

Clinical features

PP is the most common endocrine manifestation of MAS, and despite being more commonly diagnosed in females, the incidence of gonadal pathology is equal in patients of both genders

(around 83% of females and 81% of males).[251;252] PP in the setting of MAS has a peripheral (primary) origin, due to autonomous gonadal function, but some patients develop also secondary gonadotroph activation (central/secondary PP).[251] Even though most MAS patients have intermittent PP interrupted by long periods of remission, some of them show a fast progression, with growth acceleration and premature skeletal maturation, compromising the final height,[251;253] especially if FD coexists. PP in female MAS patients is caused by oestrogen production from large ovarian hyperfunctioning cysts.[254] Males develop benign testicular lesions (Leydig cell hyperplasia more commonly, and less frequently Sertoli cell hyperplasia with or without macro-orchidism or Sertoli cell intraepithelial neoplasia); malignant testicular lesions and adrenal rests are rare.[252]

Current treatment of PP in MAS female patients is based in anti-oestrogens. Medroxyprogesterone and ketoconazole might inhibit vaginal bleeding, but have no effect over skeletal maturation.[255] The aromatase inhibitor anastrozole was ineffective for the treatment of PP in a group of 28 girls with MAS,[253] but letrozole slowed down skeletal maturation, and decreased vaginal bleeding, without reduction in ovarian volume in nine patients.[254] In a group of 25 girls with MAS, tamoxifen treatment was effective to control menstrual haemorrhages, growth speed and skeletal maturation, but increased ovarian and uterine volumes were observed.[255] In patients with associated gonadotroph activation, combined therapy with long-acting GnRH analogues should be installed.[240] In cases resistant to medical treatment, surgical resection of hyperfunctioning ovarian follicles is an option, but recurrences are frequent.[255] Despite the high frequency of gonadal lesions, requiring periodic ultrasonographic surveillance and rarely surgical management, only around one fifth of the MAS male patients develop clinical signs of PP, requiring GnRH analogue therapy, aromatase inhibition or testosterone receptor blockade.[251;252]

Thirty to 50% of MAS patients develop hyperthyroidism, and even more patients bear subclinical disease. MAS-related ultrasonographic findings (diffuse heterogeneity, hypoechogenic micro and macro nodules and hyperechogenic nodules) are present in 34-54% of the patients.[256;257] Even in the absence of clinical hyperthyroidism, MAS patients show an elevated T3/T4 ratio, via increased D1 and D2 deiodinase activity, due to constitutive cAMP production.[257] Treatment with thionamides can be efficient, but these patients almost never have spontaneous remission and a definitive treatment (surgery or radioactive iodine) is frequently warranted.[240]

Cushing's syndrome in MAS is infrequent (~7%) and displays variable clinical behaviour, ranging from spontaneous resolution to more severe forms requiring adrenalectomy, with lethality in ~20% of such cases.[258;259] Hypercortisolism seems to arise during foetal life, due to tonic activity of Gsα in the adrenal cortex, so the diagnosis is usually established in the first three months of life.[259;260] Presenting features include Cushingoid facies, failure to thrive, premature delivery and low birth weight, and hepatic and cardiac abnormalities.[259] These

children tend to develop more comorbidities than other MAS patients (3.4 *vs* 2.9 MAS features), and, not infrequently, also neurocognitive disorders.[259] This endocrinopathy is unique among other MAS features because of the possibility of spontaneous resolution: cells bearing the *GNAS1* mutation are localised in the foetal zone of the adrenal cortex, which physiologically suffers complete degeneration by the first year of age.[259]

Renal phosphate wasting occurs in around one half of MAS patients.[261] Phosphaturia correlates with the degree of bone involvement and is associated with proteinuria and amiaciduria; renal cAMP is normal.[261] This feature is explained by the production of the phosphaturic factor fibroblast growth factor 23 (FGF23) by the FD lesions.[262] Treatment is based on the oral administration of phosphates at high doses, together with calcitriol or alfacalcidol.[251]

Café-au-lait macules are due to constitutive activity of the melanocyte-stimulating hormone receptor (MSHR), with active proliferation of melanocytes and increased melanin production.[238] These lesions bear no malignant potential and are not MAS specific: the can be isolated or associated with other genetic syndromes.[238] *Café-au-lait* macules in MAS are classically described as multiple lesions with variable number and size, with irregular borders (*coast of Maine* appearance) and limited to one side of the body, which usually matches the FD affection,[85;238] but morphology and distribution are widely heterogeneous. These lesions are present at birth or arise in the first years of life, the most common localisations are back or the neck, thorax and gluteus and they grow proportionally to the growth of the patient.[238] The distribution of the lesions follows Blaschko's lines, reflecting the migration pattern of endodermal cells during development.[241]

Although any bone can be involved, skull base and long bones are the most frequently affected areas in MAS-associated bone FD. FD is usually unilateral and most often includes more than one bone (polyostotic presentation), though some patients develop lesions in only one bone (monostotic) or, very rarely, the whole skeleton is affected (panostotic).[263] FD consists on focal lesions composed of bone marrow stromal cells, immature bone tissue spicules, non-mineralised osteoid and, sometimes, hyaline cartilage islands, expanding from the bone marrow cavity to surrounding cortical bone, with peripheral osteoclasts.[85;242] In the lesions, stromal cells start differentiating in the osteogenic lineage but, instead of becoming completely differentiated, they proliferate, apparently due to sustained cAMP stimulation, giving place to the lesions.[264] Initial manifestations are pain, claudication of an extremity or a pathologic fracture. Plain radiographies show cystic or lytic lesions with heterogeneous radioopacity in infants, ground glass appearance in children and peripheral sclerosis in adults.[264]

The majority of the FD extension is established between 3-10 years of age and it becomes clinically evident around the 5 years of age.[251] Lesions grow from marrow to cortex and epiphyses are usually unaffected; weight-supporting bones might undergo deformation, being characteristic the ***shepherd's crook*** femur.[240;264] In craniofacial bones, protuberances and

asymmetry might compromise cranial nerves, jeopardizing sight and hearing.[264] Treatment includes surgery to install intramedullary prostheses in long bones and to correct craniofacial lesions causing cranial nerve compromise, severe pain or disfiguration.[240;263] Intravenous pamidronate is useful as a pain reliever, but has a negligible effect over disease progression.[265] Malignant transformation of FD lesions occurs in less than 1% of cases, usually in association with GH excess and radiation exposure.[264]

Some other features have been uncommonly reported in MAS patients and are probably related to Gsα constitutive activation, including gastrointestinal reflux, gastrointestinal polyps, pancreatitis, neonatal cholestasis, sudden death, tachycardia, aortic root dilatation and platelet dysfunction.[239;240;251] Hyperparathyroidism in MAS is secondary to the abnormalities in mineral metabolism and not caused by *GNAS1* mutations.[240] A few cases of thyroid and breast cancer have been reported in association with MAS, nevertheless, a causality has not been established.[251]

Excessive GH production is part of MAS in 20-30% of patients,[266] but only 33-65% of them develop a pituitary adenoma detectable by image studies.[267;268] Originally described as mammosomatotroph hyperplasia,[269] the current concept is that pituitary involvement in MAS is widespread and diffuse, including areas of normal gland, somatotroph hyperplasia, somatotroph neoplasia, lactotroph neoplasia and mammosomatotroph neoplasia, being somatotroph hyperplasia the predominant pattern.[268] Each foci of neoplasia or hyperplasia within a single pituitary gland contain the same *GNAS1* mutation.[268] In concordance with the histopathological picture, 81-92% of the patients present with concomitant hyperprolactinaemia.[266;267] Interestingly, the proportion of patients with a positive thyrotropin-releasing hormone (TRH) test is much higher (100% in a recent series) in MAS-related acromegaly than in other populations of acromegalic patients (50-60%).[267]

One third of the MAS patients with GH excess are diagnosed before the age of 16 years, usually due to accelerated growth, with coexistent PP in 57% of them.[266] Most of the MAS patients with acromegaly and gigantism have also FD of the skull base, and around one third of them develop visual and/or audition compromise, being more severe in those patients with very high GH and insulin-like growth factor-1 (IGF-1) levels.[266;267] Surgical treatment in these cases is precluded by the presence of craniofacial bone lesions, which complicates the surgical approaches, as well as by the universal involvement of the anterior pituitary, requiring hypophysectomy.[267;268] There is a consistent response to the treatment with CBG and SSA, especially when combined, though the disease control is frequently partial.[267] Thirty percent of the patients can be controlled with SSA alone and 77% with pegvisomant alone.[266] Combined treatment with pegvisomant and radiotherapy achieved total control of the disease in five out of six patients in a series of acromegalic SSA-resistant MAS cases.[270]

Inherited pituitary adenomas (germline mutations)

The inherited conditions that, to date, are known to predispose to pituitary adenomas are multiple endocrine neoplasia (MEN) type 1 (MEN1), MEN type 4 (MEN4), pituitary blastomas due to *DICER1* mutations, Carney complex (CNC), the syndrome of pituitary adenoma and PHAEO/PGL and FIPA, including X-linked acrogigantism (X-LAG), *AIP* mutation associated FIPA or FIPA with undetermined genetic cause. Previous data suggests that approximately 2.7% of all pituitary tumours occur in the context of MEN1[271] and that FIPA accounts for another 2.5%.[272] CNC explains a few hundred cases world-wide,[272] while MEN4, pituitary adenoma and PHAEO/PGL, pituitary blastomas and X-LAG have only been described in a few individuals. Though the inheritability of these phenotypes is well known and a genetic basis has been established for each of them, the causative gene remains elusive in 5-10% of *MEN1* patients,[273;274] 27% of CNC patients[275] and 70-85% of FIPA patients.[276]

An important aspect of the study of these rare genetic syndromes is the potential role of the causative genes in the more common sporadic pituitary adenomas. Although the expression of some of the genes causing familial pituitary adenomas has been found to be altered in pituitary adenomas, somatic mutations in these genes are not common events: while somatic mutations in *MEN1* (the gene causing MEN1) have rarely been identified in pituitary adenomas (see next section) and a somatic mutation in *PRKAR1A* has only been detected in one patient (coexisting with a germline deletion in a CNC patient)[277] no somatic mutations have been described in other genes associated to familial pituitary adenomas.[9;278-280]

Multiple endocrine neoplasia

The occurrence of two or more endocrine tumours in the same patient characterises a syndrome of MEN. Currently, four main forms of MEN, all of them autosomal dominant, are recognised: MEN1, MEN2A (also referred as MEN2), MEN2B (also referred as MEN3) and MEN4 (also referred as MENX),[281] although only MEN1 and MEN4 include pituitary adenomas as part of their presentation. The spectrum of neoplasms associated to *DICER1* mutations, including pituitary blastoma, can be considered as a novel form of MEN, characterised by a predominance of malignant tumours, as opposed to other MEN syndromes. Other uncommon forms of MEN are the CNC and the syndrome of pituitary adenoma and PHAEO/PGL.

MULTIPLE ENDOCRINE NEOPLASIA TYPE 1

Definition and general description

In 1903 Erdheim reported a case of concomitant pituitary gigantism, and parathyroid tumours in one individual, and in 1954,[282] Wermer wrote the first clinical description of a family with an association of pituitary tumours, hypercalcaemia and pancreatic adenomas.[283] MEN1 (OMIM #131100) is a syndrome characterised by the development of tumours mainly in endocrine but also non-endocrine organs, with three main components: primary hyperparathyroidism (PHPT), entero-pancreatic endocrine tumours and pituitary adenomas.[283;284] The diagnosis of MEN1 is

established in the presence of two of these features or when one feature is present together with a first degree relative with established MEN1 diagnosis.[285] Other endocrine components of the syndrome are foregut carcinoids, non-functioning tumours of the adrenal cortex, and, rarely, PHAEOs, while lipomas, facial angiofibromas, collagenomas and ependymomas are non-endocrine tumours associated to MEN1.[285]

The observation of loss of heterozygosity (LOH) at 11q13 in tumours from MEN1 patients, led to the mapping, in 1988,[286] and later cloning, in 1997,[87;287] of *MEN1.* This gene spans 7.2 kb of genomic sequence, containing an 1830 base pairs (bp) coding region with ten exons (the first is not translated), encoding a 610 amino acid protein, menin.[87] Heterozygous *MEN1* mutations are detected in 90-95% of MEN1 patients.[273;274] Until 2008, 1133 germline and 203 somatic mutations had been described: 23% were nonsense, 9% splice-site, 41% frameshift deletions or insertions, 6% in-frame deletions or insertions, 20% missense and 1% whole or partial gene deletions; mutations are distributed throughout the whole gene, with mutational hotspots in exons 2, 3, 9 and 10 and intron 4.[273;288] More than 10% of the *MEN1* mutations arise *de novo* and there is no clear genotype-phenotype association in MEN1 patients.[281]

LOH in 11q13 occurs in around 90% of tumours from MEN1 patients but LOH can also be found at this region in 5-50% of sporadic endocrine tumours,[273] and somatic *MEN1* mutations are detected in some of the tumours with no LOH,[289] in line with Knudson's "two-hit" hypothesis.[290] Somatic *MEN1* mutations are also common in sporadic parathyroid (9.5-21% of cases)[291-294] and pancreatic islet cell tumours (19-44%),[294-299] but they occur only very rarely (0-3.67%, only ten mutations described) in sporadic pituitary tumours.[129-133;300-306] Seventy five percent of the *MEN1* mutations result in LOF:[273] nonsense and frameshift mutations can result either in a truncated protein, with loss of important domains such as the nuclear localization signal (NLS),[307] or in a loss of the transcript via nonsense-mediated mRNA decay (NMD).[308;309] Splice-site mutations are predicted to lead to unspliced precursor mRNA accumulation, retention of incompletely spliced precursors, aberrantly processed mRNA, or short or absent transcripts.[273;310] *MEN1* missense mutations affect the functions of menin, reducing its ability to interact with other proteins and enhancing its proteolytic degradation.[311;312]

Genetics and pathophysiology

MEN1 is considered a tumour suppressor gene because heterozygous inactivating mutations predispose to neoplasms, *Men1* knockout (KO) mice reproduce the human phenotype and the majority of MEN1-related tumours display LOH at 11q13.[274;286;289;313-315] In tumours with no LOH, other mechanisms of gene inactivation, such as hypermethylation, mutations of the promoter or non-coding regions and miRNAs may occur.[289;316] By transcriptional regulation, *MEN1* produces two transcripts: a ubiquitously expressed 2.9 kb transcript with several alternatively spliced isoforms, and a 4.2 kb transcript, present in the pancreas and thymus.[287] Menin is a 67 kilodaltons (kDa) protein without homology to any other protein,[87;317] highly conserved within species: murine menin shows 97% identity/98% similarity to human menin.[318]

Menin acts as a scaffold protein, regulating genetic expression of multiple genes involved in transcriptional regulation, genome stability, cell division and proliferation.[274;281] Due to three NLS domains,[307] menin is predominantly expressed in the nucleus, though an increased cytoplasmic expression has been described after cell division.[319] Menin expression fluctuates through the cell cycle: it is high in quiescent cells, decreases during G1 phase and increases again in S phase.[320] Menin represses the progression of cell cycle and promotes apoptosis; *in vitro*, its overexpression causes apoptosis in murine embryonic fibroblasts.[321]

The tumour suppressor activity of menin is explained by diverse mechanisms:

- Menin activates the transcription of *CDKN1B* (encoding the cyclin-dependent kinase inhibitor CDKN1B) and *CDKN2C* (encoding CDKN2C) by recruiting the histone methyltransferase mixed lineage leukaemia protein (MLL) to the promoters and coding regions of these genes, where MLL catalyses histone H3 lysine 4 methylation.[322] Although menin expression does not differ between endocrine and non-endocrine organs, MLL, CDKN1B and CDKN2C are predominantly expressed in endocrine organs and this expression profile could partially explain the selectivity of tumorigenesis in patients with MEN1.[323] Through interaction with MLL, menin also regulates the transcription of homeobox genes, particularly *HOXA9*, important for cell proliferation, differentiation and morphogenesis.[324;325] In a similar way, menin recruits polycomb group proteins to enhance methylation at the pleiotrophin (*PTN*) gene, silencing the expression of this pro-proliferative gene.[325;326]
- In the normal pituitary, menin interacts with activin, negatively regulating cell proliferation and the secretion of PRL, GH and ACTH, through inhibition of *PIT1* expression.[327;328]
- The transforming growth factor-β (TGF-β) signalling pathway inhibits cell proliferation and transcriptional activity through SMAD2 and SMAD3 proteins.[325] Menin interacts with SMAD3 and the loss of this interaction prevents SMAD3 binding to DNA, blocking the TGF-β effects.[329]
- Menin inhibits JunD protooncogene (JUND) and enhances Jun protooncogene (JUN) transactivation,[330] as well as its interaction with members of the nuclear factor kappa B (NFκB) family, modulating their transcriptional activity.[331] These regulatory activities seem to be particularly relevant for the MEN1 phenotype, as patients carrying mutations affecting the JUND-interacting domain of the protein have a higher risk of death.[332]
- Menin interacts with the nuclear receptors peroxisome proliferator-activated receptor gamma (PPARG)[333] and the vitamin D receptor (VDR),[334] enhancing the expression of their target genes.
- The expression of insulin-like growth factor binding protein 2 (IGFBP-2),[335] insulin-like growth factor 2 (IGF-2) and PTH-related protein (PTHrp),[336] important proliferative factors in endocrine tumours, is negatively modulated by menin.

- Menin inhibits transcriptional activity and cell proliferation by the wingless-type MMTV integration site family (WNT)/CTNNB1 signalling pathway by binding and translocating CTNNB1 out of the nucleus.[337]
- Menin interacts with the 32 kDa subunit of replication protein A 32 kDa (RPA2)[338] as well as with Fanconi anemia complementation group D2 (FANCD2);[339] both are proteins involved in DNA repair, and through its interaction with the promoter of the human telomerase reverse transcriptase (hTERT), menin apparently acts as a repressor of telomerase activity.[340] Other menin interactors are proteins involved in cell division, such as non-muscle myosin II-A heavy chain,[341] glial fibrillary acidic protein and vimentin.[342]
- In pancreatic endocrine cells, menin determines the effects of the K-RAS pathway, by blocking K-RAS-dependent proliferation (driven by the RAS/RAF/MEK/ERK signalling pathway), while leaving K-RAS inhibitory pathways intact.[79]

In mice, *Men1* homozygous deletion is lethal *in utero* due to multiple developmental delay and craniofacial, cardiac, neural and hepatic abnormalities.[273;313;343] Mice heterozygous for partial deletions of *Men1* develop a syndrome similar to human MEN1.[313;343] In a different model, heterozygous *MEN1* deletion restricted to the pancreas caused hyperplasia, but LOH was necessary for progression to a tumour.[314]

Clinical features

MEN1 has an autosomal dominant pattern of inheritance.[274] Eighty five percent of the cases are familial and 15% are sporadic, but the frequency of *MEN1* mutations is apparently not different between these two groups.[344] Female gender slightly predominates (52-57% of patients).[345] Within MEN1 patients, pituitary tumours are more common in females, while gastrinomas and thymic carcinomas are more common in males.[345] There is no clear genotype-phenotype correlation.[346] The penetrance of MEN1 is progressive and age and organ-specific,[285] and the clinical presentation during the first decade of life remains infrequent.[347] Parathyroid adenomas are the most constant feature of MEN1, being present in 90-100% of the patients by the age of 50 years,[285] and they are usually the first manifestation of the syndrome (72-87% of patients).[274;348;349] These tumours are frequently multiple, and require extensive surgical treatment.[285]

Thirty to 80% of MEN1 patients develop entero-pancreatic islet cell tumours.[285] In the setting of MEN1, these tumours are multicentric, hormone-secreting and may become invasive or metastatic (especially gastrinomas and glucagonomas).[285;350] Islet cell tumours are the first manifestation of the disease in around 25% of patients,[349] and arise in any part of the pancreas or the duodenal mucosa. The most common subtype is gastrinoma (in 40%-63% of patients), causing the Zollinger-Ellison syndrome.[328;348] Surgery is usually curative for insulinoma, but other entero-pancreatic islet cell tumours respond well to medical treatment with proton pump inhibitors (gastrinomas) or SSA (other entero-pancreatic tumours).[285] Carcinoids related to

MEN1 arise in bronchi, thymus and gastric or duodenal mucosa and rarely hypersecrete hormones,[285] but they may cause clinical manifestations due to ectopic GHRH or ACTH production.[351] Metastatic neuroendocrine tumours represent the main MEN1-related cause of death.[352;353]

Adrenal cortical tumours are present in 20-40% of MEN1 patients, most often are bilateral, hyperplastic and non-functional lesions; adrenal carcinomas are rare.[285] Up to one third of the patients develop lipomas, both cutaneous and visceral.[285] Multiple facial angiofibromas are found in 40-80% of cases.[285] A PGL has recently been described in a patient with genetically confirmed MEN1,[354] and a possible predisposition for breast cancer among females carrying *MEN1* mutations has been suggested by an epidemiological study.[355]

Approximately 40% of MEN1 patients develop pituitary adenomas,[344] and these tumours are the first manifestation of MEN1 in around 17% of patients[344] (ranging from 10 to 25%).[285] Pituitary adenomas in the context of MEN1 arise at a younger age (35.1±14.8 years) than in patients with sporadic pituitary adenomas;[344] the earliest age of presentation reported is five years.[356] Prolactinomas predominate (62%), but NFPAs (15%), somatotropinomas (9%), corticotropinomas (4%), and rarely thyrotropinomas can also be detected.[344;357] One case of gonadotroph cell carcinoma in an MEN1 patient has been reported.[357] Ten to 39% of tumours secrete more than one hormone, usually PRL/GH.[344;358] The majority of these tumours are macroadenomas (76-85%) and around half of them are invasive.[344;358] Four percent of patients present multiple adenomas.[358]

Pituitary adenomas in MEN1 patients are significantly larger and more invasive than in sporadic patients, but the Ki-67 index and the mitotic activity are not different.[358] Hyperplasia of somatotroph or mammosomatotroph cells has been described, but it is not common and in some cases is due to an ectopic GHRH-secreting tumour.[358;359] In an invasive tumour from a very young MEN1 patient, overexpression of genes related to tumorigenesis (*TPD52, FOS* and *SHC1*), and cell growth (*GNAS1, FOSB* and *SRF*) as well as loss of e-cadherin function were detected.[356] In general, the response of secretory pituitary adenomas to medical and/or surgical treatment is suboptimal; normalisation of hormone secretion is achieved in only 42% of patients.[344] Medical treatment of prolactinomas in MEN1 patients is difficult because they show a poor response to dopamine agonists (DA).[344]

Sequence analysis of *MEN1* (including both Sanger sequencing and multiplex ligation-dependent probe amplification [MLPA]) of index cases and their relatives is important in order to determine which individuals require follow-up, as well as to identify phenocopies (they are present in ~5% of families).[274] *MEN1* mutation carriers and MEN1 patients should have long-term follow-up, because new components of the syndrome can arise at any age.[285;353] Annual biochemical screening, including calcium, parathyroid hormone, gastrin, fasting glucose, insulin, chromogranin-A, glucagon, proinsulin, PRL and IGF-1 is recommended.[285] Imaging studies

(computed tomography, MRI and, rarely, ^{111}In-DTPA octreotide scan) should be performed at regular intervals.[285]

MULTIPLE ENDOCRINE NEOPLASIA TYPE 4

Definition and general description

The absence of *MEN1* mutations in a minority (5-10%) of patients with MEN1 clinical features drove a search for additional loci implicated in this phenotype. Homozygous mutations were found in *Cdkn1b* in association with MEN syndrome (termed MENX) showing features of both human MEN1 and MEN2, occurring spontaneously in a laboratory rat strain.[89;360] Following this discovery, mutations in the human *CDKN1B* gene were identified in a small group of patients with multiple endocrine tumours typical of MEN1 (but not of MEN2) and other neoplasms, but negative for germline mutations in *MEN1* or *RET* (the gene associated with MEN2 syndrome).[361] This infrequent MEN1-like syndrome was named MEN4 (OMIM #610755).[346;362] *CDKN1B,* localised at 12p13.1, encodes the cyclin-dependent kinase inhibitor (CDKI) CDKN1B ($p27^{Kip1}$).[363] Since the first report, mutations in *CDKN1B* have been searched in many patients with MEN1 features, negative for *MEN1* mutations, but they have rarely been found.[364-367] Those patients might have a different genetic background, not yet identified.

Genetics and pathophysiology

CDKN1B is a 27 kDa protein, highly conserved (around 90% identity) in human, mouse and mink.[368] It contains 198 amino acids, with an NLS in the C-terminal region.[368] *CDKN1B* is a tumour suppressor gene:[369] as a member of the KIP/CIP family of CDKIs, CDKN1B is implicated in the regulation of cell cycle progression from G1 to S phase[370] by binding to and regulating the activity of cyclin-dependent kinases (CDKs).[371] Subcellular localisation of CDKN1B determines its functions. In G0 and early G1, CDKN1B expression is maximal and is localised in the nucleus, where it binds and inhibits cyclin E/CDK2 complex.[370;372] In proliferating cells, CDKN1B is sequestered in the cytoplasm, with a substantial proportion bound to cyclin D/CDK4 complex.[370] As cells progress through phase G1, CDKN1B expression decreases, allowing cyclin E/CDK2 and cyclin A/CDK2 to activate the transcription of genes necessary for G1-S transition and the initiation of DNA replication.[371;372] CDKN1B exerts a dual effect over cyclin D, which is inhibitory under adverse conditions for replication, while in early G1 to mid-G1 phase it promotes cyclin D-CDK4 assembly and nuclear import.[371] In an additional anti-oncogenic activity, CDKN1B binds directly to GRB2, blocking the formation of the GRB2-SOS1/2 complex and therefore the activation of the RAS/RAF/MEK/ERK signalling pathway.[373]

CDKN1B is a substrate for tyrosine phosphorylation by the cyclin E/CDK2 complex, which triggers ubiquitination (mediated by the SKP1-CUL1-F-BOX protein complex [SCF] E3 ubiquitin ligase, containing the F-box protein SKP2) and proteasomal degradation of CDKN1B, although other proteins and also miRNAs modulate CDKN1B transcription and proteolysis.[361;362;374] For example, in tumoral cells, cytoplasmic sequestration of CDKN1B (via AKT-dependent

phosphorylation on residue T157) inhibits its activity, leading to enhanced tumour invasiveness.[361;362]

CDKN1B is a downstream element of the MEN1 signalling pathway, and menin, through its interaction with histone methyltransferases, enhances the activity of the *CDKN1B* promoter.[361] Paradoxically, CDKN1B can display oncogenic activity through a CDK-independent mechanism in experiments using knock-in mice with a mutant CDKN1B unable to bind CDKs.[375] Homozygous *Cdkn1b* KO mice have increased body size and develop multiorgan hyperplasia, retinal dysplasia, ovulatory defects, female sterility and, in 100% of the cases, hyperplasia or adenomas of the pituitary *pars intermedia,* secreting ACTH.[376-378] In addition, *Cdkn1b*$^{-/-}$ mice also show an increased susceptibility to tumour development after exposure to γ-irradiation and N-ethyl-N-nitrosourea, developing lymphomas and adenomas of the liver, intestine, lung and pituitary, ovarian granulosa cell tumours, endometrial adenocarcinomas, endometrial polyps, angiosarcomas and fibromas, as well as medullary and cortical adrenal tumours.[369] Nevertheless, *CDKN1B* somatic mutations or LOH at its locus have only rarely been described in human tumours.[89;361;379;380;380;381] Decreased CDKN1B expression, either due to heterozygous mutations or to changes in extragenic pathways regulating protein levels, is enough for tumour development in *Cdkn1b*$^{+/-}$ mice.[369] Furthermore, an important reduction in *CDKN1B* expression has been described in multiple human cancers, correlating with aggressive behaviour,[371;382-386] as well as in some endocrine malignant and benign tumours (PHAEOs, parathyroid adenomas and pancreatic and digestive endocrine tumours).[361;387-389]

Human germline *CDKN1B* mutations are extremely rare: they explain only 1.5-2.8% of MEN1 phenotype/*MEN1* mutation negative cases,[390;391] and therefore, only ~0.1-0.2% of all MEN1 cases. The first *CDKN1B* germline mutation identified in an MEN4 patient was a nonsense mutation that had been previously identified as a somatic change in an adult patient with leukaemia.[89;361] To date, eleven heterozygous *CDKN1B* germline mutations have been described in familial and sporadic patients with MEN1-like phenotype, including two frameshift, two nonsense, one non-stop, three missense, two deletions at the 5' untranslated region (UTR), one mutation at the Kozak sequence and one mutation affecting an open reading frame (ORF) located at the 5'UTR.[89;390-398] Additionally, two missense germline *CDKN1B* mutations have been reported in two patients with sporadic PHPT[380] and two more in two patients with a FIPA-like phenotype.[399] However, in the FIPA-like cases, the pathogenic association was unclear, as *CDKN1B* mutations did not segregate with the disease.[399] The functional effect of these mutations on the protein include a reduced protein level,[391;395;396] reduced mRNA and protein levels,[394] reduced protein stability,[380] abnormal electrophoretic migration,[399] loss of molecular interactions (with CDK2[392] and GRB2[391;399]) or cytoplasmic localisation,[89;397] but for some mutations the functional effect remains elusive.[380;390;393]

Clinical features

Five familial and seven sporadic MEN4 patients have been identified so far.[89;390-398] In two of the familial cases not only *CDKN1B* mutations carriers but clinically affected relatives were identified.[89;391] With this small number of patients, the penetrance, frequency of familial and sporadic cases and possible phenotype-genotype correlations cannot be determined at this moment. The patients described to date have presented one to four endocrine tumours concomitantly; nevertheless, the most common component of the syndrome is parathyroid involvement, and the presentation is similar to that of MEN1, with multiple parathyroid adenomas. Other benign and malignant tumours described as part of MEN4 are renal angiomyolipoma, adrenal non-functional tumour, uterine fibroids, gastrinoma and gastric carcinoma, gastro-entero-pancreatic neuroendocrine tumours, non-functioning pancreatic endocrine neoplasm, neuroendocrine cervical carcinoma, bronchial carcinoid and papillary thyroid carcinoma.[89;390-394;397]

Under physiological conditions, CDKN1B is especially highly expressed in the human pituitary[323] in all types of cells except normal corticotroph cells, which show a lower expression.[103] Expression of CDKN1B is significantly reduced in all pituitary adenoma types, but the protein is practically absent in corticotropinomas and pituitary carcinomas;[103] however, no somatic *CDKN1B* mutations, nor LOH of 12p13, have been found in corticotropinomas.[102;379] Only four cases of pituitary adenomas have been identified among the eleven *CDKN1B* mutation positive MEN4 patients reported to date, including two cases of acromegaly, one of gigantism, one of Cushing's disease and one NFPA,[89;390;392;395;398] and two more patients, with diagnoses of prolactinoma and acromegaly have been reported with a FIPA phenotype.[399] Due to the scarcity of cases, there is not enough data about the specific clinicopathological features of pituitary adenomas in MEN4 cases.

Due to the lack of a specific MEN4 phenotype, it is not possible to establish this diagnosis only by clinical data.[367] Because of the low prevalence of MEN4, screening for *CDKN1B* mutations in patients with MEN1 diagnosis and negative *MEN1* mutations is currently not a routine practice. However, patients previously considered as MEN1 phenocopies could be tested for *CDKN1B* mutations in a research setting.[367]

OTHER RARE MEN1-LIKE CASES

A mutation in the *CDKN1A* (*$p21^{CIP1}$*) gene was described in two sisters with an MEN1-like syndrome of PHPT and microprolactinoma, and mutations in other two genes encoding CDKIs, *CDKN2B* (*$p14^{INK4b}$*) and *CDKN2C* (*$p18^{INK4c}$*) have also been detected in the context of MEN, but none of these cases included pituitary tumours as part of the phenotype.[391]

PITUITARY BLASTOMA

Definition and general description

Pituitary blastoma is a very rare, aggressive and potentially lethal, apparently congenital pituitary tumour, which forms part of the *DICER1* syndrome or pleuropulmonary blastoma familial tumour and dysplasia syndrome (OMIM #601200), caused by germline mutations in the *DICER1* gene, a novel genetic association.[400] In addition to pituitary blastoma, the main manifestations of the *DICER1* syndrome are pleuropulmonary blastoma (PPB), ovarian sex cord-stromal tumours (Sertoli-Leydig cell tumour, juvenile granulosa cell tumour, and gynandroblastoma), cystic nephroma (CN) and thyroid gland tumours such as multinodular goitre, adenomas, or differentiated thyroid cancer. Other less frequently associated neoplasms are ciliary body medulloepithelioma, botryoid-type embryonal rhabdomyosarcoma (ERMS) of the cervix or other sites, nasal chondromesenchymal hamartoma, renal sarcoma and pineoblastoma, and in very rare cases, Wilms tumour, neuroblastoma, and other childhood cancers have been reported.[401;402] These neoplasms can also present isolated in the presence or absence of *DICER1* mutations,[401] and 66% of all the cases of PPB carry a *DICER1* germline mutation.[403]

The *DICER1* syndrome is an autosomal dominant disorder,[402] with very low penetrance (apparently 15% or less).[93;404] Eighty percent of the mutations in these patients are inherited and 20% present *de novo*; around 35% of the *DICER1* mutation carriers have a known familial history of *DICER1*-related tumours.[402] There is a predominance of female patients, perhaps due to the occurrence of ovarian and cervical tumours.[404]

A recent study reported thirteen (nine previously published and six unpublished) cases of *DICER1* syndrome with pituitary blastoma, and nine out of ten infants tested were positive for heterozygous *DICER1* mutations. Results of the genetic testing were not reported for two patients, due to either unavailability or suboptimal DNA quality. Only one of these germline mutations occurred *de novo*. In addition, somatic *DICER1* mutations were detected in seven cases, and two cases displayed LOH in the tumour, accounting for a total of nine patients with somatic alterations; seven of these cases were also positive for germline mutations.[93] This series, together with a recently reported case of isolated pituitary blastoma causing Cushing's disease in a female with *DICER1* germline and somatic mutation (and no familial history of *DICER1*-associated neoplasms),[405] account for a total of 14 genetically screened cases of this neoplasm reported to date.

Genetics and pathophysiology

DICER1 is located at 14q32.13 and contains 27 exons, encoding for a large protein (218.7 kDa), composed of 1922 amino acids. DICER1 is a multidomain enzyme with three main functions in miRNA processing: the processing of pre-miRNAs into mature miRNAs and long double stranded RNAs (dsRNAs) into small interfering RNAs (siRNAs); the loading of small RNAs onto argonaute (AGO) proteins to programme the RISC (this activity is known as RISC-

loading); and the scaffolding of interactions between different proteins implicated in the interference RNA (iRNA) mechanisms. In the miRNA biogenesis pathway, DICER1 acts downstream its nuclear homologue, the DROSHA protein. The most important functions of DICER1 are carried out by its RNaseIIIa and RNaseIIIb domains, located at its C-terminal half, which assemble into an intramolecular dimer to create the catalytic core of the enzyme.[404]

In multiple neoplastic tissues (lung, breast, skin, endometrial and ovarian cancer) reduced DICER1 levels (and in some cases, also DROSHA levels) are a marker of bad prognosis; however, overexpression of DICER1 has been found in prostate cancer metastases, in precursor lesions of lung cancers, in some oral cancers and in acute myeloid leukaemia, while DROSHA has been found upregulated in advanced stage cervical cancer and aggressive oesophageal cancers.[404] Somatic DICER1 pathogenic variants have been reported, in the presence or absence of germline mutations, in patients with PPB,[406-408] CN,[409;410] Wilms tumour, non-epithelial ovarian tumours,[411] cervical ERMS,[412] pituitary blastoma[93], prostate carcinoma, pineoblastoma[413], differentiated thyroid carcinoma[414] and testicular germ cell tumour.[415] Most of the somatic mutations detected affect the RNase IIIb catalytic domain (exons 24 and 25), specifically affecting the metal-ion binding residues or their adjacent amino acids (positions 1705, 1709, 1809 or 1813), which are therefore termed "missense hotspots".[402;404] The fact that the second hit on the WT allele almost always affects one specific region of *DICER1* distinguishes this gene from other tumour suppressors.[404]

The histopathological features of pituitary blastomas include the presence of small blastemal-like cells, small and larger glandular structures and ill-defined clusters of large epithelial cells.[416] Electron microscopy reveals the presence of folliculostellate and secretory, neuroendocrine cells. The glandular structures have the ultrastructural characteristics of Rathke's epithelium, as seen in the foetal pituitary.[417] The mitotic activity is highly variable and there is no evidence of normal adenohypohysis.[416;417] The larger, secretory cells are neuroendocrine cells, immunoreactive for synaptophysin, CgA, keratins, ACTH, β-endorphin and CRH, with rare GH positive cells.[416] Stains for other adenohypophysial hormones are negative. Ki-67 and MGMT immunoreactivity are variable. Both blastemal and glandular cells express NEUROD1, PIT1 and TBX19. [416] In summary, the histopathological appearance of pituitary blastomas resembles that of the human foetal adenohypophysis, at the age of 10-12 gestational weeks, when corticotrophs and somatotrophs are already differentiated, and α-GSU starts to emerge, but other cells types are not yet evident.[417] These findings together with the very early clinical presentation of pituitary blastomas, suggest that the development of these and possibly other *DICER1*-associated neoplasms starts *in utero.*

Clinical features

The phenotype of the *DICER1* syndrome is widely variable, but most of its manifestations occur before the age of 40 years. PPB, the most common manifestation, arises during lung development or during the neonatal stage, and it is usually diagnosed in infants and children

before the age of six years (median: 12 months, range: 0-546 months).[403;410] CN usually presents before the age of four years, while the age of onset of ovarian sex cord-stromal tumours is not well defined.[402;404]

PPB presents in infants with shortness of breath with or without pneumothorax secondary to cyst rupture, while ovarian sex cord-stromal tumours present as adnexal masses with or without signs of hormone production (PP, menstrual irregularities, or signs of virilisation). CN usually presents as a painless enlarging abdominal or flank mass; the finding of bilateral lesions strongly suggests *DICER1* mutations, and thyroid lesions usually present as palpable masses.[402] Treatment for *DICER1*-related malignant tumours usually involves surgical resection with or without chemotherapy/radiotherapy.[402]

Out of the 14 cases with pituitary blastoma and genetic screening reported to date, ten patients were females and four were males.[93;405] The first manifestation of disease appeared early in childhood (median: 12 months, range: 7-24 months), there was no familial history of that or other neoplasms and in most of the cases (9/14) pituitary blastoma was the only manifestation of the syndrome.[93;405] More than one *DICER1* syndrome-associated neoplasm can coexist in the same patient (2/14), in other cases the index patient presents one neoplasm only, but there is familial history of other tumours associated to the syndrome (3/14). Cushing's syndrome and ophtalmoplegia were the most common presenting clinical features, but in most of the patients where this parameter was available, elevated blood ACTH levels were reported, even in the absence of clinical Cushing's disease. Five out of the 14 infants died within 0-26 months of the first surgery; the maximum follow-up period in the rest of the patients is 17.4 years.[93] Pituitary blastoma is an extremely rare neoplasm and it is considered a pathognomonic feature of *DICER1* syndrome.[93]

Once a germline *DICER1* pathogenic variant has been detected in a patient, genetic testing should be offered to all the relatives at risk.[404] For the follow-up of *DICER1* mutation carriers, The International PPB Registry recommends annual physical examination and targeted review of systems, and imaging studies based on the patient's age and clinical findings, focusing on the most common components of the syndrome.[402;418]

CARNEY COMPLEX

Definition and general description

In 1985, Carney and collaborators described the clinical features and reported the first series of patients with the association of myxomas, spotty skin pigmentation and endocrine overactivity.[419] CNC (OMIM #160980 and %605244) is a syndrome characterised by the association of multiple endocrine tumours and cardiocutaneous manifestations.[420] A few patients with some components of the complex were previously described as NAME (nevi, atrial myxomas and ephelides, i.e. light-brown dermal macules) or LAMB (lentigines, atrial myxomas and blue nevi); currently all these cases are grouped as CNC.[420;421] Around 70% of the CNC

cases occur in a familial setting.[275] CNC is an infrequent clinical entity, with around 750 cases registered to date.[422] Patients are from diverse ethnicity, distributed through all the continents.[423]

The major diagnostic criteria for CNC are:[421]

- Spotty skin pigmentation with a typical distribution
- Myxoma (cutaneous and mucosal)
- Cardiac myxoma
- Breast myxomatosis or MRI suggestive image
- Primary pigmented nodular adrenal dysplasia (PPNAD) or paradoxical positive response of urinary glucocorticoids to dexamethasone
- Acromegaly
- Large-cell calcifying Sertoli cell tumours (LCCSCT) or characteristic calcification on testicular ultrasonography
- Thyroid carcinoma or multiple hypoechoic thyroid nodules in a young patient
- Psammomatous melanotic schwannoma
- Blue nevus or epithelioid blue nevus (multiple)
- Breast ductal adenoma (multiple)
- Osteochondromyxoma

The diagnosis of CNC is established if two major criteria are present or in the presence of one major criterion plus an inactivating *PRKAR1A* mutation or a first-degree relative with CNC.[421;423] Other less frequently detected clinical manifestations associated to CNC are: intense freckling, multiple blue nevus, *café-au-lait* spots, elevated IGF-1 levels, paradoxical GH response to TRH or to an oral glucose tolerance test (OGTT), cardiomyopathy, pilonidal sinus, a history of Cushing's syndrome, acromegaly or sudden death in extended family, multiple skin tags or lipomas, colonic polyps, hyperprolactinaemia, a single benign thyroid nodule in a young patient or multiple nodules in older patients, and familial history of carcinoma or other benign or malignant tumours.[423]

The genetic basis of CNC is heterogeneous, involving at least two loci, as demonstrated by linkage analysis.[424] The CNC1 gene is located at 17q24.2 and encodes the regulatory subunit 1-alpha of the protein kinase A (PRKAR1A);[88;420] seventy three percent of CNC patients present germline mutations in this gene.[275] The CNC2 gene, located at 2p16, is still unknown.[425] This locus frequently presents amplification in tumours of CNC patients, including some with known mutations in *PRKAR1A*, and thus it is suspected that an oncogene may be implicated.[426]

Genetics and pathophysiology

PRKAR1A is 21 kb in length and spans 11 exons, for a coding region of 1143 bp,[346] encoding a protein of 381 amino acids and 42.9 kDa. Protein kinase A (PKA), a main mediator of cAMP signalling is a tetramer composed of a dimer of regulatory subunits and a dimer of catalytic subunits. When four molecules of cAMP bind to the regulatory subunits, the catalytic subunits

are released to phosphorylate serine or threonine residues in their target proteins. There are four isoforms of regulatory subunits: Iα, Iβ, IIα and IIβ, which can pair up as homodimers or type I or type II heterodimers, composing holoenzyme complexes of PKA with a number of combinatorial configurations, including $RI\alpha_2C_2$, $RI\beta_2C_2$, $RII\alpha_2C_2$, $RII\beta_2C_2$ and $RI\alpha RI\beta C_2$. The dimer of catalytic subunits can contain different combinations of the three different isoforms: Cα, Cβ and Cγ.[427] Experimental downregulation of *PRKAR1A* inhibits growth in human cancer cell lines, while the overexpression of type I PKA stimulates cell growth and proliferation, via interactions with the epidermal growth factor receptor (EGFR).[428] Tumours in CNC often present LOH at 17q22-24, supporting the role or *PRKAR1A* as a tumour suppressor gene.[88]

More than 120 *PRKAR1A* mutations have been described to date in CNC patients,[422] distributed throughout the gene, with higher frequency in exons 2, 3, 5, 7 and 8.[275] Almost 80% of *PRKAR1A* mutations originate a premature stop codon, but truncated proteins are not expressed.[275;423;429] The abnormal mRNA, transcribed from the affected allele, is destroyed by a mechanism known as NMD, by which the cells degrade mRNA containing a deleterious, premature stop codon mutation prior to its translation.[428] Loss of expression of *PRKAR1A* in CNC tumours leads to a reduced regulatory activity over PKA, but also to compensatory increases in the expression of other PKA subunits.[88] These alterations derive in an increased response of PKA to cAMP, with upregulation of the cAMP signalling pathway.[428]

There is not a clear genotype-phenotype correlation for most of the *PRKAR1A* mutations in CNC,[430] although the intronic deletion exon 7 IVS del(-7→-2) is related to isolated PPNAD.[431] Differences in presentation of molecular defects and clinical features may be due to disease-modifying genes, located at other loci.[424;430] In a cohort of CNC patients, variants of the phosphodiesterase type 11A gene (*PDE11A*) showed association with a higher incidence of PPNAD and LCCSCT, suggesting that *PDE11A* can modify the phenotype.[432] No association was found with other components of the complex.

Prkar1a$^{-/-}$ mice are not viable. Lethality occurs during embryogenesis, due to a failure in mesoderm-derived structures.[280] Pituitary-conditional *Prkar1a*$^{-/-}$ mice develop pituitary adenomas with a higher frequency than their littermates. These tumours are sometimes multiple and express GH, PRL and TSH.[280] *Prkar1a*$^{+/-}$ mice are prone to develop tumours in cAMP-responsive tissues, such as bone, Schwann cells and thyroid, but not myxomas or pituitary adenomas.[433;434] *Prkar1a* haploinsufficiency in combination with *Tp53* or *Rb1* haploinsufficiency (*Prkar1a*$^{+/-}$/*Tp53*$^{+/-}$ and *Prkar1a*$^{+/-}$/*Rb1*$^{+/-}$, respectively) enhances the phenotype generated by each gene disruption, suggesting that *Prkar1a* haploinsufficiency in mice is a generic, but weak tumorigenic signal.[433;435] E2f, a downstream effector of Rb1, mediates the proliferative effects of the defective Prkar1a, and E2f activity is regulated by Tp53, providing a link between these tumour suppressor genes. [433;436] *Prkar1a* haploinsufficiency causes an increase in cAMP levels, leading to increased RAS/RAF/MEK/ERK activity, while complete *Prkar1a* deficiency causes constitutive activation of PKA and immortalisation of mouse embryonic fibroblasts through

upregulation of cyclin D1 *in vitro.*[433] A murine model with double heterozygosity for *Prkar1* and the PKA catalytic subunit alpha (*Prkar1a*$^{+/-}$/*Prkaca*$^{+/-}$) developed multiple bone lesions, including condromas, osteochondrodysplasia and rarely sarcomas.[434] This effect over bone stromal cells was mediated by PKA-II and alternative PKA catalytic subunits.

Multiple elements of the Wnt signalling pathway are overexpressed in different tumours from *Prkar1a*$^{+/-}$, *Prkar1a*$^{+/-}$/*Trp53*$^{+/-}$, *Prkar1a*$^{+/-}$/*Rb1*$^{+/-}$ and *Prkar1a*$^{+/-}$/*Prkaca*$^{+/-}$ mice, suggesting its implication in *Prkar1a*-derived tumorigenesis.[433-435] A microarray analysis of tumours from three different mouse models of *Prkar1a* haploinsufficiency (*Prkar1a*$^{+/-}$, *Prkar1a*$^{+/-}$/*Trp53*$^{+/-}$ and *Prkar1a*$^{+/-}$/*Rb1*$^{+/-}$) identified Wnt signalling as the main pathway activated by abnormal cAMP signalling, along with the mentioned cell cycle abnormalities.[433] In human tissue from PPNAD, PKA activates the expression of WISP2, a component of the WNT signalling pathway, via miRNA regulation.[437]

Twenty percent of CNC patients present *PRKAR1A* mutations in intronic sequences affecting splicing.[275] At least some of these mutations escape from NMD, leading to expression of the truncated protein.[438] LOH is not a universal finding in CNC tumours,[275] and *in vitro*, the expression of abnormal PRKAR1A without concomitant loss of the normal allele causes increased PKA activity.[438] The contribution of possible PKA-independent effects due to different protein interactions cannot be discarded.[275] *PRKAR1A* mutations have not been found in sporadic pituitary tumours;[278] however, low levels of PRKAR1A have been detected in sporadic functioning and NFPAs, despite adequate mRNA.[439]

In the pituitary, GHRH requires the cAMP/PKA pathway to stimulate GH synthesis and release.[280] The expression of other hormones is mainly regulated by different pathways, thus they are less likely to be affected by *PRKAR1A* mutations. Pituitary tumorigenesis in the context of CNC is a slow-developing process that requires mutation accumulation ("multiple hits").[440] Apparently, in CNC patients, germline mutations cause a predisposition, but other molecular events are necessary for pituitary adenoma development.[440]

Clinical features

CNC is inherited as an autosomal dominant trait.[421] Penetrance for CNC due to *PRKAR1A* is almost complete for some of the manifestations.[275;441] Clinical manifestations are variable, even within members of the same family. Thirty two percent of the *PRKAR1A* mutation positive patients present as *simplex* cases, and in more than 85% of them the mutation occurs *de novo.*[275]

Lentiginosis, consisting of 2-10 mm brown to black macules, distributed on the lips, eyelids, ears and genital area,[420] is the most common feature of CNC (70% of patients)[275] and is present in half of the patients before other components of the complex appear.[428] Lesions can exist at birth, but do not acquire their clinical characteristics until puberty.[421] Half of the patients develop

other skin lesions, such as blue, Spitz and compound nevi and *café-au-lait* spots.[275] Skin myxomas are found in 20% of the patients in eyelids, external ear canal, nipple, oropharynx, female genital tract and female pelvis.[275;421] Twenty percent of female patients present breast myxomas,[275] and also a few cases of breast ductal adenoma have been reported.[421] Cardiac myxomas are detected in 32% of cases.[275] In the setting of CNC, these tumours occur at any age, are multicentric, can be located in any cardiac chamber, tend to recur and can behave aggressively, requiring surgical resection to avoid complications such as embolism, strokes and cardiac failure.[423]

ACTH-independent Cushing's syndrome due to PPNAD is the main endocrine manifestation of CNC (60% of patients).[275;421] PPNAD almost always occurs in the context of CNC, but a very infrequent sporadic form also exists.[436] It has a bimodal age distribution: most of cases are diagnosed during the second and third decades of life and a minority present at the age of 2-3 years.[421] The disease is usually bilateral,[420] although the adrenal glands do not always show an obvious enlargement on imaging studies as nodules can be very small.[420] Hypercortisolism generally progresses subtly over years or follows a cyclic pattern, but the circadian cycle of cortisol is completely abolished, sometimes even in periods of inactive disease.[423;442] Pseudo-PP or hirsutism can appear.[442] Diagnosis is better established with the six day Liddle test, showing a paradoxical increase in the 24 hours (h) urinary free cortisol and/or 17-hydroxysteroids.[442;443] Bilateral adrenalectomy is the treatment of choice, but some patients respond to ketoconazole or mitotane.[423;442]

LCCSCT is a common (41% of male patients)[275] and almost always benign tumour in CNC, usually appears in the first decade of life, and most of the times is detected by ultrasonography, appearing as microcalcifications.[423] LCCSCT can rarely lead to gynecomastia and PP, but fertility impairment (due to obstruction of seminiferous tubules or inappropriate hormone production or aromatisation) is common. Adrenal rests and Leydig cell tumours can exist concomitantly with LCCSCT; ovarian cysts and cystadenoma have been found in some patients.[423] Thyroid nodules occur in 25% of patients and usually correspond to non-toxic adenomas of follicular type;[275;420;421] up to 10% of CNC patients with thyroid nodules develop thyroid carcinoma (follicular of papillary).[423] Psammomatous melanotic schwannomas are very rare tumours that can arise from any peripheral nerve, usually in the gastrointestinal tract and paraspinal sympathetic chain; they are pigmented, multicentric and frequently calcified.[421] These tumours are found in 8% of CNC patients[275] and they are malignant in 10% of the cases, metastasizing to lungs, liver or brain.[423] Osteochondromyxomas of the bone and tetralogy of Fallot have been found in some CNC patients and are possible components of the syndrome.[421]

A possible association between CNC and pancreatic neoplasms has recently been proposed. There is an unexpectedly high prevalence (2.5%) of pancreatic neoplasms among CNC patients, some of them of a very uncommon histological type (acinar cell carcinoma).[444] Most of the analysed cases present LOH at chromosome 17 and loss of PRKAR1A immunostaining.[444]

The main CNC-related cause of death is metastatic cancer (56% of deaths) and pancreatic cancer accounts for one third of cancer-related deaths in CNC patients.[275]

Histologically, pituitaries of CNC patients show zones of mammosomatotroph hyperplasia, that only occasionally progress to adenomas.[440] This “pro-acromegalic state” is a common characteristic shared by CNC and MAS, a syndrome in which the same molecular pathway is disturbed, though at a different level.[445] By IHC, almost all the somatotropinomas also stain positive for PRL and plurihormonal expression is frequent, but positive staining for ACTH has not been reported.[280;445] Microadenomas are much more common than macroadenomas, they are frequently multiple, sometimes microscopic and they grow surrounded by hyperplastic tissue.[440;445] Electron microscopy features are highly variable: from mammosomatotroph cells with abundant rough endoplasmic reticulum (ER), immature secretory granules and a small percentage (1%) of densely granulated cells, to sparsely granulated cells with poorly developed ER, and fibrous bodies, or a mixture of both types of cells.[445] Aggressive pituitary adenomas in CNC show genetic instability, whereas cytogenetic abnormalities are absent in hyperplasia or microadenomas;[440] LOH is not always detected.[280]

Clinically evident acromegaly is a relatively infrequent manifestation of CNC: the incidence of GH-producing pituitary tumours in CNC is 12%.[275] Nevertheless, paradoxical GH response to TRH or non-suppressible GH during a glucose challenge and/or IGF-1 elevation are present in up to 80% of patients, even in the absence of detectable tumours.[421] Acromegaly in CNC patients has a slowly progressive course,[440] and in some cases it only becomes apparent after the patient undergoes bilateral adrenalectomy for Cushing´s syndrome.[362] Pituitary tumours in CNC are almost exclusively GH or GH/PRL-secreting tumours. Around two thirds of CNC patients have mild hyperprolactinaemia (generally <100 ng/ml), but there are few cases of frank prolactinomas.[280]

Regular screening for the manifestations of the disease is recommended for patients with CNC and known carriers of *PRKAR1A* mutations. Screening for cardiac myxomas by echocardiography must start at diagnosis or during the first six months of life, and yearly thereafter.[421] If a cardiac myxoma was excised in the past, echocardiography is necessary every six months.[423] During childhood, screening for other manifestations should be performed only by clinical examination, because it is rare to detect endocrine tumours in CNC before the second decade of life.[423] Pubertal staging and growth rate must be monitored.[420] For post-pubertal patients the following annual studies are recommended: urinary free cortisol determination (plus diurnal cortisol or overnight 1mg dexamethasone test), serum IGF-1 and testicular ultrasonography in male patients.[421] Brain and spine MRI should be obtained at diagnosis and repeated only if clinical signs suggest the possibility of a schwannoma.[423] Pelvic ultrasonography in women is recommended at diagnosis and then as needed.[421] Thyroid ultrasonography is indicated at diagnosis and then as clinically indicated.[421]

PHAEOCHROMOCYTOMA/PARAGANGLIOMA AND PITUITARY ADENOMA

Definition and general description

Multiple cases reporting the coexistence of pituitary adenoma with a PHAEO or a PGL in the same patient can be found in the literature. Different causes explain the coexistence of these tumours, and a few example cases for each of them have been published: 1) a PHAEO/PGL-related gene mutation causing pituitary adenomas, 2) a pituitary adenoma-related gene mutation causing PHAEO/PGL, 3) ectopic synthesis of a hypophysiotropic hormone (GHRH or CRH) by the PHAEO/PGL and 4) pure coincidence. [92]

Recently, a cohort of 39 of such cases was screened for germline mutations in genes known to cause hereditary PHAEO/PGL (*SDHA, SDHAB, SDHAC, SDHAD, SDHAF2, RET, VHL, TMEM127, MAX, FH*) or pituitary adenomas (*MEN1, AIP, CDKN1B*), finding that mutations in *SDHB*, *SDHC*, *SDHD*, *VHL*, and *MEN1* can cause this phenotype.[92] Other few cases of the recently termed "Three P Association" (3PAs) have been reported in association with germline mutations in *SDHA*,[446] *SDHB,*[447-449] *SDHC*[450] and *SDHD.*[90;449;451-453] The *MEN1* and *VHL* mutation positive patients (one patient positive for each mutation), together with a few previously reported cases with mutations in these genes or in *RET* (causative of MEN2A),[454;455] seem to represent variants of the classic phenotypes of MEN1, the Von Hippel-Lindau disease and MEN2A respectively, whereas the patients with 3PAs and mutations in the genes encoding the subunits A, B, C and D of the succinate dehydrogenase (SDH) mitochondrial complex II (*SDHx* genes) share unique pathological features.

Germline mutations affecting multiple genes have been implicated in the pathogenesis of PHAEO/PGL: *NF1, RET, VHL, SDHD, SDHC, SDHB, EGLN1, KIF1B, SDHAF2, IDH1, TMEM127, SDHA, MAX, HIF2A and FH*.[456;457] Germline *SDHB* mutations are the most common genetic cause of PHAEO/PGL (10.3% of patients), followed by *SDHD* (8.9%) and *RET* (6.3%).[456] *SDHB* mutations are associated to a higher risk of malignancy and poor prognosis, and *SDHD* mutation carriers have a greater frequency of head and neck PGL and multiple tumours.[447;456]

Germline mutations in the *SDHx* genes are the main genetic cause of familial and sporadic cases of PHAEO/PGL (*SDHA*: paragangliomas 5 [OMIM #614165]; *SDHB*: paragangliomas 4 [OMIM #115310]; *SDHC*: paragangliomas 3 [OMIM #605373]; *SDHD*: paragangliomas 1 [OMIM #168000]),[456;458-461] but besides their association to 3PAs, so far they have not been associated to sporadic pituitary adenomas or FIPA.[92;449] Somatic *SDHx* mutations can be found in PHAEO/PGL (including one case with a germline and a somatic *SDHA* mutation),[446] but they seem to be extremely rare in pituitary adenomas, as only one positive case has been reported so far (double *SDHA* mutation in a prolactinoma).[462] Germline *SDHx* mutations are also associated to other clinical entities, such as sporadic gastrointestinal stromal tumours (GISTs),[463] the Carney-Stratakis syndrome,[464;465] and Cowden and Cowden-like syndrome,[466] and they have been detected in other neoplasms, such as multiple cases of renal cell

carcinoma,[467] a single case of adrenal medullary hyperplasia,[468] a single case of testicular seminoma,[469] two cases of neuroblastoma,[470] and a few cases of papillary thyroid carcinoma,[453] though for the last two tumour types the association remains unclear. In most of these cases there was familial or personal history of PHAEO/PGL. *SDHA* mutations are also associated to the mitochondrial complex II deficiency (OMIM #252011, progressive encephalomyopathy with variable phenotype, including the Leigh syndrome [OMIM #256000])[471] and with an autosomal recessive form of neonatal dilated cardiomyopathy (OMIM #613642).[472]

Genetics and pathophysiology

The SDH complex or succinate-coenzyme Q reductase is a heterotetrameric enzyme bound to the inner mitochondrial membrane. The catalytic core of the enzyme is composed of two hydrophilic proteins, SDHA and SDHB, and two hydrophobic proteins, SDHC and SDHD, anchor the complex to the membrane and serve as the ubiquinone site.[473] In addition, SDHAF2 is a factor required for the flavination of SDHA and for the assembly of the tetramer.[474] The SDH subunits are encoded by highly conserved nuclear genes (*SDHA*: 5p15, *SDHB*: 1p36.1-p35, *SDHC*: 1q23.3, *SDHD*: 11q23).

SDH is part of the Krebs cycle, catalysing the oxidation of succinate into fumarate. Electrons derived from this reaction are transferred to the respiratory chain complex III to reduce oxygen and form water, creating an electrochemical gradient across the mitochondrial inner membrane, which promotes adenosine triphosphate (ATP) synthesis.[473;474] Alternatively, electrons can be diverted to the ubiquinone pool (UQ pool), providing reducing equivalents necessary to reduce superoxide anions (reactive oxygen species) originated either from exogenous sources or as a result of the respiratory chain itself. A complete lack of succinate dehydrogenase activity hampers the electron flow to both respiratory chain complex III and the UQ pool, resulting in major oxidative stress.[473]

Different mechanisms can explain *SDHx*-associated tumorigenesis. The hypoxia-inducible factor (HIF) is a transcription factor composed of HIFα (oxygen-inducible) and HIFβ subunits, whose physiological function is the induction of cell adaptation to hypoxic conditions, by stimulating neovascularization and glycolysis.[475] The induction of the hypoxia pathway is the cause of the “glycolytic shift”, a feature of tumoral tissues first reported by Otto Warburg in the 1920s: even in the presence of oxygen, tumoral cells rely on anaerobic ATP production through glycolysis.[474]

The oxygen-dependent cytosolic enzymes prolyl-hydroxylases (PHDs) 1, 2 and 3 hydroxylate the HIF1α, HIF2α and HIF3α subunits, which are then bound by the von Hippel-Lindau (VHL) protein, an E3 ubiquitin-ligase, and driven to polyubiquitination and proteasomal degradation.[475] Excessive succinate accumulation, as occurs in the presence of LOF *SDHx* mutations, inhibits the function of the PHDs. In the absence of hydroxylation, HIFα subunits escape degradation, translocate to the nucleus and, after dimerising with HIFβ, induce the transcription of target

genes such as angiogenic factors and enzymes involved in glucose metabolism and cell survival, among others; this mechanism of tumorigenesis is known as “pseudohypoxia”.[475;476] In addition, in the absence of SHD function, reactive oxygen species accumulate and they can also inhibit PHDs. Succinate accumulation can also inhibit the function of KDM4D, an α-ketoglutarate-dependent histone demethylase, which could lead to tumorigenesis via a variety of epigenetic changes.[476]

In tumours carrying *SDHx* mutations, immunostaining for SDHA and SDHB is useful as a marker of involvement of the hypoxia pathway, and tumours carrying germline or somatic mutations usually display negative or decreased staining, which could be used as a screening test to triage genetic testing for *SDHx*,[462;477] though this has only been done in a small number of pituitary adenomas from *SDHB* mutation positive patients.[92]

Pituitary adenomas from *SDHx* mutation positive patients are characterised by focal oncocytic changes and by the presence of intracytoplasmic vacuoles (small and multiple or large, occupying most of the cytoplasm) in a variable number of cells (50-80%); the origin of these vacuoles remains uncertain.[92] LOH of the mutated *SDHx* gene in the tumoral tissue has been described in some of the cases, but it is not always present. The human phenotype is recapitulated by the $Sdhb^{+/-}$ mice, displaying pituitary hyperplasia of lactotroph and, to a minor extent, somatotroph cells after the age of 12 months, with blood-filled lakes and cells with large mitochondria with abnormal and/or missing cristae, intranuclear inclusions or pseudoinclusions and strong HIF1α staining, with a nuclear pattern in some cells, indicating hypoxia pathway activation.[449]

Clinical features

The phenotype can be variable among families with 3PAs: some members present both a pituitary adenoma and a PHAEO/PGL while other members harbour only one of the tumours. The phenotype of PHAEO/PGL in these patients is similar to that of other patients carrying *SDHx* mutations, usually with bilateral and/or multiple lesions, prone to recur.[449]

Twenty one cases of *SDHx* mutation positive 3PAs have been described so far.[92;446-453;476] Among them, *SDHB* and *SDHD* are the genes more frequently affected, with nine cases each, followed by *SDHC*, with two cases. Only one case has tested positive for a mutation in *SDHA*. In addition, an *SDHB* mutation was reported in a patient with a PHAEO, adrenal cortical hyperplasia and an abnormal pituitary MRI, though the pituitary diagnosis was not specified. Among the cases with available clinical data, there is a slight predominance of females (nine females vs. seven males). Sixteen cases had a familial presentation, and only one case was reported to occur in a sporadic setting. In the only two studies that have screened multiple 3PAs cases, nine out of twelve families and none of the 22 sporadic cases have tested positive for an *SDHx* mutation;[449] therefore, the presentation of this entity is almost always familial. However, only one of the families included two cases of pituitary adenoma, the rest of them had a single

case, while multiple cases of PHAEO/PGL are a more consistent finding among carriers of *SDHx* mutations.

The mean age at diagnosis of a pituitary adenoma was 44±16 years, and only two cases were diagnosed before the age of 30 years. The most common diagnosis was prolactinoma (ten cases), followed by NFPA (five cases); however, one operated NFPA stained positive for PRL. Three patients had somatotropinomas and one had a mammosomatotroph adenoma. Twelve of the patients harboured a pituitary adenoma together with a PHAEO/PGL; in one of these patients, a GIST was also detected. Five patients had only a pituitary adenoma and a PHAEO/PGL was detected in a different family member.

No phenotype-genotype associations can be established at the moment, due to the small number of cases, but it is unlikely that some *SDHx* mutations would lead specifically to PHAEO/PGL and others to 3PAs, as among members of a single *SDHx* mutation positive family, some patients present the full 3PAs phenotype while others develop PHEAO/PGL only or pituitary adenoma only, in the presence of the same mutation.

Based on the available data and in addition to the current known pathogenic implications for *SDHx* mutations, screening for *SDHx* genes is suggested in patients with 3PAs phenotype, in particular in patients with a familial presentation, as well as in families with cases of pituitary adenomas and PHAEO/PGL, even if not in the same individual. Screening for *SDHx* mutations is not recommended in patients with isolated sporadic or familial pituitary adenomas.[449] Apart of the genetic screening and close follow-up of *SDHx* mutation carriers, and possibly pituitary MRI in *SDHx* mutation positive PHAEO/PGL patients,[446] no specific indications for treatment or clinical screening of these individuals can be suggested as yet, and it would be advisable to follow the guidelines established for PHAEO/PGL patients with this genetic background.[456]

Familial isolated pituitary adenoma

Reports of familial presentation of nonsyndromic acromegaly and gigantism exist in the literature since the 18th century, even before the cause of acromegaly was known, but unfortunately, the earliest descriptions lack scientific accuracy.[478] However, by the end of the 20th century, and after the clinical description and finding of the causative genes for MEN1 and CNC, it was clear that a proportion of the pituitary adenomas in the general population, mainly somatotropinomas, could be inherited in the absence of other clinical manifestations.

FIPA (FIPA, OMIM #102200) is characterised by the presence of pituitary adenomas in two or more members of the same family in the absence of other syndromic clinical features, such as those characteristic of MEN1 and MEN4, CNC or tumours related to mutations in the *SDHx* genes. FIPA includes families previously identified as isolated familial somatotropinoma (IFS)[479] and pituitary adenoma predisposition (PAP).[8] FIPA is an autosomal dominant disease, with

incomplete penetrance and variable clinical presentation,[8;480;481] and it is estimated to account for around 2.5% of all the pituitary adenomas.[272]

Patients with known genetic cause represent around one fifth of all the FIPA cases, and include two different entities: FIPA associated to mutations in the *AIP* gene, accounting for the great majority of these cases, and patients with very young-onset GH excess and pituitary adenoma/hyperplasia due to microduplications in the Xq26.3 region (X-LAG), a novel clinical entity whose prevalence has not been determined as yet.[91 8;276;482]

Most of the FIPA families are composed of two to five affected members, and there is a first degree relationship between the affected members in about 75% of the cases.[482] Somatotropinomas and prolactinomas are the most common tumours among FIPA patients (75% of the cases), followed non-functioning pituitary adenomas (NFPA) and corticotropinomas, but functioning gonadotropinomas and one thyrotropinoma have also been diagnosed.[10;11;272] FIPA families can be classified as *homogeneous* (60% of all the reported families), when patients within the same family exhibit the same pituitary tumour type, or *heterogeneous* (40%), when two of more different tumour types are found within a family.[272;482] Families with only somatotropinomas or prolactinomas account for around 90% of all the homogeneous FIPA families.[482]

Patients from FIPA kindreds tend to be diagnosed on average four years before pituitary adenoma patients presenting in a non-familial setting,[272] and patients from IFS families are diagnosed around one decade earlier compared to MEN1 patients with pituitary adenomas.[483] In IFS families, 70% of the pituitary adenomas are diagnosed before the age of 30 years.[479] Pituitary adenomas occurring in the setting of FIPA tend to be more aggressive than those presenting as sporadic cases.[482] Despite its autosomal dominant pattern of inheritance, FIPA has a very variable penetrance and the disease is frequently not transmitted to a succeeding generation within a kindred.[483] It is not clear whether this is due to the influence of disease modifying genes (very probable), to a reduced reproductive potential among affected individuals (unlikely),[483] or to a combination of both factors.

FIPA WITH UNDETERMINED GENETIC CAUSE

Definition and general description

Around 80-85% of the FIPA families do not carry mutations in genes associated to pituitary adenomas.[276;482;484;485] Although the occurrence of two or more pituitary adenomas in the same family could be due to mere coincidence, it is possible that some of these cases could represent separate clinical entities of inherited pituitary adenomas, caused by still undetermined genetic causes.

Genetics and pathophysiology

Initial studies linked IFS to two distant loci: 11q13.1-13.3 and 2p16-12.[479] The former chromosomal region contains the *AIP* and *MEN1* genes; *MEN1* mutations were not detected, but in these and other families *AIP*muts were later discovered.[8;9] Only 8% of the sporadic somatotropinomas with LOH in 11q13 harbour *MEN1* mutations,[479] while the frequency of *AIP* mutations has not been studied in this subset of tumours. Nevertheless, LOH in 11q13 is a frequent finding in pituitary adenomas and other endocrine tumours, which can occur in the absence of *AIP* and *MEN1* mutations, suggesting the involvement of another gene at this chromosomal location in endocrine tumorigenesis.[486]

The second chromosomal region has also been implicated in the pathogenesis of some cases of CNC, in the absence of *PRKAR1A* mutations, but a pituitary adenoma causative gene in this region has not been described so far. Other chromosomal regions possibly implicated in FIPA, with significant linkage in different studies, are 8q,[8;487] and regions in chromosomes 4 and 5.[8]

Clinical features

Even though cases with undetermined genetic cause represent the wide majority of FIPA patients, their clinical features have been the less accurately described, perhaps because they represent a genetically heterogeneous population.[9] Homogeneous FIPA families with prolactinomas or Cushing's disease have only been reported to occur in the absence of *AIP*muts.[482]

These patients are 12 to 16 years older at diagnosis and their tumours are smaller, when compared to *AIP*mut positive patients.[485;488] Around half of the patients in these families have somatotropinomas, compared to three quarters of the patients with this type of tumours among *AIP*mut positive families.[485] Even though their response to treatment is relatively poor, they respond better than *AIP*mut positive patients.[488] The disease onset occurs during childhood in 11% of these families.[485]

X-LINKED ACROGIGANTISM

Definition and general description

X-LAG is characterised by childhood onset gigantism, usually manifest by the first year of life in previously normal infants, due to a pituitary adenoma or hyperplasia, caused by microduplications in Xq26.3.[91] This is a novel genetic cause of FIPA, although it can also present as sporadic disease in patients with nonsyndromic gigantism. Only 18 cases of X-LAG have been described so far, five of them occurring in a familial setting and the rest presenting as sporadic patients, and only transmission from affected mother to an affected son has been observed, while all the unaffected carriers of the duplication are females; therefore, X-LAG is considered a genetic disease with X chromosome-linked dominant inheritance pattern.[489]

Genetics and pathophysiology

The microduplicated regions of Xq26.3 in X-LAG patients encompass the genes *CD40LG, ARHGEF6, RBMX* and *GPR101. CD40LG* is not expressed in pituitary tumours and *ARHGEF6* and *RBMX* were found expressed, but not upregulated, while the expression of *GPR101* was increased by a factor as high as 1000 in the pituitary tumours of individuals with Xq26.3 microduplications, compared with normal pituitary and tumours from patients who tested negative for microduplications. In concordance, protein expression was increased in patients with Xq26.3 microduplications.[91]

In addition to the X-LAG cases, none out of 248 sporadic acromegaly patients tested carried microduplications at Xq26.13, but 11 of them carried the *GPR101* variant c.924G>C (p.E308D).[91] The minor allele frequency (MAF) of this variant is 0.004 according to the Exome Aggregation Consortium (ExAC) database,[217] but MAF is not reported in the 1000 Genomes[218] or National Heart, Lung, and Blood Institute Exome Variant Server (NHLBI EVS) databases;[216] this variant is a benign change according to *in silico* predictions. In three cases the variant was present in the germline, one of those patients presented also a somatic mutation, and three more patients had somatic mutations only.[91] One more acromegaly patient carrying this variant in the germline has recently been reported, for a global frequency of germline and somatic mutations of 2.3% (12/511), and one more *GPR101* variant, c.1098C>A (p.D366E, MAF not reported in 1000 Genomes, ExAC or NHLBI EVS databases), was reported in another sporadic acromegaly patient (among 263 tested).[490] In GH3 cells, overexpression of the p.E308D variant significantly increased cell proliferation and GH secretion compared to the WT protein, supporting a possible pathogenic role.[91]

GPR101 is composed of one exon, encoding a 508 amino acids and 56.7 kDa GPCR. GPR101 is a distant relative of the biogenic amine superfamily of GPCRs, expressed mainly in the caudate putamen and hypothalamus in the human, and in the hypothalamus, nucleus accumbens, amygdala and hippocampus in the mouse, although it was also found in other central nervous system structures.[491;492] Both murine and human GPR101 are coupled to Gs proteins, though they remain as orphan receptors.[492]

Notwithstanding the fact that the normal ligand of GPR101 is unknown, overexpression of the WT protein and of the two mutants detected in sporadic acromegaly patients resulted in increased cAMP signalling in GH3 cells, in the presence and absence of forskolin (an AC stimulator),[91] suggesting that the activation of this receptor in somatotroph cells could have similar effects to those of the GHRH receptor (GHRHR) on cell proliferation and GH secretion. The histopathological analysis of lesions from X-LAG patients reports mammosomatotroph adenomas, with a minority of the cases bearing mammosomatotroph hyperplasia.[91;489] The IHC analysis for the somatostatin receptors (SSTRs) 2, 3, and 5 and AIP is normal and there is increased expression of GPR101 and of GHRHR, but no GHRH.[91;489]

Clinical features

Gigantism in X-LAG patients characteristically develops in early childhood, in contrast with other forms of nonsyndromic gigantism, where disease onset occurs in adolescence.[91] Most of X-LAG patients are females, in contrast with other forms of pituitary gigantism, where males predominate.[489] Most of these patients have normal height and weight at birth (except one case, with length over the 97th percentile at birth), but there is an abrupt acceleration of both parameters typically by the first year of life, though it can occur as early as two months of age, an always before the age of five years.[91;489] Many of the X-LAG patients described so far developed not only tall stature, but marked acral growth and facial coarsening with hypertelorism, as well as other features that resemble those of adult acromegaly patients, including interdental separation, hyperhidrosis, skin thickening, sleep apnoea, acanthosis nigricans and hyperinsulinaemia. Interestingly, some of these patients develop increased appetite, which has not been associated to other forms of gigantism.[489] In addition to very marked hypersomatotropism, these patients display PRL co-secretion and normal or slightly elevated GHRH.[91;489] None of the patients has achieved disease control under treatment with SSA and the hyperprolactinaemia has not been controlled with DA; in most of the cases either radical surgery or multimodal therapy was necessary.[489]

AIP MUTATION-ASSOCIATED FIPA

Definition and general description

*AIP*mut-associated FIPA is an autosomal dominant disease, with incomplete and highly variable penetrance.[8;480;481] Since the late 1990s, linkage analysis and LOH studies implicated the 11q13 region in the pathogenesis of FIPA.[479;493-496] After the study of more families, the implicated locus was first narrowed down to 11q13.1-13.3,[479;483] and later to 11q13.2-13.3,[496] just next to *MEN1*, but not involving that gene. In 2006, linkage analysis identified a truncating germline *AIP*mut as the cause of several cases of pituitary adenomas (somatotropinomas and prolactinomas) in one large Finnish family.[8] Further studies identified many other novel *AIP*muts in individuals from FIPA families with gigantism, acromegaly and prolactinomas, and also in patients with apparently sporadic pituitary adenomas.[8-11;484] To date, *AIP*mut-associated FIPA and X-LAG are the two only known genetic causes of FIPA, and also the two only known causes of hereditary pituitary gigantism, defined as the occurrence of two or more cases of gigantism due to pituitary adenoma or hyperplasia in the same family.

Germline *AIP*muts have been identified in around 15-20% of the FIPA cases, with a higher prevalence among families with only cases of somatotropinomas, were mutations are found in 36-50% of the cases.[8;9;11;276;482;484] Initial studies failed to detect *AIP*muts in apparently sporadic pituitary adenomas in the general population,[279;497] but it is currently recognised that, apart from FIPA, *AIP*muts can also be found in other subsets of patients, including a small percentage (3-3.6%) of the sporadic pituitary adenomas in the general population,[6;7;12;13;13;276;498] in SSA-resistant acromegaly (8%)[14] and very rare cases of PHPT (two cases described so far).[499] Nevertheless, the most prominent pathogenic association of *AIP*muts involves pituitary

adenomas occurring in young (≤30 years old) people (11.7% of all the patients[498] and 11.7% of those with macroadenomas),[7] particularly in cases occurring in the paediatric population (20.5% of the paediatric patients with functional pituitary adenomas)[7] and in around half of the cases of gigantism.[482;500] Since the identification of *AIP* as a FIPA causative gene, 95 pathogenic or likely pathogenic mutations have been described among pituitary adenoma patients with familial and sporadic presentation (considering unpublished data from our group, part of it included in this thesis). Somatic *AIP*muts have never been detected.

The pattern of inheritance in *AIP*mut positive FIPA is autosomal dominant, but the penetrance is low and variable, calculated in around 15-33%, which is highly variable among families, as the number of affected individuals per family fluctuates between two and eleven.[8;480;482;485] The reason for the variable penetrance is unknown, but it is probable that other loci, not yet identified, could contribute to disease presentation.[487] Due to this incomplete penetrance, the phenotype can be absent in one or more generations, and reappear in subsequent generations of the same kindred.[501]

Genetics and pathophysiology

Located in the chromosomal region 11q13.2, just 2.6Mb downstream from *MEN1,* the *AIP* gene (GenBank: NG_008969.1,[502] Locus Reference Genomic: LRG_460)[503] spans six exons, encoding a protein of 37 kDa and 330 amino acids, highly conserved among species.[8;10;15] The best known function of AIP is to serve as a co-chaperone of the heat shock protein HSP90, forming part of the protein complex that regulates the function of the aryl hydrocarbon receptor (AHR).[504]

*AIP*muts in pituitary adenoma patients include deletions, insertions, segmental duplications, nonsense, missense, splice-site and promoter mutations, as well as large deletions of whole exons or the entire gene.[276] Loss of the C-terminal end of AIP occurs in the majority of the mutants, due to stop codons or frameshifts resulting in stop codons. Only one *de novo* mutation has been described, in a single patient.[6] There are three mutational hot spots in *AIP*, corresponding to C-phosphate-G (CpG) islands: mutation of both members of the c.910-911 CpG site has been described (c.910C>T [p.R304*] and c.911G>A [p.R304Q]), c.811C>T (p.R271W) and c.241C>T (p.R81*).[505] The missense variants and the in-frame segmental duplication mostly affect the tetratricopeptide repeat (TPR) domain or the C-terminal α-helix. Approximately 10% of the families that are negative for *AIP*muts by conventional methods carry large *AIP* deletions, which are only detectable by MLPA.[276] A founder effect for certain *AIP*muts has been described in different populations: Northern Irish (c.910C>G [p.R304*]),[506] Finnish (c.40C>T [p.Q14*]),[8] Italian (c.910C>G [p.R304*]),[507] English (c.805-825dup [p.F269_H275dup])[508] and Comoros islander (p.G117Afs*39).[498]

The molecular mechanism explaining the link between *AIP*muts and pituitary adenomas remains elusive, but a regulatory effect over the cAMP pathway that could affect cell

proliferation and GH secretion in somatotroph cells has been proposed.[509] More details about the normal functions of AIP and its implication in pituitary tumorigenesis are provided in the section *"Aryl hydrocarbon receptor interacting protein: association to pituitary tumorigenesis".*

Clinical features

*AIP*mut positive patients constitute a well defined group among pituitary adenoma cases. *AIP*mut positive FIPA families have more affected individuals (3.2±1.8) than families with no *AIP*muts (22±0.4).[10] *AIP*mut positive tumours are almost always macroadenomas, predominantly somatotropinomas, more than a half of them with PRL co-secretion, with disease onset during adolescence or young adulthood.[11;485] In more than a half of the patients, tumours are aggressive.[328] Pituitary adenomas in *AIPmut* positive patients show a considerably reduced response to the treatment with SSA and DA, regarding tumour size and hormone secretion, usually requiring multimodal therapy.[7]

The presence of gigantism in one third of *AIP*mut positive patients with somatotropinomas is noteworthy, given the extreme rarity of this condition among sporadic patients.[11] The frequency of gigantism, a disease which is more prevalent in males, could explain the predominance of males among *AIP*mut positive patients in different series.[11] Also, initial series proposed the occurrence of genetic anticipation among *AIP*mut FIPA families, but the observed earlier diagnosis in consequent generations is more likely to be due to patient education regarding the symptoms in other family members.[11;276]

Aryl hydrocarbon receptor interacting protein: association to pituitary tumorigenesis

Expression and structure

The reference *AIP* mRNA (NM_003977.3)[502] encodes the isoform 1 of AIP, which is the only known translated form of the protein (UniProt: O00170).[510] The Ensembl database reports three predicted alternative transcripts for this gene, two of them predicted to encode proteins[511] (these two also reported in GenBank);[502] however, the biological relevance of these alternative transcripts or their encoded proteins, if they exist, has not been demonstrated as yet. Putative phosphorylation sites for AIP have been determined by site-directed mutagenesis and two-dimensional phosphopeptide mapping analysis in serine residues 43, 53, 131, 132, and 329, but loss of any or all of these residues does not significantly affect the ability of AIP to bind AHR and to retain it in the cytoplasm, although S53 could be necessary for the nuclear translocation of AIP.[512] Many other putative phosphorylation sites have been reported by mass spectrometry (MS) studies, but they have not been experimentally tested.[513] No other posttranslational modifications for this protein are known. The structure and domains of AIP are shown in Figure 2.

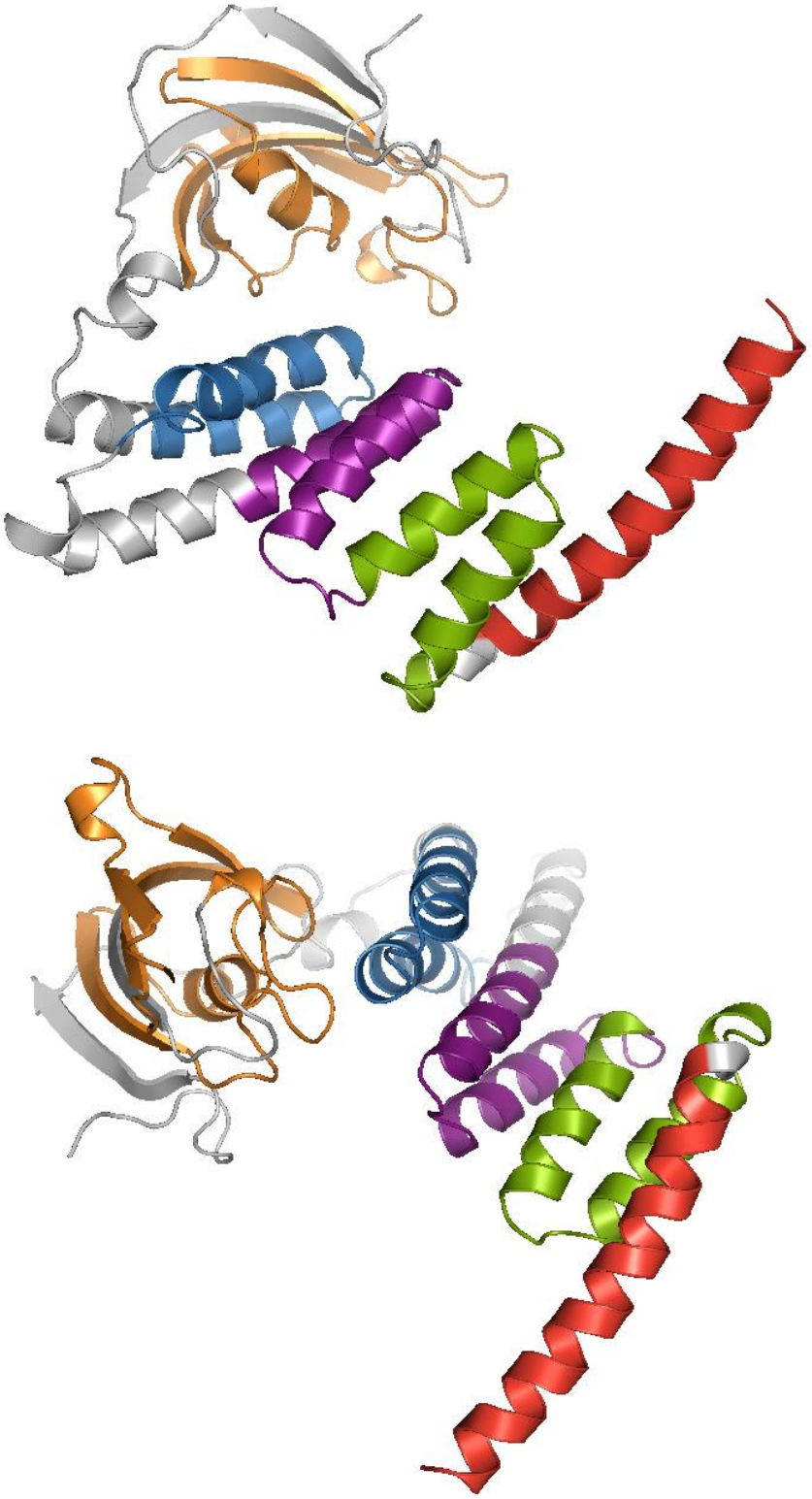

Figure 2. Prediction of the tridimensional structure of AIP (two views). Main motifs in the molecule are displayed in colours, according to UniProt annotation at 05/05/15: PPIase domain (orange, amino acids 31-121), TPR1 (blue, 179-212), TPR2 (purple, 231-264), TPR3 (green, 265-298) and C-terminal α-7 helix (red, 300-330).[510] the image was created using the PyMol software (DeLano Scientific LLC), using a prediction generated by the Phyre2 platform[514] on 04/02/13, based on the data available at the RCSB Protein Data Bank (entries: 4AWO, 4B7P, 4AWQ, 4AWP, 1Q18, 2LKN, 4AIF, 4APO).[515]

Also known as X-associated protein 2 (XAP2),[516] AHR-activated 9 protein (ARA9)[517] and FK506-binding protein 37.7 (FKBP37.7),[518] AIP was first described in 1996 as an inhibitor of hepatitis B virus X protein-mediated transactivation.[516] AIP is ubiquitously expressed in human and murine tissues, most abundantly in the cardiovascular system, brain, cerebellum, diaphragm, kidney, tongue and testis, though it is poorly expressed in the human liver.[516;519] The *AIP* gene is evolutionarily conserved among species, with orthologues in a variety of organisms, from primates (100% of protein identity for *G.g.gorilla* and *P. troglodytes*), and rodents (*R. norvegicus:* 94%, *M. musculus:* 95%) to lower organisms such as *D. rerio* (66%), *D. melanogaster* (35%) and *C. elegans* (35%).[511] AIP expression is predominantly cytoplasmic,[520] and there is nuclear expression to a lesser extent.[521] Sequence homology predicts two different domains in AIP: an N-terminal FK506-binding protein (FKBP) or peptidylprolyl *cis*-trans isomerase (PPIase)-like domain and a C-terminal TPR domain, composed of three TPR motifs and a final α-helix.[520;522;523]

FKBPs, proteins that bind the fungi-derived immunosuppressant drugs tacrolimus and rapamycin, together with cyclophilins, cyclosporine-A binding proteins, are the two largest families composing the immunophilin superfamily, with at least 16 paralogs in humans.[524] Immunophilins are highly conserved chaperones that can also display PPIase activity, but their chaperone function can occur independently of the PPIase effect.[525] Some immunophilins contain a single PPIase domain and others are multidomain proteins with one or more PPIase domains in addition to other functional domains. In *S. cerevisiae*, the deletion of 12 immunophilins individually or as a group has no effect on physiological parameters (viability at various temperatures, arrest and recovery from α-factor pheromones or glycogen, mating, sporulation) under basal conditions, but these proteins are required for specific signalling events, as for example, growth under starvation-induced stress.[525] Immunophilins play important roles as regulators of protein kinases, protein folding and retrotransport into the ER, among others.[525] Some members of the FBKP family contain a TPR through which they interact with HSP90.[526]

Frequently referred as “scaffold proteins”, due to their function as interaction modules and multiprotein complex mediators, TPR-containing proteins are abundant in the proteome and regulate several biological processes, such as organelle targeting, protein import and vesicle fusion.[527] The TPR motif consists of 3-16 tandem-repeats of 34 amino acids adopting a helix-turn-helix arrangement, with adjacent TPR motifs packed in parallel, resulting in a unique super-helix tridimensional structure formed by repeating anti-parallel α-helices.[528] The degenerate consensus sequence of TPRs has no fully invariant positions, but follows a pattern of small and large hydrophobic amino acids. Residue type is highly conserved only at positions 8 (A or G), 20 (A), and 27 (A), while positions 4, 7, 11, and 24 have a preference for large hydrophobic amino acids.[527] Positions with a strong preference for small amino acids are located in places where the helices are in close contact, and in fact there is a consistent pairing between large and small amino acids, which pack together in a complementary fashion.[527;528] Therefore, non-

conservative mutations in these positions are not tolerated and often result in LOF of the protein.[528] The exterior of the super-helix displays amino acid variety and some degree of elasticity and has a concave and a convex surface; ligand binding usually occurs via hydrophobic pockets on the concave surface.[527]

In the case of TPR-containing co-chaperones, the hydrophobic pockets on the TPR domain that bind the methionine and the valine in the MEEVD conserved sequence of the TPR domain of HSP90 can be classified depending on their relative position. When both pockets are on the same side of the TPR binding surface, as it is the case for the co-chaperone STI1 (also known as HOP), the proteins follow a *cis*-mode of binding (STI1-type). When they are on different sides, as it happens for the co-chaperones AIP and CHIP, there is a *trans*-mode of binding.[523]

The secondary structure of the FKBP domain of AIP (including amino acids 2 to 166), resolved by nuclear magnetic resonance (NMR) spectroscopy, resembles a typical FKBP domain with five antiparallel β-strands forming a half β-barrel wrapped around a central α-helix.[518;529] However, the FKBP domain of AIP has no inherent FK506 binding or PPIase activity, and displays two unusual structural elements: an N-terminal α-helix, which additionally stabilises the domain, and a long insert connecting the last two β-strands and covering the putative active site.[518] The TPR domain of AIP appears to be similar to those of STI1, CHIP, CYP40, PP5, FKBP51, FKBP52 and the aryl hydrocarbon receptor-interacting protein like 1 (AIPL1). The crystal structure of this domain shows that residues lining the TPR-binding site are highly conserved, and their spatial organisation shows a CHIP-type interaction with HSP90.[523]

Normal function and protein-protein interactions

There is strong data in the literature to support direct interaction of AIP with two viral proteins, Epstein-Barr virus (EBV)-encoded nuclear protein 3 (EBNA3)[530] and hepatitis B virus X protein,[516] and with a variety of human proteins, such as AHR,[520;531] HSP90,[520] phosphodiesterases 4A (PDE4A)[532] and 2A (PDE2A),[533] heat shock cognate 70 (HSPA8, also known as HSC70),[534] baculoviral IAP repeat-containing protein 5 (apoptosis inhibitor survivin, BIRC5),[535] peroxisome proliferator-activated receptor alpha (PPARA),[536] thyroid hormone receptor beta (THRB),[537] oestrogen receptor (ESR1),[538] mitochondrial import receptor subunit TOM20 homolog (TOMM20),[534] rearranged during transfection tyrosine-kinase receptor (RET)[539] and guanine nucleotide-binding protein subunit alpha 13 (GNA13);[540] the most studied associations are with AHR and HSP90. Other interacting partners are also reported in the BIOGRID database of protein-protein interactions, as part of datasets generated by high throughput proteomics studies, with lower levels of evidence to support the interactions, and they are not necessarily validated by other methods.[541] All the known AIP interactions with human proteins are summarised in Table 4.

Table 4: Proven and putative interacting partners of AIP (human proteins only)

UniProt entry[510]	Protein name (gene)	Reported in BIOGRID[541]	Experimental method	References
P60709	Actin, cytoplasmic 1 (*ACTB*)*	No	AC-MS	[542]
Q9UL18	Argonaute RISC catalytic component 1 (*AGO1*)	Yes	AC-MS	[543]
			Co-IP	
P35869	Aryl hydrocarbon receptor (*AHR*)	Yes	Co-IP	[520;544]
			RC	[517;520;522]
			2H	[517;520;545]
P27540	Aryl hydrocarbon receptor nuclear translocator (*ARNT*)†	Yes	Co-IP	[542]
			RC	[517;546]
			2H	[522]
O15392	Baculoviral IAP repeat-containing protein 5 (*BIRC5*)	Yes	Co-IP	[539]
Q96HB5	Coiled-coil domain containing protein 120 (*CCDC120*)	Yes	AC-MS	[547]
Q16543	Hsp90 co-chaperone cell division cycle 37 (*CDC37*)	Yes	AC-L	[548]
		Yes	AC-MS	
P50750	Cyclin-dependent kinase 9 (*CDK9*)	Yes	AC-MS	[547;549]
Q9BXN2	C-type lectin domain family 7, member A (*CLEC7A*)	Yes	2H	[550]
P68400	Casein kinase 2, alpha 1 polypeptide (*CSNK2A1*)	Yes	BA	[551]
Q9NVR5	Protein kintoun (*DNAAF2*)	Yes	AC-L	[548]
			AC-MS	
P00533	Epidermal growth factor receptor (*EGFR*)	Yes	PCA	[552]
P03372	Oestrogen receptor (*ESR1*)	No	Co-IP	[538]
P41091	Eukaryotic translation initiation factor 2 subunit 3 (*EIF2G*)	Yes	Co-F	[553]
P50395	Rab GDP dissociation inhibitor beta (*GDIB*)	Yes	Co-F	[554]
Q14344	Guanine nucleotide-binding protein subunit alpha 13 (*GNA13*)	Yes	RC	[540]
			2H	
P50148	Guanine nucleotide-binding protein G(q) subunit alpha (*GNAQ*)	Yes	RC	[540]
P11142	Heat shock cognate 71 kDa protein (*HSPA8*)‡	No	Co-IP	[534]
P07900	Heat shock protein HSP 90-alpha (*HSP90AA1*)	Yes	AC-L	[548]
			AC-MS	
			Co-IP	[522;534;555-559]¶
			RC	[523;560]
P08238	Heat shock protein HSP 90-beta (*HSP90AB1*)	Yes	AC-L	[548]
			AC-MS	
P38646	Stress-70 protein, mitochondrial (*HSPA9*)	Yes	Co-F	[553]
Q9Y6K9	NF-kappa-B essential modulator (*IKBKG*)	Yes	2H	[561]
Q92985	Interferon regulatory factor 7 (*IRF7*)	Yes	AC-MS	[562]
			RC	
P11279	Lysosome-associated membrane glycoprotein 1 (*LAMP1*)	Yes	Co-F	[553]
Q6IA69	Glutamine-dependent NAD(+) synthetase (*NADSYN1*)	Yes	AC-L	[548]
			AC-MS	
P08235	Mineralocorticoid receptor (*NR3C2*)	Yes	Co-IP	[559]
P27815	cAMP-specific 3',5'-cyclic phosphodiesterase 4A (*PDE4A*)	No	2H	[9;532]
			Co-IP	[532]

UniProt entry[510]	Protein name (gene)	Reported in BIOGRID[541]	Experimental method	References
O00408	cGMP-dependent 3',5'-cyclic phosphodiesterase 2A (*PDE2A*)	No	2H	533
			Co-IP	
			Co-loc	
Q07869	Peroxisome proliferator-activated receptor alpha (*PPARA*)	Yes	Co-IP	536
			RC	
O75170	Serine/threonine-protein phosphatase 6 regulatory subunit 2 (*PPP6R2*)	Yes	PL-MS	563
Q15185	Prostaglandin E synthase 3 (*PTGES3*)	Yes	AC-L	548
			AC-MS	
			Co-IP	559
P07949	Rearranged during transfection tyrosine-kinase receptor (*RET*)	Yes	Co-IP	539
			PCA	
P31948	Stress-induced phosphoprotein 1 (*STIP1*)	Yes	RC	560
Q9Y2Z0	Suppressor of G2 allele of SKP1 homolog (*SUGT1*)	Yes	AC-L	548
			AC-MS	
Q59H18	TNNI3 interacting kinase (*TNNI3K*)	Yes	2H	564
Q15388	Mitochondrial import receptor subunit TOM20 homolog (*TOMM20*)	No	RC	523;534
P10828	Thyroid hormone receptor beta (*THRB*)	No	2H	537
P0CG48	Polyubiquitin C (*UBC*)	Yes	AC-MS	565-569
O94966	Ubiquitin specific peptidase 19 (*USP19*)	Yes	AC-L	548
			AC-MS	

2H: two-hybrid assay, AC-MS: affinity capture (pull-down)-mass spectrometry, AC-WB: affinity capture-Western blot (co-immunoprecipitation), BA: biochemical activity (an interaction is inferred from the biochemical effect of one protein upon another), co-F: co-fractionation, co-IP: co-immunoprecipitation, co-loc: co-localisation, PCA: protein-fragment complementation assay, PL-MS: proximity label-mass spectrometry, RC: reconstituted complex (an interaction is detected between two proteins *in vitro*). Detailed explanation of all the experimental methods: http://wiki.thebiogrid.org/doku.php/experimental_systems
* Contradictive results, a direct interaction between AIP and ACTB was disproven by a different study.[570]
†Contradictive results, a direct interaction between AIP and ARNT was disproven by different studies.[517;520;555]
‡ A positive but reduced binding between AIP and HSPA8, compared to CHIP, was found in a different study.[559]
¶ Some of these experiments did not specify the HSP90 isoform used. HSP90AB1 was assumed, as this is the major form of the protein.

The best known function of the AHR is to act as a transcription factor mediating the toxic effects (immune, hepatic, cardiac, dermal, teratogenic, endocrine and carcinogenic) of the environmental toxin 2, 3, 7, 8-tetrachloro-*p*-dioxin (TCDD, dioxin).[571;572] Endogenous AHR ligands have also been described, such as indigo, indirubin, equilenin, 2-(1´H-indole-3´-carbonyl)-thiazole-4-carboxylic acid methyl ester, lipoxin 4A, prostaglandin G2, tryptamine, indole acetic acid, 6-formylindolo-carbazole,[90] bilirubin[573] and kynurenine.[574] The physiological role of AHR is, apparently, ligand, tissue and species-specific and comprises a wide variety of effects, such as regulation of the activity of nuclear receptors, transcription factors and protein kinases, modulation of cell cycle, cell adhesion and migration as well as alteration of multiple intracellular signalling pathways.[572] AHR-dependent transcription is regulated by interactions with multiple partners, thus AHR integrates signals from diverse ligands and molecular pathways.[575] Although there are some earlier controversial data, more recent studies suggest that human AIP (opposed to the murine protein) enhances the rate of nuclear translocation, but inhibits the transcriptional effects of AHR.[531;576] Some data indicate that AIP modulates AHR

levels;[521] this effect is also apparently tissue-specific[15;577] and potentially relevant for pituitary tumorigenesis.

Ligand-free AHR is localised in the cytoplasm, attached to a heterotetramer composed of a dimer of the chaperone HSP90[504;578] and one unit of each of the co-chaperone proteins translationally-controlled tumour protein (TCTP, also known as p23)[579] and AIP.[517;520;531] AIP binds to both HSP90 and AHR, but HSP90 is required to model AHR to a ligand-binding configuration.[556] The co-chaperone TCTP binds to HSP90, stabilising the complex and favouring its nuclear import.[580] After binding dioxin or other exogenous or endogenous ligands, AHR undergoes a conformational change, allowing the nuclear translocation of the protein complex.[571] Interestingly, the human AIP protein translocates to the nucleus together with the rest of the complex, while the murine protein remains in the cytoplasm.[576] In the nucleus, the aryl hydrocarbon receptor nuclear translocator (ARNT, also known as HIF1β) binds to ligand-bound AHR,[571] dissociating it from the rest of the complex. Thus, the ligand:AHR:ARNT complex is able to bind a dioxin-responsive element (also known as xenobiotic or AH-responsive element), leading to the activation of AHR-responsive genes.[572;581] AIP interacts with AHR through its TPR domain,[521;522] but the PPIase domain is required for the stability of the AHR:HSP90:AIP complex.[546]

HSP90, a highly conserved, essential and very abundant protein (it accounts for 1-2% of cytosolic proteins) is a molecular chaperone that interacts with multiple client proteins, including transcription factors, protein kinases and enzymes, therefore regulating a wide variety of cellular pathways.[526;560] HSP90 also facilitates, in concert with other chaperones, the folding and proteolytic stability of its client proteins, but it can also promote their degradation.[526] HSP90 forms complexes with different co-chaperones in a cyclical way: first STI1 binds and inhibits the adenosine triphosphatase (ATPase) activity of HSP90, but then STI1 is released and replaced by a PPIase and TCTP, in an ATP-dependent reaction.[560] Interestingly, AIP displays binding sites for HSP90 not only at the TPR but also at the PPIase domain, [518] but it does not affect the ATPase activity of HSP90.[523] The stoichiometry of the interaction between AIP and HSP90 is 0.5:1, meaning that one molecule of AIP binds two HSP90 molecules.[523]

Only 13 out of 100-150 different mitochondrial proteins are encoded by mtDNA; therefore, mitochondrial proteins synthesised in the cytosol require to be imported into these organelles. This process occurs through four different protein systems: presequence translocase-associated motor, sorting and assembly machinery of the outer membrane, translocase of the inner membrane and translocase of the outer membrane.[582] AIP forms a complex with mitochondrial pre-proteins and TOMM20, a member of the translocase of the outer membrane system, exerting a chaperone-like activity to supress the aggregation of the substrate proteins.[534] The interaction between TOMM20 and AIP involves the C-terminal EDDVE sequence of TOMM20 and the TPR domain of AIP.[523;534] One of the proteins translocated into the mitochondria by the AIP/TOMM20 complex is BIRC5, an anti-apoptotic protein.[534;535;583]

AIP also binds HSPA8, and, according to the proposed model, mitochondrial pre-proteins bound to AIP and HSPA8 would be maintained in an unfolded state, until transferred (bound to AIP) from HSPA8 to TOMM20, enabling their folding and mitochondrial translocation.[534] HSPA8 is an abundant cytosolic protein with intrinsic ATPase activity, which is part of the HSP70 family of molecular chaperones.[584] The cellular functions of HSPA8 (regulated by multiple co-chaperones) include the regulation of the dynamics of clathrin-coated vesicles and of the cell cycle (through regulation of cyclin D1), as well as protein homeostasis (maturation, folding, assembly, degradation) and translocation.[584;585] The C-terminal IEEVD sequence of HSPA8 is assumed to mediate the interaction between this protein and the TPR domain of AIP.[523]

Cyclic nucleotide phosphodiesterases (PDEs) regulate cell signalling by hydrolysing the intracellular second messengers cAMP and cyclic guanosine monophosphate (cGMP). PDE4A is a member of the PDE4 subfamily of phosphodiesterases, with cAMP-specific hydrolytic activity.[586] AIP directly binds and reversibly inhibits the enzymatic activity of PDE4A5 (the rat isoform of the human PDE4A) attenuating the ability of PKA to phosphorylate this protein.[532] This interaction involves the C-terminal α-helix of AIP, and probably the N-terminal region of PDE4A5.[523;532] Dysfunction of the cAMP molecular pathway is relevant for somatotroph function and loss of the AIP-PDE4A interaction has been demonstrated *in vitro* for different pathogenic missense and nonsense *AIP*muts.[9;10] In addition, a member of the PDE2 subfamily, PDE2A (also known as PDE2A3), which is activated by cGMP but hydrolyses both cAMP and cGMP, interacts with the TPR domain of AIP through its GAF-B domain (involved also in cGMP binding).[533;586] This interaction inhibits dioxin and cAMP-induced nuclear translocation of AHR, attenuating the AHR-dependent gene transcription.[533]

It has also been proposed that AIP could self-associate to form multimers, which could serve as a cytoplasmic reservoir of the protein.[587] However, the stoichiometric analysis of the AHR:HSP90:AIP complex has shown a ratio of 1:2:1,[504;578] and for the HSP90:AIP complex the ratio is 2:1.[523] Therefore, AIP self-association, if existent, is probably not relevant for the biological functions of the protein.

AIP functions in the pituitary gland

In the normal pituitary, AIP is predominantly expressed in somatotroph and lactotroph cells,[9;481] where it associates with GH and PRL-containing vesicles.[9] AIP has been detected in corticotropinomas and it is especially abundant in NFPAs, while it is absent in normal corticotroph and gonadotroph cells. In addition, in these adenomas AIP is not localised in the secretory vesicles but it is found free in the cytoplasm.[9]

A possible function of AIP as a regulator of the cAMP pathway has recently been proposed. Under physiological conditions, binding of GHRH to its receptor, activates a stimulatory G protein (Gs)-mediated signalling pathway, with cAMP as a central second messenger. The cAMP pathway regulates both GH secretion and the proliferation of somatotroph cells, and the

most important regulator of this pathway in the somatotroph cells is the inhibitory G protein (Gi)-mediated SS signalling pathway. The inhibition of hormone secretion and cell proliferation by the SS pathway is the basis of the use of SSA as antitumorigenic drugs in pituitary adenomas and other endocrine tumours.

The current notion about AIP function in the pituitary gland is that it exerts an inhibitory effect over the cAMP pathway. In GH3 cells (rat somatotropinoma-derived), Aip overexpression reduces the cAMP response to forskolin (a drug that produces cAMP accumulation) measured by cAMP assay and mRNA expression of downstream members of the pathway, resulting in GH secretion. Inversely, also in the presence of forskolin, Aip knockdown (KD) activates the cAMP pathway, but this effect is not coupled to increased GH secretion.[588] it is important to remark that these effects are significant under forskolin stimulation, but not in the basal conditions.

In the pituitary gland of a heterozygous *Aip* KO murine model, *AIP* deficiency leads to down-regulation of genes involved in the Gi signalling pathway (mediated by $G\alpha_{i2}$ and $G\alpha_{i3}$), and as a consequence, to cAMP accumulation.[509] However, Gi impairment is not exactly equal to Gs constitutive activity (e.g. the effect of the *gsp* oncogene), as the regulation of the cAMP pathway is complex, involving multiple steps and regulatory proteins. This could explain why the accumulation of cAMP does not cause an increased phosphorylation of the mitogen-activated protein kinases (MAPKs) 3 and 1 (also known as ERK1 and 2, respectively) and cAMP-response element binding protein (CREB), cAMP-responsive effectors of the cAMP pathway, in *AIP*mut positive somatotropinomas.[509]

AIP expression in somatotropinoma tissue is a positive predictor of responsiveness to the treatment with SSA in sporadic acromegaly patients,[16] and aggressive somatotropinomas display reduced AIP expression.[17;96;481] In concordance, *AIP* is upregulated in sporadic somatotropinomas with preoperative SSA treatment, compared to patients with no pre-treatment, and a similar effect has been found in GH3 cells treated with SSA.[589] The stimulatory effect of SSA over AIP expression is independent of the *GNAS1* status of the tumour, indicating that this response is independent of the activation status of the cAMP pathway,[17] and it is also independent of the expression of the SSTR2, the main receptor for the clinically used SSA octreotide and lanreotide.[16] Nonetheless, AIP immunostaining in pituitary adenomas is not predictive of *AIP*muts.[590]

The antiproliferative/antisecretory response to SSTR activation is carried out through multiple mechanisms; the most prominent ones regarding the somatotroph cell function are: AC inhibition, calcium channel inhibition and dephosphorylation of the cAMP effectors MAPK3/1 by phosphotyrosine phosphatases.[591] In addition, in an apparently independent mechanism of post-receptor response to SS, *AIP* overexpression upregulates *ZAC1*, an anti-proliferative target of SS, while *AIP* KD has an inverse effect.[592]

SSTRs are GPCRs, coupled to different types of G proteins: $G\alpha_{i1-3}$, $G\alpha_o$, $G\alpha_q$ and $G\alpha_{12}$. The repertoire of G proteins binding each SSTR type seems to be tissue and function-specific. For example, $G\alpha_o$ is the specific subunit necessary for the SSTR5 inhibitory effect on GH secretion and MAPK3/1 phosphorylation.[593] The $G\alpha_i$ proteins involved in the somatotroph-specific function of SSTR2 have not been described, although $G\alpha_{i1-3}$ expression has been demonstrated in all types of pituitary adenomas, where they are very infrequently mutated.[509;594] The SSTR type mediating the AIP response in pituitary adenomas remains elusive. The proposed mechanisms for the AIP tumour suppressor activity in the somatotroph cells are summarised in Figure 3.

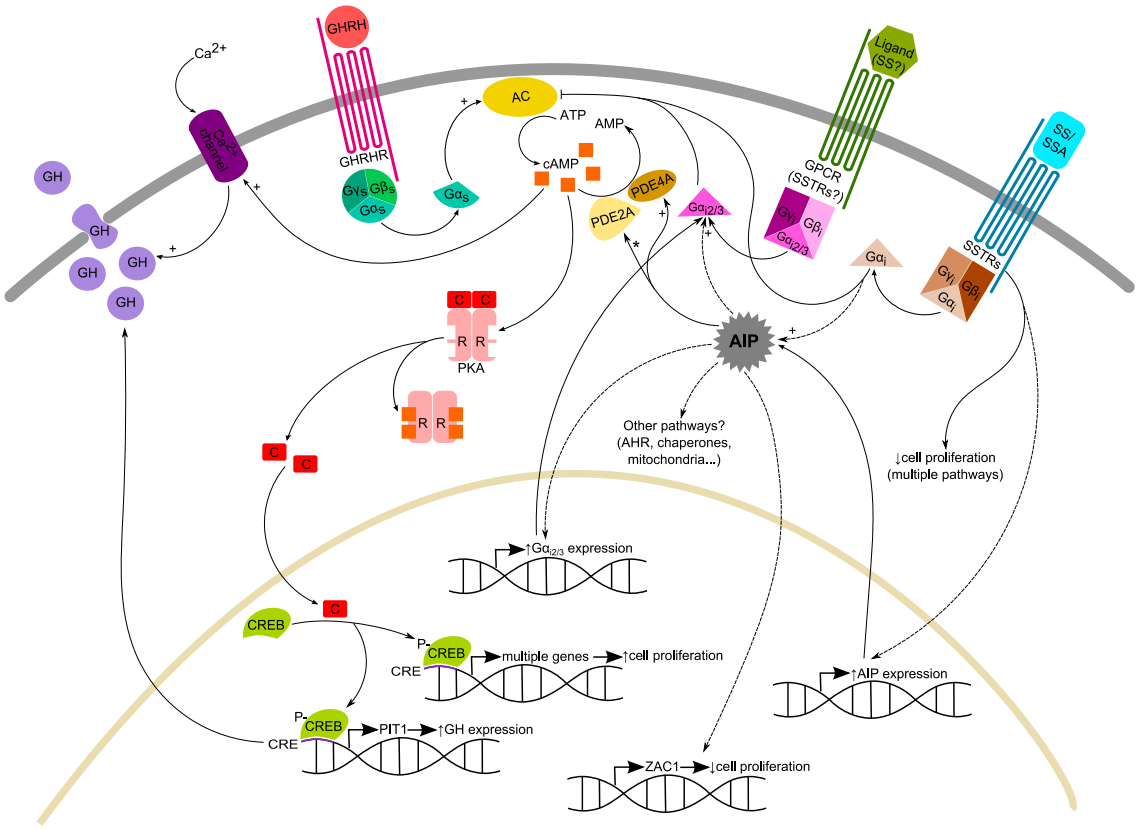

Figure 3. Summary of the proposed functions of AIP in the somatotroph cell. In response to GHRH, the GHRHR activates the cAMP pathway (via PKA) to increase GH expression and secretion and cell proliferation. In contrast, binding of SS to its receptors (mainly SSTR2 and 5) elicits multiple signalling cascades to control cell proliferation and GH expression and secretion. These effects are predominantly mediated by stimulatory G proteins in the case of GHRHR and by inhibitory G proteins for the SSTRs. AIP expression increases in response to SSTR activation, causing a rise in ZAC1 levels and therefore reduced cell proliferation and metabolism, although the signalling pathways involved in these responses remain elusive. AIP is also involved in controlling the expression and function of the inhibitory G protein subunits $G\alpha_{i2}$ and $G\alpha_{i3}$, but the mediators of these effects have not been elucidated as yet. $G\alpha_{i2}$ and $G\alpha_{i3}$ exert an inhibitory effect over AC, therefore inhibiting the cAMP pathway. The specific GPCR to which these subunits are associated in the somatotroph cells is unclear, although the SSTRs are good candidates. The AIP tumour suppressor activity could as well involve other signalling cascades, such as the AHR pathway, the HSP90 and HSP70 chaperone systems and the mitochondrial function, though this has not been studied in depth. The arrows indicate the direction of the signalling pathways, the stop ends indicate inactivation and the dashed lines indicate unknown signalling pathways; +, activation; *, molecular interaction with no functional consequence. See references in text.

Animal models of AIP deficiency

The first attempt to produce an *Aip* KO mouse model led to the discovery that this gene is necessary for embryonic development, as *Aip*$^{-/-}$ mice died *in utero* due to cardiovascular abnormalities (double-outlet right ventricle, ventricular septal defects and pericardial oedema) at the embryonic age of 10.5-14.5 days post coitum, while the *Aip*$^{+/-}$ genotype led to no apparent phenotype.[595] A hypomorphic murine model of *Aip* deficiency showed a phenotype similar to that of the *Ahr* KO mouse (patent *ductus venosus*), and the expression levels of Aip correlated with the frequency of the malformation, demonstrating that Aip is necessary for Ahr signalling during development.[596]

A mouse model with a heterozygous partial deletion of *Aip* presented pituitary adenoma predisposition, developing tumours of the *pars distalis* since the age of six months, with full penetrance by the age of 15 months. As in the human condition, the great majority of these mice (88%) developed somatotropinomas or mammosomatotroph adenomas, and a small percentage of them had prolactinomas and corticotropinomas; *AIP* LOH was detected in the tissues.[597] Some of the tumours were invasive, and in mice with GH-secreting adenomas, serum Igf-1 levels were elevated. The phenotype of this model differs from the human *AIP*mut-associated tumours in two main aspects: in mice, the disease develops in adulthood, in contrast with the young-onset of the human tumours, and the penetrance is full later in life, while in humans the penetrance remains low.[482]

Hemizygous KO (by partial deletion) of the *AIP* orthologue *CG1847* in a *D. melanogaster* model is lethal, and the phenotype can be rescued by the human WT *AIP* coding deoxyribonucleic acid sequence (CDS), but not by the CDS containing mutations that are disease-causative in humans. These results confirm the high degree of conservation of *AIP* among species and its importance of embryonic development in different species. Furthermore, this model has been proposed as a functional assay to test the pathogenicity of *AIP*muts.[598]

AIP as a pituitary-specific tumour suppressor: questions to be solved

The role of AIP as a tumour suppressor is supported by the association of multiple LOF mutations in this gene with the development of pituitary adenomas, as well as by the presence of LOH in 11q13 in pituitary adenomas from *AIP*mut positive FIPA patients.[9;10;479;496] Furthermore, *AIP,* like most of the tumour suppressor genes, is evolutionarily conserved among species,[15] and its overexpression slows down cell proliferation *in vitro,*[9] while *AIP* KD leads to increased cell proliferation.[599] As occurs with other tumour suppressor genes, *AIP* plays a role in early development: *AIP*-null mice and fruit flies are not viable.[595;596;598]

Considering that *AIP* is a tumour suppressor gene with ubiquitous expression, it would be expectable to find tumours in different organs in patients with germline *AIP*muts*.* Nevertheless, besides pituitary adenomas and a couple of cases of parathyroid adenomas,[499] no other tumour types have been consistently associated to germline *AIP*muts. Even more, the screening of a

large series of samples from different types of endocrine and non-endocrine cancer (colorectal, breast and prostate), revealed that neither germline nor somatic *AIP*muts are associated with these neoplasms.[600] Somatic mutations have not been found in pituitary adenomas either.[9;279] Therefore, pituitary tumorigenesis driven by *AIP*muts should be explained by a tumour suppressor function that is only biologically relevant for the pituitary gland, more specifically, for somatotroph cells, but not for other tissues. Overexpression of the mutant AIP p.R304* lacks the inhibitory effect of the WT protein over forskolin-stimulated cAMP response,[588] but if the final effect of AIP LOF is upregulation of the cAMP pathway, development of tumours in other cAMP-responsive tissues, as for example, the adrenal glands, would be expected in *AIP*mut carriers. Whether the AIP regulatory effect over the cAMP pathway is pituitary-specific, remains to be proven.

The LOF of AIP can occur through different mechanisms, which are not mutually exclusive. Truncating mutations, with partial or total loss of the three TPR repeats and the final α-7 helix that constitute the TPR domain of the protein, are expected to lead to unstable or non-existent proteins, with lost of molecular interactions,[523] but the occurrence of NMD is also possible. Experimental mutagenesis has proven that mutations affecting the C-terminal α-helix of AIP disrupt the interaction between AIP and some of its molecular partners, thus, the lack of function of this domain seems to be sufficient for pituitary adenoma predisposition.[523] A large percentage of the patients with *AIP*mut-related pituitary adenomas bear mutations affecting the C-terminal α-7 helix of the protein, and the repertoire of molecular partners binding AIP at this level could determine both the mechanism for tumorigenesis as well the pituitary-specific pathogenicity of such mutations. Nevertheless, even in the presence of a non-functional protein, it is difficult to determine if the loss of a specific interaction could explain the tumorigenic mechanism of *AIP*muts, as AIP interacts with a large number of independent proteins, including three different chaperone systems: HSP90, HSP70 and TOMM20.[523]

*AIP*muts, in combination with LOH in the tumour would theoretically lead to complete absence of AIP in the tissue, and in fact, in most of the *AIPmut* positive patients, AIP expression is reduced at the level of both mRNA and protein, correlating with invasiveness.[481] However, several questions remain to be answered regarding the “second hit” in *AIP*mut-associated pituitary tumours. On the one hand, LOH is not a universal finding in these tissues,[9;10] meaning that posttranscriptional mechanisms, as for example miR-34a,[235] could also be implicated, as it has been described for MEN1.[316] On the other hand, the extension of the LOH necessary to produce pituitary adenomas in these patients is not clear. In most of the cases the affected chromosomal region includes the loci for both *AIP* and *MEN1*,[601] and the combined loss of these genes could be relevant for their tumour suppressor effects. For example, combined deletion of *MEN1* and *AIP* is essential for the development of hibernomas, a rare type of brown fat tumour.[602] Nevertheless, some *AIP*mut positive pituitary adenomas display loss of only the *AIP* locus.

The comprehensive study of the clinical features of large numbers of cases of *AIP*mut-associated pituitary adenomas, in combination with studies assessing the normal molecular function of AIP in the pituitary in detail, and determining how *AIP*muts can disrupt this function, should hopefully contribute to solve these questions.

Chapter 2: The clinical and genetic landscape of familial isolated and young-onset sporadic pituitary adenomas: prospective identification of clinical disease in *AIP* mutation positive family members

Introduction

FIPA is a heterogeneous condition, encompassing cases with unknown genetic cause and patients with mutations in the *AIP* gene, with distinctive clinical characteristics, as well as the patients with the novel entity X-LAG. The phenotype of *AIP*mut-associated pituitary adenomas has been described before,[9-11;484] but a systematic follow-up of cases and families is lacking, due to the relative novelty of this pathogenic association,[8] the variable disease penetrance[10;11;480;506] and the rarity of this clinical entity. The association of *AIP*muts with pituitary tumorigenesis is relatively recent,[8] therefore there are no data available describing the clinical behaviour of this entity in the long term. The follow-up of *AIP*mut positive carriers has been described only in one FIPA family,[603] demonstrating the usefulness of clinical screening for early diagnosis and opportune treatment, but this approach has never been applied in a larger population.

Screening for *AIP*muts is not part of the routine clinical investigations done in pituitary adenoma patients in most of the centres, and because most of the case series reported in the literature include small numbers of patients, it is unlikely that they have described the whole spectrum of the disease. This has also precluded the analysis of other important features, such as possible phenotype-genotype associations, the possible influence of disease-modifying genes, complications of pituitary adenomas, other associated clinical features, and causes of death in this population. Trying to fill gaps in the knowledge about the genetic and clinical features of this rare disease, a large cohort of FIPA and *simplex* (patients with germline mutation and no family history) *AIP*mut positive patients has been studied.

Aims

General

- To confirm and extend the description of the genotype and phenotype of patients with *AIP*mut-related familial and *simplex* pituitary adenomas in a large cohort of pituitary adenoma patients, providing a comparison with *AIP*mut negative cases, and to perform a systematic follow-up of families to identify and characterise *AIP*mut positive carriers.

Specific

1. To investigate a possible genotype-phenotype association for the *AIP*muts detected in the study population.

2. To describe and compare the following features between *AIP*mut positive and negative patients from a familial and a *simplex* cohort:
    a. Frequency of specific diagnoses.
    b. Age at disease onset and at diagnosis.
    c. Tumour size and invasiveness.
    d. IHC.
    e. Apoplexy of the pituitary adenoma.
3. To calculate the penetrance of pituitary adenomas among members of *AIP*mut positive FIPA families.
4. To identify differences in the clinical presentation between *AIP*mut positive and negative patients with GH-secreting tumours and in the subset of patients with gigantism.
5. To investigate the role of two possible disease-modifying genes (*GNAS1* and *FGFR4*) on the variable phenotype and penetrance of the disease.
6. To analyse the results of the clinical screening and follow-up of *AIP*mut positive apparently unaffected individuals and to identify the characteristics of prospectively diagnosed *AIP*mut positive pituitary adenoma cases.

Hypotheses

1. In *AIP*mut positive patients, the type (truncating or non-truncating) or localisation (in the gene) of the mutation has an effect on the pituitary adenoma phenotype.
2. *AIP*mut positive patients have a well-defined phenotype, while *AIP*mut negative patients are a heterogeneous group.
3. Pituitary adenomas develop and are diagnosed earlier in life in *AIP*mut positive, compared to *AIP*mut negative patients.

Methods

Patients and carriers

Our study population (1725 subjects) was recruited via the collaborative research network of the International FIPA Consortium.[604] Between January 2007 and January 2014, we recruited patients from 35 countries from two different groups: either members of FIPA families, defined by the presence of pituitary adenomas in two or more members of a family without other associated clinical features[8;9;272;484] ('familial' cohort), or sporadically diagnosed pituitary adenoma patients with disease onset at ≤30 years of age ('sporadic' cohort). As an exception to these inclusion criteria, one *AIP*mut positive >30 years sporadic patient was found thanks to *AIP* screening in the setting of a research study, and the screening of his relatives detected a second *AIP*mut positive pituitary adenoma case; this family was included in the familial cohort. The first patient reported in each FIPA family and all the sporadic patients were considered 'probands'.

Pituitary adenoma patients were grouped into 11 clinical diagnostic categories, as listed in Table 5. The diagnoses of acromegaly, acromegaly/prolactinoma, gigantism, gigantism/ prolactinoma, and mild acromegaly[605] were grouped together under the category of 'GH excess' for some analyses.

Table 5. Definition of the clinical diagnostic categories used in the study

Diagnosis		Criteria
Cushing's disease		Evidence of ACTH-depending hypercortisolaemia with proven pituitary adenoma, in accordance to the diagnostic protocol of each institution
Clinically functioning FSH-secreting pituitary adenoma (FSHoma)		Raised serum FSH levels for age and gender and evidence of gonadal stimulation in a patient with a pituitary adenoma
GH excess	Acromegaly	Raised IGF-1 levels and unsuppressed GH during an OGTT, with cut-offs according to the protocol of each institution
	Acromegaly/prolactinoma	Diagnosis of acromegaly with concurrent hyperprolactinaemia
	Mild acromegaly*	Mild clinical features attributed to acromegaly, fulfilling the criterion of raised IGF-1 levels but not the lack of suppression of GH during an OGTT, or normal IGF-1 but lack of suppression of GH during an OGTT[605]
	Gigantism	Any of the following categories in a patient with a pituitary adenoma: (i) abnormally high growth velocity in children or teenagers with abnormal IGF-1 and OGTT, (ii) height >3SD above the mean height for age, (iii) >2SD over the calculated midparental height, using country-specific growth charts when possible
	Gigantism/prolactinoma	Diagnosis of gigantism with concurrent hyperprolactinaemia
Clinically non-functioning pituitary adenoma (NFPA)		Pituitary adenoma in the absence of clinical or biochemical evidence of pituitary hypersecretion
Pituitary tumour		Cases of pituitary tumour where the diagnosis could not be specified, due to unavailability of histopathological specimens, clinical and/or biochemical data
Prolactinoma		Hyperprolactinaemia in the presence of a pituitary adenoma and unlikely to be purely due to a stalk effect, based on either histopathology results or the relation between PRL levels and tumour size
Thyrotropinoma		Hyperthyrotropinaemia in a patient with a pituitary adenoma, with clinical and/or biochemical hyperthyroidism and no other demonstrable causes of raised TSH
* This category is important in our study, as we detected acromegaly via biochemical screening of *AIP*mut positive carriers, often not presented (yet) clinically.		

All the patients received treatment and were followed up in accordance with the guidelines and clinical criteria of their respective centres. Relevant clinical and family structure data were received from clinicians and/or patients, and genetic screening was performed in the families of all the *AIP*mut positive probands, selecting individuals according to their risk of inheriting the mutation, based on their position in the family tree, and extending the screening to as many generations as possible. In both familial and sporadic cases, other causes of familial pituitary adenomas, such as MEN1 and 4, CNC, phaeochromocytoma/paraganglioma and pituitary adenoma syndrome and X-linked acrogigantism were ruled out by clinical, biochemical and, in some cases, genetic tests, as appropriate.

The study population included a great majority of new cases, but also previously diagnosed patients being followed up by the participating centres and a few historical cases, corresponding to deceased members of FIPA families. Four *AIP*mut positive patients (two with diagnosis of acromegaly and two with gigantism) died in the post-recruitment period. Three of the deaths

were due to cardiovascular causes (stroke, chronic heart failure and acute coronary syndrome), while the exact cause of death is unknown in the fourth case, a patient with long-standing untreated familial acromegaly.

At the recruitment, relevant clinical and biochemical data were collected at each participating centre and all the information was entered into our central database. Data about the follow-up, treatments and current status of the patients were prospectively requested and collected from the collaborating centres and directly from the patients. Data about the historical cases were collected from family members and from hospital archives, when available. With a few exceptions, genetic screening results were directly sent to our centre and entered in the database. The available data did not allow a comprehensive analysis of the response to specific therapeutic modalities.

We identified subjects 'at risk' (those with the possibility of inheriting an *AIP*mut)*, '*obligate carriers' (based on their position in family tree, *AIP*muts were verified when possible) and 'unaffected carriers'. Therefore, in our analysis the term 'unaffected carrier' includes all the relatives of *AIP*mut positive patients without clinical manifestations of a pituitary adenoma and with either a genetic screening positive for the *AIP*mut present in the proband or with a position in the family tree defining them as 'obligate carriers'*.* In addition, the analysis of the family trees led to the identification of some affected individuals as 'predicted *AIP*mut positive patients', defined as individuals with an established clinical diagnosis of pituitary adenoma in whom the genetic screening could not be carried out due to unavailability of a DNA sample, but in whom the presence of the mutation was assumed based on both the phenotype and the position in the family tree. Therefore, the term '*AIP*mut positive patient' will refer to both 'predicted *AIP*mut positive patients' and '*AIP*mut positive patients' in whom the presence of the mutation was verified. Subjects 'not at risk' of inheriting an *AIP*mut were defined based on their position in the family tree. In the sporadic cohort, the *AIP*mut positive patients with no apparent familial history of pituitary disease were also referred as '*simplex'* cases as they can be considered the first case of a potentially hereditary disease. All the patients and family members included agreed to take part by providing signed informed consent forms approved by the local Ethics Committee.

Genetic screening

Pituitary adenoma patients and their apparently unaffected relatives were screened for *AIP*muts using Sanger sequencing and MLPA. Genomic DNA was obtained from blood (Ilustra DNA Extraction Kit BACC2, GE Healthcare, Little Chalfont, UK) or saliva (Oragene-DNA [collection] and prepIT-L2P [extraction] kits, DNA Genotek, Ontario, Canada) samples. The detection of the *AIP* gene variants and dosage was performed at the Molecular Genetics Laboratory, Royal Devon and Exeter, NHS Foundation Trust for the great majority of the samples, as previously described.[9;10] Although the genetic tests were performed in one of the largest Genetics laboratories in the world, with appropriate quality controls, we cannot rule out that mutations were not identified in a small number of cases, due to either technical problems or due to

location of mutations in areas not analysed (such as intronic regions). The pathogenicity of the detected variants was assessed using the Pathogenic Or Not-Pipeline (PON-P) and Alamut 2.2.1 *in silico* prediction programs, as well as considering the scientific literature concerning clinical and experimental data on the previously reported variants. We have divided the *AIP* variants into 5 classes according to the likelihood of pathogenicity, as recommended by Plon *et al*.:[606] definitely pathogenic, likely pathogenic, uncertain, unlikely pathogenic and not pathogenic. Only those variants considered as definitely or likely pathogenic[606] were included in the study. Additionally, we included one novel intronic variant with no experimental data available, for which the prediction software could not exclude pathogenicity. The variants described in this paper are listed by their position in the DNA, with the corresponding change at the protein level in parentheses, according to the nomenclature guidelines of the Human Genome Variation Society (HGVS) version 1.0[607] and the changes proposed for the version 2.0.[608] The nomenclature was verified using the Mutalyzer 2.0.beta-21 software.[609] The positions in the DNA are based on the GRCh37/hg19 assembly of the human genome and the human *AIP* reference sequence (Locus Reference Genomic code LRG_460,[503] based on NG_008969.1 and NM_003977.3). All the unaffected individuals with positive genetic screening for *AIP*muts were advised to undergo clinical, biochemical and image screening tests for the early diagnosis of possible pituitary disease, on an annual basis or as appropriate. The recommendations for screening were based on the published experience of our group[610] and others.[482]

Additional genetic tests were performed in subjects with no pituitary adenomas, but with other clinical features indicative of such tests (screening for mutations in *BRCA1* and *2* and *TP53* was performed in members of a family with breast cancer, osteosarcoma and a neuroendocrine tumour of the colon), as well as and in a randomly selected cohort of *AIP*mut negative FIPA probands, searching for mutations in other genes via direct sequencing and MLPA (*BRCA1* and *2*, *CDKN1B, MEN1, TP53, PRKAR1A)* or via a next-generation sequencing panel *(MAX, RET, SDHA, SDHAF2, SDHB, SDHC, SDHD, TMEM127,* and *VHL).*[611] Array comparative genomic hybridization analysis was performed in a group of patients with gigantism, and patients positive for Xq26 microduplications[91] were excluded from further analysis.

Disease-modifying genes

Genomic DNA (gDNA) samples from 98 *AIP*mut positive patients (55 males/43 females) and 108 unaffected *AIP*mut carriers (56 males/52 females) were subjected to polymerase chain reaction (PCR), and screened for the *FGFR4* p.G388R (rs351855) SNP, using 100 ng of each DNA sample and previously described primers: [612]

FGFR4ex9_F: 5'-GACCGCAGCAGCGCCCGAGGCCAG-3'
FGFR4ex9_R2: 5'-AGAGGGAAGCGGGAGAGCTTCTG-3'

The PCR reactions were prepared as described in Protocol 1 and ran in a thermal cycler, using the following program:

One cycle:
95°C 2 minutes (min)
35 cycles:
95°C 15 seconds (sec)
67°C 15 sec
68°C 20 sec
One cycle:
68°C 5 min
10°C Hold

Ten microliters of each PCR product (168 bp) were resolved in a 3% agarose gel, as presented in Figure 4.

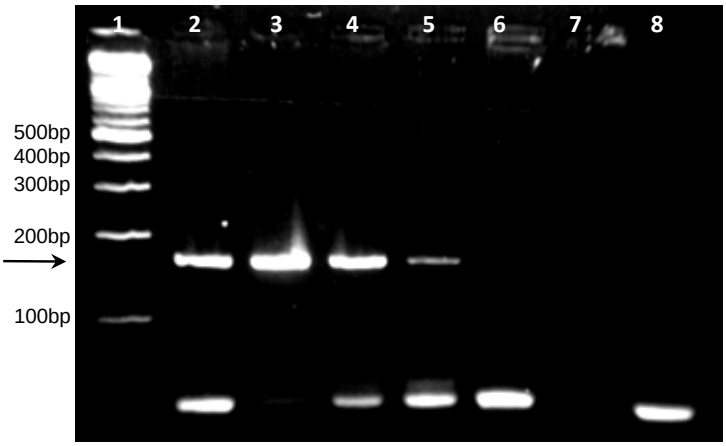

Figure 4. Example of *FGFR4* PCR. Lane 1: DNA ladder (GeneRuler,Life Technologies SM0241), lanes 2-6: samples (sample in lane 6 did not amplify), lane 7: empty, lane 8: negative control. Arrow: expected PCR product (168 bp). The lower bands appearing in some samples correspond to primer dimers.

In addition, gDNA was extracted from paraffin-embedded somatotropinomas for 23 *AIP*mut positive patients (familial and simplex), ten *AIP*mut negative FIPA patients and six *AIP*mut negative sporadic patients and cDNA was obtained from 19 frozen somatotropinomas from unselected acromegaly cases (control group, 13 males/6 females, age at diagnosis 37-77 years) as detailed in Protocol 2. All these samples were screened for mutations in the *GNAS1* codons 201 and 227 using 100 ng of each DNA sample and previously described primers for gDNA:[613]

GNAS1201_F: 5'- CCAAACTACTCCAGACCTTT-3'
GNAS1201_R: 5'- TGGAAGTTGACTTTGTCCAC-3'
GNAS1227_F: 5'- ACAGAGATCATGGTTTCTTG-3'
GNAS1227_R: 5'- TTAACCAAAGAGAGCAAAGC-3'

The primers used for cDNA were available in the laboratory stocks, and the resulting PCR product contains both codons 201 and 227:

GNAS1_F: 5'-CAAGCAGGCTGACTATGTGC-3'
GNAS1_R: 5'-ACCACGAAGATGATGGCAGT-3'

The PCR reactions with each pair of primers were prepared as described in Protocol 1 and processed in a thermal cycler, using the following program for the three pairs of primers:

One cycle:
95°C 2 min
35 cycles:
95°C 15 sec
60°C 15 sec
68°C 20 sec
One cycle:
68°C 5 min
10°C Hold

Ten microliters of each of the PCR products (164 bp for GNAS1 201 PCR, 232 bp for GNAS1 227 PCR and 189 bp for GNAS1 201 and 227 PCR from cDNA) were resolved in a 3% agarose gel, as presented in Figure 5.

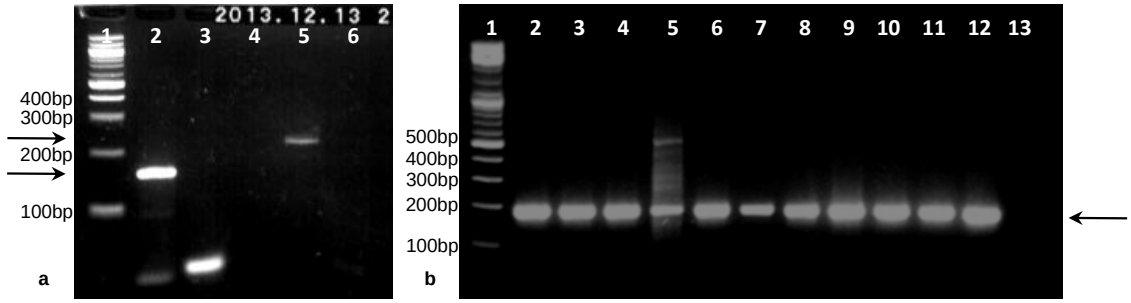

Figure 5. Examples of PCR for *GNAS1* genotyping. a) PCR products for *GNAS1* 201 and 227 PCR reactions. Lane 1: DNA ladder (GeneRuler,Life Technologies SM0241), lane 2: sample amplified for *GNAS1* 201, lane 3: negative control for GNAS1 201, lane 4: empty, lane 5: sample amplified for *GNAS1* 227, lane 6: negative control for *GNAS1* 227. Top arrow: expected PCR product for *GNAS1* 227 (232 bp); bottom arrow: expected PCR product for *GNAS1* 201 (164 bp). b) PCR products for *GNAS1* PCR reaction from cDNA. Lane 1: DNA ladder (GeneRuler,Life Technologies SM0241), lanes 2-12: samples, lane 13: negative control. Arrow: expected PCR product (189 bp) Sample in lane 5 presented non-specific amplification; the 189bp band was cut and purified before sequencing.

The sequence analysis of the *FGFR4* and *GNAS1* PCR products was carried out by Sanger sequencing (BigDye Terminator v. 3.1 kit in and ABI 3730 capillary sequencer, Applied Biosystems, Foster City, CA, USA) at the Genome Centre sequencing facility (Barts and The London School of Medicine). The obtained chromatograms were aligned against the GenBank

reference sequences NM_000516.4 (*GNAS1* variant 1 mRNA) and NG_012067 (*FGFR4* gDNA).

Statistical analysis

The qualitative, categorical variables were expressed as percentages and compared using the chi-squared test or the Fisher's exact test, as appropriate. The normal distribution of the quantitative variables was verified using the Shapiro-Wilk and the Kolmogorov-Smirnov tests for normality. Means and standard deviations were used to report parametric data, and non-parametric data were expressed as median and interquartile ranges. Parametric data were analysed with the unpaired t-test, with a 95% confidence interval, while the Mann-Whitney U test was used for the non-parametric data. Statistical significance was considered when the *P* value (*P*) was <0.05. All the statistical analyses were carried out using the GraphPad Prism 6 (GraphPad Software Inc.) and Stata 12 (StataCorp LP) statistical software.

Results

Study population

Table 6. Study population: demographics and general description

	Familial cohort	Sporadic cohort	Combined
Total individuals, no. (%)	1231 (71.4)	494 (28.6)	1725 (100)
Females, no. (%)	668 (54.3)	250 (50.6)	918 (53.2)
Current age, median (range, [IQR])	46.2 (2-97 [32-62])	35 (3-77 [26-42])	42.6 (2-97 [29-56])
Clinical status, no. (%):			
Affected	502 (40.8)	404 (81.8)	906 (52.5)
Unaffected	729 (59.2)	90 (18.2)	819 (47.5)
Affected males, no. (%)	219 (43.6)	203 (50.2)	422 (46.6)
Affected females, no. (%)	283 (56.4)	201 (49.8)	484 (53.4)
Diagnoses, no. (%):			
Acromegaly	170 (33.9)	203 (50.2)	373 (41.2)
Acromegaly/prolactinoma	17 (3.4)	12 (3)	29 (3.2)
Cushing's disease	24 (4.8)	21 (5.2)	45 (5)
FSH-secreting adenoma	2 (0.4)	1 (0.2)	3 (0.3)
Gigantism	44 (8.8)	65 (16.1)	109 (12)
Gigantism/prolactinoma	1 (0.2)	10 (2.5)	11 (1.2)
Mild acromegaly	2 (0.4)	-	2 (0.2)
NFPA	91 (18.1)	21 (5.2)	112 (12.4)
Pituitary tumour	17 (3.4)	2 (0.5)	19 (2.1)
Prolactinoma	134 (26.7)	67 (16.6)	201 (22.2)
Thyrotropinoma	-	2 (0.5)	2 (0.2)
GH excess patients, no. (%)	234 (46.6)	290 (71.8)	524 (57.8)
IQR: interquartile range.			

The familial cohort was composed of 216 FIPA families, including 156 new families (989 subjects: 337 patients and 652 unaffected family members) and 60 previously described families where 46 new subjects (15 patients and 31 unaffected family members) were added to the previously reported 196 individuals (150 patients and 46 unaffected family members, Table 6).[9;10]

The sporadic cohort originally included 409 pituitary adenoma patients ≤30 years old at disease onset, with no known familial history of pituitary adenoma, but five of these patients were excluded from further analysis due to harbouring Xq26.3 microduplications. Of the remaining 404 sporadic patients, six were reported previously.[9] In addition to the *AIP*mut screening, a subset of *AIP*mut negative FIPA (n=55) and sporadic (n=45) patients underwent genetic screening for other endocrine neoplasia-associated genes (Table 7). All of these tests were negative for pathogenic variants. After the genetic screening and follow-up of the patients and carriers, 60 individuals in the familial cohort and seven in the sporadic cohort were classified as 'not at risk' of inheriting an *AIP*mut, and were excluded from further analysis. Twenty three individuals initially thought to be unaffected were identified with pituitary abnormalities (see details in the 'Prospective diagnosis' section).

Table 7. Other genes tested

	Familial cohort			**Sporadic cohort**			**Combined, no. (%)**
	***AIP*mut positive, no. (%)**	***AIP*mut negative, no. (%)**	**Total familial, no. (%)**	***AIP*mut positive, no. (%)**	***AIP*mut negative, no. (%)**	**Total sporadic, no. (%)**	
BRCA1	1 (14.3)	2 (0.7)	3 (1)	-	-	-	3 (0.8)
BRCA2	1 (14.3)	2 (0.7)	3 (1)	-	-	-	3 (0.8)
CDKN1B	-	20 (6.5)	20 (6.4)	-	1 (2.4)	1 (2.4)	21 (5.9)
GPR101	-	-	-	-	8 (19)	8 (19)	8 (2.2)
MAX	-	23 (7.5)	23 (7.3)	-	-	-	23 (6.5)
MEN1	3 (42.9)	51 (16.6)	54 (17.2)	-	33 (78.6)	33 (78.6)	87 (24.4)
PRKAR1A	-	23 (7.5)	23 (7.3)	-	-	-	23 (6.5)
RET	-	23 (7.5)	23 (7.3)	-	-	-	23 (6.5)
SDHA	-	23 (7.5)	23 (7.3)	-	-	-	23 (6.5)
SDHAF2	-	23 (7.5)	23 (7.3)	-	-	-	23 (6.5)
SDHB	-	23 (7.5)	23 (7.3)	-	-	-	23 (6.5)
SDHC	-	23 (7.5)	23 (7.3)	-	-	-	23 (6.5)
SDHD	-	25 (8.1)	25 (8)	-	-	-	25 (7)
TMEM127	-	23 (7.5)	23 (7.3)	-	-	-	23 (6.5)
TP53	2 (28.6)	-	2 (0.6)	-	-	-	2 (0.6)
VHL	-	23 (7.5)	23 (7.3)	-	-	-	23 (6.5)
Total	7	307	314	0	42	42	712

Table 8. Screening for *AIP* mutations

	Familial cohort			Sporadic cohort			Combined		
	*AIP*mut positive familial	*AIP*mut negative familial	Total familial	*AIP*mut positive *simplex*	*AIP*mut negative sporadic	Total sporadic	*AIP*mut positive familial and *simplex*	*AIP*mut negative familial and sporadic	Total
Total number of kindreds, no (%)	37 (17.1% of familial)	179 (82.9% of familial)	216 (34.8% of total)	34 (8.4% of sporadic)	370 (91.6% of sporadic)	404 (65.2% of total)	71 (11.5% of total)	549 (88.5% of total)	620 (100)
Total individuals, no. (%):	475 (38.6% of familial)	756 (61.4% of familial)	1231 (71.4% of total)	82 (16.6% of sporadic)	412 (83.4% of sporadic)	494 (28.6% of total)	557 (32.3% of total)	1168 (67.7% of total)	1725 (100)
Genetic status, no. (%):									
*AIP*mut negative patients	3 (0.6)	389 (51.5)*	392 (31.8)	-	370 (89.8)	370 (74.9)	3 (0.5)	759 (65)	762 (44.2)
*AIP*mut positive tested patients	95 (20)	-	95 (7.7)	34 (41.5)	-	34 (6.9)	129 (23.2)	-	129 (7.5)
At risk, but not tested	33 (6.9)	-	33 (2.7)	8 (9.8)	-	8 (1.6)	41 (7.4)	-	41 (2.4)
Not at risk	48 (10.1)	12 (1.6)	60 (4.9)	7 (8.5)	-	7 (1.4)	55 (9.9)	12 (1)	67 (3.9)
Obligate unaffected carriers, not tested	8 (1.7)	-	8 (0.6)	2 (2.4)	-	2 (0.4)	10 (1.8)	-	10 (0.6)
Predicted *AIP*mut positive patients	15 (3.2)	-	15 (1.2)	-	-	-	15 (2.7)	-	15 (0.9)
Unaffected *AIP*mut tested carriers	120 (25.3)	-	120 (9.7)	16 (19.5)	-	16 (3.2)	136 (24.4)	-	136 (7.9)
Unaffected and *AIP*mut negative	153 (32.2)	-	153 (12.4)	15 (18.3)	-	15 (3)	168 (30.2)	-	168 (9.7)
Unaffected relatives of *AIP*mut negative patients	-	355 (47)	355 (28.8)	-	42 (10.2)	42 (8.5)	-	397 (34)	397 (23)
Summary of *AIP*mut positive individuals, no. (%):									
Total *AIP*mut positive patients:†	110 (23.2)	-	110 (8.9)	34 (41.5)	-	34 (6.9)	144 (25.9)	-	144 (8.3)
Total unaffected *AIP*mut carriers:‡	128 (26.9)	-	128 (10.4)	18 (22)	-	18 (3.6)	146 (26.2)	-	146 (8.5)

* In *AIP*mut negative FIPA families, 199 patients were tested for *AIP*muts, the rest (n=190) were assumed to be negative.
†This is equal to the sum of tested *AIP*mut positive patients plus the predicted *AIP*mut positive patients.
‡ Sum of tested unaffected carriers plus obligate unaffected carriers.

Genetic screening results

Thirty-seven (17.1%) out of 216 FIPA families screened and 34 out of 404 sporadic patients (8.4%) were positive for pathogenic or likely pathogenic *AIP*muts, accounting for a total of 71 *AIP*mut positive kindreds and 144 *AIP*mut positive patients (76.4% familial and 23.6% *simplex*, Table 8). We also identified 164 *AIP*mut positive apparently unaffected family members (see 'Follow-up and prospective diagnosis'). Samples were not available from family members of 25 *AIP*mut positive *simplex* cases to establish the presence or lack of *de novo* mutations. We identified three pituitary adenoma patients (two with clinically NFPA and one with a microprolactinoma) belonging to *AIP*mut positive FIPA families and being 'at risk' of inheriting, but not carrying an *AIP*mut, therefore they were considered as phenocopies.

Thirty-one different AIPmuts (ten not previously reported) were identified in our study population: 12 exclusively in familial cases, 12 in *simplex* cases only and seven in both settings (Table 9 and Figure 6). Of the total mutations, 70.8% (22/31) predicted a truncated or missing protein, and were termed as 'truncating *AIP*muts' (Figure 7). There were no exclusive associations of specific *AIP*muts with particular diagnoses. However, 77.4% of all the mutations (24/31) were found in cases of gigantism (with or without prolactin (PRL) co-secretion), being this the diagnosis with the highest number of associated *AIP*muts. Furthermore, all the mutations were found in at least one patient with GH excess, supporting this diagnostic category as the most frequent *AIP*mut pathogenic association. Patients with diagnosis of NFPA harboured 29% (9/31) of the *AIP*muts found in the study, and 22.6% of them (7/31) were detected in prolactinoma cases. As expected based on previous data,[482;614] the commonest mutation in both cohorts was c.910C>T (p.R304*), found in 33.3% of the *AIP*mut patients and in 35.9% of all the *AIP*mut positive individuals (affected plus unaffected carriers).

Table 9. *AIP* pathogenic or likely pathogenic mutations in familial and *simplex* cohorts

Mutation (DNA level [protein level])	Mutation type	Pathogenic	Location in protein	Familial cohort (n=238)*	Sporadic cohort (n=52)*	Combined (n=290)*	References
g.4856_4857CG>AA	Promoter	Yes†	Not in protein (5' UTR)	3 (1.3)	-	3 (1)	9;10;496
c.3G>A (p.?)	Start codon	Likely†	N-terminus	2 (0.8)	-	2 (0.7)	This thesis
c.40C>T (p.Q14*)	Nonsense	Yes†	N-terminus	2 (0.8)	-	2 (0.7)	8;615;616
c.70G>T (p.E24*)	Nonsense	Yes†	N-terminus	9 (3.8)	-	9 (3.1)	9;495
c.74_81delins7 (p.L25Pfs*130)	Frameshift	Yes†	PPIase domain	10 (4.2)	-	10 (3.4)	10;617
c.100-1025_279+357del (ex2del) (p.A34_K93del)	Large genomic deletion	Yes†	PPIase domain	12 (5)	2 (4)	14 (4.8)	618
c.100-18C>T	Intronic	Likely	Not in protein (intron 1)	-	3 (6)	3 (1)	7;9;14;615
c.241C>T (p.R81*)	Nonsense	Yes†	PPIase domain	12 (5)	4 (8)	16 (5.5)	9;496;590;619;620
c.249G>T	Splice site	Yes†	PPIase	4 (1.7)	-	4 (1.4)	10

Mutation (DNA level [protein level])	Mutation type	Pathogenic	Location in protein	Familial cohort (n=238)*	Sporadic cohort (n=52)*	Combined (n=290)*	References
(p.G83Afs*15)	(cryptic splice site)		domain				
c.338_341dup (p.L115Pfs*16)	Frameshift	Yes†	PPIase domain	-	2 (4)	2 (0.7)	6
c.427C>T (p.Q143*)	Nonsense	Yes†	Between PPIase and TPR1 domains	-	1 (2)	1 (0.3)	This thesis
c.469-2A>G (p.E158_Q184del)	Splice site	Likely	TPR1 domain	-	1 (2)	1 (0.3)	12;13;621
c.490C>T (p.Q164*)	Nonsense	Yes†	Between PPIase and TPR1 domains	3 (1.3)	-	3 (1)	10
c.570C>G (p.Y190*)	Nonsense	Yes†	TPR1 domain	9 (3.8)	-	9 (3.1)	This thesis
c.662dupC (p.E222*)	Nonsense	Yes†	Between TPR1 and 2 domains	3 (1.3)	-	3 (1)	10
c.713G>A (p.C238Y)	Missense	Yes	TPR2 domain	4 (1.7)	-	4 (1.4)	9;495
c.783C>G (p.Y261*)	Nonsense	Yes†	TPR2 domain	4 (1.7)	-	4 (1.4)	13;498;622;623
c.787+9C>T	Intronic	Uncertain	Not in protein (intron 5)	-	1 (2)	1 (0.3)	This thesis
c.804C>A (p.Y268*)	Nonsense	Yes†	TPR3 domain	19 (8)	3 (6)	22 (7.6)	624;625
c.805_825dup (p.F269_H275dup)	In-frame insertion	Yes	TPR3 domain	16 (6.7)	2 (4)	18 (6.2)	9;13;496;626
c.807C>T (p.(=))	Splice site (reduced transcript level)	Yes	TPR3 domain	7 (2.9)	4 (8)	11 (3.8)	7;9;10;12;14;627;628
c.811C>T (p.R271W)	Missense	Yes	TPR3 domain	-	1 (2)	1 (0.3)	7;10;484;629
c.816delC (p.K273Rfs*30)	Frameshift	Yes†	TPR3 domain	-	1 (2)	1 (0.3)	This thesis
c.868A>T (p.K290*)	Nonsense	Yes†	TPR3 domain	-	1 (2)	1 (0.3)	This thesis
c.872_877delTGCTGG (p.V291_L292del)	In-frame deletion	Yes	TPR3 domain	-	1 (2)	1 (0.3)	This thesis
c.910C>T (p.R304*)	Nonsense	Yes†	C-terminal α-helix	88 (37)	16 (31)	104 (35.9)	7-10;12;13;484;498;506;507;630;631
c.911G>A (p.R304Q)	Missense	Yes	C-terminal α-helix	20 (8.4)	3 (6)	23 (7.9)	7;7;9;10;12;13;13;498;539;615;632
c.967delC (p.R323Gfs*39)	Frameshift	Yes†	C-terminal α-helix	-	4 (8)	4 (1.4)	This thesis
c.976_977insC (p.G326Afs*?)	Frameshift	Yes†	C-terminal α-helix	-	1 (2)	1 (0.3)	This thesis
c.978dupG (p.I327Dfs*?)	Frameshift	Yes†	C-terminal α-helix	-	1 (2)	1 (0.3)	This thesis
c.1-?_993+?del- (whole gene deletion)	Large genomic deletion	Yes†	Absence of the whole protein	11 (4.6)	-	11 (3.8)	10

* Number of positive individuals for each mutation, considering the *AIP*mut positive tested individuals, the obligate carriers and the predicted *AIP*mut patients. † Truncating mutation.
PPIase, peptidylprolyl isomerase.

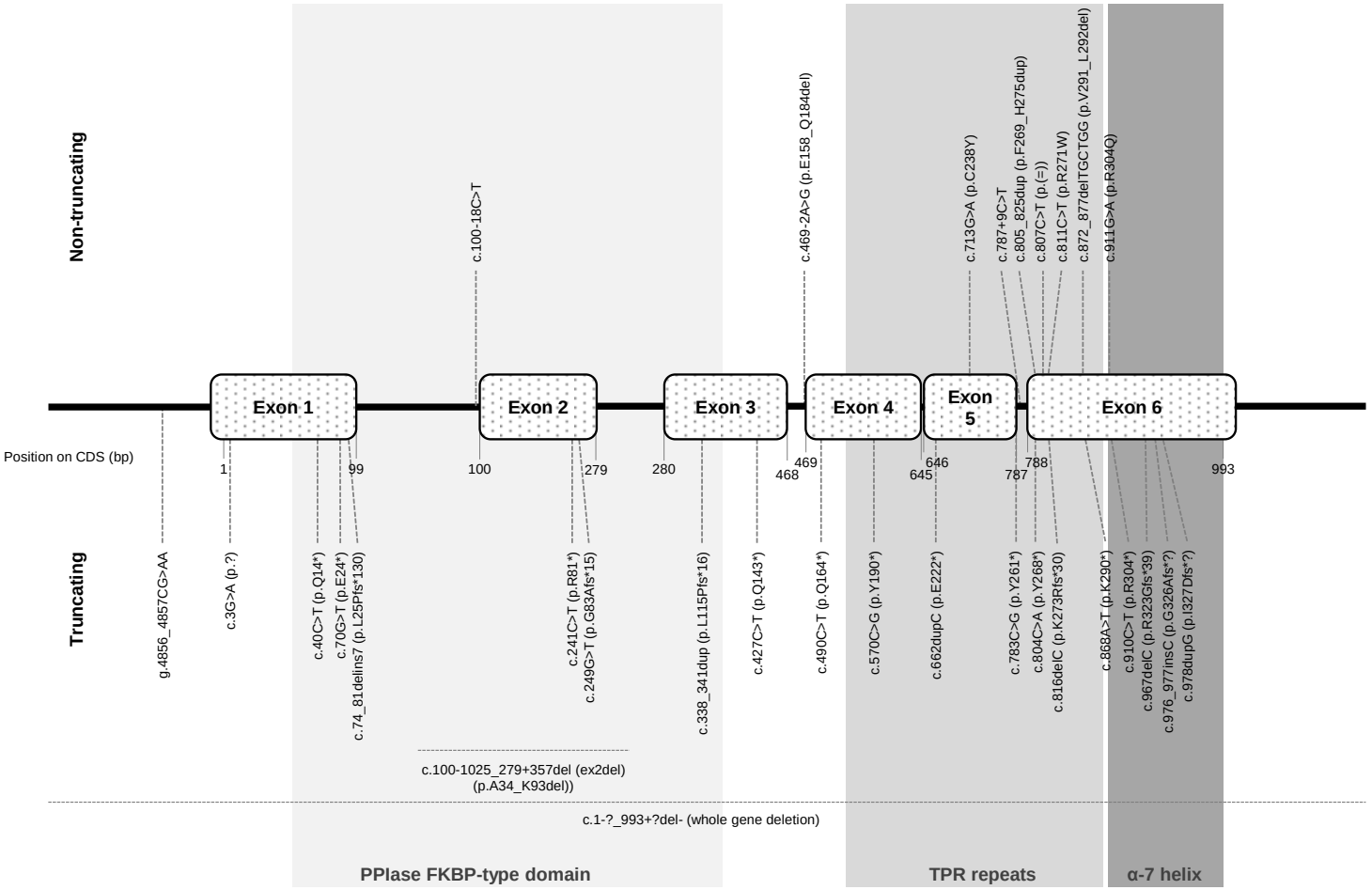

Figure 6. *AIP*muts detected in the study population and their position on the *AIP* gene. Shadowed areas indicate the protein domains codified by each region of the gene. Mutations producing a truncated or missing protein are shown at the bottom of the scheme, and non-truncating mutations are at the top. Even though we identified variants throughout the whole AIP gene, mutations tended to cluster in the genomic regions encoding the TPR domains and the C-terminal α-helix of the protein. Furthermore, the mutations located at the N-terminal extreme and inside the peptidylprolyl isomerase (PPIase) domain were essentially truncating mutations, resulting in short and unstable proteins, lacking the TPR domains.

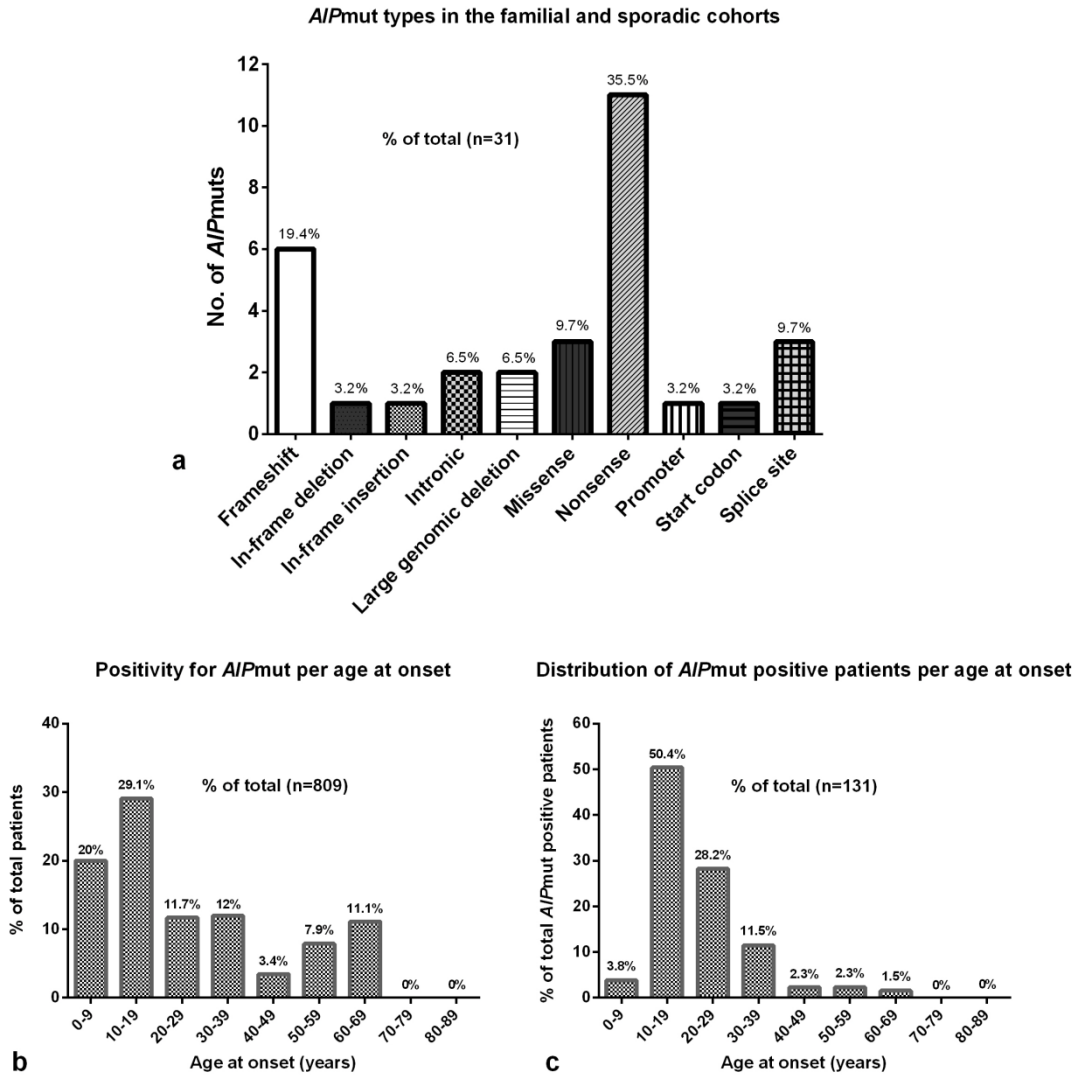

Figure 7. *AIP*mut types and frequency according to age at disease onset in the familial and sporadic cohorts (whole study population). a) Number of *AIP*muts per mutation type, note the predominance of nonsense mutations. b) The probability of finding an *AIP*mut was higher when testing patients with disease onset during the second decade of life; c) in concordance, three quarters of all the *AIP*mut positive patients had disease onset during the second and third decades of life.

We also identified 11 apparently non-pathogenic *AIP* variants (three of them novel) in our population (Table 10).

A multiple regression analysis was performed to determine which clinical features could more accurately predict the likelihood of a patient to carry an *AIP*mut. An age at diagnosis ≥10 and <20 years conferred an odds ratio (OR) of 5.8 (*P*=0.000, 95% CI 3.1-10.8) of having an *AIP*mut, while the OR was 2.8 if the age at diagnosis was ≥20 and <30 years (*P*=0.000, 95% CI 1.3-5.7); thus, an age at diagnosis between 10 and 30 years is the best predictor of *AIP*muts. Inversely, a diagnosis of prolactinoma resulted in an OR of 0.2 (*P*=0.000, 95% CI 0.1-0.5).

Table 10 *AIP* non-pathogenic mutations in the familial and *simplex* cohorts.

Variant (DNA level [protein level])	Variant type	Pathogenic	Location in protein	Familial cohort* (N=19)	Sporadic cohort* (N=37)	Combined* (N=56)	References
c.47G>A (p.R16H)	Missense	No	N-terminus	0	2	2	7;12;13;484;600;615;633-636
c.132C>T (p.(=))	Synonymous	No	PPIase domain	0	3	3	12;637
c.144C>T (p.(=))	Synonymous	No	PPIase domain	0	1	1	632;637-639
c.516C>T (p.(=))	Synonymous	No	Between PPIase and TPR1 domains	8	13	21	10;12;279;633;636;637;639;640
c.573C>T (p.(=))	Synonymous	No	TPR1 domain	0	0	0	This thesis
c.579G>T (p.(=))	Synonymous	No	TPR1 domain	1	0	1	This thesis
c.682A>C (p.K228Q) †	Missense	No	Between TPR1 and 2 domains	2	16	18	12;279;636;637
c.831C>T (p.(=))	Synonymous	Unlikely	TPR3 domain	1	0	1	This thesis
c.891C>A (p.(=))	Synonymous	No	TPR3 domain	0	2	2	12;637
C.896C>T (p.A299V)	Missense	Unlikely	TPR3 domain	5	0	5	10;615
c.906G>A (p.(=))	Synonymous	No	C-terminal α-helix	2	0	2	615;637

* Number of positive individuals for each mutation, considering the *AIP*mut positive tested individuals, the obligate carriers and the predicted *AIP*mut patients.
† There is a Q at this position in the *AIP* reference sequence, but we consider K as the WT amino acid, due to its higher prevalence in the population screened so far (Stals K., unpublished data).
PPIase, peptidylprolyl isomerase.

Genotype-phenotype correlation within the *AIP*mut positive cohort

Truncating mutations accounted for 78.9% (15/19) of the *AIP*muts found in the familial cohort, and for 57.9% (11/19) of those detected in the sporadic cohort. To study a possible difference in disease penetrance between truncating and non-truncating mutations, we compared the number of affected individuals with truncating *AIP*muts in the familial (85/110 [77.3%]) and *simplex* cohorts (21/34 [61.8%]), finding no significant difference, although a trend was observed (*P*=0.0729, analysis included prospectively diagnosed patients). No significant differences were found regarding the proportion of GH excess cases, number of patients per family, maximum tumoral diameter, frequency of macroadenomas, extrasellar invasion or number of treatments received between the patients with truncating and non-truncating mutations. However, patients with truncating mutations were significantly younger at disease onset (median 16 [IQR 15-25] vs. 22 [IQR 17.3-27.8] years, *P*=0.0046, Figure 8a) and at diagnosis (median 21 [IQR 16-30] vs. 27 [IQR 20.8-37] years, *P*=0.0028, Figure 8b), and the occurrence of paediatric cases was more common in this group (60% [57/95], Figure 8c), compared to the patients with non-truncating *AIP*muts (33.3% [12/36], *P*=0.0064).

In concordance with these differences, gigantism accounted for a significantly higher proportion of the GH excess cases in the patients with truncating *AIP*muts (54.7% [47/86]), compared to those with non-truncating *AIP*muts (30% [9/30], *P*=0.0200). As p.R304* was the most common

*AIP*mut in our study population (20 kindreds), we analysed if these patients behaved differently to other patients with truncating mutations. We found more affected individuals per family (median 4 [IQR 2.5-5]) among families carrying the p.R304* *AIP*mut, compared to families with other *AIP*muts (median 2 [IQR 2-3], *P*=0.0133). When considering all the *AIP*mut positive patients together (familial and sporadic), we found a higher proportion of paediatric patients among those with the *AIP* p.R304* mutation (65.8% [25/38] vs. 46.5% [40/86], *P*=0.0475).

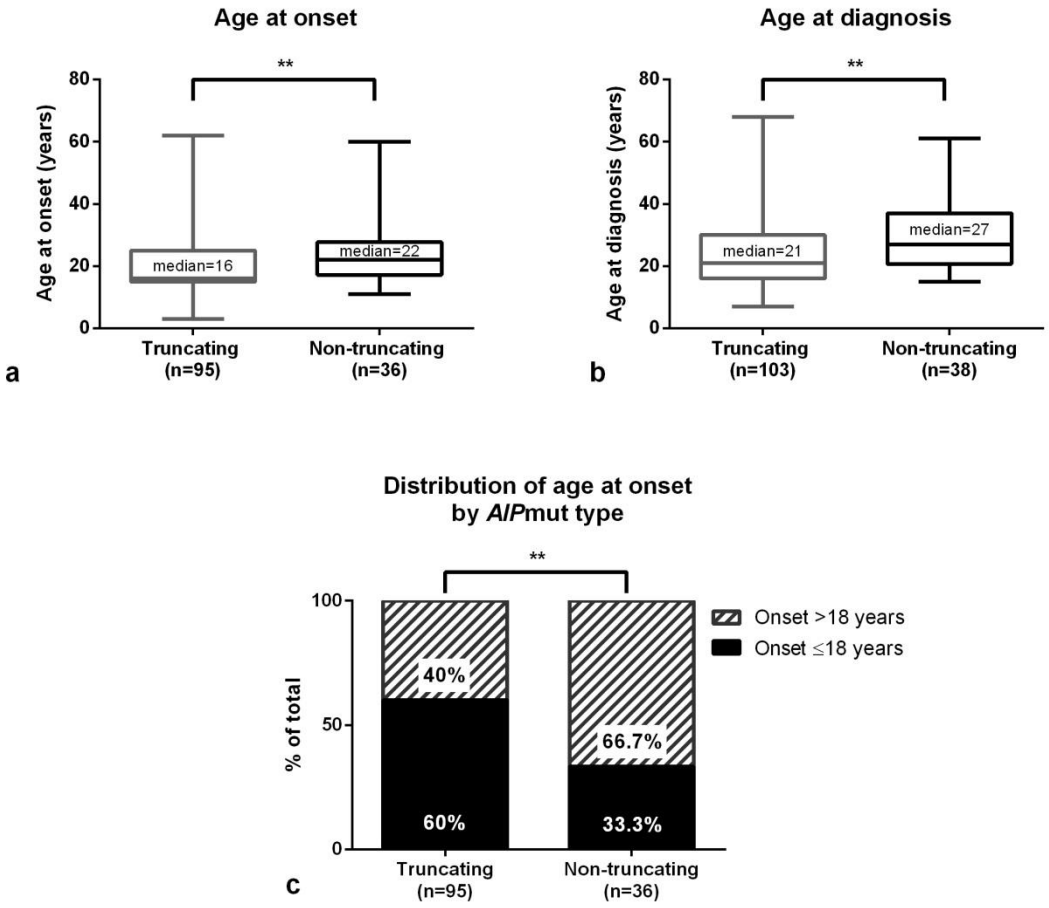

Figure 8. Patients with truncating vs. non-truncating *AIP*muts. a) Patients with truncating *AIP*muts present with a more aggressive phenotype, characterised by an earlier age at onset (*P*=0.005) and b) at diagnosis (*P*=0.003). c) This earlier disease onset results in a higher frequency of paediatric cases (n [total]= 131); in fact, the majority of the patients with truncating mutations present in childhood and adolescence. **, *P*<0.01.

Clinical and histopathological features

Gender distribution

Among the familial patients, there was a significantly different gender distribution of the affected individuals between the *AIP*mut positive and negative subgroups (*P*=0.0015, Figure 9a), showing a predominance of females in the *AIP*mut negative families. This difference is unlikely to be due to a selection bias, as the gender distribution was not significantly different between affected and unaffected individuals in the whole study population (*P*=0.8581), or, in the familial cohort, between unaffected *AIP*mut positive and negative individuals (*P*=0.4421, Figure 9b), or

between *AIP*mut positive affected and unaffected individuals (*P*=0.1367). We did not see a difference in gender distribution between the *AIP*mut positive and negative sporadic patients either (*P*=0.1605, Figure 9c).

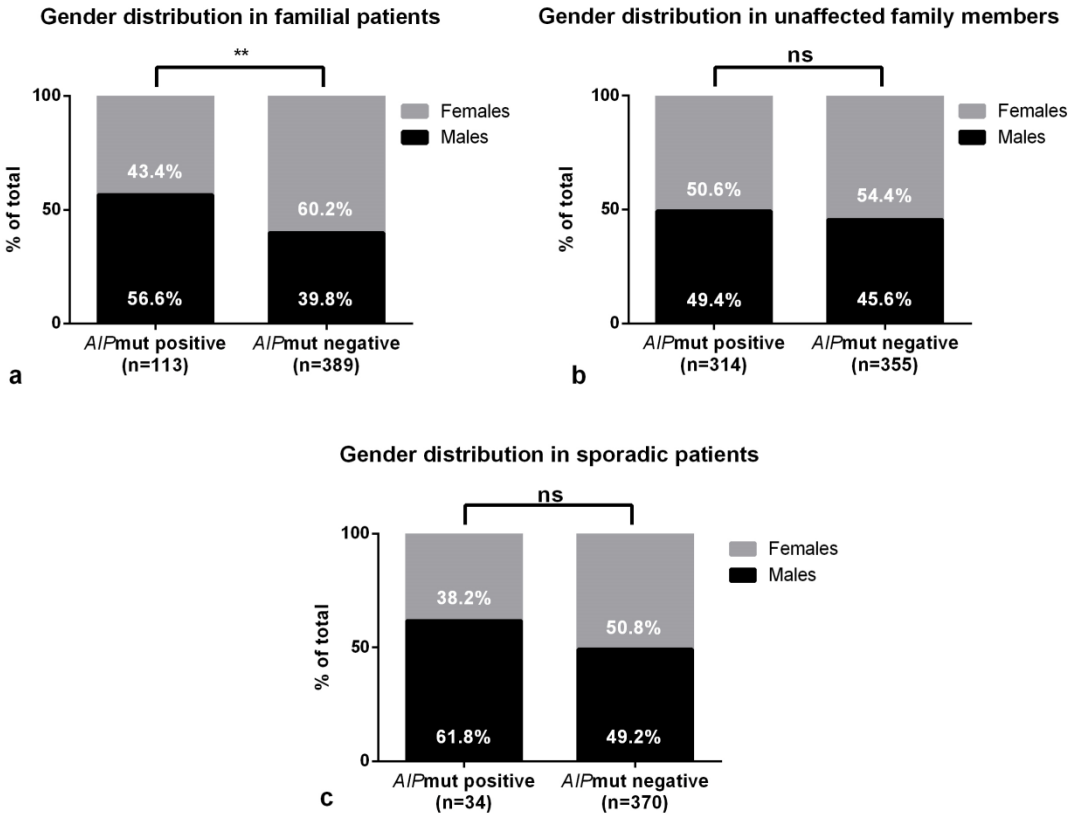

Figure 9. Gender distribution in FIPA families and sporadic patients: a) Gender distribution was different between the *AIP*mut positive and negative FIPA patients, due to a predominance of female patients within the *AIP*mut negative families. b) This difference cannot be explained by a selection bias towards one specific gender, as there were similar numbers of males and females within the unaffected family members (excluding 'not at risk' individuals) of *AIP*mut positive and negative FIPA families. c) The gender distribution was not significantly different between *AIP*mut positive and negative patients, despite a slight prevalence of males in the *AIP*mut positive subgroup. ns, not significant, **, *P*<0.01.

Age

Familial patients

FIPA *AIP*mut positive patients were younger at disease onset (Figure 10) compared to *AIP*mut negative FIPA patients. In the *AIP*mut positive subgroup, the earliest age at onset was three years, while in the *AIP*mut negative families a female patient with Cushing's disease had the earliest disease onset at seven years. Most of the *AIP*mut positive FIPA patients (71.7% [71/99]) developed their pituitary adenomas during the second and third decades of life (10-29 years), whereas only 39.2% (121/309) of the *AIP*mut negative FIPA patients had their first signs/symptoms of pituitary adenoma during the same stage of life (*P*<0.0001, Figure 10a and b). The age at diagnosis was also significantly different (*P*<0.0001): 68.2% (75/110) of the *AIP*mut positive FIPA patients were diagnosed at ≤30 years of age, whereas the diagnosis was

established in only 36.7% (116/316) of the *AIP*mut negative patients by that age. The earlier disease presentation was also reflected in a much higher frequency of paediatric cases (disease onset at ≤18 years of age, Figure 10c) in the *AIP*mut positive FIPA families, compared with the *AIP*mut negative FIPA families (44.1 vs. 11.8%, $P<0.0001$). These distributions were calculated taking into consideration the prospectively diagnosed *AIP*mut positive patients; however, the statistical analysis results were not significantly different when those patients were excluded.

Sporadic patients

Even though our sporadic cohort included only young-onset pituitary adenoma patients, a significant younger age at onset was still found within this young group in the *AIP*mut positive simplex patients in comparison with the *AIP*mut negative ones (median 16 [IQR 14.8-22.3] vs. 22 [IQR 16-26] years, $P=0.0054$, Figure 10d), and there was a higher proportion of paediatric cases within the *AIP*mut positive subgroup (58.8% vs. 35.9%, $P=0.0085$). Nevertheless, while the youngest age at onset in the *AIP*mut positive *simplex* patients was nine years, 3% (11/369) of the *AIP*mut negative patients had disease onset before the nine years of age, with a minimum age of three years.

Clinical diagnoses

GH excess patients accounted for 57.8% (524/906) of the total affected individuals in the entire cohort: 46.6% (234/502) of the familial and 71.8% (290/404) of the sporadic cases. Patients with GH excess, prolactinomas and NFPAs were present in both *AIP*mut positive and negative subgroups, but Cushing's disease, functioning gonadotropinomas and TSHomas were not found in patients bearing *AIP*muts.

Familial patients

We classified the FIPA families as 'homogeneous', when all the affected individuals within the family had the same diagnosis (GH excess was considered as a single category), or 'heterogeneous', when different diagnoses were found in the same family.[272] Around one half of the families in our cohort were homogeneous FIPA families (families with only one pituitary adenoma type) in both the *AIP*mut positive (48.6%) and negative (52.5%) subgroups (Table 11). The most common family type in both subgroups (according to the diagnostic categories found in the affected members) was the pure GH excess family, but it was significantly more frequent within the *AIP*mut positive FIPA families ($P=0.0249$). The most common diagnoses in *AIP*mut positive and negative families were the different categories of GH excess; nevertheless, these cases were significantly more frequent in the *AIP*mut positive subgroup, with at least one case of GH excess in 91.9% (34/37) of the *AIP*mut positive and in 53.1% (95/179) of the *AIP*mut negative FIPA families ($P<0.0001$, Figure 10e). There was a higher frequency of PRL co-secretion among the *AIP*mut positive patients with acromegaly or gigantism, compared to the *AIP*mut negative ones ($P=0.0158$, Figure 10f). In the *AIP*mut negative FIPA patients the most frequent diagnosis was acromegaly, in 35.3% (137/389) of the patients, with prolactinoma in the

second place of frequency (30.9%, 120/389). In sharp contrast to *AIP*mut positive families, where 31% (35/113) of the patients had gigantism, only 2.1% (8/389) of the *AIP*mut negative FIPA patients had this diagnosis.

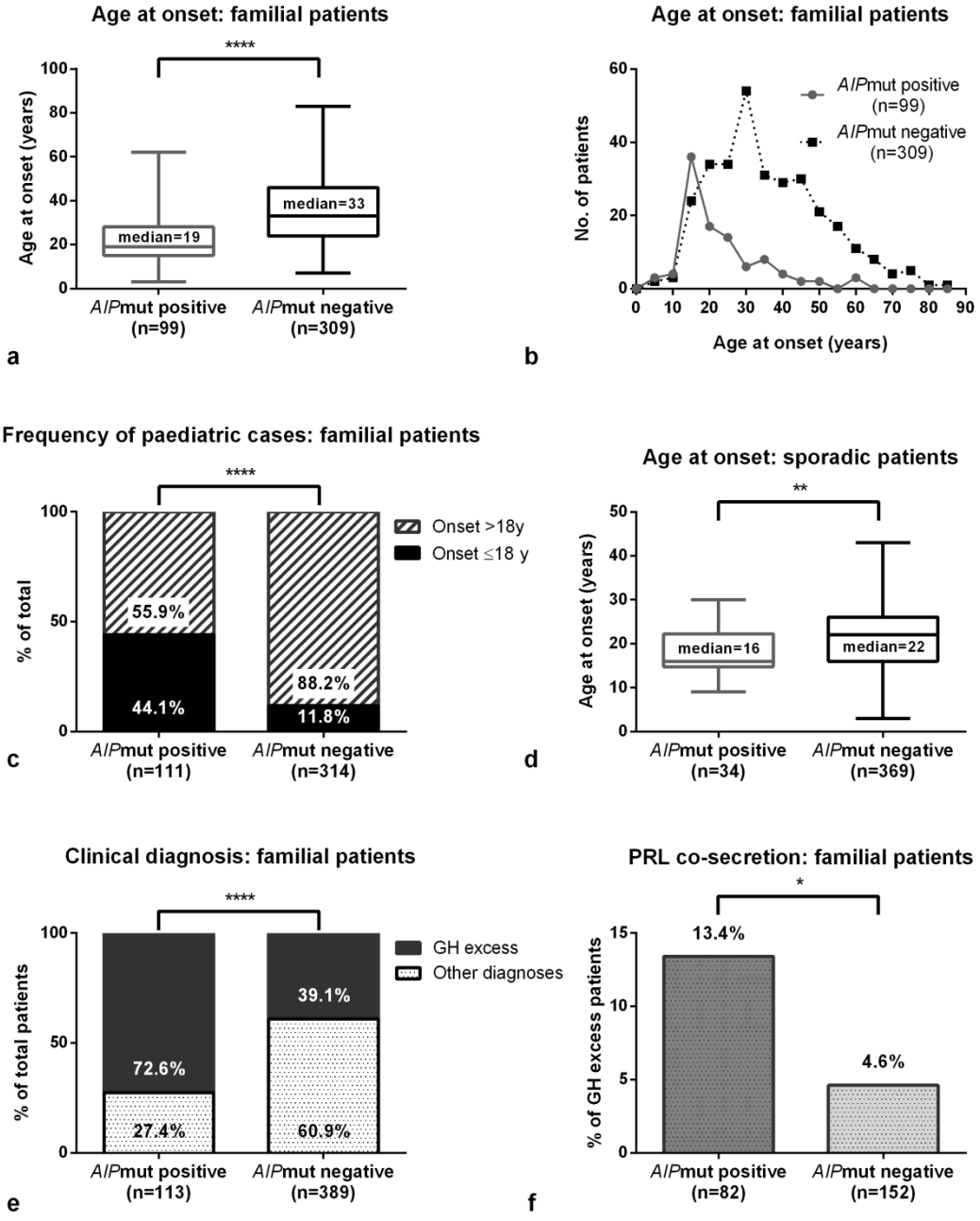

Figure 10. Clinical features in FIPA families and sporadic patients: a) *AIP*mut positive familial patients were younger at disease onset (*P*<0.0001), b) as most of them developed symptoms after the age of 10 and before the age of 40. c) There was a higher frequency of paediatric cases (n [total]=425) in the *AIP*mut positive FIPA families, compared with the *AIP*mut negative FIPA families. d) In the sporadic group, although all these patients were <30 years at disease onset, *AIP*mut positive individuals were significantly younger at disease onset than the *AIP*mut negative ones. e) GH excess and f) presence of GH and PRL co-secretion were significantly more frequent in *AIP*mut positive familial patients. *, *P*<0.05, **, *P*<0.01, ****, *P*<0.0001.

Table 11. Classification of FIPA families by diagnoses

	***AIP*mut positive**	***AIP*mut negative**	**Total**
Total families, no.:	37	179	216
Diagnoses:			
Cushing's disease only, no. (%)	-	3 (1.7)	3 (1.4)
Cushing's disease + FSHoma, no. (%)	-	1 (0.6)	1 (0.5)
Cushing's disease + NFPA, no. (%)	-	1 (0.6)	1 (0.5)
Cushing's disease + NFPA + pituitary tumour, no. (%)	-	1 (0.6)	1 (0.5)
Cushing's disease + prolactinoma, no. (%)	-	5 (2.8)	5 (2.3)
FSHoma + prolactinoma, no. (%)	-	1 (0.6)	1 (0.5)
Cushing's disease+ GH excess, no. (%)	-	7 (3.9)	7 (3.2)
GH excess only, no. (%)	16 (43.2)	44 (24.6)	60 (27.8)
GH excess + NFPA, no. (%)	8 (21.6)	12 (6.7)	20 (9.3)
GH excess + NFPA + prolactinoma, no. (%)	1 (2.7%)	3 (1.7)	4 (1.9)
GH excess + pituitary tumour, no. (%)	-	5 (2.8)	5 (2.3)
GH excess + pituitary tumour + prolactinoma, no. (%)	-	1 (0.6)	1 (0.5)
GH excess + prolactinoma, no. (%)	9 (24.3)	30 (16.8)	39 (18.1)
NFPA only, no. (%)	2 (5.4)	17 (9.5)	19 (8.8)
NFPA + pituitary tumour, no. (%)	-	7 (3.9)	7 (3.2)
NFPA + prolactinoma, no. (%)	1 (2.7)	10 (5.6)	11 (5.1)
Pituitary tumour + prolactinoma, no. (%)	-	1 (0.6)	1 (0.5)
Prolactinoma, no. (%)	-	30 (16.8)	30 (13.9)

* The category "GH excess" includes the following diagnoses: acromegaly, acromegaly/ prolactinoma, gigantism, gigantism/ prolactinoma and mild acromegaly.
FSHoma, FSH secreting adenoma. NFPA, non-functioning pituitary adenoma.

Sporadic patients

In the sporadic cohort, all the *AIP*mut positive simplex patients harboured GH-secreting adenomas (vs. 69.2% of the *AIP*mut negative cases), as proven by the clinical diagnosis and IHC report. The predominance of GH excess cases in both groups could be due to a selection bias, as the previously reported association between *AIP*muts and acromegaly/gigantism could have influenced the referral of these patients for the study.

Histopathology

Familial patients

The IHC analysis of the operated pituitary adenomas confirmed the clinical/biochemical picture in the vast majority of the cases, reporting a predominance of somatotropinomas and mammosomatotroph adenomas in FIPA patients, more evident in the *AIP*mut positive subgroup (*P*= 0.0304, Figure 11a and b). There was a unique case of a double adenoma (one tumour positive for GH and another one for PRL) and one unusual case of somatotroph hyperplasia in a patient with gigantism within the *AIP*mut positive patients. None of the few *AIP*mut positive clinically NFPA cases were gonadotroph or null cell adenomas. In contrast, in the *AIP*mut negative FIPA families, 48.3% of the NFPAs analysed were reported as gonadotropinomas and 31% were null cell adenomas (based on negative immunostaining for GH, ACTH, PRL, TSH, LH

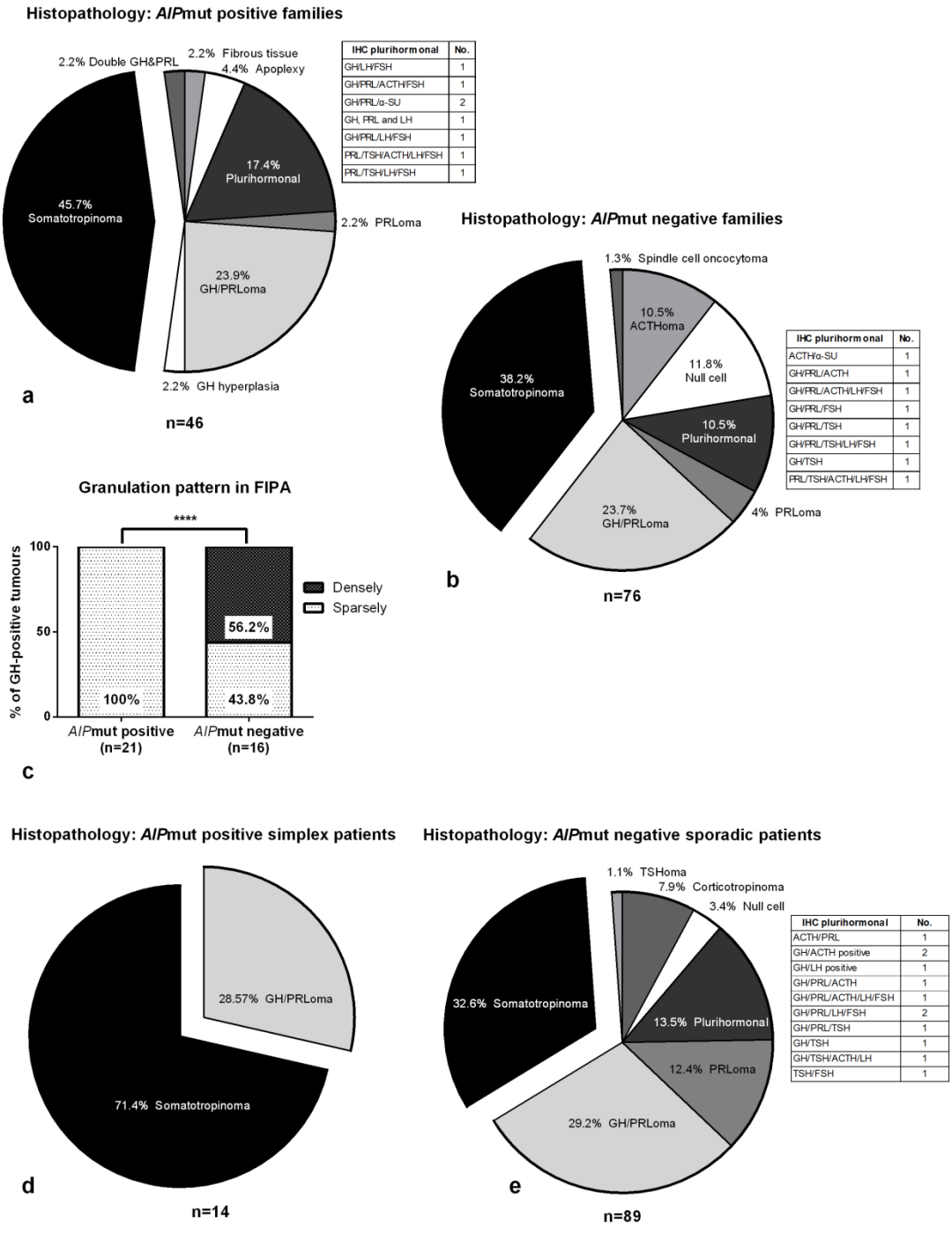

Figure 11. Histopathological diagnoses in FIPA families and sporadic patients. The distribution of the IHC diagnoses was different between *AIP*mut positive (a) and negative (b) familial patients, though GH positive tumours predominated in both subgroups. c) The analysis of the granulation pattern reported sparsely granulated tumours in all the *AIP*mut positive and in 43.8% of the *AIP*mut negative familial adenomas (P<0.0001). d) *AIP*mut simplex patients had GH positive adenomas (with or without positive PRL staining), while e) the *AIP*mut negative sporadic patients had a variety of other tumour types. PRLoma, prolactinoma; GH/PRLoma, mammosomatotroph adenoma; ns, not significant; ****, P<0.0001.

and FSH). There was a similar prevalence of plurihormonal tumours in both subgroups (17.4% in the *AIP*mut positive and 10.5% in the *AIP*mut negative families, P=0.2763). Seventy five percent of all the plurihormonal tumours in both subgroups had positive GH staining. There was

a significant difference among the *AIP*mut positive and negative FIPA patients involving the granulation pattern in GH positive adenomas. All the *AIP*mut positive FIPA patients for whom this parameter was available (22/22) had sparsely granulated adenomas, while 43.8% (7/16) of the *AIP*mut negative patients harboured densely granulated adenomas (*P*<0.0001, Figure 11c); this difference could correspond to the response to the treatment with SSA, as suggested by previous reports.[202] We found no difference in the proportion of patients with Ki-67 index ≥3% between the two subgroups (global 28.1%, *P*=1.0000).

Sporadic patients

All the *AIP*mut positive patients with available histopathology results (n=14) had GH positive pituitary adenomas by IHC, 28.6% of them (n=4) were mammosomatotroph adenomas (Figure 11d). In contrast, the *AIP*mut negative subgroup (n=89) included corticotropinomas (7.9%), null cell adenomas (3.4%), plurihormonal tumours (13.5%), prolactinomas (12.4%), somatotropinomas (32.6%), mammosomatotroph adenomas (29.2%), as well as a TSHoma (1.1%, Figure 11e). In the *AIP*mut positive subgroup, one third (2/6) of the somatotroph adenomas with available cytokeratin staining had a densely granulated pattern and the rest were sparsely granulated. The distribution was similar in the *AIP*mut negative subgroup, where 31.6% of the GH adenomas presented a densely granulated pattern (6/19) and 68.4% were sparsely granulated. Additionally, one *AIP*mut negative patient had a somatotropinoma with a mixed granulation pattern.

Pituitary adenoma size and extension

Familial patients

We compared size and extension of pituitary adenomas between *AIP*mut positive and negative FIPA patients (Figure 12), and for this purpose, the prospectively diagnosed *AIP*mut positive patients were excluded from the analysis. Despite macroadenomas being predominant in both FIPA patient groups, the *AIP*mut positive FIPA patients had larger tumours, demonstrated by a larger maximum diameter (*P*=0.0404, Figure 12a) and a higher prevalence of macroadenomas (*P*<0.0001, Figure 12b). The proportion of giant (maximum diameter ≥40 mm) adenomas (6.3% in *AIP*mut positive and 3% in *AIP*mut negative patients) was not significantly different (*P*=0.1766). There was a higher frequency of extrasellar extension in *AIP*mut positive FIPA patients with pituitary adenomas (*P*=0.004, Figure 12c). Three of the *AIP*mut negative, but none of the *AIP*mut positive patients, harboured tumours with extensive invasion (defined as involvement of intracranial areas beyond the perisellar region); two of them had somatotropinomas and the third one harboured a gonadotropinoma. None of the patients in our cohort had evidence of metastases to justify a diagnosis of pituitary carcinoma.

Sporadic patients

In the sporadic cohort, the maximum diameter of the tumours and the proportion of giant adenomas were similar between *AIP*mut positive and negative sporadic cases (*P*=0.6965 and 0.7859, respectively). All the *AIP*mut positive patients had macroadenomas (29/29) vs. 86.3%

(283/328) of the *AIP*mut negative subgroup, and the presence of extrasellar extension was more common in the former group (95% vs. 58.9%, *P*=0.0011).

Apoplexy of the pituitary adenoma

Excluding the prospectively diagnosed patients, symptomatic apoplexy of the pituitary adenoma occurred in 8.3% of the *AIP*mut positive cases (9.1% of the familial cases, including three families with two cases per family, and 5.9% of the sporadic patients) and in only 1.3% of the patients in the *AIP*mut negative subgroup (*P*<0.0001) and this difference remained significant when only the familial cases were analysed (10.6% of the AIPmut positive vs. 2.3% of the AIPmut negative patients, *P*=0.0002, Figure 12d).

Eight (72.7%) of the *AIP*mut positive patients with a history of pituitary apoplexy had a diagnosis of gigantism, and in three of them (27.2%) apoplexy was the manifestation that led to the diagnosis of pituitary disease (Figure 12e). There were no significant differences in the age at onset/diagnosis or in the tumoral size between the *AIP*mut positive patients that developed pituitary apoplexy and those who did not have this complication. Out of ten *AIP*mut negative pituitary adenoma patients with a history of apoplexy, six had NFPA, two had acromegaly, one had gigantism and the specific diagnosis was unknown in the last patient.

GH excess patients

With the purpose of analysing a relatively homogeneous population of patients, we compared the main clinical features of the *AIP*mut positive and negative GH excess patients from both cohorts, excluding the prospectively diagnosed patients. Similar to the whole study population, the GH excess *AIP*mut positive patients had an earlier disease onset and diagnosis, had significantly more apoplexy cases (8.4 vs. 1.2%, *P*<0.0001) and a higher frequency of sparsely granulated tumours (91.7 vs. 57.1%, *P*=0.0073). In the *AIP*mut positive subgroup there is a preponderance of males (60.7% [65/107]), in contrast with the gender distribution found in patients with all the diagnostic categories. PRL co-secretion was more common in *AIP*mut positive patients (14 vs. 5.9%, *P*=0.0046).

There were no differences in tumour size, frequency of extrasellar extension, or giant tumours, though most of the tumours in both subgroups (89.5%) were macroadenomas. There was no significant difference in the number of therapeutic modalities employed between the two subgroups, but there were fewer patients cured or controlled in the *AIP*mut negative subgroup (41/66 vs. 86/192, *P*=0.0151). Given that the *AIP*mut positive patients had a significantly longer follow-up duration, we decided to evaluate the current status (i.e. effect of the therapies) only in patients with zero to five years of follow-up. In this subset of patients, there was no significant difference in the percentage of cured or controlled patients between the *AIP*mut positive (57.1%) and the *AIP*mut negative (41.7%) subgroups.

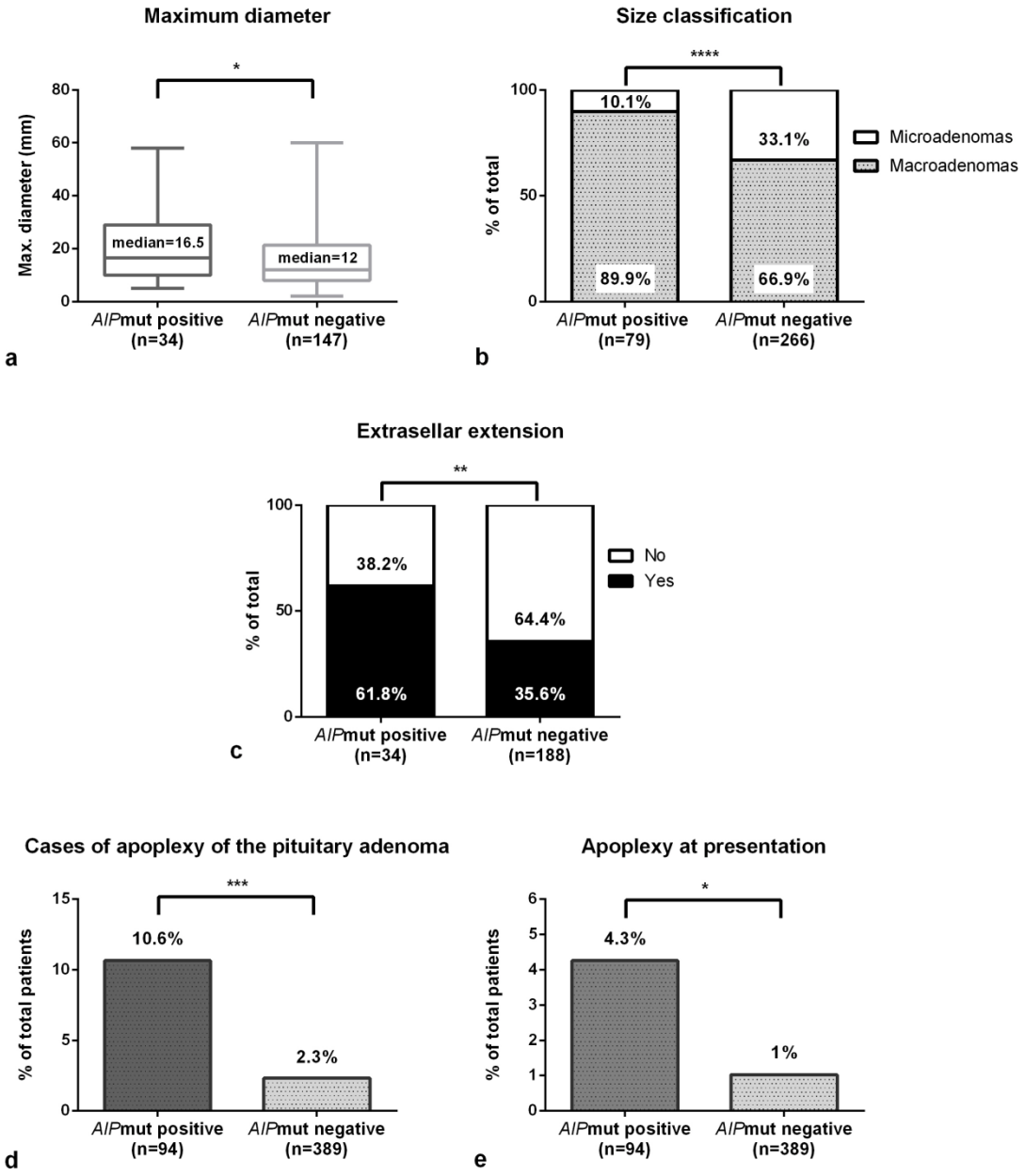

Figure 12. Tumour size and pituitary apoplexy in FIPA families (excluding prospectively diagnosed AIPmut positive patients): *AIP*mut positive vs. *AIP*mut negative patients. a) Pituitary adenomas were larger in *AIP*mut positive familial patients (P=0.040), b) what was reflected in a higher frequency of macroadenomas (P=0.0001). c) In concordance with this, there was a higher frequency of extrasellar extension within *AIP*mut positive patients (P=0.004). d) The occurrence of symptomatic apoplexy of the pituitary adenoma was significantly more common among the *AIP*mut positive families, occurring in 10.6% of these patients (vs. 2.3% of the *AIP*mut negative FIPA patients, (P=0.0002), including one phenocopy NFPA patient. e) Apoplexy was the first sign of pituitary disease in 4.3% of the *AIP*mut positive familial patients, but only in 1% of the *AIP*mut negative ones. * P<0.05, **, P<0.01, ***, P<0.001, ****, P<0.0001.

Gigantism

This study included 120 patients with gigantism, 45 of them, (37.5%) were part of FIPA families and 75 (62.5%) presented as sporadic patients. Overall, 46.7% (56/120) of the patients with gigantism were *AIP*mut positive. Males were predominant among *AIP*mut positive and negative patients (global 67.5%), as expected for gigantism cases. Childhood-onset GH excess resulting

in gigantism was more prevalent among the *AIP*mut positive patients (48.3% [56/116]) than GH excess with no pathological body height, while the opposite pattern was observed in the *AIP*mut negative subgroup (only 16.7% [64/408] had gigantism, *P*<0.0001). Sixty percent of the *AIP*mut positive families had at least one patient with gigantism.

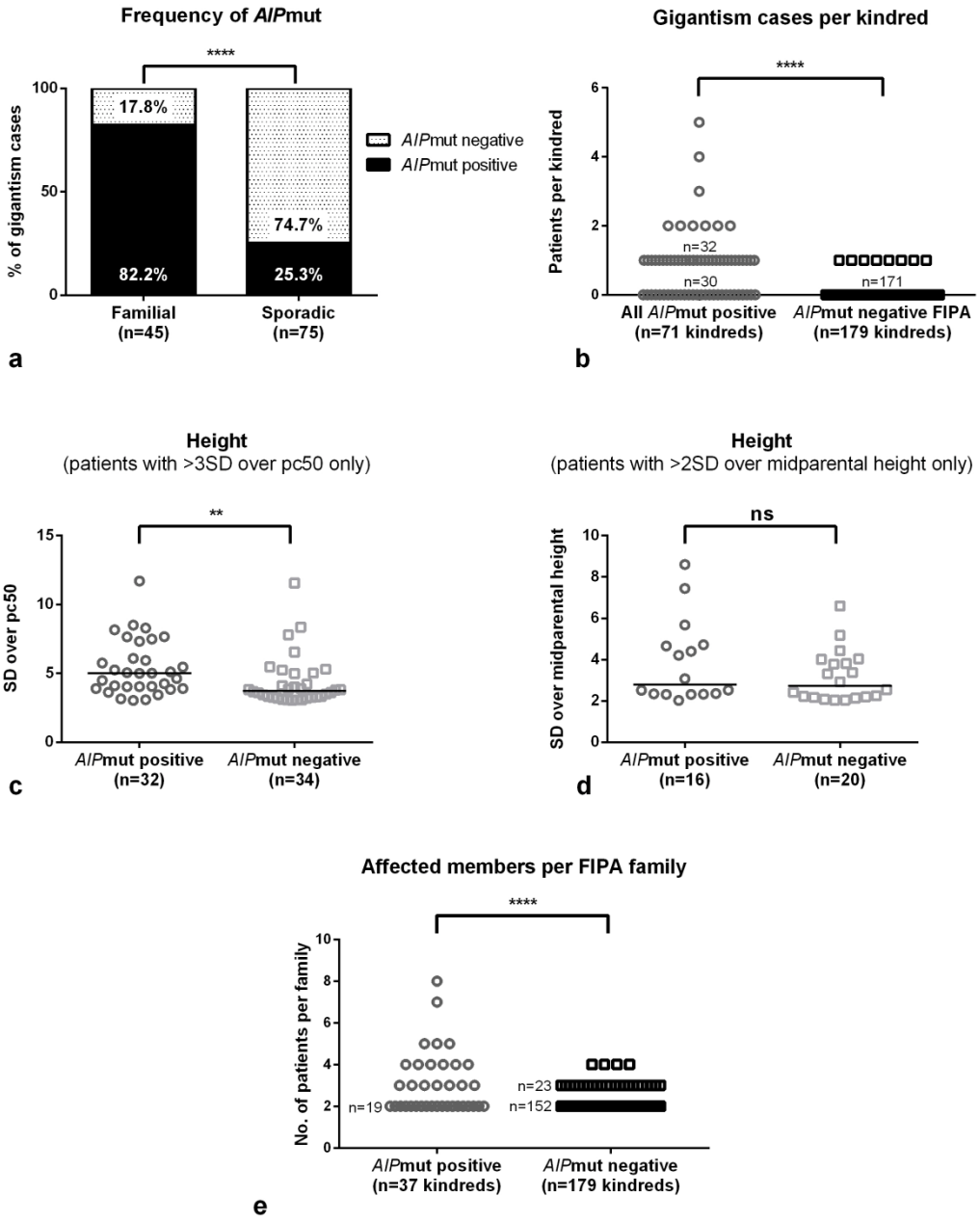

Figure 13. Characteristics of gigantism cases (familial n=45, sporadic n=75) and penetrance. a) The great majority of the gigantism cases occurring in a familial setting were *AIP*mut positive vs. only one quarter of those cases presenting sporadically (*P*<0.0001). b) In our study population, all the kindreds including more than one case of gigantism carried *AIP*muts (this graph includes all the *AIP*mut positive kindreds, FIPA and simplex patients, and the *AIP*mut negative FIPA families). c) Considering only those patients fulfilling the criterion of height ≥3SD over percentile 50, *AIP*mut positive patients were taller at diagnosis than the *AIP*mut negative ones (*P*=0.0164); however, d) there was no significant difference in height when the comparison was done among patients fulfilling the criterion of >2SD over midparental height. e) In average, there were more affected individuals per family in the *AIP*mut positive families (*P*<0.0001). ns, not significant, * *P*<0.05, ** *P*<0.01, ****, *P*<0.0001.

The frequency of *AIP*muts was much higher in the gigantism cases occurring in a familial setting (Figure 13a), where 82.2% (37/45) of the patients were *AIP*mut positive, in comparison with the sporadic cohort, where *AIP*mut positive patients accounted for only 25.3% (19/75) of the patients (P<0.0001). Familial gigantism, defined as the occurrence of two or more gigantism cases due to pituitary adenoma in the same family, occurred only in *AIP*mut positive FIPA families (9/37 families, 24.3%, Figure 13b). Four of these families harboured the p.R304* *AIP*mut, and the *AIP*muts g.4856_4857CG>AA, p.Q164*, p.269_H275dup, p.E24* and a whole gene deletion accounted for one family each. *AIP*mut positive gigantism patients were taller than their *AIP*mut negative counterparts if we considered the criterion of height >3SD over percentile 50 but not when considering >2SD over midparental height (Figure 13c and d).

There was no difference in the age at diagnosis (global median 18 [IQR 15-23]) between the *AIP*mut positive and negative gigantism subgroups. Differences in the frequency of disease onset and diagnosis during the first decade of life did not reach statistical significance (onset: *AIP*mut positive 9.1% vs. *AIP*mut negative 9.5%; diagnosis: 3.6% vs. 1.6%). There were no significant differences in the parameters of tumour size and extension either (maximum diameter, frequency of giant adenomas and extrasellar invasion). However, it is worth noting that the vast majority of the tumours in both subgroups were macroadenomas (global 91.5%), and most of them displayed extrasellar invasion (77.6%). A small percentage of the patients had PRL co-secretion at diagnosis (9.2% global, not significantly different between *AIP*mut positive and negative patients). There were no significant differences in the number of treatments received or the frequency of controlled patients between the two subgroups. Overall, 43.2% of all the patients with gigantism have currently active or only partially controlled disease.

Disease penetrance

To calculate the penetrance of pituitary adenomas among *AIP*mut positive families, complete data is needed both for phenotype and genotype. Therefore, we have selected three families (two with p.R304*, and one with p.A34_K39del mutations) where complete data was available in three or more generations for consenting 'at risk' individuals. The *AIP* genotype was known in 76.6% (range 68.4-94.7%) of the individuals at risk; of them, 16.8% were patients and 83.2% were unaffected carriers. The gender distribution was similar between patients and unaffected carriers. The mean penetrance in these three families was 28.6% (19-38.1), and it decreased to 22.7% (18.2-26.7) when 50% of the individuals at risk with unknown genotype were considered as unaffected carriers. When the prospectively diagnosed patients were omitted from this calculation, the total penetrance of pituitary adenomas was 12.5%, highlighting the importance of the follow-up of apparently unaffected carriers for the correct calculation of the disease penetrance.

As penetrance cannot be appropriately calculated for *AIP*mut negative families, we assessed the number of affected family members. The *AIP*mut positive families had more affected individuals per family than the *AIP*mut negative families (P<0.0001, Figure 13e). While 84.9%

(152/179) of the *AIP*mut negative families had only two affected members, 48.6% (18/37) of the *AIP*mut positive families had three or more pituitary adenoma patients per family. The maximum number of affected individuals within the same family was eight (six of them prospectively diagnosed) in a family carrying the p.R304* *AIP*mut, and the maximum number of cases of gigantism in the same family was five, in a FIPA family with the p.E24* *AIP*mut.

Disease-modifying genes

We have studied the role of two possible disease-modifying genes: *GNAS1*[95] (somatic) and *FGFR4* (germline).[221] *GNAS1* mutations were absent in all the studied *AIP*mut positive somatotropinomas (n=23), but were detected in 50% of the *AIP*mut negative familial somatotropinomas (5/10), 16.7% of the *AIP*mut negative young-onset cases (1/6), and 26.3% of the unselected acromegaly cases studied (5/19). All the mutations detected, detailed in Figure 14, have been previously reported in the literature.

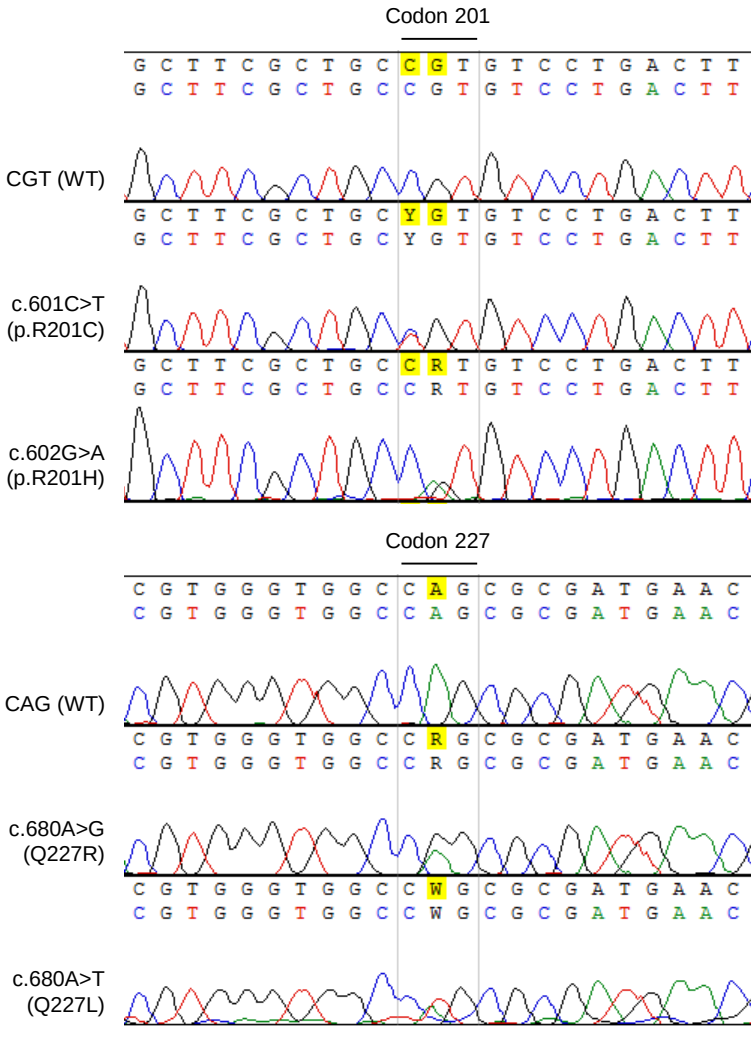

Figure 14. *GNAS1* mutations detected in the study population. Top panel: mutations in codon 201. Bottom panel: mutation in codon 227. All these mutations have previously been reported in the literature. WT sequence is at the top of each panel.

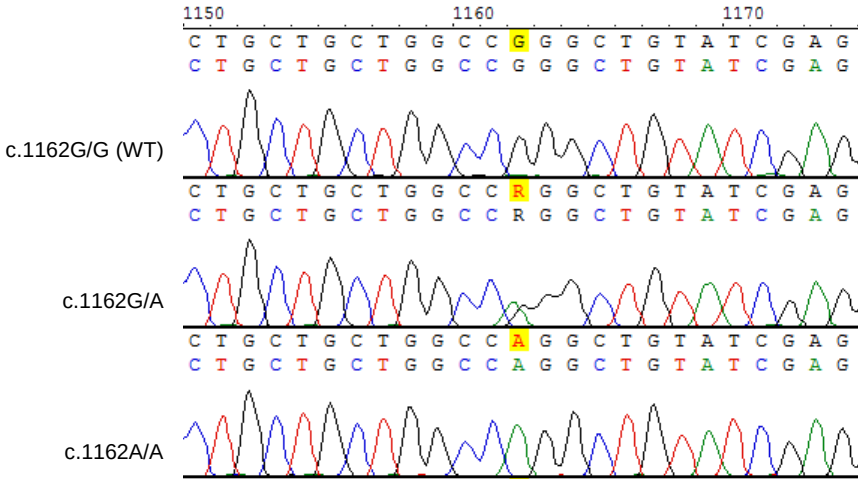

Figure 15. *FGFR4* genotyping. Top: chromatogram of a WT individual. Middle: individual heterozygous for the SNP of risk. Bottom: individual homozygous for the SNP of risk.

The distribution of the *FGFR4* p.G388R SNP conserved the Hardy-Weinberg equilibrium (*P*=0.5509)[641] and the genotype distribution was similar between patients (n=98) and *AIP*mut carriers (n=108) (*P*=0.523). The age at onset and at diagnosis, tumour size and frequency of extrasellar invasion were not significantly different between the GG (WT) and GR/RR patients.

Extra-pituitary neoplasms in *AIP*mut positive individuals

To explore the possibility of a syndromic presentation, we looked for additional neoplasms in the affected and unaffected *AIP*mut positive individuals (n=290). We found a total of ten cases of eight different extra-pituitary neoplasms (osteosarcoma, breast cancer, neuroendocrine tumour of the colon, GIST, glioma, meningioma, non-Hodgkin's lymphoma and spinal ependymoma) in nine subjects (four patients and five unaffected *AIP*mut carriers, Table 12), accounting for 3.1% of the *AIP*mut positive individuals studied. *AIP*mut positive GH excess patients accounted for 44.4% (4/9) of the individuals with extra-pituitary neoplasms, while the rest were unaffected *AIP*mut positive carriers. We note that the association of these tumours with *AIP*muts could be coincidental.

Table 12. Extrapituitary neoplasms in *AIP*mut positive individuals.

Pituitary diagnosis	Cohort	Gender	*AIP*mut	Extrapituitary neoplasm
Unaffected	Familial	Male	c.910C>T (p.R304*)	Osteosarcoma and neuroendocrine tumour of the colon†
Unaffected	Familial	Female	c.910C>T (p.R304*)	Breast cancer†
Unaffected	Familial	Female	c.910C>T (p.R304*)	Breast cancer†
Acromegaly	Familial	Male	c.805_825dup (p.F269_H275dup)	GIST
Acromegaly	Familial	Male	c.241C>T (p.R81*)	GIST*
Unaffected	Sporadic	Male	c.910C>T (p.R304*)	Glioma
Acromegaly	Familial	Female	c.241C>T (p.R81*)	Meningioma*
Gigantism	Familial	Male	c.74_81delins7 (p.L25Pfs*130)	Non-Hodgkin's lymphoma
Unaffected	Familial	Female	c.100-1025_279+357del (ex2del) (p.A34_K93del)	Spinal ependymoma

* Brother and sister. † Brother and 2 sisters.

An increased risk of malignancy among unselected pituitary adenoma patients has been previously reported.[642;643] We have also found neoplasms within the *AIP*mut positive individuals with no pituitary adenomas, where hormonal excess, especially GH, does not play a role. Further analyses are needed to establish whether there is a possible association between *AIP*muts and these neoplasms. Recently, germline *AIP*muts have been associated with three cases of parathyroid adenomas (two middle aged women in the setting of non-familial, isolated PHPT and a young male with acromegaly).[393;499] An MEN-1 like phenotype was an exclusion criterion in our study, therefore, it was not possible to assess this novel pathogenic association, and none of our patients or carriers developed PHPT during the follow-up.

Follow-up and prospective diagnosis

Out of the 164 originally identified unaffected *AIP*mut carriers, 160 were available and advised to undergo biochemical and clinical screening. Prospective diagnosis of a pituitary adenoma was established in 11.3% (18 subjects, 11 males) of the individuals originally considered as unaffected *AIP*mut carriers. Six of the prospectively diagnosed patients had acromegaly (one of them with PRL co-secretion), one patient had gigantism, two patients were diagnosed with mild acromegaly[605] and nine patients harboured NFPAs. Out of the 142 individuals remaining as apparently unaffected *AIP*mut carriers, 79 (55.6%) underwent clinical assessment and one or more biochemical or imaging tests, while 63 subjects (44.4%) had only clinical evaluation.

The prospective cases were diagnosed at an older age than the rest of the patients (median 30 [IQR 22.8-39.5] vs. 23 [IQR 16-33] years, P=0.025). At diagnosis, seven of the prospectively diagnosed patients were symptomatic (headaches, arthralgias, acral growth, facial changes, weight gain or hyperhidrosis). Five of the 18 prospectively diagnosed tumours were macroadenomas, in contrast with a predominance of macroadenomas (89.9%, 71/79) in the rest of the *AIP*mut positive FIPA patients (P<0.0001). The maximum diameter was significantly smaller for prospective cases (median 5.8 [IQR 4.7-14.4] vs. 16.5 [IQR 10-29] mm, P=0.0002). Four of the patients with macroadenomas had surgery and the histopathological study confirmed GH or GH/PRL positive adenomas. The fifth macroadenoma was identified in a 68-year-old male patient with high IGF-1, well-controlled hypertension and diabetes mellitus and no other comorbidities or symptoms, who did not want to receive any treatment. In addition, one *AIP*mut negative pituitary adenoma patient, harbouring a 25mm NFPA, was prospectively diagnosed as part of an *AIP*mut positive family (brother of the *AIP*mut positive proband).

Further seven subjects had abnormalities in their screening tests, but a pituitary disease was not confirmed: five individuals had slightly elevated IGF-1 levels for their age/gender, one patient displayed acromegaloid features but normal pituitary MRI and biochemistry, and a 17-year-old female had repeatedly borderline high IGF-1 and incompletely suppressed GH on OGTT, but her bulky pituitary gland (11mm in height), normal at this age group, is not changing during follow-up and her biochemical results are now within the normal range, after three years of follow-up.

The global penetrance of pituitary adenomas among the individuals initially considered as unaffected *AIP*mut carriers was 11.3% (18/160). However, the penetrance was higher in the group of carriers who underwent biochemical and imaging investigations varying between 18.6 and 28.1% depending on the depth of screening (Figure 16). Overall, these data suggest that approximately 20-25% of the apparently unaffected *AIP*mut carriers screened with biochemical or imaging tests will be identified with a pituitary adenoma at some point in their lives.

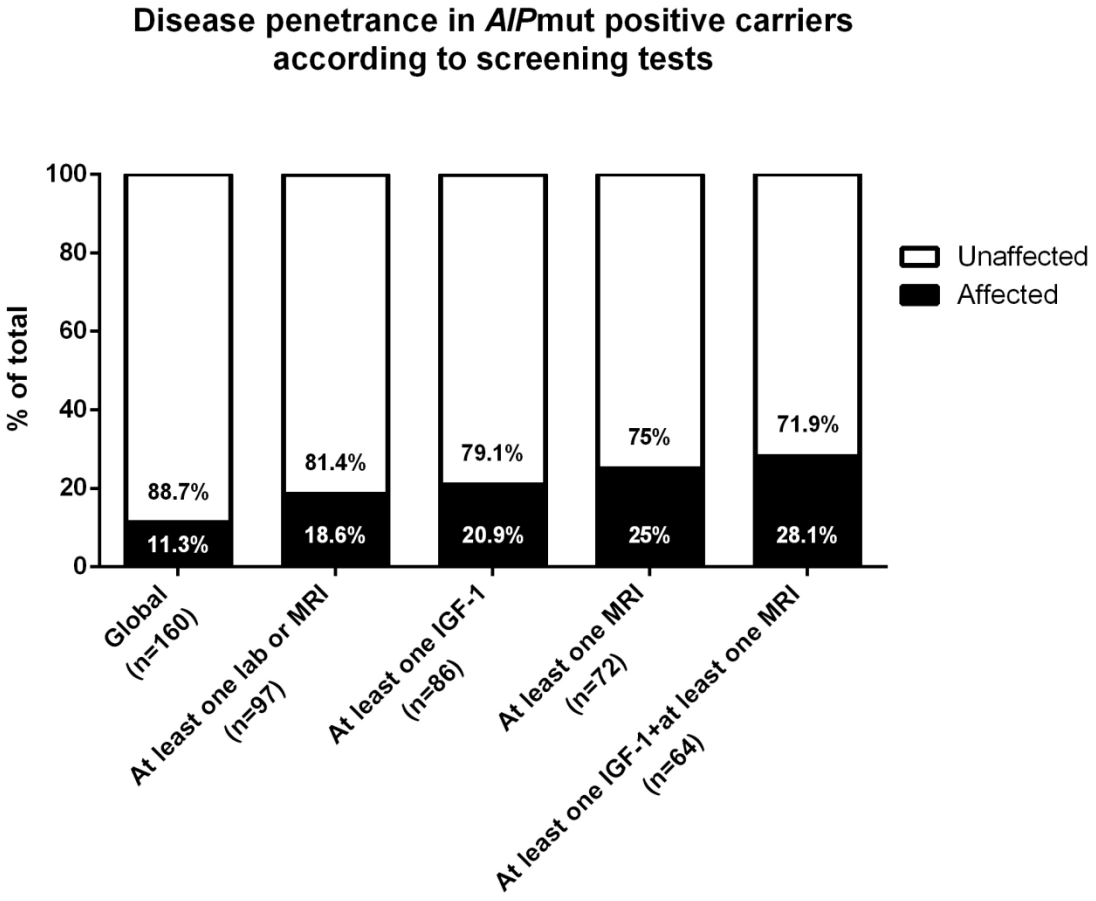

Figure 16. Penetrance in screened *AIP*mut positive carriers (n [total]=160). The probability of detecting new cases of pituitary adenomas within apparently unaffected *AIP*mut carriers depends on the clinical assessment and the type of complementary biochemical/imaging studies included in the screening protocol (see text).

Clinical screening was not systematically performed in the *AIP*mut negative FIPA unaffected family members. Nevertheless, due to the increased disease awareness given by the existence of previous pituitary adenoma cases within their families, four individuals (three females and one male) from three different *AIP*mut negative FIPA families were prospectively diagnosed. Three of them harboured NFPAs, but we lack complete information about the fourth patient. The mean age at diagnosis in the three NFPA cases was 37 years, and only one patient referred symptoms at diagnosis (galactorrhoea, not clearly associated to stalk compression, and lethargy). All of them had microadenomas, with a mean diameter of 6.5mm, and did not require

any therapeutic intervention other than hormonal replacement in one case. The characteristics of these cases resemble those of incidentalomas; however, the occurrence of two prospective cases in the same family supports an apparent inherited component.

Discussion

*AIP*muts are prevalent in young-onset GH-excess patients (24%) and FIPA (17.1%), with more than double frequency in patients with gigantism (46.7%) in our cohort, in concordance with other studies.[7;498;500;644] However, in contrast to previous reports, in this large and extensively studied cohort there was no predominance of male patients among the *AIP*mut positive familial cases, and equal numbers of male and female unaffected carriers were identified. Earlier studies[9-11;488] may have had an ascertainment bias for families with cases of gigantism, a disease that is more prevalent in males, at least partly due to the physiologically later puberty and therefore later cessation of growth in boys. In addition, we have found some interesting clinical features among *AIP*mut positive patients, which are described in the next paragraphs.

The presence of two different types of pituitary adenomas in the same gland is infrequent (2.3% of all the cases and 3.3% of the cases of Cushing's disease).[645] Multiple pituitary adenomas have been previously described in a few cases of MEN1 and FIPA (not screened for *AIP*muts) patients.[358;646-649] Although somatotroph hyperplasia has been described before in the setting of *AIP*muts,[6;650] this finding does not seem to be particularly frequent, as in our cohort it was found only in one patient with acromegaly and PRL co-secretion.

There was a marked predominance of sparsely granulated GH-secreting adenomas among the *AIP*mut positive patients, compared to the *AIP*mut negative ones. Patients with sparsely granulated tumours are usually younger at diagnosis than those with a densely granulated pattern,[651;652] have increased invasiveness[202;651-653] and reduced response to the treatment with SSA,[202;653] though the strength of these associations has been variable among different studies. The mechanism proposed for this effect in sporadic adenomas implies a reduced expression of the SS receptor subtype 2 (SSTR2).[654;655] Since the expression of the SSTR2 and other SSTR subtypes is not reduced in somatotropinomas from *AIP*mut positive patients, other molecular mechanisms must be involved in the association of these mutations with decreased responsiveness to SSA and a sparsely granulated pattern, such as ZAC1 activation[589;591] or an impaired inhibitory G protein subunit function in these tumours.[509]

The original description of multiple cases of pituitary adenoma apoplexy in *AIP*mut positive patients[9] was later confirmed in other studies[10;11;276;603;650;656] as well as now in this larger cohort. Although the prevalence of 8.3% does not seem to be higher than the prevalence reported in populations of unselected pituitary adenomas (7.9%),[68] in the latter study patients were older (mean age 60.5 years) and harboured NFPAs, while in our cohort the majority had gigantism and the rest, acromegaly or prolactinoma, with a mean age at diagnosis of 23.4 years. Our three familial apoplexy families, together with a recently reported family with three apoplexy

cases[56] provide support for the phenotype of young-onset, familial apoplexy in *AIP*mut positive patients. To our knowledge, there are no previously known genetic causes of familial pituitary adenoma apoplexy, and this remains an uncommon finding. The mechanism why *AIP*mut positive cases are more prone to apoplexy needs further study.

We have demonstrated that around a quarter of the individuals initially identified as unaffected *AIP*mut carriers who underwent clinical screening tests were diagnosed with pituitary abnormalities. Full clinical screening identified 28.1% of the carriers, with fewer tests understandably resulting in fewer positive cases. Our data suggest that not all the *AIP*mut-associated pituitary adenomas have a rapidly growing, aggressive phenotype. The follow-up of these patients allowed us to observe some probably very early cases of acromegaly, where the current clinical scenario had not indicated intervention at data closure. We cannot rule out that some of the small NFPAs are indeed incidentalomas, similar to those frequently observed in *AIP*mut negative subjects of the general population.

This frequency of prospective diagnosis may justify the clinical screening and, possibly, follow-up of all the *AIP*mut positive unaffected carriers. Our data would support the assessment of all the newly identified *AIP*mut carriers (clinical examination/history, PRL and IGF-1, as a minimum, up to a full screening, including also an OGTT and contrast-enhanced pituitary MRI). Follow-up of the younger family members should continue until at least the 30 years of age, preferably annually, with clinical assessment and basal pituitary hormonal levels, leaving stimulation tests for cases with suspicion of pituitary disease and a follow-up MRI if necessary.[603;610] The cost-effectiveness and the possible psychological burden of this approach will need future study. Stopping the follow-up should be considered in older patients, given the low possibility of detecting new pituitary adenoma patients in these individuals after the fifth decade of life.[603;610] Once a case has been prospectively diagnosed, the treatment and follow-up should proceed as for the general population of pituitary adenoma patients, as there are no data to suggest a different type of treatment in *AIP*mut positive patients.[482]

The genetic and clinical screening of *AIP*mut negative FIPA families is uncertain at this point. Baseline screening and follow-up of obligate carriers could be considered, keeping in mind that the age of onset is considerably older in these families. Education on possible signs and symptoms of family members is a viable option in the routine setting. We expect that the identification of further genes implicated in the pathogenesis of FIPA in the next years will allow us to tailor these recommendations in accordance with the clinical behaviour of each genetic entity.

Patients with GH excess starting before the age of 5 years should be tested for the recently identified Xq26.3 chromosomal microduplications.[91] The genetic screening of other sporadic young-onset pituitary adenoma patients with no evidence of other endocrine tumours should be focused on *AIP*muts in first instance in cases of GH excess (with or without PRL co-secretion)

and on *MEN1* mutations, especially in cases of prolactinoma,[498] as this can be the first manifestation of MEN1[657]. Whether it would be advisable to continue screening young patients with other diagnoses for *AIP*muts out of the setting of research studies needs longer follow-up.

To explain the variable clinical phenotype in our *AIP*mut positive patients, we evaluated the possible influence of two disease-modifying genes, *GNAS1* and *FGFR4*. While somatic *GNAS1* mutations are common in unselected somatotropinomas, we have not identified any in adenomas from *AIP*mut positive patients, suggesting that germline *AIP*muts and somatic *GNAS1* mutations are mutually exclusive in somatotropinomas. A previous study in two isolated familial acromegaly cases, carrying the *AIP* c.804C>A (p.Y268*) mutation, reported similar results.[624] *GNAS1* mutations have previously been rarely studied in paediatric patients with acromegaly and gigantism, and they seem to be an extremely infrequent finding in this age-group.[658;659] *GNAS1* mutations have rarely been studied in paediatric patients with acromegaly and gigantism, and they seem to be an extremely infrequent finding in this age-group.[658;659] A recent study has shown no change in the AIP immunostaining in sporadic somatotropinomas in the presence of *GNAS1* mutations.[17] The characteristic phenotype of adenomas containing the *GNAS1* seems to be in contrast with the typical *AIP*mut positive tumour phenotype. On the other hand, in somatotroph adenomas of *AIP*mut negative FIPA patients, half of the tested samples had *GNAS1* mutations. This suggests that in *AIP*mut negative FIPA, somatic *GNAS1* mutations could exist in a similar frequency as to in unselected somatotropinomas and possibly, in addition to a germline predisposing mutation, may play a role in their pathogenesis.

The *FGFR4* gene SNP rs351855 (c.1162G>A, p.G388R), with a minor allele frequency of 0.3, is a predictor of progression and poor prognosis in a variety of human neoplasms.[219] A role for rs351855 as a facilitator of somatotroph cell tumorigenesis has been recently proposed,[221] and we hypothesised that this variant could increase the penetrance and/or size and extension of *AIP*mut positive pituitary adenomas. The screening for this SNP in our *AIP*mut positive patients failed to show increase in size, extension or apoplexy, even though this association had previously been suggested in sporadic acromegaly patients,[221] and no earlier onset or higher penetrance were observed. The lack of association with these two potentially disease-modifying genes suggests that *AIP*mut-related pituitary adenomas are regulated by different pathogenic mechanisms than unselected somatotropinomas.

The numerous limitations of our study are fully acknowledged. We chose an arbitrary age cut-off (≤ 30 years), in concordance with previous *AIP*-related publications, but our data shows that only 13.2% of the *AIP*mut positive patients had disease onset after the age of 30 years. Our patients were recruited from different genetic backgrounds and this could have influenced the disease penetrance and presentation. On the other hand, 19.7% of the *AIP*mut positive kindreds (24.3% of the *AIP*mut positive patients) belong to a cohort with a founder *AIP*mut (p.R304*), originally from Northern Ireland.[506] The larger number of subjects screened in these families provided a higher number of carriers and chance for detection of affected individuals.

Additional genetic traits possibly co-segregating with this founder mutation could modify the phenotype and thus introduce a bias into our results. Full genotype and phenotype data were not available for all the families; therefore, we limited our penetrance calculations to three large, well-characterised families. A better assessment of the prevalence of pituitary apoplexy and extrapituitary adenomas in *AIP*mut positive patients would require a large control group, screened *ad hoc*, which was beyond the scope of this study. Finally, the data about therapeutic modalities was limited, hampering the analysis of the response to different treatments.

Conclusions

The analysis of this large cohort of FIPA patients allowed us establishing a number of novel aspects of FIPA. A phenotype-genotype correlation was found with younger onset of disease in patients with truncating *AIP*muts. We identified a surprisingly high percentage of somatic *GNAS1* mutations in the *AIP*mut negative somatotropinomas, and their absence in *AIP*mut positive tumours. The lack of influence of the germline *FGFR4* p.G388R variant on disease penetrance/severity suggests that currently unknown factors drive penetrance and variable phenotype in *AIP*mut positive pituitary adenomas. The presence of milder, more indolent disease in some *AIP*mut positive subjects has been established. Genetic and clinical screening leads to the prospective identification of an unexpectedly high proportion of affected patients in the originally apparently unaffected carrier group, resulting in earlier diagnosis and treatment and, possibly, better long-term outcome[603]. The recruitment of a large study population with this uncommon disease has only been possible thanks to world-wide collaboration.

Chapter 3:
An integral analysis of the panel of molecular partners of AIP in the pituitary: the role of AIP in pituitary tumorigenic pathways

Introduction

The mechanism by which *AIP* LOF disrupts pituitary function has remained elusive ever since disease causality was established between *AIP*muts and pituitary adenomas. AIP is a co-chaperone of HSP90 and HSPA8, with a promiscuous repertoire of molecular interactions.[15] More functional studies are needed to explain the role of *AIPmut* in pituitary tumorigenesis, in order to determine how the loss of tumour suppression activity occurs and to clarify the mechanism for the apparent pituitary specificity of this effect.

The diverse experimental approaches used to describe AIP functions have been focused, in most of the cases, on addressing the function of AIP in the AHR signalling pathway in the setting of toxicological studies.[521;570;587] The role of AHR in tumorigenesis is complex, but the current hypothesis is that increased AHR expression or activity correlates with tumour progression in most human tissues.[660] *AIP*mut positive pituitary adenomas show loss of nuclear AHR staining, indicating that *AIP*mut-associated tumorigenesis is very probably not driven via increased AHR signalling.[481] An epidemiological study suggested an association between environmental pollution by dioxins and a higher frequency of acromegaly,[661] and an AHR SNP has been described as a possible disease modifier in somatotropinomas.[662] However, animal models of AHR deficiency do not display a pituitary phenotype,[596] and it is clear from other studies that the role of AHR on pituitary tumorigenesis, if existent, is not prominent, neither in the setting of AIP LOF,[509] nor in other types of pituitary adenomas.[663]

Two recent studies reported an apparent regulatory role of AIP in the cAMP pathway,[509;588] which could be mediated by activation of GNAI2 and GNAI3.[509] These results are supported by the clinical and experimental observation that AIP expression is enhanced by the treatment with drugs activating the SS pathway, the main regulator of cAMP in the pituitary gland. Nevertheless, the experimental approaches used to address these questions have been based on the study of expression patterns under different conditions, such as AIP KD or KO, pharmacological phosphodiesterase blocking or cAMP overactivation, among others. Although these techniques have rendered important data regarding the functional changes in signalling pathways under those stimuli, they have been unable to determine which specific molecular interactions must occur (or stop occurring) for those functional changes to take place.

Considering the fact that AIP is a ubiquitously expressed protein, that it is not known to be a transcription factor and that *AIP*muts are associated to pituitary adenomas only, it is very probable that the pituitary specific function of AIP is not due to the protein itself or to its expression pattern, but explained by its possible intervention on signalling pathways regulating cell proliferation specifically in the pituitary gland. On these bases, the present study has been focused on studying the specific repertoire of AIP interacting proteins in the pituitary gland, using a proteomic approach.

Aims

General

To identify the molecular partners of *AIP* in the pituitary gland using a proteomic approach and to analyse the potential role of *AIP* in the pathways that drive pituitary tumorigenesis.

Specific

1. To produce a glutathione-S-transferase (GST)-fused WT AIP and six AIP variants (p.E192R, p.C238Y, p.K266A, p.A299V, p.R304* and p.R304Q) using a GST tag-mediated affinity purification system.
2. To perform pull-down assays in a somatotropinoma cell line using the purified proteins as baits.
3. To identify relevant AIP interacting proteins in a somatotropinoma cell line through quantitative MS (qMS), analysing differences in the repertoire of protein interactions among WT AIP and its variants.
    – To determine if the differences in AIP interactions are only due to loss of normal interactions or if new interactions are generated by variants.
4. To validate qMS results through co-immunoprecipitation (co-IP) and co-localisation assays.
5. To analyse the identified AIP interacting proteins using a pathway analysis software.
    – To define if the identified AIP interacting proteins are involved in pathways which are relevant for pituitary tumorigenesis.
6. To explore the role of AIP in pituitary tumorigenic pathways.

Hypotheses

1. AIP interacts with proteins that regulate the cell cycle in somatotroph cells.
    a. Pathogenic AIP variants lose some of these protein-protein interactions, supporting the role of AIP as a tumour suppressor factor.
2. Variants with a questionable pathogenic effect do not differ to WT AIP in their interacting proteins repertoire.
3. Proteins related to pituitary tumorigenesis interact with some AIP variants but neither with other variants, nor with WT AIP.
    a. Those abnormal interactions favour uncontrolled cell proliferation.

4. The effect of certain variants is double: disruption of tumour suppressor function and enhancement of uncontrolled cell proliferation.

Methods

Selection of AIP variants

Six AIP variants were selected for the study, as detailed below.

AIP p.E192R (chr11:67257614-67257615)

The possibility that AIP could dimerise has been proposed, but remains unproven. If this occurs, the residue E192 is expected to be essential for binding another AIP molecule, through its interaction with R312 (*in silico* analysis by C. Prodromou). The variant p.E192R (c.574-575GA>CG) at *AIP* exon 4 has never been found in patients, but it is predicted to disrupt the hypothetical AIP dimerisation ability.

p.C238Y (rs267606569, Genbank EF643648, chr11:67257854)

This transition (c.713G>A), located at *AIP* exon 5, was detected for the first time in a FIPA family.[9;495] This variant is considered a missense mutation, predicted to destabilise the packaging of α and β helices of the second TPR motif.[10] Functional studies have shown a reduced ability of AIP p.C238Y to block cell proliferation *in vitro,*[9] as well as a complete disruption the AIP-PDE4A5 interaction.[10] All the available information supports its pathogenic potential.

p.K266A (chr11:67258267-67258268)

The residue K266 in AIP is essential for the interaction between AIP and HSP90.[556] The experimental mutation p.K266A (c.796-797AA>GC) at exon 6 disrupts this interaction *in vitro*, though it has never been found in patients.[556] Loss of HSP90 binding significantly reduces the ability of AIP to interact with AHR,[556] but it is unknown if this affects other signalling pathways. We decided to include this mutation as an approach to analyse the importance of HSP90 for AIP function.

p.A299V (rs148986773, Genbank EF203235, chr11:67258367)

This variant is a transition (c.896C>T) at the exon 6 of *AIP*, first described in a patient with sporadic acromegaly.[615] Although it was initially considered a missense mutation, two apparently healthy individuals are compound heterozygotes for p.R304* and p.A299V.[9] Furthermore, one FIPA patient has been found to bear p.A299V and a microprolactinoma, so the probability of a phenocopy cannot be discarded.[10] This variant is localised at the beginning of the C-terminal α-7 helix of the protein. Functional studies for p.A299V showed only slight reduction in PDE4A5 binding *in vitro.*[10] This variant in currently not considered pathogenic, mainly based on clinical data, but there is not enough experimental evidence to support this.

p.R304* (rs104894195, Genbank AM236344, chr11:67258381)

The codon 304 is a mutational hotspot in AIP and p.R304* is the most frequent mutation found in *AIP*mut positive pituitary adenoma patients. This transition (c.910C>T) at *AIP* exon 6 was originally described in a family with IFS.[8] Since then, p.R304* has been reported in both patients (familial and *simplex*) and apparently healthy carriers. Functional studies for R304* proved complete disruption in PDE4A5 binding and loss of the ability of the mutant AIP to block cell proliferation *in vitro.*[9] This variant is considered a nonsense mutation, resulting in a truncated protein, and all the available data support its pathogenic potential.

p.R304Q (rs104894190, Genbank EF203236, chr11:67258382)

This variant is also a transition (c.911G>A) at *AIP* codon 304. The p.R304Q variant was first found in an apparently sporadic case of Cushing´s disease[615] and since then it has been reported in several FIPA families and *simplex* patients. This variant is relatively conservative, changing a longer side chain, positively charged amino acid, to a slightly shorter, uncharged, hydrophilic one at the C-terminal α-7 helix.[10] Although it does not affect PDE4A5 binding by AIP *in vitro*,[10] other functional studies are not available and clinical data support the role of p.R304Q as a missense pathogenic mutation. Interestingly, the ExAC database reports the presence of this variant in homozygosity in two European individuals,[217] increasing the uncertainty about its pathogenic effect.

Generation of plasmids for protein production

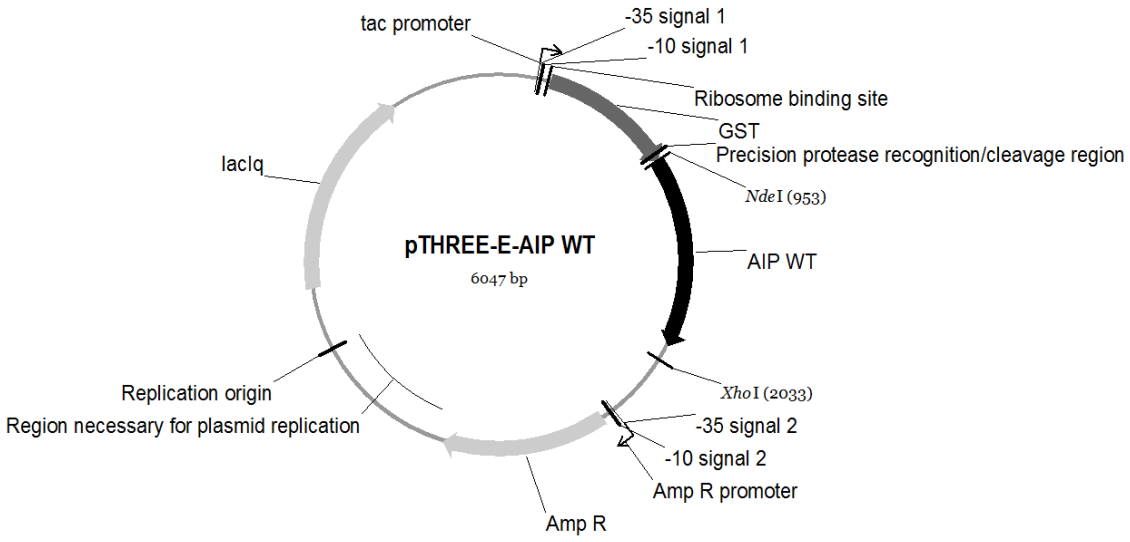

Figure 17. Plasmid for expression of GST- tagged AIP. The pTHREE-E plasmid is based on the commercial plasmid pGEX-6P-1 and confers ampicillin resistance to the transformed bacteria. The CDS cloned into the multiple cloning site, in this case AIP, is positioned downstream the CDS of *S. japonicum* GST, to express a fused GST-AIP protein. The expression of the GST-AIP CDS is regulated by the *tac* promoter. The plasmid constitutively expresses the lacIq repressor, which binds and represses the *tac* promoter (containing a lac operator). When IPTG is supplemented to the medium, it binds the lacIq repressor, inactivating it, and thus allowing tac promoter-driven transcription to take place.[664;665]

A set of plasmids based on the non-commercial p-THREE-E plasmid (A. Oliver, University of Sussex. Figure 17) was generated, carrying the *AIP* CDS (WT and variants) downstream the *S. japonicum GST* gene. In this plasmid, the transcription of the fused cDNA *GST-AIP* is under the control of the isopropyl-β-thiogalactoside (IPTG)-inducible *lac* promoter. The plasmids for WT AIP and the mutants p.C238Y, p.A299V, p.R304* and p.R304Q and the empty plasmid (codifying GST only) were a kind gift of C. Prodromou and collaborators (University of Sussex).

Calcium competent JM109 *E.coli* (strain pre-existent in the laboratory stocks, prepared as described in Protocol 3) were transformed with each of the GST-AIP plasmids, as described in Protocol 4, and grown overnight at 37°C. Colonies were selected and inoculated in 10 ml of LB broth with 100 µg/ml ampicillin, to be grown overnight at 37°C/250 rpm. One millilitre of each culture was used to inoculate 200 ml of LB broth with 100 µg/ml ampicillin to obtain large-scale cultures and the remaining volume was used for DNA extraction, as specified in Protocol 5. The large-scale cultures were incubated overnight and then centrifuged at 4000rpm for 10 min at room temperature (RT). The pellets were stored at -80°C until the sequences of the plasmids were confirmed.

To obtain the plasmids for the AIP mutants p.E192R and p.K266A, site-directed mutagenesis of the WT plasmid was performed using the QuikChange II XL kit (Agilent Technologies 200521), following the manufacturer's instructions, as detailed in Protocol 6. The mutagenic primers were designed using the QuikChange Primer Design tool:[666]

AIP_E192R_F: 5'- ACCGGTTGTACCGCCGGGGGCATGTGAAGG-3'
AIP_E192R_R: 5'-CCTTCACATGCCCCCGGCGGTACAACCGGT-3'
AIP_K266A_F: 5'-GTACGACGACAACGTCGCGGCCTACTTCAAGCGG-3'
AIP_K266A_R: 5'-CCGCTTGAAGTAGGCCGCGACGTTGTCGTCGTAC-3'

Colonies of XL10-Gold *E.coli* transformed with the mutagenised plasmids were selected and inoculated in 10 ml of LB broth with 100 µg/ml ampicillin, to be grown overnight at 37°C/250 rpm. As for the rest of the plasmids, these cultures were used for inoculating large-scale cultures and for DNA extraction, and pellets obtained from the large scale cultures were stored frozen at -80°C. The plasmids for p.E192R and p.K266A were submitted for Sanger sequencing at the Genome Centre sequencing facility (Barts and The London School of Medicine), using the following primers:

pGEX-5_F: 5'-CTGGCAAGCCACGTTTGG
pGEX-5_R: 5'-GGAGCTGCATGTGTCAGAG

The sequences of the rest of the plasmids were obtained from C. Prodromou and collaborators (University of Sussex). Once all the sequences had been confirmed, the frozen bacterial pellets were used for DNA extraction, as described in Protocol 7.

Production and purification of GST-AIP proteins

To optimise the conditions for protein production, calcium competent protease-negative BL-21 *E. coli* (Bioline BIO-85031) were transformed with p.THREE-E-WT_AIP (as described in Protocol 4). Two colonies were selected, inoculated in 5 ml of LB broth with 100 µg/ml ampicillin and grown at 37°C/250 rpm. Twelve hours later, 1 M IPTG was added to one of the tubes to a final concentration of 1 mM, and the incubation was continued at 20, 22 or 28°C. At, 0, 5, 10, 20, 30 and 40 h after the addition of IPTG, 500 µl samples were taken from each culture, pelleted (13000 g for 2 min) and stored at -20°C until the end of the experiment. Finally, the bacterial pellets were defrosted, the cells were disrupted in 100 µl of 1X SDS gel loading buffer, denatured for 5 min at 100°C and resolved by polyacrylamide gel electrophoresis (PAGE), as detailed in Protocol 8. The PAGE gels underwent Coomassie staining (see Protocol 9) and the band corresponding to the size of AIP was compared between the IPTG-induced and the non-induced cultures at each time point for each induction temperature (Figure 18). Based on these results, an induction temperature of 20°C was selected, and used for protein production.

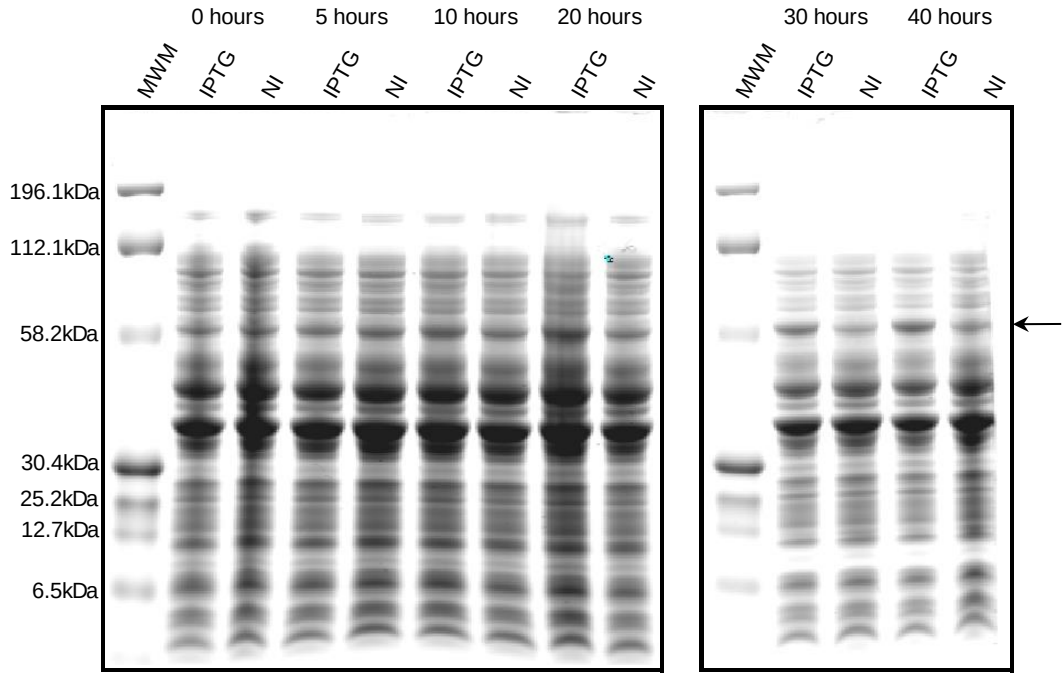

Figure 18. Optimisation of growth and IPTG induction conditions for protein production. Bacteria transformed with pTHREE-E-WT_AIP plasmid were grown for 12 h and then induced with 1 mM IPTG (IPTG) or not induced (NI) at 20°C. Samples were taken at 0, 5, 10, 20, 30 and 40 h post-induction. Whole bacterial lysates were resolved in a 10% bis-tris polyacrylamide gel and Commassie blue stained. The arrow indicates the location of the expected AIP band (64.8 kDa). MWM: molecular weight marker.

Protein production and purification were carried out at the Genome Damage and Stability Centre, University of Sussex, following the procedures detailed in Protocol 10. For each of the GST-AIP and GST plasmids, calcium competent protease deficient BL21-PLyss *E. coli* were transformed, and all the transformed colonies were collected and used as a starter culture to inoculate 3 l of LB broth with 100 µg/ml ampicillin. Bacteria were grown at 37°C/250 rpm until OD600 0.6-0.8, then IPTG was added to a final concentration of 1 mM and incubation was

continued at 20°C overnight. Bacteria were pelleted and lysed by sonication, and the lysates were cleared by centrifugation. Lysates underwent affinity purification using glutathione sepharose, and the purified proteins were eluted with a glutathione-containing buffer and concentrated. The affinity-purified samples, except the GST protein, underwent gel filtration chromatography to eliminate protein aggregates, with reduced biological activity. Chromatography fractions were resolved by PAGE and Coomassie blue staining, and the fractions containing the expected proteins were pooled, concentrated and frozen for later use (Figure 19 and Figure 20). The yield of GST-AIP C238Y was poor and the protein looked insufficiently purified, so it was not used in subsequent experiments. GST protein, eluted in glutathione-containing buffer, was dialysed against 1 l of 1M NaCl/1M Tris-HCl pH 7.5 overnight at 4°C in agitation (10K MWCO Slide-A-Lyzer dialysis cassette [Thermo Scientific 66383]), and concentrated; 5% glycerol was added and the sample was frozen for later use.

The identity of the synthetic proteins obtained was verified by Western blot (WB, details in Protocol 11), using the following antibodies and concentrations (Figure 21):

- Primary antibodies: mouse monoclonal anti-AIP/ARA9 antibody (35-2) (Novus Biologicals NB100-127) and rabbit polyclonal anti-GST antibody (1-109) (Santa Cruz Biotechnologies sc-33613), both 1:1000 (v/v).
- Secondary antibodies: IRDye® 680 RD Goat anti-Mouse IgM (µ chain specific) (LI-COR 926-68180) IRDye® 800CW Goat anti-Rabbit IgG (H + L) (LI-COR 926-32211), both 1:20000 (v/v).

GST pull-down assays

The experimental procedure was based on a classic protocol[667] and optimised by varying the starting material and washes to obtain a consistent pattern of visible bands in Coomassie blue stained polyacrylamide gels. Using the experimental conditions detailed in Protocol 12, six different assays were performed, using no bait or GST, GST-WT AIP, GST-AIP K266A, GST-AIP A299V, GST-AIP R304* and GST-AIP R304Q as bait proteins, respectively. Briefly, cell lysates obtained from $12X10^6$ GH3 cells (*R.norvegicus* somatotropinoma-derived) were pre-cleaned with glutathione beads, and then incubated for 4 h with 10 µl of each bait protein, pre-bound to glutathione beads. The beads were washed and eluted in a glutathione-containing buffer. The pull-down assay was repeated four times for each bait protein and the eluates of the four experiments were pooled together and dialysed against 1X PBS, as reduced glutathione and Tris-HCl present in the elution buffer are not compatible with isobaric mass tagging reagents. Finally, the samples and the unbound fractions were resolved by PAGE and analysed in Coomassie-stained gels (Figure 22). The total protein content of the cleared lysate used for each pull-down experiment was ~2 mg. Additionally, samples from all the steps of one of the pull-down experiments using GST- WT AIP as bait were analysed by WB to verify the presence of HSP90, a known molecular partner of AIP, using the mouse monoclonal HSP 90α/β (F-8) antibody (Santa Cruz Biotechnologies sc-13119) at a concentration of 1:1000 (v/v), according to Protocol 11 (Figure 23).

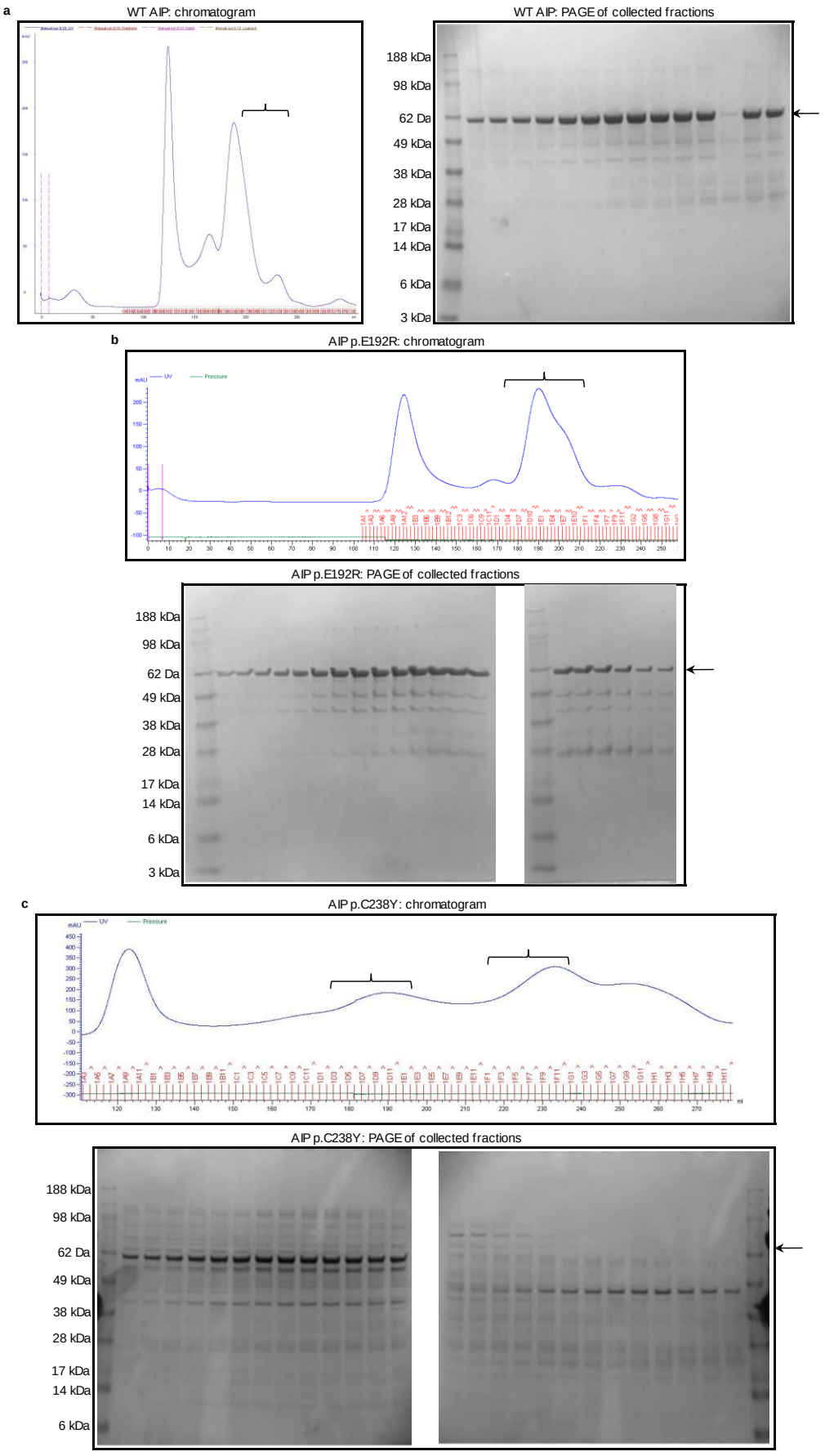

Figure 19. Gel filtration chromatography 1. WT AIP (a), AIP p.E192R (b) and AIP p.C238Y (C). Collected fractions are marked with brackets in the chromatograms, 5 µl of each fraction were resolved in a 4-12% bis-tris gel and Coomassie blue stained. Arrow: expected size of GST-AIP. Ladder is in the first lane of each gel, except for the last gel.

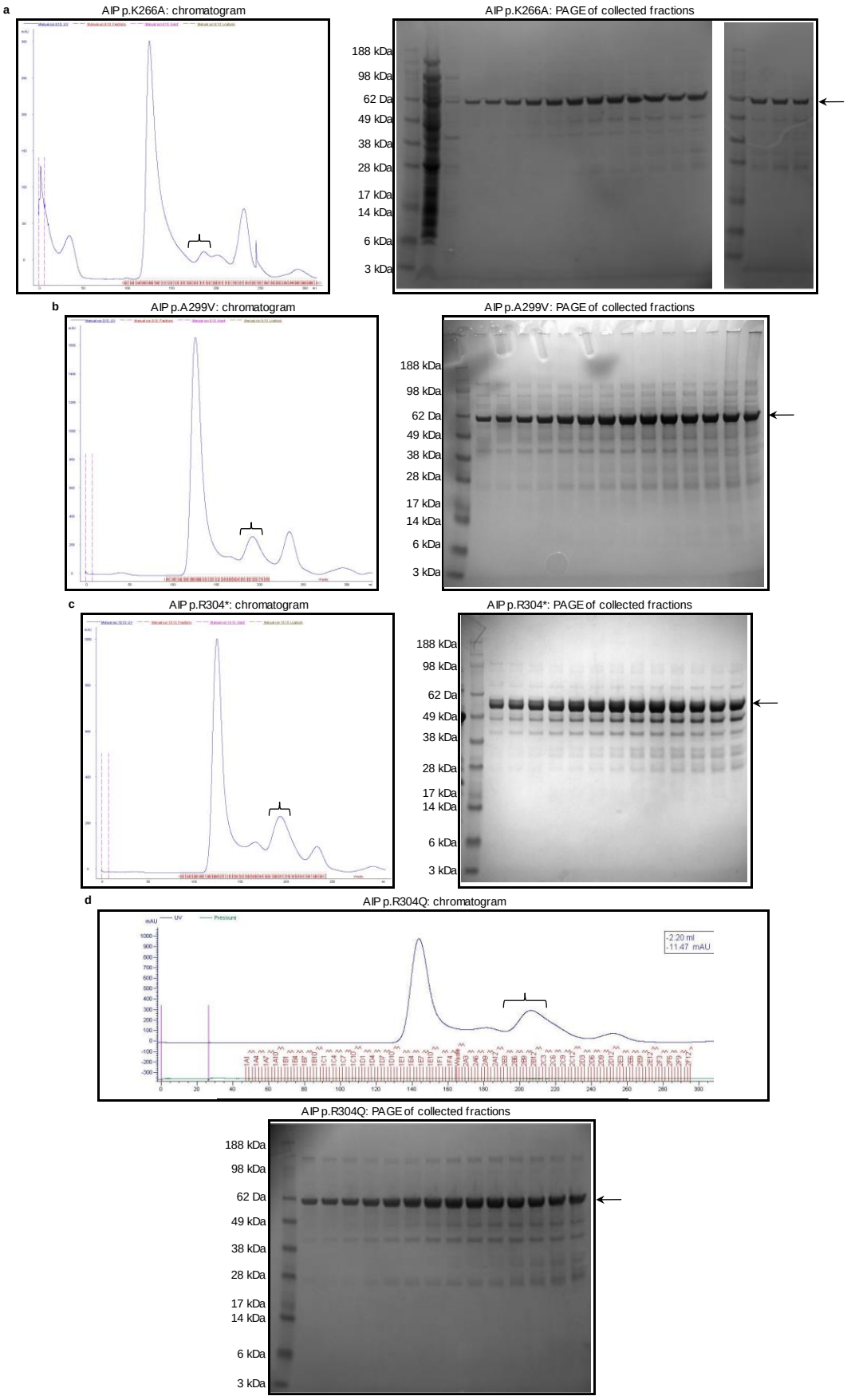

Figure 20. Gel filtration chromatography 2. AIP K266A (a), AIP p.A299V (b), AIP p.R304Q (c) and AIP p.R304* (d). Collected fractions are marked with brackets in the chromatograms, 5 µl of each fraction were resolved in a 4-12% bis-tris gel and Coomassie blue stained. Arrow: expected size of GST-AIP. Ladder is in the first lane of each gel. Gel for p.K266A includes a sample of the flow-through of the affinity purification (second lane).

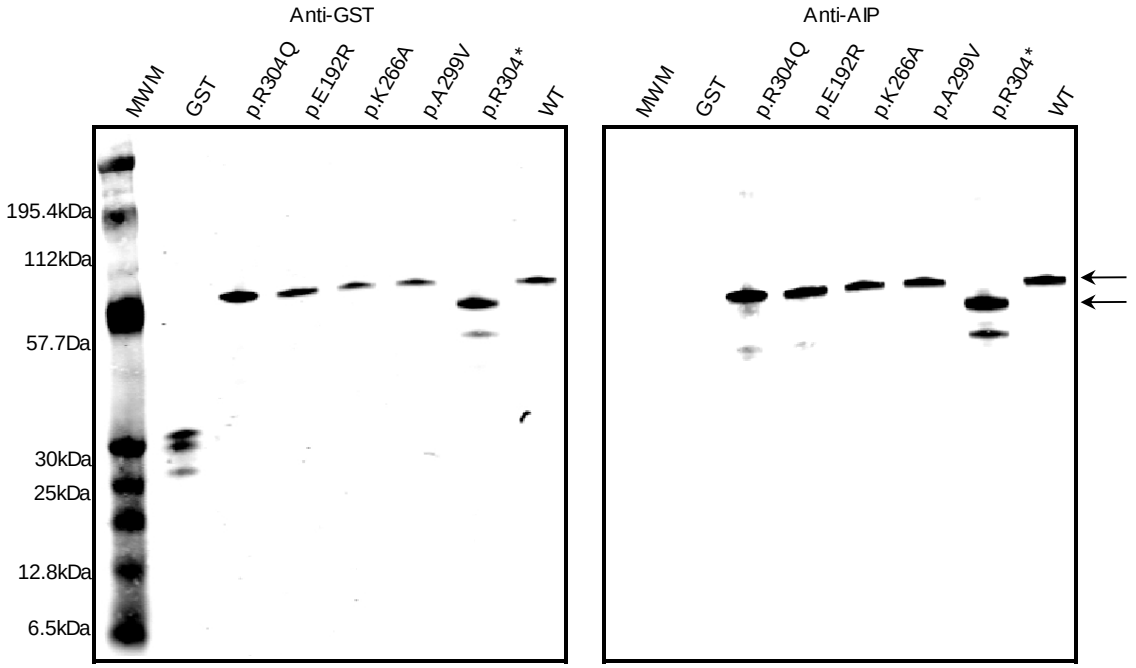

Figure 21. WB to confirm the identity of the synthetic GST-proteins. Two hundred nanograms of each purified protein were resolved in an 4-12% bis-tris polyacrylamide gel and used for WB (see text). The membrane for the anti-GST WB is on the left panel, and the membrane for the anti-AIP WB is on the right panel. The arrows mark the position of the normal-sized GST-AIP proteins (upper arrow, 64.8 kDa) and the truncated GST-AIP p.R304* protein (lower arrow, 61.5 kDa). Mass of GST (second lane of the left panel) is 26.8 kDa.

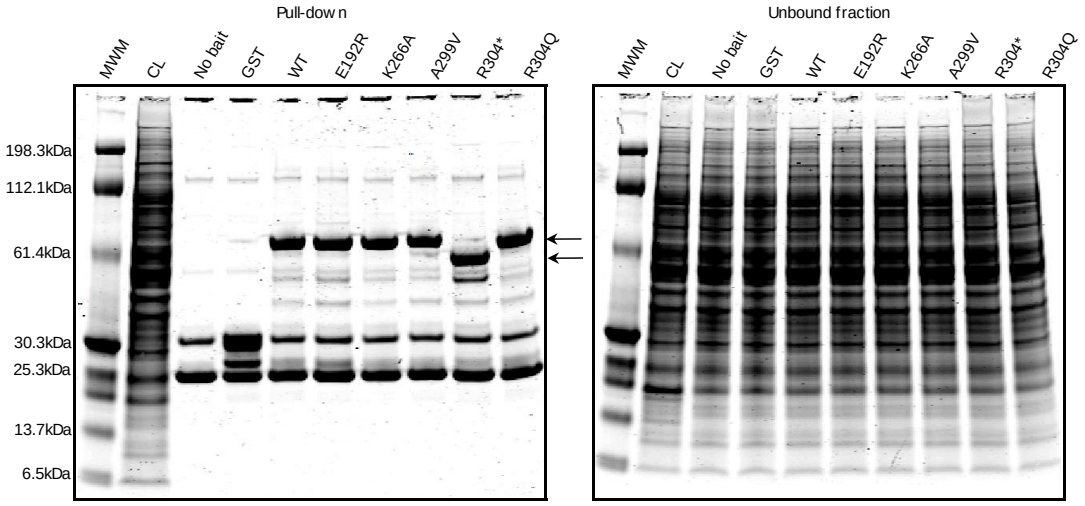

Figure 22. Pull-down assays. Pull-down experiments were carried out using the final experimental conditions. On the left panel, the total pull-down products, eluted in loading buffer, are shown. The arrows mark the position of the normal-sized GST-AIP proteins (upper arrow, 64.8 kDa) and the truncated GST-AIP p.R304* protein (lower arrow, 61.5 kDa). On the right panel, the unbound fractions are presented for comparison. The samples were resolved in a 4-12% bis-tris polyacrylamide gel and Commassie blue stained. CL: cleared lysate.

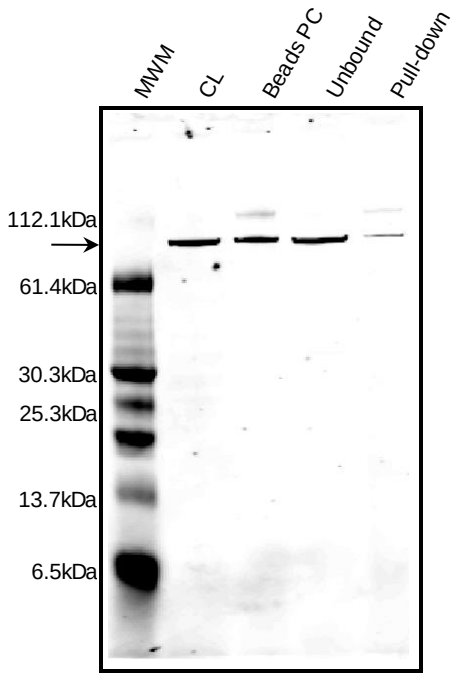

Figure 23. Anti-HSP90 WB in pull-down fractions. HSP90 was detected in a sample of cleared lysate (CL, ~15 µg), in an eluate from the beads used to pre-clean the lysate (beads PC, ~20 µl), in the unbound fraction (20 µl) and in the pull-down (total reaction eluted in 20 µl). The samples were resolved in a 4-12% bis-tris polyacrylamide gel and used for anti-HSP90 WB (see text).

Tandem mass tagging and quantitative mass spectrometry analysis

Tandem mass tagging (TMT)[668] and qMS were carried out at the King's College London Denmark Hill Proteomics Facility. Ten micrograms of each of the six protein eluates obtained from the pull-down experiment were labelled with a different TMT tag, and the six samples were pooled together after labelling. The pooled sample was loaded in two lanes of a 4-12% bis-tris polyacrylamide gel and separated by PAGE. The gel was stained with Coomassie blue and the two lanes containing the samples were cut in 15 transversal slices. The samples were then lyophilised, rehydrated, destained and trypsin-digested. Finally, the resulting peptides were extracted from the gel and stored at -80°C until analysed. The complete method for TMT, in gel trypsin digestion and peptide extraction can be found in Protocol 15.

For MS analysis, the samples were separated by liquid chromatography (LC) in a gradient of acetonitrile in formic acid. Peptides underwent electrospray ionisation (ESI) using a Z-spray source and ion trap MS/MS was conducted using an Orbitrap Velos Pro (Thermo Scientific) instrument. The MS/MS analyses were conducted using collision energy profiles that were chosen based on the mass-to-charge ratio (*m/z*) and the charge state of the peptide. The qMS data were processed using the Proteome Discoverer version 1.3.0.339 (Thermo Scientific) software, obtaining the following number of filtered/unfiltered result items:

- 102/117 Protein groups
- 2568/2568 Merged proteins
- 2377/2377 Peptides
- 3967/3967 PSM

- 6981/6981 Search inputs

The following parameters were applied to generate the spectrum files:

- Peptide Grouping Options
    - Show peptide groups: True
    - Group peptides by: Mass and Sequence
- Protein Grouping Options
    - Enable protein grouping: True
    - Consider leucine and isoleucine as equal: True
    - Consider only PSMs with confidence at least: Medium
    - Consider only PSMs with delta Cn better than: 0.15
    - Apply strict maximum parsimony principle: True

Then, spectra were selected using the following filters:

- Min. Precursor Mass: 700 Da
- Max. Precursor Mass: 10000 Da
- Total Intensity Threshold: 100
- Minimum Peak Count: 8

The peptides' sequences generated were searched in the UniProt[510] database using the Mascot v.2.2 platform.[669] The following Mascot search parameters were used:

- Protein Database: uniprot_sprot
- Enzyme Name: Trypsin
- Maximum Missed Cleavage Sites: 3
- Instrument: ESI-TRAP
- Taxonomy: all entries
- Peptide Scoring Options:
    - Peptide Cut Off Score: 10
    - Peptide Without Protein Cut Off Score: 5
- Protein Scoring Options:
- Use MudPIT Scoring: Automatic
- Protein Relevance Threshold: 20
- Protein Relevance Factor: 1
- Tolerances:
    - Precursor Mass Tolerance: 5 ppm
    - Fragment Mass Tolerance: 0.5 Da
- Dynamic Modifications: deamidated (NQ), oxidation (M), TMT6plex intact labelling (K)
- Static Modifications: carbamidomethyl (C), TMT6plex intact labelling (Protein N-term)
- Taxonomy: *Rattus norvegicus*.
- Variable modifications: carbamidomethyl (C), Gln->pyro=Glu (N-termQ), oxidation (M), TMT6plex (K), TMT6plex (protein N-term)

The list of peptides generated was quantitatively analysed by performing a new search which omitted the variable modifications TMT6plex [K] and TMT6plex [protein N-term] and adding quantitation using the parameter “TMT6plex intact protein labelling”.

Results were filtered using the Percolator function in the platform

- Maximum Delta Cn: 0.05
- Decoy Database Search:
- Target false discovery rate (FDR) (Strict): 0.01
- Target FDR (Relaxed): 0.05
- Validation based on: q-value

For reporting the quantifier ions, the following parameters were entered:

- Quantification Method: TMT 6plex PS (Custom)
- Peak Integration:
    - Integration Window Tolerance: 20 ppm
    - Integration Method: most confident centroid

All data files were processed through the in-house Perl script Mmunger (King’s College London Denmark Hill Proteomics Facility), which extracted the absolute intensity values of the TMT reporter ions from the .dat file generated by the Proteome Discoverer platform. CSV files were produced and saved, and these results were exported to a Microsoft Excel 97 file for further analysis. A manual analysis of the MS fragmentation spectra of all the peptides obtained from the Mascot search was performed by the MS Facility staff using the Scaffold (Proteome Software) software. Only peptides with the following criteria were considered valid further analysis: a Mascot score ≥20 and a valid MS spectrum. The Mascot score is defined as the probability that the observed match is a random event, reported as -10*log10 (probability). Proteins with three or more assigned peptides were considered as highly probable candidates.

Selection of candidates

The peptides considered valid were grouped in proteins, and these proteins were listed in decreasing order, according to the number of assigned peptides. Those proteins with three or more assigned peptides were considered as highly probable candidates. The intensity values for each TMT tag were matched to the corresponding *AIPmut* and GST control used in the pull-down experiments and labelled as follows: TMT126=GST, TMT127=WT, TMT128=K266A, TMT129=A299V, TMT130=R304*, TMT131=R304Q. When a single peptide was reported several times, an average of the intensity values was calculated for each tag. For normalisation against the negative control, the intensity value obtained for the GST experiment was subtracted from the value obtained for WT AIP and each of the mutants. Peptides showing intensity values below 0 for all the tags after normalisation were discarded. Then, the normalised values for each of the mutants were divided by the normalised value for the WT

protein. Those peptides showing significant differences between the intensity values for AIP and the pathogenic variant R304* (≥1.5 fold, positive or negative) or present in the WT protein and absent in the mutant, or vice versa, were also considered of interest. When none of the peptides assigned to one candidate protein was identified in the WT AIP pull-down experiment, or when the normalised intensity value for all the peptides assigned to one protein was ≤0, the protein was discarded from the list of candidates. The Ingenuity Pathways Analysis platform[670] was used for grouping the identified proteins in signalling pathways. The human homologues of the candidates selected were identified using the Blast tool in the UniProt database.[510] The best match was selected in each case, and the rest of the experiments are based on these human homologues.

Generation of plasmids for co-immunoprecipitation

Candidate AIP partners selected from the previous analysis underwent a validation process using co-IP and/or co-localisation. For the co-IP experiments, a previously existent plasmid containing the Myc tag upstream the WT AIP CDS (pcDNA3.0-Myc-AIP_WT) was co-transfected in HEK293 cells (human embryo kidney, ECACC 85120602) together with the human influenza hemagglutinin (HA) tag-containing plasmid pSF-CMV-NH2-HA-EKT-NcoI (Oxford Genetics OG93), in which the CDS of each of the candidate AIP partners was cloned downstream the tag. Additionally, a previously existent plasmid containing the Flag tag at the 3' end of the WT AIP CDS (pCI-neo-AIP_WT-Flag) was used for testing the dimerisation of AIP. A scheme of these plasmids is shown in Figure 24.

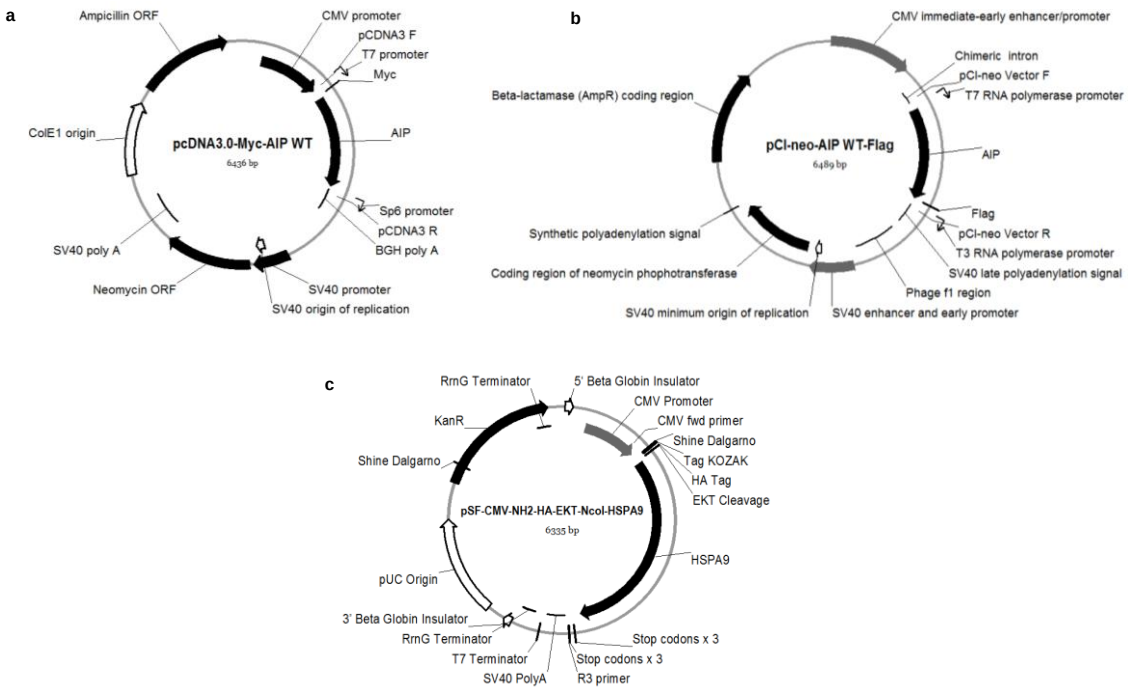

Figure 24. Map of the plasmids used in the co-IP experiments. AIP was expressed with an N-terminal Myc (a) and a C-terminal Flag (b) tags. c) Candidate AIP partners were expressed as N-terminal HA-tagged (as HSPA9 in this example). Antibiotics used for colony selection were ampicillin for plasmids a and b, and kanamycin for plasmid c.

A pcDNA3.0-Myc plasmid carrying the p.R304* AIP mutation (previously existent in the laboratory stocks) was also used for some experiments.

Three different strategies were employed for cloning the CDS of AIP candidate partners in the pSF-CMV-NH2-HA-EKT-NcoI plasmid, based on the available source of the CDS for each candidate partner: cloning from cDNA, subcloning from other plasmids using two restriction enzyme sites and creating one restriction enzyme site by PCR and then subcloning using two restriction enzyme sites. The procedures used to create each plasmid are presented in Table 13. Sequences used matched the reference sequence for each mRNA (with some exceptions, as detailed in Table 14), and codified the exact proteins reported in the candidate partners list. Mutations were corrected by site-directed mutagenesis when necessary.

Cloning from cDNA was used only for the SOD1 plasmid. As shown in Table 13, primers to amplify the whole CDS from cDNA were designed using the Primer3 v.4.0.0 software.[671] Total RNA was extracted from HEK293 cells as specified in Protocol 16. One microgram of total RNA was reverse transcribed, following the procedure specified in Protocol 18. High-fidelity PCR was carried out with 40 ng of cDNA, 3' A-overhangs were added and the PCR product was visualised in an agarose gel, according to Protocol 19. The band containing the expected PCR product was cut and DNA was extracted, according to Protocol 20. The purified band was used for TA cloning into the plasmid pCR2.1, according to Protocol 21, and calcium competent DH5α *E.coli* were transformed with the whole ligation reaction, according to Protocol 4. Bacteria were plated on agar containing 0.1 mM IPTG, 20 µg/ml 5-bromo-4-chloro-3-indolyl-beta-D-galacto-pyranoside (X-gal) and 100 µg/ml ampicillin for blue-white colony screening. White colonies were screened by colony PCR (Protocol 22), using the following primers:

pUC/M13_F: 5´-GTTTTCCCAGTCACGAC-3´
pUC/M13_R: 5´-CAGGAAACAGCTATGAC-3´

Positive colonies were inoculated in 10 ml of LB broth with 100 µg/ml ampicillin, to be grown overnight at 37°C/250 rpm, and DNA was extracted from one culture (Protocol 5); the rest of them were stored at 4°C. The purified plasmid was sent for sequencing (Genome Centre, Barts and The London School of Medicine) using the pUC/M13 primers.

The pCR2.1-SOD1 plasmid was used as a template for high-fidelity PCR (Protocol 19) to add a 5' NcoI restriction enzyme site, as specified in Table 13. The PCR product was visualised in an agarose gel, cut and purified (Protocol 20), the whole sample volume was digested with NcoI and SpeI restriction enzymes, as detailed in Protocol 23. The plasmid of destination (psF-CMV-NH2-HA-EKT-NcoI) was digested likewise, using the restriction enzymes NcoI and NheI (SpeI and NheI create complementary ends), and dephosphorylated (Protocol 23). The digestion products were resolved in a 1% agarose gel and the bands were cut and purified, as before. Finally, the purified bands were ligated (see Protocol 24).

Table 13. Plasmids used for co-immunoprecipitation of candidate AIP partners

Human protein	CDS origin	Plasmid of destination	Subcloning method	Primers	Final plasmid
AIP	-	-	-	-	pcDNA3.0-Myc-AIP_WT (1026 bp)
AIP	-	-	-	-	pCI-Neo-AIP_WT-Flag (1014 bp)
CBR1	pDONR221-CBR1 (PlasmID HsCD00044416)	pSF-CMV-NH2-HA-EKT-NcoI	PCR adding a 5' XbaI site, then XbaI digestion of PCR product and ligation in XbaI-EcoRV- digested plasmid	CBR1-XbaI_F CCGTTCTAGAATGTCGTCCGGCATCCA pUC/M13_rev CAGGAAACAGCTATGAC	pSF-CMV-NH2-HA-EKT-NcoI-CBR1
DSTN	pOTB7-DSTN (PlasmID HsCD00328071)	pSF-CMV-NH2-HA-EKT-NcoI	PCR adding a 5' NcoI site, then NcoI digestion of PCR product and ligation in NcoI-EcoRV-digested plasmid	DSTN-NcoI_F GCGACCATGGCCTCAGGAGTGCAAG pUC/M13_rev CAGGAAACAGCTATGAC	pSF-CMV-NH2-HA-EKT-NcoI-DSTN
EEF1G	pOTB7-EEF1G (PlasmID HsCD00321611)	pSF-CMV-NH2-HA-EKT-NcoI	NcoI-HincII digestion of plasmid of origin and ligation in NcoI-EcoRV-digested plasmid	-	pSF-CMV-NH2-HA-EKT-NcoI-EEF1G
FBXO3	pDONR221-FBXO3 (PlasmID HsCD00296315)	pSF-CMV-NH2-HA-EKT-NcoI	PCR adding a 5' KpnI site, then KpnI digestion of PCR product and ligation in KpnI-EcoRV-digested plasmid	FBX3-KpnI_F CGGGGTACCCCATGGCGGCCATGGAGA pUC/M13_rev CAGGAAACAGCTATGAC	pSF-CMV-NH2-HA-EKT-NcoI-FBXO3
HSPA5	pDONR221-HSPA5 (PlasmID HsCD00044236)	pSF-CMV-NH2-HA-EKT-NcoI	PCR adding a 5' KpnI site, then KpnI digestion of PCR product and ligation in KpnI-EcoRV-digested plasmid	HSPA5-KpnI_F CTGGGGTACCAGATGAAGCTCTCCCTG pUC/M13_rev CAGGAAACAGCTATGAC	pSF-CMV-NH2-HA-EKT-NcoI-HSPA5
HSPA8	pGEMT-HSPA8 (Paul Chapple's lab)	pSF-CMV-NH2-HA-EKT-NcoI	NcoI-XhoI digestion of both plasmids and ligation	-	pSF-CMV-NH2-HA-EKT-NcoI-HSPA8
HSPA9	pOTB7-HSPA9 (PlasmID HsCD00322446)	pSF-CMV-NH2-HA-EKT-NcoI	1. PCR adding a 5' NcoI site, HindIII digestion of PCR product (to eliminate 3' sequence after stop codon), NcoI digestion and ligation in NcoI-EcoRV-digested plasmid. 2. Site-directed mutagenesis to revert p.74Q>R, present in the original plasmid	Subcloning: HSPA9-NcoI_F CATGCCATGGCAATGATAAGTGCCAGCCGAG pUC/M13_rev CAGGAAACAGCTATGAC Site-directed mutagenesis: HSPA9-p.74R>Q_F CAGTTATGGAAGGTAAACAAGCAAAGGTGCTGGAGAA HSPA9-p.72R>Q_R TTCTCCAGCACCTTTGCTTGTTTACCTTCCATAACTG	pSF-CMV-NH2-HA-EKT-NcoI-HSPA9
HSP90A	pGEMT-HSP90A (Paul Chapple's lab)	pSF-CMV-NH2-HA-EKT-NcoI	NcoI-XhoI digestion of both plasmids and ligation	-	pSF-CMV-NH2-HA-EKT-NcoI-HSP90A
HSP90B	pGEMT-HSP90β (Paul Chapple's lab)	pSF-CMV-NH2-HA-EKT-NcoI	PCR adding a 5'XbaI site, then XbaI-SpeI digestion of PCR product and ligation in XbaI-NheI-digested plasmid	HSP90β-XbaI_F TGCTCTAGAATGCCTGAGGAAGTGCAC pUC/M13_rev CAGGAAACAGCTATGAC	pSF-CMV-NH2-HA-EKT-NcoI-HSP90β
NEFL	pDONR221-NEFL (PlasmID HsCD00044698)	pSF-CMV-NH2-HA-EKT-NcoI	PCR adding a 5' NcoI site, then NcoI-EcoRV digestion of PCR product and plasmid and ligation	NEFL-NcoI_F CGGCCATGGCCATGAGTTCCTTCAGC pUC/M13_rev CAGGAAACAGCTATGAC	pSF-CMV-NH2-HA-EKT-NcoI-NEFL

Human protein	CDS origin	Plasmid of destination	Subcloning method	Primers	Final plasmid
NME1	pDONR201-NME1 (PlasmID HsCD00001213)	pSF-CMV-NH2-HA-EKT-NcoI	PCR adding a 5' KpnI site, then KpnI digestion of PCR product and ligation in KpnI-EcoRV-digested plasmid	NDKA-KpnI_F CGGGGTACCCCATGGCCAACTGTGAGCG pDONRE01_R: GTAACATCAGAGATTTTGAGACAC	pSF-CMV-NH2-HA-EKT-NcoI-NME1
SKP1	pDONR221-SKP1 (PlasmID HsCD00295916)	pSF-CMV-NH2-HA-EKT-NcoI	1. PCR adding a 5' NcoI site, then NcoI digestion of PCR product and ligation in NcoI-EcoRV-digested plasmid. 2. Site-directed mutagenesis to revert c.299T>C(p.L100P), present in the original plasmid	Subcloning: SKP1-NcoI_F2 TATGCCATGGCCATGCCTTCAATTAAGTT pUC/M13_rev CAGGAAACAGCTATGAC Site-directed mutagenesis: SKP1_c.299C>T_F GAAAGTTGACCAAGGAACACTTTTTGAACTCATTCTGGCTG SKP1_c.299C>T_R CAGCCAGAATGAGTTCAAAAAGTGTTCCTTGGTCAACTTTC	pSF-CMV-NH2-HA-EKT-NcoI-SKP1
SOD1	cDNA from HEK293 cells	pSF-CMV-NH2-HA-EKT-NcoI	PCR from cDNA and TA ligation in pCR2.1. PCR adding a 5' NcoI site, then NcoI-SpeI digestion of PCR product and ligation in NcoI-NheI-digested plasmid	Cloning from cDNA: SOD1_F: GTTTGCGTCGTAGTCTCCTG SOD1_R2: GGGCCTCAGACTACATCCAA Subcloning: SOD1-NcoI_F: CGAGCCATGGCGACGAAGGCC	pSF-CMV-NH2-HA-EKT-NcoI-SOD1
TUBB	pDONR221-TUBB (PlasmID HsCD00043911)	pSF-CMV-NH2-HA-EKT-NcoI	PCR adding a 5'KpnI site, then KpnI digestion of PCR product and ligation in KpnI-EcoRV-digested plasmid	TUBB-KpnI_F CGGGGTACCCCATGAGGGAAATCGTGCACA pUC/M13_rev CAGGAAACAGCTATGAC	pSF-CMV-NH2-HA-EKT-NcoI-TUBB
TUBB2A	pDONR221-TUBB2A (PlasmID HsCD00044406)	pSF-CMV-NH2-HA-EKT-NcoI	PCR adding a 5' KpnI site, then KpnI digestion of PCR product and ligation in KpnI-EcoRV-digested plasmid	TUBB2A-KpnI_F GCAGGGTACCCCATGCGCGAGATCG pUC/M13_rev CAGGAAACAGCTATGAC	pSF-CMV-NH2-HA-EKT-NcoI-TUBB2A
VAPA	pOTB7-VAPA (PlasmID HsCD00321764)	pSF-CMV-NH2-HA-EKT-NcoI	PCR adding a 5' KpnI site, then KpnI digestion of PCR product and ligation in KpnI-EcoRV-digested plasmid	VAPA-KpnI_F CGGGGTACCCCATGGCGTCCGCCTCAG pUC/M13_rev CAGGAAACAGCTATGAC	pSF-CMV-NH2-HA-EKT-NcoI-VAPA

Table 14. Details of CDS sequences used in HA-tagged expression plasmids

Protein	Genbank reference sequence (mRNA)	Genbank entry name	CDS (bp)	Amino acids	Notes
AIP	NM_003977.3	Aryl hydrocarbon receptor interacting protein (AIP), transcript variant 1	993	330	The plasmid carries the changes c.19A>C and c.21A>C, in codon 7 (AGA to CGC), with no effect on amino acid R7.This plasmid carries also the c.682C>A (Q228K) variant, which has been found in the majority of the individuals when sequencing AIP (see Chapter 2)
CBR1	NM_001757.3	Carbonyl reductase [NADPH] 1 isoform 1	834	277	Termination codon in the plasmid is TAG, instead of TGA in the reference sequence
DSTN	NM_006870.3	Destrin (actin depolymerizing factor) (DSTN), transcript variant 1	498	165	-
EEF1G	NM_001404.4	Eukaryotic translation elongation factor 1 gamma (EEF1G)	1314	437	-
FBXO3	NM_012175.3	F-box protein 3 (FBXO3), transcript variant 1	1416	471	Termination codon in the plasmid is TGA, instead of TAG in the reference sequence
HSPA5	NM_005347.4	Heat shock 70 kDa protein 5 (glucose-regulated protein, 78 kDa) (HSPA5)	1965	654	-
HSPA8	NM_006597.5	Heat shock 70 kDa protein 8 (HSPA8), transcript variant 1	1941	646	-
HSPA9	NM_004134.6	Heat shock 70 kDa protein 9 (mortalin) (HSPA9)	2040	679	The plasmid carries c.1933C>T, causing no change on L645
HSP90A	NM_005348.3	Heat shock protein 90 kDa alpha (cytosolic), class A member 1 (HSP90AA1), transcript variant 2	2199	732	-
HSP90B	NM_007355.3	Heat shock protein 90 kDa alpha (cytosolic), class B member 1 (HSP90AB1), transcript variant 2	2175	724	-
NEFL	NM_006158.4	Neurofilament, light polypeptide (NEFL)	1632	543	Termination codon in the plasmid is TAG, instead of TGA in the reference sequence
NME1	NM_000269.2	NME/NM23 nucleoside diphosphate kinase 1 (NME1), transcript variant 2	459	152	-
SKP1	NM_170679.2	S-phase kinase-associated protein 1 (SKP1), transcript variant 2	492	163	Termination codon in the plasmid is TAG, instead of TGA in the reference sequence
SOD1	NM_000454.4	Superoxide dismutase 1, soluble (SOD1)	465	154	-
TUBB	NM_178014.3	Tubulin, beta class I (TUBB), transcript variant 2	1335	444	Termination codon in the plasmid is TAG, instead of TAA in the reference sequence
TUBB2A	NM_001069.2	Tubulin, beta 2A class IIa (TUBB2A)	1338	445	The plasmid carries c.564T>G, causing no change on S188 (synonymous variant). Termination codon in the plasmid is TAG, instead of TAA in the reference sequence
VAPA	NM_194434.2	VAMP (vesicle-associated membrane protein)-associated protein A, 33 kDa (VAPA), transcript variant 2	750	249	-

The plasmids of origin for HSPA8, HSP90A and HSP90B (pGEMT-HSPA8 and pGEMT-HSP90A and pGEMT-HSP90B) were kindly donated by P. Chapple (Barts and The London School of Medicine). For HSPA8 and HSP90A, the plasmids of origin and destination were digested with the restriction enzymes NcoI and XhoI, dephosphorylating the plasmid of destination (Protocol 23), and then ligating the gel-extracted fragments (Protocol 24). For HSP90B, a forward primer was designed to create a 5' XbaI restriction site and amplify the CDS with pUC/M13_R as a reverse primer (Protocol 19). The gel-extracted PCR product was digested with XbaI and Spe I and the plasmid of destination underwent XbaI-NheI digestion and dephosphorylation (Protocol 23). The gel-extracted fragments were ligated as above.

To obtain the CDS for the rest of the candidate partners to be tested, a set of plasmids was acquired from the PlasmID Repository (DNA Resource Core, Harvard Medical School). Direct subcloning with restriction enzymes was done for the plasmid containing the EEF1G CDS (pOTB7-EEF1G), by digesting the plasmid of origin with NcoI and HincII and the plasmid of destination with NcoI and EcoRV (EcoRV leaves a blunt end, that can be ligated in a cohesive end at the 3' end). The plasmid of destination was dephosphorylated and both digestion products were gel-extracted and ligated. For the rest of the plasmids, a forward primer was designed to create a 5' restriction enzyme site suitable for subcloning the CDS contained in each plasmid. Primers normally used for sequencing these plasmids were employed as reverse primers for CDS amplification. The PCR products were purified, digested and gel-extracted and finally ligated in appropriately digested and dephosphorylated pSF-CMV-NH2-HA-EKT-NcoI (see Table 13 for details).

For all the inserts subcloned in pSF-CMV-NH2-Ha-EKT-NcoI, the whole ligation reactions were used for transforming DH5α *E.coli* (Protocol 4). Bacteria were plated on 50 µg/ml kanamycin-containing agar plates and grown overnight at 37°C. Colonies were screened by colony PCR (Protocol 22), using the following primers:

CMV_F: 5'- CGCAAATGGGCGGTAGGCGTG-3'
R3: 5'- AGCTGAAGGTACGCTGTATC-3'

Positive colonies were inoculated in 10 ml of LB broth with 50 µg/ml kanamycin and grown overnight at 37°C/250 rpm. DNA was extracted from nine millilitres of one of these cultures (Protocol 5), and 1 ml was inoculated in 200 ml of LB broth with 50 µg/ml kanamycin to be grown overnight at 37°C/250 rpm, pelleted and frozen, awaiting sequence confirmation. The rest of the cultures were kept at 4°C. Finally, the plasmids were sent for sequencing using the CMV_F and R3 primers (Genome Centre, Barts and The London School of Medicine). DNA extraction from the frozen bacterial pellets for all the plasmids (large-scale cultures) was carried out once the sequences had been confirmed, as described in Protocol 7. The plasmids pSF-CMV-NH2-HA-EKT-NcoI-HSPA9 and SKP1 underwent site-directed mutagenesis (Protocol 6) to

correct probably damaging changes in the CDS that were present in the plasmids of origin (see Table 13 for details).

Co-immunoprecipitation

For most of the experiments, a total of 20 µg of an equimolar mixture (considering the size of the CDS) of plasmids containing AIP and one or more plasmids containing the candidate partners were transfected in $10X10^6$ HEK293 cells, plated 24 h before in a T175 flask. The cells were harvested one day later by trypsinisation and lysed in 1.5ml of lysis buffer. The crude lysates were cleared by centrifugation and then cleaned by incubation with 50 µl of Protein G beads. The cleared lysate was divided in three 1.5ml tubes and mixed with 5 µg anti-Myc or anti-HA mouse monoclonal antibodies, or mouse anti-IgG, as appropriate. A small volume of cleared lysate was reserved for protein quantification and WB. The reactions were incubated for 1 h at 4°C and then transferred to a tube with 50 µl of protein G beads and incubated overnight at 4°C on a rotator. The supernatant was discarded and the beads were washed three times with lysis buffer and once with PBS, and finally the samples were denatured and eluted in 30 µl of 2X SDS loading buffer at 95°C. The eluates were resolved by PAGE and anti-Myc and anti-HA WB, including a sample of the cleared lysate (input).

Only those experiments with positive bands for the anti-Myc and anti-HA co-IP in both WBs, and negative IgG controls, were considered as real interactions by this method. The general co-IP protocol is detailed in Protocol 25. Co-IP was also done with this method to test AIP dimerisation, using the Myc-tagged and Flag-tagged AIP expression plasmids. The amount of DNA transfected and the number of cells varied between experiments to ensure the presence of clear bands in the WB images. Positive co-IP experiments for new protein partners were repeated at least once for confirmation.

Co-IP experiments in GH3 cells with a TOMM20 10mer peptide (AQSLAEDDVE) or 0.8% formaldehyde as crosslinkers were also carried out to test AIP dimerisation, using the Myc-tagged and Flag-tagged AIP plasmids, as detailed in Protocol 26 and Protocol 27.

AIP indirect protein-protein interactions

To investigate possible HSP90-mediated indirect interactions of AIP, a triple co-IP experiment was performed, involving AIP, HSP90 and a known HSP90 partner, the cAMP-dependent PKA catalytic subunit alpha (PRKACA). For this purpose, two-step site directed mutagenesis (following Protocol 6) of the pSF-CMV-NH2-HA-EKT-NcoI-PRKACA (plasmid pre-existent in the laboratory stocks) was carried out to obtain a Flag-tagged plasmid (pSF-CMV-NH2-Flag-EKT-NcoI-PRKACA), as shown in Figure 25. The primers used for the first step of site-directed mutagenesis were:

del882-899_F: 5’-GGAGGTACTCACGATGGATTATGCGGATGACG-3’

del882-899_R: 5’-CGTCATCCGCATAATCCATCGTGAGTACCTCC-3’

The mutagenised plasmid underwent a second site-directed mutagenesis using the primers:

HA_to_Flag_F 5’-GGAGGTACTCACGATGGATTATAAGGATGACG-3’
HA_to_Flag_R 5’-CGTCATCCTTATAATCCATCGTGAGTACCTCC-3’

The expected sequences were confirmed and the plasmid was produced as described before.

Figure 25. HA to Flag site-directed mutagenesis. In the plasmid of origin (top panel), the sequence between the end of the HA tag and the NcoI restriction site (PDYADDDD) is very similar to the sequence of the Flag tag (MDYKDDDD). Therefore, the HA tag was deleted from Y to P, and in a second step, A (GCG) was mutagenised to K (AAG) to obtain a Flag tag. Black background: HA and Flag tags; grey background: start of the AIP CDS.

Co-localisation

Co-localisation experiments using immunocytofluorescence were carried out to verify interactions with the proteins NEFL and TUBB2A, which are known to have a specific cellular distribution (cytoskeletal filaments), different to the distribution described for AIP. For these experiments, $5X10^4$ HEK293 cells were plated on each of the wells of a chamber slide and grown for 48 h. The cells were fixed with 4% formaldehyde, permeabilised, blocked with goat serum and incubated overnight with primary antibodies against AIP and one of the candidate partners. The cells were washed, incubated with fluorescent secondary antibodies, washed again, counterstained with 4',6-diamidino-2-phenylindole (DAPI) and mounted for confocal microscopy analysis, as detailed in Protocol 28. Z-stack images were obtained and reconstructed using the ImageJ v.1.47 software.[672] Co-localisation was analysed on representative slices of the z-stacks, employing the JACoP (Just Another Colocalization Plugin) plugin,[673] using the Pearson’s correlation coefficient and the overlap coefficient.[673;674]

Results

Identification of candidate partners for AIP

The manually validated qualitative MS results (peptides grouped by proteins) are presented in Table 25 (Appendix 1), accounting for a total of 155 proteins identified. For some of the proteins with low coverage, one peptide was assigned to more than one protein. The qualitative analysis was used with two purposes: first, to filter the results, eliminating those peptides present with higher intensity values in the negative control (GST) compared to the samples, and second, to compare the normalised values (once the values for the negative control had been subtracted)

between the different pull-down baits. Table 15 lists the 35 proteins identified as candidate AIP partners (considering the results for the WT protein only) after the filters were applied, according to the Mascot search with taxonomy *R. norvegicus*. The proteins in grey cells are considered highly probable candidates (including two known AIP partners), because of having three or more assigned peptides. Different isoforms of GST were identified, but they were considered artefacts due to the use of a GST tag for the pull-down experiments. The peptides identified for each protein are listed in the last column. The human homologues for each of the candidate AIP partners identified were searched in UniProt[510]. The human homologues and the percentage of identity with the rat proteins are presented in Table 16.

Table 15. Candidate AIP partners and peptides identified by qMS

#	UniProt entry[510]	Protein description (gene name)	Mass (kDa)[510]	Peptides identified
1	P60711	ACTB_RAT Actin, cytoplasmic 1(*Actb*)	41.7	VAPEEHPVLLTEAPLNPKANR
				KDLYANTVLSGGTTMYPGIADR
2	Q5FWY5	AIP_RAT AH receptor-interacting protein (*Aip*)	37.6	EDGIQK
				AKAVPLIHQEGNR
				GELPEFQDGTK
				GKAHAAVWNAQEAQADFAK
				GKAHAAVWNAQEAQADFAKVLELDPALAPVVSR
3	P29419	ATP5I_RAT ATP synthase subunit e, mitochondrial (*Atp5i*)	8.3	ELAEAEDVSIFK
4	P15999	ATPA_RAT ATP synthase subunit alpha, mitochondrial (*Atp5a1*)	59.8	VGLKAPGIIPR
5	P35434	ATPD_RAT ATP synthase subunit delta, mitochondrial (*Atp5d*)	17.6	ANLEKAQSELSGAADEAAR
6	P47727	CBR1_RAT Carbonyl reductase [NADPH] 1 (*Cbr1*)	30.6	EDKILLNACCPGWVR
				ELLPIIKPQGR
				GHEAVKQLQTEGLSPR
				GVHAKEGWPNSAYGVTKIGVTVLSR
				KFLGDVVLTAR
				REDKILLNACCPGWVR
				SCSPELQQKFR
7	P08649	CO4_RAT Complement C4 (*C4*)	192.2	ADLEKLTSLSDR
8	Q497C3	CP013_RAT UPF0585 protein C16orf13 homolog	22.6	MVDMPANNKCLIFR
				NKEPILCVLR
9	P63255	CRIP1_RAT Cysteine-rich protein 1(*Crip1*)	8.6	GGAESHTFK
10	Q68FR6	EF1G_RAT Elongation factor 1-gamma (*Eef1g*)	50.1	KLDPGSEETQTLVR
				AFKALIAAQYSGAQIR
				ILGLLDTHLKTR
				KFPAGKVPAFEGDDGFCVFESNAIAYYVSNEELR
11	D4ABP9	FBX3_RAT F-box only protein 3 (*Fbxo3*)	55.4	EEDLDAVEAQIGCKLPDDYR
				ITNAKGDVEEVQGPGVVGEFPIISPGR
12	Q99PF5	FUBP2_RAT Far upstream element-binding	74.2	KDAFADAVQR

#	UniProt entry[510]	Protein description (gene name)	Mass (kDa)[510]	Peptides identified
		protein 2 (*Khsrp*)		
13	P48721	GRP75_RAT Stress-70 protein, mitochondrial (*Hspa9*)	73.9	EMAGDNKLLGQFTLIGIPPAPR
				QATKDAGQISGLNVLR
				MPKVQQTVQDLFGR
				KDSETGENIR
				QAVTNPNNTFYATKR
14	P06761	GRP78_RAT 78 kDa glucose-regulated protein (*Hspa5*)	72.3	KSDIDEIVLVGGSTR
				IINEPTAAAIAYGLDKR
				NQLTSNPENTVFDAKR
				AKFEELNMDLFR
15	P14942	GSTA4_RAT Glutathione S-transferase alpha-4 (*Gsta4*)	25.5	APQEKEESLALAVKR
				EESLALAVKR
16	P04905	GSTM1_RAT Glutathione S-transferase Mu 1 (*Gstm1*)	25.9	FKLGLDFPNLPYLIDGSR
				LAQWSNK
				KHHLCGETEEER
				KITQSNAIMR
				ISAYMKSSR
				YLSTPIFSKLAQWSNK
17	P08009	GSTM4_RAT Glutathione S-transferase Yb-3 (*Gstm3*)	25.7	MAIWGSK
				LKPGYLEQLPGMMR
				FLPRPLFTKMAIWGSK
				NQVFEATCLDAFPNLKDFIAR
18	P04906	GSTP1_RAT Glutathione S-transferase P (*Gstp1*)	23.4	SLGLYGKDQKEAALVDMVNDGVEDLR
				AFLSSPDHLNRPINGNGKQ
				DQKEAALVDMVNDGVEDLR
				STCLYGQLPKFEDGDLTLYQSNAILR
19	P34058	HS90B_RAT Heat shock protein HSP 90-beta (*Hsp90ab1*)	83.3	ELISNASDALDKIR
20	P63018	HSP7C_RAT Heat shock cognate 71 kDa protein (*Hspa8*)	70.9	MVNHFIAEFKR
				QATKDAGTIAGLNVLR
				NQVAMNPTNTVFDAKR
				GTLDPVEKALR
				LIGDAAKNQVAMNPTNTVFDAKR
21	Q5FVL7	KTU_RAT Protein kintoun (*Dnaaf2*)	89.3	EWYWGLNKDSLEER
22	Q9QX69	LANC1_RAT LanC-like protein 1 (*Lancl1*)	45.2	AFPNPYADYNKSLAENYFDSTGR
23	Q05982	NDKA_RAT Nucleoside diphosphate kinase A (*Nme1*)	17.2	TFIAIKPDGVQR
24	P19527	NFL_RAT Neurofilament light polypeptide (*Nefl*)	61.3	KGADEAALAR
				LAAEDATNEKQALQGER
				FTVLTESAAKNTDAVR
				AAKDEVSESR
				QKHSEPSR
25	P63324	RS12_RAT 40S ribosomal protein S12 (*Rps12*)	14.5	LGEWVGLCKIDR
26	P13471	RS14_RAT 40S ribosomal protein S14 (*Rps14*)	16.3	TKTPGPGAQSALR

#	UniProt entry[510]	Protein description (gene name)	Mass (kDa)[510]	Peptides identified
27	P60868	RS20_RAT 40S ribosomal protein S20 (*Rps20*)	13.4	SLEKVCADLIR
28	P05765	RS21_RAT 40S ribosomal protein S21 (*Rps21*)	9.1	LAKADGIVSKNF
29	P62859	RS28_RAT 40S ribosomal protein S28 (*Rps28*)	7.8	NVKGPVREGDVLTLLESER
30	Q6PEC4	SKP1_RAT S-phase kinase-associated protein 1 (*Skp1*)	18.7	KTFNIKNDFTEEEEAQVR
31	P07632	SODC_RAT Superoxide dismutase [Cu-Zn] (*Sod1*)	15.9	GGNEESTKTGNAGSR
32	P85108	TBB2A_RAT Tubulin beta-2A chain (*Tubb2a*)	49.9	INVYYNEAAGNKYVPR
33	Q6P9T8	TBB4B_RAT Tubulin beta-4B chain (*Tubb4b*)	49.8	INVYYNEATGGKYVPR
34	P69897	TBB5_RAT Tubulin beta-5 chain (*Tubb5*)	49.7	ISVYYNEATGGKYVPR
35	Q9Z270	VAPA_RAT Vesicle-associated membrane protein-associated protein A (*Vapa*)	27.8	FKGPFTDVVTTNLKLQNPSDR
				QDGPLPKPHSVSLNDTETR

Table 16. Candidate AIP partners in *R. norvegicus* and their human homologues

#	*R. norvegicus proteins*		*Human homologues*			
	UniProt entry[510]	Protein description (gene name)	% of identity	UniProt entry[510]	Protein description (gene name)	Mass (kDa)
1	P60711	ACTB_RAT Actin, cytoplasmic 1 (*Actb*)	100	P60709	ACTB_HUMAN Actin, cytoplasmic 1 (*ACTB*)	41.7
2	Q5FWY5	AIP_RAT AH receptor-interacting protein (*Aip*)	94	O00170	AIP_HUMAN AH receptor-interacting protein (*AIP*)	37.6
3	P29419	ATP5I_RAT ATP synthase subunit e, mitochondrial (*Atp5i*)	83	P56385	ATP5I_HUMAN ATP synthase subunit e, mitochondrial (*ATP5I*)	7.9
4	P15999	ATPA_RAT ATP synthase subunit alpha, mitochondrial (*Atp5a1*)	97	P25705	ATPA_HUMAN ATP synthase subunit alpha, mitochondrial (*ATP5A1*)	59.8
5	P35434	ATPD_RAT ATP synthase subunit delta, mitochondrial (*Atp5d*)	87	P30049	ATPD_HUMAN ATP synthase subunit delta, mitochondrial (*ATP5D*)	17.5
6	P47727	CBR1_RAT Carbonyl reductase [NADPH] 1 (*Cbr1*)	86	P16152	CBR1_HUMAN Carbonyl reductase [NADPH] 1 (*CBR1*)	30.4
7	P08649	CO4_RAT Complement C4 (*C4*)	80	P0C0L4	CO4A_HUMAN Complement C4-A (*C4A*)	192.8
8	Q497C3	CP013_RAT UPF0585 protein C16orf13 homolog	90	Q96S19	CP013_HUMAN UPF0585 protein C16orf13 (*C16orf13*)	22.6
9	P63255	CRIP1_RAT Cysteine-rich protein 1 (*Crip1*)	97	P50238	CRIP1_HUMAN Cysteine-rich protein 1 (*CRIP1*)	8.5
10	Q68FR6	EF1G_RAT Elongation factor 1-gamma (*Eef1g*)	98	P26641	EF1G_HUMAN Elongation factor 1-gamma (*EEF1G*)	50.1
11	D4ABP9	FBX3_RAT F-box only protein 3 (*Fbxo3*)	91	Q9UK99	FBX3_HUMAN F-box only protein 3 (*FBXO3*)	54.6
12	Q99PF5	FUBP2_RAT Far upstream element-binding protein 2 (*Khsrp*)	98	Q92945	FUBP2_HUMAN Far upstream element-binding protein 2 (*KHSRP*)	73.1
13	P48721	GRP75_RAT Stress-70 protein, mitochondrial (*Hspa9*)	98	P38646	GRP75_HUMAN Stress-70 protein, mitochondrial (*HSPA9*)	73.7

#	*R. norvegicus proteins*		*Human homologues*			
	UniProt entry[510]	**Protein description (gene name)**	**% of identity**	**UniProt entry[510]**	**Protein description (gene name)**	**Mass (kDa)**
14	P06761	GRP78_RAT 78 kDa glucose-regulated protein (*Hspa5*)	98	P11021	GRP78_HUMAN 78 kDa glucose-regulated protein (*HSPA5*)	72.3
15	P14942	GSTA4_RAT Glutathione S-transferase alpha-4 (*Gsta4*)	60	P08263	GSTA1_HUMAN Glutathione S-transferase A1 (*GSTA1*)	25.6
16	P04905	GSTM1_RAT Glutathione S-transferase Mu 1 (*Gstm1*)	79	P09488	GSTM1_HUMAN Glutathione S-transferase Mu 1 (*GSTM1*)	25.7
17	P08009	GSTM4_RAT Glutathione S-transferase Yb-3 (*Gstm3*)	85	P28161	GSTM2_HUMAN Glutathione S-transferase Mu 2 (*GSTM2*)	25.7
18	P04906	GSTP1_RAT Glutathione S-transferase P (*Gstp1*)	86	P09211	GSTP1_HUMAN Glutathione S-transferase P (*GSTP1*)	23.4
19	P34058	HS90B_RAT Heat shock protein HSP 90-beta (*Hsp90ab1*)	99	P08238	HS90B_HUMAN Heat shock protein HSP 90-beta (*HSP90AB1*)	83.3
20	P63018	HSP7C_RAT Heat shock cognate 71 kDa protein (*Hspa8*)	99	P11142	HSP7C_HUMAN Heat shock cognate 71 kDa protein (*HSPA8*)	70.9
21	Q5FVL7	KTU_RAT Protein kintoun (*Dnaaf2*)	65	Q9NVR5	KTU_HUMAN Protein kintoun (*DNAAF2*)	91.1
22	Q9QX69	LANC1_RAT LanC-like protein 1 (*Lancl1*)	91	O43813	LANC1_HUMAN LanC-like protein 1 (*LANCL1*)	45.3
23	Q05982	NDKA_RAT Nucleoside diphosphate kinase A (*Nme1*)	95	P15531	NDKA_HUMAN Nucleoside diphosphate kinase A (*NME1*)	17.1
24	P19527	NFL_RAT Neurofilament light polypeptide (*Nefl*)	97	P07196	NFL_HUMAN Neurofilament light polypeptide (*NEFL*)	61.5
25	P63324	RS12_RAT 40S ribosomal protein S12 (*Rps12*)	99	P25398	RS12_HUMAN 40S ribosomal protein S12 (*RPS12*)	14.5
26	P13471	RS14_RAT 40S ribosomal protein S14 (*Rps14*)	99	P62263	RS14_HUMAN 40S ribosomal protein S14 (*RPS14*)	16.3
27	P60868	RS20_RAT 40S ribosomal protein S20 (*Rps20*)	100	P60866	RS20_HUMAN 40S ribosomal protein S20 (*RPS20*)	13.4
28	P05765	RS21_RAT 40S ribosomal protein S21 (*Rps21*)	95	P63220	RS21_HUMAN 40S ribosomal protein S21 (*RPS21*)	9.1
29	P62859	RS28_RAT 40S ribosomal protein S28 (*Rps28*)	100	P62857	RS28_HUMAN 40S ribosomal protein S28 (*RPS28*)	7.8
30	Q6PEC4	SKP1_RAT S-phase kinase-associated protein 1 (*Skp1*)	99	P63208	SKP1_HUMAN S-phase kinase-associated protein 1 (*SKP1*)	18.7
31	P07632	SODC_RAT Superoxide dismutase [Cu-Zn] (*Sod1*)	83	P00441	SODC_HUMAN Superoxide dismutase [Cu-Zn] (*SOD1*)	15.9
32	P85108	TBB2A_RAT Tubulin beta-2A chain (*Tubb2a*)	100	Q13885	TBB2A_HUMAN Tubulin beta-2A chain (*TUBB2A*)	49.9
33	Q6P9T8	TBB4B_RAT Tubulin beta-4B chain (*Tubb4b*)	99	P68371	TBB4B_HUMAN Tubulin beta-4B chain (*TUBB4B*)	49.8
34	P69897	TBB5_RAT Tubulin beta-5 chain (*Tubb5*)	100	P07437	TBB5_HUMAN Tubulin beta chain (*TUBB*)	49.7
35	Q9Z270	VAPA_RAT Vesicle-associated membrane protein-associated protein A (*Vapa*)	97	Q9P0L0	VAPA_HUMAN Vesicle-associated membrane protein-associated protein A (*VAPA*)	27.9

Pathways analysis

The final list of human homologues of the AIP candidate partners identified was submitted for pathway analysis, using the Ingenuity Pathways Analysis software.[670] The results of this analysis are summarised in Table 17.

Table 17. Summary of pathway analysis results

Top networks		
Associated network functions	**ID**	**Score**
Cellular assembly and organisation, nervous system development and function, free radical scavenging	1	30
Cancer, gastrointestinal disease, organismal injury and abnormalities	2	22
Cancer, reproductive system disease, cell morphology	3	2
Cell morphology, developmental disorder, drug metabolism	4	2
Hereditary disorder, neurological disease, cell death and survival	5	2
Top diseases and disorders		
Name	***P***	**No. of molecules**
Cancer	1.11E-07 - 4.48E-02	18
Gastrointestinal disease	1.11E-07 - 4.88E-02	9
Respiratory disease	2.34E-07 - 4.16E-03	7
Organismal injury and abnormalities	5.39E-07 - 4.88E-02	16
Reproductive system disease	5.39E-07 - 3.48E-02	13
Top molecular and cellular functions		
Name	***P***	**No. of molecules**
Drug metabolism	1.95E-09 - 1.24E-02	6
Protein synthesis	9.16E-06 - 4.26E-02	7
Small molecule biochemistry	1.26E-05 - 2.57E-02	9
Cell death and survival	4.15E-04 - 4.88E-02	13
Cell cycle	2.08E-03 - 3.48E-02	4
Top physiological system development and function		
Name	***P***	**No. of molecules**
Organ development	3.92E-05 - 5.01E-03	6
Behaviour	2.08E-03 - 2.88E-02	1
Tissue development	2.08E-03 - 4.88E-02	3
Tumour morphology	2.08E-03 - 2.27E-02	2
Organism survival	2.20E-03 - 2.20E-03	4
Top canonical pathways		
Name	***P***	**Ratio**
NRF2-mediated oxidative stress response	6.53E-08	7/187 (0.037)
Glutathione-mediated detoxification	1.35E-07	4/23 (0.174)
Remodelling of epithelial adherens junctions	2.34E-07	5/66 (0.076)
Aryl hydrocarbon receptor signalling	2.90E-07	6/141 (0.043)
Regulation or eIF4 and p70S6K signalling	1.05E-05	5/158 (0.032)

The top two networks reported in the analysis, including most of the protein in the list, are presented in Figure 26.

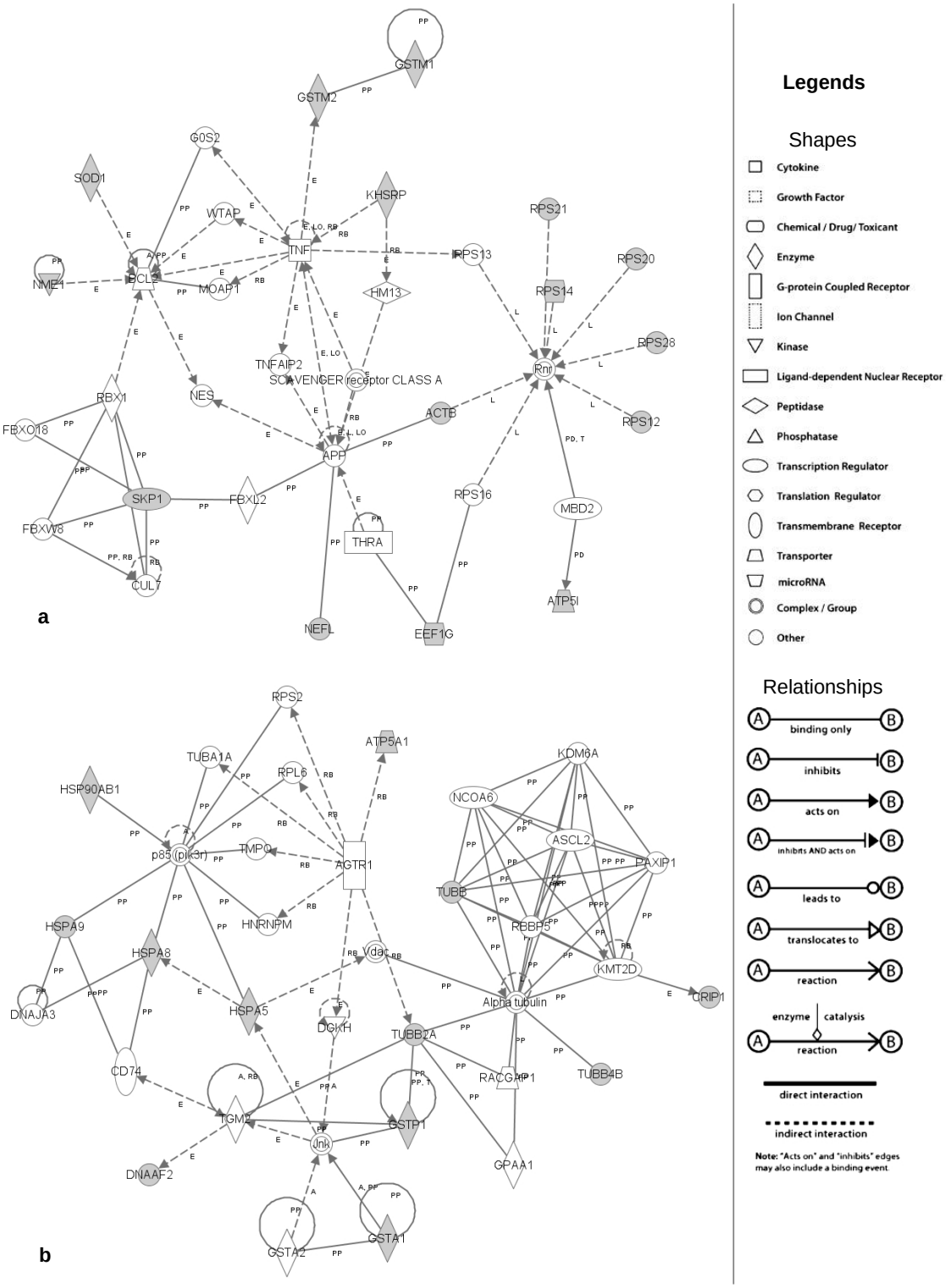

Figure 26. Pathway analysis top networks. Networks 1 (a) and 2 (b) included the majority of AIP interacting partners. Note that networks in this type of analysis denote functional relationships, and not necessarily protein-protein interactions. Proteins in grey are included in the list of AIP candidate interacting partners.

Differential interaction repertoire among AIP variants

For each pull-down experiment, a list including the normalised intensity values for all the peptides identified, grouped in proteins, was created. Intensity values for the peptides were

compared between the different experiments and expressed as fold change, considering the intensity value for each peptide in the experiment done with the WT protein as 1, as presented in Table 18; only proteins present in the WT experiment were included (all the peptides detected for those proteins, even if not present in the WT experiment, are shown). Negative normalised intensity values (higher intensity in the negative control than in the experiment) were not compared, and are shown as grey squares. Comparisons were not possible in cases where the normalised intensity value in the WT experiment was negative, and they are shown as hyphens in the table. Finally, peptides not detected at all in one experiment are presented as black squares.

The comparative table of results (Table 18) includes peptides found in all the experiments and peptides present in only one, two, three or four of the pull-down assays for AIP variants. It is difficult to analyse the relevance of these differences, as some peptides for some of the proteins were not detected in the experiment for the WT protein. Therefore, comparative results including only those proteins for which at least one peptide was detected in the WT AIP pull-down are presented as a graph in Figure 27. The differences in the intensity values of the peptides among the pull-down experiments were interpreted as differential binding of the corresponding proteins for each bait AIP protein. Proteins in bold characters in Table 18 were considered of interest, either because one or more of their assigned peptides showed a ≥1.5 fold difference in binding (positive or negative) when comparing the pathogenic AIP mutant p.R304* to the WT protein, and the other peptides in the same protein did not show an opposite pattern, or because they bound the WT but not the mutant protein.

Validation experiments

As it would be technically complex to confirm by other experimental methods all the protein-protein interactions identified, certain proteins showing differential binding were selected for validation. On this regard, the loss of interactions by the p.R304* AIP mutant was of special interest, as this is a clearly pathogenic variant. Plasmids containing the CDS for the proteins of interest were constructed as detailed in Methods. The characteristics of the tagged proteins expressed after the transfection of these plasmids are summarised in Table 19.

Validation of protein-protein interactions

AIP self-association occurs only in the presence of a chemical crosslinker

The ability of AIP to self-associate to form dimers or oligomers, in the absence of HSP90 or AHR, had been suggested before.[587] Additionally, the crystal structure of AIP TPR domain in complex with a 10mer of TOMM20 suggested the possibility that the TPR could form a biological dimer.[523] Co-IP experiments were carried out to test AIP self-association in GH3 cells (Figure 28).

Table 18. Comparative intensity values of peptides identified per bait protein

#	Protein description (gene name)	Peptide sequence	GST-normalised intensity value/WT				
			WT	K266A	A299V	R304*	R304Q
1	1433T_RAT 14-3-3 protein theta (*Ywhaq*)	EKVESELR			-		
2	1433Z_RAT 14-3-3 protein zeta/delta (*Ywhaz*)	NLLSVAYKNVVGAR		-	-		
3	**ACTB_RAT Actin, cytoplasmic 1 (*Actb*)**	VAPEEHPVLLTEAPLNPKANR	1.0	0.8	0.8	0.3	0.6
		KDLYANTVLSGGTTMYPGIADR			-		
4	AIP_RAT AH receptor-interacting protein (*Aip*)	EDGIQK	1.0	1.1	1.9	2.4	0.5
		AKAVPLIHQEGNR	1.0	26.1	36.2	11.7	8.3
		GELPEFQDGTK		-	-	-	
		GKAHAAVWNAQEAQADFAK				-	
		GKAHAAVWNAQEAQADFAKVLELDPALAPVVSR	1.0	1.9			
5	ALBU_RAT Serum albumin (*Alb*)	AFKAWAVAR		-	-	-	-
6	**ATP5I_RAT ATP synthase subunit e, mitochondrial (*Atp5i*)**	ELAEAEDVSIFK	1.0	1.3	1.9	3.0	
7	**ATPA_RAT ATP synthase subunit alpha, mitochondrial (*Atp5a1*)**	VGLKAPGIIPR	1.0	0.9	1.8	0.3	0.1
8	**ATPD_RAT ATP synthase subunit delta, mitochondrial (*Atp5d*)**	ANLEKAQSELSGAADEAAR	1.0	2.7	4.7	4.2	6.9
9	CBR1_RAT Carbonyl reductase [NADPH] 1 (*Cbr1*)	EDKILLNACCPGWVR			-		
		ELLPIIKPQGR	1.0		0.8		0.2
		GHEAVKQLQTEGLSPR			-		-
		GVHAKEGWPNSAYGVTKIGVTVLSR			-		
		KFLGDVVLTAR				-	
		REDKILLNACCPGWVR	1.0		4.1	6.4	
		SCSPELQQKFR		-	-		-
10	**CO4_RAT Complement C4 (*C4*)**	ADLEKLTSLSDR	1.0	0.3	5.7	4.2	3.2
11	CP013_RAT UPF0585 protein C16orf13 homolog	MVDMPANNKCLIFR	1.0		2.1	1.1	
		NKEPILCVLR				-	

#	Protein description (gene name)	Peptide sequence	GST-normalised intensity value/WT				
			WT	K266A	A299V	R304*	R304Q
12	**CRIP1_RAT Cysteine-rich protein 1 (*Crip1*)**	GGAESHTFK	1.0		80.5		
13	DEFI8_RAT Differentially expressed in FDCP 8 homolog (*Def8*)	QTCDK		-	-		
14	DEST_RAT Destrin (*Dstn*)	YALYDASFETKESR			-	-	
15	ECHA_RAT Trifunctional enzyme subunit alpha, mitochondrial (*Hadha*)	DLANNSSKKFYQ				-	
		LPAKPEVSSDEDIQYR			-	-	
16	EF1A2_RAT Elongation factor 1-alpha 2 (*Eef1a2*)	EGNASGVSLLEALDTILPPTRPTDKPLR			-		
17	EF1G_RAT Elongation factor 1-gamma (*Eef1g*)	KLDPGSEETQTLVR	1.0		1.7	1.1	
		AFKALIAAQYSGAQIR		-	-	-	
		ILGLLDTHLKTR			-	-	
		KFPAGKVPAFEGDDGFCVFESNAIAYYVSNEELR	1.0			0.1	
18	EF2_RAT Elongation factor 2 (*Eef2*)	YLAEKYEWDVAEAR		-	-	-	
19	**FBX3_RAT F-box only protein 3 (*Fbxo3*)**	EEDLDAVEAQIGCKLPDDYR	1.0	0.8	1.8	1.5	0.6
		ITNAKGDVEEVQGPGVVGEFPIISPGR			-	-	
20	FUBP2_RAT Far upstream element-binding protein 2 (*Khsrp*)	KDAFADAVQR	1.0	2.6	10.0	0.8	1.5
21	GRP75_RAT Stress-70 protein, mitochondrial (*Hspa9*)	EMAGDNKLLGQFTLIGIPPAPR	1.0	2.1	5.2	0.9	2.7
		QATKDAGQISGLNVLR			-		
		MPKVQQTVQDLFGR			-		
		KDSETGENIR			-		
		QAVTNPNNTFYATKR			-		
22	GRP78_RAT 78 kDa glucose-regulated protein (*Hspa5*)	KSDIDEIVLVGGSTR	1.0	1.0	4.7	1.3	1.4
		IINEPTAAAIAYGLDKR			-		
		NQLTSNPENTVFDAKR	1.0	2.9	8.1		
		AKFEELNMDLFR	1.0	7.7	35.0	1.9	
23	GSTA4_RAT Glutathione S-transferase alpha-4 (*Gsta4*)	APQEKEESLALAVKR			-	-	

#	Protein description (gene name)	Peptide sequence	GST-normalised intensity value/WT				
			WT	K266A	A299V	R304*	R304Q
		EESLALAVKR	1.0	1.6	3.5	0.7	1.5
24	GSTA6_RAT Glutathione S-transferase A6 (*Gsta6*)	FIHTNEDLEKLR			-	-	
25	GSTM1_RAT Glutathione S-transferase Mu 1 (Gstm1)	FKLGLDFPNLPYLIDGSR			-		
		LAQWSNK	1.0	2.6	2.9	0.2	4.0
		KHHLCGETEEER		-	-	-	-
		KITQSNAIMR			-	-	
		ISAYMKSSR	1.0	6.0	12.5		12.1
		YLSTPIFSKLAQWSNK				-	
26	GSTM4_RAT Glutathione S-transferase Yb-3 (*Gstm3*)	MAIWGSK	1.0	1.5	1.1		2.3
		LKPGYLEQLPGMMR	1.0		4.0		
		FLPRPLFTKMAIWGSK	1.0	1.1	3.9	3.9	0.1
		NQVFEATCLDAFPNLKDFIAR				-	
27	GSTM5_RAT Glutathione S-transferase Mu 5 (*Gstm5*)	NKITQSNAILR			-		
		FEALEKIAAFLQSDR			-	-	
		MLLEFTDTSYEEKQYTCGEAPDYDR			-	-	
28	GSTP1_RAT Glutathione S-transferase P (*Gstp1*)	SLGLYGKDQKEAALVDMVNDGVEDLR	1.0			2.4	
		AFLSSPDHLNRPINGNGKQ	1.0		14.7	8.1	6.1
		DQKEAALVDMVNDGVEDLR			-		
		STCLYGQLPKFEDGDLTLYQSNAILR	1.0			2.8	7.9
29	**HS90B_RAT Heat shock protein HSP 90-beta (*Hsp90ab1*)**	ELISNASDALDKIR	1.0	1.0	2.8	0.3	0.3
30	**HSP7C_RAT Heat shock cognate 71 kDa protein (*Hspa8*)**	MVNHFIAEFKR	1.0	0.1	0.9		0.3
		QATKDAGTIAGLNVLR	1.0	0.3	1.6	0.0	0.5
		NQVAMNPTNTVFDAKR	1.0	0.3	1.8		0.5
		GTLDPVEKALR	1.0	0.5	1.6		5.8

#	Protein description (gene name)	Peptide sequence	GST-normalised intensity value/WT				
			WT	K266A	A299V	R304*	R304Q
		LIGDAAKNQVAMNPTNTVFDAKR	1.0		1.5		
31	**KTU_RAT Protein kintoun (*Dnaaf2*)**	EWYWGLNKDSLEER	1.0	1.0	3.5	2.1	0.5
32	LANC1_RAT LanC-like protein 1 (*Lancl1*)	AFPNPYADYNKSLAENYFDSTGR	1.0	1.9	2.8	0.9	
33	**NDKA_RAT Nucleoside diphosphate kinase A (*Nme1*)**	TFIAIKPDGVQR	1.0	0.9	0.2		
34	**NFL_RAT Neurofilament light polypeptide (*Nefl*)**	KGADEAALAR	1.0	1.3	0.5	2.1	1.9
		LAAEDATNEKQALQGER	1.0	0.5		1.5	1.1
		FTVLTESAAKNTDAVR	1.0	0.9	438.9	2.1	1.2
		AAKDEVSESR	1.0	1.5	1287.4	4.6	2.4
		QKHSEPSR	1.0	143.9	354.0	303.7	242.6
35	RS12_RAT 40S ribosomal protein S12 (*Rps12*)	LGEWVGLCKIDR	1.0	1.2	2.4	0.7	0.7
36	**RS14_RAT 40S ribosomal protein S14 (*Rps14*)**	TKTPGPGAQSALR	1.0	0.1	75.8	0.3	
37	RS20_RAT 40S ribosomal protein S20 (*Rps20*)	SLEKVCADLIR	1.0	2.2	1.2	1.0	0.9
38	**RS21_RAT 40S ribosomal protein S21 (*Rps21*)**	LAKADGIVSKNF	1.0	2.0	2.0	2.8	
39	RS25_RAT 40S ribosomal protein S25 (*Rps25*)	NTKGGDAPAAGEDA		-	-		
40	RS27A_RAT Ubiquitin-40S ribosomal protein S27a (*Rps27a*)	LIFAGKQLEDGR			-	-	
41	RS28_RAT 40S ribosomal protein S28 (*Rps28*)	NVKGPVREGDVLTLLESER	1.0				0.7
42	RSSA_RAT 40S ribosomal protein SA (*Rpsa*)	AVLKFAAATGATPIAGR		-	-	-	-
46	**SKP1_RAT S-phase kinase-associated protein 1 (*Skp1*)**	KTFNIKNDFTEEEEAQVR	1.0	0.5	6.8	3.3	
44	SODC_RAT Superoxide dismutase [Cu-Zn] (*Sod1*)	GGNEESTKTGNAGSR	1.0	1.1	1.4		
45	SSRG_RAT Translocon-associated protein subunit gamma (*Ssr3*)	APKGGSKQQSEEDLLLQDFSR			-	-	
46	**TBB2A_RAT Tubulin beta-2A chain (*Tubb2a*)**	INVYYNEAAGNKYVPR	1.0	1.8		0.2	1.1
47	TBB4B_RAT Tubulin beta-4B chain (*Tubb4b*)	INVYYNEATGGKYVPR	1.0	2.2	1.6	0.9	1.1
48	**TBB5_RAT Tubulin beta-5 chain (*Tubb5*)**	ISVYYNEATGGKYVPR	1.0	2.4		0.3	1.3
49	THIO_RAT Thioredoxin (*Txn*)	EKLEATITEFA			-		

#	Protein description (gene name)	Peptide sequence	GST-normalised intensity value/WT				
			WT	K266A	A299V	R304*	R304Q
		VGEFSGANKEKLEATITEFA			-		
50	TPIS_RAT Triosephosphate isomerase (*Tpi1*)	VNHALSEGLGVIACIGEKLDER			-		
		TATPQQAQEVHEKLR			-		
		GWLKCNVSEGVAQCTR			-	-	
51	UCHL1_RAT Ubiquitin carboxyl-terminal hydrolase isozyme L1 (*Uchl1*)	MPFPVNHGASSEDSLLQDAAKVCR			-		
52	VAPA_RAT Vesicle-associated membrane protein-associated protein A (*Vapa*)	FKGPFTDVVTTNLKLQNPSDR	1.0		0.8	0.6	
		QDGPLPKPHSVSLNDTETR			-		
53	VAPB_RAT Vesicle-associated membrane protein-associated protein B (*Vapb*)	QLKEEDGLR			-	-	

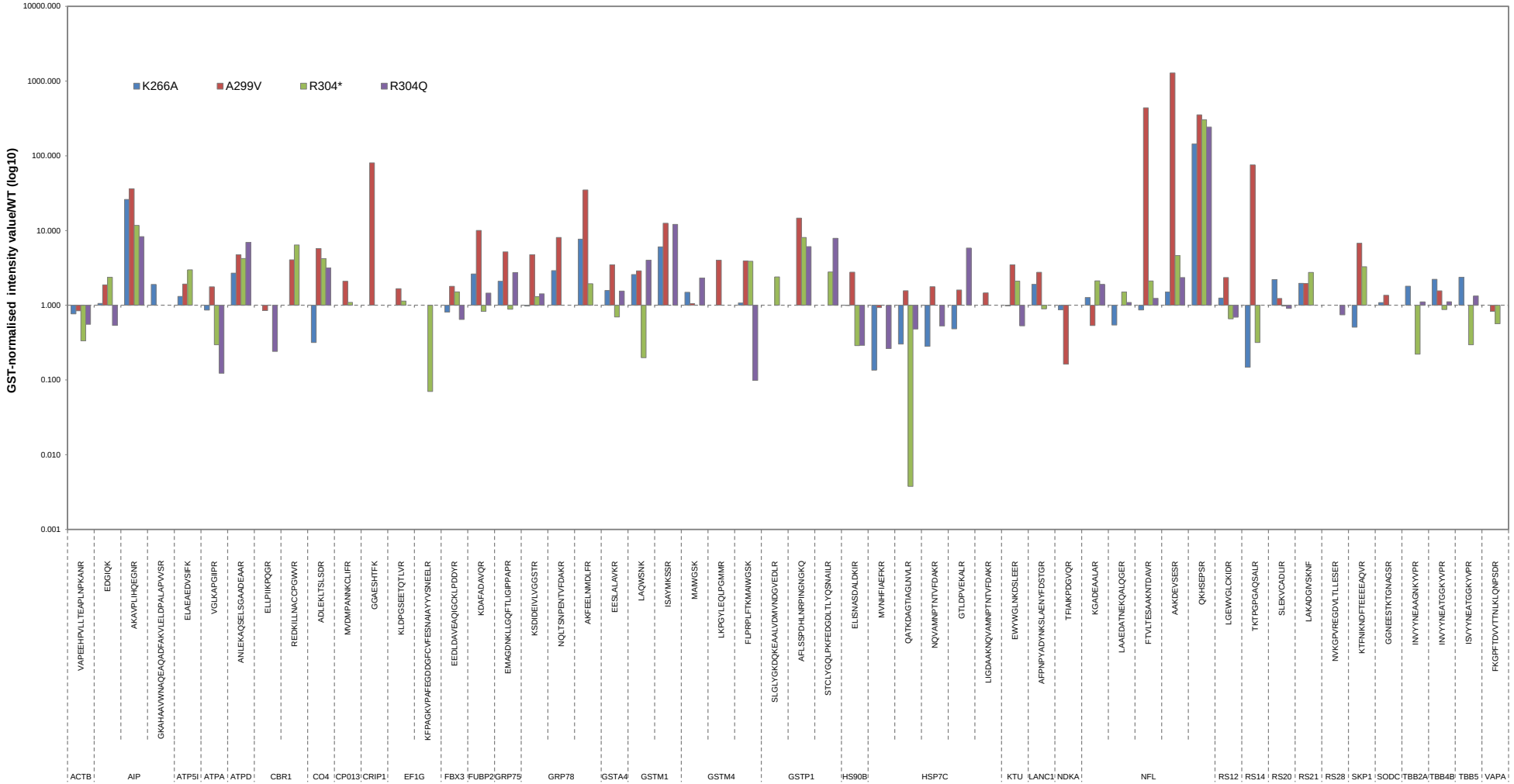

Figure 27. Graphic representation of the comparative intensity values of peptides identified per bait protein: candidate partners of WT AIP only. In a broad sense, proteins whose peptides were underrepresented in the experiments for the mutant proteins, compared to the WT, can be interpreted as lost interactions.

Table 19: Tagged proteins selected for co-immunoprecipitation

Protein	CDS (bp)	Amino acids	pI	Mass (kDa)
Myc-AIP	1026	341	5.8	39.0
AIP-Flag	1017	338	5.7	38.7
HA-CBR1	918	305	6.3	33.8
HA-DSTN	546	181	5.6	20.4
HA-EEF1G	1362	453	5.6	52.0
HA-FBXO3	1476	491	4.8	56.9
HA-HSPA5	2025	674	5.0	74.7
HA-HSPA8	2043	680	5.2	74.6
HA-HSPA9	2094	697	5.5	75.8
HA-HSP90A	2253	750	4.9	86.8
HA-HSP90B	2259	752	4.9	86.7
HA-NEFL	1686	561	4.6	63.6
HA-NME1	519	172	5.0	19.5
HA-SOD1	513	170	5.0	17.8
HA-SKP1	546	181	4.3	20.8
HA-TUBB	1395	464	4.7	52.5
HA-TUBB2A	1398	465	4.7	52.3
HA-VAPA	810	269	6.5	30.2

Under standard experimental conditions (i.e., without adding a crosslinker), it was not possible to co-immunoprecipitate Myc and Flag tagged AIP (Figure 28a), and the addition of a 10mer peptide of TOMM20 did not change the results (Figure 28b). However, in the presence of 0.8% formaldehyde as a crosslinker, only very weak co-immunoprecipitated bands were observed (Figure 28c). These results are supported by isothermal calorimetry assays, demonstrating that the stoichiometry of the interaction between the TPR domain of AIP and HSP90 is 0.3:1, thus implying that one molecule of AIP interacts with an HSP90 dimer.[523] In conclusion, AIP self-association, if existent, might not be biologically relevant.

AIP interacts with multiple molecular chaperones of the HSP70 and HSP90 families

Originally described as stress-responsive proteins, involved in the response to thermal and other proteotoxic stresses, human heat shock proteins (HSPs) are also constitutively expressed[675] and are abundantly represented in the proteome. Two of the best known molecular partners of AIP are the heat shock proteins HSP90 and HSPA8 (HSC70). Both HSPA8, a constitutively expressed protein of the HSPA (HSP70) family, and the constitutive isoform of HSP90, HSP90B, were detected in the MS analysis. Co-IP of these proteins was carried out to validate the experimental protocol (i.e. they were used as positive controls). Additionally, the inducible form of HSP90, HSP90A,[676] was also tested. A successful co-IP of AIP and HSPA8, with a clean negative control, was obtained, as shown in Figure 29. Also, the co-IP experiments confirmed an interaction of AIP with both the inducible and the constitutive isoforms of HSP90 (Figure 30).

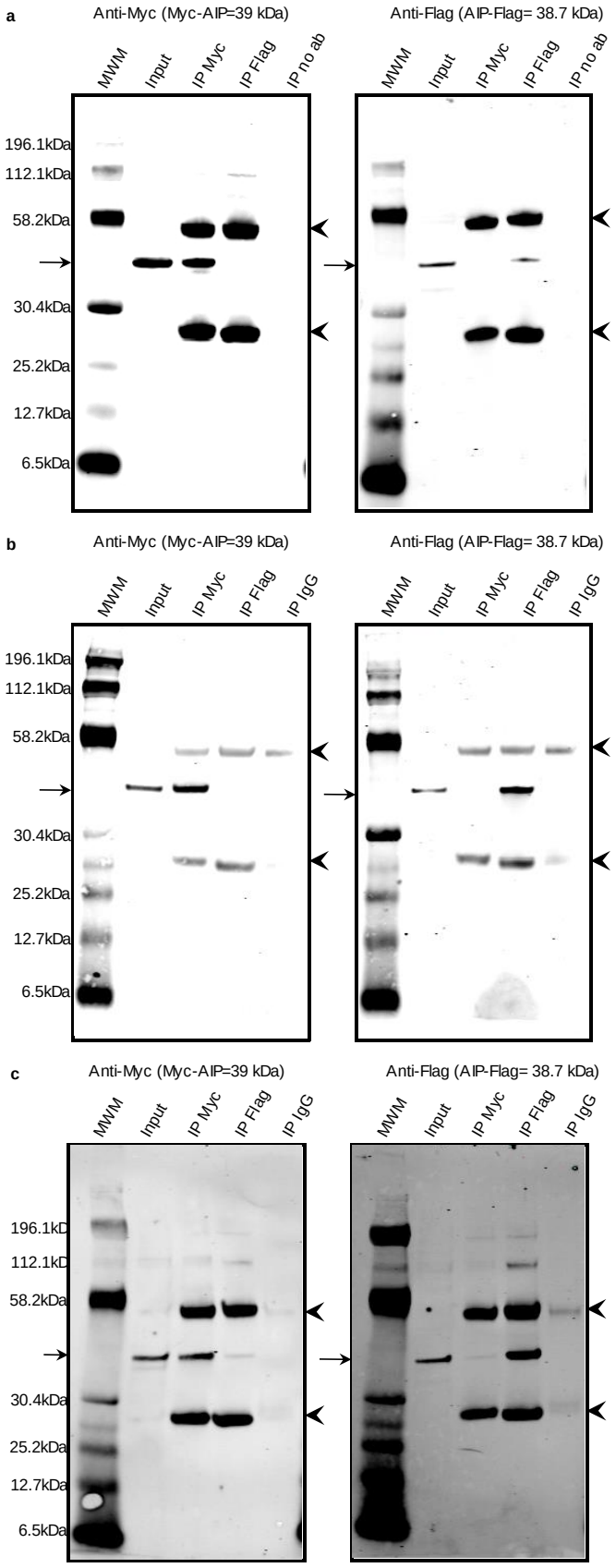

Figure 28. Myc-AIP and AIP-Flag co-immunoprecipitation. a) Standard protocol, b) with 1 µg of a TOMM20 10mer, and c) with 0.8% formaldehyde. Cells were co-transfected with pcDNA3.0-Myc-WT_AIP and pCI-Neo-WT_AIP-Flag and IP was performed using anti-Myc, anti-Flag or no antibody (or mouse IgG). Left panels: anti-Myc WB, right panels: anti-Flag WB. Arrow on the left panel: Myc-AIP, arrow on the right panel: AIP-Flag. Arrowheads on both panels: heavy (top) and light (bottom) chains of mouse immunoglobulins. IP: immunoprecipitation, MWM: molecular weight marker.

The qMS results predicted total loss of HSPA8 binding and partial loss of HSP90B binding to the AIP mutant p.R304*, when compared to the WT protein. To determine the reliability of the comparative analysis for assuming loss of interaction, a co-IP experiment was carried out to verify the loss of interaction between HSPA8 and AIP p.R304* (Figure 31). An apparent loss of co-immunoprecipitated HA-HSPA8 was observed when immunoprecipitating with anti-Myc antibody. Likewise, the co-immunoprecipitated Myc-AIP band when immunoprecipitating with anti-HA antibody was weaker than in the experiment done with the WT protein. Although these results are only qualitative, they seem to confirm a reduced HSPA8 binding by the mutant p.R304*, as shown by qMS.

Interactions of AIP with two other members of the HSP70 family, HSPA5 and HSPA9, were also detected. HSPA5 (also know as GRP78 and BiP) is a molecular chaperone resident in the ER, involved in protein quality control by regulating the folding and assembly of nascent proteins and the retention of misfolded proteins.[677] By co-IP an interaction between AIP and HSPA5 was confirmed (Figure 32). The interaction of HSPA5 and AIP has not been reported before. HSPA9, also known as GRP75 or mortalin, is also a member of the HSP70 family of chaperones. HSPA9 in localised mainly in the mitochondria, but it can also be found in the ER, cytoplasmic vesicles, and cytosol in human transformed cell lines.[678] HSPA9 interacts with the tumour suppressor TP53, inactivating its functions as a transcriptional activator and pro-apoptotic molecule.[679] An interaction between AIP and HSPA9 was confirmed by the co-IP experiment (Figure 33).

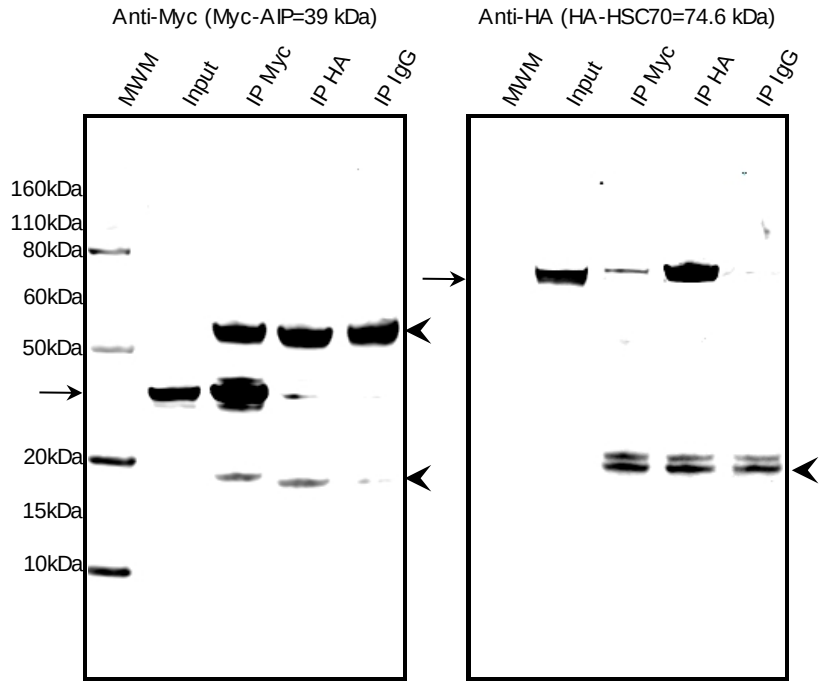

Figure 29. Myc-AIP and HA-HSPA8 co-immunoprecipitation. Cells were co-transfected with pcDNA3.0-Myc-WT_AIP and pSF-CMV-NH2-HA-EKT-NcoI-HSPA8 and the IP was performed using anti-Myc, anti-HA or mouse IgG. Left panel: anti-Myc WB, right panel: anti-HA WB. Arrow on the left panel: Myc-AIP, arrow on the right panel: HA-HSPA8. Arrowheads on both panels: heavy (top) and light (bottoms) chains of mouse immunoglobulins. IP: immunoprecipitation, MWM: molecular weight marker.

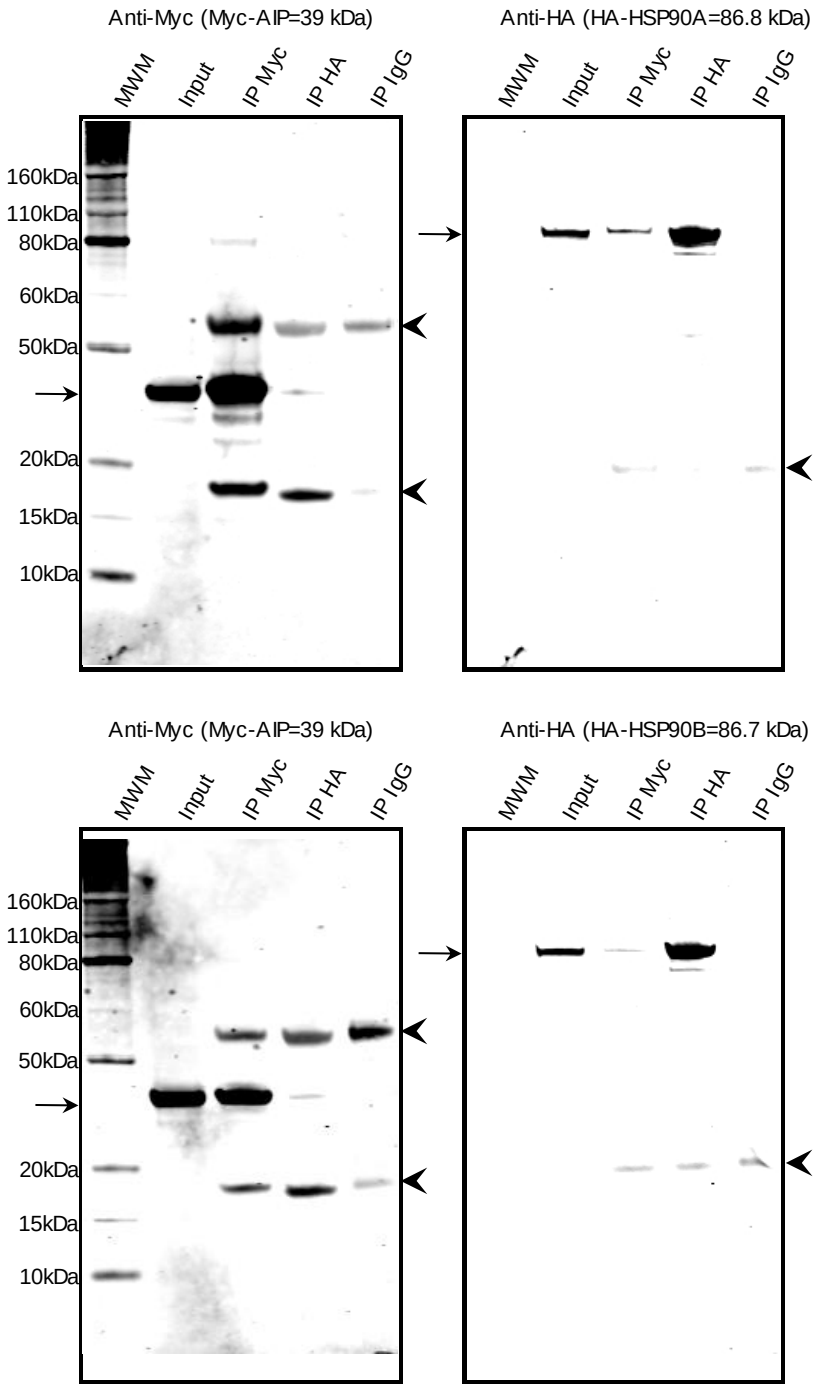

Figure 30. Myc-AIP and HA-HSP90A/B co-immunoprecipitation. Top panels: co-IP experiment for HSP90A, bottom panels: co-IP for HSP90B. In both cases, the cells were co-transfected with pcDNA3.0-Myc-WT_AIP and pSF-CMV-NH2-HA-EKT-NcoI-HSP90A (top) or pSF-CMV-NH2-HA-EKT-NcoI-HSP90B (bottom) and IP was carried out using anti-Myc, anti-HA or mouse IgG. Left panels: anti-Myc WB, right panels: anti-HA WB. Arrow on the left panels: Myc-AIP, arrow on the right panels: HA-HSP90A (top) or HA-HSP90B (bottom). Arrowheads on both panels: heavy (top) and light (bottom) chains of mouse immunoglobulins. IP: immunoprecipitation, MWM: molecular weight marker.

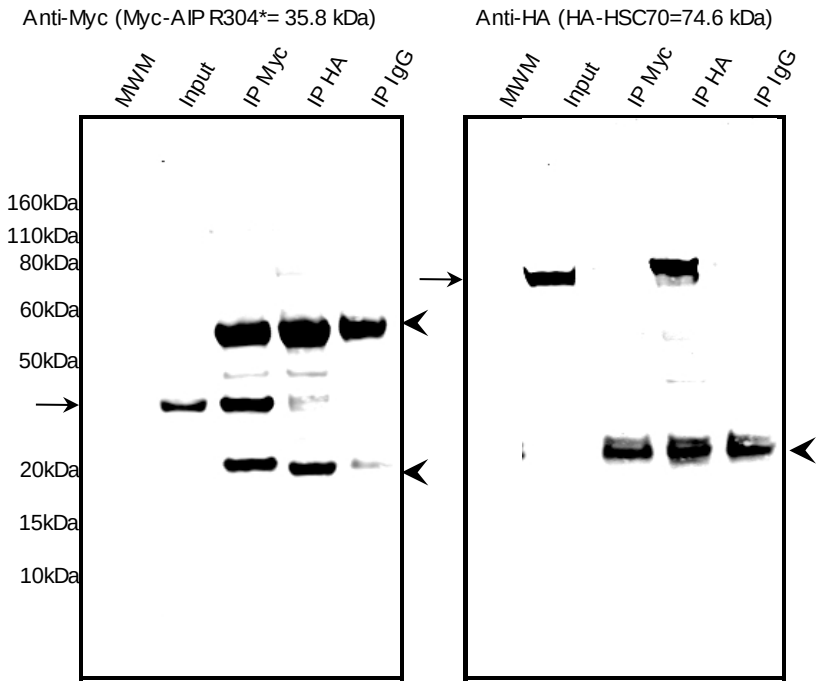

Figure 31. Myc-AIP p.R304* and HA-HSPA8 co-immunoprecipitation. Cells were co-transfected with pcDNA3.0-Myc-AIP_p.R304* and pSF-CMV-NH2-HA-EKT-NcoI-HSPA8 and the IP was performed using anti-Myc, anti-HA or mouse IgG. Left panel: anti-Myc WB, right panel: anti-HA WB. Arrow on the left panel: Myc-AIP, arrow on the right panel: HA-HSPA8. Arrowheads on both panels: heavy (top) and light (bottom) chains of mouse immunoglobulins. The molecular weight marker is not visible in these images, as it was loaded in a different part of the gel, but the marks indicating the size of the bands were placed accordingly. IP: immunoprecipitation, MWM: molecular weight marker.

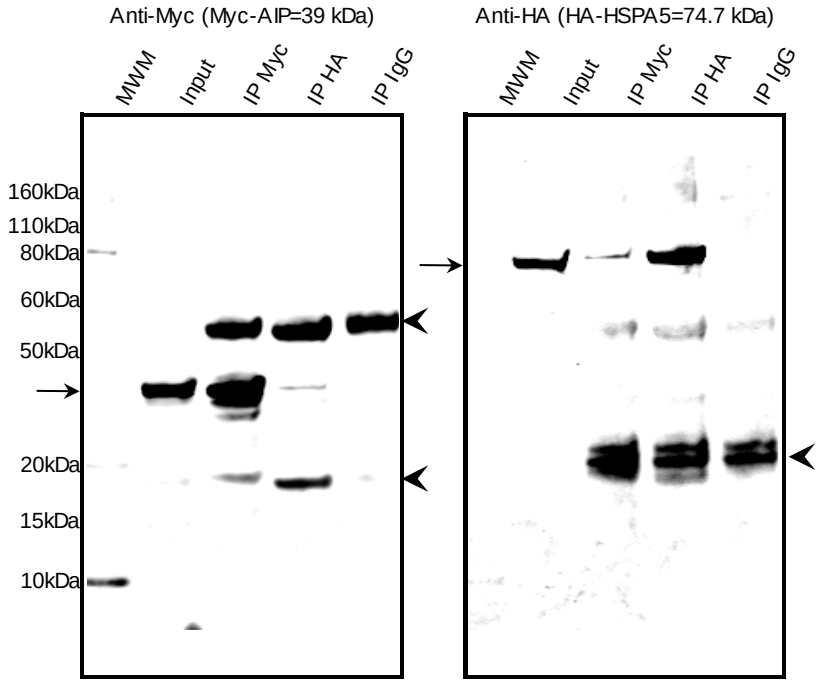

Figure 32. Myc-AIP and HA-HSPA5 co-immunoprecipitation. Cells were co-transfected with pcDNA3.0-Myc-WT_AIP and pSF-CMV-NH2-HA-EKT-NcoI-HSPA5 and the IP was performed using anti-Myc, anti-HA or mouse IgG. Left panel: anti-Myc WB, right panel: anti-HA WB. Arrow on the left panel: Myc-AIP, arrow on the right panel: HA-HSPA5. Arrowheads on both panels: heavy (top) and light (bottom) chains of mouse immunoglobulins. IP: immunoprecipitation, MWM: molecular weight marker.

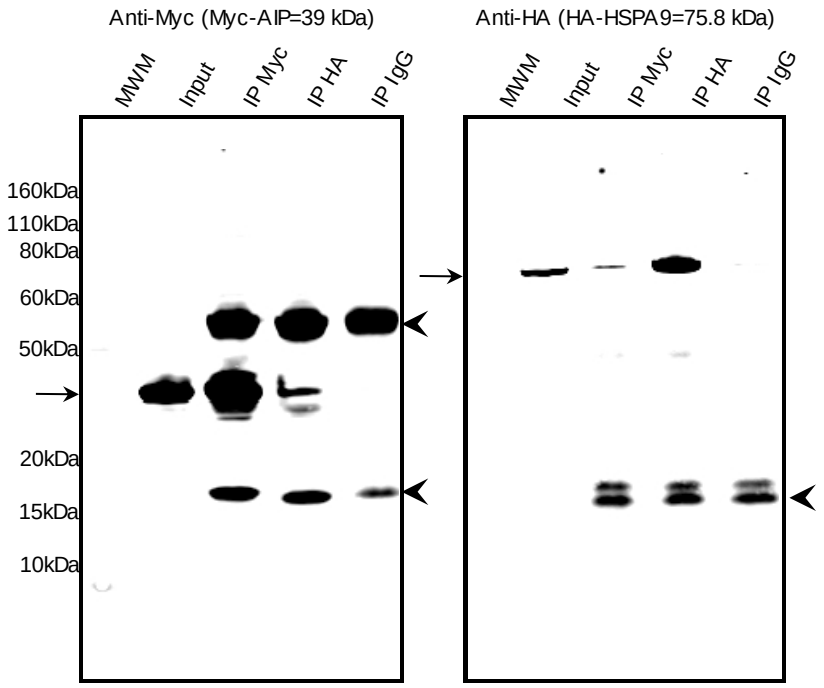

Figure 33. Myc-AIP and HA-HSPA9 co-immunoprecipitation. Cells were co-transfected with pcDNA3.0-Myc-WT_AIP and pSF-CMV-NH2-HA-EKT-NcoI-HSPA9 and the IP was performed using anti-Myc, anti-HA or mouse IgG. Left panel: anti-Myc WB, right panel: anti-HA WB. Arrow on the left panel: Myc-AIP, arrow on the right panel: HA-HSPA9. Arrowheads on both panels: heavy (top) and light (bottom) chains of mouse immunoglobulins. IP: immunoprecipitation, MWM: molecular weight marker.

Cytoskeletal proteins are novel AIP partners, and also experimental artefacts

Multiple cytoskeletal proteins were reported in the MS results. These proteins are abundantly expressed in all the cells, and therefore they are frequently found artefacts in pull-down assays. However, some of these proteins displayed differential binding between WT AIP and the mutant proteins, pointing out the need for validation of these interactions.

Microtubules are essential cytoskeletal structures composed of heterodimers of beta tubulins and alpha tubulins; these structures are involved in mitosis, intracellular transport and cellular motility.[680] Microtubules are also targets of anti-cancer drugs and the impaired expression of tubulins in cancer cells is a frequent cause of tumour progression and drug resistance.[681] Two isotypes of beta tubulins were found underrepresented in the pull-down experiment for the mutant p.R304*, compared to WT AIP: TUBB and TUBB2A. TUBB is constitutively expressed in multiple cell lines, while TUBB2A is the major isotype in neurons and in prostate adenocarcinoma.[681]

In the AIP-TUBB co-IP experiment (Figure 34), Myc-AIP was co-immunoprecipitated when using anti-HA antibody, while the immunoprecipitation with anti-Myc failed to co-immunoprecipitate HA-TUBB (the experiment was repeated, with identical results), which could indicate a positive but weak protein-protein interaction. On the other hand, the co-IP experiment clearly confirmed the interaction of AIP with TUBB2A (Figure 35, top). In the confocal immunocytofluorescence images (Figure 35, bottom), TUBB2A appears distributed in cytoplasmic filaments, while AIP

has a predominantly cytoplasmic diffuse distribution. There is clear overlap of both proteins (yellow areas) in the cytoplasmic network constituted by TUBB2A. Calculation of the co-localisation in the whole z-stack rendered a Pearson's coefficient of 0.642 and an overlap coefficient of 0.763, for an apparently positive co-localisation.

Actins are proteins highly expressed in most of the cell types, involved in cell motility.[510] In the cell, monomeric ATP-bound actin assembles in polymers (nucleation), which elongate into filaments, and these processes are regulated by actin-binding proteins.[682] ACTB was reported as an AIP partner in the MS experiments, underrepresented in the experiments for the mutants AIP p.R304Q and AIP p.R304*.

Validation of this interaction was attempted by co-IP of Myc-AIP and endogenous ACTB, using the anti-Myc antibody, as before, and a mouse monoclonal anti-ACTB antibody (SIGMA A1978). Although the co-IP reactions were positive in both directions, bands for the co-immunoprecipitated proteins were also observed in the negative control (mouse IgG), indicating a non-specific binding of ACTB to mouse IgG (Figure 36). Therefore, it was not possible to confirm or disprove an interaction between AIP and ACTB by this method. In order to overcome this limitation, the experiment should be repeated using antibodies from a different origin, or a different experimental approach could be employed.

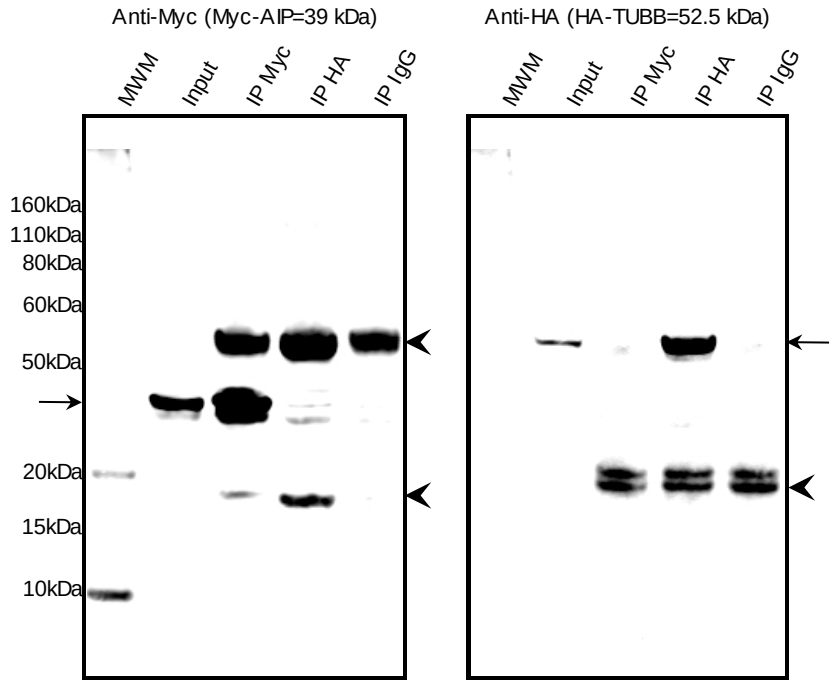

Figure 34. Myc-AIP and HA-TUBB co-immunoprecipitation. Cells were co-transfected with pcDNA3.0-Myc-WT_AIP and pSF-CMV-NH2-HA-EKT-NcoI-TUBB and the IP was performed using anti-Myc, anti-HA or mouse IgG. Left panel: anti-Myc WB, right panel: anti-HA WB. Arrow on the left panel: Myc-AIP, arrow on the right panel: HA-TUBB. Arrowheads on both panels: heavy (top) and light (bottom) chains of mouse immunoglobulins. IP: immunoprecipitation, MWM: molecular weight marker.

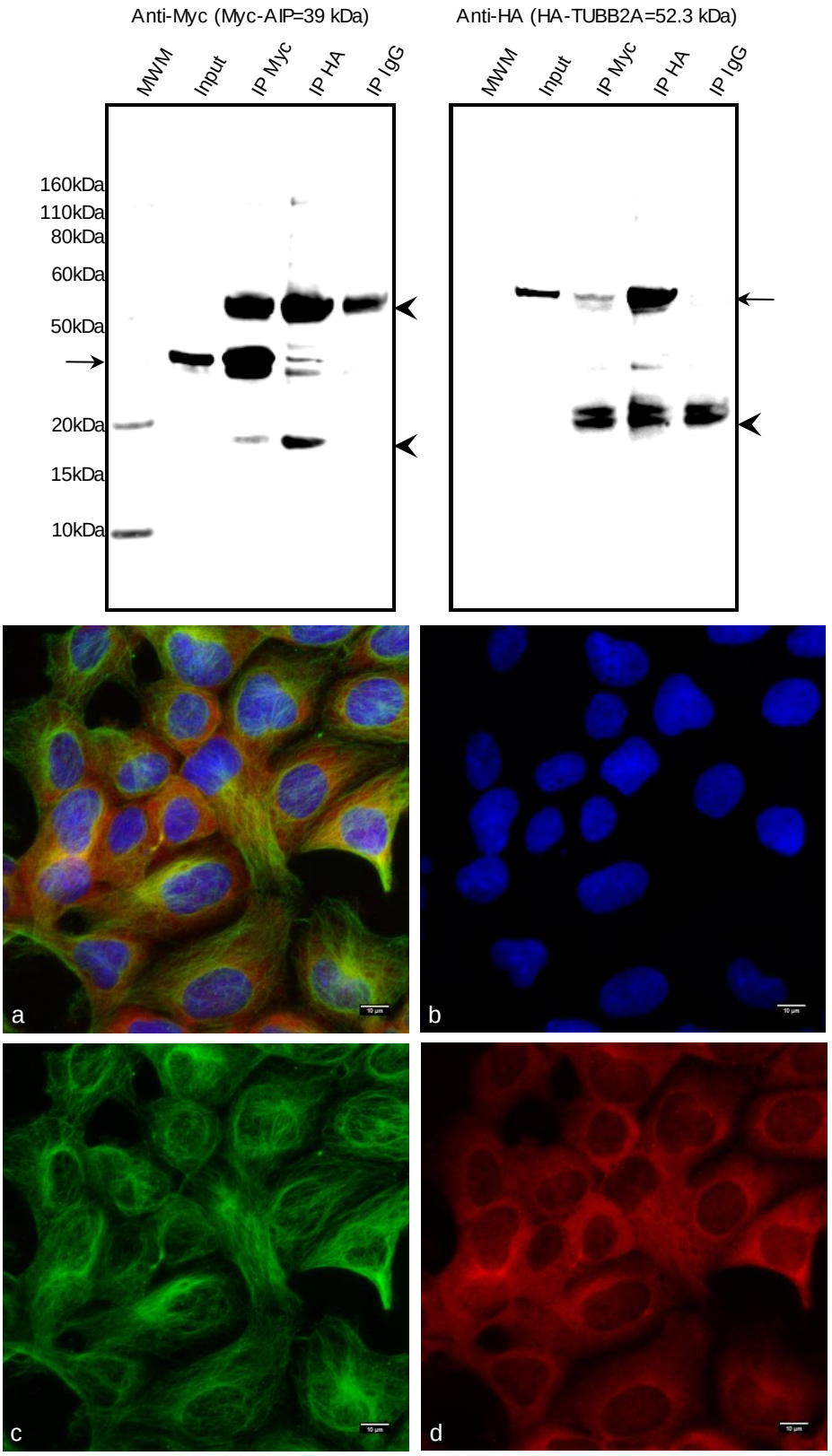

Figure 35. Myc-AIP and HA-TUBB2A validation experiments. Top panel: co-IP. Cells were co-transfected with pcDNA3.0-Myc-WT_AIP and pSF-CMV-NH2-HA-EKT-NcoI-TUBB2A; IP was performed with anti-Myc, anti-HA or mouse IgG. Left panel: anti-Myc WB, right panel: anti-HA WB. Arrow on the left panel: Myc-AIP, arrow on the right panel: HA-TUBB2A. Arrowheads on both panels: heavy (top) and light (bottom) chains of mouse immunoglobulins. IP: immunoprecipitation, MWM: molecular weight marker. Bottom panel: co-localisation of endogenous AIP and TUBB2A, 63X z-stack reconstruction. a) Merged image, b) nuclei (DAPI), c) TUBB2A, d) AIP. Antibodies: 1:100 (v/v) rabbit polyclonal anti-AIP (Novus NBP1-31347) and 1:100 (v/v) mouse monoclonal anti-TUBB2A (Abnova H00007280-M03).

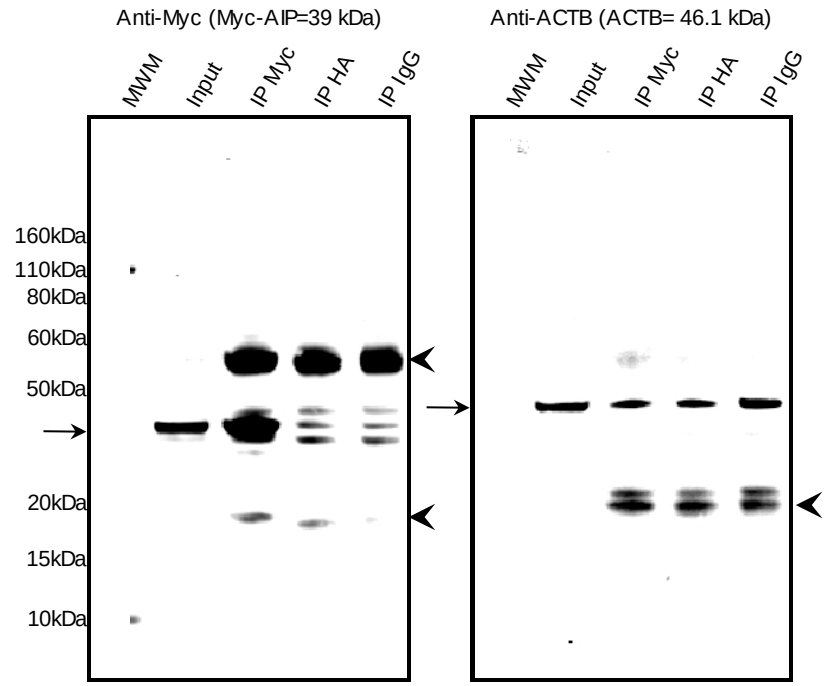

Figure 36: Co-immunoprecipitation Myc-AIP and ACTB. Cells were transfected with pcDNA3.0-Myc-WT_AIP and the IP was performed using anti-Myc, anti-ACTB or mouse IgG. Left panels: anti-Myc WB, right panels: anti-ACTB WB. Arrow on the left panel: Myc-AIP, arrow on the right panel: ACTB. Arrowheads on both panels: heavy (top) and light (bottom) chains of mouse immunoglobulins. IP: immunoprecipitation, MWM: molecular weight marker.

NEFL forms intermediate filaments in the neural cells and it may have a tumour suppressor activity in cancer cells, inducing apoptosis and inhibiting invasion.[683] The co-IP experiment between NEFL protein and AIP failed to prove an interaction (Figure 37, top). In the confocal immunocytofluorescence experiment, the reconstructed z-stack image presents very few areas of overlap between the two proteins by direct visualisation (yellow areas). Likewise, the co-localisation analysis reported a Pearson's coefficient of 0.347 and an overlap coefficient of 0.538. These data can be interpreted as apparently absent or minimal intracellular co-localisation of both endogenous proteins.

The protein DSTN was included among the validation experiments, because it was found as a candidate interacting partner for one of the mutants (p.R304*) but not for the WT AIP. DSTN, also known as ADF or cofilin, is involved in the organisation of the cytoskeleton, and it can either promote actin assembly or disassembly depending of the concentration of DSTN relative to actin and also depending on other actin-binding proteins.[684] Co-IP experiments for this protein were carried out using the WT or p.R304* AIP, but none of them confirmed an interaction (Figure 38). Therefore, it can be concluded that the presence of DSTN in the pull-down fraction of p.R304* represents an artefact and not a real protein-protein interaction.

The E3 ubiquitin-ligase FBXO3 interacts with AIP

Two members of the SCF E3 ubiquitin-ligase complex were detected in the pull-down results: the F-box containing protein FBXO3 and SKP1, with differential representation among different pull-down experiments. Validation by co-IP with AIP was positive for FBXO3 (Figure 39), but not

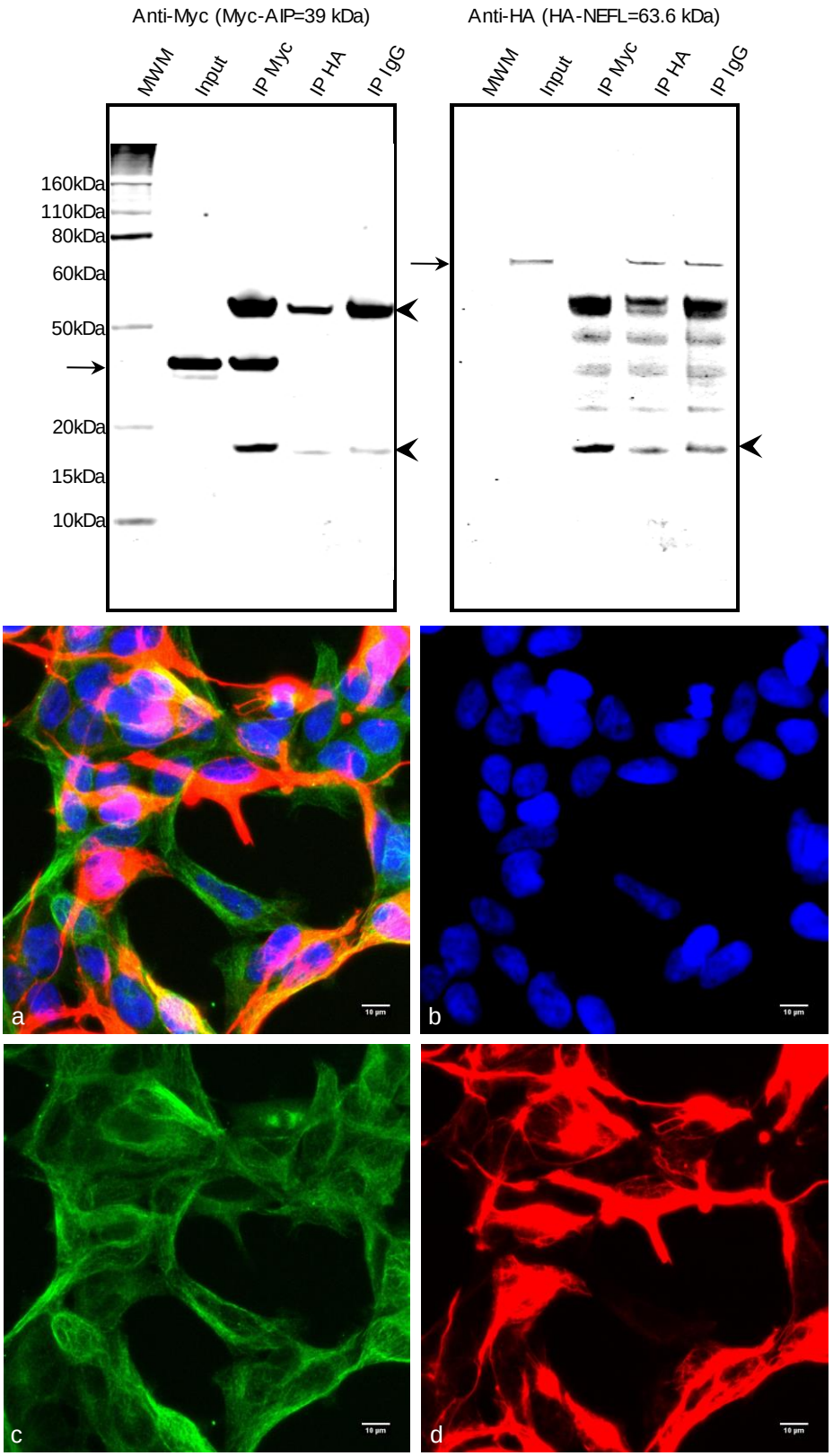

Figure 37. Myc-AIP and HA-NEFL validation experiments. Top panel: co-IP. Cells were co-transfected with pcDNA3.0-Myc-WT_AIP and pSF-CMV-NH2-HA-EKT-NcoI-NEFL, and the IP was performed using anti-Myc, anti-HA or mouse IgG. Left panels: anti-Myc WB, right panels: anti-HA WB. Arrow on the left panel: Myc-AIP, arrow on the right panel: NEFL. Arrowheads on both panels: heavy (top) and light (bottom) chains of mouse immunoglobulins. IP: immunoprecipitation, MWM: molecular weight marker. Bottom panel: co-localisation of endogenous AIP and NEFL, 63X z-stack reconstruction. a) Merged image, b) nuclei (DAPI), c) AIP, d) NEFL. Antibodies: 1:100 (v/v) mouse monoclonal anti-AIP (Novus NB100-127) and 1:50 rabbit monoclonal anti-NEFL (Cell Signalling CST2837).

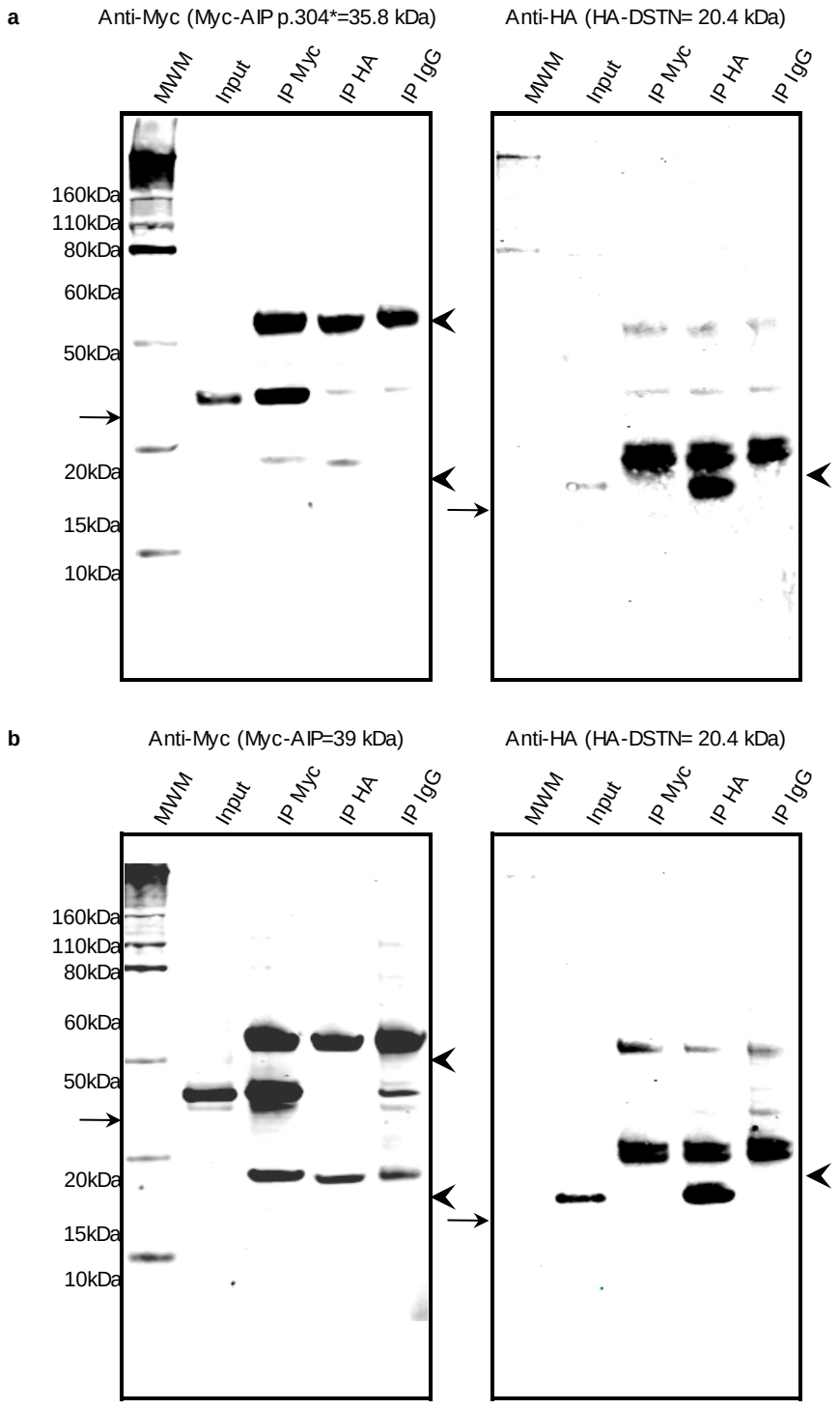

Figure 38. Co-immunoprecipitation HA-DSTN and Myc-AIP p.R304* (a) and HA-DSTN and Myc-WT AIP (b). Cells were co-transfected with pcDNA3.0-Myc-AIP_p.R304* or pcDNA3.0-Myc-WT_AIP and pSF-CMV-NH2-HA-EKT-NcoI-DSTN, and the IP was performed using anti-Myc, anti-HA or mouse IgG. Left panels: anti-Myc WB, right panels: anti-HA WB. Arrow on the left panel: Myc-AIP, arrow on the right panel: NEFL. Arrowheads on both panels: heavy (top) and light (bottom) chains of mouse immunoglobulins. IP: immunoprecipitation, MWM: molecular weight marker.

for SKP1 (Figure 40). However, if AIP is directed to ubiquitination by the SCF complex, it would be expected to be bound by FBXO3 and not by SKP1. These data suggests that AIP undergoes ubiquitination and posterior proteasomal degradation, initiated by an FBXO3 containing SCF E3 ubiquitin-ligase complex. Although these results are a good proof of this mechanism, further

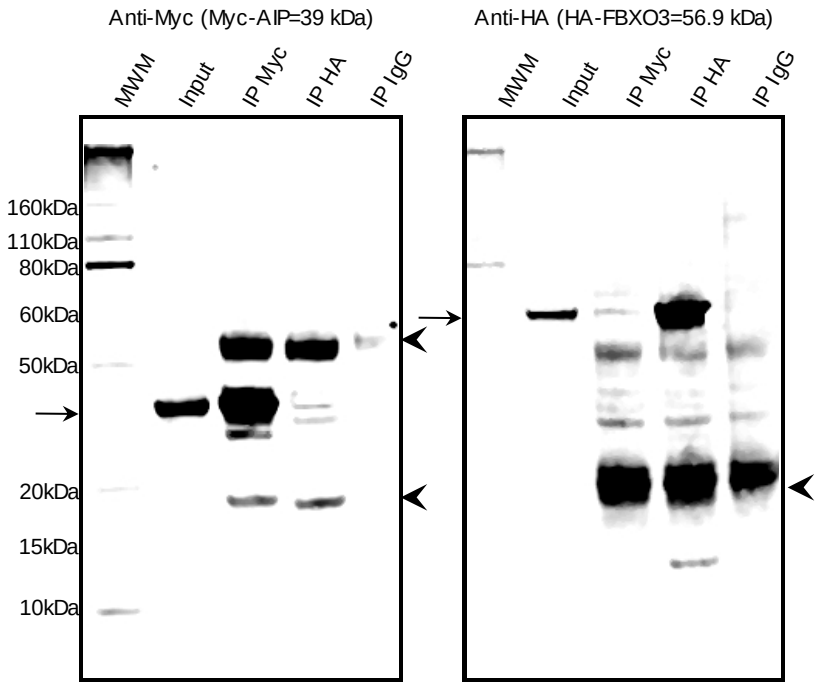

Figure 39. Myc-AIP and HA-FBXO3 co-immunoprecipitation. Cells were co-transfected with pcDNA3.0-Myc-WT_AIP and pSF-CMV-NH2-HA-EKT-NcoI-FBXO3, and IP was performed using anti-Myc, anti-HA or mouse IgG. Left panels: anti-Myc WB, right panels: anti-HA WB. Arrow on the left panel: Myc-AIP, arrow on the right panel: FBXO3. Arrowheads on both panels: heavy (top) and light (bottom) chains of mouse immunoglobulins. IP: immunoprecipitation, MWM: molecular weight marker.

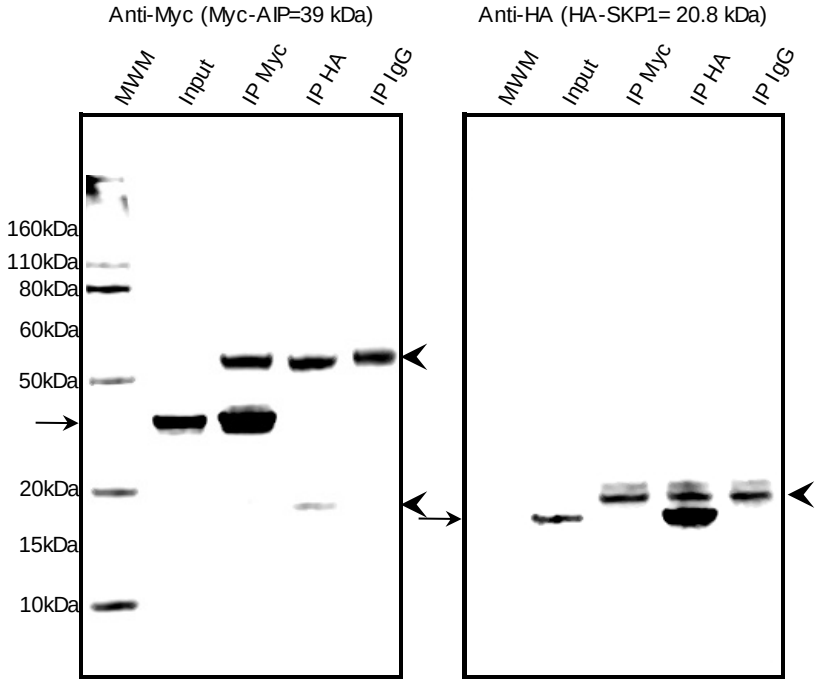

Figure 40. Myc-AIP and HA-SKP1 co-immunoprecipitation. Cells were co-transfected with pcDNA3.0-Myc-WT_AIP and pSF-CMV-NH2-HA-EKT-NcoI-SKP1, and IP was performed using anti-Myc, anti-HA or mouse IgG. Left panels: anti-Myc WB, right panels: anti-HA WB. Arrow on the left panel: Myc-AIP, arrow on the right panel: SKP1. Arrowheads on both panels: heavy (top) and light (bottom) chains of mouse immunoglobulins. IP: immunoprecipitation, MWM: molecular weight marker.

experiments should be done to ensure that FBXO3 is indeed the specific protein directing AIP to ubiquitination, considering the very large number of E3 ubiquitin-ligases encoded in the human genome (reviewed in Chapter 4).

Miscellaneous interacting partners, not confirmed

Also known as VAP-33, VAPA is a protein implicated in vesicle docking and fusion, localised in intracellular vesicles and at the tight junctions.[685] VAPA binds SNARE proteins, thereby contributing to the secretory process.[686] This protein was detected as an AIP interacting partner, underrepresented in the pull-down experiments for some of the AIP mutants. Considering the function of this protein, an interaction between AIP and VAPA could be important for GH secretion in the somatotroph cells, where AIP has been localised surrounding GH secretory vesicles. However, the co-IP experiment has discarded a direct interaction between AIP and VAPA (Figure 41).

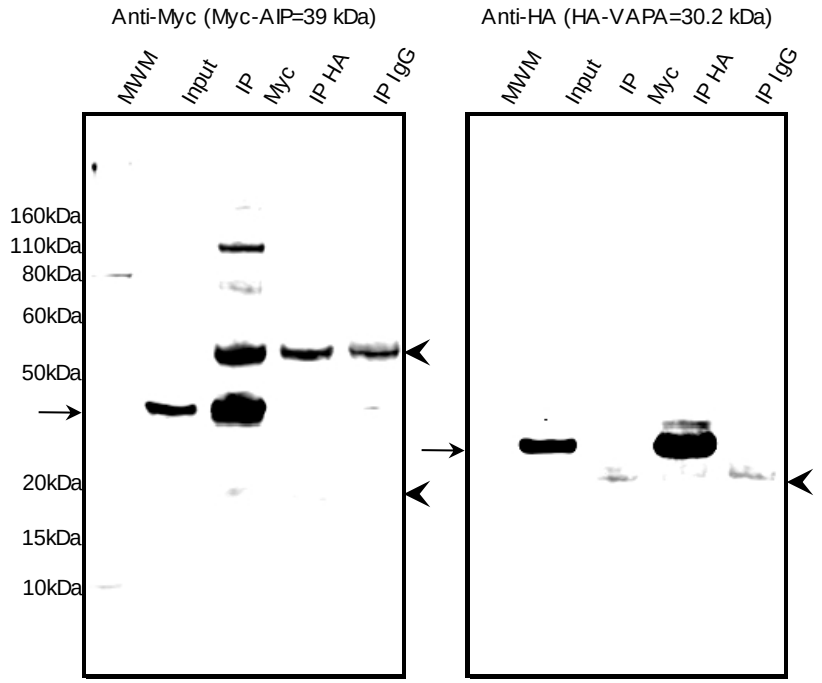

Figure 41. Myc-AIP and HA-VAPA co-immunoprecipitation. Cells were co-transfected with pcDNA3.0-Myc-WT_AIP and pSF-CMV-NH2-HA-EKT-NcoI-VAPA, and IP was performed using anti-Myc, anti-HA or mouse IgG. Left panels: anti-Myc WB, right panels: anti-HA WB. Arrow on the left panel: Myc-AIP, arrow on the right panel: VAPA. Arrowheads on both panels: heavy (top) and light (bottom) chains of mouse immunoglobulins. IP: immunoprecipitation, MWM: molecular weight marker.

CBR1 is an NADPH-dependent reductase, catalysing the reduction of several carbonyl compounds.[510] Human CBR1 is highly expressed in the liver, placenta and central nervous system and it apparently has a protective role, involving the metabolic reduction of xenobiotic carbonyls and quinones.[687] Co-IP experiments for this protein showed no interaction with WT AIP. CBR1 can bind glutathione,[510] so this protein could constitute an artefact due to the GST tag and glutathione elution used in the pull-down experiments.

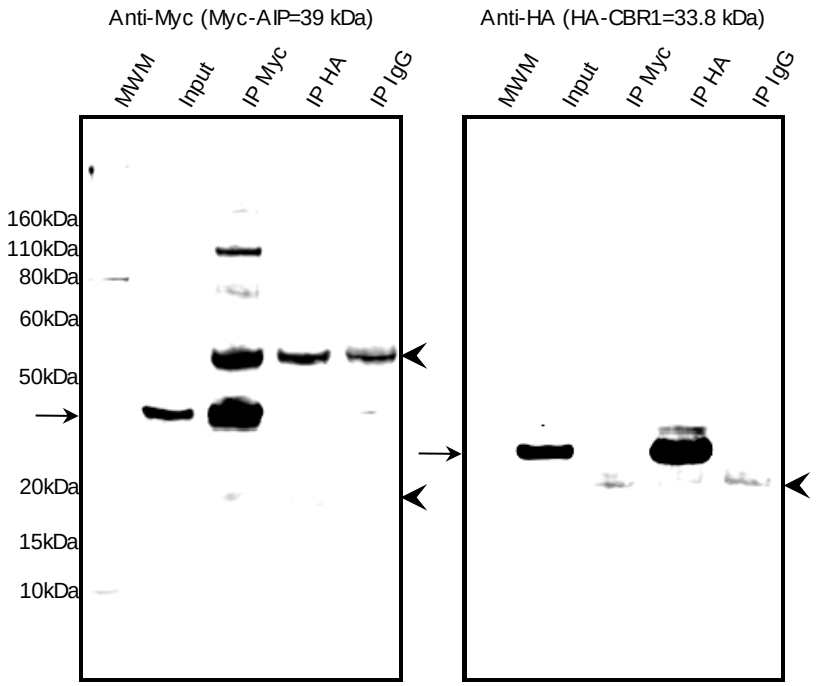

Figure 42. Myc-AIP and HA-CBR1 co-immunoprecipitation. Cells were co-transfected with pcDNA3.0-Myc-WT_AIP and pSF-CMV-NH2-HA-EKT-NcoI-CBR1, and IP was performed using anti-Myc, anti-HA or mouse IgG. Left panels: anti-Myc WB, right panels: anti-HA WB. Arrow on the left panel: Myc-AIP, arrow on the right panel: CBR1. Arrowheads on both panels: heavy (top) and light (bottom) chains of mouse immunoglobulins. IP: immunoprecipitation, MWM: molecular weight marker.

EEF1G is a component of the translational apparatus, together with eIF4A, eIF4E, eEF1A and eEF1; this complex is frequently overexpressed in tumoral cells.[688] WB bands for both EEF1G and AIP were detected when immunoprecipitating with anti-Myc and anti-HA antibodies, but the immunoprecipitation with mouse IgG (negative control) was also positive for both proteins (Figure 43). With these results it is not possible to discard or to prove the interaction reported in the MS data. It is important to mention that EEF1G contains a GST domain,[689] and therefore it could have been pulled-down and eluted due to its affinity for glutathione.

NME1 (NM23, NDKA) is a regulator of the cell cycle progression (from G2 to M), through downregulation of cyclin B, and this activity is inhibited by cAMP.[77] In pituitary adenomas, the expression of NME1 (measured by IHC) is inversely correlated with invasiveness.[690] Co-IP of NME1 was negative when immunoprecipitating with anti-Myc, but co-IP of AIP was positive when immunoprecipitating with anti-HA, though AIP was also detected in the negative control (Figure 44). These results were interpreted as no direct interaction between AIP and NME1. Finally, validation of an interaction between AIP and the mitochondrial protein SOD1 was also attempted (Figure 45). Co-IP of AIP when immunoprecipitating with anti-HA was detected, but there was no co-immunoprecipitation of SOD1 when immunoprecipitating with anti-Myc. These results could possibly be interpreted as a weak interaction between these two proteins.

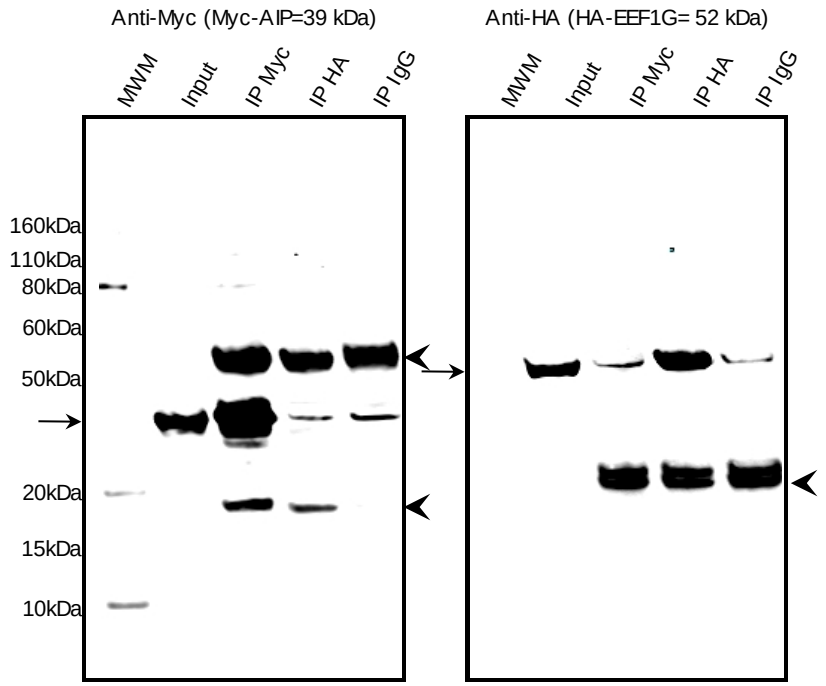

Figure 43. Myc-AIP and HA-EEF1G co-immunoprecipitation. Cells were co-transfected with pcDNA3.0-Myc-WT AIP and pSF-CMV-NH2-HA-EKT-NcoI-EEF1G, and IP was performed using anti-Myc, anti-HA or mouse IgG. Left panels: anti-Myc WB, right panels: anti-HA WB. Arrow on the left panel: Myc-AIP, arrow on the right panel: EEF1G. Arrowheads on both panels: heavy (top) and light (bottom) chains of mouse immunoglobulins. IP: immunoprecipitation, MWM: molecular weight marker.

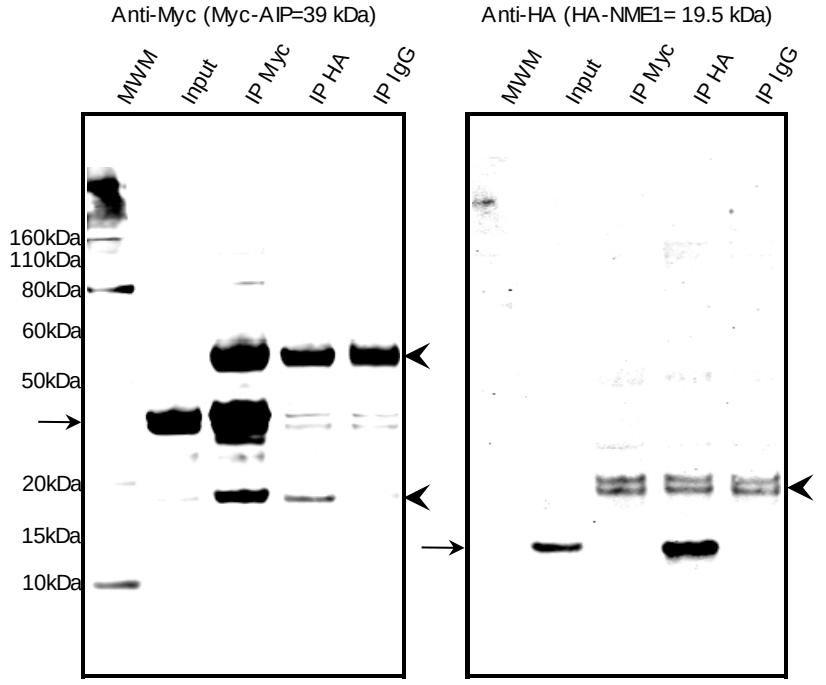

Figure 44. Myc-AIP and HA-NME1 co-immunoprecipitation. Cells were co-transfected with pcDNA3.0-Myc-WT AIP and pSF-CMV-NH2-HA-EKT-NcoI-NME1, and IP was performed using anti-Myc, anti-HA or mouse IgG. Left panels: anti-Myc WB, right panels: anti-HA WB. Arrow on the left panel: Myc-AIP, arrow on the right panel: NME1. Arrowheads on both panels: heavy (top) and light (bottom) chains of mouse immunoglobulins. IP: immunoprecipitation, MWM: molecular weight marker.

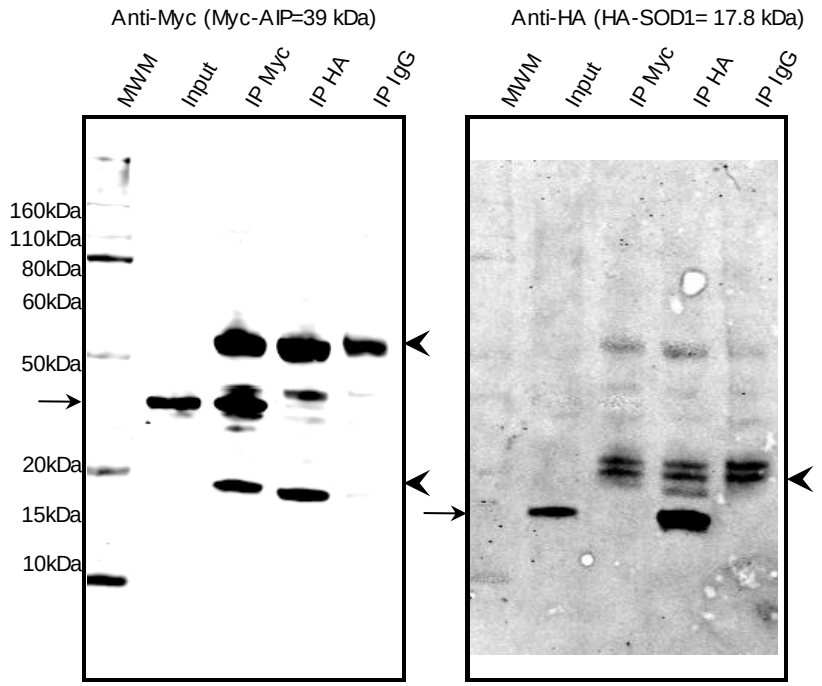

Figure 45. Myc-AIP and HA-SOD1 co-immunoprecipitation. Cells were co-transfected with pcDNA3.0-Myc-WT AIP and pSF-CMV-NH2-HA-EKT-NcoI-SOD1, and IP was performed using anti-Myc, anti-HA or mouse IgG. Left panels: anti-Myc WB, right panels: anti-HA WB. Arrow on the left panel: Myc-AIP, arrow on the right panel: SOD1. Arrowheads on both panels: heavy (top) and light (bottom) chains of mouse immunoglobulins. IP: immunoprecipitation, MWM: molecular weight marker.

The pituitary-specific function of AIP could occur via chaperone client proteins

AIP could exert functions relevant for pituitary physiology via indirect interactions with client proteins of molecular chaperones of the HSP90 or HSP70 families. For this reason, a possible indirect interaction of AIP with PRKACA, an HSP90 client protein with an important role in the somatotroph cell function, was explored. This protein was not part of the list of candidate partners for AIP, but it was selected after finding some similarities between its protein partners and those of AIP in the BIOGRID protein-protein interaction database.[541]

PRKACA is part of the complex of proteins that constitute PKA, a key member of the cAMP pathway. An important role for this pathway in the tumorigenesis of different endocrine organs is well established.[81] Recently, the activating PRKACA mutation p.L206R has been shown to be causative of cortisol-producing adrenal tumours, leading to Cushing's syndrome.[691]

AIP and PRKACA do not interact directly (Figure 46), but when a triple co-IP experiment including AIP, PRKACA and HSP90A was attempted, the three proteins were successfully co-immunoprecipitated (Figure 47). Although these findings support a possible interaction between the three proteins, they do not prove the existence of a complex containing the three proteins in the cell.

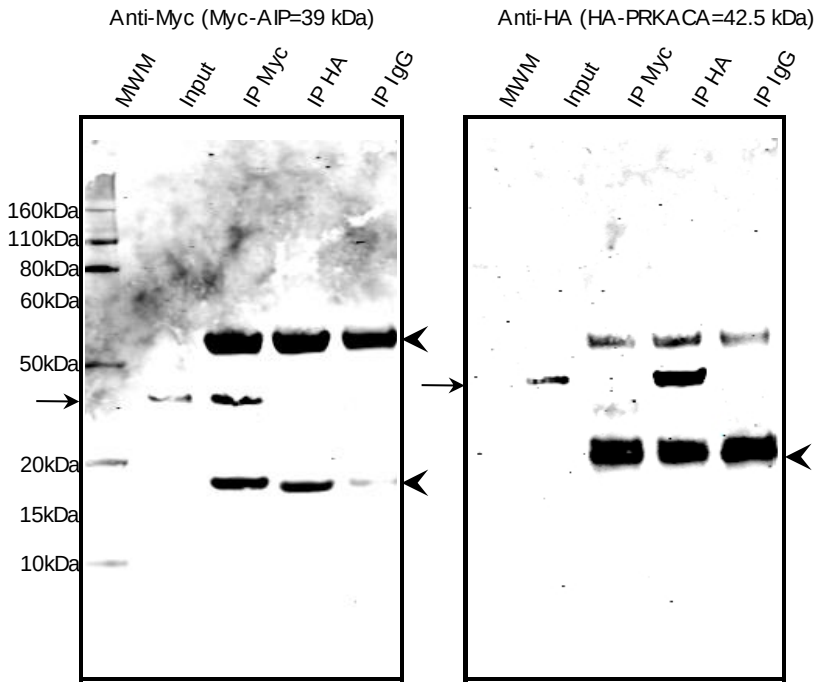

Figure 46. Myc-AIP and HA-PRKACA co-immunoprecipitation. Cells were co-transfected with pcDNA3.0-Myc-WT_AIP and pSF-CMV-NH2-HA-EKT-NcoI-PRKACA, and IP was performed using anti-Myc, anti-HA or mouse IgG. Left panel: anti-Myc WB, right panel: anti-HA WB. Arrow on the left panel: Myc-AIP, arrow on the right panel: HA-PRKACA. Arrowheads on both panels: heavy (top arrowheads) and light (bottom arrowheads) chains of mouse immunoglobulins. IP: immunoprecipitation, MWM: molecular weight marker.

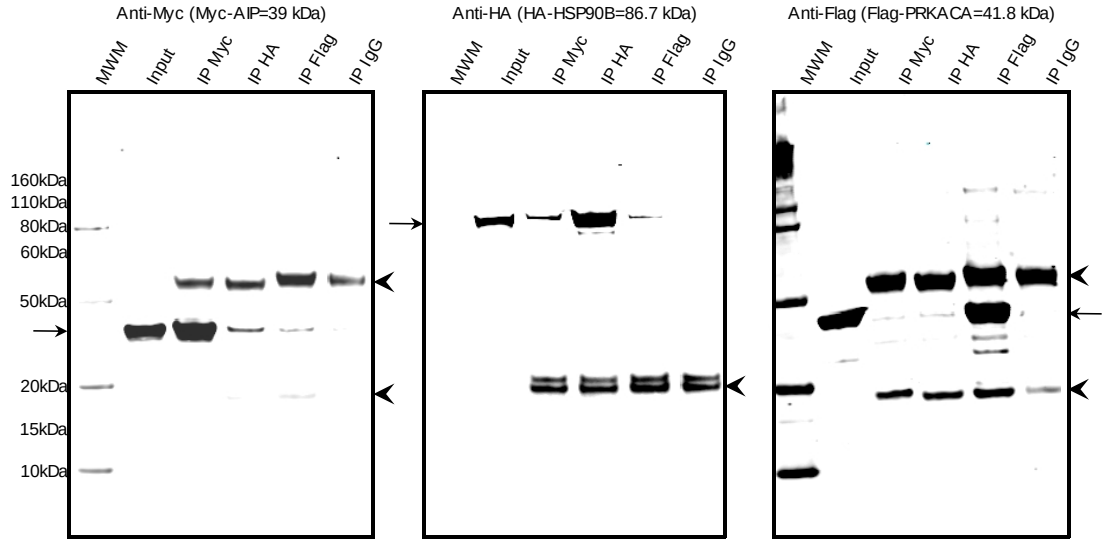

Figure 47. Myc-AIP, HA-HSP90B and Flag-PRKACA co-immunoprecipitation. Cells were co-transfected with pcDNA3.0-Myc-WT_AIP, pSF-CMV-NH2-HA-EKT-NcoI-HSP90B and pSF-CMV-NH2-Flag-EKT-NcoI-PRKACA and IP was performed using anti-Myc, anti-HA, anti-Flag or mouse IgG. Left panel: anti-Myc WB, central panel: anti-HA WB, right panel: anti-Flag WB. Arrow on the left panel: Myc-AIP, arrow on the central panel: HA-HSP90B, arrow on the right panel: Flag-PRKACA. Arrowheads on all the panels: heavy (top arrowheads) and light (bottom arrowheads) chains of mouse immunoglobulins. IP: immunoprecipitation, MWM: molecular weight marker.

Discussion

Biological functions are orchestrated and regulated by dynamic networks of interacting proteins, and a wide variety of proteomic methods are currently available for the study of protein-protein interactions.[692] The two-hybrid (2H) system, originally employing yeast and therefore termed yeast-2H assay, is one of the most common methods for testing protein-protein interactions.[693] In this system, plasmids are constructed to express two proteins whose interaction is being tested. In one of them, a functional domain that binds a promoter DNA sequence is fused to the CDS for one of the proteins of interest. In the other plasmid, the CDS for the other protein is fused to a transcriptional activator. Both proteins are co-expressed in a cell and, if interaction exists, the transcription of a reporter gene will be activated.[694] Although this method can only screen interactions of two proteins at a time, it can be scaled-up to create libraries of interacting partners.[693] A limitation of this system is that, if yeasts are used (heterologous system), the mammalian proteins expressed may not carry all the posttranslational modifications relevant for their function.[695]

The gold-standard assay for protein-protein interactions is the co-IP of untagged proteins at their endogenous level. However, this is frequently difficult to do, due to the variable expression of the proteins of interest in the cells, and it is limited by the availability of suitable antibodies. Even more, only two proteins can be studied at a time by co-IP.[695]

For “fishing” experiments, trying to investigate protein interactions in a proteome scale, high-throughput methods are required. For these purposes, proteins complexes are first isolated from an appropriate biological sample and purified, using a variety of techniques, and protein identification is carried out in a second step, generally involving peptide identification by MS.[692] Affinity fusion-based techniques for protein purification take advantage of the use of genetically fused affinity tags, and in these methods proteins of interest are expressed in frame with an epitope tag.[692] Plasmids encoding the tagged proteins are transfected into cells and left to be expressed for a certain period of time. The cells are then lysed, and the tagged bait along with its interacting partners (“prey”) is isolated using a chemical or biological ligand linked to a solid support, and then eluted.[694] Proteins in the eluted fraction can be resolved by PAGE and then identified by MS.

A variant of this method is tandem affinity purification (TAP). In this method, a so called TAP-tag, composed of two sequential affinity tags spaced by a cleavage site of tobacco etch virus (TEV) protease, is fused to the CDS for the protein of interest.[694] After expression of the bait protein and cell lysis, a first affinity purification step is done, using the protein A moiety in the TAP tag, which binds IgG-sepharose.[692] Then, TEV protease is added, cleaving the TEV tag and therefore eluting the proteins. These samples undergo a second affinity purification step via the calmodulin binding peptide present in the TAP tag (using calmodulin-sepharose), and they are finally eluted. This method reduces the background due by nonspecific interactions; however, given the need of two purification steps, transient interactions are frequently lost.[694]

Other types of TAP tags have been described, with variable structure, but following the same principle.[696]

An advantage of affinity purification is that the proteins are expressed *in vivo,* and therefore they can undergo posttranslational modifications that could possibly affect the binding to certain partners. However, after cell lysis, the bait protein is put in contact with proteins that are not normally expressed in the same subcellular compartment. Also, due to the purification step and the stringent washes required to eliminate contaminants during the purification step, this method is biased towards proteins that interact with high affinity, and is therefore not useful to detect transient protein interactions. Because the tagged bait protein is overexpressed, its assembly could be compromised, and this could result in high levels of chaperones interacting with the misfolded protein, obscuring interactions with other less abundant proteins.[694] Also, affinity purification approaches can only generate a list of proteins detected at a given time, not revealing the composition of individual protein complexes. This is due to the fact that only protein interactions that are resistant to the lysis and purification conditions can survive to be detected by MS. This problem can be solved by the use of chemical crosslinkers, which stabilise the proteins in complexes. However, crosslinking can also frequently introduce false positive results.[692]

The pull-down assay, which was the method used in the present study, also includes affinity purification, but in this method a synthetic protein, usually fused to an affinity tag, is exposed to a cell lysate, and proteins interacting with the bait are then recovered by affinity purification.[667] The GST tag is frequently used in this method, both for protein production and for pull-down. The pull-down asssay does not require transfection, allowing the use of a wider diversity of starting material (cells, tissues) for the lysates and facilitating the use of different amounts of bait protein, according to the experimental needs. However, tags used for protein production, as GST, are usually long and therefore they can modify the interactions of the normal protein. Also, false positive results can be introduced due to proteins interacting not with the protein of interest, but with the tag instead.

MS is the method of choice for peptide sequencing because of its high sensitivity and compatibility with high-throughput experimental strategies. Mass spectrometric analyses take place in the gas phase of ionised analytes.[697] Two main strategies to ionise and volatilise peptides, previously separated by reverse phase liquid chromatography, are currently used: ESI and matrix-assisted laser desorption/ionisation (MALDI).[692] The mass spectrometer is composed of an ion source, a mass analyser that separates ionised analytes based on their mass-to-charge ratio (*m/z*), and a detector that registers the number of ions at each *m/z* value.[698] For proteomic analyses, it is necessary to have sensitive instruments, providing high resolution/mass accuracy and with the ability to generate information-rich ion mass spectra from peptide fragments, which is referred to as the tandem mass or MS/MS spectra.[697] Four basic types of mass spectrometers are currently used, and they can be used separately or in tandem:

quadrupole, ion trap (quadrupole ion trap or linear ion trap), time-of-flight, quadrupole and Fourier-transform ion cyclotron resonance, together with a variant of ion trap, Orbitrap.[698] The instrument used in the present study was a hybrid linear ion trap-Orbitrap mass analyser. The ion-trap technology consists on "trapping" the ions for a certain period of time, before subjecting them to MS or MS/MS analysis.[697] In the Orbitrap, the ions are trapped and orbit around a spindle-like electrode, oscillating harmonically along its axis with a frequency characteristic of their *m/z* values. This induces an image current in the outer electrodes that is transformed into the time domain, producing mass spectra. This technology improves the mass accuracy and high resolution or MS.[698] The most frequently used fragmentation method in MS/MS is collision-induced dissociation. In this technique, gas-phase peptide/protein cations are internally heated by multiple collisions with rare gas atoms, causing peptide backbone fragmentation and resulting in a series of b-fragment and y-fragment ions. Other fragmentation methods are electron-capture dissociation and electron-transfer dissociation.[698]

Two main approaches exist regarding the type of samples that are submitted for MS. In the bottom-up approach the proteins of interest are subjected to enzymatic digestion (e.g. trypsin) and the resulting peptides are submitted for ionisation. The analysis of the ionised peptides takes place in two steps: first the masses of the peptides are determined and then the peptide ions are fragmented to produce information on their sequence and modifications. As only a very small fraction of the peptides produces useful fragmentation ladders, this method is not optimal for the study of posttranslational modifications and alternative splice variants.[699] In the present study, a bottom-up approach was used, based on in-gel trypsin digestion. The top-down approach consists on submitting intact proteins for ionisation, to be subsequently fragmented in the mass spectrometer, reporting the masses of both the protein and the fragmented ions, which under optimal conditions provides a complete description of the protein sequence and its posttranslational modifications.[699]

High throughput interaction data derived from affinity purification experiments are enriched in proteins of high abundance. The best way of distinguishing true interaction partners from non-specific contaminants is the use of quantitative proteomics. The rationale for this technology is to compare the abundance of proteins identified in a sample with a suitable control.[695] The present study has used qMS based on isotopomer labels, named TMT or isobaric mass tags.[668] TMT are a set of structurally identical tags which label the free N-terminus and ε-amino functions of K residues.[700] Different samples can be labelled with different TMT and then combined and processed as one sample, whose results can be quantitatively analysed. The tags are composed of a reactive group, which binds amino groups in the peptide, a mass normalisation group (balancer group), balancing the mass differences from individual ion reporters to ensure the same overall mass of the label reagents, a cleavable linker, enabling the release of the reporter ion from the tag during MS/MS fragmentation, and a reporter ion. "Heavy" isotopes (^{13}C or ^{15}N) are contained in the reporter group and in the balancer ion. The 6-

plex TMT tags used in the present study have specific reporters that appear at *m/z*=126.1, 127.1, 128.1, 129.1, 130.1 and 131.1.[700]

Once a protein-protein interaction has been identified, it is necessary to verify the binding by additional methods. One frequently used method is immunofluorescent staining to detect co-localisation in confocal microscopy images. The purpose of this method is to determine if two proteins display overlapping distribution within the cell, which would make their interaction more plausible. Imaging can be done in the intact cells, expressing endogenous proteins, or in previously transfected cells overexpressing the proteins of interest, though the first approach is usually preferred. Another confirmatory method is co-IP, where one of the proteins of interest (endogenous or overexpressed) is immunoprecipitated with a specific antibody, and the interacting protein is searched in the immunoprecipitated material by WB or MS.[694] The finding of multiple qMS artefacts in this study, with negative co-IP assays, points out one of the weaknesses of proteomics studies, and emphasises the need for validation.

The novel interacting partners of AIP identified and confirmed in this study correspond to three different categories. The first category is heat shock proteins. In addition to the previously known AIP partners HSPA8 and HSP90, interactions with two more heat shock proteins of the HSP70 family, HSPA5 and HSPA9, have been demonstrated. In contrast with HSPA8 and HSP90, which are widely distributed in the cytoplasm, these two HSP70 proteins have specific subcellular distributions: HSPA5 preferentially resides in the ER, while HSPA9 is mainly expressed in the mitochondria, though small amounts of both proteins can also be observed in other subcellular localisations (see below). Interestingly, the proteins HSPA5 and HSPA9 do not contain a MEEVD (like HSP90) or IEEVD (like HSPA8) domain, and according to the qMS data, none of the variants studied disturbed these interactions. A member of the HSP70 family, HSPA2 (HSP72), is expressed in around 90% of all the pituitary adenomas (including all subtypes), showing areas of focal induction when detected by IHC,[701] but this protein was not identified as an AIP interacting partner. Further experiments should be done, involving HSPA5 and HSPA9 mutagenesis, to better characterise these novel AIP interactions (i.e. defining residues involved in the interaction, studying co-localisation in pituitary adenoma tissue).

Under physiological conditions, HSPA5 and other ER resident chaperones serve to ensure an adequate folding of the nascent proteins, preventing their aggregation. Stressful factors such as hypoxia, pH changes, and reduced nutrient supply impair the ER function and activate a cellular mechanism known as unfolded protein response (UPR).[702] The function of the UPR is to limit damage to other organelles and to the whole organism, and this is accomplished by limiting the accumulation of unfolded proteins, targeting them to degradation, and eliminating cells subjected to prolonged stress, therefore including both cytoprotective and apoptotic responses.[703] In the absence of ER stress, HSPA5 binds the luminal domain of the UPR transducers inositol-requiring gene 1 (IRE1), PKR-like ER kinase (PERK) and activating transcription factor 6 (ATF6), keeping them inactive.[704] When unfolded proteins accumulate in

the ER, HSPA5 is released and the transducers are activated, causing activation of NF-κB, caspase-12 and MAPK1, as well as G1 arrest and increased angiogenesis. In the presence of sustained ER stress, these responses may elicit the selective proliferation of transformed cells, with anti-apoptotic mutations and angiogenic abilities.[703]

UPR activation is a key event in solid tumours, and HSPA5, overexpressed in various human cancer types (acute lymphoblastic leukaemia, lung, breast, prostate, colon, stomach and liver), exhibits oncogenic abilities and is associated with poor prognosis and drug resistance.[702;703;705] In a rat gliosarcoma cell line, HSPA5 expression is induced by PKA and MAPK1.[706] In addition to its ER localisation, HSPA5 is also localised on the cell surface in different cancer types, were it is activated by the binding to α_2-macroglobulin and acts as an oncogene, promoting cell proliferation (via RAS/RAF/MEK/ERK and phosphatidylinositol 3-kinase [PI3K] signalling) and survival (mediated by Akt and NF-κB).[707] HSPA5 has recently been identified as a therapeutic target in cancer: adenoviral E1A-induced HSPA5 ubiquitination and proteasomal degradation suppresses the metastatic potential of human breast cancer cells[708] and treatment with the synthetic HSPA5 inhibitor (OSU-03012), in combination with sildenafil, induces lethality on a human glioblastoma cell line.[709]

Cell surface HSPA5 also responds to other stimuli, such as plasminogen kringle 5, microplasminogen and angiogenic peptides, and is involved in viral entry of coxsackie B and dengue fever viruses.[710] The co-chaperone MTJ-1 is one of the regulators of HSPA5 function in the ER, and it is also essential for the HSPA5 localisation on the cell surface.[711] No data exists about the role of the UPR or specifically HSPA5 on pituitary function or tumorigenesis; therefore, it is not possible to make assumptions about the possible functional role of the interaction between this chaperone and AIP.

HSPA9 was originally identified as a mitochondrial chaperone, but it is also expressed in other subcellular localisations (nucleus, cell membrane, ER, and cytosol), mainly in cancer cells, which may be relevant for its function as a regulator of cell growth and survival.[712-714] HSPA9 overexpression is induced by cellular stress and is a frequent finding in different types of human neoplasms, including colon, prostate, cervix, lung, liver, brain, breast, skin and medullary thyroid cancer.[679;715] In the late G1 phase of the cell cycle, HSPA9 is localised at the centrosomes, remains there during S and G2 and dissociates from the centrosomes during M.[716] In cancer cells subjected to stress (either due to *TP53* mutations or to stress-inducing chemicals), the tumour suppressor protein TP53 interacts with HSPA9 and this chaperone regulates the intracellular location of TP53 during the cell cycle.[679;716] Overexpressed HSPA9 sequesters TP53 in the cytoplasm, preventing its nuclear translocation and thus abrogating the regulation of cell cycle progression by TP53.[717] Overexpressed HSPA9 is also a negative regulator of the CDKN1A-mediated tumour suppressive MAPK1 signalling pathway in a TP53-dependent or independent manner, an important mechanism for CDKN1A silencing in BRAF p.V600E-transformed cancers, such as melanoma and medullary thyroid carcinoma.[713;718] When located

in the nucleus, HSPA9 exerts an additional pro-oncogenic activity, by interacting with the telomerase transcriptase (hTERT) and the heterogeneous ribonucleoprotein K (hnRNP-K) proteins, activating them.[719]

Due to these pro-tumorigenic activities, HSPA9 represents a potential therapeutic target for cancer. In contrast, missense mutations in the *HSPA9* gene are associated to Parkinson's disease: mutant HSPA9 increases the endogenous oxidative stress and the sensitivity to exogenous oxidative stress, resulting in neuronal senescence.[714] Normal levels of HSPA9 are necessary for normal B lymphopoiesis, and the HSPA9 locus (5q31.1) is included in a region frequently deleted in in patients with myeloid malignancies, such as myelodysplastic syndrome.[720] Besides the multiple studies addressing the HSPA9 functions in normal and neoplastic cells, there is no information available about the co-chaperones that regulate HSPA9 cellular localisation and functions in different settings. By acting as a co-chaperone of HSPA9, AIP could possibly regulate HSPA9-mediated TP53 trafficking or its interaction with members of the RAS/RAF/MEK/ERK signalling pathway. However, it would be necessary to first study the expression and the function of this chaperone in the normal pituitary gland and in pituitary adenomas, an issue that has not been addressed before.

HSP90 has been found overexpressed in adrenocorticotropinomas, impairing the sensitivity of the glucocorticoid receptor and therefore adrenal-pituitary negative feedback, and the C-terminal HSP90 inhibitor silibinin showed anti-tumorigenic effects in an allograft mouse model of Cushing's disease, by releasing GR from HSP90,[721] but the role of HSP90 in *AIP*mut-associated pituitary adenomas has not been explored. Previously reported co-IP experiments, and now our data, showed that the TPR domain of AIP is required for the interaction with HSP90.[546] The highly conserved residue of HSP90 G272 seems to be necessary for this interaction.[521] Under our experimental conditions, the AIP p.K266A, also predicted to be necessary for this interaction to occur, did not impair the binding of HSP90 to AIP, while mutations affecting the C-terminal α-helix of the protein (p.R304* and p.R304Q) resulted in a reduced binding. Although these mutations do not affect the HSP90 binding site directly, an abnormal C-terminal α-helix could possibly disrupt the folding of the TPR3, affecting the interaction with the HSP90 MEEVD motif. An interaction of HSP90 with the PPIase-like domain of AIP has recently been described,[518] but our data seem to indicate that the binding through the TPR domain might be more important for this protein-protein interaction to occur. Also interestingly, the binding to HSPA8 was one of the interactions more strikingly affected by the pathogenic AIP mutation p.R304* in the pull-down experiments.

Both chaperones, HSP90 and HSPA8, have a large list of interacting partners, and it would be necessary to perform another "fishing" experiment to identify the specific client proteins that can bind HSP90 or HSPA8 and AIP concomitantly in pituitary cells. In this sense, our triple co-IP experiment has identified an interaction between AIP, HSP90 and PRKACA, a known HSP90 client protein with a central role in somatotroph cell function. PRKACA forms part of the

heterotetrameric enzyme PKA. Upon activation by cAMP, the catalytic subunits of the enzyme (PRKACA and other isoforms) are translocated to the cell nucleus, where they phosphorylate CREB at the residue S133; activated CREB can then induce the transcription of genes containing a cAMP response element (CRE).[722] Subcellular localisation of the catalytic subunits of PKA is regulated by A-kinase anchor proteins (AKAPs), but its nuclear translocation is considered to be a passive process.[723] The interaction between HSP90 and PRKACA was found in a high throughput proteomic study[549] and has not been further functionally or structurally characterised. Considering the effect of the HSP90/AIP complex over the AHR function, it is feasible that this complex could regulate PKA localisation, by maintaining it in the cytoplasm, in which case they would possibly also interact with the PRKAR1A, as it has recently been suggested.[724]

The second category of interacting partners includes cytoskeletal proteins. Interaction of AIP with the microtubule structural proteins TUBB and TUBB2A has been validated, while interaction with other cytoskeletal proteins has been found by pull-down and MS, but not confirmed. This is not the first time that a role of AIP or other immunophilins as regulators of the cytoskeleton is proposed. The HSP90-binding immunophilin FKBP2 mediates the nuclear translocation of nuclear receptors by interacting with dynein, a regulator or the organisation of tubulin networks, through its PPIase domain.[725] However, previous studies addressing the interaction of AIP with cytoskeletal proteins rendered contradictory results. While no binding or very weak binding of the PPIase-like domain of AIP to dynein was found by one group,[726] a different study demonstrated that the AIP-mediated cytoplasmic localisation of the AHR requires the anchoring of the complex to actin filaments.[542] Even more, while the latter study proved a direct interaction between AIP and actin when AHR is inactive, a different group disproved this interaction.[570]

The microtubules are structures formed by heterodimers of α and β-tubulins of various isotypes (six of α and seven of β-tubulin), involved in cell movement, intracellular transport and cell division.[681;727] The microtubule-associated proteins regulate microtubule dynamics and also the interactions between microtubules and other cellular components.[728] Posttranslational modifications define distinctive groups of microtubules within the cell, and shape them to form structures with specific functions, e.g. mitotic spindle, cilia, flagella, basal bodies.[727] Microtubules forming the mitotic spindle are the target of anti-mitotic drugs used in the treatment of cancer, including microtubule-stabilising (taxanes and epothilones) and microtubule-destabilising (vincristine, vinblastine and vinorelbine) drugs; changes in the expression of β-tubulin isotypes and microtubule-associated proteins can modify the response to those drugs.[681]

Cytoskeletal disorganisation is a key feature of epithelial-mesenchymal transition (EMT), a process by which polarised epithelial cells develop increased migratory capacity, invasiveness, resistance to apoptosis and increased production of extracellular matrix, ultimately acquiring a mesenchymal cell phenotype.[729] One of the hallmarks of EMT is the loss of expression of e-

cadherin, a protein implicated in the formation of the adherens junction, and in somatotropinomas, e-cadherin expression correlates positively with GH and IGF-1 levels and response to SSA treatment, and negatively with tumour size and invasiveness.[730] The characteristics of somatotropinomas with low e-cadherin expression recapitulate the phenotype described in the *AIP*mut positive setting.[730] The EMT phenotype in somatotropinomas depends on the expression of ESRP1, an epithelial-specific splicing regulator.[730;731] A function of AIP as a microtubule-associated protein in the somatotroph cells, suggested by our results, would explain why the cells acquire an EMT phenotype in the setting of *AIP*mut positive pituitary adenomas (unpublished data by our group).

The third group is composed of proteins belonging to the ubiquitination pathway: FBXO3, SKP1 and RS27A. FBXO3 and SKP1 are part of the SCF E3 ubiquitin-ligase complex, while RS27A forms part of the ubiquitin chains. These findings suggest that AIP is degraded by the ubiquitin-proteasome system (UPS) via the SCF complex, and that this interaction is mediated by specific recognition of AIP via the F-box containing protein FBXO3. The cullin-really interesting new gene (RING) E3 ubiquitin-ligases (CRLs) are protein complexes composed of one of seven cullin family scaffold proteins, a RING domain enzyme (RBX1 or RBX2) bound to the C-terminal domain of the cullin protein, an adaptor protein, bound to the N-terminal cullin-repeat motifs of the cullin protein, and an F-box containing protein, bound to the adaptor protein.[732;733] The RING domain is responsible for binding to the E2 enzyme and stimulating ubiquitin transfer.[732] The SCF is the prototypical CRL, composed of the RING-containing enzyme RBX1, the cullin scaffold CUL1, the adaptor protein SKP1 and a variable F-box containing protein; this last protein regulates the specificity of the protein degradation via the UPS (reviewed in Chapter 4).[733;734]

F-box containing proteins are divided in three classes according to the domain used for interacting with the substrate: Fbxl (containing a C-terminal leucine-rich repeat domain), Fbxw (C-terminal WD40 repeat domain) and Fbxo (other domains or no recognisable domains).[735] Besides AIP, other proteins recognised by FBXO3 are the tumour necrosis factor receptor-associated factor inhibitor Fbxl2,[736] the Smurf1 ubiquitin ligase,[737] the serine/threonine-protein kinase homeodomain-interacting protein kinase 2 (HIPK2) and the histone acetyltransferase p300 HAT.[738] Given the great diversity of E3 ubiquitin-ligases encoded in the genome, further studies should be carried out to completely characterise this interaction. Interestingly, the qMS data showed an increased binding of FBXO3 and SKP1 to AIP p.R304* when compared to the WT protein. This differential affinity could possibly mean that the AIP p.R304* mutant protein is more prone to be ubiquitinated than the WT protein, a theory that will be further explored in Chapter 4.

Among the candidate AIP interacting partners not fully validated, two proteins, NME1 and SOD1, displayed positive co-IP only when using one of the anti-tag antibodies, but not when using the other one, and therefore, these molecular interactions cannot be discarded at the

moment. Of particular interest is NME1, the first metastasis suppressor gene identified, which is now also considered a tumour suppressor.[739-741] NME1 negatively regulates cell migration and motility, and displays both nucleoside diphosphate kinase and histidine protein kinase activity.[740] NME1 expression is upregulated by the G protein signalling regulator RGS19, and it phosphorylates the kinase suppressor of HRAS (KSR1), inhibiting the activity of HRAS and therefore the RAS/RAF/MEK/ERK signalling pathway;[742] for this reason, NME1 is also considered a tumour suppressor.[741]

NME1 mRNA levels are high in cell lines with low metastatic potential (murine K-1735 melanoma and N-nitroso-Nmethylurea-induced rat mammary carcinomas).[739] In contrast, LOH involving the NME1 locus (17q21.3), resulting in reduced protein expression, increases the risk of metastasis in colorectal cancer.[743] Low NME1 expression correlates with metastasis and poor clinical prognosis in different human epithelial cancer types, but in other tumour types (neuroblastoma and haematological malignancies) NME1 overexpression correlates with bad prognosis.[744] Moreover, NME1 KD in various human cancer cell lines disrupts e-cadherin-mediated cell adhesion, resulting in CTNNB1 nuclear translocation and transactivation of the T-cell factor/lymphoid-enhancing factor-1, a component of the WNT signalling pathway.[745] In contrast, overexpression of NME1 inhibits the metastatic potential of TP53-deficient HeLa cells.[741] NME1 co-localises with e-cadherin in epithelial cancer cell lines, suggesting a possible regulatory role of NME1 in the stabilisation of the adherens junction.[745] In pituitary adenomas, NME1 expression inversely correlates with tumour extension into the cavernous sinus.[690] A possible interaction between AIP and NME1 with a positive effect on NME1 function is feasible, as *AIP*mut positive pituitary adenomas are characterised by increased invasiveness. Low e-cadherin expression in pituitary adenomas, together with other markers of EMT, is an indicator of tumour progression and bone destruction, and NME1 could have a role in regulating e-cadherin function and therefore the organisation of the adherens junction in these tumours.

The enzyme SOD1, required for the conversion of superoxide to hydrogen peroxide, is located mainly in the cytoplasm, but also in the nucleus and in the intermembrane space of the mithochondria.[746] Mutations in the *SOD1* gene cause one fifth of the cases of familial amyotrophic lateral sclerosis.[747] SOD1 is overexpressed in breast and lung cancer cells. Treatment of non-small-cell lung cancer with a SOD1 inhibitor (ATN-224) induces MAPK1-mediated cell death *in vitro* and *in vivo.*[748] SOD1 is secreted by many cell lines, including the rat somatotropinoma-derived GH3 cells, both constitutively and in response to depolarisation through calcium-dependent mechanisms.[749] In GH3 cells, extracellular SOD1, through activation of a muscarinic M1 receptor, reduces the activity of the MAPK1 signalling pathway, via inhibition of MAPK3 phosphorylation, which resembles the effect of SSA on pituitary adenoma cells.[749;750] Therefore, SOD1 seems to be an interesting target for the effect of AIP on the SS pathway.

Conclusions

New molecular partners of AIP have been described. In line with the previously known function of AIP as a co-chaperone of HSP90 and HSPA8, interactions with two new members of the HSP70 families, HSPA5 and HSPA9 have been validated. These new interactions expand the repertoire of interactions between heat shock proteins and client proteins that could be modulated by AIP, but also opens a new window for possible anti-tumorigenic functions of AIP, as a regulator of stress-induced heat-shock protein functions. In addition, novel molecular interactions with the cytoskeletal proteins TUBB and TUBB2A indicate a possible role for AIP as a regulator of microtubule organisation, cell motility and adhesion, cellular functions which become of primordial importance in tumour development. Interactions with the proteins NME1 and SOD1 were only partially validated, and will require further study. Finally, an interaction of AIP with the SCF E3 ubiquitin-ligase complex indicates that AIP is processed via ubiquitination and proteasomal degradation, a pathway that will be further explored in the next chapter.

Chapter 4: Missense AIP variants and protein stability: implications for pituitary tumorigenesis

Introduction

The great majority of the *AIP*muts identified in patients are truncating mutations, and multiple mechanisms have been postulated to explain why they lead to LOF of the protein (see "*AIP as a pituitary-specific tumour suppressor: questions to be solved*"). While the functional effects of truncating mutations are usually evident, predicting the possible pathogenic effect of missense variants can be challenging. The amino acid substitutions caused by missense mutations can alter the structure, folding or stability of the protein, but they may also have no functional effect on the protein. In addition to *in silico* prediction platforms (reviewed in[751]), different methods can be used to determine whether missense variants are indeed pathogenic or not.

One option is evaluating the variant segregation in association with the phenotype,[752] but this should ideally be studied in large pedigrees with full familial medical history, which are not available for most of the patients. In the setting of a germline variant in a tumour suppressor gene, the finding of LOH involving that locus in a tumoral tissue is usually considered as a confirmation of involvement of the genetic variant on tumorigenesis.[753] Nevertheless, LOH is not an invariable finding in *AIP*mut-associated pituitary adenomas, even in those associated to clearly pathogenic variants; therefore, this parameter does not accurately determine pathogenicity. Functional studies could also be useful;[752] however, it is not clear which would be the most appropriate functional assay to evaluate *AIP*muts. Variants located in a mutational hotspot are more likely to be pathogenic,[754] but this parameter would be helpful to predict pathogenicity only for a minority of variants. The evaluation of protein stability could help to determine if the mutant protein is produced and if it has a normal turnover, regardless of its function.[755] The protein half-life depends on the rate of protein degradation and it is expected to be reduced in truncated or misfolded proteins, which is the role of the protein quality control system.

Missense *AIP*muts probably lead to unstable, rapidly degraded proteins, which is a possible mechanism for losing AIP tumour suppressor activity. This effect could be assessed by measuring the half-lives of mutant proteins. A similar study has been carried out before to characterise missense *MEN1* variants, showing that menin also degraded by the UPS, and that proteasome inhibitors rescue the short-lived mutants. Mutant menin is bound by HSC70 and then recognised by the E3 ubiquitin ligase CHIP, which drives the defective protein to ubiquitination and proteasomal degradation.[756] AIP might be degraded by ubiquitination and proteasomal degradation, based on its affinity for ubiquitin and the E3-ligase FBXO3 (see Chapter 2), but this degradation mechanism has not been proven before.

Aims

General

- To analyse the mechanism and speed of protein turnover of WT AIP and AIP missense variants, and to correlate the protein half-life with the phenotype, using protein stability as an indicator of LOF.

Specific

1. To determine the half-life under cycloheximide (CHX) treatment of the endogenous WT AIP protein in different cell lines.
2. To determine the half-life under CHX treatment of the endogenous AIP protein in a cell line derived from a p.R304* AIP mutation carrier.
3. To determine the half-life under CHX treatment of WT AIP, missense AIP variants and the nonsense AIP variant p.R304* overexpressed in a cell line.
4. To analyse the correlation between the half-life and the clinical phenotype in *AIP*mut positive patients.
5. To study the effect of the proteasome inhibitor MG-132 over the half-life of unstable AIP variants.

Hypotheses

- Missense *AIP* variants catalogued as pathogenic or likely pathogenic by *in silico prediction* are unstable proteins, and this is translated into reduced half-life.
- Missense mutant affecting conserved residues on the TPR domain are more likely to be unstable.
- AIP is degraded via ubiquitination and proteasomal degradation.
- Missense mutants with reduced half-life can be rescued by the treatment with a proteasome inhibitor.

Methods

Determining the half-life of endogenous AIP

The half-life of the endogenous AIP protein was measured in three different cell lines: HEK293 (human embryo kidney, ECACC 85120602) and two EBV-immortalised human B-lymphoblastoid cell (LC) lines: a commercially available cell line, derived from a healthy control (ECACC C0137, referred as EBV-LC-WT AIP), and a similar cell line, EBV-immortalised by ECACC, derived from an *AIP* c.910C>T (p.R304*) mutation carrier, member of a FIPA family (F70M38), with no pituitary adenoma (referred as EBV-LC-AIP p.R304*).

For experiments with HEK293, 12-well plates were plated with $5X10^5$ cells per well in complete medium (minimum essential medium [MEM] supplemented with 10% foetal bovine serum [FBS]/1X non-essential amino acids [NEAA]/2mM L-glutamine) and grown at 37°C/5% CO_2. Forty-eight hours later, the cells were treated with 100 µg/ml CHX diluted in complete medium,

or a similar volume of vehicle (dimethyl sulfoxide [DMSO]). Considering time 0 as the moment when the treatment started, three wells of cells were harvested at 0, 6, and 24 h for each experimental condition (cells harvested at time 0 received no treatment). For this purpose, the medium was removed, the cells were washed with 1X phosphate buffered saline (PBS), 75 µl of ice-cold lysis buffer were added, the cells were scraped from the wells and the content of each well was transferred to a microcentrifuge tube. After incubation at 4°C and centrifugation to pellet cell debris, 20 µg of total protein from these cell lysates were used for WB for AIP and beta actin (ACTB) as a loading control.

The amount of protein for each repeat at each time point was calculated by band densitometry, using the Odyssey application software v.2.1.12 (LI-COR Biosciences). The integrated density values for AIP were copied in an individual Excel spreadsheet for each experiment, and normalised by dividing each value by the value for the loading control in the same well. The values for the different time points were compared with the one-way ANOVA test for matched measures, followed by the post-hoc Tukey's test for multiple comparisons, using the GraphPad software.

The procedure for the EBV-LC-WT-AIP and AIP p.R304* cells was similar, but $3x10^6$ cells per well, plated in 6-well plates in suspension, were used, and the time points for cell harvesting were 0, 6, and 24 h for the WT AIP cell line and 0, 2, 4, 10, 12 and 24 h AIP p.R304*. In the AIP p.R304* experiment, 40 µg of total protein were used for WB. The experimental procedures are detailed in Protocol 30 (HEK293) and Protocol 31 (EBV-LC-WT AIP and AIP p.R304*).

Selection of AIP *variants*

A group of 14 missense *AIP* variants detected in pituitary adenoma patients from our cohort or reported in the literature was selected for the study. The variants were classified according to their pathogenicity likelihood, based on *in silico* prediction (see "Genetic screening"). Comments on the specific effect on the protein structure were kindly provided by C. Prodromou (some of them included in[523]), as shown in Table 20. Additionally, we included the WT AIP protein, as a "normal half-life control" (negative control) and the pathogenic nonsense *AIP*mut as a "short half-life" control (positive control), as this variant has been reported to be rapidly degraded in previous half-life experiments (unpublished data by F. Martucci and M. Korbonits).

Preparation of expression plasmids

A plasmid for the expression of the variant c.769A>G (p.I257V) was created by site directed mutagenesis from the pcDNA3.0-Myc-AIP plasmid. The following primers for site-directed mutagenesis were designed using the QuikChange Primer Design tool:[666]

c.769A>G_F: 5'-TGGACCACTGTTCTTCCGTCCTCAACAAGTACGAC-3'
c.769A>G_R: 5'-GTCGTACTTGTTGAGGACGGAAGAACAGTGGTCCA-3'

Table 20. Missense variants included in the study

Variant	Location in protein	Pathogenic	Effect on protein structure
c.47G>A (p.R16H)	N-terminus	No	No effect, protein out in solvent
c.145G>A (p.V49M)	PPIase domain	Unlikely	Out in solvent, strange for a hydrophobic change. Probably involved in interactions
c.509T>C (p.M170T)	Between PPIase and TPR1 domains	Likely	No structure available*
c.562C>T (p.R188W)	TPR1 domain	Likely	No prediction available
c.713G>A (p.C238Y)	TPR2 domain	Yes	Mutation causes severe steric clashes, disrupts packing of hydrophobic core[523]
c.760 C>T (p.C254R)	TPR2 domain	Likely	No prediction available
c.762C>G (p.C254W)	TPR2 domain	Likely	No prediction available
c.769A>G (p.I257V)	TPR2 domain	Likely	Disrupts packing of hydrophobic core[523]
c.811C>T (p.R271W)	TPR3 domain	Yes	Involved in packing by numerous polar interactions. W at this position is likely to be disruptive[523]
c.827C>T (p.A276V)	TPR3 domain	Unlikely	Involved in packing, some steric clash with V, but difficult to draw a definitive conclusion on the effect
c.871G>A (p.V291M)	TPR3 domain	Likely	Disrupts packing of hydrophobic core (forms base of hydrophobic pocket interacting with bound peptide)[523]
c.896C>T (p.A299V)	TPR3 domain	Unlikely	At start of C-terminal α-7 helix and may disrupt some small degree of packing with L292[523]
c.911G>A (p.R304Q)	TPR3 domain	Yes	Not involved in packing, but probably required for client protein interaction[523]
c.974G>A (p.R325Q)	C-terminal α-helix	Likely	Part of the C-terminal α-7 helix, may affect client protein binding[523]
*This residue is neither included in the NMR structure of the PPIase domain, nor in the crystal structure of the TPR domain.			

Site-directed mutagenesis was carried out using the QuikChange II XL Site-Directed Mutagenesis Kit (Agilent Technologies 200521), according to the protocol suggested by the manufacturer (details in Protocol 6). Colonies were selected and grown overnight at 250 rpm/37°C in 10 ml LB broth supplied with 100 µg/ml ampicillin; 1 ml of this bacterial culture was used to seed 250 ml of LB broth supplied with 100 µg/ml ampicillin (grown overnight at 250 rpm/37°C). The remaining 9 ml were centrifuged at for 10 min at 4000 g/4°C, and the bacterial pellets were used for plasmid DNA extraction, using the QIAprep Spin Miniprep Kit, as detailed in Protocol 5. The 250 ml cultures were pelleted likewise, the supernatants were discarded and the pellets were stored at 80°C until sequence confirmation.

Samples of 100 ng/µl plasmid DNA were submitted for Sanger sequencing at the Genome Centre, Barts and The London School of Medicine (BigDye Terminator v.3.1 kit in an ABI 3730 capillary sequencer, Applied Biosystems, Foster City, CA, USA) using the following primers:

pcDNA3.0_F: 5'-TCACTATAGGGAGACCCAAGC-3'
pcDNA3.0_R: 5'-CAACAGATGGCTGGCAACTA-3'

A contig was built using the ContigExpress software (Life Technologies), including the obtained sequences and the sequence of the WT plasmid, and the presence of the expected single nucleotide change was verified (Figure 48).

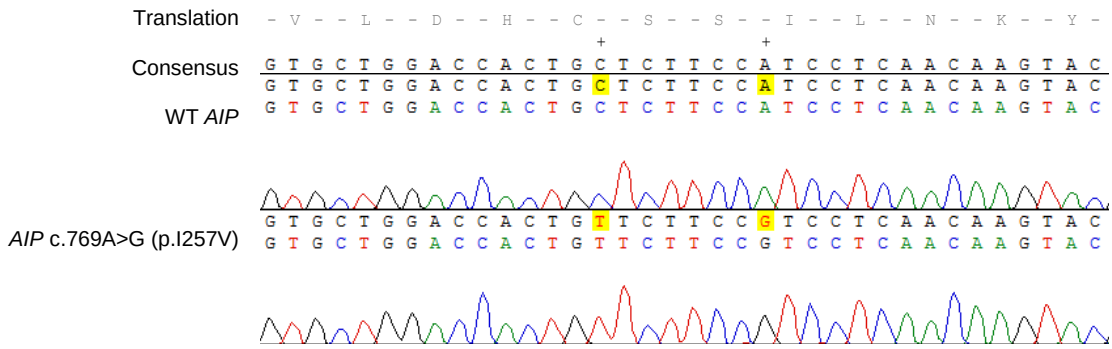

Figure 48. Chromatograms of WT *AIP* and *AIP* c.769A>G (p.I257V). These are the sequencing results for the CDS of the WT and the variant, cloned in pcDNA3.0. The mutant plasmid presents an unexpected nucleotide change probably induced during the SDM reaction (c.762C>T, highlighted C) resulting in a synonymous variant (at C254) that does not affect the protein sequence; therefore, the plasmid was used carrying this variant. The expected single nucleotide change is also observed (highlighted A).

After confirmation of the expected sequences, plasmid DNA was extracted from the frozen bacterial pellets using the GenElute™ HP Plasmid Maxiprep Kit according to the manufacturer's instructions (details in Protocol 7). For the rest of the mutants, a pre-existent collection of plasmids expressing Myc-tagged AIP missense mutants (obtained by site-directed mutagenesis from the pcDNA3.0-Myc-AIP plasmid), was used. When necessary, DH5α *E.*coli were transformed with plasmids from the pre-existent collection (Protocol 4) and plasmid DNA maxipreps were obtained after sequence confirmation, as described before.

Determining the half-life of overexpressed AIP

To determine the concentration of CHX to be used in these experiments, 12-well plates were plated with $2.5X10^5$ HEK293 cells per well in complete medium. Twenty-four hours later, the cells were transfected with 1 µg per well of the pcDNA3.0-Myc-WT_AIP plasmid, using Lipofectamine 2000, according to the manufacturer's instructions. Twenty-four hours later, the cells were treated with 5, 10, 20 or 50 µg/ml CHX, or a similar volume of DMSO. Considering time 0 as the moment when the treatment started, three wells of cells were harvested at 0, 6, 12 and 24 h for each experimental condition, and protein extraction, WB and protein quantification were performed as described before. Experiments using the WT AIP plasmid had an extra time point at 48 h. The experiment with DMSO was done with the WT AIP plasmid only. Using the same parameters than for the experiments with endogenous protein, the concentration of 20 µg/ml of CHX was chosen. Experiments using the WT and each of the mutant plasmids were performed at least twice with the chosen CHX, for a total of at least six repeats of each condition. The final experimental procedure used is detailed in Protocol 32.

Calculation and comparison of the protein half-lives

For all the experiments, the normalised protein levels were converted to percentages, considering time 0 as 100%, in a single Excel spreadsheet per experiment, as shown in Table 21. The results of all the experiments (expressed as percentages) were copied into a GraphPad

XY table, resulting in at least six repeats of each time point, for a total of three to four time points. These results were fit to a non-linear curve using the One Phase Decay equation, with the following parameters:

X: time
Y: starts at Y0 and decays (with one phase) down to plateau
Y0 and plateau: same units as Y
K: rate constant equal to the reciprocal of the X axis units
Initial value of Y0: 1 (*YMAX)
Initial value of plateau: 1 (*YMIN)
Initial value of K: 1 (/(value of X at YMID)
Constrains: Y0=100, plateau=0

These results were plotted as curves (with SEM for each time point) for each WT or mutant protein (including two experiments per mutation, in triplicates). The half-life of each protein was calculated based on these curves, using the formula: half-life=ln(2)/k. The degradation speed, represented by the K value, was compared between each mutant protein and the WT protein using the extra sum-of-squares F test. P <0.05 was considered significant and the variants tested were classified according to this values as “normal half-life” (P>0.05), “intermediate half-life” (P<0.05 but >0.0001) and “very short half-life” (P<0.0001).

Correlating half-life with phenotype

To analyse the possible impact of the half-life on the clinical phenotype in pituitary adenoma patients, clinical data from pituitary adenoma patients carrying the mutations in study was collected, including individuals from our cohorts of FIPA and young-onset sporadic pituitary adenomas and also cases reported in the literature by other research groups. Using the GraphPad software, the Spearman R test was employed to establish correlations between half-life and age at disease onset, age at diagnosis and maximum tumour diameter. The frequency of macroadenomas was compared between variants with very short half-life and normal or reduced half-life, using the Fisher’s exact test. Results were considered statistically significant when P was <0.05.

Rescuing very short-lived mutants

Experiments to counteract the degradation via the UPS of AIP variants with very short half-life were done using the proteasome inhibitor MG-132. To optimise the conditions for these experiments, HEK293 cells were plated, transfected with plasmids to express the short-lived variants (as described before) and treated with 20 µg/ml of CHX. After 6 h of treatment, MG-132 was added to a final concentration of 0, 20, 40 or 80 µM, the cells were harvested at 0 and 6 h and the results were plotted as a dose curve. The concentration of 20 µM, corresponding to the exponential phase of the curve, was chosen for the next experiments.

Table 21: Normalisation of integrated density values and conversion to percentages of the value at time 0

Integrated density of WB bands												
Sample:	AIPWT1 0-A	AIPWT1 6-A	AIPWT1 12-A	AIPWT1 24-A	AIPWT1 0-B	AIPWT1 6-B	AIPWT1 12-B	AIPWT1 24-B	AIPWT1 0-C	AIPWT1 6-C	AIPWT1 12-C	AIPWT1 24-C
Integrated density AIP:	B3	C3	D3	E3	F3	G3	H3	I3	J3	K3	L3	M3
Integrated density ACTB:	B4	C4	D4	E4	F4	G4	H4	I4	J4	K4	L4	M4
Ratio (AIP/ACTB):	=B3/B4	=C3/C4	=D3/D4	=E3/E4	=F3/F4	=G3/G4	=H3/H4	=I3/I4	=J3/J4	=K3/K4	=L3/L4	=M3/M4
Time point:	0 h	6 h	12 h	24 h								
Average ratio (AIP/ACTB):	=AVERAGE (B5,F5,J5)	=AVERAGE (C5,G5,K5)	=AVERAGE (D5,H5,L5)	=AVERAGE (E5,I5,M5)								
Standard error of the mean (SEM):	=STDEV (B5,F5,J5)/ SQRT(3)	=STDEV (C5,G5,K5)/ SQRT(3)	=STDEV (D5,H5,L5)/ SQRT(3)	=STDEV (E5,I5,M5)/ SQRT(3)								
Results expressed as percentages (time 0=100%)												
Sample:	=B2	=C2	=D2	=E2	=F2	=G2	=H2	=I2	=J2	=K2	=L2	=M2
Percentage of time 0:	=((B5*100)/ (AVERAGE ($B$5,$F$5, $J$5)))	=((C5*100)/ (AVERAGE ($B$5,$F$5, $J$5)))	=((D5*100)/ (AVERAGE ($B$5,$F$5, $J$5)))	=((E5*100)/ (AVERAGE ($B$5,$F$5, $J$5)))	=((F5*100)/ (AVERAGE ($B$5,$F$5, $J$5)))	=((G5*100)/ (AVERAGE ($B$5,$F$5, $J$5)))	=((H5*100)/ (AVERAGE ($B$5,$F$5, $J$5)))	=((H5*100)/ (AVERAGE ($B$5,$F$5, $J$5)))	=((J5*100)/ (AVERAGE ($B$5,$F$5, $J$5)))	=((K5*100)/ (AVERAGE ($B$5,$F$5, $J$5)))	=((L5*100)/ (AVERAGE ($B$5,$F$5, $J$5)))	=((M5*100)/ (AVERAGE ($B$5,$F$5, $J$5)))
Time point:	0 h	6 h	12 h	24 h								
Average percentage:	=AVERAGE (B14,F14, J14)	=AVERAGE (C13,G13, K13)	=AVERAGE (D13,H13, L13)	=AVERAGE (E13,I13, M13)								
Standard error of the mean (SEM):	=STDEV (B14,F14, J14)/ SQRT(3)	=STDEV (C13,G13, K13)/ SQRT(3)	=STDEV (D13,H13, L13)/ SQRT(3)	=STDEV (E13,I13, M13)/ SQRT(3)								

The experiment was also done for 20 µM MG-132, using a CHX pre-treatment time of 3 h, but the difference between the protein level at 0 and 6 h (using a Student's t test) was not significant for any of the doses. The final protocol consisted of CHX pre-treatment for 6 h, followed by addition of 20 µM MG-132, harvesting cells at 0, 6, 12 and 24 h after the addition of the proteasome inhibitor (Protocol 33).

The results were normalised and analysed as for the half-life experiments, except that they were expressed as percentages of the last time point (value at 24 h=100%) and also as fold-change from time 0 (value at time 0=1). The results of the independent experiments for each protein were pooled and the protein levels at different time points were compared using the one-way ANOVA test for repeated measures (Geisser-Greenhouse correction) and the post-hoc Dunnett's test to compare results at each time point with results at time 0. The Spearman R test was used to correlate the half-life of each variant with the results of the MG-132 "rescue" (expressed as fold-change) at 6, 12 and 24 h. Results were considered statistically significant when P was <0.05.

Results

Half-life of endogenous AIP in different cell lines

Half-life of AIP in HEK293 cells (68.2 h) was not significantly different to the value obtained in EBV-LC-WT AIP cells (33.1 h, P=0.1644). The average of the values at each time point in these two cell lines resulted in an average half-life of 34.1 h. In both cell lines the measured AIP half-life was significantly lower under CHX treatment compared to the DMSO control (P=0.0006 for CHX vs. DMSO in HEK293 cells and P<0.0001 in EBV-LC-WT AIP, confirming that the findings under this experimental conditions are due to the effect of CHX.

AIP half-life was practically identical in EBV-LC-WT AIP and in AIP heterozygous p.R304* cells (33.1 and 33.2 h, respectively). However, the measured WB bands corresponded to the WT protein in both cell lines, while the expected band for the mutant protein was not visible. Assuming biallelic expression, bands of 37.6 kDa for WT AIP and 34.5 kDa for the truncated protein AIP p.R304* (as calculated by the Expasy Compute pI/Mw tool)[757] would be expected in the WB images (Figure 49).

Findings were similar when repeating the experiment using 80 µg of total protein (data not shown), indicating that the mutant protein is either not expressed or very rapidly degraded. The later possibility was further explored in proteasome inhibition experiments (see "Rescuing very short-lived mutants"). However, the finding that the half-life of the WT protein is normal in these cells excludes the possibility of a dominant negative effect of the heterozygous nonsense mutation on the normal protein, at least regarding protein stability, under these experimental conditions.

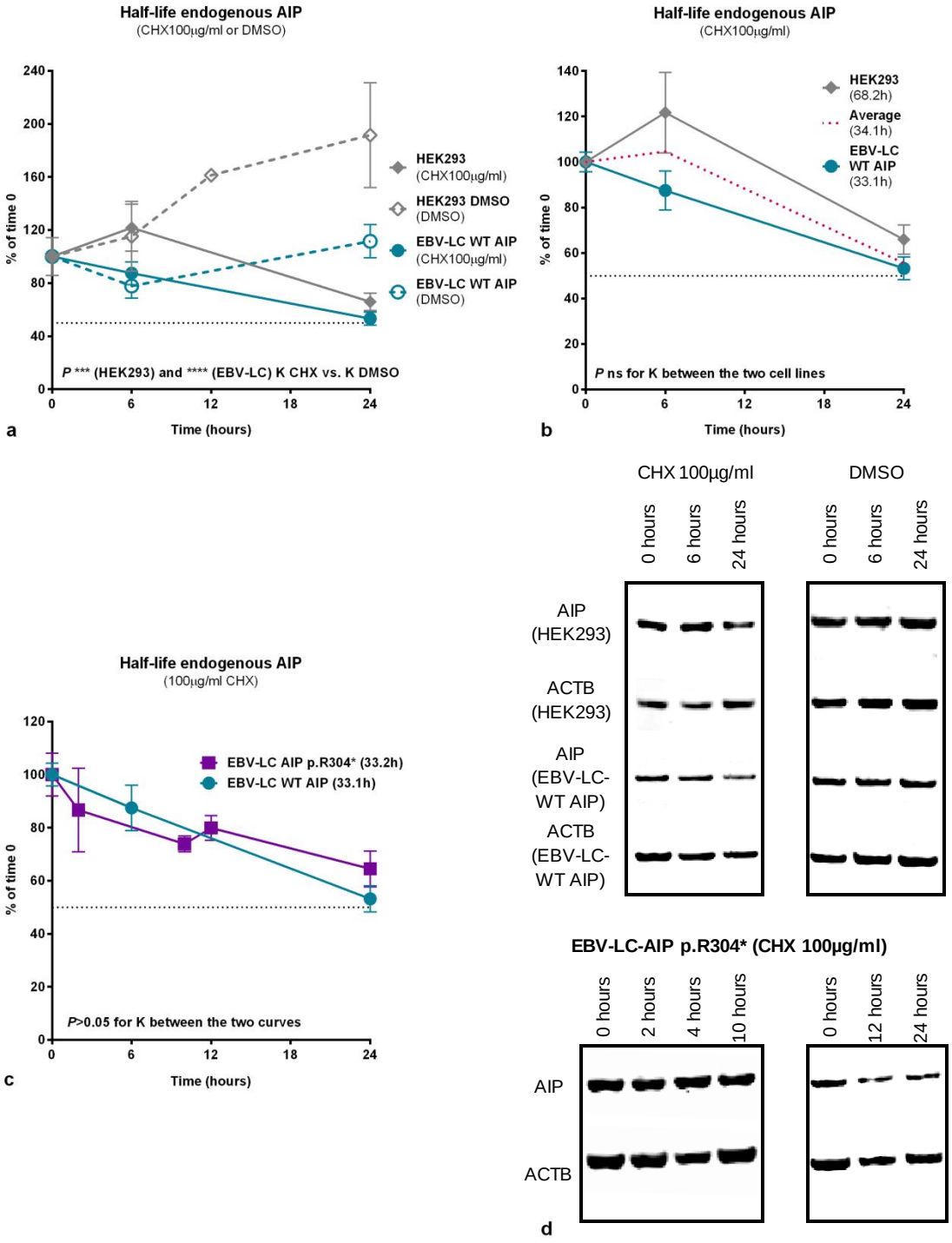

Figure 49. Half-life of endogenous AIP in different cell lines. a) AIP half-life was significantly lower under CHX treatment compared to the DMSO control in HEK293 and EBV-LC-WT AIP cells. b) AIP half-life in HEK293 cells was not significantly different to the half-life in EBV-LC-WT AIP. c) AIP half-life was almost the same in EBV-LC-WT AIP and AIP p.304* cells, when considering band densitometry for the normal protein. d) Representative WB images. The top panels are for the experiments with CHX and DMSO in HEK293 and EBV-LC-WT AIP cells, and the bottom panels are for EBV-LC-AIP p.R304* cells. WB bands for AIP (37.6kDa) and the loading control ACTB (41.7kDa) are shown in each case. Note the absence of the band for the mutant AIP p.R304* (expected mass: 34.5 kDa).

Half-life of overexpressed WT AIP and missense variants

The results of the half-life of the overexpressed proteins in HEK293 cells are summarised in Table 22 and Figure 50. Comparisons with the WT protein were established by means of the degradation speed (K) calculated from each half-life curve (Figure 50a and b). The AIP missense variants p.R16H, p.M170T, p.R304Q and p.R325Q behaved as stable proteins, with a similar half-life compared to the WT protein (normal half-lived variants, Figure 50c). The rest of the missense variants tested displayed a reduced half-life when compared to the WT protein. A group of variants (p.V49M, p.I257V, p.A299V) was considered to have an "intermediate" or "short" half-life, as the difference between their K and that of the WT protein resulted in $P<0.05$ but >0.0001 (Figure 50d). Variants whose K displayed maximum statistical significance ($P<0.0001$) when compared to the WT protein where considered to have "very short" half-life: p.R188W, p.C238Y, p.C254R, p.C254W, p.R271W, p.A276V, p.V291M, Figure 51). The variants with the shortest half-lives (p.C238Y and p.C254R) were located in the second TPR motif of the protein.

The pathogenic nonsense AIP variant p.R304* had a "very short" half-life (5.9 h), compatible with the proposed unstable behaviour of this variant (F. Martucci and M. Korbonits, unpublished). Interestingly, all the missense variants with "very short" half-life, except p.R188W and p.V291M, had degradation speeds comparable to that of the p.R304* variant (Figure 51 and Table 23). Also similar to p.R304*, their degradation curves were characterised for a fast decay of the protein in the first 6 h, followed by a plateau. In contrast, the curves for p.R188W and p.V291M displayed gradual decay throughout the duration of the experiment, similar in shape to that of the variants with "intermediate" half-life.

Table 22. Half-life of overexpressed AIP (WT and variants) in HEK293 cells

Variant	Location in protein	Half-life transfected protein (h)	Degradation speed (K)	*P* value (K *vs*. WT K)
c.47G>A (p.R16H)	N-terminus	94.2	0.0074	0.0512
c.145G>A (p.V49M)	PPIase domain	27.0	0.0257	**0.0359**
c.509T>C (p.M170T)	Between PPIase and TPR1 domains	66.6	0.0104	0.2931
c.562C>T (p.R188W)	TPR1 domain	21.0	0.0331	**< 0.0001**
c.713G>A (p.C238Y)	TPR2 domain	5.5	0.1270	**< 0.0001**
c.760 C>T (p.C254R)	TPR2 domain	4.7	0.1467	**< 0.0001**
c.762C>G (p.C254W)	TPR2 domain	8.4	0.0830	**< 0.0001**
c.769A>G (p.I257V)	TPR2 domain	28.7	0.0241	**0.0222**
c.811C>T (p.R271W)	TPR3 domain	8.2	0.0849	**< 0.0001**
c.827C>T (p.A276V)	TPR3 domain	7.2	0.0957	**< 0.0001**
c.871G>A (p.V291M)	TPR3 domain	11.2	0.0621	**< 0.0001**
c.896C>T (p.A299V)	TPR3 domain	21.6	0.0321	**0.0002**
c.911G>A (p.R304Q)	TPR3 domain	58.7	0.0118	0.5644
c.910C>T (p.R304*)	C-terminal α-helix	5.9	0.1183	**< 0.0001**
c.974G>A (p.R325Q)	C-terminal α-helix	88.8	0.0078	0.0948

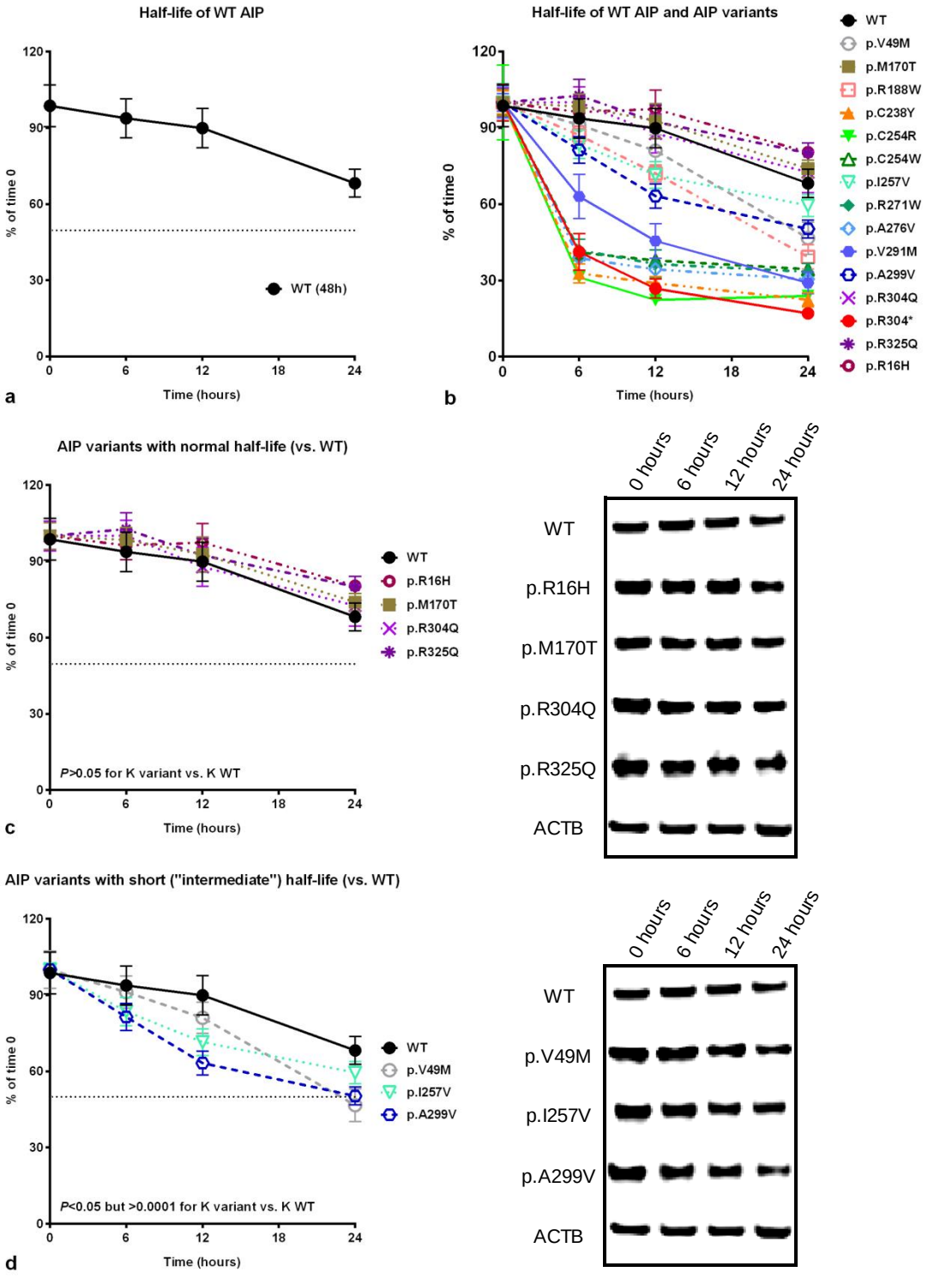

Figure 50. Half-life of WT AIP and variants, overexpressed in HEK293 cells (part 1). a) The WT AIP protein had a half-life of 48 h under the experimental conditions used. b) Half-life curves for all the variants studied, compared to the WT protein. c) Half-life curves for missense AIP variants with normal half-life (p.R16H, p.M170T, p.R304Q and p.R325Q) and representative WB images, compared to the WT protein. d) Half-life curves for variants with short or "intermediate" half-life (p.V49M, p.I257V, p.A299V) and representative WB images, compared to the WT protein. Myc-AIP=39 kDa, ACTB=41.7 kDa (the representative ACTB loading control shown corresponds to the WT experiment in each case).

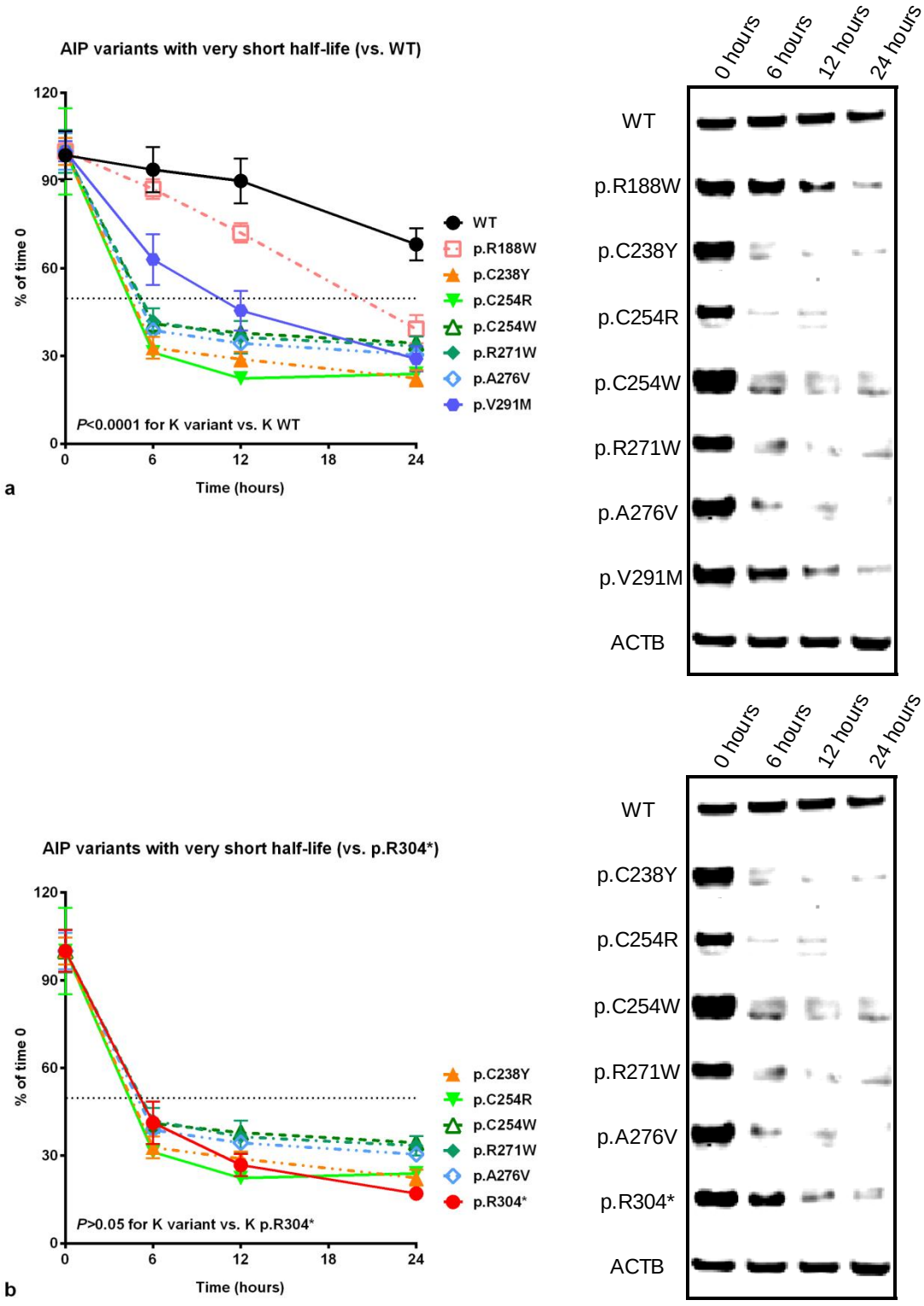

Figure 51. Half-life of WT AIP and variants, overexpressed in HEK 293 cells (part 2). a) Half-life curves for missense AIP variants with "very short" half-life (p.R188W, p.C238Y, p.C254R, p.C254W, p.R271W, p.A276V, p.V291M) and representative WB images, compared to the WT protein. d) Half-life curves for variants with half-life similar to the nonsense variant p.R304* (p.C238Y, p.C254R, p.C254W, p.R271W, p.A276V) and representative WB images, compared to p.R304*. Myc-AIP=39 kDa, Myc-AIP p.R304*=35.8 kDa, ACTB=41.7 kDa (ACTB loading control shown corresponds to the WT experiment in each case).

Table 23. Half-life of missense AIP variants with very short half-life

Variant	Location in protein	Half-life transfected protein (h)	Degradation speed (K)	*P* (K* *vs.* p.R304*)
c.562C>T (p.R188W)	TPR1 domain	21.0	0.0331	**< 0.0001**
c.713G>A (p.C238Y)	TPR2 domain	5.5	0.1270	0.7065
c.760 C>T (p.C254R)	TPR2 domain	4.7	0.1467	0.3735
c.762C>G (p.C254W)	TPR2 domain	8.4	0.0830	0.0652
c.811C>T (p.R271W)	TPR3 domain	8.2	0.0849	0.1141
c.827C>T (p.A276V)	TPR3 domain	7.2	0.0957	0.2749
c.871G>A (p.V291M)	TPR3 domain	11.2	0.0621	**0.0003**
* K= degradation speed				

Correlating protein half-life and phenotype

Clinical data of 100 pituitary adenoma patients (60 from our cohort and 40 cases reported in the literature) carrying the missense *AIP* variants and the nonsense variant included in the half-life experiments (Table 24). The variants c.47G>A (p.R16H), c.145G>A (p.V49M) and c.896C>T (p.A299V) were not included, as they are not considered pathogenic. The variant c.827C>T (p.A276V) was also excluded, as it has never been found in pituitary adenoma patients (detected only in a screening for *AIP* SNPs in DNA samples from different populations).[637]

Table 24: Missense *AIP* variants in pituitary adenoma patients: clinical features

Variant	No. of cases			Clinical presentation	Gender (M/F)	Age at onset, median (IQR)	Age at diagnosis, median (IQR)	Macro/ micro, no.	References
	Our cases	Other cases	Total						
c.509T>C (p.M170T)	0	1	1	Simplex	1/0	NA	32	NA	[13]
c.562C>T (p.R188W)	1	0	1	Simplex	1/0	10	12	NA	Unpublished
c.713G>A (p.C238Y)	3	0	3	Familial	3/0	20 (18-22)	21 (19-23)	2/0	[9;495]
c.760 C>T (p.C254R)	1	0	1	Familial	0/1	14	17	1/0	Unpublished
c.762C>G (p.C254W)	2	0	2	Familial	1/1	26 (21-31)	28 (23-33)	1/0	Unpublished
c.769A>G (p.I257V)	0	1	1	Simplex	1/0	NA	NA	NA	[11]
c.811C>T (p.R271W)	1	8	9	Both	7/2	15.5 (12.8-18.3)	22 (14-28)	9/0	[7;10;484;629]
c.871G>A (p.V291M)	0	1	1	Simplex	0/1	NA	30	NA	[632]
c.911G>A (p.R304Q)	13	8	21	Both	6/13	27 (22-37)	36 (24.3-39.5)	14/3	[7;9;10;12;13;498;539;615;632]
c.910C>T (p.R304*)	39	18	57	Both	31/26	17 (15-25.8)	19.5 (17-28.5)	43/5	[7;9;10;12;13;498;507;631]
c.974G>A (p.R325Q)	0	3	3	Both	1/2	16 (7-33)	18 (16-35)	3/0	[13;758]
Total:	60	40	100		52/46	18 (15-27)	23 (17-32)	73/8	
Age at onset and at diagnosis is expressed in years. Macro/micro: macroadenomas/microadenomas.									

Spearman correlation tests were ran to determine whether the half-life of the mutant proteins could correlate with the clinical features in these patients (age at onset, age at diagnosis, tumour size), expecting that less stable proteins would lead to a more aggressive phenotype

(Figure 52). A direct correlation between age at diagnosis and protein half-life was found (r=0.3810, *P*=0.0015), which remained significant after excluding patients carrying the p.R304* nonsense variant (r=0.3478, *P*=0.0259). The significance of this correlation increased when only patients with GH excess (acromegaly or gigantism) were considered (r=0.411, *P*=0.002). Correlation between half-life and maximum tumoral diameter or age at disease onset did not reach statistical significance (r=0.1399 [*P*=0.3788] and r=0.2205 [*P*=0.0540]); however, clinical data for these parameters was missing in a large number of patients. The proportion of patients with macroadenomas (vs. microadenomas) was similar for very short half-lived variants and other variants (*P*=0.4007).

Short-lived AIP variants are partially rescued by proteasome inhibition

Stable WT AIP protein levels were found under proteasome inhibition with MG-132, with minimal, but not significant increase at 0, 6, 12 and 24 h of treatment (fold change at 24 h: 1.1, global *P*=0.3592). Likewise, levels of the AIP variants p.R188W (fold change at 24 h: 1.1, global *P*=0.5080) and p.V291M (fold change at 24 h: 1.4, global *P*=0.1263) remained stable. In contrast, levels of the rest of the variants studied, including the p.R304* nonsense variant, significantly raised in response to MG-132: p.C238Y (fold change at 24 h: 2.1, *P*=0.0403, 0.0170 and 0.0015 at 6, 12 and 24 h, respectively), p.C254R (fold change at 24 h: 2.6, *P*= 0.0087, 0.0008 and 0.0094), p.C254W (fold change at 24 h: 1.7, *P*=0.0910, 0.0006 and 0.0087), p.R271W (fold change at 24 h: 1.7, *P*=0.1796, 0.0229 and 0.0676), p.A276V (fold change at 24 h: 3.9, *P*=0.0072, 0.0120 and 0.0225) and p.R304* (fold change at 24 h: 2.4, *P*=0.0055, 0.0041 and <0.0001, Figure 53a, b and c).

Pooling all these results together, a significant indirect correlation was found between protein half-life and protein levels at 6 (r=-0.6279), 12 (r=-0.8292) and 24 h (r=-0.8022) of MG-132 treatment (*P*<0.0001 for all the time points), meaning that proteins with shorter half-lives displayed a more dramatic response to proteasome inhibition (Figure 53d). These findings confirm that WT AIP is a very stable protein, whose degradation is driven by the proteasome system, and that an enhanced proteasomal degradation is responsible for the reduced half-life shown by some missense variants.

After the treatment of EBV-LC-AIP p.R304* cells with the proteasome inhibitor MG-132 for 3 or 6 h, the WB images displayed an additional band with a slightly faster migration, compared to the WT protein (Figure 54). A third extra band, below the second one was present at 0 h and disappeared after treatment with the proteasome inhibitor. Though both of these bands could represent degradation products (a frequent finding in WB images), it is possible that one of them, (more likely the highest one) could correspond to the mutant protein p.R304*, meaning that the mutant protein is expressed, but rapidly degraded via the proteasome system, and therefore it is not visible in basal conditions. A similar behaviour could be assumed for the unstable missense AIP variants.

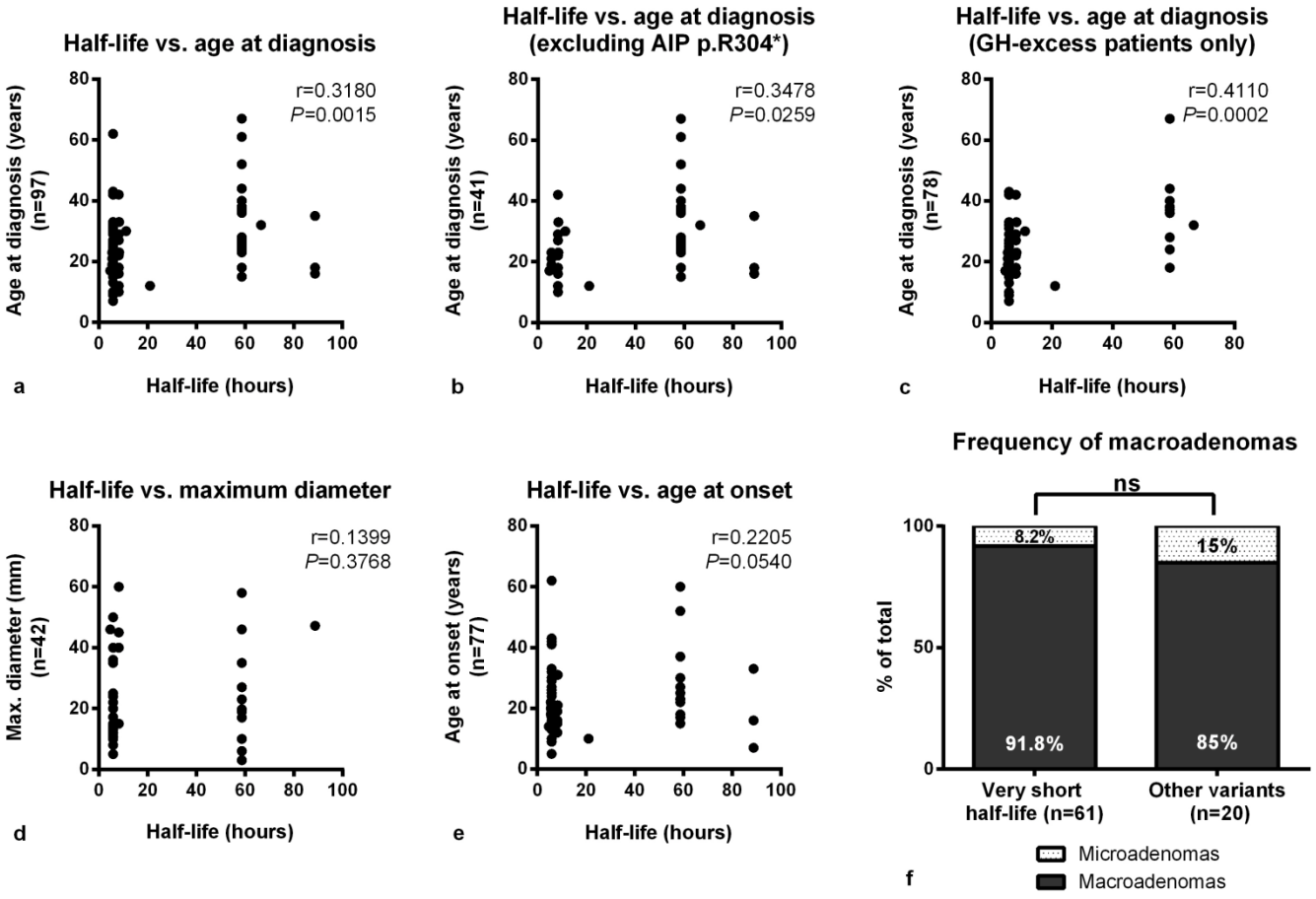

Figure 52. Implications of AIP half-life for the phenotype in pituitary adenoma patients. a) The half-life of very AIP variants directly correlated with the age at diagnosis, b) even when excluding patients with the p.R304* mutant; c) the significance increased when considering only patients with acromegaly or gigantism. d) There was no significant correlation between half-life and maximum tumoral diameter or e) age at onset. f) The frequency of macroadenomas did not differ between patients with very short half-lived variants and other variants.

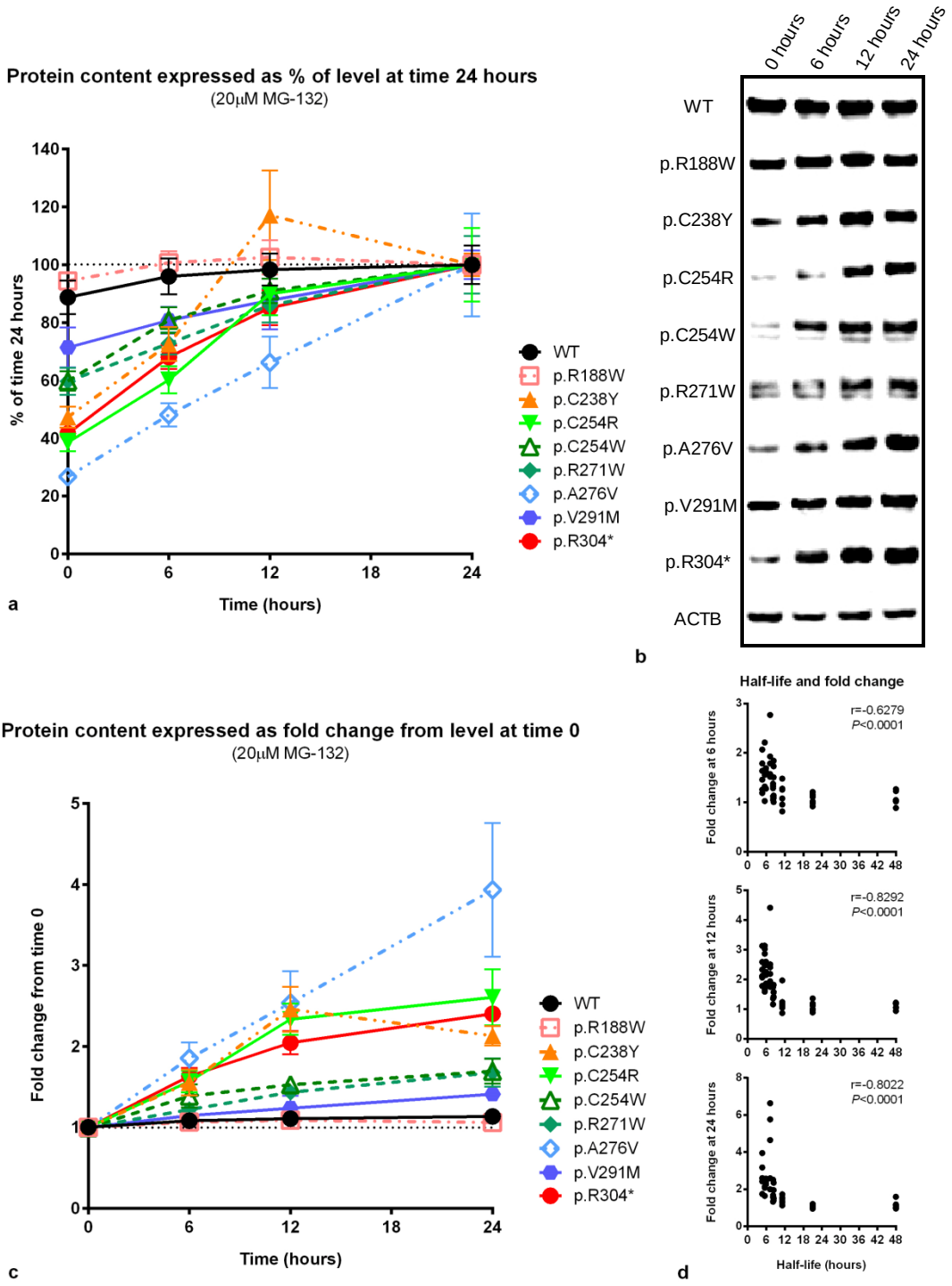

Figure 53. Blocking of proteasomal degradation with MG-132 ("rescue experiments"). a) Curves of protein contents for the experiments with the variants and WT protein, expressed as percentages (level at time 24 h was considered as 100% for each protein) and b) representative WB images. c) Same results, expressed at fold change from time 0 for each protein (time 0=1). d) Correlation between half-life and fold change after MG-132 treatment at 6, 12 and 24 h. A significant indirect correlation was found at the three time points, indicating proteins with shorter half-lives responded better to proteasome inhibition.

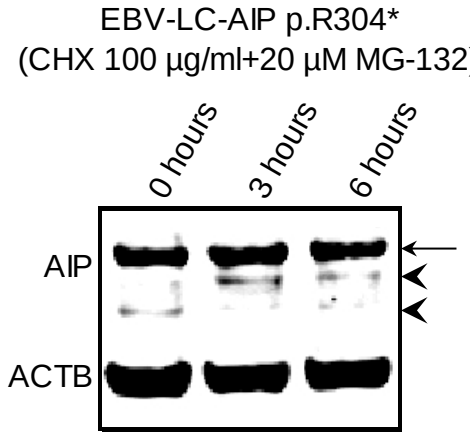

Figure 54. MG-132 treatment of EBV-LC-AIP p.R304* cells. In the AIP WB (using 40 µg of total protein) the strongest band (arrow) corresponds to the WT protein (37.6 kDa). Two faint extra bands can be observed: a first band which is absent at time 0 and appears after the treatment with MG-132 (top arrowhead) and a second, lower band (bottom arrowhead), which is more evident at time 0. Though both bands could correspond to degradation products, the largest band could possibly be given by a small amount of truncated protein, appearing after proteasomal degradation is stopped (expected size: 34.5 kDa). Loading control: ACTB (41.7 kDa).

Discussion

Although the four fundamental cellular processes involved in gene expression, i.e. transcription, mRNA degradation, translation and protein degradation, are targets for regulatory events, cellular abundance of proteins is predominantly controlled at the level of translation. Protein stability seems to have a smaller role in cellular protein abundance under basal conditions, but could be important under stimulation.[759] The maintenance of intracellular proteostasis requires the correct functioning of complex regulatory mechanisms, which are frequently disrupted in human diseases.

Different *in vitro* experimental approaches can be used to determine protein turnover, usually expressed as half-life, i.e. the time it takes for the protein of interest to be reduced by 50% relative to its level at time 0. Pulse-labelling (pulse-chase analysis) is considered the "gold standard" method for this purpose),[759] with the advantage of causing minimal disruption on cell growth and metabolism. In this method the protein of interest is labelled in previously amino acid starved cells (to deplete the pool of the amino acid to be used for labelling) using a radioactive precursor (e.g. ^{35}S-methinine or cysteine) or heavy stable-isotope versions of essential amino acids (stable isotope labelling by amino acids in cell culture [SILAC]), and after a time period, an excess of a non-labelled precursor is added to prevent further incorporation of the labelled amino acid.[759;760] Cells are harvested at different time points and then they are either immunoprecipitated, resolved by PAGE and quantified by phosphor imaging or autoradiography, or quantified by qMS.[760;761] A disadvantage of this method is the requirement of either radioactive reagents or costly MS reagents and equipment. Another problem is a possibly enhanced ubiquitin-proteasomal activity after amino acid starvation, which can influence the results.[760]

Another frequently used technique is blocking protein synthesis with CHX (CHX chase), a chemical translation inhibitor, which exerts its effect by blocking eEF2-mediated tRNA translocation.[762;763] In this approach, protein synthesis is stopped at some point by the addition of CHX, and the decay of the target protein over time is measured by harvesting cells at different time points and determining the amount of target protein in WB membranes by protein band densitometry. When antibodies against the protein of interest are not available or when studying the effect of mutations on protein stability (and there are no cell lines available endogenously expressing these mutants) tagged proteins can be expressed in cell lines and detected with antibodies raised against the tag. Small tags (e.g. Myc, Flag, HA, V5) are usually employed, but the location of the tag in the protein (N- or C-terminal) could interfere with the normal protein structure.[760]

A disadvantage of this method is that, given that the protein half-life is measured when protein synthesis has been stopped, the results might not reflect the real turnover rate under physiological conditions, as the abundance of the proteolytic enzymes can also be affected.[761] Inhibition of protein synthesis also activates (via the PI3K signalling pathway) the serine/threonine kinase AKT (transforming murine retrovirus AKT8-related oncogene), resulting in phosphorylation of AKT target substrates such as FoxO1,GSK-3α/β, p70S6 kinase, AS160 and the E3 ubiquitin ligase MDM2, and this leads to altered degradation of some proteins.[764] Although this means that half-life measurements obtained under CHX treatment might not accurately reflect the values under physiological conditions, these problems can be partially solved by comparing the results against a control protein. Moreover, good correlation of half-lives obtained by SILAC and CHX chase experiments was recently reported for high turnover proteins in a proteome-scale protein/mRNA half-life quantification study.[759]

Protein and mRNA half-lives are not randomly regulated. Genes with stable mRNAs and stable proteins, such as housekeeping genes, are enriched in constitutive cell functions (translation, respiration and metabolism), while genes with unstable mRNAs and unstable proteins are enriched among transcription factors, signalling, chromatin modifying enzymes and genes with cell-cycle specific functions. Abundant proteins are more stable than the less abundant ones, and highly structured proteins are more stable than the less structured ones.[759] Determining which proteins are to be repaired or degraded, often referred as “protein quality control”, depends on different co-translational and posttranslational mechanisms to repair or remove misfolded proteins.[765] Protein folding, unfolding, disaggregation and remodelling are functions carried out by the chaperone network of proteins.[766] Cells use two main mechanisms for protein degradation: autophagy and the UPS.

Cytoplasmic contents are degraded by lysosomes through a mechanism known as autophagy or “self-eating”, which is divided in three types according to their substrates and mechanisms of sequestration: microautophagy, chaperone-mediated autophagy (CMA) and macroautophagy.[765;767] In microautophagy, cytoplasmic materials are transported into the lysosomes by invagination of the lysosomal membrane and posterior formation of intralysosomal vesicles, which are then degraded.[765] CMA starts by the binding of an individual cytoplasmic protein to HSC70 through a pentapeptide motif located on the target protein (KFERQ-like); then the chaperone-substrate complex is recognised by the lysosomal membrane associated protein 2A (LAMP2A), the substrate is unfolded and translocated into the lysosome via polymerised LAMP2A, and finally degraded into the lysosomal lumen. Macroautophagy can be selective or nonselective and it is regulated by several intracellular and extracellular stimuli.[767] In this process large portions of cytoplasm, sometimes including organelles, are engulfed within a compartment termed as phagophore, which matures into a double-membrane enclosed structure known as an autophagosome that fuses with the lysosomal membrane, allowing degradation of the cargo.[765;767] Independently of the delivery process, proteins processed by autophagy are degraded by hydrolases in the lysosome and the breakdown products are released back into the cytosol through permeases, therefore allowing their recycling for protein synthesis or energy production.[767]

The ubiquitin-proteasome pathway follows two steps: a specific recognition process, involving the ubiquitin conjugation cascade, and a proteolytic step, carried out by the proteasome core. Ubiquitin, a highly conserved 8.5 kDa protein, is activated by the ubiquitin-activating E1 enzyme, which, in an ATP-dependent reaction, forms a thioester bound with the ubiquitin G76 (C-terminus).[732] Ubiquitin is then transferred by transacylation to a thiol group of an active C residue of an E2 enzyme (ubiquitin carrier protein or ubiquitin-conjugating enzyme), to yield an E2-Ub thioester intermediate.[732;768] Finally, an E3 ubiquitin-ligase (or ubiquitin-protein ligase) enzyme, consisting of either a single protein or a protein complex, catalyses the transfer of the ubiquitin from the E2 to the substrate, where it binds either an ε-amino group of a K or the N-terminus.[732;768] E3 ubiquitin-ligases can catalyse direct transfer of ubiquitin from E2 to the substrate (binding both the E2-Ub complex and the substrate) or function in a two-step reaction, in which ubiquitin is transferred from the E2 to an active site C on E3 and then from the E3 to the substrate.[732] Once the substrate is mono-ubiquitinated, a polyubiquitin chain of four or more ubiquitin subunits bound through their K48 residues is formed to serve as a recognition signal for proteasomal degradation, a process counteracted by the removal of ubiquitin subunits from ubiquitinated proteins by more than 100 different deubiquitinating enzymes (DUBs).[765]

The specificity of ubiquitination is determined by a variety of E1, E2 and, more importantly, E3 enzymes. The E1 function can be performed by two E1 enzymes in humans, binding different E2s: ubiquitin-like modifier-activating enzyme 1 (UBA1) and ubiquitin-like modifier-activating enzyme 6 (UBA6), while thirty-five different E2 enzymes exist in humans, with

specificity for different E3 enzymes.[769] In contrast, more than 1000 human E3 enzymes have been described, divided in five classes: the cullin-RING and U-box containing E3 ubiquitin-ligases families, the homology to E6AP C-terminus (HECT), the RING-between-RING (RBR) family and the PHD-containing E3 ubiquitin-ligases.[732;769-771]

The proteasome is a large multi-subunit protease formed by ~33 different proteins, which is found free in the cytosol and also attached to the ER, as well as in the nucleus of eukaryotic cells.[765] The eukaryotic proteasome is formed by two subunits: a catalytic core particle (20S proteasome) and a regulatory subunit (19S proteasome, 11S proteasome or both). The ~700 kDa core particle of the proteasome is composed of 28 subunits, arranged into four stacked heptameric rings (two rings consisting of related α-subunits and two consisting of related β-subunits) forming a compact hollow cylinder.[772] There are a total of six proteolytic sites on the proteasome, located on three of the β-subunits in the central cavity, with relatively weak preferences for specific target amino acids, being able to cleave almost any sequence; however, their location makes them inaccessible for folded proteins due to the narrow pores at the entrance to the core particle.[768;772] The proteasome β-subunits with proteolytic activity are sometimes referred as caspase-like (β1), trypsin-like (β2), and chymotrypsin-like (β5) subunits, due to their mechanisms of action.[773] The pores at the entrance of the core particle are usually closed in the inactive state, and open after activators or caps bind the core particle. Two types of activators, the 11S cap (proteasome activator 28 [PA28, also known as REG] in mammals) and bleomycin-sensitive 10 cap (Blm10, also known as PA200 in humans) trigger ATP-independent protein degradation of non-ubiquitinated substrates. The 19S regulatory particle recognises ubiquitinated proteins, unfolds them (requiring ATP hydrolysis) and translocates them into the core particle. Most of the eukaryotic proteasomes are formed by one 20S and one or two 19S proteasome subunits, forming together the 26S proteasome.[772]

The 19S regulatory particle (~900 kDa) is formed by at least 19 subunits organised in a “base and lid” conformation. The base consists of six ATPases, two large organising and two established ubiquitin receptors (Rpn10 and Rpn13), binding polyubiquitin via their ubiquitin interacting motif (UIM).[765;772] The lid consists of the deubiquitinating enzyme Rpn11 and, in addition to proteasome subunits, a large number of proteins associate with the 19S regulatory particle to modulate degradation.[772]

In addition to ubiquitin, proteasomal degradation can also be triggered by ubiquitin-like proteins, such as neural precursor cell expressed developmentally down-regulated protein 8 (NEDD8), small ubiquitin-like modifier (SUMO) and interferon-induced 15 kDa protein (ISG15), following a similar activation cascade.[769] Misfolded or unassembled proteins located in the ER can also be directed to ubiquitination and proteasomal degradation by the process termed as ER-associated protein degradation (ERAD).[774] A crosstalk between the UPS and

autophagy exists, as ubiquitination can serve as a posttranscriptional modification regulating autophagy.[767]

Considering all these factors, the CHX-mediated synthesis inhibition approach was used for studying AIP half-life. Under the experimental conditions used, WT AIP behaved as a stable protein, either studied as an endogenous or an overexpressed protein, with a half-life of 33.1-68.2 h (median: 48 h), which is near the median half-life of 46 h calculated for the whole mammalian proteome (range of <30 min to >200 h).[759] The half-life of human AIP in EBV-LC-WT AIP cells (33.1 h) was very similar to the half-life of mouse Aip, measured by SILAC in NIH 3T3 cells (mouse fibroblast), which is 30.4 h.[759]

Co-chaperones play important roles as regulators of protein quality control. Different co-chaperones, by their interaction with HSP90 or HSP70, can enhance the ubiquitination and proteasomal degradation of client proteins. Examples of proteins with this function include FKBP25,[775] cyclophilin B[776] and the TPR-containing protein AIPL1, which shares around 50% amino acid homology with AIP.[777] Interestingly, the co-chaperone CHIP is itself, an E3-ubiquitin ligase.[778] However, AIP has no structural characteristics compatible with any of the E3-ubiquitin ligase classes, and its function as a co-chaperone seems to be more directed to stabilise its client proteins, and not to promote their degradation, though the later possibility has not been explored. On the other hand, immunophilins, such as FKBP12 can also be degraded via ubiquitination,[779] and this has now been proven also for AIP.

The amino acid sequence of the TPR motifs of AIP is important to ensure a correct interaction of residues in contiguous chains, and therefore, a correct protein folding.[528] The amino acids located in the pocket between TPRs 2 and 3 are essential for the interaction of AIP with HSP90, and amino acids at this location are among the most conserved ones.[523] Missense mutations affecting residues involved in folding of the TPR domain could lose their ability to interact with other proteins. Moreover, misfolded proteins could be unstable, and display a rapid turnover, when compared to the WT protein, which was the case of most of the missense variants studied.

Half-life experiments are only one of many possible approaches for evaluating protein functionality, and therefore, the possible pathogenicity of gene variants. While for most of the variants the pathogenicity predictions (based on *in silico* prediction and other functional/clinical data, as explained in Chapter 2) matched the half-life results (i.e. pathogenic variants had very short half-life). Considering that defining the pathogenicity of missense mutants is not an easy process and there are no experimental methods that could possibly render “black and white” results, we observed some discrepancies. First, only one of the four variants included in the group with normal half-life is currently considered a non-pathogenic variant (p.R16H), while the other three (p.M170T, p.R304Q, p.R325Q) are considered truly pathogenic. While the variant p.M170T has only been reported in one

patient,[13] and p.R325Q has been detected in three cases,[13;758] p.R304Q seems to be much more common (21 patients reported so far).[7;9;10;12;13;498;539;615;632] Apart of the *in silico* prediction and clinical data, no functional data are available for p.R325Q (MAF 0.0001)[217] and p.M170T (MAF not available at the NHLBI EVS, ExAC or 1000 Genomes databases). For p.R304Q (MAF 0.0007[216] and 0.0015[217] according to two different databases), though clinical data supports a pathogenic role, experimental results are against a negative effect on protein function.[10;539] If these variants are really pathogenic, the mechanism should be related to loss of protein function, independent of protein stability.

Second, the definition of "intermediate half-life" was arbitrary (based on statistical significance) but it is important to remark that the three variants included in this group had reduced half-life, two of them considered unlikely pathogenic (p.A299V and p.V49M) and one considered truly pathogenic (p.I257V). The study of the AIP 3D molecule predicted a possible structural effect for p.A299V and p.I257V (Table 20), and, though no prediction was available for p.V49M, the change of a hydrophobic (V) for a polar (M) amino acid could possibly disrupt the folding of the PPIase domain. While for p.I257V the half-life results match the pathogenicity prediction, this is not the case for p.A299V and p.V49M. The AIP variant c.896C>T (p.A299V) is an apparently non-pathogenic SNP (MAF of 0.001[216;218] and 0.0004[217] according to three databases) and the analysis of the clinical data of variant carriers, together with the results of different functional studies support an apparently benign behaviour of this variant.[9;10;539] On the other hand, p.V49M is an uncommon SNP (MAF 0.0002[216;217]) which has only been reported in one patient, a male with gigantism presenting as a *simplex* case, with no LOH in the tumour.[640] The clinical data available, the rarity of the SNP and now the half-life data support a pathogenic role for this variant, and its classification as unlikely pathogenic should be reconsidered.

In the half-life experiments with the cell line EBV-LC-AIP p.R304* the mutant protein was not detected by WB, except (probably) when the cells were treated with a proteasome inhibitor, supporting the finding of a very unstable behaviour of this protein. The p.R304* mutant is a truncated protein with loss of the C-terminal α-helix. While no direct effect of the mutation is expected on the TPR motifs of the protein, protein interaction studies (see Chapter 3) have shown a partial loss of interaction with HSP90 and HSC70 for this mutant. Considering that the main interaction site for those chaperones is located on the TPR motif, it is probable that the loss of the C-terminal α-helix could somehow disrupt also the folding of the TPR motifs. This is also supported by the fact that the effect of this nonsense mutation on protein half-life has similar to that of the missense mutations affecting the TPR 2 and 3. Also, the loss of certain protein interactions can make proteins more prone to ubiquitination and proteasomal degradation. It has been shown that AIP TPR mutants unable to bind HSP90 or to assemble AHR/HSP90 complexes apparently have a normal half-life, meaning that AIP stability is probably independent of HSP90 binding,[521] though other ligands could possibly stabilise the protein. Conversely, if a short half-life is translated into an almost absent protein under

physiological conditions, it could be assumed that the endogenously expressed short half-lived missense variants would be present also at very low levels in the cells. As it was pointed out in the results, some of the studied variants behaved as unstable as p.R304*, while others had a still reduced, but longer half-life. Whether these “intermediate” half-lived variants could be endogenously expressed at higher levels compared to “very short” half-lived variants would be an interesting avenue for further research.

As mentioned before, LOH is not a universal finding in *AIP*mut positive pituitary adenomas. As *AIP*muts are always found in the heterozygous state, other mechanisms inhibiting the function of the normal allele should be explored. On this regard, the half-life experiments have two different implications. First, the fact the half-life of the WT AIP is normal in the presence of a heterozygous unstable variant, rules out the possibility of a dominant negative effect of the mutant protein, an effect which accounts, for example, for the loss of tumour suppressor function of TP53.[780] Second, as the expression of AIP is apparently biallelic, the expression of both alleles might be necessary for AIP to perform its tumour suppressor function, under basal or stimulated conditions, and the reduction on total AIP expression could be translated on an insufficient anti-tumorigenic response (haploinsufficiency) in the pituitary gland.[781] It would also be interesting to determine whether the apparently pathogenic variants with normal half-life behave in a similar way, or if in those cases the proteins are expressed at normal levels, but interfere with the stability or function of the normal protein (i.e. if they have dominant negative effect).

Interestingly, the half-life of the AIP variants studied directly correlated with the age at diagnosis in pituitary adenoma patients carrying those mutations. Correlation with age at disease onset and tumour size was not statistically significant, perhaps due to the small number of patients for whom those parameters were available. This finding contributes to validate the half-life assay as a method for determining the pathogenicity of *AIP* variants, and it suggests that disease penetrance in the setting of *AIP*muts can be determined by the amount of functional protein available. Nevertheless, protein stability is a parameter that cannot be evaluated with routine diagnostic histopathological procedures. As IHC represents a static image of a tissue, pituitary adenomas with very unstable missense *AIP*muts and LOH could display normal immunostaining for AIP, and still be almost devoid of functional AIP. The use of a protein stability assay as a means to evaluate the pathogenic effect of missense variants has also been applied for *MEN1.*[756;782]

Dysfunction of the ubiquitination pathway is related to a variety of human disorders, such as different cancer types (tumour-suppressing and tumour-promoting pathways are regulated by ubiquitination and DUBs, such as A20, CYLD and BAP1 are tumour suppressors frequently mutated in cancer), autoimmune, neurodegenerative and metabolic diseases.[783] Of special interest for endocrine tumorigenesis, mutations in the *VHL* gene, an E3 ubiquitin-ligase lead to accumulation of HIF-1α, which stimulates rapid vascularization of tumours,

promoting the development of the neoplasms characteristic of the Von Hippel-Lindau syndrome.[475;783] Different steps of the ubiquitin-proteasome pathway are targets for recently developed drugs for the treatment of human neoplasms and other conditions.[773]

Considering the interaction of AIP with FBXO3, a member of the SCF E3 ubiquitin-ligase complex described in Chapter 3 and the response of unstable AIP variants to proteasome inhibition, is now clear that AIP is processed via ubiquitination and proteasomal degradation. The proteasome inhibitor MG-132 acts at the chymotrypsin-like site of the proteasome (and also at the caspase-like site at high concentrations), in a similar way to the clinically available proteasome inhibitor Bortezomib (PS-341).[784] Bortezomib is the first proteasome inhibitor approved for clinical use, currently indicated in the treatment of relapsed multiple myeloma and mantle cell lymphoma and under study for as an anticancer drug in other haematological malignancies, prostate, breast and non-small-cell lung cancers, as well as for the treatment of amyloidosis.[785;786] The second-generation proteasome inhibitor Carfizomib is now approved for the treatment of Bortezomib-resistant multiple myeloma cases and other second-generation proteasome inhibitors (Ixazomib, Delanzomib, Oprozomib and Marizomib) are under investigation.[786] Proteasome inhibitors could theoretically restore the levels of mutant AIP, as it has recently been proposed also for menin,[756] and therefore they could have a role in the treatment of aggressive pituitary adenomas. However, the effects of these drugs include regulation of multiple pathways implicated in tumorigenesis, and therefore this possible pre-clinical application should be explored in depth.

Conclusions

Human AIP is a stable protein with an endogenous half-life between 33.1 and 68.2 h whose degradation is driven by ubiquitination and proteasomal degradation, probably mediated by the FBXO3-containing SCF1 E3 ubiquitin-ligase complex. Multiple clinically relevant missense AIP variants, especially those affecting the TPR domain of the protein, and the nonsense mutant p.R304* display reduced half-lives due to enhanced proteasomal degradation. These unstable proteins can be partially rescued by proteasome inhibition. Interestingly, a direct correlation between protein half-life and age at diagnosis in *AIP*mut positive pituitary patients was found. Unstable AIP variants seem to be present only at very low levels in cells with heterozygous *AIP*muts, indicating that, under physiological conditions, the function of these variants is very probably completely lost. However, the presence of an unstable AIP mutant does not seem to affect the function of the WT AIP protein. The reduced half-life of missense AIP mutants is an additional pathogenic mechanism for *AIP*muts, not described before.

General conclusions and avenues for future research

Although the studies presented in this thesis have hopefully helped to better understand the function of AIP in the pituitary gland, as well as to further address the pathogenic mechanisms of *AIP*muts and the clinical presentation of *AIP*mut-associated pituitary adenomas, some questions remain still open and represent excellent avenues for future research. The next paragraphs summarise the main results of the three research projects presented in this thesis, emphasising the novel findings and establishing questions to be addressed by future studies.

Phenotype of *AIP*mut positive pituitary adenomas

Besides the familial presentation, the distinctive characteristics of pituitary adenomas associated to *AIP*muts are the disease onset between the second and third decades of life, an overrepresentation of cases of gigantism (a rather uncommon clinical presentation), along with acromegaly, and the great predominance of macroadenomas. Based on this and on the results of previous studies, genetic testing for *AIP*muts should be directed to FIPA families, cases of gigantism and pituitary adenoma patients with disease onset in adolescence and early adulthood. There is currently no apparent indication for testing other subgroups of patients out of the setting of research studies.

In this sense, it is important to remark that *AIP*mut testing is not widely available in clinical centres worldwide, and this is probably hampering the recognition of more *AIP*mut positive cases, and therefore a better characterisation of the disease features. This could also limit the application of strategies for the follow-up of patients and carriers, or specific therapies based on the molecular basis of these tumours in the future. The development of affordable genetic tests, not only for *AIP* but for other inherited conditions that could benefit from preclinical diagnosis, is therefore required.

Usefulness of clinical screening of *AIP*mut positive apparently unaffected carriers

Up to one quarter of the apparently unaffected individuals carrying *AIP*muts develop a pituitary adenoma at some point in their lives. The detection of such cases is primordial, to ensure early treatment and therefore better prognosis. However, clinical testing means an investment from the public health systems on individuals that are otherwise healthy. Although it is true than treating small, non-invasive pituitary adenomas is safer and less costly than treating large, complicated tumours, this study was not focused on calculating the economic impact of clinical testing on public health systems. This issue should be addressed in future studies, considering the clinical experience with the long-term follow-up of unaffected *AIP*mut carriers.

No role for the *gsp* oncogene in *AIP*mut positive pituitary adenomas

Interestingly, the most common disease modifier in pituitary adenomas, the *gsp* oncogene (*GNAS1* mutations) was not detected in *AIP*mut positive pituitary adenomas. This finding enforces the idea that *AIP*mut positive pituitary adenomas are originated by a unique molecular mechanism, different from other sporadic somatotropinomas. It is now apparent that AIP somehow regulates the cAMP pathway in the pituitary gland and it has generally been accepted that an overactive cAMP pathway is a hallmark of somatotroph tumorigenesis. At the moment, there is no good theoretical explanation to address the question of why mutations in two genes affecting the same pathway are mutually exclusive in these tumours. This is an interesting point to investigate, as the discovery of more regulatory events in the cAMP pathway, including crosstalk with other signalling pathways, could be useful for the development of new therapeutic targets.

***AIP*mut positive pituitary adenomas are prone to apoplexy**

This is not a new observation, but it has been reinforced by the recruitment and analysis of a large number of *AIP*mut positive cases. It could be assumed that the increased frequency of this complication among *AIP*mut positive individuals is due to the high prevalence of macroadenomas among this population. However, there are some unusual features suggesting that this is not the case, including the type of tumours, the age at presentation and the presence of multiple cases in the same family. Whether LOF of AIP could have an effect on the pattern and organisation of the tumoral vessels in pituitary adenomas, is a matter to be investigated.

AIP is a co-chaperone of multiple heat shock proteins of the HSP90 and HSP70 families

While the finding of new chaperones interacting with AIP has shed light on the repertoire of interacting partners of AIP, it has also increased the number of chaperone-client proteins that could be regulated by the co-chaperone activity of AIP. Although mapping all these possible indirect interactions would be complicated, future studies could concentrate on determining which interactions of these chaperones in the somatotroph cells are mediated by AIP, as has been shown for PRKACA. On the other hand, the expression of these heat shock proteins in the normal pituitary gland and in pituitary adenomas should be further investigated, as they represent potential therapeutic targets.

The regulation of the cytoskeletal organisation might be a mechanism for the tumour suppressor function of AIP

Disorganisation of the cytoskeletal network and of the cell-cell junctions is a characteristic of invasive tumours. The possible function of AIP as a microtubule-associated protein could explain why loss of AIP function produces pituitary adenomas with an EMT phenotype. However, it is necessary to determine whether this function occurs specifically in the pituitary gland, and the reason for that, as it could represent a potential therapeutic target for invasive pituitary adenomas.

The E3 ubiquitin-ligase complex SCF targets AIP

It has been demonstrated that AIP degradation occurs via ubiquitination and proteasomal degradation, and the specific E3 ubiquitin-ligase complex mediating this mechanism has been identified. Rapid degradation of unstable AIP mutants can be partially reverted by the treatment with a proteasome inhibitor. However, it is not clear whether restoring the protein stability means restoring the normal function, as those proteins could still be abnormal, due to loss of protein-protein interactions.

Human AIP is a stable protein

In general, proteins with stable half-life are stably expressed, and proteins whose expression fluctuates during the cell cycle have been found to be less stable.[759] This finding is probably an indicator that the tumour suppressor function of AIP does not implicate direct regulation of the proteins involved in cell-cycle progression. The specific proteins mediating the AIP tumour suppressor function remain elusive.

Short half-life is a mechanism for LOF in missense *AIP* variants and the expression of unstable *AIP* variants under physiological conditions is probably negligible

It has been hypothesised that LOF of AIP missense mutants could lead to loss of protein-protein interactions. However, considering the very low or null endogenous level of the short half-lived AIP nonsense mutant p.R304*, it is very probable that very short half-lived mutants are also present in the cells at negligible levels under physiological conditions. This means that the final effect of these mutations on the protein would be loss of the protein. However, it is not clear why pituitary adenomas can develop in some cases in absence of LOH, in the presence of one normal, half-lived allele. Further studies to address this issue are required.

Reference List

1. Ezzat S, Asa SL, Couldwell WT, Barr CE, Dodge WE, Vance ML, McCutcheon IE. The prevalence of pituitary adenomas: a systematic review. *Cancer.* 2004;101(3):613-619.
2. Gadelha MR, Trivellin G, Hernández-Ramírez LC, Korbonits M. Genetics of pituitary adenomas. *Front Horm Res.* 2013;41:111-140.
3. Melmed S. Acromegaly pathogenesis and treatment. *J Clin Invest.* 2009;119(11):3189-3202.
4. Couldwell WT, Cannon-Albright L. A heritable predisposition to pituitary tumors. *Pituitary.* 2010;13(2):130-137.
5. Nozieres C, Berlier P, Dupuis C, Raynaud-Ravni C, Morel Y, Borson-Chazot F, Nicolino M. Sporadic and genetic forms of paediatric somatotropinoma: a retrospective analysis of seven cases and a review of the literature. *Orphanet J Rare Dis.* 2011;6(1):67.
6. Stratakis CA, Tichomirowa MA, Boikos S, Azevedo MF, Lodish M, Martari M, Verma S, Daly AF, Raygada M, Keil MF, Papademetriou J, Drori-Herishanu L, Horvath A, Tsang KM, Nesterova M, Franklin S, Vanbellinghen JF, Bours V, Salvatori R, Beckers A. The role of germline *AIP*, *MEN1*, *PRKAR1A*, *CDKN1B* and *CDKN2C* mutations in causing pituitary adenomas in a large cohort of children, adolescents, and patients with genetic syndromes. *Clin Genet.* 2010;78(5):457-463.
7. Tichomirowa MA, Barlier A, Daly AF, Jaffrain-Rea ML, Ronchi C, Yaneva M, Urban JD, Petrossians P, Elenkova A, Tabarin A, Desailloud R, Maiter D, Schurmeyer T, Cozzi R, Theodoropoulou M, Sievers C, Bernabeu I, Naves LA, Chabre O, Montanana CF, Hana V, Halaby G, Delemer B, Aizpun JI, Sonnet E, Longas AF, Hagelstein MT, Caron P, Stalla GK, Bours V, Zacharieva S, Spada A, Brue T, Beckers A. High prevalence of *AIP* gene mutations following focused screening in young patients with sporadic pituitary macroadenomas. *Eur J Endocrinol.* 2011;165(4):509-515.
8. Vierimaa O, Georgitsi M, Lehtonen R, Vahteristo P, Kokko A, Raitila A, Tuppurainen K, Ebeling TM, Salmela PI, Paschke R, Gundogdu S, De ME, Makinen MJ, Launonen V, Karhu A, Aaltonen LA. Pituitary adenoma predisposition caused by germline mutations in the *AIP* gene. *Science.* 2006;312(5777):1228-1230.
9. Leontiou CA, Gueorguiev M, van der Spuy J, Quinton R, Lolli F, Hassan S, Chahal HS, Igreja SC, Jordan S, Rowe J, Stolbrink M, Christian HC, Wray J, Bishop-Bailey D, Berney DM, Wass JA, Popovic V, Ribeiro-Oliveira A, Jr., Gadelha MR, Monson JP, Akker SA, Davis JR, Clayton RN, Yoshimoto K, Iwata T, Matsuno A, Eguchi K, Musat M, Flanagan D, Peters G, Bolger GB, Chapple JP, Frohman LA, Grossman AB, Korbonits M. The role of the aryl hydrocarbon receptor-interacting

protein gene in familial and sporadic pituitary adenomas. *J Clin Endocrinol Metab.* 2008;93(6):2390-2401.

10. Igreja S, Chahal HS, King P, Bolger GB, Srirangalingam U, Guasti L, Chapple JP, Trivellin G, Gueorguiev M, Guegan K, Stals K, Khoo B, Kumar AV, Ellard S, Grossman AB, Korbonits M. Characterization of aryl hydrocarbon receptor interacting protein (*AIP*) mutations in familial isolated pituitary adenoma families. *Hum Mutat.* 2010;31(8):950-960.
11. Daly AF, Tichomirowa MA, Petrossians P, Heliovaara E, Jaffrain-Rea ML, Barlier A, Naves LA, Ebeling T, Karhu A, Raappana A, Cazabat L, De ME, Montanana CF, Raverot G, Weil RJ, Sane T, Maiter D, Neggers S, Yaneva M, Tabarin A, Verrua E, Eloranta E, Murat A, Vierimaa O, Salmela PI, Emy P, Toledo RA, Sabate MI, Villa C, Popelier M, Salvatori R, Jennings J, Longas AF, Labarta Aizpun JI, Georgitsi M, Paschke R, Ronchi C, Valimaki M, Saloranta C, De HW, Cozzi R, Guitelman M, Magri F, Lagonigro MS, Halaby G, Corman V, Hagelstein MT, Vanbellinghen JF, Barra GB, Gimenez-Roqueplo AP, Cameron FJ, Borson-Chazot F, Holdaway I, Toledo SP, Stalla GK, Spada A, Zacharieva S, Bertherat J, Brue T, Bours V, Chanson P, Aaltonen LA, Beckers A. Clinical characteristics and therapeutic responses in patients with germ-line *AIP* mutations and pituitary adenomas: an international collaborative study. *J Clin Endocrinol Metab.* 2010;95(11):E373-E383.
12. Cazabat L, Libe R, Perlemoine K, Rene-Corail F, Burnichon N, Gimenez-Roqueplo AP, Dupasquier-Fediaevsky L, Bertagna X, Clauser E, Chanson P, Bertherat J, Raffin-Sanson ML. Germline inactivating mutations of the aryl hydrocarbon receptor-interacting protein gene in a large cohort of sporadic acromegaly: mutations are found in a subset of young patients with macroadenomas. *Eur J Endocrinol.* 2007;157(1):1-8.
13. Cazabat L, Bouligand J, Salenave S, Bernier M, Gaillard S, Parker F, Young J, Guiochon-Mantel A, Chanson P. Germline *AIP* mutations in apparently sporadic pituitary adenomas: prevalence in a prospective single-center cohort of 443 patients. *J Clin Endocrinol Metab.* 2012;97(4):E663-E670.
14. Oriola J, Lucas T, Halperin I, Mora M, Perales MJ, Alvarez-Escola C, Paz de MN, Diaz SG, Salinas I, Julian MT, Olaizola I, Bernabeu I, Marazuela M, Puig-Domingo M. Germline mutations of *AIP* gene in somatotropinomas resistant to somatostatin analogues. *Eur J Endocrinol.* 2013;168(1):9-13.
15. Trivellin G, Korbonits M. AIP and its interacting partners. *J Endocrinol.* 2011;210(2):137-155.
16. Kasuki L, Vieira NL, Wildemberg LE, Colli LM, De CM, Takiya CM, Gadelha MR. AIP expression in sporadic somatotropinomas is a predictor of the response to octreotide LAR therapy independent of SSTR2 expression. *Endocr Relat Cancer.* 2012;19(3):L25-L29.

17. Jaffrain-Rea ML, Rotondi S, Turchi A, Occhi G, Barlier A, Peverelli E, Rostomyan L, Defilles C, Angelini M, Oliva MA, Ceccato F, Maiorani O, Daly AF, Esposito V, Buttarelli F, Figarella-Branger D, Giangaspero F, Spada A, Scaroni C, Alesse E, Beckers A. Somatostatin analogues increase AIP expression in somatotropinomas, irrespective of Gsp mutations. *Endocr Relat Cancer.* 2013;20(5):753-766.
18. Melmed S, Kleinberg D. Anterior Pituitary. In: Kronenberg HM, Melmed S, Polonsky KS, Larsen PR, eds. *Williams Textbook of Endocrinology*. 11 ed. Philadelphia, PA: Elsevier Inc.; 2008;155-263.
19. Lechan, R. M. and Toni, R.Endotext: Functional anatomy of the hypothalamus and pituitary. http://www.endotext.org/chapter/functional-anatomy-of-the-hypothalamus-and-pituitary/2/. Accessed 6/12/2014.
20. Ben-Shlomo A, Melmed S. Hypothalamic regulation of anterior pituitary function. In: Melmed S, ed. *The Pituitary*. 3rd ed. San Diego, CA, USA: Academic Press; 2011;21-45.
21. Nussey S, Whitehead S. The pituitary gland. Oxford: Oxford: BIOS Scientific Publishers; 2001.
22. Horvath E, Kovacs K, Scheithauer BW. Pituitary hyperplasia. *Pituitary.* 1999;1(3-4):169-179.
23. Al-Gahtany M, Horvath E, Kovacs K. Pituitary hyperplasia. *Hormones (Athens).* 2003;2(3):149-158.
24. Allaerts W, Vankelecom H. History and perspectives of pituitary folliculo-stellate cell research. *Eur J Endocrinol.* 2005;153(1):1-12.
25. Devnath S, Inoue K. An insight to pituitary folliculo-stellate cells. *J Neuroendocrinol.* 2008;20(6):687-691.
26. Perez-Castro C, Renner U, Haedo MR, Stalla GK, Arzt E. Cellular and molecular specificity of pituitary gland physiology. *Physiol Rev.* 2012;92(1):1-38.
27. Horvath E, Kovacs K, Penz G, Ezrin C. Origin, possible function and fate of "follicular cells" in the anterior lobe of the human pituitary. *Am J Pathol.* 1974;77(2):199-212.
28. Nishioka H, Ito H, Hirano A, Kato Y. Immunocytochemical demonstration of oncocytes in normal adenohypophysis. *Acta Neuropathol.* 1999;97(1):40-44.
29. Horvath E, Kovacs K, Lloyd R. Pars intermedia of the human pituitary revisited: Morphologic aspects and frequency of hyperplasia of POMC-peptide immunoreactive cells. *Endocr Pathol.* 1999;10(1):55-64.
30. Drouin J. Pituitary development. In: Melmed S, ed. *The Pituitary*. 3rd ed. San Diego, CA, USA: Academic Press; 2011;3-19.
31. Cordoba-Chacon J, Gahete MD, Pozo-Salas AI, Martinez-Fuentes AJ, de LL, Gracia-Navarro F, Kineman RD, Castano JP, Luque RM. Cortistatin is not a somatostatin analogue but stimulates prolactin release and inhibits GH and ACTH

in a gender-dependent fashion: potential role of ghrelin. *Endocrinology.* 2011;152(12):4800-4812.

32. Lanfranco F, Motta G, Baldi M, Gasco V, Grottoli S, Benso A, Broglio F, Ghigo E. Ghrelin and anterior pituitary function. *Front Horm Res.* 2010;38:206-211.
33. Bagosi Z, Csabafi K, Palotai M, Jaszberenyi M, Foldesi I, Gardi J, Szabo G, Telegdy G. The effect of urocortin I on the hypothalamic ACTH secretagogues and its impact on the hypothalamic-pituitary-adrenal axis. *Neuropeptides.* 2014;48(1):15-20.
34. Cohen LE, Radovick S. Molecular basis of combined pituitary hormone deficiencies. *Endocr Rev.* 2002;23(4):431-442.
35. Kelberman D, Rizzoti K, Lovell-Badge R, Robinson IC, Dattani MT. Genetic regulation of pituitary gland development in human and mouse. *Endocr Rev.* 2009;30(7):790-829.
36. Treier M, Gleiberman AS, O'Connell SM, Szeto DP, McMahon JA, McMahon AP, Rosenfeld MG. Multistep signaling requirements for pituitary organogenesis in vivo. *Genes Dev.* 1998;12(11):1691-1704.
37. di Iorgi N, Secco A, Napoli F, Calandra E, Rossi A, Maghnie M. Developmental abnormalities of the posterior pituitary gland. *Endocr Dev.* 2009;14:83-94.
38. Kovacs K, Horvath E, Vidal S. Classification of pituitary adenomas. *J Neurooncol.* 2001;54(2):121-127.
39. Lloyd RV, Kovacs K, Young WF et al. Tumours of the Pituitary Gland. *World Health Organization Classification of tumours.Pathology and Genetics of Tumours of Endocrine Organs*. 3 ed. Lyon: IARC Press; 2004.
40. Scheithauer BW, Gaffey TA, Lloyd RV, Sebo TJ, Kovacs KT, Horvath E, Yapicier O, Young WF, Jr., Meyer FB, Kuroki T, Riehle DL, Laws ER, Jr. Pathobiology of pituitary adenomas and carcinomas. *Neurosurgery.* 2006;59(2):341-353.
41. Alexander JM, Biller BM, Bikkal H, Zervas NT, Arnold A, Klibanski A. Clinically nonfunctioning pituitary tumors are monoclonal in origin. *J Clin Invest.* 1990;86(1):336-340.
42. Herman V, Fagin J, Gonsky R, Kovacs K, Melmed S. Clonal origin of pituitary adenomas. *J Clin Endocrinol Metab.* 1990;71(6):1427-1433.
43. Jacoby LB, Hedley-Whyte ET, Pulaski K, Seizinger BR, Martuza RL. Clonal origin of pituitary adenomas. *J Neurosurg.* 1990;73(5):731-735.
44. Clayton RN, Pfeifer M, Atkinson AB, Belchetz P, Wass JA, Kyrodimou E, Vanderpump M, Simpson D, Bicknell J, Farrell WE. Different patterns of allelic loss (loss of heterozygosity) in recurrent human pituitary tumors provide evidence for multiclonal origins. *Clin Cancer Res.* 2000;6(10):3973-3982.
45. Korbonits M, Morris DG, Nanzer A, Kola B, Grossman AB. Role of regulatory factors in pituitary tumour formation. *Front Horm Res.* 2004;32:63-95.
46. Fowkes RC, Vlotides G. Hypoxia-induced VEGF production 'RSUMEs' in pituitary adenomas. *Endocr Relat Cancer.* 2012;19(1):C1-C5.

47. Melmed S. Pathogenesis of pituitary tumors. *Nat Rev Endocrinol.* 2011;7(5):257-266.
48. Orciani M, Davis S, Appolloni G, Lazzarini R, Mattioli-Belmonte M, Ricciuti RA, Boscaro M, Di PR, Arnaldi G. Isolation and characterization of progenitor mesenchymal cells in human pituitary tumors. *Cancer Gene Ther.* 2015;22(1):9-16.
49. Raverot G, Jouanneau E, Trouillas J. Management of endocrine disease: clinicopathological classification and molecular markers of pituitary tumours for personalized therapeutic strategies. *Eur J Endocrinol.* 2014;170(4):R121-R132.
50. Freda PU, Beckers AM, Katznelson L, Molitch ME, Montori VM, Post KD, Vance ML. Pituitary incidentaloma: an endocrine society clinical practice guideline. *J Clin Endocrinol Metab.* 2011;96(4):894-904.
51. Asa SL. Practical pituitary pathology: what does the pathologist need to know? *Arch Pathol Lab Med.* 2008;132(8):1231-1240.
52. Hardy J. Transsphenoidal surgery of hypersecreting pituitary tumors. In: Kohler PO, Ross GT, eds. *Diagnosis and treatment of pituitary tumors*. 303 ed. Amsterdam: Excerpta Medica; 1973;179-198.
53. Knosp E, Steiner E, Kitz K, Matula C. Pituitary adenomas with invasion of the cavernous sinus space: a magnetic resonance imaging classification compared with surgical findings. *Neurosurgery.* 1993;33(4):610-617.
54. Micko AS, Wohrer A, Wolfsberger S, Knosp E. Invasion of the cavernous sinus space in pituitary adenomas: endoscopic verification and its correlation with an MRI-based classification. *J Neurosurg.* 2015;122(4):803-811.
55. Di IA, Rotondo F, Syro LV, Cusimano MD, Kovacs K. Aggressive pituitary adenomas--diagnosis and emerging treatments. *Nat Rev Endocrinol.* 2014;10(7):423-435.
56. Scheithauer BW, Kovacs KT, Laws ER, Jr., Randall RV. Pathology of invasive pituitary tumors with special reference to functional classification. *J Neurosurg.* 1986;65(6):733-744.
57. Meij BP, Lopes MB, Ellegala DB, Alden TD, Laws ER, Jr. The long-term significance of microscopic dural invasion in 354 patients with pituitary adenomas treated with transsphenoidal surgery. *J Neurosurg.* 2002;96(2):195-208.
58. Al-Shraim M, Asa SL. The 2004 World Health Organization classification of pituitary tumors: what is new? *Acta Neuropathol.* 2006;111(1):1-7.
59. Saeger W, Ludecke DK, Buchfelder M, Fahlbusch R, Quabbe HJ, Petersenn S. Pathohistological classification of pituitary tumors: 10 years of experience with the German Pituitary Tumor Registry. *Eur J Endocrinol.* 2007;156(2):203-216.
60. Erickson D, Scheithauer B, Atkinson J, Horvath E, Kovacs K, Lloyd RV, Young WF, Jr. Silent subtype 3 pituitary adenoma: a clinicopathologic analysis of the Mayo Clinic experience. *Clin Endocrinol (Oxf).* 2009;71(1):92-99.

61. Trouillas J. In search of a prognostic classification of endocrine pituitary tumors. *Endocr Pathol.* 2014;25(2):124-132.
62. Lloyd RV, Jin L, Fields K, Chandler WF, Horvath E, Stefaneanu L, Kovacs K. Analysis of pituitary hormones and chromogranin A mRNAs in null cell adenomas, oncocytomas, and gonadotroph adenomas by in situ hybridization. *Am J Pathol.* 1991;139(3):553-564.
63. Porcelli AM, Ghelli A, Ceccarelli C, Lang M, Cenacchi G, Capristo M, Pennisi LF, Morra I, Ciccarelli E, Melcarne A, Bartoletti-Stella A, Salfi N, Tallini G, Martinuzzi A, Carelli V, Attimonelli M, Rugolo M, Romeo G, Gasparre G. The genetic and metabolic signature of oncocytic transformation implicates HIF1alpha destabilization. *Hum Mol Genet.* 2010;19(6):1019-1032.
64. Kurelac I, MacKay A, Lambros MB, Di CE, Cenacchi G, Ceccarelli C, Morra I, Melcarne A, Morandi L, Calabrese FM, Attimonelli M, Tallini G, Reis-Filho JS, Gasparre G. Somatic complex I disruptive mitochondrial DNA mutations are modifiers of tumorigenesis that correlate with low genomic instability in pituitary adenomas. *Hum Mol Genet.* 2013;22(2):226-238.
65. Trouillas J, Roy P, Sturm N, Dantony E, Cortet-Rudelli C, Viennet G, Bonneville JF, Assaker R, Auger C, Brue T, Cornelius A, Dufour H, Jouanneau E, Francois P, Galland F, Mougel F, Chapuis F, Villeneuve L, Maurage CA, Figarella-Branger D, Raverot G, Barlier A, Bernier M, Bonnet F, Borson-Chazot F, Brassier G, Caulet-Maugendre S, Chabre O, Chanson P, Cottier JF, Delemer B, Delgrange E, Di TL, Eimer S, Gaillard S, Jan M, Girard JJ, Lapras V, Loiseau H, Passagia JG, Patey M, Penfornis A, Poirier JY, Perrin G, Tabarin A. A new prognostic clinicopathological classification of pituitary adenomas: a multicentric case-control study of 410 patients with 8 years post-operative follow-up. *Acta Neuropathol.* 2013;126(1):123-135.
66. Daly AF, Rixhon M, Adam C, Dempegioti A, Tichomirowa MA, Beckers A. High prevalence of pituitary adenomas: a cross-sectional study in the province of Liege, Belgium. *J Clin Endocrinol Metab.* 2006;91(12):4769-4775.
67. Fontana E, Gaillard R. [Epidemiology of pituitary adenoma: results of the first Swiss study]. *Rev Med Suisse.* 2009;5(223):2172-2174.
68. Fernandez A, Karavitaki N, Wass JA. Prevalence of pituitary adenomas: a community-based, cross-sectional study in Banbury (Oxfordshire, UK). *Clin Endocrinol (Oxf).* 2010;72(3):377-382.
69. Raappana A, Koivukangas J, Ebeling T, Pirila T. Incidence of pituitary adenomas in Northern Finland in 1992-2007. *J Clin Endocrinol Metab.* 2010;95(9):4268-4275.
70. Gruppetta M, Mercieca C, Vassallo J. Prevalence and incidence of pituitary adenomas: a population based study in Malta. *Pituitary.* 2013;16(4):545-553.
71. Gold EB. Epidemiology of pituitary adenomas. *Epidemiol Rev.* 1981;3:163-183.
72. Keil MF, Stratakis CA. Pituitary tumors in childhood: update of diagnosis, treatment and molecular genetics. *Expert Rev Neurother.* 2008;8(4):563-574.

73. Mindermann T, Wilson CB. Age-related and gender-related occurrence of pituitary adenomas. *Clin Endocrinol (Oxf).* 1994;41(3):359-364.
74. Aflorei ED, Korbonits M. Epidemiology and etiopathogenesis of pituitary adenomas. *J Neurooncol.* 2014;117(3):379-394.
75. Hérincs M, Owusu-Antwi S, Chahal HS, Kumar SR, Ozfirat Z, Grossman AB, Druce MR, Akker SA, Drake WM, Korbonits M. Prevalence of familial isolated pituitary adenomas [abstract]. *Endocrine Abstracts* 2013;31(Society for Endocrinology BES 2013):258.
76. Cano DA, Soto-Moreno A, Leal-Cerro A. Genetically engineered mouse models of pituitary tumors. *Front Oncol.* 2014;4:203.
77. Suhardja A, Kovacs K, Rutka J. Genetic basis of pituitary adenoma invasiveness: a review. *J Neurooncol.* 2001;52(3):195-204.
78. Ewing I, Pedder-Smith S, Franchi G, Ruscica M, Emery M, Vax V, Garcia E, Czirjak S, Hanzely Z, Kola B, Korbonits M, Grossman AB. A mutation and expression analysis of the oncogene BRAF in pituitary adenomas. *Clin Endocrinol (Oxf).* 2007;66(3):348-352.
79. Chamberlain CE, Scheel DW, McGlynn K, Kim H, Miyatsuka T, Wang J, Nguyen V, Zhao S, Mavropoulos A, Abraham AG, O'Neill E, Ku GM, Cobb MH, Martin GR, German MS. Menin determines K-RAS proliferative outputs in endocrine cells. *J Clin Invest.* 2014;124(9):4093-4101.
80. Cabrera-Vera TM, Vanhauwe J, Thomas TO, Medkova M, Preininger A, Mazzoni MR, Hamm HE. Insights into G protein structure, function, and regulation. *Endocr Rev.* 2003;24(6):765-781.
81. Peverelli E, Mantovani G, Lania AG, Spada A. cAMP in the pituitary: an old messenger for multiple signals. *J Mol Endocrinol.* 2014;52(1):R67-R77.
82. Kleuss C, Raw AS, Lee E, Sprang SR, Gilman AG. Mechanism of GTP hydrolysis by G-protein alpha subunits. *Proc Natl Acad Sci U S A.* 1994;91(21):9828-9831.
83. Hayward BE, Moran V, Strain L, Bonthron DT. Bidirectional imprinting of a single gene: *GNAS1* encodes maternally, paternally, and biallelically derived proteins. *Proc Natl Acad Sci U S A.* 1998;95(26):15475-15480.
84. Hayward BE, Bonthron DT. An imprinted antisense transcript at the human GNAS1 locus. *Hum Mol Genet.* 2000;9(5):835-841.
85. Weinstein LS, Yu S, Warner DR, Liu J. Endocrine manifestations of stimulatory G protein alpha-subunit mutations and the role of genomic imprinting. *Endocr Rev.* 2001;22(5):675-705.
86. Hayward BE, Kamiya M, Strain L, Moran V, Campbell R, Hayashizaki Y, Bonthron DT. The human *GNAS1* gene is imprinted and encodes distinct paternally and biallelically expressed G proteins. *Proc Natl Acad Sci U S A.* 1998;95(17):10038-10043.
87. Chandrasekharappa SC, Guru SC, Manickam P, Olufemi SE, Collins FS, Emmert-Buck MR, Debelenko LV, Zhuang Z, Lubensky IA, Liotta LA, Crabtree JS, Wang

Y, Roe BA, Weisemann J, Boguski MS, Agarwal SK, Kester MB, Kim YS, Heppner C, Dong Q, Spiegel AM, Burns AL, Marx SJ. Positional cloning of the gene for multiple endocrine neoplasia-type 1. *Science.* 1997;276(5311):404-407.

88. Kirschner LS, Carney JA, Pack SD, Taymans SE, Giatzakis C, Cho YS, Cho-Chung YS, Stratakis CA. Mutations of the gene encoding the protein kinase A type I-alpha regulatory subunit in patients with the Carney complex. *Nat Genet.* 2000;26(1):89-92.
89. Pellegata NS, Quintanilla-Martinez L, Siggelkow H, Samson E, Bink K, Hofler H, Fend F, Graw J, Atkinson MJ. Germ-line mutations in *p27Kip1* cause a multiple endocrine neoplasia syndrome in rats and humans. *Proc Natl Acad Sci U S A.* 2006;103(42):15558-15563.
90. Xekouki P, Pacak K, Almeida M, Wassif CA, Rustin P, Nesterova M, de la Luz SM, Matro J, Ball E, Azevedo M, Horvath A, Lyssikatos C, Quezado M, Patronas N, Ferrando B, Pasini B, Lytras A, Tolis G, Stratakis CA. Succinate dehydrogenase (SDH) D subunit (SDHD) inactivation in a growth-hormone-producing pituitary tumor: a new association for SDH? *J Clin Endocrinol Metab.* 2012;97(3):E357-E366.
91. Trivellin G, Daly AF, Faucz FR, Yuan B, Rostomyan L, Larco DO, Schernthaner-Reiter MH, Szarek E, Leal LF, Caberg JH, Castermans E, Villa C, Dimopoulos A, Chittiboina P, Xekouki P, Shah N, Metzger D, Lysy PA, Ferrante E, Strebkova N, Mazerkina N, Zatelli MC, Lodish M, Horvath A, de Alexandre RB, Manning AD, Levy I, Keil MF, Sierra MD, Palmeira L, Coppieters W, Georges M, Naves LA, Jamar M, Bours V, Wu TJ, Choong CS, Bertherat J, Chanson P, Kamenicky P, Farrell WE, Barlier A, Quezado M, Bjelobaba I, Stojilkovic SS, Wess J, Costanzi S, Liu P, Lupski JR, Beckers A, Stratakis CA. Gigantism and Acromegaly Due to Xq26 Microduplications and *GPR101* Mutation. *N Engl J Med.* 2014;371(25):2363-2374.
92. Denes J, Swords F, Rattenberry E, Stals K, Owens M, Cranston T, Xekouki P, Moran L, Kumar A, Wassif C, Fersht N, Baldeweg SE, Morris D, Lightman S, Agha A, Rees A, Grieve J, Powell M, Boguszewski CL, Dutta P, Thakker RV, Srirangalingam U, Thompson CJ, Druce M, Higham C, Davis J, Eeles R, Stevenson M, O'Sullivan B, Taniere P, Skordilis K, Gabrovska P, Barlier A, Webb SM, Aulinas A, Drake WM, Bevan JS, Preda C, Dalantaeva N, Ribeiro-Oliveira A, Jr., Garcia IT, Yordanova G, Iotova V, Evanson J, Grossman AB, Trouillas J, Ellard S, Stratakis CA, Maher ER, Roncaroli F, Korbonits M. Heterogeneous genetic background of the association of pheochromocytoma/paraganglioma and pituitary adenoma: results from a large patient cohort. *J Clin Endocrinol Metab.* 2015;100(3):E531-E541.
93. de KL, Sabbaghian N, Plourde F, Srivastava A, Weber E, Bouron-Dal SD, Hamel N, Choi JH, Park SH, Deal CL, Kelsey MM, Dishop MK, Esbenshade A, Kuttesch JF, Jacques TS, Perry A, Leichter H, Maeder P, Brundler MA, Warner J, Neal J,

Zacharin M, Korbonits M, Cole T, Traunecker H, McLean TW, Rotondo F, Lepage P, Albrecht S, Horvath E, Kovacs K, Priest JR, Foulkes WD. Pituitary blastoma: a pathognomonic feature of germ-line *DICER1* mutations. *Acta Neuropathol.* 2014;128(1):111-122.

94. Reincke M, Sbiera S, Hayakawa A, Theodoropoulou M, Osswald A, Beuschlein F, Meitinger T, Mizuno-Yamasaki E, Kawaguchi K, Saeki Y, Tanaka K, Wieland T, Graf E, Saeger W, Ronchi CL, Allolio B, Buchfelder M, Strom TM, Fassnacht M, Komada M. Mutations in the deubiquitinase gene *USP8* cause Cushing's disease. *Nat Genet.* 2015;47(1):31-38.
95. Landis CA, Masters SB, Spada A, Pace AM, Bourne HR, Vallar L. GTPase inhibiting mutations activate the alpha chain of Gs and stimulate adenylyl cyclase in human pituitary tumours. *Nature.* 1989;340(6236):692-696.
96. Kasuki Jomori de PL, Vieira NL, Armondi Wildemberg LE, Gasparetto EL, Marcondes J, de Almeida NB, Takiya CM, Gadelha MR. Low aryl hydrocarbon receptor-interacting protein expression is a better marker of invasiveness in somatotropinomas than Ki-67 and p53. *Neuroendocrinology.* 2011;94(1):39-48.
97. Paez-Pereda M, Giacomini D, Refojo D, Nagashima AC, Hopfner U, Grubler Y, Chervin A, Goldberg V, Goya R, Hentges ST, Low MJ, Holsboer F, Stalla GK, Arzt E. Involvement of bone morphogenetic protein 4 (BMP-4) in pituitary prolactinoma pathogenesis through a Smad/estrogen receptor crosstalk. *Proc Natl Acad Sci U S A.* 2003;100(3):1034-1039.
98. Neto AG, McCutcheon IE, Vang R, Spencer ML, Zhang W, Fuller GN. Elevated expression of p21 (WAF1/Cip1) in hormonally active pituitary adenomas. *Ann Diagn Pathol.* 2005;9(1):6-10.
99. Qian X, Jin L, Grande JP, Lloyd RV. Transforming growth factor-beta and p27 expression in pituitary cells. *Endocrinology.* 1996;137(7):3051-3060.
100. Lloyd RV, Jin L, Qian X, Kulig E. Aberrant p27kip1 expression in endocrine and other tumors. *Am J Pathol.* 1997;150(2):401-407.
101. Jin L, Qian X, Kulig E, Sanno N, Scheithauer BW, Kovacs K, Young WF, Jr., Lloyd RV. Transforming growth factor-beta, transforming growth factor-beta receptor II, and p27Kip1 expression in nontumorous and neoplastic human pituitaries. *Am J Pathol.* 1997;151(2):509-519.
102. Bamberger CM, Fehn M, Bamberger AM, Ludecke DK, Beil FU, Saeger W, Schulte HM. Reduced expression levels of the cell-cycle inhibitor p27Kip1 in human pituitary adenomas. *Eur J Endocrinol.* 1999;140(3):250-255.
103. Lidhar K, Korbonits M, Jordan S, Khalimova Z, Kaltsas G, Lu X, Clayton RN, Jenkins PJ, Monson JP, Besser GM, Lowe DG, Grossman AB. Low expression of the cell cycle inhibitor p27Kip1 in normal corticotroph cells, corticotroph tumors, and malignant pituitary tumors. *J Clin Endocrinol Metab.* 1999;84(10):3823-3830.

104. Komatsubara K, Tahara S, Umeoka K, Sanno N, Teramoto A, Osamura RY. Immunohistochemical analysis of p27 (Kip1) in human pituitary glands and in various types of pituitary adenomas. *Endocr Pathol.* 2001;12(2):181-188.
105. Nakabayashi H, Sunada I, Hara M. Immunohistochemical analyses of cell cycle-related proteins, apoptosis, and proliferation in pituitary adenomas. *J Histochem Cytochem.* 2001;49(9):1193-1194.
106. Korbonits M, Chahal HS, Kaltsas G, Jordan S, Urmanova Y, Khalimova Z, Harris PE, Farrell WE, Claret FX, Grossman AB. Expression of phosphorylated p27(Kip1) protein and Jun activation domain-binding protein 1 in human pituitary tumors. *J Clin Endocrinol Metab.* 2002;87(6):2635-2643.
107. Musat M, Korbonits M, Kola B, Borboli N, Hanson MR, Nanzer AM, Grigson J, Jordan S, Morris DG, Gueorguiev M, Coculescu M, Basu S, Grossman AB. Enhanced protein kinase B/Akt signalling in pituitary tumours. *Endocr Relat Cancer.* 2005;12(2):423-433.
108. Woloschak M, Yu A, Xiao J, Post KD. Frequent loss of the *P16INK4a* gene product in human pituitary tumors. *Cancer Res.* 1996;56(11):2493-2496.
109. Jaffrain-Rea ML, Ferretti E, Toniato E, Cannita K, Santoro A, Di SD, Ricevuto E, Maroder M, Tamburrano G, Cantore G, Gulino A, Martinotti S. *p16* (*INK4a, MTS-1*) gene polymorphism and methylation status in human pituitary tumours. *Clin Endocrinol (Oxf).* 1999;51(3):317-325.
110. Simpson DJ, Bicknell JE, McNicol AM, Clayton RN, Farrell WE. Hypermethylation of the *p16/CDKN2A/MTSI* gene and loss of protein expression is associated with nonfunctional pituitary adenomas but not somatotrophinomas. *Genes Chromosomes Cancer.* 1999;24(4):328-336.
111. Ruebel KH, Jin L, Zhang S, Scheithauer BW, Lloyd RV. Inactivation of the *p16* gene in human pituitary nonfunctioning tumors by hypermethylation is more common in null cell adenomas. *Endocr Pathol.* 2001;12(3):281-289.
112. Seemann N, Kuhn D, Wrocklage C, Keyvani K, Hackl W, Buchfelder M, Fahlbusch R, Paulus W. *CDKN2A/p16* inactivation is related to pituitary adenoma type and size. *J Pathol.* 2001;193(4):491-497.
113. Ogino A, Yoshino A, Katayama Y, Watanabe T, Ota T, Komine C, Yokoyama T, Fukushima T. The p15(INK4b)/p16(INK4a)/RB1 pathway is frequently deregulated in human pituitary adenomas. *J Neuropathol Exp Neurol.* 2005;64(5):398-403.
114. Yoshino A, Katayama Y, Ogino A, Watanabe T, Yachi K, Ohta T, Komine C, Yokoyama T, Fukushima T. Promoter hypermethylation profile of cell cycle regulator genes in pituitary adenomas. *J Neurooncol.* 2007;83(2):153-162.
115. Machiavelli G, Cotignola J, Danilowicz K, Carbonara C, Paes de LA, Basso A, Bruno OD, Szijan I. Expression of *p16*(*INK4A*) gene in human pituitary tumours. *Pituitary.* 2008;11(1):71-75.

116. Kirsch M, Morz M, Pinzer T, Schackert HK, Schackert G. Frequent loss of the CDKN2C (p18INK4c) gene product in pituitary adenomas. *Genes Chromosomes Cancer.* 2009;48(2):143-154.
117. Morris DG, Musat M, Czirjak S, Hanzely Z, Lillington DM, Korbonits M, Grossman AB. Differential gene expression in pituitary adenomas by oligonucleotide array analysis. *Eur J Endocrinol.* 2005;153(1):143-151.
118. Hossain MG, Iwata T, Mizusawa N, Qian ZR, Shima SW, Okutsu T, Yamada S, Sano T, Yoshimoto K. Expression of p18(INK4C) is down-regulated in human pituitary adenomas. *Endocr Pathol.* 2009;20(2):114-121.
119. Simpson DJ, Clayton RN, Farrell WE. Preferential loss of Death Associated Protein kinase expression in invasive pituitary tumours is associated with either CpG island methylation or homozygous deletion. *Oncogene.* 2002;21(8):1217-1224.
120. Bellodi C, Krasnykh O, Haynes N, Theodoropoulou M, Peng G, Montanaro L, Ruggero D. Loss of function of the tumor suppressor DKC1 perturbs p27 translation control and contributes to pituitary tumorigenesis. *Cancer Res.* 2010;70(14):6026-6035.
121. Michaelis KA, Knox AJ, Xu M, Kiseljak-Vassiliades K, Edwards MG, Geraci M, Kleinschmidt-DeMasters BK, Lillehei KO, Wierman ME. Identification of growth arrest and DNA-damage-inducible gene beta (GADD45beta) as a novel tumor suppressor in pituitary gonadotrope tumors. *Endocrinology.* 2011;152(10):3603-3613.
122. Zhang X, Sun H, Danila DC, Johnson SR, Zhou Y, Swearingen B, Klibanski A. Loss of expression of GADD45 gamma, a growth inhibitory gene, in human pituitary adenomas: implications for tumorigenesis. *J Clin Endocrinol Metab.* 2002;87(3):1262-1267.
123. Bahar A, Bicknell JE, Simpson DJ, Clayton RN, Farrell WE. Loss of expression of the growth inhibitory gene GADD45gamma, in human pituitary adenomas, is associated with CpG island methylation. *Oncogene.* 2004;23(4):936-944.
124. Zhang X, Zhou Y, Mehta KR, Danila DC, Scolavino S, Johnson SR, Klibanski A. A pituitary-derived MEG3 isoform functions as a growth suppressor in tumor cells. *J Clin Endocrinol Metab.* 2003;88(11):5119-5126.
125. Zhao J, Dahle D, Zhou Y, Zhang X, Klibanski A. Hypermethylation of the promoter region is associated with the loss of MEG3 gene expression in human pituitary tumors. *J Clin Endocrinol Metab.* 2005;90(4):2179-2186.
126. Gejman R, Batista DL, Zhong Y, Zhou Y, Zhang X, Swearingen B, Stratakis CA, Hedley-Whyte ET, Klibanski A. Selective loss of MEG3 expression and intergenic differentially methylated region hypermethylation in the MEG3/DLK1 locus in human clinically nonfunctioning pituitary adenomas. *J Clin Endocrinol Metab.* 2008;93(10):4119-4125.

127. Cheunsuchon P, Zhou Y, Zhang X, Lee H, Chen W, Nakayama Y, Rice KA, Tessa Hedley-Whyte E, Swearingen B, Klibanski A. Silencing of the imprinted DLK1-MEG3 locus in human clinically nonfunctioning pituitary adenomas. *Am J Pathol.* 2011;179(4):2120-2130.
128. Mezzomo LC, Gonzales PH, Pesce FG, Kretzmann FN, Ferreira NP, Oliveira MC, Kohek MB. Expression of cell growth negative regulators MEG3 and GADD45gamma is lost in most sporadic human pituitary adenomas. *Pituitary.* 2012;15(3):420-427.
129. Zhuang Z, Ezzat SZ, Vortmeyer AO, Weil R, Oldfield EH, Park WS, Pack S, Huang S, Agarwal SK, Guru SC, Manickam P, Debelenko LV, Kester MB, Olufemi SE, Heppner C, Crabtree JS, Burns AL, Spiegel AM, Marx SJ, Chandrasekharappa SC, Collins FS, Emmert-Buck MR, Liotta LA, Asa SL, Lubensky IA. Mutations of the *MEN1* tumor suppressor gene in pituitary tumors. *Cancer Res.* 1997;57(24):5446-5451.
130. Tanaka C, Kimura T, Yang P, Moritani M, Yamaoka T, Yamada S, Sano T, Yoshimoto K, Itakura M. Analysis of loss of heterozygosity on chromosome 11 and infrequent inactivation of the MEN1 gene in sporadic pituitary adenomas. *J Clin Endocrinol Metab.* 1998;83(8):2631-2634.
131. Wenbin C, Asai A, Teramoto A, Sanno N, Kirino T. Mutations of the *MEN1* tumor suppressor gene in sporadic pituitary tumors. *Cancer Lett.* 1999;142(1):43-47.
132. Schmidt MC, Henke RT, Stangl AP, Meyer-Puttlitz B, Stoffel-Wagner B, Schramm J, von DA. Analysis of the MEN1 gene in sporadic pituitary adenomas. *J Pathol.* 1999;188(2):168-173.
133. McCabe CJ, Gittoes NJ, Sheppard MC, Franklyn JA. Increased *MEN1* mRNA expression in sporadic pituitary tumours. *Clin Endocrinol (Oxf).* 1999;50(6):727-733.
134. Pagotto U, Arzberger T, Theodoropoulou M, Grubler Y, Pantaloni C, Saeger W, Losa M, Journot L, Stalla GK, Spengler D. The expression of the antiproliferative gene ZAC is lost or highly reduced in nonfunctioning pituitary adenomas. *Cancer Res.* 2000;60(24):6794-6799.
135. Noh TW, Jeong HJ, Lee MK, Kim TS, Kim SH, Lee EJ. Predicting recurrence of nonfunctioning pituitary adenomas. *J Clin Endocrinol Metab.* 2009;94(11):4406-4413.
136. Simpson DJ, Hibberts NA, McNicol AM, Clayton RN, Farrell WE. Loss of pRb expression in pituitary adenomas is associated with methylation of the RB1 CpG island. *Cancer Res.* 2000;60(5):1211-1216.
137. Bahar A, Simpson DJ, Cutty SJ, Bicknell JE, Hoban PR, Holley S, Mourtada-Maarabouni M, Williams GT, Clayton RN, Farrell WE. Isolation and characterization of a novel pituitary tumor apoptosis gene. *Mol Endocrinol.* 2004;18(7):1827-1839.

138. Bilodeau S, Vallette-Kasic S, Gauthier Y, Figarella-Branger D, Brue T, Berthelet F, Lacroix A, Batista D, Stratakis C, Hanson J, Meij B, Drouin J. Role of Brg1 and HDAC2 in GR trans-repression of the pituitary *POMC* gene and misexpression in Cushing disease. *Genes Dev.* 2006;20(20):2871-2886.
139. Corbetta S, Ballare E, Mantovani G, Lania A, Losa M, Di Blasio AM, Spada A. Somatostatin receptor subtype 2 and 5 in human GH-secreting pituitary adenomas: analysis of gene sequence and mRNA expression. *Eur J Clin Invest.* 2001;31(3):208-214.
140. Ando S, Sarlis NJ, Oldfield EH, Yen PM. Somatic mutation of TRbeta can cause a defect in negative regulation of TSH in a TSH-secreting pituitary tumor. *J Clin Endocrinol Metab.* 2001;86(11):5572-5576.
141. Ando S, Sarlis NJ, Krishnan J, Feng X, Refetoff S, Zhang MQ, Oldfield EH, Yen PM. Aberrant alternative splicing of thyroid hormone receptor in a TSH-secreting pituitary tumor is a mechanism for hormone resistance. *Mol Endocrinol.* 2001;15(9):1529-1538.
142. Tanizaki Y, Jin L, Scheithauer BW, Kovacs K, Roncaroli F, Lloyd RV. P53 gene mutations in pituitary carcinomas. *Endocr Pathol.* 2007;18(4):217-222.
143. Kawashima ST, Usui T, Sano T, Iogawa H, Hagiwara H, Tamanaha T, Tagami T, Naruse M, Hojo M, Takahashi JA, Shimatsu A. **P53** gene mutation in an atypical corticotroph adenoma with Cushing's disease. *Clin Endocrinol (Oxf).* 2009;70(4):656-657.
144. Pinto EM, Siqueira SA, Cukier P, Fragoso MC, Lin CJ, de Mendonca BB. Possible role of a radiation-induced p53 mutation in a Nelson's syndrome patient with a fatal outcome. *Pituitary.* 2011;14(4):400-404.
145. Murakami M, Mizutani A, Asano S, Katakami H, Ozawa Y, Yamazaki K, Ishida Y, Takano K, Okinaga H, Matsuno A. A mechanism of acquiring temozolomide resistance during transformation of atypical prolactinoma into prolactin-producing pituitary carcinoma: case report. *Neurosurgery.* 2011;68(6):E1761-E1767.
146. Elston MS, Gill AJ, Conaglen JV, Clarkson A, Shaw JM, Law AJ, Cook RJ, Little NS, Clifton-Bligh RJ, Robinson BG, McDonald KL. Wnt pathway inhibitors are strongly down-regulated in pituitary tumors. *Endocrinology.* 2008;149(3):1235-1242.
147. Sanchez-Beato M, Sanchez E, Gonzalez-Carrero J, Morente M, Diez A, Sanchez-Verde L, Martin MC, Cigudosa JC, Vidal M, Piris MA. Variability in the expression of polycomb proteins in different normal and tumoral tissues. A pilot study using tissue microarrays. *Mod Pathol.* 2006;19(5):684-694.
148. Westerman BA, Blom M, Tanger E, van d, V, Song JY, van SM, Gadiot J, Cornelissen-Steijger P, Zevenhoven J, Prosser HM, Uren A, Aronica E, van LM. GFAP-Cre-mediated transgenic activation of Bmi1 results in pituitary tumors. *PLoS One.* 2012;7(5):e35943.

149. Palumbo T, Faucz FR, Azevedo M, Xekouki P, Iliopoulos D, Stratakis CA. Functional screen analysis reveals miR-26b and miR-128 as central regulators of pituitary somatomammotrophic tumor growth through activation of the PTEN-AKT pathway. *Oncogene.* 2013;32(13):1651-1659.
150. Turner HE, Nagy Z, Sullivan N, Esiri MM, Wass JA. Expression analysis of cyclins in pituitary adenomas and the normal pituitary gland. *Clin Endocrinol (Oxf).* 2000;53(3):337-344.
151. Wierinckx A, Auger C, Devauchelle P, Reynaud A, Chevallier P, Jan M, Perrin G, Fevre-Montange M, Rey C, Figarella-Branger D, Raverot G, Belin MF, Lachuer J, Trouillas J. A diagnostic marker set for invasion, proliferation, and aggressiveness of prolactin pituitary tumors. *Endocr Relat Cancer.* 2007;14(3):887-900.
152. De M, I, Visone R, Wierinckx A, Palmieri D, Ferraro A, Cappabianca P, Chiappetta G, Forzati F, Lombardi G, Colao A, Trouillas J, Fedele M, Fusco A. HMGA proteins up-regulate *CCNB2* gene in mouse and human pituitary adenomas. *Cancer Res.* 2009;69(5):1844-1850.
153. Hibberts NA, Simpson DJ, Bicknell JE, Broome JC, Hoban PR, Clayton RN, Farrell WE. Analysis of cyclin D1 (CCND1) allelic imbalance and overexpression in sporadic human pituitary tumors. *Clin Cancer Res.* 1999;5(8):2133-2139.
154. Jordan S, Lidhar K, Korbonits M, Lowe DG, Grossman AB. Cyclin D and cyclin E expression in normal and adenomatous pituitary. *Eur J Endocrinol.* 2000;143(1):R1-R6.
155. Simpson DJ, Fryer AA, Grossman AB, Wass JA, Pfeifer M, Kros JM, Clayton RN, Farrell WE. Cyclin D1 (CCND1) genotype is associated with tumour grade in sporadic pituitary adenomas. *Carcinogenesis.* 2001;22(11):1801-1807.
156. Bertherat J, Chanson P, Montminy M. The cyclic adenosine 3',5'-monophosphate-responsive factor CREB is constitutively activated in human somatotroph adenomas. *Mol Endocrinol.* 1995;9(7):777-783.
157. Chaidarun SS, Eggo MC, Sheppard MC, Stewart PM. Expression of epidermal growth factor (EGF), its receptor, and related oncoprotein (erbB-2) in human pituitary tumors and response to EGF in vitro. *Endocrinology.* 1994;135(5):2012-2021.
158. Theodoropoulou M, Arzberger T, Gruebler Y, Jaffrain-Rea ML, Schlegel J, Schaaf L, Petrangeli E, Losa M, Stalla GK, Pagotto U. Expression of epidermal growth factor receptor in neoplastic pituitary cells: evidence for a role in corticotropinoma cells. *J Endocrinol.* 2004;183(2):385-394.
159. McCabe CJ, Khaira JS, Boelaert K, Heaney AP, Tannahill LA, Hussain S, Mitchell R, Olliff J, Sheppard MC, Franklyn JA, Gittoes NJ. Expression of pituitary tumour transforming gene (PTTG) and fibroblast growth factor-2 (FGF-2) in human pituitary adenomas: relationships to clinical tumour behaviour. *Clin Endocrinol (Oxf).* 2003;58(2):141-150.

160. Zhu X, Lee K, Asa SL, Ezzat S. Epigenetic silencing through DNA and histone methylation of fibroblast growth factor receptor 2 in neoplastic pituitary cells. *Am J Pathol.* 2007;170(5):1618-1628.
161. Ezzat S, Zheng L, Zhu XF, Wu GE, Asa SL. Targeted expression of a human pituitary tumor-derived isoform of FGF receptor-4 recapitulates pituitary tumorigenesis. *J Clin Invest.* 2002;109(1):69-78.
162. Evans CO, Young AN, Brown MR, Brat DJ, Parks JS, Neish AS, Oyesiku NM. Novel patterns of gene expression in pituitary adenomas identified by complementary deoxyribonucleic acid microarrays and quantitative reverse transcription-polymerase chain reaction. *J Clin Endocrinol Metab.* 2001;86(7):3097-3107.
163. Williamson EA, Daniels M, Foster S, Kelly WF, Kendall-Taylor P, Harris PE. Gs alpha and Gi2 alpha mutations in clinically non-functioning pituitary tumours. *Clin Endocrinol (Oxf).* 1994;41(6):815-820.
164. Williamson EA, Ince PG, Harrison D, Kendall-Taylor P, Harris PE. G-protein mutations in human pituitary adrenocorticotrophic hormone-secreting adenomas. *Eur J Clin Invest.* 1995;25(2):128-131.
165. Vallar L, Spada A, Giannattasio G. Altered Gs and adenylate cyclase activity in human GH-secreting pituitary adenomas. *Nature.* 1987;330(6148):566-568.
166. Tordjman K, Stern N, Ouaknine G, Yossiphov Y, Razon N, Nordenskjold M, Friedman E. Activating mutations of the Gs alpha-gene in nonfunctioning pituitary tumors. *J Clin Endocrinol Metab.* 1993;77(3):765-769.
167. Hamacher C, Brocker M, Adams EF, Lei T, Fahlbusch R, Buchfelder M, Derwahl M. Overexpression of stimulatory G protein alpha-subunit is a hallmark of most human somatotrophic pituitary tumours and is associated with resistance to GH-releasing hormone. *Pituitary.* 1998;1(1):13-23.
168. Hayward BE, Barlier A, Korbonits M, Grossman AB, Jacquet P, Enjalbert A, Bonthron DT. Imprinting of the G(s)alpha gene *GNAS1* in the pathogenesis of acromegaly. *J Clin Invest.* 2001;107(6):R31-R36.
169. Riminucci M, Collins MT, Lala R, Corsi A, Matarazzo P, Gehron RP, Bianco P. An R201H activating mutation of the *GNAS1* (Gsalpha) gene in a corticotroph pituitary adenoma. *Mol Pathol.* 2002;55(1):58-60.
170. Picard C, Silvy M, Gerard C, Buffat C, Lavaque E, Figarella-Branger D, Dufour H, Gabert J, Beckers A, Brue T, Enjalbert A, Barlier A. Gs alpha overexpression and loss of Gs alpha imprinting in human somatotroph adenomas: association with tumor size and response to pharmacologic treatment. *Int J Cancer.* 2007;121(6):1245-1252.
171. Finelli P, Pierantoni GM, Giardino D, Losa M, Rodeschini O, Fedele M, Valtorta E, Mortini P, Croce CM, Larizza L, Fusco A. The High Mobility Group A2 gene is amplified and overexpressed in human prolactinomas. *Cancer Res.* 2002;62(8):2398-2405.

172. Pierantoni GM, Finelli P, Valtorta E, Giardino D, Rodeschini O, Esposito F, Losa M, Fusco A, Larizza L. High-mobility group A2 gene expression is frequently induced in non-functioning pituitary adenomas (NFPAs), even in the absence of chromosome 12 polysomy. *Endocr Relat Cancer.* 2005;12(4):867-874.
173. Karga HJ, Alexander JM, Hedley-Whyte ET, Klibanski A, Jameson JL. Ras mutations in human pituitary tumors. *J Clin Endocrinol Metab.* 1992;74(4):914-919.
174. Cai WY, Alexander JM, Hedley-Whyte ET, Scheithauer BW, Jameson JL, Zervas NT, Klibanski A. ras mutations in human prolactinomas and pituitary carcinomas. *J Clin Endocrinol Metab.* 1994;78(1):89-93.
175. Pei L, Melmed S, Scheithauer B, Kovacs K, Prager D. H-ras mutations in human pituitary carcinoma metastases. *J Clin Endocrinol Metab.* 1994;78(4):842-846.
176. Lin Y, Jiang X, Shen Y, Li M, Ma H, Xing M, Lu Y. Frequent mutations and amplifications of the *PIK3CA* gene in pituitary tumors. *Endocr Relat Cancer.* 2009;16(1):301-310.
177. Ezzat S, Yu S, Asa SL. Ikaros isoforms in human pituitary tumors: distinct localization, histone acetylation, and activation of the 5' fibroblast growth factor receptor-4 promoter. *Am J Pathol.* 2003;163(3):1177-1184.
178. Zhu X, Asa SL, Ezzat S. Fibroblast growth factor 2 and estrogen control the balance of histone 3 modifications targeting MAGE-A3 in pituitary neoplasia. *Clin Cancer Res.* 2008;14(7):1984-1996.
179. Alvaro V, Levy L, Dubray C, Roche A, Peillon F, Querat B, Joubert D. Invasive human pituitary tumors express a point-mutated alpha-protein kinase-C. *J Clin Endocrinol Metab.* 1993;77(5):1125-1129.
180. Zhang X, Horwitz GA, Heaney AP, Nakashima M, Prezant TR, Bronstein MD, Melmed S. Pituitary tumor transforming gene (*PTTG*) expression in pituitary adenomas. *J Clin Endocrinol Metab.* 1999;84(2):761-767.
181. Salehi F, Kovacs K, Scheithauer BW, Cantelmi D, Horvath E, Lloyd RV, Cusimano M. Immunohistochemical expression of pituitary tumor transforming gene (PTTG) in pituitary adenomas: a correlative study of tumor subtypes. *Int J Surg Pathol.* 2010;18(1):5-13.
182. Caccavelli L, Feron F, Morange I, Rouer E, Benarous R, Dewailly D, Jaquet P, Kordon C, Enjalbert A. Decreased expression of the two D2 dopamine receptor isoforms in bromocriptine-resistant prolactinomas. *Neuroendocrinology.* 1994;60(3):314-322.
183. Asa SL, DiGiovanni R, Jiang J, Ward ML, Loesch K, Yamada S, Sano T, Yoshimoto K, Frank SJ, Ezzat S. A growth hormone receptor mutation impairs growth hormone autofeedback signaling in pituitary tumors. *Cancer Res.* 2007;67(15):7505-7511.
184. Thapar K, Kovacs K, Stefaneanu L, Scheithauer B, Killinger DW, Lioyd RV, Smyth HS, Barr A, Thorner MO, Gaylinn B, Laws ER, Jr. Overexpression of the growth-

hormone-releasing hormone gene in acromegaly-associated pituitary tumors. An event associated with neoplastic progression and aggressive behavior. *Am J Pathol.* 1997;151(3):769-784.

185. Hashimoto K, Koga M, Motomura T, Kasayama S, Kouhara H, Ohnishi T, Arita N, Hayakawa T, Sato B, Kishimoto T. Identification of alternatively spliced messenger ribonucleic acid encoding truncated growth hormone-releasing hormone receptor in human pituitary adenomas. *J Clin Endocrinol Metab.* 1995;80(10):2933-2939.
186. Karl M, Von WG, Kempter E, Katz DA, Reincke M, Monig H, Ali IU, Stratakis CA, Oldfield EH, Chrousos GP, Schulte HM. Nelson's syndrome associated with a somatic frame shift mutation in the glucocorticoid receptor gene. *J Clin Endocrinol Metab.* 1996;81(1):124-129.
187. Huizenga NA, de LP, Koper JW, Clayton RN, Farrell WE, van der Lely AJ, Brinkmann AO, de Jong FH, Lamberts SW. Human adrenocorticotropin-secreting pituitary adenomas show frequent loss of heterozygosity at the glucocorticoid receptor gene locus. *J Clin Endocrinol Metab.* 1998;83(3):917-921.
188. Acunzo J, Roche C, Defilles C, Thirion S, Quentien MH, Figarella-Branger D, Graillon T, Dufour H, Brue T, Pellegrini I, Enjalbert A, Barlier A. Inactivation of PITX2 transcription factor induced apoptosis of gonadotroph tumoral cells. *Endocrinology.* 2011;152(10):3884-3892.
189. Palmieri D, Valentino T, De M, I, Esposito F, Cappabianca P, Wierinckx A, Vitiello M, Lombardi G, Colao A, Trouillas J, Pierantoni GM, Fusco A, Fedele M. PIT1 upregulation by HMGA proteins has a role in pituitary tumorigenesis. *Endocr Relat Cancer.* 2012;19(2):123-135.
190. Ma ZY, Song ZJ, Chen JH, Wang YF, Li SQ, Zhou LF, Mao Y, Li YM, Hu RG, Zhang ZY, Ye HY, Shen M, Shou XF, Li ZQ, Peng H, Wang QZ, Zhou DZ, Qin XL, Ji J, Zheng J, Chen H, Wang Y, Geng DY, Tang WJ, Fu CW, Shi ZF, Zhang YC, Ye Z, He WQ, Zhang QL, Tang QS, Xie R, Shen JW, Wen ZJ, Zhou J, Wang T, Huang S, Qiu HJ, Qiao ND, Zhang Y, Pan L, Bao WM, Liu YC, Huang CX, Shi YY, Zhao Y. Recurrent gain-of-function *USP8* mutations in Cushing's disease. *Cell Res.* 2015;25(3):306-317.
191. Ishikawa Y, Bianchi C, Nadal-Ginard B, Homcy CJ. Alternative promoter and 5' exon generate a novel Gs alpha mRNA. *J Biol Chem.* 1990;265(15):8458-8462.
192. Lyons J, Landis CA, Harsh G, Vallar L, Grunewald K, Feichtinger H, Duh QY, Clark OH, Kawasaki E, Bourne HR, . Two G protein oncogenes in human endocrine tumors. *Science.* 1990;249(4969):655-659.
193. Weinstein LS, Liu J, Sakamoto A, Xie T, Chen M. Minireview: *GNAS*: normal and abnormal functions. *Endocrinology.* 2004;145(12):5459-5464.
194. Landis CA, Harsh G, Lyons J, Davis RL, McCormick F, Bourne HR. Clinical characteristics of acromegalic patients whose pituitary tumors contain mutant Gs protein. *J Clin Endocrinol Metab.* 1990;71(6):1416-1420.

195. Hosoi E, Yokogoshi Y, Hosoi E, Horie H, Sano T, Yamada S, Saito S. Analysis of the Gs alpha gene in growth hormone-secreting pituitary adenomas by the polymerase chain reaction-direct sequencing method using paraffin-embedded tissues. *Acta Endocrinol (Copenh).* 1993;129(4):301-306.
196. Yoshimoto K, Iwahana H, Fukuda A, Sano T, Itakura M. Rare mutations of the Gs alpha subunit gene in human endocrine tumors. Mutation detection by polymerase chain reaction-primer-introduced restriction analysis. *Cancer.* 1993;72(4):1386-1393.
197. Shi Y, Tang D, Deng J, Su C. Detection of gsp oncogene in growth hormone-secreting pituitary adenomas and the study of clinical characteristics of acromegalic patients with gsp-positive pituitary tumors. *Chin Med J (Engl).* 1998;111(10):891-894.
198. Buchfelder M, Fahlbusch R, Merz T, Symowski H, Adams EF. Clinical correlates in acromegalic patients with pituitary tumors expressing *GSP* oncogenes. *Pituitary.* 1999;1(3-4):181-185.
199. Park C, Yang I, Woo J, Kim S, Kim J, Kim Y, Sohn S, Kim E, Lee M, Park H, Jung J, Park S. Somatostatin (SRIF) receptor subtype 2 and 5 gene expression in growth hormone-secreting pituitary adenomas: the relationship with endogenous srif activity and response to octreotide. *Endocr J.* 2004;51(2):227-236.
200. Mendoza V, Sosa E, Espinosa-de-los-Monteros AL, Salcedo M, Guinto G, Cheng S, Sandoval C, Mercado M. *GSPalpha* mutations in Mexican patients with acromegaly: potential impact on long term prognosis. *Growth Horm IGF Res.* 2005;15(1):28-32.
201. Freda PU, Chung WK, Matsuoka N, Walsh JE, Kanibir MN, Kleinman G, Wang Y, Bruce JN, Post KD. Analysis of *GNAS* mutations in 60 growth hormone secreting pituitary tumors: correlation with clinical and pathological characteristics and surgical outcome based on highly sensitive GH and IGF-I criteria for remission. *Pituitary.* 2007;10(3):275-282.
202. Larkin S, Reddy R, Karavitaki N, Cudlip S, Wass J, Ansorge O. Granulation pattern, but not GSP or GHR mutation, is associated with clinical characteristics in somatostatin-naive patients with somatotroph adenomas. *Eur J Endocrinol.* 2013;168(4):491-499.
203. Spada A, Arosio M, Bochicchio D, Bazzoni N, Vallar L, Bassetti M, Faglia G. Clinical, biochemical, and morphological correlates in patients bearing growth hormone-secreting pituitary tumors with or without constitutively active adenylyl cyclase. *J Clin Endocrinol Metab.* 1990;71(6):1421-1426.
204. Mayr B, Buslei R, Theodoropoulou M, Stalla GK, Buchfelder M, Schofl C. Molecular and functional properties of densely and sparsely granulated GH-producing pituitary adenomas. *Eur J Endocrinol.* 2013;169(4):391-400.

205. Taboada GF, Tabet AL, Naves LA, de Carvalho DP, Gadelha MR. Prevalence of *gsp* oncogene in somatotropinomas and clinically non-functioning pituitary adenomas: our experience. *Pituitary.* 2009;12(3):165-169.
206. Suarez HG, du Villard JA, Caillou B, Schlumberger M, Parmentier C, Monier R. *gsp* mutations in human thyroid tumours. *Oncogene.* 1991;6(4):677-679.
207. Williamson EA, Johnson SJ, Foster S, Kendall-Taylor P, Harris PE. G protein gene mutations in patients with multiple endocrinopathies. *J Clin Endocrinol Metab.* 1995;80(5):1702-1705.
208. Fragoso MC, Latronico AC, Carvalho FM, Zerbini MC, Marcondes JA, Araujo LM, Lando VS, Frazzatto ET, Mendonca BB, Villares SM. Activating mutation of the stimulatory G protein (gsp) as a putative cause of ovarian and testicular human stromal Leydig cell tumors. *J Clin Endocrinol Metab.* 1998;83(6):2074-2078.
209. Turan S, Bastepe M. *GNAS* Spectrum of Disorders. *Curr Osteoporos Rep.* 2015.
210. Weinstein LS, Shenker A, Gejman PV, Merino MJ, Friedman E, Spiegel AM. Activating mutations of the stimulatory G protein in the McCune-Albright syndrome. *N Engl J Med.* 1991;325(24):1688-1695.
211. Mantovani G, Bondioni S, Lania AG, Corbetta S, de SL, Cappa M, Di BE, Chanson P, Beck-Peccoz P, Spada A. Parental origin of *Gsalpha* mutations in the McCune-Albright syndrome and in isolated endocrine tumors. *J Clin Endocrinol Metab.* 2004;89(6):3007-3009.
212. Turan S, Bastepe M. The *GNAS* complex locus and human diseases associated with loss-of-function mutations or epimutations within this imprinted gene. *Horm Res Paediatr.* 2013;80(4):229-241.
213. Turner N, Grose R. Fibroblast growth factor signalling: from development to cancer. *Nat Rev Cancer.* 2010;10(2):116-129.
214. Morita K, Takano K, Yasufuku-Takano J, Yamada S, Teramoto A, Takei M, Osamura RY, Sano T, Fujita T. Expression of pituitary tumour-derived, N-terminally truncated isoform of fibroblast growth factor receptor 4 (ptd-FGFR4) correlates with tumour invasiveness but not with G-protein alpha subunit (*gsp*) mutation in human GH-secreting pituitary adenomas. *Clin Endocrinol (Oxf).* 2008;68(3):435-441.
215. Qian ZR, Sano T, Asa SL, Yamada S, Horiguchi H, Tashiro T, Li CC, Hirokawa M, Kovacs K, Ezzat S. Cytoplasmic expression of fibroblast growth factor receptor-4 in human pituitary adenomas: relation to tumor type, size, proliferation, and invasiveness. *J Clin Endocrinol Metab.* 2004;89(4):1904-1911.
216. NHLBI GO Exome Sequencing Project (ESP).Exome Variant Server. http://evs.gs.washington.edu/EVS/. Accessed 18/5/2015.
217. Exome Aggregation Consortium. http://exac.broadinstitute.org. Accessed 3/6/2015.

218. Abecasis GR, Auton A, Brooks LD, DePristo MA, Durbin RM, Handsaker RE, Kang HM, Marth GT, McVean GA. An integrated map of genetic variation from 1,092 human genomes. *Nature.* 2012;491(7422):56-65.
219. Frullanti E, Berking C, Harbeck N, Jezequel P, Haugen A, Mawrin C, Parise O, Jr., Sasaki H, Tsuchiya N, Dragani TA. Meta and pooled analyses of *FGFR4* Gly388Arg polymorphism as a cancer prognostic factor. *Eur J Cancer Prev.* 2011;20(4):340-347.
220. Wang J, Yu W, Cai Y, Ren C, Ittmann MM. Altered fibroblast growth factor receptor 4 stability promotes prostate cancer progression. *Neoplasia.* 2008;10(8):847-856.
221. Tateno T, Asa SL, Zheng L, Mayr T, Ullrich A, Ezzat S. The FGFR4-G388R polymorphism promotes mitochondrial STAT3 serine phosphorylation to facilitate pituitary growth hormone cell tumorigenesis. *PLoS Genet.* 2011;7(12):e1002400.
222. Bartel DP. MicroRNAs: genomics, biogenesis, mechanism, and function. *Cell.* 2004;116(2):281-297.
223. Lewis BP, Burge CB, Bartel DP. Conserved seed pairing, often flanked by adenosines, indicates that thousands of human genes are microRNA targets. *Cell.* 2005;120(1):15-20.
224. Farazi TA, Spitzer JI, Morozov P, Tuschl T. miRNAs in human cancer. *J Pathol.* 2011;223(2):102-115.
225. Gadelha MR, Kasuki L, Denes J, Trivellin G, Korbonits M. MicroRNAs: Suggested role in pituitary adenoma pathogenesis. *J Endocrinol Invest.* 2013;36(10):889-895.
226. Bottoni A, Piccin D, Tagliati F, Luchin A, Zatelli MC, degli Uberti EC. miR-15a and miR-16-1 down-regulation in pituitary adenomas. *J Cell Physiol.* 2005;204(1):280-285.
227. Qian ZR, Asa SL, Siomi H, Siomi MC, Yoshimoto K, Yamada S, Wang EL, Rahman MM, Inoue H, Itakura M, Kudo E, Sano T. Overexpression of HMGA2 relates to reduction of the let-7 and its relationship to clinicopathological features in pituitary adenomas. *Mod Pathol.* 2009;22(3):431-441.
228. Butz H, Liko I, Czirjak S, Igaz P, Khan MM, Zivkovic V, Balint K, Korbonits M, Racz K, Patocs A. Down-regulation of Wee1 kinase by a specific subset of microRNA in human sporadic pituitary adenomas. *J Clin Endocrinol Metab.* 2010;95(10):E181-E191.
229. Trivellin G, Butz H, Delhove J, Igreja S, Chahal HS, Zivkovic V, McKay T, Patocs A, Grossman AB, Korbonits M. MicroRNA miR-107 is overexpressed in pituitary adenomas and inhibits the expression of aryl hydrocarbon receptor-interacting protein in vitro. *Am J Physiol Endocrinol Metab.* 2012;303(6):E708-E719.
230. Palmieri D, D'Angelo D, Valentino T, De M, I, Ferraro A, Wierinckx A, Fedele M, Trouillas J, Fusco A. Downregulation of HMGA-targeting microRNAs has a critical role in human pituitary tumorigenesis. *Oncogene.* 2012;31(34):3857-3865.

231. D'Angelo D, Palmieri D, Mussnich P, Roche M, Wierinckx A, Raverot G, Fedele M, Croce CM, Trouillas J, Fusco A. Altered microRNA expression profile in human pituitary GH adenomas: down-regulation of miRNA targeting HMGA1, HMGA2, and E2F1. *J Clin Endocrinol Metab.* 2012;97(7):E1128-E1138.
232. Gentilin E, Tagliati F, Filieri C, Mole D, Minoia M, Rosaria AM, degli Uberti EC, Zatelli MC. miR-26a plays an important role in cell cycle regulation in ACTH-secreting pituitary adenomas by modulating protein kinase Cdelta. *Endocrinology.* 2013;154(5):1690-1700.
233. Leone V, Langella C, D'Angelo D, Mussnich P, Wierinckx A, Terracciano L, Raverot G, Lachuer J, Rotondi S, Jaffrain-Rea ML, Trouillas J, Fusco A. Mir-23b and miR-130b expression is downregulated in pituitary adenomas. *Mol Cell Endocrinol.* 2014;390(1-2):1-7.
234. Renjie W, Haiqian L. MiR-132, miR-15a and miR-16 synergistically inhibit pituitary tumor cell proliferation, invasion and migration by targeting Sox5. *Cancer Lett.* 2015;356(2 Pt B):568-578.
235. Denes J, Kasuki L, Trivellin G, Colli LM, Takiya CM, Stiles CE, Barry S, De CM, Gadelha MR, Korbonits M. Regulation of aryl hydrocarbon receptor interacting protein (*AIP*) protein expression by MiR-34a in sporadic somatotropinomas. *PLoS One.* 2015;10(2):e0117107.
236. McCune D.J. Osteitis fibrosa cystica: the case of a nine year old girl who also exhibits precocious puberty, multiple pigmentation of the skin and hyperthyroidism. *Am J Dis Child.* 1936;52:743-744.
237. Albright F, Butler AM, Hampton AO, Smith P. Syndrome characterized by osteitis fibrosa disseminata, areas of pigmentation and endocrine dysfunction, with precocious puberty in females - Report of five cases. *N Engl J Med.* 1937;216(17):727-746.
238. Shah KN. The diagnostic and clinical significance of cafe-au-lait macules. *Pediatr Clin North Am.* 2010;57(5):1131-1153.
239. Lumbroso S, Paris F, Sultan C. Activating Gsalpha mutations: analysis of 113 patients with signs of McCune-Albright syndrome--a European Collaborative Study. *J Clin Endocrinol Metab.* 2004;89(5):2107-2113.
240. Dumitrescu CE, Collins MT. McCune-Albright syndrome. *Orphanet J Rare Dis.* 2008;3:12.
241. Happle R. The McCune-Albright syndrome: a lethal gene surviving by mosaicism. *Clin Genet.* 1986;29(4):321-324.
242. Bianco P, Kuznetsov SA, Riminucci M, Fisher LW, Spiegel AM, Robey PG. Reproduction of human fibrous dysplasia of bone in immunocompromised mice by transplanted mosaics of normal and Gsalpha-mutated skeletal progenitor cells. *J Clin Invest.* 1998;101(8):1737-1744.
243. Campbell R, Gosden CM, Bonthron DT. Parental origin of transcription from the human *GNAS1* gene. *J Med Genet.* 1994;31(8):607-614.

244. Weinstein LS. The stimulatory G protein alpha-subunit gene: mutations and imprinting lead to complex phenotypes. *J Clin Endocrinol Metab.* 2001;86(10):4622-4626.
245. Davies SJ, Hughes HE. Imprinting in Albright's hereditary osteodystrophy. *J Med Genet.* 1993;30(2):101-103.
246. Yu S, Yu D, Lee E, Eckhaus M, Lee R, Corria Z, Accili D, Westphal H, Weinstein LS. Variable and tissue-specific hormone resistance in heterotrimeric Gs protein alpha-subunit (Gsalpha) knockout mice is due to tissue-specific imprinting of the gsalpha gene. *Proc Natl Acad Sci U S A.* 1998;95(15):8715-8720.
247. Zheng H, Radeva G, McCann JA, Hendy GN, Goodyer CG. *Galphas* transcripts are biallelically expressed in the human kidney cortex: implications for pseudohypoparathyroidism type 1b. *J Clin Endocrinol Metab.* 2001;86(10):4627-4629.
248. Mantovani G, Ballare E, Giammona E, Beck-Peccoz P, Spada A. The *gsalpha* gene: predominant maternal origin of transcription in human thyroid gland and gonads. *J Clin Endocrinol Metab.* 2002;87(10):4736-4740.
249. Candeliere GA, Roughley PJ, Glorieux FH. Polymerase chain reaction-based technique for the selective enrichment and analysis of mosaic arg201 mutations in *G alpha s* from patients with fibrous dysplasia of bone. *Bone.* 1997;21(2):201-206.
250. Riminucci M, Fisher LW, Majolagbe A, Corsi A, Lala R, De SC, Robey PG, Bianco P. A novel *GNAS1* mutation, R201G, in McCune-albright syndrome. *J Bone Miner Res.* 1999;14(11):1987-1989.
251. Collins MT, Singer FR, Eugster E. McCune-Albright syndrome and the extraskeletal manifestations of fibrous dysplasia. *Orphanet J Rare Dis.* 2012;7 Suppl 1:S4.
252. Boyce AM, Chong WH, Shawker TH, Pinto PA, Linehan WM, Bhattacharryya N, Merino MJ, Singer FR, Collins MT. Characterization and management of testicular pathology in McCune-Albright syndrome. *J Clin Endocrinol Metab.* 2012;97(9):E1782-E1790.
253. Mieszczak J, Lowe ES, Plourde P, Eugster EA. The aromatase inhibitor anastrozole is ineffective in the treatment of precocious puberty in girls with McCune-Albright syndrome. *J Clin Endocrinol Metab.* 2008;93(7):2751-2754.
254. Feuillan P, Calis K, Hill S, Shawker T, Robey PG, Collins MT. Letrozole treatment of precocious puberty in girls with the McCune-Albright syndrome: a pilot study. *J Clin Endocrinol Metab.* 2007;92(6):2100-2106.
255. Eugster EA, Rubin SD, Reiter EO, Plourde P, Jou HC, Pescovitz OH. Tamoxifen treatment for precocious puberty in McCune-Albright syndrome: a multicenter trial. *J Pediatr.* 2003;143(1):60-66.
256. Feuillan PP, Shawker T, Rose SR, Jones J, Jeevanram RK, Nisula BC. Thyroid abnormalities in the McCune-Albright syndrome: ultrasonography and hormonal studies. *J Clin Endocrinol Metab.* 1990;71(6):1596-1601.

257. Celi FS, Coppotelli G, Chidakel A, Kelly M, Brillante BA, Shawker T, Cherman N, Feuillan PP, Collins MT. The role of type 1 and type 2 5'-deiodinase in the pathophysiology of the 3,5,3'-triiodothyronine toxicosis of McCune-Albright syndrome. *J Clin Endocrinol Metab.* 2008;93(6):2383-2389.
258. Gillis D, Rosler A, Hannon TS, Koplewitz BZ, Hirsch HJ. Prolonged remission of severe Cushing syndrome without adrenalectomy in an infant with McCune-Albright syndrome. *J Pediatr.* 2008;152(6):882-4, 884.
259. Brown RJ, Kelly MH, Collins MT. Cushing syndrome in the McCune-Albright syndrome. *J Clin Endocrinol Metab.* 2010;95(4):1508-1515.
260. Carney JA, Young WF, Stratakis CA. Primary bimorphic adrenocortical disease: cause of hypercortisolism in McCune-Albright syndrome. *Am J Surg Pathol.* 2011;35(9):1311-1326.
261. Collins MT, Chebli C, Jones J, Kushner H, Consugar M, Rinaldo P, Wientroub S, Bianco P, Robey PG. Renal phosphate wasting in fibrous dysplasia of bone is part of a generalized renal tubular dysfunction similar to that seen in tumor-induced osteomalacia. *J Bone Miner Res.* 2001;16(5):806-813.
262. Riminucci M, Collins MT, Fedarko NS, Cherman N, Corsi A, White KE, Waguespack S, Gupta A, Hannon T, Econs MJ, Bianco P, Gehron RP. FGF-23 in fibrous dysplasia of bone and its relationship to renal phosphate wasting. *J Clin Invest.* 2003;112(5):683-692.
263. Glorieux FH, Rauch F. Medical therapy of children with fibrous dysplasia. *J Bone Miner Res.* 2006;21 Suppl 2:110-113.
264. Leet AI, Collins MT. Current approach to fibrous dysplasia of bone and McCune-Albright syndrome. *J Child Orthop.* 2007;1(1):3-17.
265. Plotkin H, Rauch F, Zeitlin L, Munns C, Travers R, Glorieux FH. Effect of pamidronate treatment in children with polyostotic fibrous dysplasia of bone. *J Clin Endocrinol Metab.* 2003;88(10):4569-4575.
266. Salenave S, Boyce AM, Collins MT, Chanson P. Acromegaly and McCune-Albright syndrome. *J Clin Endocrinol Metab.* 2014;99(6):1955-1969.
267. Akintoye SO, Chebli C, Booher S, Feuillan P, Kushner H, Leroith D, Cherman N, Bianco P, Wientroub S, Robey PG, Collins MT. Characterization of gsp-mediated growth hormone excess in the context of McCune-Albright syndrome. *J Clin Endocrinol Metab.* 2002;87(11):5104-5112.
268. Vortmeyer AO, Glasker S, Mehta GU, Abu-Asab MS, Smith JH, Zhuang Z, Collins MT, Oldfield EH. Somatic *GNAS* mutation causes widespread and diffuse pituitary disease in acromegalic patients with McCune-Albright Syndrome. *J Clin Endocrinol Metab.* 2012.
269. Kovacs K, Horvath E, Thorner MO, Rogol AD. Mammosomatotroph hyperplasia associated with acromegaly and hyperprolactinemia in a patient with the McCune-Albright syndrome. A histologic, immunocytologic and ultrastructural study of the

surgically-removed adenohypophysis. *Virchows Arch A Pathol Anat Histopathol.* 1984;403(1):77-86.

270. Galland F, Kamenicky P, Affres H, Reznik Y, Pontvert D, Le BY, Young J, Chanson P. McCune-Albright syndrome and acromegaly: effects of hypothalamopituitary radiotherapy and/or pegvisomant in somatostatin analog-resistant patients. *J Clin Endocrinol Metab.* 2006;91(12):4957-4961.
271. Scheithauer BW, Laws ER, Jr., Kovacs K, Horvath E, Randall RV, Carney JA. Pituitary adenomas of the multiple endocrine neoplasia type I syndrome. *Semin Diagn Pathol.* 1987;4(3):205-211.
272. Daly AF, Jaffrain-Rea ML, Ciccarelli A, Valdes-Socin H, Rohmer V, Tamburrano G, Borson-Chazot C, Estour B, Ciccarelli E, Brue T, Ferolla P, Emy P, Colao A, De ME, Lecomte P, Penfornis F, Delemer B, Bertherat J, Wemeau JL, De HW, Archambeaud F, Stevenaert A, Calender A, Murat A, Cavagnini F, Beckers A. Clinical characterization of familial isolated pituitary adenomas. *J Clin Endocrinol Metab.* 2006;91(9):3316-3323.
273. Lemos MC, Thakker RV. Multiple endocrine neoplasia type 1 (*MEN1*): analysis of 1336 mutations reported in the first decade following identification of the gene. *Hum Mutat.* 2008;29(1):22-32.
274. Thakker RV. Multiple endocrine neoplasia type 1 (MEN1). *Best Pract Res Clin Endocrinol Metab.* 2010;24(3):355-370.
275. Bertherat J, Horvath A, Groussin L, Grabar S, Boikos S, Cazabat L, Libe R, Rene-Corail F, Stergiopoulos S, Bourdeau I, Bei T, Clauser E, Calender A, Kirschner LS, Bertagna X, Carney JA, Stratakis CA. Mutations in regulatory subunit type 1A of cyclic adenosine 5'-monophosphate-dependent protein kinase (*PRKAR1A*): phenotype analysis in 353 patients and 80 different genotypes. *J Clin Endocrinol Metab.* 2009;94(6):2085-2091.
276. Chahal HS, Chapple JP, Frohman LA, Grossman AB, Korbonits M. Clinical, genetic and molecular characterization of patients with familial isolated pituitary adenomas (FIPA). *Trends Endocrinol Metab.* 2010;21(7):419-427.
277. Iwata T, Tamanaha T, Koezuka R, Tochiya M, Makino H, Kishimoto I, Mizusawa N, Ono S, Inoshita N, Yamada S, Shimatsu A, Yoshimoto K. Germline deletion and a somatic mutation of the *PRKAR1A* gene in a Carney complex-related pituitary adenoma. *Eur J Endocrinol.* 2015;172(1):K5-10.
278. Kaltsas GA, Kola B, Borboli N, Morris DG, Gueorguiev M, Swords FM, Czirjak S, Kirschner LS, Stratakis CA, Korbonits M, Grossman AB. Sequence analysis of the *PRKAR1A* gene in sporadic somatotroph and other pituitary tumours. *Clin Endocrinol (Oxf).* 2002;57(4):443-448.
279. Barlier A, Vanbellinghen JF, Daly AF, Silvy M, Jaffrain-Rea ML, Trouillas J, Tamagno G, Cazabat L, Bours V, Brue T, Enjalbert A, Beckers A. Mutations in the aryl hydrocarbon receptor interacting protein gene are not highly prevalent among

subjects with sporadic pituitary adenomas. *J Clin Endocrinol Metab.* 2007;92(5):1952-1955.

280. Kirschner LS. *PRKAR1A* and the evolution of pituitary tumors. *Mol Cell Endocrinol.* 2010;326(1-2):3-7.
281. Thakker RV. Multiple endocrine neoplasia type 1 (MEN1) and type 4 (MEN4). *Mol Cell Endocrinol.* 2014;386(1-2):2-15.
282. Erdheim J. Zur normalen und pathologischen Histologie der Glandula thyreoidea, parathyroidea und Hypophysis. *Beitr Pathol Anat.* 2015.
283. Wermer P. Genetic aspects of adenomatosis of endocrine glands. *Am J Med.* 1954;16(3):363-371.
284. Thakker RV. The molecular genetics of the multiple endocrine neoplasia syndromes. *Clin Endocrinol (Oxf).* 1993;38(1):1-14.
285. Brandi ML, Gagel RF, Angeli A, Bilezikian JP, Beck-Peccoz P, Bordi C, Conte-Devolx B, Falchetti A, Gheri RG, Libroia A, Lips CJ, Lombardi G, Mannelli M, Pacini F, Ponder BA, Raue F, Skogseid B, Tamburrano G, Thakker RV, Thompson NW, Tomassetti P, Tonelli F, Wells SA, Jr., Marx SJ. Guidelines for diagnosis and therapy of MEN type 1 and type 2. *J Clin Endocrinol Metab.* 2001;86(12):5658-5671.
286. Larsson C, Skogseid B, Oberg K, Nakamura Y, Nordenskjold M. Multiple endocrine neoplasia type 1 gene maps to chromosome 11 and is lost in insulinoma. *Nature.* 1988;332(6159):85-87.
287. Lemmens I, Van de Ven WJ, Kas K, Zhang CX, Giraud S, Wautot V, Buisson N, De WK, Salandre J, Lenoir G, Pugeat M, Calender A, Parente F, Quincey D, Gaudray P, De Wit MJ, Lips CJ, Hoppener JW, Khodaei S, Grant AL, Weber G, Kytola S, Teh BT, Farnebo F, Thakker RV, . Identification of the multiple endocrine neoplasia type 1 (*MEN1*) gene. The European Consortium on MEN1. *Hum Mol Genet.* 1997;6(7):1177-1183.
288. Bassett JH, Forbes SA, Pannett AA, Lloyd SE, Christie PT, Wooding C, Harding B, Besser GM, Edwards CR, Monson JP, Sampson J, Wass JA, Wheeler MH, Thakker RV. Characterization of mutations in patients with multiple endocrine neoplasia type 1. *Am J Hum Genet.* 1998;62(2):232-244.
289. Pannett AA, Thakker RV. Somatic mutations in MEN type 1 tumors, consistent with the Knudson "two-hit" hypothesis. *J Clin Endocrinol Metab.* 2001;86(9):4371-4374.
290. Knudson AG, Jr. Mutation and cancer: statistical study of retinoblastoma. *Proc Natl Acad Sci U S A.* 1971;68(4):820-823.
291. Heppner C, Kester MB, Agarwal SK, Debelenko LV, Emmert-Buck MR, Guru SC, Manickam P, Olufemi SE, Skarulis MC, Doppman JL, Alexander RH, Kim YS, Saggar SK, Lubensky IA, Zhuang Z, Liotta LA, Chandrasekharappa SC, Collins FS, Spiegel AM, Burns AL, Marx SJ. Somatic mutation of the *MEN1* gene in parathyroid tumours. *Nat Genet.* 1997;16(4):375-378.

292. Farnebo F, Teh BT, Kytola S, Svensson A, Phelan C, Sandelin K, Thompson NW, Hoog A, Weber G, Farnebo LO, Larsson C. Alterations of the *MEN1* gene in sporadic parathyroid tumors. *J Clin Endocrinol Metab.* 1998;83(8):2627-2630.
293. Carling T, Correa P, Hessman O, Hedberg J, Skogseid B, Lindberg D, Rastad J, Westin G, Akerstrom G. Parathyroid *MEN1* gene mutations in relation to clinical characteristics of nonfamilial primary hyperparathyroidism. *J Clin Endocrinol Metab.* 1998;83(8):2960-2963.
294. Shan L, Nakamura Y, Nakamura M, Yokoi T, Tsujimoto M, Arima R, Kameya T, Kakudo K. Somatic mutations of multiple endocrine neoplasia type 1 gene in the sporadic endocrine tumors. *Lab Invest.* 1998;78(4):471-475.
295. Hessman O, Lindberg D, Skogseid B, Carling T, Hellman P, Rastad J, Akerstrom G, Westin G. Mutation of the multiple endocrine neoplasia type 1 gene in nonfamilial, malignant tumors of the endocrine pancreas. *Cancer Res.* 1998;58(3):377-379.
296. Wang EH, Ebrahimi SA, Wu AY, Kashefi C, Passaro E Jr, Sawicki MP. Mutation of the MENIN gene in sporadic pancreatic endocrine tumors. *Cancer Res.* 1998;58(19):4417-4420.
297. Mailman MD, Muscarella P, Schirmer WJ, Ellison EC, O'Dorisio TM, Prior TW. Identification of *MEN1* mutations in sporadic enteropancreatic neuroendocrine tumors by analysis of paraffin-embedded tissue. *Clin Chem.* 1999;45(1):29-34.
298. Fujii T, Kawai T, Saito K, Hishima T, Hayashi Y, Imura J, Hironaka M, Hosoya Y, Koike M, Fukayama M. *MEN1* gene mutations in sporadic neuroendocrine tumors of foregut derivation. *Pathol Int.* 1999;49(11):968-973.
299. Cupisti K, Hoppner W, Dotzenrath C, Simon D, Berndt I, Roher HD, Goretzki PE. Lack of *MEN1* gene mutations in 27 sporadic insulinomas. *Eur J Clin Invest.* 2000;30(4):325-329.
300. Prezant TR, Levine J, Melmed S. Molecular characterization of the *Men1* tumor suppressor gene in sporadic pituitary tumors. *J Clin Endocrinol Metab.* 1998;83(4):1388-1391.
301. Farrell WE, Simpson DJ, Bicknell J, Magnay JL, Kyrodimou E, Thakker RV, Clayton RN. Sequence analysis and transcript expression of the *MEN1* gene in sporadic pituitary tumours. *Br J Cancer.* 1999;80(1-2):44-50.
302. Fukino K, Kitamura Y, Sanno N, Teramoto A, Emi M. Analysis of the *MEN1* gene in sporadic pituitary adenomas from Japanese patients. *Cancer Lett.* 1999;144(1):85-92.
303. Poncin J, Stevenaert A, Beckers A. Somatic *MEN1* gene mutation does not contribute significantly to sporadic pituitary tumorigenesis. *Eur J Endocrinol.* 1999;140(6):573-576.
304. Bergman L, Boothroyd C, Palmer J, Grimmond S, Walters M, Teh B, Shepherd J, Hartley L, Hayward N. Identification of somatic mutations of the *MEN1* gene in sporadic endocrine tumours. *Br J Cancer.* 2000;83(8):1003-1008.

305. Evans CO, Brown MR, Parks JS, Oyesiku NM. Screening for *MEN1* tumor suppressor gene mutations in sporadic pituitary tumors. *J Endocrinol Invest.* 2000;23(5):304-309.
306. Wrocklage C, Gold H, Hackl W, Buchfelder M, Fahlbusch R, Paulus W. Increased menin expression in sporadic pituitary adenomas. *Clin Endocrinol (Oxf).* 2002;56(5):589-594.
307. La P, Desmond A, Hou Z, Silva AC, Schnepp RW, Hua X. Tumor suppressor menin: the essential role of nuclear localization signal domains in coordinating gene expression. *Oncogene.* 2006;25(25):3537-3546.
308. Zetoune AB, Fontaniere S, Magnin D, Anczukow O, Buisson M, Zhang CX, Mazoyer S. Comparison of nonsense-mediated mRNA decay efficiency in various murine tissues. *BMC Genet.* 2008;9:83.
309. Luzi E, Marini F, Tognarini I, Carbonell SS, Galli G, Falchetti A, Brandi ML. Ribozyme-mediated compensatory induction of menin-oncosuppressor function in primary fibroblasts from MEN1 patients. *Cancer Gene Ther.* 2010;17(11):814-825.
310. Turner JJ, Leotlela PD, Pannett AA, Forbes SA, Bassett JH, Harding B, Christie PT, Bowen-Jones D, Ellard S, Hattersley A, Jackson CE, Pope R, Quarrell OW, Trembath R, Thakker RV. Frequent occurrence of an intron 4 mutation in multiple endocrine neoplasia type 1. *J Clin Endocrinol Metab.* 2002;87(6):2688-2693.
311. Agarwal SK, Guru SC, Heppner C, Erdos MR, Collins RM, Park SY, Saggar S, Chandrasekharappa SC, Collins FS, Spiegel AM, Marx SJ, Burns AL. Menin interacts with the AP1 transcription factor JunD and represses JunD-activated transcription. *Cell.* 1999;96(1):143-152.
312. Yaguchi H, Ohkura N, Takahashi M, Nagamura Y, Kitabayashi I, Tsukada T. Menin missense mutants associated with multiple endocrine neoplasia type 1 are rapidly degraded via the ubiquitin-proteasome pathway. *Mol Cell Biol.* 2004;24(15):6569-6580.
313. Crabtree JS, Scacheri PC, Ward JM, Garrett-Beal L, Emmert-Buck MR, Edgemon KA, Lorang D, Libutti SK, Chandrasekharappa SC, Marx SJ, Spiegel AM, Collins FS. A mouse model of multiple endocrine neoplasia, type 1, develops multiple endocrine tumors. *Proc Natl Acad Sci U S A.* 2001;98(3):1118-1123.
314. Crabtree JS, Scacheri PC, Ward JM, McNally SR, Swain GP, Montagna C, Hager JH, Hanahan D, Edlund H, Magnuson MA, Garrett-Beal L, Burns AL, Ried T, Chandrasekharappa SC, Marx SJ, Spiegel AM, Collins FS. Of mice and MEN1: Insulinomas in a conditional mouse knockout. *Mol Cell Biol.* 2003;23(17):6075-6085.
315. Bertolino P, Tong WM, Galendo D, Wang ZQ, Zhang CX. Heterozygous Men1 mutant mice develop a range of endocrine tumors mimicking multiple endocrine neoplasia type 1. *Mol Endocrinol.* 2003;17(9):1880-1892.

316. Luzi E, Marini F, Giusti F, Galli G, Cavalli L, Brandi ML. The negative feedback-loop between the oncomir Mir-24-1 and menin modulates the Men1 tumorigenesis by mimicking the "Knudson's second hit". *PLoS One.* 2012;7(6):e39767.
317. Guru SC, Goldsmith PK, Burns AL, Marx SJ, Spiegel AM, Collins FS, Chandrasekharappa SC. Menin, the product of the *MEN1* gene, is a nuclear protein. *Proc Natl Acad Sci U S A.* 1998;95(4):1630-1634.
318. Guru SC, Crabtree JS, Brown KD, Dunn KJ, Manickam P, Prasad NB, Wangsa D, Burns AL, Spiegel AM, Marx SJ, Pavan WJ, Collins FS, Chandrasekharappa SC. Isolation, genomic organization, and expression analysis of *Men1*, the murine homolog of the *MEN1* gene. *Mamm Genome.* 1999;10(6):592-596.
319. Huang SC, Zhuang Z, Weil RJ, Pack S, Wang C, Krutzsch HC, Pham TA, Lubensky IA. Nuclear/cytoplasmic localization of the multiple endocrine neoplasia type 1 gene product, menin. *Lab Invest.* 1999;79(3):301-310.
320. Kaji H, Canaff L, Goltzman D, Hendy GN. Cell cycle regulation of menin expression. *Cancer Res.* 1999;59(20):5097-5101.
321. Schnepp RW, Mao H, Sykes SM, Zong WX, Silva A, La P, Hua X. Menin induces apoptosis in murine embryonic fibroblasts. *J Biol Chem.* 2004;279(11):10685-10691.
322. Milne TA, Hughes CM, Lloyd R, Yang Z, Rozenblatt-Rosen O, Dou Y, Schnepp RW, Krankel C, Livolsi VA, Gibbs D, Hua X, Roeder RG, Meyerson M, Hess JL. Menin and MLL cooperatively regulate expression of cyclin-dependent kinase inhibitors. *Proc Natl Acad Sci U S A.* 2005;102(3):749-754.
323. Taguchi R, Yamada M, Horiguchi K, Tomaru T, Ozawa A, Shibusawa N, Hashimoto K, Okada S, Satoh T, Mori M. Haploinsufficient and predominant expression of multiple endocrine neoplasia type 1 (MEN1)-related genes, *MLL, p27*(*Kip1*) and *p18*(*Ink4C*) in endocrine organs. *Biochem Biophys Res Commun.* 2011.
324. Chen YX, Yan J, Keeshan K, Tubbs AT, Wang H, Silva A, Brown EJ, Hess JL, Pear WS, Hua X. The tumor suppressor menin regulates hematopoiesis and myeloid transformation by influencing *Hox* gene expression. *Proc Natl Acad Sci U S A.* 2006;103(4):1018-1023.
325. Wu T, Hua X. Menin represses tumorigenesis via repressing cell proliferation. *Am J Cancer Res.* 2011;1(6):726-739.
326. Gao SB, Feng ZJ, Xu B, Wu Y, Yin P, Yang Y, Hua X, Jin GH. Suppression of lung adenocarcinoma through menin and polycomb gene-mediated repression of growth factor pleiotrophin. *Oncogene.* 2009;28(46):4095-4104.
327. Lacerte A, Lee EH, Reynaud R, Canaff L, De GC, Devost D, Ali S, Hendy GN, Lebrun JJ. Activin inhibits pituitary prolactin expression and cell growth through Smads, Pit-1 and menin. *Mol Endocrinol.* 2004;18(6):1558-1569.
328. Vasilev V, Daly AF, Petrossians P, Zacharieva S, Beckers A. Familial pituitary tumor syndromes. *Endocr Pract.* 2011;17 Suppl 3:41-46.

329. Kaji H, Canaff L, Lebrun JJ, Goltzman D, Hendy GN. Inactivation of menin, a Smad3-interacting protein, blocks transforming growth factor type beta signaling. *Proc Natl Acad Sci U S A.* 2001;98(7):3837-3842.
330. Ikeo Y, Yumita W, Sakurai A, Hashizume K. JunD-menin interaction regulates c-Jun-mediated AP-1 transactivation. *Endocr J.* 2004;51(3):333-342.
331. Heppner C, Bilimoria KY, Agarwal SK, Kester M, Whitty LJ, Guru SC, Chandrasekharappa SC, Collins FS, Spiegel AM, Marx SJ, Burns AL. The tumor suppressor protein menin interacts with NF-kappaB proteins and inhibits NF-kappaB-mediated transactivation. *Oncogene.* 2001;20(36):4917-4925.
332. Thevenon J, Bourredjem A, Faivre L, Cardot-Bauters C, Calender A, Murat A, Giraud S, Niccoli P, Odou MF, Borson-Chazot F, Barlier A, Lombard-Bohas C, Clauser E, Tabarin A, Parfait B, Chabre O, Castermans E, Beckers A, Ruszniewski P, Le BM, Delemer B, Bouchard P, Guilhem I, Rohmer V, Goichot B, Caron P, Baudin E, Chanson P, Groussin L, Du BH, Weryha G, Lecomte P, Penfornis A, Bihan H, Archambeaud F, Kerlan V, Duron F, Kuhn JM, Verges B, Rodier M, Renard M, Sadoul JL, Binquet C, Goudet P. Higher risk of death among MEN1 patients with mutations in the JunD interacting domain: a Groupe d'etude des Tumeurs Endocrines (GTE) cohort study. *Hum Mol Genet.* 2013;22(10):1940-1948.
333. Dreijerink KM, Varier RA, van BO, Jeninga EH, Hoppener JW, Lips CJ, Kummer JA, Kalkhoven E, Timmers HT. The multiple endocrine neoplasia type 1 (MEN1) tumor suppressor regulates peroxisome proliferator-activated receptor gamma-dependent adipocyte differentiation. *Mol Cell Biol.* 2009;29(18):5060-5069.
334. Dreijerink KM, Varier RA, van NR, Broekhuizen R, Valk GD, van der Wal JE, Lips CJ, Kummer JA, Timmers HT. Regulation of vitamin D receptor function in MEN1-related parathyroid adenomas. *Mol Cell Endocrinol.* 2009;313(1-2):1-8.
335. La P, Schnepp RW, Petersen D, Silva C, Hua X. Tumor suppressor menin regulates expression of insulin-like growth factor binding protein 2. *Endocrinology.* 2004;145(7):3443-3450.
336. Fontaniere S, Tost J, Wierinckx A, Lachuer J, Lu J, Hussein N, Busato F, Gut I, Wang ZQ, Zhang CX. Gene expression profiling in insulinomas of Men1 beta-cell mutant mice reveals early genetic and epigenetic events involved in pancreatic beta-cell tumorigenesis. *Endocr Relat Cancer.* 2006;13(4):1223-1236.
337. Cao Y, Liu R, Jiang X, Lu J, Jiang J, Zhang C, Li X, Ning G. Nuclear-cytoplasmic shuttling of menin regulates nuclear translocation of {beta}-catenin. *Mol Cell Biol.* 2009;29(20):5477-5487.
338. Sukhodolets KE, Hickman AB, Agarwal SK, Sukhodolets MV, Obungu VH, Novotny EA, Crabtree JS, Chandrasekharappa SC, Collins FS, Spiegel AM, Burns AL, Marx SJ. The 32-kilodalton subunit of replication protein A interacts with menin, the product of the *MEN1* tumor suppressor gene. *Mol Cell Biol.* 2003;23(2):493-509.

339. Jin S, Mao H, Schnepp RW, Sykes SM, Silva AC, D'Andrea AD, Hua X. Menin associates with FANCD2, a protein involved in repair of DNA damage. *Cancer Res.* 2003;63(14):4204-4210.
340. Hashimoto M, Kyo S, Hua X, Tahara H, Nakajima M, Takakura M, Sakaguchi J, Maida Y, Nakamura M, Ikoma T, Mizumoto Y, Inoue M. Role of menin in the regulation of telomerase activity in normal and cancer cells. *Int J Oncol.* 2008;33(2):333-340.
341. Obungu VH, Lee BA, Agarwal SK, Chandrasekharapa SC, Adelstein RS, Marx SJ. Menin, a tumor suppressor, associates with nonmuscle myosin II-A heavy chain. *Oncogene.* 2003;22(41):6347-6358.
342. Lopez-Egido J, Cunningham J, Berg M, Oberg K, Bongcam-Rudloff E, Gobl A. Menin's interaction with glial fibrillary acidic protein and vimentin suggests a role for the intermediate filament network in regulating menin activity. *Exp Cell Res.* 2002;278(2):175-183.
343. Bertolino P, Radovanovic I, Casse H, Aguzzi A, Wang ZQ, Zhang CX. Genetic ablation of the tumor suppressor menin causes lethality at mid-gestation with defects in multiple organs. *Mech Dev.* 2003;120(5):549-560.
344. Verges B, Boureille F, Goudet P, Murat A, Beckers A, Sassolas G, Cougard P, Chambe B, Montvernay C, Calender A. Pituitary disease in MEN type 1 (MEN1): data from the France-Belgium MEN1 multicenter study. *J Clin Endocrinol Metab.* 2002;87(2):457-465.
345. Goudet P, Bonithon-Kopp C, Murat A, Ruszniewski P, Niccoli P, Menegaux F, Chabrier G, Borson-Chazot F, Tabarin A, Bouchard P, Cadiot G, Beckers A, Guilhem I, Chabre O, Caron P, Du BH, Verges B, Cardot-Bauters C. Gender-related differences in MEN1 lesion occurrence and diagnosis: a cohort study of 734 cases from the Groupe d'etude des Tumeurs Endocrines. *Eur J Endocrinol.* 2011;165(1):97-105.
346. Horvath A, Stratakis CA. Clinical and molecular genetics of acromegaly: MEN1, Carney complex, McCune-Albright syndrome, familial acromegaly and genetic defects in sporadic tumors. *Rev Endocr Metab Disord.* 2008;9(1):1-11.
347. Goudet P, Dalac A, Le BM, Cardot-Bauters C, Niccoli P, Levy-Bohbot N, Du BH, Bertagna X, Ruszniewski P, Borson-Chazot F, Verges B, Sadoul JL, Menegaux F, Tabarin A, Kuhn JM, d'Anella P, Chabre O, Christin-Maitre S, Cadiot G, Binquet C, Delemer B. MEN1 Disease Occurring Before 21 Years Old: A 160-Patient Cohort Study From the Groupe d'etude des Tumeurs Endocrines. *J Clin Endocrinol Metab.* 2015;100(4):1568-1577.
348. Trump D, Farren B, Wooding C, Pang JT, Besser GM, Buchanan KD, Edwards CR, Heath DA, Jackson CE, Jansen S, Lips K, Monson JP, O'Halloran D, Sampson J, Shalet SM, Wheeler MH, Zink A, Thakker RV. Clinical studies of multiple endocrine neoplasia type 1 (MEN1). *QJM.* 1996;89(9):653-669.

349. Pieterman CR, Schreinemakers JM, Koppeschaar HP, Vriens MR, Rinkes IH, Zonnenberg BA, van der Luijt RB, Valk GD. Multiple endocrine neoplasia type 1 (MEN1): its manifestations and effect of genetic screening on clinical outcome. *Clin Endocrinol (Oxf).* 2009;70(4):575-581.
350. Marini F, Falchetti A, Del MF, Carbonell SS, Gozzini A, Luzi E, Brandi ML. Multiple endocrine neoplasia type 1. *Orphanet J Rare Dis.* 2006;1:38.
351. Ghazi AA, Dezfooli AA, Mohamadi F, Yousefi SV, Amirbaigloo A, Ghazi S, Pourafkari M, Berney D, Ellard S, Grossman AB. Cushing syndrome secondary to a thymic carcinoid tumor due to multiple endocrine neoplasia type 1. *Endocr Pract.* 2011;17(4):e92-e96.
352. Dean PG, van Heerden JA, Farley DR, Thompson GB, Grant CS, Harmsen WS, Ilstrup DM. Are patients with multiple endocrine neoplasia type I prone to premature death? *World J Surg.* 2000;24(11):1437-1441.
353. Machens A, Schaaf L, Karges W, Frank-Raue K, Bartsch DK, Rothmund M, Schneyer U, Goretzki P, Raue F, Dralle H. Age-related penetrance of endocrine tumours in multiple endocrine neoplasia type 1 (MEN1): a multicentre study of 258 gene carriers. *Clin Endocrinol (Oxf).* 2007;67(4):613-622.
354. Jamilloux Y, Favier J, Pertuit M, Delage-Corre M, Lopez S, Teissier MP, Mathonnet M, Galinat S, Barlier A, Archambeaud F. A MEN1 syndrome with a paraganglioma. *Eur J Hum Genet.* 2014;22(2):283-285.
355. Dreijerink KM, Goudet P, Burgess JR, Valk GD. Breast-cancer predisposition in multiple endocrine neoplasia type 1. *N Engl J Med.* 2014;371(6):583-584.
356. Farrell WE, Azevedo MF, Batista DL, Smith A, Bourdeau I, Horvath A, Boguszewski M, Quezado M, Stratakis CA. Unique gene expression profile associated with an early-onset multiple endocrine neoplasia (MEN1)-associated pituitary adenoma. *J Clin Endocrinol Metab.* 2011;96(11):E1905-E1914.
357. Benito M, Asa SL, Livolsi VA, West VA, Snyder PJ. Gonadotroph tumor associated with multiple endocrine neoplasia type 1. *J Clin Endocrinol Metab.* 2005;90(1):570-574.
358. Trouillas J, Labat-Moleur F, Sturm N, Kujas M, Heymann MF, Figarella-Branger D, Patey M, Mazucca M, Decullier E, Verges B, Chabre O, Calender A. Pituitary tumors and hyperplasia in multiple endocrine neoplasia type 1 syndrome (MEN1): a case-control study in a series of 77 patients versus 2509 non-MEN1 patients. *Am J Surg Pathol.* 2008;32(4):534-543.
359. Capella C, Riva C, Leutner M, La RS. Pituitary lesions in multiple endocrine neoplasia syndrome (MENS) type 1. *Pathol Res Pract.* 1995;191(4):345-347.
360. Piotrowska K, Pellegata NS, Rosemann M, Fritz A, Graw J, Atkinson MJ. Mapping of a novel MEN-like syndrome locus to rat chromosome 4. *Mamm Genome.* 2004;15(2):135-141.
361. Marinoni I, Pellegata NS. *p27kip1*: a new multiple endocrine neoplasia gene? *Neuroendocrinology.* 2011;93(1):19-28.

362. Xekouki P, Azevedo M, Stratakis CA. Anterior pituitary adenomas: inherited syndromes, novel genes and molecular pathways. *Expert Rev Endocrinol Metab.* 2010;5(5):697-709.
363. Ponce-Castaneda MV, Lee MH, Latres E, Polyak K, Lacombe L, Montgomery K, Mathew S, Krauter K, Sheinfeld J, Massague J, . *p27Kip1*: chromosomal mapping to 12p12-12p13.1 and absence of mutations in human tumors. *Cancer Res.* 1995;55(6):1211-1214.
364. Ozawa A, Agarwal SK, Mateo CM, Burns AL, Rice TS, Kennedy PA, Quigley CM, Simonds WF, Weinstein LS, Chandrasekharappa SC, Collins FS, Spiegel AM, Marx SJ. The parathyroid/pituitary variant of multiple endocrine neoplasia type 1 usually has causes other than *p27Kip1* mutations. *J Clin Endocrinol Metab.* 2007;92(5):1948-1951.
365. Igreja S, Chahal HS, Akker SA, Gueorguiev M, Popovic V, Damjanovic S, Burman P, Wass JA, Quinton R, Grossman AB, Korbonits M. Assessment of *p27* (cyclin-dependent kinase inhibitor 1B) and aryl hydrocarbon receptor-interacting protein (*AIP*) genes in multiple endocrine neoplasia (MEN1) syndrome patients without any detectable MEN1 gene mutations. *Clin Endocrinol (Oxf).* 2009;70(2):259-264.
366. Owens M, Stals K, Ellard S, Vaidya B. Germline mutations in the *CDKN1B* gene encoding p27 Kip1 are a rare cause of multiple endocrine neoplasia type 1. *Clin Endocrinol (Oxf).* 2009;70(3):499-500.
367. Georgitsi M. MEN-4 and other multiple endocrine neoplasias due to cyclin-dependent kinase inhibitors (*p27*(*Kip1*) and *p18*(*INK4C*)) mutations. *Best Pract Res Clin Endocrinol Metab.* 2010;24(3):425-437.
368. Polyak K, Lee MH, Erdjument-Bromage H, Koff A, Roberts JM, Tempst P, Massague J. Cloning of *p27Kip1*, a cyclin-dependent kinase inhibitor and a potential mediator of extracellular antimitogenic signals. *Cell.* 1994;78(1):59-66.
369. Fero ML, Randel E, Gurley KE, Roberts JM, Kemp CJ. The murine gene *p27Kip1* is haplo-insufficient for tumour suppression. *Nature.* 1998;396(6707):177-180.
370. Polyak K, Kato JY, Solomon MJ, Sherr CJ, Massague J, Roberts JM, Koff A. p27Kip1, a cyclin-Cdk inhibitor, links transforming growth factor-beta and contact inhibition to cell cycle arrest. *Genes Dev.* 1994;8(1):9-22.
371. Chu IM, Hengst L, Slingerland JM. The Cdk inhibitor p27 in human cancer: prognostic potential and relevance to anticancer therapy. *Nat Rev Cancer.* 2008;8(4):253-267.
372. Hengst L, Reed SI. Translational control of p27Kip1 accumulation during the cell cycle. *Science.* 1996;271(5257):1861-1864.
373. Moeller SJ, Head ED, Sheaff RJ. p27Kip1 inhibition of GRB2-SOS formation can regulate Ras activation. *Mol Cell Biol.* 2003;23(11):3735-3752.
374. Tsvetkov LM, Yeh KH, Lee SJ, Sun H, Zhang H. p27(Kip1) ubiquitination and degradation is regulated by the SCF(Skp2) complex through phosphorylated Thr187 in p27. *Curr Biol.* 1999;9(12):661-664.

375. Besson A, Hwang HC, Cicero S, Donovan SL, Gurian-West M, Johnson D, Clurman BE, Dyer MA, Roberts JM. Discovery of an oncogenic activity in p27Kip1 that causes stem cell expansion and a multiple tumor phenotype. *Genes Dev.* 2007;21(14):1731-1746.
376. Kiyokawa H, Kineman RD, Manova-Todorova KO, Soares VC, Hoffman ES, Ono M, Khanam D, Hayday AC, Frohman LA, Koff A. Enhanced growth of mice lacking the cyclin-dependent kinase inhibitor function of p27(Kip1). *Cell.* 1996;85(5):721-732.
377. Nakayama K, Ishida N, Shirane M, Inomata A, Inoue T, Shishido N, Horii I, Loh DY, Nakayama K. Mice lacking p27(Kip1) display increased body size, multiple organ hyperplasia, retinal dysplasia, and pituitary tumors. *Cell.* 1996;85(5):707-720.
378. Fero ML, Rivkin M, Tasch M, Porter P, Carow CE, Firpo E, Polyak K, Tsai LH, Broudy V, Perlmutter RM, Kaushansky K, Roberts JM. A syndrome of multiorgan hyperplasia with features of gigantism, tumorigenesis, and female sterility in p27(Kip1)-deficient mice. *Cell.* 1996;85(5):733-744.
379. Dahia PL, Aguiar RC, Honegger J, Fahlbush R, Jordan S, Lowe DG, Lu X, Clayton RN, Besser GM, Grossman AB. Mutation and expression analysis of the *p27/kip1* gene in corticotrophin-secreting tumours. *Oncogene.* 1998;16(1):69-76.
380. Costa-Guda J, Marinoni I, Molatore S, Pellegata NS, Arnold A. Somatic mutation and germline sequence abnormalities in *CDKN1B*, encoding p27Kip1, in sporadic parathyroid adenomas. *J Clin Endocrinol Metab.* 2011;96(4):E701-E706.
381. Lee M, Pellegata NS. Multiple endocrine neoplasia syndromes associated with mutation of *p27*. *J Endocrinol Invest.* 2013;36(9):781-787.
382. Catzavelos C, Bhattacharya N, Ung YC, Wilson JA, Roncari L, Sandhu C, Shaw P, Yeger H, Morava-Protzner I, Kapusta L, Franssen E, Pritchard KI, Slingerland JM. Decreased levels of the cell-cycle inhibitor p27Kip1 protein: prognostic implications in primary breast cancer. *Nat Med.* 1997;3(2):227-230.
383. Tan P, Cady B, Wanner M, Worland P, Cukor B, Magi-Galluzzi C, Lavin P, Draetta G, Pagano M, Loda M. The cell cycle inhibitor p27 is an independent prognostic marker in small (T1a,b) invasive breast carcinomas. *Cancer Res.* 1997;57(7):1259-1263.
384. Esposito V, Baldi A, De LA, Groger AM, Loda M, Giordano GG, Caputi M, Baldi F, Pagano M, Giordano A. Prognostic role of the cyclin-dependent kinase inhibitor p27 in non-small cell lung cancer. *Cancer Res.* 1997;57(16):3381-3385.
385. Mori M, Mimori K, Shiraishi T, Tanaka S, Ueo H, Sugimachi K, Akiyoshi T. p27 expression and gastric carcinoma. *Nat Med.* 1997;3(6):593.
386. Porter PL, Malone KE, Heagerty PJ, Alexander GM, Gatti LA, Firpo EJ, Daling JR, Roberts JM. Expression of cell-cycle regulators p27Kip1 and cyclin E, alone and in combination, correlate with survival in young breast cancer patients. *Nat Med.* 1997;3(2):222-225.

387. Canavese G, Azzoni C, Pizzi S, Corleto VD, Pasquali C, Davoli C, Crafa P, Delle FG, Bordi C. p27: a potential main inhibitor of cell proliferation in digestive endocrine tumors but not a marker of benign behavior. *Hum Pathol.* 2001;32(10):1094-1101.
388. Pellegata NS, Quintanilla-Martinez L, Keller G, Liyanarachchi S, Hofler H, Atkinson MJ, Fend F. Human pheochromocytomas show reduced p27Kip1 expression that is not associated with somatic gene mutations and rarely with deletions. *Virchows Arch.* 2007;451(1):37-46.
389. Grabowski P, Schrader J, Wagner J, Horsch D, Arnold R, Arnold CN, Georgieva I, Stein H, Zeitz M, Daniel PT, Sturm I. Loss of nuclear p27 expression and its prognostic role in relation to *cyclin E* and *p53* mutation in gastroenteropancreatic neuroendocrine tumors. *Clin Cancer Res.* 2008;14(22):7378-7384.
390. Georgitsi M, Raitila A, Karhu A, van der Luijt RB, Aalfs CM, Sane T, Vierimaa O, Makinen MJ, Tuppurainen K, Paschke R, Gimm O, Koch CA, Gundogdu S, Lucassen A, Tischkowitz M, Izatt L, Aylwin S, Bano G, Hodgson S, De ME, Launonen V, Vahteristo P, Aaltonen LA. Germline *CDKN1B/p27Kip1* mutation in multiple endocrine neoplasia. *J Clin Endocrinol Metab.* 2007;92(8):3321-3325.
391. Agarwal SK, Mateo CM, Marx SJ. Rare germline mutations in cyclin-dependent kinase inhibitor genes in multiple endocrine neoplasia type 1 and related states. *J Clin Endocrinol Metab.* 2009;94(5):1826-1834.
392. Molatore S, Marinoni I, Lee M, Pulz E, Ambrosio MR, degli Uberti EC, Zatelli MC, Pellegata NS. A novel germline *CDKN1B* mutation causing multiple endocrine tumors: clinical, genetic and functional characterization. *Hum Mutat.* 2010;31(11):E1825-E1835.
393. Belar O, De la Hoz C, Perez-Nanclares G, Castano L, Gaztambide S. Novel mutations in *MEN1*, *CDKN1B* and *AIP* genes in patients with multiple endocrine neoplasia type 1 syndrome in Spain. *Clin Endocrinol (Oxf).* 2012;76(5):719-724.
394. Malanga D, De GS, Riccardi M, Scrima M, De MC, Robledo M, Viglietto G. Functional characterization of a rare germline mutation in the gene encoding the cyclin-dependent kinase inhibitor *p27Kip1* (*CDKN1B*) in a Spanish patient with multiple endocrine neoplasia (MEN)-like phenotype. *Eur J Endocrinol.* 2012;166(3):551-560.
395. Occhi G, Regazzo D, Trivellin G, Boaretto F, Ciato D, Bobisse S, Ferasin S, Cetani F, Pardi E, Korbonits M, Pellegata NS, Sidarovich V, Quattrone A, Opocher G, Mantero F, Scaroni C. A novel mutation in the upstream open reading frame of the *CDKN1B* gene causes a MEN4 phenotype. *PLoS Genet.* 2013;9(3):e1003350.
396. Tonelli F, Giudici F, Giusti F, Marini F, Cianferotti L, Nesi G, Brandi ML. A heterozygous frameshift mutation in exon 1 of *CDKN1B* gene in a patient affected by MEN4 syndrome. *Eur J Endocrinol.* 2014;171(2):K7-K17.
397. Pardi E, Mariotti S, Pellegata NS, Benfini K, Borsari S, Saponaro F, Torregrossa L, Cappai A, Satta C, Mastinu M, Marcocci C, Cetani F. Functional

characterization of a *CDKN1B* mutation in a Sardinian kindred with multiple endocrine neoplasia type 4 (MEN4). *Endocr Connect.* 2015;4(1):1-8.

398. Sambugaro S, Di RM, Ambrosio MR, Pellegata NS, Bellio M, Guerra A, Buratto M, Foschini MP, Tagliati F, degli UE, Zatelli MC. Early onset acromegaly associated with a novel deletion in *CDKN1B* 5'UTR region. *Endocrine.* 2015;49(1):58-64.
399. Tichomirowa MA, Lee M, Barlier A, Daly AF, Marinoni I, Jaffrain-Rea ML, Naves LA, Rodien P, Rohmer V, Faucz FR, Caron P, Estour B, Lecomte P, Borson-Chazot F, Penfornis A, Yaneva M, Guitelman M, Castermans E, Verhaege C, Wemeau JL, Tabarin A, Fajardo MC, Delemer B, Kerlan V, Sadoul JL, Cortet RC, Archambeaud F, Zacharieva S, Theodoropoulou M, Brue T, Enjalbert A, Bours V, Pellegata NS, Beckers A. Cyclin dependent kinase inhibitor 1B (*CDKN1B*) gene variants in *AIP* mutation-negative familial isolated pituitary adenomas (FIPA) kindreds. *Endocr Relat Cancer.* 2012;19:233-241.
400. Wildi-Runge S, Bahubeshi A, Carret A, Crevier L, Robitaille. New phenotype in the familial DICER1 tumor syndrome: pituitary blastoma presenting at age 9 months. *Endocr Rev.* 2011;32((03_MeetingAbstracts)):P1-777.
401. Slade I, Bacchelli C, Davies H, Murray A, Abbaszadeh F, Hanks S, Barfoot R, Burke A, Chisholm J, Hewitt M, Jenkinson H, King D, Morland B, Pizer B, Prescott K, Saggar A, Side L, Traunecker H, Vaidya S, Ward P, Futreal PA, Vujanic G, Nicholson AG, Sebire N, Turnbull C, Priest JR, Pritchard-Jones K, Houlston R, Stiller C, Stratton MR, Douglas J, Rahman N. DICER1 syndrome: clarifying the diagnosis, clinical features and management implications of a pleiotropic tumour predisposition syndrome. *J Med Genet.* 2011;48(4):273-278.
402. Doros L, Schultz KA, Stewart DR et al. DICER1-Related Disorders. In: Pagon RA, Adam MP, Ardinger HH et al., eds. Seattle, WA: University of Washington, Seattle; 2014.
403. Messinger YH, Stewart DR, Priest JR, Williams GM, Harris AK, Schultz KA, Yang J, Doros L, Rosenberg PS, Hill DA, Dehner LP. Pleuropulmonary blastoma: a report on 350 central pathology-confirmed pleuropulmonary blastoma cases by the International Pleuropulmonary Blastoma Registry. *Cancer.* 2015;121(2):276-285.
404. Foulkes WD, Priest JR, Duchaine TF. *DICER1*: mutations, microRNAs and mechanisms. *Nat Rev Cancer.* 2014;14(10):662-672.
405. Sahakitrungruang T, Srichomthong C, Pornkunwilai S, Amornfa J, Shuangshoti S, Kulawonganunchai S, Suphapeetiporn K, Shotelersuk V. Germline and somatic *DICER1* mutations in a pituitary blastoma causing infantile-onset Cushing's disease. *J Clin Endocrinol Metab.* 2014;99(8):E1487-E1492.
406. de KL, Plourde F, Carter MT, Hamel N, Srivastava A, Meyn MS, Arseneau J, Bouron-Dal SD, Foulkes WD. Germ-line and somatic *DICER1* mutations in a pleuropulmonary blastoma. *Pediatr Blood Cancer.* 2013;60(12):2091-2092.

407. Murray MJ, Bailey S, Raby KL, Saini HK, de KL, Burke GA, Foulkes WD, Enright AJ, Coleman N, Tischkowitz M. Serum levels of mature microRNAs in *DICER1*-mutated pleuropulmonary blastoma. *Oncogenesis.* 2014;3:e87.
408. Pugh TJ, Yu W, Yang J, Field AL, Ambrogio L, Carter SL, Cibulskis K, Giannikopoulos P, Kiezun A, Kim J, McKenna A, Nickerson E, Getz G, Hoffher S, Messinger YH, Dehner LP, Roberts CW, Rodriguez-Galindo C, Williams GM, Rossi CT, Meyerson M, Hill DA. Exome sequencing of pleuropulmonary blastoma reveals frequent biallelic loss of *TP53* and two hits in *DICER1* resulting in retention of 5p-derived miRNA hairpin loop sequences. *Oncogene.* 2014;33(45):5295-5302.
409. Wu MK, Sabbaghian N, Xu B, Addidou-Kalucki S, Bernard C, Zou D, Reeve AE, Eccles MR, Cole C, Choong CS, Charles A, Tan TY, Iglesias DM, Goodyer PR, Foulkes WD. Biallelic *DICER1* mutations occur in Wilms tumours. *J Pathol.* 2013;230(2):154-164.
410. Doros LA, Rossi CT, Yang J, Field A, Williams GM, Messinger Y, Cajaiba MM, Perlman EJ, Schultz A, Cathro HP, Legallo RD, LaFortune KA, Chikwava KR, Faria P, Geller JI, Dome JS, Mullen EA, Gratias EJ, Dehner LP, Hill DA. *DICER1* mutations in childhood cystic nephroma and its relationship to DICER1-renal sarcoma. *Mod Pathol.* 2014;27(9):1267-1280.
411. Heravi-Moussavi A, Anglesio MS, Cheng SW, Senz J, Yang W, Prentice L, Fejes AP, Chow C, Tone A, Kalloger SE, Hamel N, Roth A, Ha G, Wan AN, Maines-Bandiera S, Salamanca C, Pasini B, Clarke BA, Lee AF, Lee CH, Zhao C, Young RH, Aparicio SA, Sorensen PH, Woo MM, Boyd N, Jones SJ, Hirst M, Marra MA, Gilks B, Shah SP, Foulkes WD, Morin GB, Huntsman DG. Recurrent somatic *DICER1* mutations in nonepithelial ovarian cancers. *N Engl J Med.* 2012;366(3):234-242.
412. Tomiak E, de KL, Grynspan D, Ramphal R, Foulkes WD. *DICER1* mutations in an adolescent with cervical embryonal rhabdomyosarcoma (cERMS). *Pediatr Blood Cancer.* 2014;61(3):568-569.
413. de KL, Sabbaghian N, Druker H, Weber E, Hamel N, Miller S, Choong CS, Gottardo NG, Kees UR, Rednam SP, van Hest LP, Jongmans MC, Jhangiani S, Lupski JR, Zacharin M, Bouron-Dal SD, Huang A, Priest JR, Perry A, Mueller S, Albrecht S, Malkin D, Grundy RG, Foulkes WD. Germ-line and somatic *DICER1* mutations in pineoblastoma. *Acta Neuropathol.* 2014;128(4):583-595.
414. de KL, Sabbaghian N, Soglio DB, Guillerman RP, Park BK, Chami R, Deal CL, Priest JR, Foulkes WD. Exploring the association between *DICER1* mutations and differentiated thyroid carcinoma. *J Clin Endocrinol Metab.* 2014;99(6):E1072-E1077.
415. de Boer CM, Eini R, Gillis AM, Stoop H, Looijenga LH, White SJ. DICER1 RNase IIIb domain mutations are infrequent in testicular germ cell tumours. *BMC Res Notes.* 2012;5:569.

416. Scheithauer BW, Horvath E, Abel TW, Robital Y, Park SH, Osamura RY, Deal C, Lloyd RV, Kovacs K. Pituitary blastoma: a unique embryonal tumor. *Pituitary.* 2011.
417. Scheithauer BW, Kovacs K, Horvath E, Kim DS, Osamura RY, Ketterling RP, Lloyd RV, Kim OL. Pituitary blastoma. *Acta Neuropathol.* 2008;116(6):657-666.
418. The International Pleuropulmonary Blastoma Registry. http://www.ppbregistry.org/families/familygenetic-issues. Accessed 29/4/2014.
419. Carney JA, Gordon H, Carpenter PC, Shenoy BV, Go VL. The complex of myxomas, spotty pigmentation, and endocrine overactivity. *Medicine (Baltimore).* 1985;64(4):270-283.
420. Bertherat J. Carney complex (CNC). *Orphanet J Rare Dis.* 2006;1:21-26.
421. Stratakis CA, Kirschner LS, Carney JA. Clinical and molecular features of the Carney complex: diagnostic criteria and recommendations for patient evaluation. *J Clin Endocrinol Metab.* 2001;86(9):4041-4046.
422. Schernthaner-Reiter MH, Trivellin G, Stratakis CA. MEN1, MEN4, and Carney Complex: Pathology and Molecular Genetics. *Neuroendocrinology.* 2015.
423. Rothenbuhler A, Stratakis CA. Clinical and molecular genetics of Carney complex. *Best Pract Res Clin Endocrinol Metab.* 2010;24(3):389-399.
424. Kirschner LS, Sandrini F, Monbo J, Lin JP, Carney JA, Stratakis CA. Genetic heterogeneity and spectrum of mutations of the *PRKAR1A* gene in patients with the carney complex. *Hum Mol Genet.* 2000;9(20):3037-3046.
425. Toledo RA, Sekiya T, Horvath A, Faucz F, Fragoso MC, Longuini VC, Lourenco Jr DM, Toledo SP, Stratakis CA. Assessing the emerging oncogene protein kinase C epsilon as a candidate gene in families with Carney complex-2. *Clin Endocrinol (Oxf).* 2012;76:147-150.
426. Matyakhina L, Pack S, Kirschner LS, Pak E, Mannan P, Jaikumar J, Taymans SE, Sandrini F, Carney JA, Stratakis CA. Chromosome 2 (2p16) abnormalities in Carney complex tumours. *J Med Genet.* 2003;40(4):268-277.
427. Tasken K, Skalhegg BS, Solberg R, Andersson KB, Taylor SS, Lea T, Blomhoff HK, Jahnsen T, Hansson V. Novel isozymes of cAMP-dependent protein kinase exist in human cells due to formation of RI alpha-RI beta heterodimeric complexes. *J Biol Chem.* 1993;268(28):21276-21283.
428. Sandrini F, Stratakis C. Clinical and molecular genetics of Carney complex. *Mol Genet Metab.* 2003;78(2):83-92.
429. Cazabat L, Guillaud-Bataille M, Bertherat J, Raffin-Sanson ML. Mutations of the gene for the aryl hydrocarbon receptor-interacting protein in pituitary adenomas. *Horm Res.* 2009;71(3):132-141.
430. Stratakis CA. Mutations of the gene encoding the protein kinase A type I-alpha regulatory subunit (PRKAR1A) in patients with the "complex of spotty skin pigmentation, myxomas, endocrine overactivity, and schwannomas" (Carney complex). *Ann N Y Acad Sci.* 2002;968:3-21.

431. Groussin L, Horvath A, Jullian E, Boikos S, Rene-Corail F, Lefebvre H, Cephise-Velayoudom FL, Vantyghem MC, Chanson P, Conte-Devolx B, Lucas M, Gentil A, Malchoff CD, Tissier F, Carney JA, Bertagna X, Stratakis CA, Bertherat J. A *PRKAR1A* mutation associated with primary pigmented nodular adrenocortical disease in 12 kindreds. *J Clin Endocrinol Metab.* 2006;91(5):1943-1949.
432. Libe R, Horvath A, Vezzosi D, Fratticci A, Coste J, Perlemoine K, Ragazzon B, Guillaud-Bataille M, Groussin L, Clauser E, Raffin-Sanson ML, Siegel J, Moran J, Drori-Herishanu L, Faucz FR, Lodish M, Nesterova M, Bertagna X, Bertherat J, Stratakis CA. Frequent phosphodiesterase 11A gene (PDE11A) defects in patients with Carney complex (CNC) caused by *PRKAR1A* mutations: PDE11A may contribute to adrenal and testicular tumors in CNC as a modifier of the phenotype. *J Clin Endocrinol Metab.* 2011;96(1):E208-E214.
433. Almeida MQ, Muchow M, Boikos S, Bauer AJ, Griffin KJ, Tsang KM, Cheadle C, Watkins T, Wen F, Starost MF, Bossis I, Nesterova M, Stratakis CA. Mouse Prkar1a haploinsufficiency leads to an increase in tumors in the Trp53+/- or Rb1+/- backgrounds and chemically induced skin papillomas by dysregulation of the cell cycle and Wnt signaling. *Hum Mol Genet.* 2010;19(8):1387-1398.
434. Tsang KM, Starost MF, Nesterova M, Boikos SA, Watkins T, Almeida MQ, Harran M, Li A, Collins MT, Cheadle C, Mertz EL, Leikin S, Kirschner LS, Robey P, Stratakis CA. Alternate protein kinase A activity identifies a unique population of stromal cells in adult bone. *Proc Natl Acad Sci U S A.* 2010;107(19):8683-8688.
435. Azevedo MF, Stratakis CA. The transcriptome that mediates increased cyclic adenosine monophosphate signaling in PRKAR1A defects and other settings. *Endocr Pract.* 2011;17 Suppl 3:2-7.
436. Almeida MQ, Stratakis CA. How does cAMP/protein kinase A signaling lead to tumors in the adrenal cortex and other tissues? *Mol Cell Endocrinol.* 2011;336(1-2):162-168.
437. Iliopoulos D, Bimpaki EI, Nesterova M, Stratakis CA. MicroRNA signature of primary pigmented nodular adrenocortical disease: clinical correlations and regulation of Wnt signaling. *Cancer Res.* 2009;69(8):3278-3282.
438. Groussin L, Kirschner LS, Vincent-Dejean C, Perlemoine K, Jullian E, Delemer B, Zacharieva S, Pignatelli D, Carney JA, Luton JP, Bertagna X, Stratakis CA, Bertherat J. Molecular analysis of the cyclic AMP-dependent protein kinase A (PKA) regulatory subunit 1A (*PRKAR1A*) gene in patients with Carney complex and primary pigmented nodular adrenocortical disease (PPNAD) reveals novel mutations and clues for pathophysiology: augmented PKA signaling is associated with adrenal tumorigenesis in PPNAD. *Am J Hum Genet.* 2002;71(6):1433-1442.
439. Lania AG, Mantovani G, Ferrero S, Pellegrini C, Bondioni S, Peverelli E, Braidotti P, Locatelli M, Zavanone ML, Ferrante E, Bosari S, Beck-Peccoz P, Spada A. Proliferation of transformed somatotroph cells related to low or absent expression

of protein kinase a regulatory subunit 1A protein. *Cancer Res.* 2004;64(24):9193-9198.

440. Pack SD, Kirschner LS, Pak E, Zhuang Z, Carney JA, Stratakis CA. Genetic and histologic studies of somatomammotropic pituitary tumors in patients with the "complex of spotty skin pigmentation, myxomas, endocrine overactivity and schwannomas" (Carney complex). *J Clin Endocrinol Metab.* 2000;85(10):3860-3865.
441. Stratakis CA. Clinical genetics of multiple endocrine neoplasias, Carney complex and related syndromes. *J Endocrinol Invest.* 2001;24(5):370-383.
442. Cazabat L, Ragazzon B, Groussin L, Bertherat J. *PRKAR1A* mutations in primary pigmented nodular adrenocortical disease. *Pituitary.* 2006;9(3):211-219.
443. Stratakis CA, Sarlis N, Kirschner LS, Carney JA, Doppman JL, Nieman LK, Chrousos GP, Papanicolaou DA. Paradoxical response to dexamethasone in the diagnosis of primary pigmented nodular adrenocortical disease. *Ann Intern Med.* 1999;131(8):585-591.
444. Gaujoux S, Tissier F, Ragazzon B, Rebours V, Saloustros E, Perlemoine K, Vincent-Dejean C, Meurette G, Cassagnau E, Dousset B, Bertagna X, Horvath A, Terris B, Carney JA, Stratakis CA, Bertherat J. Pancreatic ductal and acinar cell neoplasms in Carney complex: a possible new association. *J Clin Endocrinol Metab.* 2011;96(11):E1888-E1895.
445. Stergiopoulos SG, Abu-Asab MS, Tsokos M, Stratakis CA. Pituitary pathology in Carney complex patients. *Pituitary.* 2004;7(2):73-82.
446. Dwight T, Mann K, Benn DE, Robinson BG, McKelvie P, Gill AJ, Winship I, Clifton-Bligh RJ. Familial *SDHA* mutation associated with pituitary adenoma and pheochromocytoma/paraganglioma. *J Clin Endocrinol Metab.* 2013;98(6):E1103-E1108.
447. Benn DE, Richardson AL, Marsh DJ, Robinson BG. Genetic testing in pheochromocytoma- and paraganglioma-associated syndromes. *Ann N Y Acad Sci.* 2006;1073:104-111.
448. Majumdar S, Friedrich CA, Koch CA, Megason GC, Fratkin JD, Moll GW. Compound heterozygous mutation with a novel splice donor region DNA sequence variant in the succinate dehydrogenase subunit B gene in malignant paraganglioma. *Pediatr Blood Cancer.* 2010;54(3):473-475.
449. Xekouki P, Szarek E, Bullova P, Giubellino A, Quezado M, Mastroyannis SA, Mastorakos P, Wassif CA, Raygada M, Rentia N, Dye L, Cougnoux A, Koziol D, de la Luz SM, Lyssikatos C, Belyavskaya E, Malchoff C, Moline J, Eng C, Maher LT, Pacak K, Lodish M, Stratakis CA. Pituitary adenoma with paraganglioma/pheochromocytoma (3PAs) and succinate dehydrogenase defects in human and mice. *J Clin Endocrinol Metab.* 2015;jc20144297.
450. Lopez-Jimenez E, de Campos JM, Kusak EM, Landa I, Leskela S, Montero-Conde C, Leandro-Garcia LJ, Vallejo LA, Madrigal B, Rodriguez-Antona C, Robledo M,

Cascon A. *SDHC* mutation in an elderly patient without familial antecedents. *Clin Endocrinol (Oxf).* 2008;69(6):906-910.

451. Dematti S, Branz G, Casagranda G, Recla M, Sartorato P, Zovato S, Schiavi S, Opocher G. Pituitary tumors in *SDH* mutation carriers [abstract]. *12th ENSAT Meeting* 2013;29.
452. Varsavsky M, Sebastian-Ochoa A, Torres VE. Coexistence of a pituitary macroadenoma and multicentric paraganglioma: a strange coincidence. *Endocrinol Nutr.* 2013;60(3):154-156.
453. Papathomas TG, Gaal J, Corssmit EP, Oudijk L, Korpershoek E, Heimdal K, Bayley JP, Morreau H, van DM, Papaspyrou K, Schreiner T, Hansen T, Andresen PA, Restuccia DF, van K, I, van Leenders GJ, Kros JM, Looijenga LH, Hofland LJ, Mann W, van Nederveen FH, Mete O, Asa SL, de Krijger RR, Dinjens WN. Non-pheochromocytoma (PCC)/paraganglioma (PGL) tumors in patients with succinate dehydrogenase-related PCC-PGL syndromes: a clinicopathological and molecular analysis. *Eur J Endocrinol.* 2014;170(1):1-12.
454. Saito T, Miura D, Taguchi M, Takeshita A, Miyakawa M, Takeuchi Y. Coincidence of multiple endocrine neoplasia type 2A with acromegaly. *Am J Med Sci.* 2010;340(4):329-331.
455. Naziat A, Karavitaki N, Thakker R, Ansorge O, Sadler G, Gleeson F, Cranston T, McCormack A, Grossman AB, Shine B. Confusing genes: a patient with MEN2A and Cushing's disease. *Clin Endocrinol (Oxf).* 2013;78(6):966-968.
456. Lenders JW, Duh QY, Eisenhofer G, Gimenez-Roqueplo AP, Grebe SK, Murad MH, Naruse M, Pacak K, Young WF, Jr. Pheochromocytoma and paraganglioma: an endocrine society clinical practice guideline. *J Clin Endocrinol Metab.* 2014;99(6):1915-1942.
457. Castro-Vega LJ, Buffet A, De Cubas AA, Cascon A, Menara M, Khalifa E, Amar L, Azriel S, Bourdeau I, Chabre O, Curras-Freixes M, Franco-Vidal V, Guillaud-Bataille M, Simian C, Morin A, Leton R, Gomez-Grana A, Pollard PJ, Rustin P, Robledo M, Favier J, Gimenez-Roqueplo AP. Germline mutations in *FH* confer predisposition to malignant pheochromocytomas and paragangliomas. *Hum Mol Genet.* 2014;23(9):2440-2446.
458. Niemann S, Muller U. Mutations in *SDHC* cause autosomal dominant paraganglioma, type 3. *Nat Genet.* 2000;26(3):268-270.
459. Baysal BE, Ferrell RE, Willett-Brozick JE, Lawrence EC, Myssiorek D, Bosch A, van der Mey A, Taschner PE, Rubinstein WS, Myers EN, Richard CW, III, Cornelisse CJ, Devilee P, Devlin B. Mutations in *SDHD*, a mitochondrial complex II gene, in hereditary paraganglioma. *Science.* 2000;287(5454):848-851.
460. Astuti D, Latif F, Dallol A, Dahia PL, Douglas F, George E, Skoldberg F, Husebye ES, Eng C, Maher ER. Gene mutations in the succinate dehydrogenase subunit *SDHB* cause susceptibility to familial pheochromocytoma and to familial paraganglioma. *Am J Hum Genet.* 2001;69(1):49-54.

461. Burnichon N, Briere JJ, Libe R, Vescovo L, Riviere J, Tissier F, Jouanno E, Jeunemaitre X, Benit P, Tzagoloff A, Rustin P, Bertherat J, Favier J, Gimenez-Roqueplo AP. *SDHA* is a tumor suppressor gene causing paraganglioma. *Hum Mol Genet.* 2010;19(15):3011-3020.
462. Gill AJ, Toon CW, Clarkson A, Sioson L, Chou A, Winship I, Robinson BG, Benn DE, Clifton-Bligh RJ, Dwight T. Succinate dehydrogenase deficiency is rare in pituitary adenomas. *Am J Surg Pathol.* 2014;38(4):560-566.
463. Janeway KA, Kim SY, Lodish M, Nose V, Rustin P, Gaal J, Dahia PL, Liegl B, Ball ER, Raygada M, Lai AH, Kelly L, Hornick JL, O'Sullivan M, de Krijger RR, Dinjens WN, Demetri GD, Antonescu CR, Fletcher JA, Helman L, Stratakis CA. Defects in succinate dehydrogenase in gastrointestinal stromal tumors lacking *KIT* and *PDGFRA* mutations. *Proc Natl Acad Sci U S A.* 2011;108(1):314-318.
464. McWhinney SR, Pasini B, Stratakis CA. Familial gastrointestinal stromal tumors and germ-line mutations. *N Engl J Med.* 2007;357(10):1054-1056.
465. Pasini B, McWhinney SR, Bei T, Matyakhina L, Stergiopoulos S, Muchow M, Boikos SA, Ferrando B, Pacak K, Assie G, Baudin E, Chompret A, Ellison JW, Briere JJ, Rustin P, Gimenez-Roqueplo AP, Eng C, Carney JA, Stratakis CA. Clinical and molecular genetics of patients with the Carney-Stratakis syndrome and germline mutations of the genes coding for the succinate dehydrogenase subunits *SDHB, SDHC,* and *SDHD*. *Eur J Hum Genet.* 2008;16(1):79-88.
466. Ni Y, Zbuk KM, Sadler T, Patocs A, Lobo G, Edelman E, Platzer P, Orloff MS, Waite KA, Eng C. Germline mutations and variants in the succinate dehydrogenase genes in Cowden and Cowden-like syndromes. *Am J Hum Genet.* 2008;83(2):261-268.
467. Vanharanta S, Buchta M, McWhinney SR, Virta SK, Peczkowska M, Morrison CD, Lehtonen R, Januszewicz A, Jarvinen H, Juhola M, Mecklin JP, Pukkala E, Herva R, Kiuru M, Nupponen NN, Aaltonen LA, Neumann HP, Eng C. Early-onset renal cell carcinoma as a novel extraparaganglial component of SDHB-associated heritable paraganglioma. *Am J Hum Genet.* 2004;74(1):153-159.
468. Grogan RH, Pacak K, Pasche L, Huynh TT, Greco RS. Bilateral adrenal medullary hyperplasia associated with an *SDHB* mutation. *J Clin Oncol.* 2011;29(8):e200-e202.
469. Galera-Ruiz H, Gonzalez-Campora R, Rey-Barrera M, Rollon-Mayordomo A, Garcia-Escudero A, Fernandez-Santos JM, DeMiguel M, Galera-Davidson H. W43X *SDHD* mutation in sporadic head and neck paraganglioma. *Anal Quant Cytol Histol.* 2008;30(2):119-123.
470. Schimke RN, Collins DL, Stolle CA. Paraganglioma, neuroblastoma, and a SDHB mutation: Resolution of a 30-year-old mystery. *Am J Med Genet A.* 2010;152A(6):1531-1535.
471. Bourgeron T, Rustin P, Chretien D, Birch-Machin M, Bourgeois M, Viegas-Pequignot E, Munnich A, Rotig A. Mutation of a nuclear succinate dehydrogenase

gene results in mitochondrial respiratory chain deficiency. *Nat Genet.* 1995;11(2):144-149.

472. Levitas A, Muhammad E, Harel G, Saada A, Caspi VC, Manor E, Beck JC, Sheffield V, Parvari R. Familial neonatal isolated cardiomyopathy caused by a mutation in the flavoprotein subunit of succinate dehydrogenase. *Eur J Hum Genet.* 2010;18(10):1160-1165.
473. Rustin P, Munnich A, Rotig A. Succinate dehydrogenase and human diseases: new insights into a well-known enzyme. *Eur J Hum Genet.* 2002;10(5):289-291.
474. Raimundo N, Baysal BE, Shadel GS. Revisiting the TCA cycle: signaling to tumor formation. *Trends Mol Med.* 2011;17(11):641-649.
475. Selak MA, Armour SM, MacKenzie ED, Boulahbel H, Watson DG, Mansfield KD, Pan Y, Simon MC, Thompson CB, Gottlieb E. Succinate links TCA cycle dysfunction to oncogenesis by inhibiting HIF-alpha prolyl hydroxylase. *Cancer Cell.* 2005;7(1):77-85.
476. Xekouki P, Stratakis CA. Succinate dehydrogenase (*SDHx*) mutations in pituitary tumors: could this be a new role for mitochondrial complex II and/or Krebs cycle defects? *Endocr Relat Cancer.* 2012;19(6):C33-C40.
477. Gill AJ, Hes O, Papathomas T, Sedivcova M, Tan PH, Agaimy A, Andresen PA, Kedziora A, Clarkson A, Toon CW, Sioson L, Watson N, Chou A, Paik J, Clifton-Bligh RJ, Robinson BG, Benn DE, Hills K, Maclean F, Niemeijer ND, Vlatkovic L, Hartmann A, Corssmit EP, van Leenders GJ, Przybycin C, McKenney JK, Magi-Galluzzi C, Yilmaz A, Yu D, Nicoll KD, Yong JL, Sibony M, Yakirevich E, Fleming S, Chow CW, Miettinen M, Michal M, Trpkov K. Succinate dehydrogenase (SDH)-deficient renal carcinoma: a morphologically distinct entity: a clinicopathologic series of 36 tumors from 27 patients. *Am J Surg Pathol.* 2014;38(12):1588-1602.
478. de Herder WW. Acromegaly and gigantism in the medical literature. Case descriptions in the era before and the early years after the initial publication of Pierre Marie (1886). *Pituitary.* 2009;12(3):236-244.
479. Gadelha MR, Une KN, Rohde K, Vaisman M, Kineman RD, Frohman LA. Isolated familial somatotropinomas: establishment of linkage to chromosome 11q13.1-11q13.3 and evidence for a potential second locus at chromosome 2p16-12. *J Clin Endocrinol Metab.* 2000;85(2):707-714.
480. Naves LA, Daly AF, Vanbellinghen JF, Casulari LA, Spilioti C, Magalhaes AV, Azevedo MF, Giacomini LA, Nascimento PP, Nunes RO, Rosa JW, Jaffrain-Rea ML, Bours V, Beckers A. Variable pathological and clinical features of a large Brazilian family harboring a mutation in the aryl hydrocarbon receptor-interacting protein gene. *Eur J Endocrinol.* 2007;157(4):383-391.
481. Jaffrain-Rea ML, Angelini M, Gargano D, Tichomirowa MA, Daly AF, Vanbellinghen JF, D'Innocenzo E, Barlier A, Giangaspero F, Esposito V, Ventura L, Arcella A, Theodoropoulou M, Naves LA, Fajardo C, Zacharieva S, Rohmer V, Brue T, Gulino A, Cantore G, Alesse E, Beckers A. Expression of aryl

hydrocarbon receptor (AHR) and AHR-interacting protein in pituitary adenomas: pathological and clinical implications. *Endocr Relat Cancer.* 2009;16(3):1029-1043.

482. Beckers A, Aaltonen LA, Daly AF, Karhu A. Familial isolated pituitary adenomas (FIPA) and the pituitary adenoma predisposition due to mutations in the aryl hydrocarbon receptor interacting protein (*AIP*) gene. *Endocr Rev.* 2013;34(2):239-277.
483. Frohman LA. Isolated familial somatotropinomas: clinical and genetic considerations. *Trans Am Clin Climatol Assoc.* 2003;114:165-177.
484. Daly AF, Vanbellinghen JF, Khoo SK, Jaffrain-Rea ML, Naves LA, Guitelman MA, Murat A, Emy P, Gimenez-Roqueplo AP, Tamburrano G, Raverot G, Barlier A, De HW, Penfornis A, Ciccarelli E, Estour B, Lecomte P, Gatta B, Chabre O, Sabate MI, Bertagna X, Garcia BN, Stalldecker G, Colao A, Ferolla P, Wemeau JL, Caron P, Sadoul JL, Oneto A, Archambeaud F, Calender A, Sinilnikova O, Montanana CF, Cavagnini F, Hana V, Solano A, Delettieres D, Luccio-Camelo DC, Basso A, Rohmer V, Brue T, Bours V, Teh BT, Beckers A. Aryl hydrocarbon receptor-interacting protein gene mutations in familial isolated pituitary adenomas: analysis in 73 families. *J Clin Endocrinol Metab.* 2007;92(5):1891-1896.
485. Cain J, Miljic D, Popovic V, Korbonits M. Role of the aryl hydrocarbon receptor-interacting protein in familial isolated pituitary adenoma. *Expert Rev Endocrinol Metab.* 2010;5(5):681-695.
486. Lecoq AL, Kamenicky P, Guiochon-Mantel A, Chanson P. Genetic mutations in sporadic pituitary adenomas--what to screen for? *Nat Rev Endocrinol.* 2015;11(1):43-54.
487. Khoo SK, Pendek R, Nickolov R, Luccio-Camelo DC, Newton TL, Massie A, Petillo D, Menon J, Cameron D, Teh BT, Chan SP. Genome-wide scan identifies novel modifier loci of acromegalic phenotypes for isolated familial somatotropinoma. *Endocr Relat Cancer.* 2009;16(3):1057-1063.
488. Beckers A, Daly AF. The clinical, pathological, and genetic features of familial isolated pituitary adenomas. *Eur J Endocrinol.* 2007;157(4):371-382.
489. Beckers A, Lodish M, Giampaolo T, Rostomyan L, Lee M, Faucz FR, Yuan B, Choong C, Caberg JH, Verrua E, Naves LA, Cheetham T, Young J, Lysy P, Petrossians P, Cotterill A, Shah N, Metzger D, Castermans E, Ambrosio MR, Villa C, Strebkova N, Mazerkina N, Gaillard S, Barcelos BG, Casulari LA, Neggers S, Salvatori R, Jaffrain-Rea ML, Zacharin M, Lecumberri SB, Zacharieva S, Lim EM, Mantovani G, Zatelli MC, Collins MT, Bonneville JF, Quezado M, Chittiboina P, Oldfield E, Bours V, Liu P, de Herder WW, Pellegata NS, Lupski JR, Daly AF, Stratakis CA. X-linked acrogigantism (X-LAG) syndrome: clinical profile and therapeutic responses. *Endocr Relat Cancer.* 2015;22:353-367.
490. Kamenicky P, Bouligand J, Chanson P. Gigantism, acromegaly, and *GPR101* mutations. *N Engl J Med.* 2015;372(13):1264.

491. Lee DK, Nguyen T, Lynch KR, Cheng R, Vanti WB, Arkhitko O, Lewis T, Evans JF, George SR, O'Dowd BF. Discovery and mapping of ten novel G protein-coupled receptor genes. *Gene.* 2001;275(1):83-91.
492. Bates B, Zhang L, Nawoschik S, Kodangattil S, Tseng E, Kopsco D, Kramer A, Shan Q, Taylor N, Johnson J, Sun Y, Chen HM, Blatcher M, Paulsen JE, Pausch MH. Characterization of Gpr101 expression and G-protein coupling selectivity. *Brain Res.* 2006;1087(1):1-14.
493. Benlian P, Giraud S, Lahlou N, Roger M, Blin C, Holler C, Lenoir G, Sallandre J, Calender A, Turpin G. Familial acromegaly: a specific clinical entity--further evidence from the genetic study of a three-generation family. *Eur J Endocrinol.* 1995;133(4):451-456.
494. Yamada S, Yoshimoto K, Sano T, Takada K, Itakura M, Usui M, Teramoto A. Inactivation of the tumor suppressor gene on 11q13 in brothers with familial acrogigantism without multiple endocrine neoplasia type 1. *J Clin Endocrinol Metab.* 1997;82(1):239-242.
495. Gadelha MR, Prezant TR, Une KN, Glick RP, Moskal SF, Vaisman M, Melmed S, Kineman RD, Frohman LA. Loss of heterozygosity on chromosome 11q13 in two families with acromegaly/gigantism is independent of mutations of the multiple endocrine neoplasia type I gene. *J Clin Endocrinol Metab.* 1999;84(1):249-256.
496. Soares BS, Eguchi K, Frohman LA. Tumor deletion mapping on chromosome 11q13 in eight families with isolated familial somatotropinoma and in 15 sporadic somatotropinomas. *J Clin Endocrinol Metab.* 2005;90(12):6580-6587.
497. DiGiovanni R, Serra S, Ezzat S, Asa SL. *AIP* Mutations are not identified in patients with sporadic pituitary adenomas. *Endocr Pathol.* 2007;18(2):76-78.
498. Cuny T, Pertuit M, Sahnoun-Fathallah M, Daly AF, Occhi G, Odou MF, Tabarin A, Nunes ML, Delemer B, Rohmer V, Desailloud R, Kerlan V, Chabre O, Sadoul JL, Cogne M, Caron P, Cortet C, Lienhardt-Roussie A, Raingeard I, Guedj AM, Brue T, Beckers A, Weryha G, Enjalbert A, Barlier A. Genetic analysis in young patients with sporadic pituitary macroadenomas: Beside *AIP* don't forget *MEN1* genetic analysis. *Eur J Endocrinol.* 2013;168(4):533-541.
499. Pardi E, Marcocci C, Borsari S, Saponaro F, Torregrossa L, Tancredi M, Raspini B, Basolo F, Cetani F. Aryl hydrocarbon receptor-interacting protein (*AIP*) mutations occur rarely in sporadic parathyroid adenomas. *J Clin Endocrinol Metab.* 2013;98(7):2800-2810.
500. Rostomyan L, Daly AF, Lila A, Lecoq AL, Nachev E, Moraitis A, Naves LA, Kranenburg D, MacMurray Holdaway I, Filipponi S, Jung-Sievers C, Sahnoun-Fathallah M, Ojaniemi M, Sorkina E, Tichomirowa MI, I, Zacharin M, Bertherat J, Malchiodi E, Salvatori R, Laboureau-Soares Barbosa S, Maiter D, McCormack AI, Von Werder K, Dal J, Nazzari E, Auriemma RS, Metzger DL, Jorgensen JO, Ebeling T, Ferone D, Stalla GK, Beck-Peccoz P, Aaltonen LA, Colao A, Pronin V, Barlier A, Brue T, Rohmer V, Mukhopadhyay S, Borson-Chazot F, Neggers S,

Jaffrain-Rea ML, Stratakis CA, Chanson P, Zacharieva S, Petrossians P, Shah N, Beckers A. Gigantism: Results of an international clinical and genetic study [abstract]. *Endocr Rev* 2013;34(03_MeetingAbstracts):OR20-6.

501. Cooper DN, Krawczak M, Polychronakos C, Tyler-Smith C, Kehrer-Sawatzki H. Where genotype is not predictive of phenotype: towards an understanding of the molecular basis of reduced penetrance in human inherited disease. *Hum Genet.* 2013;132(10):1077-1130.
502. NCBI Gene: *AIP* aryl hydrocarbon receptor interacting protein [Homo sapiens (human)]. http://www.ncbi.nlm.nih.gov/gene/9049#reference-sequences. Accessed 4/5/2015.
503. Locus Reference Genomic LRG_460 - AIP. http://ftp.ebi.ac.uk/pub/databases/lrgex/LRG_460.xml. Accessed 21/8/2014.
504. Perdew GH. Association of the Ah receptor with the 90-kDa heat shock protein. *J Biol Chem.* 1988;263(27):13802-13805.
505. Ozfirat Z, Korbonits M. *AIP* gene and familial isolated pituitary adenomas. *Mol Cell Endocrinol.* 2010;326(1-2):71-79.
506. Chahal HS, Stals K, Unterlander M, Balding DJ, Thomas MG, Kumar AV, Besser GM, Atkinson AB, Morrison PJ, Howlett TA, Levy MJ, Orme SM, Akker SA, Abel RL, Grossman AB, Burger J, Ellard S, Korbonits M. *AIP* mutation in pituitary adenomas in the 18th century and today. *N Engl J Med.* 2011;364(1):43-50.
507. Occhi G, Jaffrain-Rea ML, Trivellin G, Albiger N, Ceccato F, De ME, Angelini M, Ferasin S, Beckers A, Mantero F, Scaroni C. The R304X mutation of the aryl hydrocarbon receptor interacting protein gene in familial isolated pituitary adenomas: Mutational hot-spot or founder effect? *J Endocrinol Invest.* 2010;33(11):800-805.
508. Salvatori R, Gabrovska P, Weber A, Quinton R, Crowne EC, Corazzini V, Radian S, Sinha K, Lecoq AL, Chanson P, Thomas MG, Baborie A, Ansorge O, Bussel M, Stals K, Ellard S, Trainer PJ, Korbonits M. Founder Effect in Recurring *AIP* Mutation Causing Familial Isolated Pituitary Adenoma Syndrome [abstract]. *Endocrine Reviews* 2015;35(3 Supplement):SUN-0698.
509. Tuominen I, Heliovaara E, Raitila A, Rautiainen MR, Mehine M, Katainen R, Donner I, Aittomaki V, Lehtonen HJ, Ahlsten M, Kivipelto L, Schalin-Jantti C, Arola J, Hautaniemi S, Karhu A. AIP inactivation leads to pituitary tumorigenesis through defective Galpha-cAMP signaling. *Oncogene.* 2014;34(9):1174-1184.
510. The Uniprot Consortium. UniProt: a hub for protein information (http://www.uniprot.org/). *Nucleic Acids Res.* 2015;43(Database issue):D204-D212.
511. Cunningham F, Amode MR, Barrell D, Beal K, Billis K, Brent S, Carvalho-Silva D, Clapham P, Coates G, Fitzgerald S, Gil L, Giron CG, Gordon L, Hourlier T, Hunt SE, Janacek SH, Johnson N, Juettemann T, Kahari AK, Keenan S, Martin FJ, Maurel T, McLaren W, Murphy DN, Nag R, Overduin B, Parker A, Patricio M,

Perry E, Pignatelli M, Riat HS, Sheppard D, Taylor K, Thormann A, Vullo A, Wilder SP, Zadissa A, Aken BL, Birney E, Harrow J, Kinsella R, Muffato M, Ruffier M, Searle SM, Spudich G, Trevanion SJ, Yates A, Zerbino DR, Flicek P. Ensembl 2015. *Nucleic Acids Res.* 2015;43(Database issue):D662-D669.

512. Dull AB, Carlson DB, Petrulis JR, Perdew GH. Characterization of the phosphorylation status of the hepatitis B virus X-associated protein 2. *Arch Biochem Biophys.* 2002;406(2):209-221.
513. Hornbeck PV, Kornhauser JM, Tkachev S, Zhang B, Skrzypek E, Murray B, Latham V, Sullivan M. PhosphoSitePlus: a comprehensive resource for investigating the structure and function of experimentally determined post-translational modifications in man and mouse. *Nucleic Acids Res.* 2012;40(Database issue):D261-D270.
514. Kelley LA, Sternberg MJ. Protein structure prediction on the Web: a case study using the Phyre server (http://www.sbg.bio.ic.ac.uk/phyre2/html/page.cgi?id=index). *Nat Protoc.* 2009;4(3):363-371.
515. Berman HM, Westbrook J, Feng Z, Gilliland G, Bhat TN, Weissig H, Shindyalov IN, Bourne PE. The Protein Data Bank (www.rcsb.org). *Nucleic Acids Res.* 2000;28(1):235-242.
516. Kuzhandaivelu N, Cong YS, Inouye C, Yang WM, Seto E. XAP2, a novel hepatitis B virus X-associated protein that inhibits X transactivation. *Nucleic Acids Res.* 1996;24(23):4741-4750.
517. Carver LA, Bradfield CA. Ligand-dependent interaction of the aryl hydrocarbon receptor with a novel immunophilin homolog in vivo. *J Biol Chem.* 1997;272(17):11452-11456.
518. Linnert M, Lin YJ, Manns A, Haupt K, Paschke AK, Fischer G, Weiwad M, Lucke C. The FKBP-type domain of the human aryl hydrocarbon receptor-interacting protein reveals an unusual Hsp90 interaction. *Biochemistry.* 2013;52(12):2097-2107.
519. EMBL-EBI.Expression Atlas. http://www.ebi.ac.uk/gxa/query?geneQuery=AIP&exactMatch=true&_exactMatch=on&organism=Homo+sapiens&condition=. Accessed 4/5/2015.
520. Ma Q, Whitlock JP, Jr. A novel cytoplasmic protein that interacts with the Ah receptor, contains tetratricopeptide repeat motifs, and augments the transcriptional response to 2,3,7,8-tetrachlorodibenzo-p-dioxin. *J Biol Chem.* 1997;272(14):8878-8884.
521. Meyer BK, Petrulis JR, Perdew GH. Aryl hydrocarbon (Ah) receptor levels are selectively modulated by hsp90-associated immunophilin homolog XAP2. *Cell Stress Chaperones.* 2000;5(3):243-254.
522. Carver LA, LaPres JJ, Jain S, Dunham EE, Bradfield CA. Characterization of the Ah receptor-associated protein, ARA9. *J Biol Chem.* 1998;273(50):33580-33587.

523. Morgan RM, Hernandez-Ramirez LC, Trivellin G, Zhou L, Roe SM, Korbonits M, Prodromou C. Structure of the TPR Domain of AIP: Lack of Client Protein Interaction with the C-Terminal alpha-7 Helix of the TPR Domain of AIP Is Sufficient for Pituitary Adenoma Predisposition. *PLoS One.* 2012;7(12):e53339.
524. Cox MB, Smith MF. Functions of the Hsp90-Binding FKBP immunophilins. In: Blatch G.L., ed. *Networking of Chaperones by Co-Chaperones*. First ed. Austin, Texas: Landes Bioscience/Eurekah.com; 2000;13-25.
525. Barik S. Immunophilins: for the love of proteins. *Cell Mol Life Sci.* 2006;63(24):2889-2900.
526. Guy NC, Garcia YA, Sivils JC, Galigniana MD, Cox MB. Functions of the Hsp90-binding FKBP immunophilins. *Subcell Biochem.* 2015;78:35-68.
527. Zeytuni N, Zarivach R. Structural and functional discussion of the tetra-trico-peptide repeat, a protein interaction module. *Structure.* 2012;20(3):397-405.
528. D'Andrea LD, Regan L. TPR proteins: the versatile helix. *Trends Biochem Sci.* 2003;28(12):655-662.
529. Linnert M, Haupt K, Lin YJ, Kissing S, Paschke AK, Fischer G, Weiwad M, Lucke C. NMR assignments of the FKBP-type PPIase domain of the human aryl-hydrocarbon receptor-interacting protein (AIP). *Biomol NMR Assign.* 2012;6(2):209-212.
530. Kashuba E, Kashuba V, Pokrovskaja K, Klein G, Szekely L. Epstein-Barr virus encoded nuclear protein EBNA-3 binds XAP-2, a protein associated with Hepatitis B virus X antigen. *Oncogene.* 2000;19(14):1801-1806.
531. Meyer BK, Pray-Grant MG, Vanden Heuvel JP, Perdew GH. Hepatitis B virus X-associated protein 2 is a subunit of the unliganded aryl hydrocarbon receptor core complex and exhibits transcriptional enhancer activity. *Mol Cell Biol.* 1998;18(2):978-988.
532. Bolger GB, Peden AH, Steele MR, MacKenzie C, McEwan DG, Wallace DA, Huston E, Baillie GS, Houslay MD. Attenuation of the activity of the cAMP-specific phosphodiesterase PDE4A5 by interaction with the immunophilin XAP2. *J Biol Chem.* 2003;278(35):33351-33363.
533. de Oliveira SK, Hoffmeister M, Gambaryan S, Muller-Esterl W, Guimaraes JA, Smolenski AP. Phosphodiesterase 2A forms a complex with the co-chaperone XAP2 and regulates nuclear translocation of the aryl hydrocarbon receptor. *J Biol Chem.* 2007;282(18):13656-13663.
534. Yano M, Terada K, Mori M. AIP is a mitochondrial import mediator that binds to both import receptor Tom20 and preproteins. *J Cell Biol.* 2003;163(1):45-56.
535. Kang BH, Altieri DC. Regulation of survivin stability by the aryl hydrocarbon receptor-interacting protein. *J Biol Chem.* 2006;281(34):24721-24727.
536. Sumanasekera WK, Tien ES, Turpey R, Vanden Heuvel JP, Perdew GH. Evidence that peroxisome proliferator-activated receptor alpha is complexed with

the 90-kDa heat shock protein and the hepatitis virus B X-associated protein 2. *J Biol Chem.* 2003;278(7):4467-4473.

537. Froidevaux MS, Berg P, Seugnet I, Decherf S, Becker N, Sachs LM, Bilesimo P, Nygard M, Pongratz I, Demeneix BA. The co-chaperone XAP2 is required for activation of hypothalamic thyrotropin-releasing hormone transcription in vivo. *EMBO Rep.* 2006;7(10):1035-1039.
538. Cai W, Kramarova TV, Berg P, Korbonits M, Pongratz I. The immunophilin-like protein XAP2 is a negative regulator of estrogen signaling through interaction with estrogen receptor alpha. *PLoS One.* 2011;6(10):e25201.
539. Vargiolu M, Fusco D, Kurelac I, Dirnberger D, Baumeister R, Morra I, Melcarne A, Rimondini R, Romeo G, Bonora E. The tyrosine kinase receptor RET interacts in vivo with aryl hydrocarbon receptor-interacting protein to alter survivin availability. *J Clin Endocrinol Metab.* 2009;94(7):2571-2578.
540. Nakata A, Urano D, Fujii-Kuriyama Y, Mizuno N, Tago K, Itoh H. G-protein signalling negatively regulates the stability of aryl hydrocarbon receptor. *EMBO Rep.* 2009;10(6):622-628.
541. Stark C, Breitkreutz BJ, Reguly T, Boucher L, Breitkreutz A, Tyers M. BioGRID: a general repository for interaction datasets. *Nucleic Acids Res.* 2006;34(Database issue):D535-D539.
542. Berg P, Pongratz I. Two parallel pathways mediate cytoplasmic localization of the dioxin (aryl hydrocarbon) receptor. *J Biol Chem.* 2002;277(35):32310-32319.
543. Li S, Wang L, Fu B, Berman MA, Diallo A, Dorf ME. TRIM65 regulates microRNA activity by ubiquitination of TNRC6. *Proc Natl Acad Sci U S A.* 2014;111(19):6970-6975.
544. Petrulis JR, Hord NG, Perdew GH. Subcellular localization of the aryl hydrocarbon receptor is modulated by the immunophilin homolog hepatitis B virus X-associated protein 2. *J Biol Chem.* 2000;275(48):37448-37453.
545. Dunham EE, Stevens EA, Glover E, Bradfield CA. The aryl hydrocarbon receptor signaling pathway is modified through interactions with a Kelch protein. *Mol Pharmacol.* 2006;70(1):8-15.
546. Kazlauskas A, Poellinger L, Pongratz I. Two distinct regions of the immunophilin-like protein XAP2 regulate dioxin receptor function and interaction with hsp90. *J Biol Chem.* 2002;277(14):11795-11801.
547. Huttlin, E. L., Ting, L., Bruckner, R. J., Paulo, J. A., Gygi, M. P., Rad, R., Kolippakkam, D., Szpyt, J., Zarraga, G., Tam, S., Gebreab, F., Colby, G., Pontano-Vaites, L., Obar, R. A., Guarani-Pereira, V., Artavanis-Tsakonas, S., Sowa, M. E., Harper, J. W., and Gygi, S. P.High-Throughput Proteomic Mapping of Human Interaction Networks via Affinity-Purification Mass Spectrometry (Pre-Publication). http://thebiogrid.org/166968/publication/high-throughput-proteomic-mapping-of-human-interaction-networks-via-affinity-purification-mass-spectrometry.html. Accessed 5/5/2014.

548. Taipale M, Tucker G, Peng J, Krykbaeva I, Lin ZY, Larsen B, Choi H, Berger B, Gingras AC, Lindquist S. A quantitative chaperone interaction network reveals the architecture of cellular protein homeostasis pathways. *Cell.* 2014;158(2):434-448.
549. Varjosalo M, Sacco R, Stukalov A, van DA, Planyavsky M, Hauri S, Aebersold R, Bennett KL, Colinge J, Gstaiger M, Superti-Furga G. Interlaboratory reproducibility of large-scale human protein-complex analysis by standardized AP-MS. *Nat Methods.* 2013;10(4):307-314.
550. Wang J, Huo K, Ma L, Tang L, Li D, Huang X, Yuan Y, Li C, Wang W, Guan W, Chen H, Jin C, Wei J, Zhang W, Yang Y, Liu Q, Zhou Y, Zhang C, Wu Z, Xu W, Zhang Y, Liu T, Yu D, Zhang Y, Chen L, Zhu D, Zhong X, Kang L, Gan X, Yu X, Ma Q, Yan J, Zhou L, Liu Z, Zhu Y, Zhou T, He F, Yang X. Toward an understanding of the protein interaction network of the human liver. *Mol Syst Biol.* 2011;7:536.
551. Zhang M, Han G, Wang C, Cheng K, Li R, Liu H, Wei X, Ye M, Zou H. A bead-based approach for large-scale identification of in vitro kinase substrates. *Proteomics.* 2011;11(24):4632-4637.
552. Deribe YL, Wild P, Chandrashaker A, Curak J, Schmidt MH, Kalaidzidis Y, Milutinovic N, Kratchmarova I, Buerkle L, Fetchko MJ, Schmidt P, Kittanakom S, Brown KR, Jurisica I, Blagoev B, Zerial M, Stagljar I, Dikic I. Regulation of epidermal growth factor receptor trafficking by lysine deacetylase HDAC6. *Sci Signal.* 2009;2(102):ra84.
553. Kristensen AR, Gsponer J, Foster LJ. A high-throughput approach for measuring temporal changes in the interactome. *Nat Methods.* 2012;9(9):907-909.
554. Havugimana PC, Hart GT, Nepusz T, Yang H, Turinsky AL, Li Z, Wang PI, Boutz DR, Fong V, Phanse S, Babu M, Craig SA, Hu P, Wan C, Vlasblom J, Dar VU, Bezginov A, Clark GW, Wu GC, Wodak SJ, Tillier ER, Paccanaro A, Marcotte EM, Emili A. A census of human soluble protein complexes. *Cell.* 2012;150(5):1068-1081.
555. Meyer BK, Perdew GH. Characterization of the AhR-hsp90-XAP2 core complex and the role of the immunophilin-related protein XAP2 in AhR stabilization. *Biochemistry.* 1999;38(28):8907-8917.
556. Bell DR, Poland A. Binding of aryl hydrocarbon receptor (AhR) to AhR-interacting protein. The role of hsp90. *J Biol Chem.* 2000;275(46):36407-36414.
557. Kazlauskas A, Poellinger L, Pongratz I. The immunophilin-like protein XAP2 regulates ubiquitination and subcellular localization of the dioxin receptor. *J Biol Chem.* 2000;275(52):41317-41324.
558. Laenger A, Lang-Rollin I, Kozany C, Zschocke J, Zimmermann N, Ruegg J, Holsboer F, Hausch F, Rein T. XAP2 inhibits glucocorticoid receptor activity in mammalian cells. *FEBS Lett.* 2009;583(9):1493-1498.

559. Schulke JP, Wochnik GM, Lang-Rollin I, Gassen NC, Knapp RT, Berning B, Yassouridis A, Rein T. Differential impact of tetratricopeptide repeat proteins on the steroid hormone receptors. *PLoS One.* 2010;5(7):e11717.

560. Li J, Richter K, Buchner J. Mixed Hsp90-cochaperone complexes are important for the progression of the reaction cycle. *Nat Struct Mol Biol.* 2011;18(1):61-66.

561. Ravasi T, Suzuki H, Cannistraci CV, Katayama S, Bajic VB, Tan K, Akalin A, Schmeier S, Kanamori-Katayama M, Bertin N, Carninci P, Daub CO, Forrest AR, Gough J, Grimmond S, Han JH, Hashimoto T, Hide W, Hofmann O, Kamburov A, Kaur M, Kawaji H, Kubosaki A, Lassmann T, van NE, MacPherson CR, Ogawa C, Radovanovic A, Schwartz A, Teasdale RD, Tegner J, Lenhard B, Teichmann SA, Arakawa T, Ninomiya N, Murakami K, Tagami M, Fukuda S, Imamura K, Kai C, Ishihara R, Kitazume Y, Kawai J, Hume DA, Ideker T, Hayashizaki Y. An atlas of combinatorial transcriptional regulation in mouse and man. *Cell.* 2010;140(5):744-752.

562. Li S, Wang L, Berman M, Kong YY, Dorf ME. Mapping a dynamic innate immunity protein interaction network regulating type I interferon production. *Immunity.* 2011;35(3):426-440.

563. Couzens AL, Knight JD, Kean MJ, Teo G, Weiss A, Dunham WH, Lin ZY, Bagshaw RD, Sicheri F, Pawson T, Wrana JL, Choi H, Gingras AC. Protein interaction network of the mammalian Hippo pathway reveals mechanisms of kinase-phosphatase interactions. *Sci Signal.* 2013;6(302):rs15.

564. Zhao Y, Meng XM, Wei YJ, Zhao XW, Liu DQ, Cao HQ, Liew CC, Ding JF. Cloning and characterization of a novel cardiac-specific kinase that interacts specifically with cardiac troponin I. *J Mol Med (Berl).* 2003;81(5):297-304.

565. Danielsen JM, Sylvestersen KB, Bekker-Jensen S, Szklarczyk D, Poulsen JW, Horn H, Jensen LJ, Mailand N, Nielsen ML. Mass spectrometric analysis of lysine ubiquitylation reveals promiscuity at site level. *Mol Cell Proteomics.* 2011;10(3):M110.

566. Kim W, Bennett EJ, Huttlin EL, Guo A, Li J, Possemato A, Sowa ME, Rad R, Rush J, Comb MJ, Harper JW, Gygi SP. Systematic and quantitative assessment of the ubiquitin-modified proteome. *Mol Cell.* 2011;44(2):325-340.

567. Udeshi ND, Mani DR, Eisenhaure T, Mertins P, Jaffe JD, Clauser KR, Hacohen N, Carr SA. Methods for quantification of in vivo changes in protein ubiquitination following proteasome and deubiquitinase inhibition. *Mol Cell Proteomics.* 2012;11(5):148-159.

568. Povlsen LK, Beli P, Wagner SA, Poulsen SL, Sylvestersen KB, Poulsen JW, Nielsen ML, Bekker-Jensen S, Mailand N, Choudhary C. Systems-wide analysis of ubiquitylation dynamics reveals a key role for PAF15 ubiquitylation in DNA-damage bypass. *Nat Cell Biol.* 2012;14(10):1089-1098.

569. Stes E, Laga M, Walton A, Samyn N, Timmerman E, De S, I, Goormachtig S, Gevaert K. A COFRADIC protocol to study protein ubiquitination. *J Proteome Res.* 2014;13(6):3107-3113.
570. Petrulis JR, Kusnadi A, Ramadoss P, Hollingshead B, Perdew GH. The hsp90 Co-chaperone XAP2 alters importin beta recognition of the bipartite nuclear localization signal of the Ah receptor and represses transcriptional activity. *J Biol Chem.* 2003;278(4):2677-2685.
571. Whitlock JP, Jr. Mechanistic aspects of dioxin action. *Chem Res Toxicol.* 1993;6(6):754-763.
572. Denison MS, Soshilov AA, He G, DeGroot DE, Zhao B. Exactly the same but different: promiscuity and diversity in the molecular mechanisms of action of the aryl hydrocarbon (dioxin) receptor. *Toxicol Sci.* 2011;124(1):1-22.
573. Nguyen LP, Bradfield CA. The search for endogenous activators of the aryl hydrocarbon receptor. *Chem Res Toxicol.* 2008;21(1):102-116.
574. Opitz CA, Litzenburger UM, Sahm F, Ott M, Tritschler I, Trump S, Schumacher T, Jestaedt L, Schrenk D, Weller M, Jugold M, Guillemin GJ, Miller CL, Lutz C, Radlwimmer B, Lehmann I, von DA, Wick W, Platten M. An endogenous tumour-promoting ligand of the human aryl hydrocarbon receptor. *Nature.* 2011;478(7368):197-203.
575. de Oliveira SK, Smolenski A. Phosphodiesterases link the aryl hydrocarbon receptor complex to cyclic nucleotide signaling. *Biochem Pharmacol.* 2009;77(4):723-733.
576. Ramadoss P, Petrulis JR, Hollingshead BD, Kusnadi A, Perdew GH. Divergent roles of hepatitis B virus X-associated protein 2 (XAP2) in human versus mouse Ah receptor complexes. *Biochemistry.* 2004;43(3):700-709.
577. Nukaya M, Lin BC, Glover E, Moran SM, Kennedy GD, Bradfield CA. The aryl hydrocarbon receptor-interacting protein (AIP) is required for dioxin-induced hepatotoxicity but not for the induction of the Cyp1a1 and Cyp1a2 genes. *J Biol Chem.* 2010;285(46):35599-35605.
578. Chen HS, Perdew GH. Subunit composition of the heteromeric cytosolic aryl hydrocarbon receptor complex. *J Biol Chem.* 1994;269(44):27554-27558.
579. Nair SC, Toran EJ, Rimerman RA, Hjermstad S, Smithgall TE, Smith DF. A pathway of multi-chaperone interactions common to diverse regulatory proteins: estrogen receptor, Fes tyrosine kinase, heat shock transcription factor Hsf1, and the aryl hydrocarbon receptor. *Cell Stress Chaperones.* 1996;1(4):237-250.
580. Kazlauskas A, Sundstrom S, Poellinger L, Pongratz I. The hsp90 chaperone complex regulates intracellular localization of the dioxin receptor. *Mol Cell Biol.* 2001;21(7):2594-2607.
581. Beischlag TV, Luis MJ, Hollingshead BD, Perdew GH. The aryl hydrocarbon receptor complex and the control of gene expression. *Crit Rev Eukaryot Gene Expr.* 2008;18(3):207-250.

582. Baker MJ, Frazier AE, Gulbis JM, Ryan MT. Mitochondrial protein-import machinery: correlating structure with function. *Trends Cell Biol.* 2007;17(9):456-464.
583. Kang BH, Xia F, Pop R, Dohi T, Socolovsky M, Altieri DC. Developmental control of apoptosis by the immunophilin aryl hydrocarbon receptor-interacting protein (AIP) involves mitochondrial import of the survivin protein. *J Biol Chem.* 2011;286(19):16758-16767.
584. Liu T, Daniels CK, Cao S. Comprehensive review on the HSC70 functions, interactions with related molecules and involvement in clinical diseases and therapeutic potential. *Pharmacol Ther.* 2012;136(3):354-374.
585. Truman AW, Kristjansdottir K, Wolfgeher D, Hasin N, Polier S, Zhang H, Perrett S, Prodromou C, Jones GW, Kron SJ. CDK-dependent Hsp70 Phosphorylation controls G1 cyclin abundance and cell-cycle progression. *Cell.* 2012;151(6):1308-1318.
586. Lugnier C. Cyclic nucleotide phosphodiesterase (PDE) superfamily: a new target for the development of specific therapeutic agents. *Pharmacol Ther.* 2006;109(3):366-398.
587. Hollingshead BD, Petrulis JR, Perdew GH. The aryl hydrocarbon (Ah) receptor transcriptional regulator hepatitis B virus X-associated protein 2 antagonizes p23 binding to Ah receptor-Hsp90 complexes and is dispensable for receptor function. *J Biol Chem.* 2004;279(44):45652-45661.
588. Formosa R, Xuereb-Anastasi A, Vassallo J. Aip regulates cAMP signalling and GH secretion in GH3 cells. *Endocr Relat Cancer.* 2013;20(4):495-505.
589. Chahal HS, Trivellin G, Leontiou CA, Alband N, Fowkes RC, Tahir A, Igreja SC, Chapple JP, Jordan S, Lupp A, Schulz S, Ansorge O, Karavitaki N, Carlsen E, Wass JA, Grossman AB, Korbonits M. Somatostatin analogs modulate AIP in somatotroph adenomas: the role of the ZAC1 pathway. *J Clin Endocrinol Metab.* 2012;97(8):E1411-E1420.
590. Guaraldi F, Corazzini V, Gallia GL, Grottoli S, Stals K, Dalantaeva N, Frohman LA, Korbonits M, Salvatori R. Genetic analysis in a patient presenting with meningioma and familial isolated pituitary adenoma (FIPA) reveals selective involvement of the R81X mutation of the *AIP* gene in the pathogenesis of the pituitary tumor. *Pituitary.* 2012;15 Suppl 1:S61-S67.
591. Gadelha MR, Kasuki L, Korbonits M. Novel pathway for somatostatin analogs in patients with acromegaly. *Trends Endocrinol Metab.* 2013;24(5):238-246.
592. Theodoropoulou M, Zhang J, Laupheimer S, Paez-Pereda M, Erneux C, Florio T, Pagotto U, Stalla GK. Octreotide, a somatostatin analogue, mediates its antiproliferative action in pituitary tumor cells by altering phosphatidylinositol 3-kinase signaling and inducing Zac1 expression. *Cancer Res.* 2006;66(3):1576-1582.

593. Peverelli E, Busnelli M, Vitali E, Giardino E, Gales C, Lania AG, Beck-Peccoz P, Chini B, Mantovani G, Spada A. Specific roles of G(i) protein family members revealed by dissecting SST5 coupling in human pituitary cells. *J Cell Sci.* 2013;126(Pt 2):638-644.
594. Ruggeri RM, Santarpia L, Curto L, Torre ML, Galatioto M, Galatioto S, Trimarchi F, Cannavo S. Non-functioning pituitary adenomas infrequently harbor G-protein gene mutations. *J Endocrinol Invest.* 2008;31(11):946-949.
595. Lin BC, Sullivan R, Lee Y, Moran S, Glover E, Bradfield CA. Deletion of the aryl hydrocarbon receptor-associated protein 9 leads to cardiac malformation and embryonic lethality. *J Biol Chem.* 2007;282(49):35924-35932.
596. Lin BC, Nguyen LP, Walisser JA, Bradfield CA. A hypomorphic allele of aryl hydrocarbon receptor-associated protein-9 produces a phenocopy of the AHR-null mouse. *Mol Pharmacol.* 2008;74(5):1367-1371.
597. Raitila A, Lehtonen HJ, Arola J, Heliovaara E, Ahlsten M, Georgitsi M, Jalanko A, Paetau A, Aaltonen LA, Karhu A. Mice with inactivation of aryl hydrocarbon receptor-interacting protein (Aip) display complete penetrance of pituitary adenomas with aberrant ARNT expression. *Am J Pathol.* 2010;177(4):1969-1976.
598. Aflorei ED, Radian S, Chen C, Klapholz B, Brown N, Stanewsky R, Korbonits M. Functional homology between human and fruitfly *AIP* protein - an in vivo assay system to test the pathogenicity of *AIP* mutations [abstract]. *Endocrine Reviews* 2015;36(2_MeetingAbstracts):SAT-440.
599. Heliovaara E, Raitila A, Launonen V, Paetau A, Arola J, Lehtonen H, Sane T, Weil RJ, Vierimaa O, Salmela P, Tuppurainen K, Makinen M, Aaltonen LA, Karhu A. The expression of AIP-related molecules in elucidation of cellular pathways in pituitary adenomas. *Am J Pathol.* 2009;175(6):2501-2507.
600. Georgitsi M, Karhu A, Winqvist R, Visakorpi T, Waltering K, Vahteristo P, Launonen V, Aaltonen LA. Mutation analysis of aryl hydrocarbon receptor interacting protein (*AIP*) gene in colorectal, breast, and prostate cancers. *Br J Cancer.* 2007;96(2):352-356.
601. Iwata T, Yamada S, Ito J, Inoshita N, Mizusawa N, Ono S, Yoshimoto K. A novel C-terminal nonsense mutation, Q315X, of the aryl hydrocarbon receptor-interacting protein gene in a Japanese familial isolated pituitary adenoma family. *Endocr Pathol.* 2014;25(3):273-281.
602. Nord KH, Magnusson L, Isaksson M, Nilsson J, Lilljebjorn H, Domanski HA, Kindblom LG, Mandahl N, Mertens F. Concomitant deletions of tumor suppressor genes *MEN1* and *AIP* are essential for the pathogenesis of the brown fat tumor hibernoma. *Proc Natl Acad Sci U S A.* 2010;107(49):21122-21127.
603. Williams F, Hunter S, Bradley L, Chahal HS, Storr HL, Akker SA, Kumar AV, Orme SM, Evanson J, Abid N, Morrison PJ, Korbonits M, Atkinson AB. Clinical experience in the screening and management of a large kindred with familial

isolated pituitary adenoma due to an aryl hydrocarbon receptor interacting protein (*AIP*) mutation. *J Clin Endocrinol Metab.* 2014;99(4):1122-1131.

604. The International FIPA Consortium. http://www.fipapatients.org/fipaconsortium/. Accessed 17/11/2014.
605. Dimaraki EV, Jaffe CA, DeMott-Friberg R, Chandler WF, Barkan AL. Acromegaly with apparently normal GH secretion: implications for diagnosis and follow-up. *J Clin Endocrinol Metab.* 2002;87(8):3537-3542.
606. Plon SE, Eccles DM, Easton D, Foulkes WD, Genuardi M, Greenblatt MS, Hogervorst FB, Hoogerbrugge N, Spurdle AB, Tavtigian SV. Sequence variant classification and reporting: recommendations for improving the interpretation of cancer susceptibility genetic test results. *Hum Mutat.* 2008;29(11):1282-1291.
607. den Dunnen JT, Antonarakis SE. Mutation nomenclature extensions and suggestions to describe complex mutations: a discussion. *Hum Mutat.* 2000;15(1):7-12.
608. Human Genome Variation Society.Nomenclature for the description of sequence variants. http://www.hgvs.org/mutnomen/. Accessed 1/6/2013.
609. Wildeman M, van OE, den Dunnen JT, Taschner PE. Improving sequence variant descriptions in mutation databases and literature using the Mutalyzer sequence variation nomenclature checker. *Hum Mutat.* 2008;29(1):6-13.
610. Korbonits M, Storr H, Kumar AV. Familial pituitary adenomas - who should be tested for *AIP* mutations? *Clin Endocrinol (Oxf).* 2012;77(3):351-356.
611. Rattenberry E, Vialard L, Yeung A, Bair H, McKay K, Jafri M, Canham N, Cole TR, Denes J, Hodgson SV, Irving R, Izatt L, Korbonits M, Kumar AV, Lalloo F, Morrison PJ, Woodward ER, Macdonald F, Wallis Y, Maher ER. A comprehensive next generation sequencing-based genetic testing strategy to improve diagnosis of inherited pheochromocytoma and paraganglioma. *J Clin Endocrinol Metab.* 2013;98(7):E1248-E1256.
612. Bange J, Prechtl D, Cheburkin Y, Specht K, Harbeck N, Schmitt M, Knyazeva T, Muller S, Gartner S, Sures I, Wang H, Imyanitov E, Haring HU, Knayzev P, Iacobelli S, Hofler H, Ullrich A. Cancer progression and tumor cell motility are associated with the *FGFR4* Arg(388) allele. *Cancer Res.* 2002;62(3):840-847.
613. Lania A, Persani L, Ballare E, Mantovani S, Losa M, Spada A. Constitutively active Gs alpha is associated with an increased phosphodiesterase activity in human growth hormone-secreting adenomas. *J Clin Endocrinol Metab.* 1998;83(5):1624-1628.
614. Stals K, Trivellin G, Korbonits M. *AIP* mutation in pituitary adenomas. *N Engl J Med.* 2011;364(20):1974-1975.
615. Georgitsi M, Raitila A, Karhu A, Tuppurainen K, Makinen MJ, Vierimaa O, Paschke R, Saeger W, van der Luijt RB, Sane T, Robledo M, De ME, Weil RJ, Wasik A, Zielinski G, Lucewicz O, Lubinski J, Launonen V, Vahteristo P, Aaltonen LA. Molecular diagnosis of pituitary adenoma predisposition caused by aryl

hydrocarbon receptor-interacting protein gene mutations. *Proc Natl Acad Sci U S A.* 2007;104(10):4101-4105.

616. Raitila A, Georgitsi M, Karhu A, Tuppurainen K, Makinen MJ, Birkenkamp-Demtroder K, Salmenkivi K, Orntoft TF, Arola J, Launonen V, Vahteristo P, Aaltonen LA. No evidence of somatic aryl hydrocarbon receptor interacting protein mutations in sporadic endocrine neoplasia. *Endocr Relat Cancer.* 2007;14(3):901-906.
617. Pestell RG, Alford FP, Best JD. Familial acromegaly. *Acta Endocrinol (Copenh).* 1989;121(2):286-289.
618. Georgitsi M, Heliovaara E, Paschke R, Kumar AV, Tischkowitz M, Vierimaa O, Salmela P, Sane T, De ME, Cannavo S, Gundogdu S, Lucassen A, Izatt L, Aylwin S, Bano G, Hodgson S, Koch CA, Karhu A, Aaltonen LA. Large genomic deletions in *AIP* in pituitary adenoma predisposition. *J Clin Endocrinol Metab.* 2008;93(10):4146-4151.
619. Luccio-Camelo DC, Une KN, Ferreira RE, Khoo SK, Nickolov R, Bronstein MD, Vaisman M, Teh BT, Frohman LA, Mendonca BB, Gadelha MR. A meiotic recombination in a new isolated familial somatotropinoma kindred. *Eur J Endocrinol.* 2004;150(5):643-648.
620. Toledo RA, Mendonca BB, Fragoso MC, Soares IC, Almeida MQ, Moraes MB, Lourenco DM, Jr., Alves VA, Bronstein MD, Toledo SP. Isolated familial somatotropinoma: 11q13-loh and gene/protein expression analysis suggests a possible involvement of *AIP* also in non-pituitary tumorigenesis. *Clinics (Sao Paulo).* 2010;65(4):407-415.
621. Martucci F, Trivellin G, Korbonits M. Familial isolated pituitary adenomas: an emerging clinical entity. *J Endocrinol Invest.* 2012;35(11):1003-1014.
622. Fukuoka H, Iguchi G., Suda K., Yamamoto M., Nishizawa H., Takahashi M, Seino S., Yamada S, Takahashi Y. A novel missense mutation of *AIP* gene in a patient with octreotide-resistant non-familial gigantism [abstract]. *Endocr Rev* 2012;33(03_MeetingAbstracts):SUN-713.
623. Nishizawa H, Fukuoka H, Iguchi G, Inoshita N, Yamada S, Takahashi Y. AIP mutation identified in a patient with acromegaly caused by pituitary somatotroph adenoma with neuronal choristoma. *Exp Clin Endocrinol Diabetes.* 2013;121(5):295-299.
624. Jorge BH, Agarwal SK, Lando VS, Salvatori R, Barbero RR, Abelin N, Levine MA, Marx SJ, Toledo SP. Study of the multiple endocrine neoplasia type 1, growth hormone-releasing hormone receptor, Gs alpha, and Gi2 alpha genes in isolated familial acromegaly. *J Clin Endocrinol Metab.* 2001;86(2):542-544.
625. Toledo RA, Lourenco DM, Jr., Liberman B, Cunha-Neto MB, Cavalcanti MG, Moyses CB, Toledo SP, Dahia PL. Germline mutation in the aryl hydrocarbon receptor interacting protein gene in familial somatotropinoma. *J Clin Endocrinol Metab.* 2007;92(5):1934-1937.

626. Prescott RWG, Spruce BA, Kendall-Taylor P, Hall K, Hall R. Acromegaly and gigantism presenting in two brothers [abstract]. *1st Joint Mtg Brit Endocr Soc* 1982;49
627. McCarthy MI, Noonan K, Wass JA, Monson JP. Familial acromegaly: studies in three families. *Clin Endocrinol (Oxf).* 1990;32(6):719-728.
628. Georgitsi M, De ME, Cannavo S, Makinen MJ, Tuppurainen K, Pauletto P, Curto L, Weil RJ, Paschke R, Zielinski G, Wasik A, Lubinski J, Vahteristo P, Karhu A, Aaltonen LA. Aryl hydrocarbon receptor interacting protein (*AIP*) gene mutation analysis in children and adolescents with sporadic pituitary adenomas. *Clin Endocrinol (Oxf).* 2008;69(4):621-627.
629. Jennings JE, Georgitsi M, Holdaway I, Daly AF, Tichomirowa M, Beckers A, Aaltonen LA, Karhu A, Cameron FJ. Aggressive pituitary adenomas occurring in young patients in a large Polynesian kindred with a germline R271W mutation in the *AIP* gene. *Eur J Endocrinol.* 2009;161(5):799-804.
630. de Lima DS, Martins CS, Paixao BM, Amaral FC, Colli LM, Saggioro FP, Neder L, Machado HR, dos Santos AR, Pinheiro DG, Moreira AC, Silva WA, Jr., Castro M. SAGE analysis highlights the putative role of underexpression of ribosomal proteins in GH-secreting pituitary adenomas. *Eur J Endocrinol.* 2012;167(6):759-768.
631. Niyazoglu M, Sayitoglu M, Firtina S, Hatipoglu E, Gazioglu N, Kadioglu P. Familial acromegaly due to aryl hydrocarbon receptor-interacting protein (*AIP*) gene mutation in a Turkish cohort. *Pituitary.* 2013;17(3):220-226.
632. Occhi G, Trivellin G, Ceccato F, De LP, Giorgi G, Dematte S, Grimaldi F, Castello R, Davi MV, Arnaldi G, Salviati L, Opocher G, Mantero F, Scaroni C. Prevalence of *AIP* mutations in a large series of sporadic Italian acromegalic patients and evaluation of *CDKN1B* status in acromegalic patients with multiple endocrine neoplasia. *Eur J Endocrinol.* 2010;163(3):369-376.
633. Buchbinder S, Bierhaus A, Zorn M, Nawroth PP, Humpert P, Schilling T. Aryl hydrocarbon receptor interacting protein gene (*AIP*) mutations are rare in patients with hormone secreting or non-secreting pituitary adenomas. *Exp Clin Endocrinol Diabetes.* 2008;116(10):625-628.
634. Raitila A, Georgitsi M, Bonora E, Vargiolu M, Tuppurainen K, Makinen MJ, Vierimaa O, Salmela PI, Launonen V, Vahteristo P, Aaltonen LA, Romeo G, Karhu A. Aryl hydrocarbon receptor interacting protein mutations seem not to associate with familial non-medullary thyroid cancer. *J Endocrinol Invest.* 2009;32(5):426-429.
635. Guaraldi F, Salvatori R. Familial isolated pituitary adenomas: from genetics to therapy. *Clin Transl Sci.* 2011;4(1):55-62.
636. Zatelli MC, Torre ML, Rossi R, Ragonese M, Trimarchi F, degli UE, Cannavo S. Should *aip* gene screening be recommended in family members of FIPA patients with R16H variant? *Pituitary.* 2013;16(2):238-244.

637. Rowlands JC, Urban JD, Wikoff DS, Budinsky RA. An evaluation of single nucleotide polymorphisms in the human aryl hydrocarbon receptor-interacting protein (*AIP*) gene. *Drug Metab Pharmacokinet.* 2011;26(4):431-439.
638. Ceccato F, Occhi G, Albiger NM, Rizzati S, Ferasin S, Trivellin G, Mantero F, Scaroni C. Adrenal lesions in acromegaly: do metabolic aspects and aryl hydrocarbon receptor interacting protein gene have a role? Evaluation at baseline and after long-term follow-up. *J Endocrinol Invest.* 2011;34(5):353-360.
639. Cai F, Zhang YD, Zhao X, Yang YK, Ma SH, Dai CX, Liu XH, Yao Y, Feng M, Wei JJ, Xing B, Jiao YH, Wei ZQ, Yin ZM, Zhang B, Gu F, Wang RZ. Screening for *AIP* gene mutations in a Han Chinese pituitary adenoma cohort followed by LOH analysis. *Eur J Endocrinol.* 2013;169(6):867-884.
640. Iwata T, Yamada S, Mizusawa N, Golam HM, Sano T, Yoshimoto K. The aryl hydrocarbon receptor-interacting protein gene is rarely mutated in sporadic GH-secreting adenomas. *Clin Endocrinol (Oxf).* 2007;66(4):499-502.
641. Hardy-Weinberg Equilibrium Calculator. http://www.koonec.com/k-blog/2010/06/20/hardy-weinberg-equilibrium-calculator/. Accessed 1/3/2014.
642. Popovic V, Damjanovic S, Micic D, Nesovic M, Djurovic M, Petakov M, Obradovic S, Zoric S, Simic M, Penezic Z, Marinkovic J. Increased incidence of neoplasia in patients with pituitary adenomas. The Pituitary Study Group. *Clin Endocrinol (Oxf).* 1998;49(4):441-445.
643. Hemminki K, Forsti A, Ji J. Incidence and familial risks in pituitary adenoma and associated tumors. *Endocr Relat Cancer.* 2007;14(1):103-109.
644. Schofl C, Honegger J, Droste M, Grussendorf M, Finke R, Plockinger U, Berg C, Willenberg HS, Lammert A, Klingmuller D, Jaursch-Hancke C, Tonjes A, Schneidewind S, Flitsch J, Bullmann C, Dimopoulou C, Stalla G, Mayr B, Hoeppner W, Schopohl J. Frequency of *AIP* gene mutations in young patients with acromegaly: a registry-based study. *J Clin Endocrinol Metab.* 2014;99(12):E2789-E2793.
645. Iacovazzo D, Bianchi A, Lugli F, Milardi D, Giampietro A, Lucci-Cordisco E, Doglietto F, Lauriola L, De ML. Double pituitary adenomas. *Endocrine.* 2013;43(2):452-457.
646. Kannuki S, Matsumoto K, Sano T, Shintani Y, Bando H, Saito S. Double pituitary adenoma--two case reports. *Neurol Med Chir (Tokyo).* 1996;36(11):818-821.
647. Ratliff JK, Oldfield EH. Multiple pituitary adenomas in Cushing's disease. *J Neurosurg.* 2000;93(5):753-761.
648. Sahdev A, Jager R. Bilateral pituitary adenomas occurring with multiple endocrine neoplasia type one. *AJNR Am J Neuroradiol.* 2000;21(6):1067-1069.
649. Kim K, Yamada S, Usui M, Sano T. Preoperative identification of clearly separated double pituitary adenomas. *Clin Endocrinol (Oxf).* 2004;61(1):26-30.
650. Villa C, Lagonigro MS, Magri F, Koziak M, Jaffrain-Rea ML, Brauner R, Bouligand J, Junier MP, Di RF, Sainte-Rose C, Beckers A, Roux FX, Daly AF, Chiovato L.

Hyperplasia-adenoma sequence in pituitary tumorigenesis related to aryl hydrocarbon receptor interacting protein gene mutation. *Endocr Relat Cancer.* 2011;18(3):347-356.

651. Mazal PR, Czech T, Sedivy R, Aichholzer M, Wanschitz J, Klupp N, Budka H. Prognostic relevance of intracytoplasmic cytokeratin pattern, hormone expression profile, and cell proliferation in pituitary adenomas of akromegalic patients. *Clin Neuropathol.* 2001;20(4):163-171.
652. Obari A, Sano T, Ohyama K, Kudo E, Qian ZR, Yoneda A, Rayhan N, Mustafizur RM, Yamada S. Clinicopathological features of growth hormone-producing pituitary adenomas: difference among various types defined by cytokeratin distribution pattern including a transitional form. *Endocr Pathol.* 2008;19(2):82-91.
653. Bakhtiar Y, Hirano H, Arita K, Yunoue S, Fujio S, Tominaga A, Sakoguchi T, Sugiyama K, Kurisu K, Yasufuku-Takano J, Takano K. Relationship between cytokeratin staining patterns and clinico-pathological features in somatotropinomae. *Eur J Endocrinol.* 2010;163(4):531-539.
654. Kato M, Inoshita N, Sugiyama T, Tani Y, Shichiri M, Sano T, Yamada S, Hirata Y. Differential expression of genes related to drug responsiveness between sparsely and densely granulated somatotroph adenomas. *Endocr J.* 2012;59(3):221-228.
655. Brzana J, Yedinak CG, Gultekin SH, Delashaw JB, Fleseriu M. Growth hormone granulation pattern and somatostatin receptor subtype 2A correlate with postoperative somatostatin receptor ligand response in acromegaly: a large single center experience. *Pituitary.* 2013;16(4):490-498.
656. Xekouki P, Mastroyiannis SA, Avgeropoulos D, de la Luz SM, Trivellin G, Gourgari EA, Lyssikatos C, Quezado M, Patronas N, Kanaka-Gantenbein C, Chrousos GP, Stratakis CA. Familial pituitary apoplexy as the only presentation of a novel *AIP* mutation. *Endocr Relat Cancer.* 2013;20(5):L11-L14.
657. Thakker RV, Newey PJ, Walls GV, Bilezikian J, Dralle H, Ebeling PR, Melmed S, Sakurai A, Tonelli F, Brandi ML. Clinical practice guidelines for multiple endocrine neoplasia type 1 (MEN1). *J Clin Endocrinol Metab.* 2012;97(9):2990-3011.
658. Johnson MC, Codner E, Eggers M, Mosso L, Rodriguez JA, Cassorla F. Gps mutations in Chilean patients harboring growth hormone-secreting pituitary tumors. *J Pediatr Endocrinol Metab.* 1999;12(3):381-387.
659. Metzler M, Luedecke DK, Saeger W, Grueters A, Haberl H, Kiess W, Repp R, Rascher W, Doetsch J. Low prevalence of Gs alpha mutations in somatotroph adenomas of children and adolescents. *Cancer Genet Cytogenet.* 2006;166(2):146-151.
660. Murray IA, Patterson AD, Perdew GH. Aryl hydrocarbon receptor ligands in cancer: friend and foe. *Nat Rev Cancer.* 2014;14(12):801-814.
661. Cannavo S, Ferrau F, Ragonese M, Curto L, Torre ML, Magistri M, Marchese A, Alibrandi A, Trimarchi F. Increased prevalence of acromegaly in a highly polluted area. *Eur J Endocrinol.* 2010;163(4):509-513.

662. Cannavo S, Ferrau F, Ragonese M, Romeo PD, Torre ML, Puglisi S, De ME, Arnaldi G, Salpietro C, Cotta OR, Albani A, Ruggeri RM, Trimarchi F. Increased frequency of the rs2066853 variant of aryl hydrocarbon receptor gene in patients with acromegaly. *Clin Endocrinol (Oxf).* 2014;81(2):249-253.
663. Zhan X, Desiderio DM. Signaling pathway networks mined from human pituitary adenoma proteomics data. *BMC Med Genomics.* 2010;3:13.
664. Terpe K. Overview of bacterial expression systems for heterologous protein production: from molecular and biochemical fundamentals to commercial systems. *Appl Microbiol Biotechnol.* 2006;72(2):211-222.
665. Wilson CJ, Zhan H, Swint-Kruse L, Matthews KS. The lactose repressor system: paradigms for regulation, allosteric behavior and protein folding. *Cell Mol Life Sci.* 2007;64(1):3-16.
666. Agilent Technologies.QuikChange Primer Design tool. http://www.genomics.agilent.com/primerDesignProgram.jsp. Accessed 17/9/2014.
667. Detection of protein-protein interactions using the GST fusion protein pull-down technique. *Nat Methods.* 2004;1(3):275-276.
668. Thompson A, Schafer J, Kuhn K, Kienle S, Schwarz J, Schmidt G, Neumann T, Johnstone R, Mohammed AK, Hamon C. Tandem mass tags: a novel quantification strategy for comparative analysis of complex protein mixtures by MS/MS. *Anal Chem.* 2003;75(8):1895-1904.
669. Perkins DN, Pappin DJ, Creasy DM, Cottrell JS. Probability-based protein identification by searching sequence databases using mass spectrometry data. *Electrophoresis.* 1999;20(18):3551-3567.
670. QIAGEN.Ingenuity Pathways Analysis. www.qiagen.com/ingenuity. Accessed 17/12/2013.
671. Untergasser A, Cutcutache I, Koressaar T, Ye J, Faircloth BC, Remm M, Rozen SG. Primer3--new capabilities and interfaces. *Nucleic Acids Res.* 2012;40(15):e115.
672. Schneider CA, Rasband WS, Eliceiri KW. NIH Image to ImageJ: 25 years of image analysis. *Nat Methods.* 2012;9(7):671-675.
673. Bolte S, Cordelieres FP. A guided tour into subcellular colocalization analysis in light microscopy. *J Microsc.* 2006;224(Pt 3):213-232.
674. Dunn KW, Kamocka MM, McDonald JH. A practical guide to evaluating colocalization in biological microscopy. *Am J Physiol Cell Physiol.* 2011;300(4):C723-C742.
675. Kampinga HH, Hageman J, Vos MJ, Kubota H, Tanguay RM, Bruford EA, Cheetham ME, Chen B, Hightower LE. Guidelines for the nomenclature of the human heat shock proteins. *Cell Stress Chaperones.* 2009;14(1):105-111.
676. Sreedhar AS, Kalmar E, Csermely P, Shen YF. Hsp90 isoforms: functions, expression and clinical importance. *FEBS Lett.* 2004;562(1-3):11-15.

677. Laitusis AL, Brostrom MA, Brostrom CO. The dynamic role of GRP78/BiP in the coordination of mRNA translation with protein processing. *J Biol Chem.* 1999;274(1):486-493.
678. Wadhwa R, Taira K, Kaul SC. An Hsp70 family chaperone, mortalin/mthsp70/PBP74/Grp75: what, when, and where? *Cell Stress Chaperones.* 2002;7(3):309-316.
679. Lu WJ, Lee NP, Kaul SC, Lan F, Poon RT, Wadhwa R, Luk JM. Mortalin-p53 interaction in cancer cells is stress dependent and constitutes a selective target for cancer therapy. *Cell Death Differ.* 2011;18(6):1046-1056.
680. Leandro-Garcia LJ, Leskela S, Landa I, Montero-Conde C, Lopez-Jimenez E, Leton R, Cascon A, Robledo M, Rodriguez-Antona C. Tumoral and tissue-specific expression of the major human beta-tubulin isotypes. *Cytoskeleton (Hoboken).* 2010;67(4):214-223.
681. Kavallaris M. Microtubules and resistance to tubulin-binding agents. *Nat Rev Cancer.* 2010;10(3):194-204.
682. Staiger CJ, Blanchoin L. Actin dynamics: old friends with new stories. *Curr Opin Plant Biol.* 2006;9(6):554-562.
683. Huang Z, Zhuo Y, Shen Z, Wang Y, Wang L, Li H, Chen J, Chen W. The role of NEFL in cell growth and invasion in head and neck squamous cell carcinoma cell lines. *J Oral Pathol Med.* 2014;43(3):191-198.
684. Bernstein BW, Bamburg JR. ADF/cofilin: a functional node in cell biology. *Trends Cell Biol.* 2010;20(4):187-195.
685. Lapierre LA, Tuma PL, Navarre J, Goldenring JR, Anderson JM. VAP-33 localizes to both an intracellular vesicle population and with occludin at the tight junction. *J Cell Sci.* 1999;112 (Pt 21):3723-3732.
686. Weir ML, Klip A, Trimble WS. Identification of a human homologue of the vesicle-associated membrane protein (VAMP)-associated protein of 33 kDa (VAP-33): a broadly expressed protein that binds to VAMP. *Biochem J.* 1998;333 (Pt 2):247-251.
687. Oppermann U. Carbonyl reductases: the complex relationships of mammalian carbonyl- and quinone-reducing enzymes and their role in physiology. *Annu Rev Pharmacol Toxicol.* 2007;47:293-322.
688. Matassa DS, Amoroso MR, Agliarulo I, Maddalena F, Sisinni L, Paladino S, Romano S, Romano MF, Sagar V, Loreni F, Landriscina M, Esposito F. Translational control in the stress adaptive response of cancer cells: a novel role for the heat shock protein TRAP1. *Cell Death Dis.* 2013;4:e851.
689. Koonin EV, Mushegian AR, Tatusov RL, Altschul SF, Bryant SH, Bork P, Valencia A. Eukaryotic translation elongation factor 1 gamma contains a glutathione transferase domain--study of a diverse, ancient protein superfamily using motif search and structural modeling. *Protein Sci.* 1994;3(11):2045-2054.

690. Pan LX, Chen ZP, Liu YS, Zhao JH. Magnetic resonance imaging and biological markers in pituitary adenomas with invasion of the cavernous sinus space. *J Neurooncol.* 2005;74(1):71-76.
691. Goh G, Scholl UI, Healy JM, Choi M, Prasad ML, Nelson-Williams C, Kunstman JW, Korah R, Suttorp AC, Dietrich D, Haase M, Willenberg HS, Stalberg P, Hellman P, Akerstrom G, Bjorklund P, Carling T, Lifton RP. Recurrent activating mutation in *PRKACA* in cortisol-producing adrenal tumors. *Nat Genet.* 2014;46(6):613-617.
692. Gingras AC, Gstaiger M, Raught B, Aebersold R. Analysis of protein complexes using mass spectrometry. *Nat Rev Mol Cell Biol.* 2007;8(8):645-654.
693. Parrish JR, Gulyas KD, Finley RL, Jr. Yeast two-hybrid contributions to interactome mapping. *Curr Opin Biotechnol.* 2006;17(4):387-393.
694. Berggard T, Linse S, James P. Methods for the detection and analysis of protein-protein interactions. *Proteomics.* 2007;7(16):2833-2842.
695. Paul FE, Hosp F, Selbach M. Analyzing protein-protein interactions by quantitative mass spectrometry. *Methods.* 2011;54(4):387-395.
696. Gavin AC, Maeda K, Kuhner S. Recent advances in charting protein-protein interaction: mass spectrometry-based approaches. *Curr Opin Biotechnol.* 2011;22(1):42-49.
697. Aebersold R, Mann M. Mass spectrometry-based proteomics. *Nature.* 2003;422(6928):198-207.
698. Han X, Aslanian A, Yates JR, III. Mass spectrometry for proteomics. *Curr Opin Chem Biol.* 2008;12(5):483-490.
699. Chait BT. Chemistry. Mass spectrometry: bottom-up or top-down? *Science.* 2006;314(5796):65-66.
700. Dayon L, Hainard A, Licker V, Turck N, Kuhn K, Hochstrasser DF, Burkhard PR, Sanchez JC. Relative quantification of proteins in human cerebrospinal fluids by MS/MS using 6-plex isobaric tags. *Anal Chem.* 2008;80(8):2921-2931.
701. Kontogeorgos G, Stefaneanu L, Kovacs K. Stress-response proteins in human pituitary adenomas. Expression of heat-shock protein 72 (HSP-72). *Endocrine.* 1997;6(1):25-29.
702. Fu Y, Lee AS. Glucose regulated proteins in cancer progression, drug resistance and immunotherapy. *Cancer Biol Ther.* 2006;5(7):741-744.
703. Ma Y, Hendershot LM. The role of the unfolded protein response in tumour development: friend or foe? *Nat Rev Cancer.* 2004;4(12):966-977.
704. Zhu G, Lee AS. Role of the unfolded protein response, GRP78 and GRP94 in organ homeostasis. *J Cell Physiol.* 2015;230(7):1413-1420.
705. Uckun FM, Qazi S, Ozer Z, Garner AL, Pitt J, Ma H, Janda KD. Inducing apoptosis in chemotherapy-resistant B-lineage acute lymphoblastic leukaemia cells by targeting HSPA5, a master regulator of the anti-apoptotic unfolded protein response signalling network. *Br J Haematol.* 2011;153(6):741-752.

706. Chen KD, Chen LY, Huang HL, Lieu CH, Chang YN, Chang MD, Lai YK. Involvement of p38 mitogen-activated protein kinase signaling pathway in the rapid induction of the 78-kDa glucose-regulated protein in 9L rat brain tumor cells. *J Biol Chem.* 1998;273(2):749-755.
707. Misra UK, Deedwania R, Pizzo SV. Activation and cross-talk between Akt, NF-kappaB, and unfolded protein response signaling in 1-LN prostate cancer cells consequent to ligation of cell surface-associated GRP78. *J Biol Chem.* 2006;281(19):13694-13707.
708. Chang YW, Chen HA, Tseng CF, Hong CC, Ma JT, Hung MC, Wu CH, Huang MT, Su JL. De-acetylation and degradation of HSPA5 is critical for E1A metastasis suppression in breast cancer cells. *Oncotarget.* 2014;5(21):10558-10570.
709. Booth L, Roberts JL, Tavallai M, Nourbakhsh A, Chuckalovcak J, Carter J, Poklepovic A, Dent P. OSU-03012 and Viagra Treatment Inhibits the Activity of Multiple Chaperone Proteins and Disrupts the Blood-Brain Barrier: Implications for Anti-Cancer Therapies. *J Cell Physiol.* 2015;230(8):1982-1998.
710. Gonzalez-Gronow M, Selim MA, Papalas J, Pizzo SV. GRP78: a multifunctional receptor on the cell surface. *Antioxid Redox Signal.* 2009;11(9):2299-2306.
711. Misra UK, Gonzalez-Gronow M, Gawdi G, Pizzo SV. The role of MTJ-1 in cell surface translocation of GRP78, a receptor for alpha 2-macroglobulin-dependent signaling. *J Immunol.* 2005;174(4):2092-2097.
712. Wadhwa R, Yaguchi T, Hasan MK, Taira K, Kaul SC. Mortalin-MPD (mevalonate pyrophosphate decarboxylase) interactions and their role in control of cellular proliferation. *Biochem Biophys Res Commun.* 2003;302(4):735-742.
713. Starenki D, Hong SK, Lloyd RV, Park JI. Mortalin (GRP75/HSPA9) upregulation promotes survival and proliferation of medullary thyroid carcinoma cells. *Oncogene.* 2014.
714. Wadhwa R, Ryu J, Ahn HM, Saxena N, Chaudhary A, Yun CO, Kaul SC. Functional significance of point mutations in stress chaperone mortalin and their relevance to Parkinson disease. *J Biol Chem.* 2015;290(13):8447-8456.
715. Wadhwa R, Takano S, Kaur K, Deocaris CC, Pereira-Smith OM, Reddel RR, Kaul SC. Upregulation of mortalin/mthsp70/Grp75 contributes to human carcinogenesis. *Int J Cancer.* 2006;118(12):2973-2980.
716. Ma Z, Izumi H, Kanai M, Kabuyama Y, Ahn NG, Fukasawa K. Mortalin controls centrosome duplication via modulating centrosomal localization of p53. *Oncogene.* 2006;25(39):5377-5390.
717. Wadhwa R, Takano S, Robert M, Yoshida A, Nomura H, Reddel RR, Mitsui Y, Kaul SC. Inactivation of tumor suppressor p53 by mot-2, a hsp70 family member. *J Biol Chem.* 1998;273(45):29586-29591.
718. Wu PK, Hong SK, Veeranki S, Karkhanis M, Starenki D, Plaza JA, Park JI. A mortalin/HSPA9-mediated switch in tumor-suppressive signaling of

Raf/MEK/extracellular signal-regulated kinase. *Mol Cell Biol.* 2013;33(20):4051-4067.

719. Ryu J, Kaul Z, Yoon AR, Liu Y, Yaguchi T, Na Y, Ahn HM, Gao R, Choi IK, Yun CO, Kaul SC, Wadhwa R. Identification and functional characterization of nuclear mortalin in human carcinogenesis. *J Biol Chem.* 2014;289(36):24832-24844.
720. Krysiak K, Tibbitts JF, Shao J, Liu T, Ndonwi M, Walter MJ. Reduced levels of Hspa9 attenuate Stat5 activation in mouse B cells. *Exp Hematol.* 2015;43(4):319-330.
721. Riebold M, Kozany C, Freiburger L, Sattler M, Buchfelder M, Hausch F, Stalla GK, Paez-Pereda M. A C-terminal HSP90 inhibitor restores glucocorticoid sensitivity and relieves a mouse allograft model of Cushing disease. *Nat Med.* 2015;21(3):276-280.
722. Rosenberg D, Groussin L, Jullian E, Perlemoine K, Bertagna X, Bertherat J. Role of the PKA-regulated transcription factor CREB in development and tumorigenesis of endocrine tissues. *Ann N Y Acad Sci.* 2002;968:65-74.
723. Griffioen G, Thevelein JM. Molecular mechanisms controlling the localisation of protein kinase A. *Curr Genet.* 2002;41(4):199-207.
724. Schernthaner-Reiter MH, Trivellin G, Hernández-Ramírez LC, Korbonits M, Stratakis C. Interaction between AIP and the cAMP-dependent protein kinase (PKA) pathway in pituitary tumor formation [abstract]. *Endocr Rev* 2015;SAT-427.
725. Galigniana MD, Radanyi C, Renoir JM, Housley PR, Pratt WB. Evidence that the peptidylprolyl isomerase domain of the hsp90-binding immunophilin FKBP52 is involved in both dynein interaction and glucocorticoid receptor movement to the nucleus. *J Biol Chem.* 2001;276(18):14884-14889.
726. Galigniana MD, Harrell JM, Murphy PJ, Chinkers M, Radanyi C, Renoir JM, Zhang M, Pratt WB. Binding of hsp90-associated immunophilins to cytoplasmic dynein: direct binding and in vivo evidence that the peptidylprolyl isomerase domain is a dynein interaction domain. *Biochemistry.* 2002;41(46):13602-13610.
727. Garnham CP, Roll-Mecak A. The chemical complexity of cellular microtubules: tubulin post-translational modification enzymes and their roles in tuning microtubule functions. *Cytoskeleton (Hoboken).* 2012;69(7):442-463.
728. Akhmanova A, Steinmetz MO. Tracking the ends: a dynamic protein network controls the fate of microtubule tips. *Nat Rev Mol Cell Biol.* 2008;9(4):309-322.
729. Kalluri R, Weinberg RA. The basics of epithelial-mesenchymal transition. *J Clin Invest.* 2009;119(6):1420-1428.
730. Lekva T, Berg JP, Fougner SL, Olstad OK, Ueland T, Bollerslev J. Gene expression profiling identifies ESRP1 as a potential regulator of epithelial mesenchymal transition in somatotroph adenomas from a large cohort of patients with acromegaly. *J Clin Endocrinol Metab.* 2012;97(8):E1506-E1514.
731. Tavanez JP, Valcarcel J. A splicing mastermind for EMT. *EMBO J.* 2010;29(19):3217-3218.

732. Berndsen CE, Wolberger C. New insights into ubiquitin E3 ligase mechanism. *Nat Struct Mol Biol.* 2014;21(4):301-307.
733. Lee EK, Diehl JA. SCFs in the new millennium. *Oncogene.* 2014;33(16):2011-2018.
734. Sandoval D, Hill S, Ziemba A, Lewis S, Kuhlman B, Kleiger G. Ubiquitin-conjugating enzyme Cdc34 and ubiquitin ligase Skp1-cullin-F-box ligase (SCF) interact through multiple conformations. *J Biol Chem.* 2015;290(2):1106-1118.
735. Jin J, Cardozo T, Lovering RC, Elledge SJ, Pagano M, Harper JW. Systematic analysis and nomenclature of mammalian F-box proteins. *Genes Dev.* 2004;18(21):2573-2580.
736. Chen BB, Coon TA, Glasser JR, McVerry BJ, Zhao J, Zhao Y, Zou C, Ellis B, Sciurba FC, Zhang Y, Mallampalli RK. A combinatorial F box protein directed pathway controls TRAF adaptor stability to regulate inflammation. *Nat Immunol.* 2013;14(5):470-479.
737. Li D, Xie P, Zhao F, Shu J, Li L, Zhan Y, Zhang L. F-box protein Fbxo3 targets Smurf1 ubiquitin ligase for ubiquitination and degradation. *Biochem Biophys Res Commun.* 2015;458(4):941-945.
738. Shima Y, Shima T, Chiba T, Irimura T, Pandolfi PP, Kitabayashi I. PML activates transcription by protecting HIPK2 and p300 from SCFFbx3-mediated degradation. *Mol Cell Biol.* 2008;28(23):7126-7138.
739. Steeg PS, Bevilacqua G, Kopper L, Thorgeirsson UP, Talmadge JE, Liotta LA, Sobel ME. Evidence for a novel gene associated with low tumor metastatic potential. *J Natl Cancer Inst.* 1988;80(3):200-204.
740. Takacs-Vellai K. The metastasis suppressor Nm23 as a modulator of Ras/ERK signaling. *J Mol Signal.* 2014;9:4.
741. Tong Y, Yung LY, Wong YH. Metastasis suppressors Nm23H1 and Nm23H2 differentially regulate neoplastic transformation and tumorigenesis. *Cancer Lett.* 2015;361(2):207-217.
742. Tso PH, Wang Y, Yung LY, Tong Y, Lee MM, Wong YH. RGS19 inhibits Ras signaling through Nm23H1/2-mediated phosphorylation of the kinase suppressor of Ras. *Cell Signal.* 2013;25(5):1064-1074.
743. Berney CR, Fisher RJ, Yang J, Russell PJ, Crowe PJ. Genomic alterations (LOH, MI) on chromosome 17q21-23 and prognosis of sporadic colorectal cancer. *Int J Cancer.* 2000;89(1):1-7.
744. Boissan M, Lacombe ML. Learning about the functions of NME/NM23: lessons from knockout mice to silencing strategies. *Naunyn Schmiedebergs Arch Pharmacol.* 2011;384(4-5):421-431.
745. Boissan M, De WO, Lizarraga F, Wendum D, Poincloux R, Chignard N, Desbois-Mouthon C, Dufour S, Nawrocki-Raby B, Birembaut P, Bracke M, Chavrier P, Gespach C, Lacombe ML. Implication of metastasis suppressor NM23-H1 in

maintaining adherens junctions and limiting the invasive potential of human cancer cells. *Cancer Res.* 2010;70(19):7710-7722.

746. Papa L, Manfredi G, Germain D. SOD1, an unexpected novel target for cancer therapy. *Genes Cancer.* 2014;5(1-2):15-21.

747. Rosen DR, Siddique T, Patterson D, Figlewicz DA, Sapp P, Hentati A, Donaldson D, Goto J, O'Regan JP, Deng HX, . Mutations in Cu/Zn superoxide dismutase gene are associated with familial amyotrophic lateral sclerosis. *Nature.* 1993;362(6415):59-62.

748. Glasauer A, Sena LA, Diebold LP, Mazar AP, Chandel NS. Targeting SOD1 reduces experimental non-small-cell lung cancer. *J Clin Invest.* 2014;124(1):117-128.

749. Secondo A, De MM, Zirpoli L, Santillo M, Mondola P. The Cu-Zn superoxide dismutase (SOD1) inhibits ERK phosphorylation by muscarinic receptor modulation in rat pituitary GH3 cells. *Biochem Biophys Res Commun.* 2008;376(1):143-147.

750. Hubina E, Nanzer AM, Hanson MR, Ciccarelli E, Losa M, Gaia D, Papotti M, Terreni MR, Khalaf S, Jordan S, Czirjak S, Hanzely Z, Nagy GM, Goth MI, Grossman AB, Korbonits M. Somatostatin analogues stimulate p27 expression and inhibit the MAP kinase pathway in pituitary tumours. *Eur J Endocrinol.* 2006;155(2):371-379.

751. Thusberg J, Olatubosun A, Vihinen M. Performance of mutation pathogenicity prediction methods on missense variants. *Hum Mutat.* 2011;32(4):358-368.

752. MacArthur DG, Manolio TA, Dimmock DP, Rehm HL, Shendure J, Abecasis GR, Adams DR, Altman RB, Antonarakis SE, Ashley EA, Barrett JC, Biesecker LG, Conrad DF, Cooper GM, Cox NJ, Daly MJ, Gerstein MB, Goldstein DB, Hirschhorn JN, Leal SM, Pennacchio LA, Stamatoyannopoulos JA, Sunyaev SR, Valle D, Voight BF, Winckler W, Gunter C. Guidelines for investigating causality of sequence variants in human disease. *Nature.* 2014;508(7497):469-476.

753. Murthy SK, DiFrancesco LM, Ogilvie RT, Demetrick DJ. Loss of heterozygosity associated with uniparental disomy in breast carcinoma. *Mod Pathol.* 2002;15(12):1241-1250.

754. Walker DR, Bond JP, Tarone RE, Harris CC, Makalowski W, Boguski MS, Greenblatt MS. Evolutionary conservation and somatic mutation hotspot maps of *p53*: correlation with p53 protein structural and functional features. *Oncogene.* 1999;18(1):211-218.

755. DePristo MA, Weinreich DM, Hartl DL. Missense meanderings in sequence space: a biophysical view of protein evolution. *Nat Rev Genet.* 2005;6(9):678-687.

756. Canaff L, Vanbellinghen JF, Kanazawa I, Kwak H, Garfield N, Vautour L, Hendy GN. Menin missense mutants encoded by the *MEN1* gene that are targeted to the proteasome: restoration of expression and activity by CHIP siRNA. *J Clin Endocrinol Metab.* 2012;97(2):E282-E291.

757. Artimo P, Jonnalagedda M, Arnold K, Baratin D, Csardi G, de CE, Duvaud S, Flegel V, Fortier A, Gasteiger E, Grosdidier A, Hernandez C, Ioannidis V, Kuznetsov D, Liechti R, Moretti S, Mostaguir K, Redaschi N, Rossier G, Xenarios I, Stockinger H. ExPASy: SIB bioinformatics resource portal. *Nucleic Acids Res.* 2012;40(Web Server issue):W597-W603.
758. Garcia-Arnes JA, Gonzalez-Molero I, Oriola J, Mazuecos N, Luque R, Castano J, Arraez MA. Familial isolated pituitary adenoma caused by a *Aip* gene mutation not described before in a family context. *Endocr Pathol.* 2013;24(4):234-238.
759. Schwanhausser B, Busse D, Li N, Dittmar G, Schuchhardt J, Wolf J, Chen W, Selbach M. Global quantification of mammalian gene expression control. *Nature.* 2011;473(7347):337-342.
760. Alvarez-Castelao B, Ruiz-Rivas C, Castano JG. A critical appraisal of quantitative studies of protein degradation in the framework of cellular proteostasis. *Biochem Res Int.* 2012;2012:823597.
761. Zhou P. Determining protein half-lives. *Methods Mol Biol.* 2004;284:67-77.
762. Hillman RT, Green RE, Brenner SE. An unappreciated role for RNA surveillance. *Genome Biol.* 2004;5(2):R8.
763. Schneider-Poetsch T, Ju J, Eyler DE, Dang Y, Bhat S, Merrick WC, Green R, Shen B, Liu JO. Inhibition of eukaryotic translation elongation by cycloheximide and lactimidomycin. *Nat Chem Biol.* 2010;6(3):209-217.
764. Dai CL, Shi J, Chen Y, Iqbal K, Liu F, Gong CX. Inhibition of protein synthesis alters protein degradation through activation of protein kinase B (AKT). *J Biol Chem.* 2013;288(33):23875-23883.
765. Wang X, Terpstra EJ. Ubiquitin receptors and protein quality control. *J Mol Cell Cardiol.* 2013;55:73-84.
766. Doyle SM, Genest O, Wickner S. Protein rescue from aggregates by powerful molecular chaperone machines. *Nat Rev Mol Cell Biol.* 2013;14(10):617-629.
767. Feng Y, Yao Z, Klionsky DJ. How to control self-digestion: transcriptional, post-transcriptional, and post-translational regulation of autophagy. *Trends Cell Biol.* 2015.
768. Myung J, Kim KB, Crews CM. The ubiquitin-proteasome pathway and proteasome inhibitors. *Med Res Rev.* 2001;21(4):245-273.
769. van Wijk SJ, Timmers HT. The family of ubiquitin-conjugating enzymes (E2s): deciding between life and death of proteins. *FASEB J.* 2010;24(4):981-993.
770. Cyr DM, Hohfeld J, Patterson C. Protein quality control: U-box-containing E3 ubiquitin ligases join the fold. *Trends Biochem Sci.* 2002;27(7):368-375.
771. Coscoy L, Ganem D. PHD domains and E3 ubiquitin ligases: viruses make the connection. *Trends Cell Biol.* 2003;13(1):7-12.
772. Bhattacharyya S, Yu H, Mim C, Matouschek A. Regulated protein turnover: snapshots of the proteasome in action. *Nat Rev Mol Cell Biol.* 2014;15(2):122-133.

773. Moore BS, Eustaquio AS, McGlinchey RP. Advances in and applications of proteasome inhibitors. *Curr Opin Chem Biol.* 2008;12(4):434-440.
774. Meusser B, Hirsch C, Jarosch E, Sommer T. ERAD: the long road to destruction. *Nat Cell Biol.* 2005;7(8):766-772.
775. Ochocka AM, Kampanis P, Nicol S, Allende-Vega N, Cox M, Marcar L, Milne D, Fuller-Pace F, Meek D. FKBP25, a novel regulator of the p53 pathway, induces the degradation of MDM2 and activation of p53. *FEBS Lett.* 2009;583(4):621-626.
776. Jeong K, Kim H, Kim K, Kim SJ, Hahn BS, Jahng GH, Yoon KS, Kim SS, Ha J, Kang I, Choe W. Cyclophilin B is involved in p300-mediated degradation of CHOP in tumor cell adaptation to hypoxia. *Cell Death Differ.* 2014;21(3):438-450.
777. Hidalgo-de-Quintana J, Evans RJ, Cheetham ME, van der Spuy J. The Leber congenital amaurosis protein AIPL1 functions as part of a chaperone heterocomplex. *Invest Ophthalmol Vis Sci.* 2008;49(7):2878-2887.
778. Matsumura Y, Sakai J, Skach WR. Endoplasmic reticulum protein quality control is determined by cooperative interactions between Hsp/c70 protein and the CHIP E3 ligase. *J Biol Chem.* 2013;288(43):31069-31079.
779. Egeler EL, Urner LM, Rakhit R, Liu CW, Wandless TJ. Ligand-switchable substrates for a ubiquitin-proteasome system. *J Biol Chem.* 2011;286(36):31328-31336.
780. Valastyan JS, Lindquist S. Mechanisms of protein-folding diseases at a glance. *Dis Model Mech.* 2014;7(1):9-14.
781. Payne SR, Kemp CJ. Tumor suppressor genetics. *Carcinogenesis.* 2005;26(12):2031-2045.
782. Nagamura Y, Yamazaki M, Shimazu S, Tsukada T, Sakurai A. Application of an intracellular stability test of a novel missense menin mutant to the diagnosis of multiple endocrine neoplasia type 1. *Endocr J.* 2012;59(12):1093-1098.
783. Popovic D, Vucic D, Dikic I. Ubiquitination in disease pathogenesis and treatment. *Nat Med.* 2014;20(11):1242-1253.
784. Goldberg AL. Development of proteasome inhibitors as research tools and cancer drugs. *J Cell Biol.* 2012;199(4):583-588.
785. Nalepa G, Rolfe M, Harper JW. Drug discovery in the ubiquitin-proteasome system. *Nat Rev Drug Discov.* 2006;5(7):596-613.
786. Dou QP, Zonder JA. Overview of proteasome inhibitor-based anti-cancer therapies: perspective on bortezomib and second generation proteasome inhibitors versus future generation inhibitors of ubiquitin-proteasome system. *Curr Cancer Drug Targets.* 2014;14(6):517-536.

Appendix 1: Supplementary mass spectrometry results

Table 25. Qualitative mass spectrometry results after manual validation

#	Protein description (gene name)	UniProt entry	Mass (kDa)[483]	Protein ID probability	% of total spectra	Assigned spectra	Unique peptides	Unique spectra	Coverage	Best Mascot ion score	Calculated +1H peptide mass (AMU)
1	AIP_RAT AH receptor-interacting protein (*Aip)*	Q5FWY5	37.6	100%	0.2%	223	29	42	41.0%		
	AHAAVWNAQEAQADFAK									89.6	1827.9
	AHAAVWNAQEAQADFAKVLELDPALAPVVSR									47	3516.9
	AKAVPLIHQEGNR									27.3	1662.0
	AVPLIHQEGNR									41.2	1233.7
	DPLEGQR									31.4	814.4
	EAAAKYYDAIACLK									34.5	1816.0
	EAAAKYYDAIACLKNLQMK									51.1	2675.4
	EDGIQK									24.1	918.5
	FRGIFSH									26.4	863.5
	GELPEFQDGTK									23.4	1449.7
	GKAHAAVWNAQEAQADFAK									81.2	2242.2
	GKAHAAVWNAQEAQADFAKVLELDPALAPVVSR									83.6	3702.0
	GKPMELIIGK									48.6	1101.6
	GKPMELIIGKK									35.1	1442.9
	IRQKDEEDKAR									27.6	1616.9
	LREDGIQK									24.5	958.5
	LREDGIQKR									41	1114.6
	MADLIAR									47.5	789.4
	QKDEEDK									26	1103.5
	QKDEEDKAR									45.9	1330.7

#	Protein description (gene name)	UniProt entry	Mass (kDa)[483]	Protein ID probability	% of total spectra	Assigned spectra	Unique peptides	Unique spectra	Coverage	Best Mascot ion score	Calculated +1H peptide mass (AMU)
	RGKAHAAVWNAQEAQADFAK									42.4	2398.3
	VESPGTYQQDPWAMTDEEK									50.7	2226.9
	VESPGTYQQDPWAMTDEEKAK									77.4	2655.2
	VIQEGR									41.7	701.4
	VLELDPALAPVVSR									67.7	1478.9
	VLELDPALAPVVSRELR									43.8	1877.1
	YDDNVKAYFK									21	1491.8
	YYDAIACLK									42.9	1116.5
	YYDAIACLKNLQMK									48.2	1960.0
2	GSTP1_RAT Glutathione S-transferase P (*Gstp1)*	P04906	23.4	100%	0.2%	135	22	33	70.0%		
	AFLSSPDHLNRPINGNGK									30.3	1937.0
	AFLSSPDHLNRPINGNGKQ									21.5	2294.2
	ALPGHLKPFETLLSQNQGGK									46.6	2364.3
	CKYGTLIYTNYENGK									55.7	2053.0
	CKYGTLIYTNYENGKDDYVK									60.9	2673.3
	DQKEAALVDMVNDGVEDLR									93	2346.2
	EAALVDMVNDGVEDLR									123	1761.8
	FEDGDLTLYQSNAILR									112	1854.9
	FEDGDLTLYQSNAILRHLGR									46.4	2318.2
	IKAFLSSPDHLNRPINGNGK									22.8	2407.3
	LSARPKIK									24.1	1141.8
	MLLADQGQSWK									35.8	1276.6
	MPPYTIVYFPVR									79.8	1498.8
	PPYTIVYFPVR									42.4	1351.7

#	Protein description (gene name)	UniProt entry	Mass (kDa)[483]	Protein ID probability	% of total spectra	Assigned spectra	Unique peptides	Unique spectra	Coverage	Best Mascot ion score	Calculated +1H peptide mass (AMU)
	PPYTIVYFPVRGR									41.9	1564.9
	SLGLYGK									47.1	737.4
	SLGLYGKDQK									37.3	1108.6
	SLGLYGKDQKEAALVDMVNDGVEDLR									80.5	3064.6
	STCLYGQLPK									37.4	1166.6
	STCLYGQLPKFEDGDLTLYQSNAILR									63.2	3231.7
	YGTLIYTNYENGK									44.8	1535.7
	YGTLIYTNYENGKDDYVK									71.4	2156.0
3	GSTM4_RAT Glutathione S-transferase Yb-3 (*Gstm3)*	P08009	25.7	100%	0.0%	37	14	18	48.0%		
	FLPRPLFTK									25.7	1118.7
	FLPRPLFTKMAIWGSK									24.2	2366.4
	IRVDILENQLMDNR									50	1728.9
	ISDYMKSSR									19.8	1331.7
	KISDYMKSSR									28.2	1443.8
	LCYNPDFEK									39.8	1185.5
	LCYNPDFEKLKPGYLEQLPGMMR									22	3028.5
	LKPGYLEQLPGMMR									53.1	1878.0
	MAIWGSK									38.9	1021.6
	NQVFEATCLDAFPNLK									48.6	1866.9
	NQVFEATCLDAFPNLKDFIAR									49.9	2698.4
	VDILENQLMDNR									107	1459.7
	YTMGDAPDFDR									66.9	1303.5
	YTMGDAPDFDRSQWLNEKFK									33.8	2693.3
4	GSTA4_RAT Glutathione S-transferase alpha-4 (*Gsta4)*	P14942	25.5	100%	0.1%	75	19	23	38.0%		

#	Protein description (gene name)	UniProt entry	Mass (kDa)[483]	Protein ID probability	% of total spectra	Assigned spectra	Unique peptides	Unique spectra	Coverage	Best Mascot ion score	Calculated +1H peptide mass (AMU)
	AILSYLAAK									38.4	949.6
	AILSYLAAKYNLYGK									29.7	1917.1
	AILSYLAAKYNLYGKDLK									32	2502.5
	AKNRYFPVFEK									18.9	1627.9
	APQEKEESLALAVK									65.3	1512.8
	APQEKEESLALAVKR									25.1	2127.3
	EESLALAVK									43	959.5
	EESLALAVKR									32.5	1344.8
	GRMESIR									21.8	848.4
	ISNIPTIK									52.3	885.5
	ISNIPTIKK									36.1	1242.8
	KPPPDGHYVDVVR									59.5	1707.9
	KPPPDGHYVDVVRTVLKF									17.3	2296.3
	LYYFQGR									25.5	946.5
	NRYFPVFEK									23.8	1199.6
	WLLATAGVEFEEEFLETR									81.5	2140.1
	YFPVFEK									21.6	929.5
	YNLYGKDLK									20	1342.8
	YNLYGKDLKER									20.3	1627.9
5	FIBA_RAT Fibrinogen alpha chain (*Fga)*	P06399	86.7	85%	0.0%	6	1	1	1.3%		
	LEVDIDIKIR									37.1	1442.9
6	CBR1_RAT Carbonyl reductase [NADPH] 1 (*Cbr1)*	P47727	30.6	100%	0.1%	75	28	31	78.0%		
	ALKSCSPELQQK									28.9	1617.9
	EDKILLNACCPGWVR									52.2	2060.1

#	Protein description (gene name)	UniProt entry	Mass (kDa)[483]	Protein ID probability	% of total spectra	Assigned spectra	Unique peptides	Unique spectra	Coverage	Best Mascot ion score	Calculated +1H peptide mass (AMU)
	EGWPNSAYGVTK									41.2	1308.6
	ELLPIIKPQGR									21.5	1492.9
	FHQLDIDNPQSIR									57.5	1582.8
	FIEDAK									30.5	722.4
	FIEDAKK									24.3	1079.6
	FLGDVVLTAR									50.4	1090.6
	FRSETITEEELVGLMNK									54.1	1996.0
	GHEAVKQLQTEGLSPR									45	1979.1
	GIGFAIVR									33.7	832.5
	GVHAKEGWPNSAYGVTK									37.3	2030.1
	GVHAKEGWPNSAYGVTKIGVTVLSR									25.9	3084.7
	IGVTVLSR									60.1	844.5
	ILLNACCPGWVR									56.4	1458.7
	KFLGDVVLTAR									21	1447.9
	KFLGDVVLTAR									51.5	1447.9
	QLQTEGLSPR									67.3	1128.6
	REDKILLNACCPGWVR									40.7	2216.2
	SCSPELQQK									20.8	1076.5
	SCSPELQQKFR									30.9	1608.8
	SETITEEELVGLMNK									62.4	1708.8
	SETITEEELVGLMNKFIEDAKK									19.1	2982.6
	SPEEGAETPVYLALLPPGAEGPHGQFVQDKK									50.9	3490.8
	TDMAGPKATK									38.6	1264.7
	TNFFGTQDVCK									61.9	1316.6

#	Protein description (gene name)	UniProt entry	Mass (kDa)[483]	Protein ID probability	% of total spectra	Assigned spectra	Unique peptides	Unique spectra	Coverage	Best Mascot ion score	Calculated +1H peptide mass (AMU)
	VVDPTPFHIQAEVTMK									47	1811.9
	VVNVSSSVSLR									63.4	1146.6
7	EF1G_RAT Elongation factor 1-gamma (*Eef1g)*	Q68FR6	50.1	100%	0.1%	79	22	26	38.0%		
	AFKALIAAQYSGAQIR									64.7	1937.1
	AILGEVK									32.8	729.5
	AILGEVKLCEK									24.4	1488.9
	AKDPFAHLPK									31.9	1352.8
	ALIAAQYSGAQIR									74.4	1361.8
	DPFAHLPKSTFVLDEFK									36.4	2220.2
	DPFAHLPKSTFVLDEFKR									24.5	2376.3
	EEKQKPQTER									18.1	1501.8
	EYFSWEGAFQHVGK									52.8	1684.8
	ILGLLDTHLK									41.2	1122.7
	ILGLLDTHLKTR									26.5	1609.0
	KFAESQPK									23.3	1163.7
	KFPAGKVPAFEGDDGFCVFESNAIAYYVSNEELR									65.7	4285.1
	KLDPGSEETQTLVR									67.3	1802.0
	LDPGSEETQTLVR									98.6	1444.7
	QAFPNTNR									36.8	947.5
	QATENAKEEVK									25.5	1458.8
	STFVLDEFK									30.5	1085.6
	STFVLDEFKR									40.7	1241.7
	TFLVGER									47.8	821.5
	TPEFLR									35.8	762.4

#	Protein description (gene name)	UniProt entry	Mass (kDa)[483]	Protein ID probability	% of total spectra	Assigned spectra	Unique peptides	Unique spectra	Coverage	Best Mascot ion score	Calculated +1H peptide mass (AMU)
	VLSAPPHFHFGQTNR									37	1707.9
8	GSTM5_RAT Glutathione S-transferase Mu 5 (*Gstm5)*	Q9Z1B2	26.6	100%	0.1%	71	22	25	72.0%		
	CLDEFPNLKAFMCR									19.9	2030.0
	FEALEK									39.7	736.4
	FEALEKIAAFLQSDR									49.8	1967.1
	FKLDLDFPNLPYLMDGK									21.3	2271.2
	FTWFAGEK									33.7	985.5
	IAAFLQSDR									70.6	1020.5
	KHNMCGDTEEEK									52.6	1706.8
	LCYNSNHESLKPQYLEQLPAQLK									38.2	2773.4
	LDLDFPNLPYLMDGK									31.4	1766.9
	LDLDFPNLPYLMDGKNK									46.8	2222.2
	MFEPKCLDEFPNLK									19	2013.0
	MLLEFTDTSYEEK									69.3	1621.7
	MLLEFTDTSYEEKQYTCGEAPDYDR									55.9	3306.5
	MPINNKMAK									22.5	1307.7
	NKITQSNAILR									50.2	1486.9
	QFSLFLGK									20.1	939.5
	QYTCGEAPDYDR									97.4	1474.6
	QYTCGEAPDYDRSQWLDVK									24.3	2331.0
	SMVLGYWDIR									46.7	1239.6
	SQWLDVK									30.4	875.5
	SQWLDVKFK									22.9	1379.8
	VDIMENQIMDFR									119	1510.7

#	Protein description (gene name)	UniProt entry	Mass (kDa)[483]	Protein ID probability	% of total spectra	Assigned spectra	Unique peptides	Unique spectra	Coverage	Best Mascot ion score	Calculated +1H peptide mass (AMU)
9	GSTM1_RAT Glutathione S-transferase Mu 1 (*Gstm1)*	P04905	25.9	100%	0.0%	39	19	23	65.0%		
	ADIVENQVMDNR									89.4	1419.7
	CLDAFPNLKDFLAR									49.8	1679.9
	FKLGLDFPNLPYLIDGSR									48.8	2294.3
	GLTHPIR									25.2	793.5
	HHLCGETEEER									54.9	1396.6
	IRADIVENQVMDNR									49.2	1688.8
	ISAYMKSSR									21.2	1271.7
	ITQSNAIMR									51.5	1033.5
	KHHLCGETEEER									44.6	1753.8
	KISAYMKSSR									19.8	1629.0
	KITQSNAIMR									41.9	1406.8
	LAQWSNK									35.5	1075.6
	LGLDFPNLPYLIDGSR									96	1789.9
	MQLIMLCYNPDFEK									40.6	1833.8
	PMILGYWNVR									37.7	1264.7
	YAMGDAPDYDR									70.3	1289.5
	YAMGDAPDYDRSQWLNEKFK									24.2	2679.3
	YLSTPIFSK									43	1055.6
	YLSTPIFSKLAQWSNK									28.4	2112.2
10	HSP7C_RAT Heat shock cognate 71 kDa protein (*Hspa8)*	P63018	70.9	100%	0.0%	39	20	20	30.0%		
	ARFEELNADLFR									46.9	1480.8
	DAGTIAGLNVLR									51.6	1199.7
	DAKLDKSQIHDIVLVGGSTR									31.2	2381.3

#	Protein description (gene name)	UniProt entry	Mass (kDa)[483]	Protein ID probability	% of total spectra	Assigned spectra	Unique peptides	Unique spectra	Coverage	Best Mascot ion score	Calculated +1H peptide mass (AMU)
	FEELNADLFR									70.8	1253.6
	GTLDPVEKALR									20.2	1427.8
	IINEPTAAAIAYGLDKK									64	2017.2
	LDKSQIHDIVLVGGSTR									61.7	1838.0
	LIGDAAKNQVAMNPTNTVFDAKR									27.7	2932.6
	LLQDFFNGKELNK									33.9	1795.0
	LSKEDIER									36.8	989.5
	MVNHFIAEFKR									21	1620.9
	NQVAMNPTNTVFDAK									88.8	1649.8
	NQVAMNPTNTVFDAKR									42.1	2051.1
	NSLESYAFNMK									32.7	1303.6
	QATKDAGTIAGLNVLR									64.9	1857.1
	STAGDTHLGGEDFDNR									42	1691.7
	TTPSYVAFTDTER									75.9	1487.7
	TVTNAVVTVPAYFNDSQR									80.4	1982.0
	VQVEYKGETK									22.2	1409.8
	YKAEDEKQR									22.8	1395.7
11	HLF_RAT Hepatic leukaemia factor (*Hlf)*	Q64709	33.1	91%	0.0%	15	1	1	2.7%		
	QEVADLRK									28.3	958.5
12	TBA8_RAT Tubulin alpha-8 chain (*Tuba8)*	Q6AY56	50.0	91%	0.0%	7	1	1	3.6%		
	GHYTVGKESIDLVLDR									21.3	1801.9
13	EF1A2_RAT Elongation factor 1-alpha 2 (*Eef1a2)*	P62632	50.5	100%	0.0%	9	7	7	19.0%		
	EGNASGVSLLEALDTILPPTRPTDKPLR									51.5	3189.8
	KLEDNPKSLK									21.8	1630.0

#	Protein description (gene name)	UniProt entry	Mass (kDa)[483]	Protein ID probability	% of total spectra	Assigned spectra	Unique peptides	Unique spectra	Coverage	Best Mascot ion score	Calculated +1H peptide mass (AMU)
	LEDNPKSLK									22.6	1272.7
	QTVAVGVIKNVEK									43.1	1614.0
	VETGILRPGMVVTFAPVNITTEVK									62.2	2571.4
	YDEIVK									27.9	766.4
	YDEIVKEVSAYIK									22.9	1786.0
14	TPIS_RAT Triosephosphate isomerase (*Tpi1)*	P48500	26.8	100%	0.0%	23	15	17	70.0%		
	DLGATWVVLGHSER									45.7	1539.8
	ELASQPDVDGFLVGGASLKPEFVDIINAK									31.4	3258.7
	GWLKCNVSEGVAQCTR									47.6	2094.0
	HIFGESDELIGQK									43.9	1472.7
	IIYGGSVTGATCK									81.8	1326.7
	KFFVGGNWK									19	1311.7
	KFFVGGNWKMNGR									28.1	1999.1
	LPADTEVVCAPPTAYIDFAR									80.3	2206.1
	TATPQQAQEVHEK									53.1	1466.7
	TATPQQAQEVHEKLR									43.6	1965.1
	VNHALSEGLGVIACIGEKLDER									41.2	2609.4
	VTNGAFTGEISPGMIK									31.8	1637.8
	VVFEQTK									34.2	850.5
	VVLAYEPVWAIGTGK									49.1	1602.9
	VVLAYEPVWAIGTGKTATPQQAQEVHEK									41	3279.8
15	CP013_RAT UPF0585 protein C16orf13 homolog	Q497C3	22.6	100%	0.0%	15	8	9	45.0%		
	AFPNAEWQPSDVDQR									89.3	1759.8
	CRNPEWGLR									23.4	1187.6

#	Protein description (gene name)	UniProt entry	Mass (kDa)[483]	Protein ID probability	% of total spectra	Assigned spectra	Unique peptides	Unique spectra	Coverage	Best Mascot ion score	Calculated +1H peptide mass (AMU)
	DTALLEELGQASGLTLER									105	1916.0
	MVDMPANNKCLIFR									20.4	1970.0
	NKEPILCVLR									44.4	1241.7
	NPEWGLR									46.2	871.4
	QYVDPAQR									53.5	976.5
	VLEVASGSGQHAAHFAR									58.1	1736.9
16	GRP75_RAT Stress-70 protein, mitochondrial (*Hspa9)*	P48721	73.9	100%	0.0%	13	10	11	20.0%		
	AQFEGIVTDLIKR									26.9	1719.0
	DAGQISGLNVLR									57.5	1242.7
	EMAGDNKLLGQFTLIGIPPAPR									27.6	2567.4
	KDSETGENIR									50.5	1377.7
	MPKVQQTVQDLFGR									50.5	1892.0
	NAVITVPAYFNDSQR									64	1694.8
	QATKDAGQISGLNVLR									53.6	1900.1
	QAVTNPNNTFYATKR									39.5	1954.0
	TTPSVVAFTPDGER									59	1476.7
	VEAVNMAEGIIHDTETK									60.8	1856.9
17	LANC1_RAT LanC-like protein 1 (*Lancl1)*	Q9QX69	45.2	100%	0.0%	14	5	6	9.8%		
	AFPNPYADYNK									34.5	1299.6
	AFPNPYADYNKSLAENYFDSTGR									46.8	2869.4
	ELLQQMER									63.9	1046.5
	QAEDCITR									60.5	992.4
	SLAENYFDSTGR									70.5	1359.6
18	HEXB_RAT Beta-hexosaminidase subunit beta (*Hexb)*	Q6AXR4	61.5	90%	0.0%	8	1	1	2.0%		

#	Protein description (gene name)	UniProt entry	Mass (kDa)[483]	Protein ID probability	% of total spectra	Assigned spectra	Unique peptides	Unique spectra	Coverage	Best Mascot ion score	Calculated +1H peptide mass (AMU)
	AEPLNFEGSEK									26.5	1220.6
19	ATPA_RAT ATP synthase subunit alpha, mitochondrial (*Atp5a1)*	P15999	59.8	100%	0.0%	15	8	8	14.0%		
	AVDSLVPIGR									39.1	1026.6
	ELIIGDR									47	815.5
	ILGADTSVDLEETGR									105	1575.8
	SDGKISEQSDAK									36.4	1493.8
	TGAIVDVPVGDELLGR									77.3	1610.9
	VGLKAPGIIPR									28	1349.9
	VLSIGDGIAR									46.7	1000.6
	VVDALGNAIDGK									58.4	1171.6
20	ACTB_RAT Actin, cytoplasmic 1 (*Actb)* ACTG_RAT Actin, cytoplasmic 2 (*Actg1)*	P60711 P63259	41.7, 41.8	100%	0.0%	15	9	9	32.0%		
	AGFAGDDAPR									79.2	976.4
	AVFPSIVGRPR									33.1	1198.7
	GYSFTTTAER									40.8	1132.5
	IIAPPER									34	795.5
	KDLYANTVLSGGTTMYPGIADR									50.2	2588.3
	SYELPDGQVITIGNER									81.6	1790.9
	TTGIVMDSGDGVTHTVPIYEGYALPHAILR									52	3199.6
	VAPEEHPVLLTEAPLNPK									33.9	1954.1
	VAPEEHPVLLTEAPLNPKANR									23.9	2524.4
21	ALBU_RAT Serum albumin (*Alb*)	P02770	68.7	98%	0.0%	3	2	2	2.3%		
	AFKAWAVAR									25.2	1248.7
	ECCHGDLLECADDR									35.7	1749.7
22	HS90B_RAT Heat shock protein HSP 90-beta, (*Hsp90ab1*)	P34058	83.3	100%	0.0%	5	3	3	4.3%		

#	Protein description (gene name)	UniProt entry	Mass (kDa)[483]	Protein ID probability	% of total spectra	Assigned spectra	Unique peptides	Unique spectra	Coverage	Best Mascot ion score	Calculated +1H peptide mass (AMU)
	ALLFIPR									33.4	829.5
	ELISNASDALDKIR									31.9	1774.0
	IDIIPNPQER									47.9	1194.6
23	RS28_RAT 40S ribosomal protein S28, (*Rps28*)	P62859	7.8	100%	0.0%	8	4	5	45.0%		
	EGDVLTLLESER									87	1360.7
	EGDVLTLLESEREAR									21.8	1716.9
	NVKGPVREGDVLTLLESER									30.8	2340.3
	VEFMDDTSR									48.4	1099.5
24	GRP78_RAT 78 kDa glucose-regulated protein, (*Hspa5*)	P06761	72.3	100%	0.0%	8	8	8	19.0%		
	AKFEELNMDLFR									70.3	1741.9
	IINEPTAAAIAYGLDKR									37.8	2045.2
	ITPSYVAFTPEGER									51	1566.8
	KSDIDEIVLVGGSTR									26.5	1818.0
	KSQIFSTASDNQPTVTIK									30.7	2194.2
	NQLTSNPENTVFDAKR									37.6	2063.1
	TWNDPSVQQDIK									48.1	1430.7
	VTHAVVTVPAYFNDAQR									38.2	1888.0
25	SYFA_RAT Phenylalanyl-tRNA synthetase alpha chain (*Farsa*)	Q505J8	57.7	90%	0.0%	3	2	2	2.2%		
	ADNPVLEQLLR									22.9	1267.7
	VVDSIEDEVQR									25.2	1288.6
26	VAPA_RAT Vesicle-associated membrane protein-associated protein A (*Vapa)*	Q9Z270	27.8	100%	0.0%	6	5	5	26.0%		
	FKGPFTDVVTTNLKLQNPSDR									38.7	2835.6
	HLRDEGLR									21.4	995.5
	KVAHSDKPGSTSAVSFR									49.1	2003.1

#	Protein description (gene name)	UniProt entry	Mass (kDa)[483]	Protein ID probability	% of total spectra	Assigned spectra	Unique peptides	Unique spectra	Coverage	Best Mascot ion score	Calculated +1H peptide mass (AMU)
	QDGPLPKPHSVSLNDTETR									56	2320.2
	VAHSDKPGSTSAVSFR									24.6	1645.8
27	CO4_RAT Complement C4 (*C4)*	P08649	192.2	100%	0.0%	9	2	2	1.3%		
	ADLEKLTSLSDR									40.4	1576.9
	VEYGFQVKVLR									34.5	1566.9
28	PRDX1_RAT Peroxiredoxin-1 (*Prdx1*)	Q63716	22.1	100%	0.0%	9	6	6	19.0%		
	ADEGISFR									51.9	894.4
	GLFIIDDK									35.7	920.5
	GLFIIDDKGILR									19.3	1589.0
	QITINDLPVGR									54	1225.7
	SVDEILR									29	831.5
	TIAQDYGVLK									28.7	1107.6
29	SKA2_RAT Spindle and kinetochore-associated protein 2 (*Ska2*)	Q5I0J4	16.5	83%	0.0%	1	1	1	4.9%		
	NAVAILK									23.3	728.5
30	THIO_RAT Thioredoxin (*Txn*)	P11232	11.7	100%	0.0%	8	5	5	31.0%		
	EAFQEALAAAGDK									49.5	1320.6
	EKLEATITEFA									62.5	1480.8
	VGEFSGANK									51.5	908.4
	VGEFSGANKEK									30.3	1394.7
	VGEFSGANKEKLEATITEFA									21.2	2599.4
31	PYGM_RAT Glycogen phosphorylase, muscle form (*Pygm*)	P09812	97.3	100%	0.0%	6	3	3	4.3%		
	ARPEFTLPVHFYGR									27	1689.9
	DYYFALAHTVR									29.9	1355.7
	HLQIIYEINQR									41.1	1426.8

#	Protein description (gene name)	UniProt entry	Mass (kDa)[483]	Protein ID probability	% of total spectra	Assigned spectra	Unique peptides	Unique spectra	Coverage	Best Mascot ion score	Calculated +1H peptide mass (AMU)
32	SEBP2_RAT Selenocysteine insertion sequence-binding protein 2 (*Secisbp2*)	Q9QX72	93.3	89%	0.0%	4	1	1	0.8%		
	TMLETMR									24	913.4
33	CALD1_RAT Non-muscle caldesmon (*Cald1*)	Q62736	60.6	82%	0.0%	2	1	1	1.9%		
	LSRSGSQGRR									27	1103.6
34	ECHA_RAT Trifunctional enzyme subunit alpha, mitochondrial (*Hadha*)	Q64428	82.7	100%	0.0%	6	6	6	10.0%		
	DLANNSSKKFYQ									28.2	1873.0
	ILQEGVDPK									32.3	998.6
	LPAKPEVSSDEDIQYR									36.8	2076.1
	NLNSEIDNILVNLR									34	1626.9
	TIEYLEEVAVNFAK									29.7	1625.8
	TLLKDTTVTGLGR									19.6	1604.0
35	GSTA6_RAT Glutathione S-transferase A6 (*Gsta6*)	Q6AXY0	25.8	100%	0.0%	5	5	5	16.0%		
	AIMNYFSSKYNLYGK									26.1	2028.0
	FIHTNEDLEK									40	1245.6
	FIHTNEDLEKLR									37.8	1744.0
	QPPVDEKSIQK									20.8	1480.8
	VFESHGQDYLVGNK									46.4	1592.8
36	MYH10_RAT Myosin-10 (*Myh10*)	Q9JLT0	229.0	90%	0.0%	4	1	1	0.5%		
	ARDEVIKQLR									22.2	1227.7
37	GSTM2_RAT Glutathione S-transferase Mu 2 (*Gstm2*)	P08010	25.7	100%	0.0%	4	2	2	4.1%		
	SQWLSEK									23.8	877.4
	SQWLSEKFK									21.1	1381.8
38	GRPE1_RAT GrpE protein homolog 1, mitochondrial (*Grpel1*)	P97576	24.3	100%	0.0%	4	2	2	8.3%		
	ALADTENLR									69.8	1002.5

#	Protein description (gene name)	UniProt entry	Mass (kDa)[483]	Protein ID probability	% of total spectra	Assigned spectra	Unique peptides	Unique spectra	Coverage	Best Mascot ion score	Calculated +1H peptide mass (AMU)
	SQKLVEEAK									20.8	1260.7
39	G3P_RAT Glyceraldehyde-3-phosphate dehydrogenase (*Gapdh*)	P04797	35.8	100%	0.0%	6	2	2	8.7%		
	GAAQNIIPASTGAAK									51.8	1369.7
	VPTPNVSVVDLTCR									87.3	1556.8
40	ATPB_RAT ATP synthase subunit beta, mitochondrial (*Atp5b*)	P10719	56.4	100%	0.0%	5	5	5	12.0%		
	AIAELGIYPAVDPLDSTSR									53.1	1988.0
	FTQAGSEVSALLGR									79.4	1435.8
	IMDPNIVGSEHYDVAR									38.4	1815.9
	IMNVIGEPIDER									46.9	1385.7
	TIAMDGTEGLVR									72.4	1262.6
41	PRDX2_RAT Peroxiredoxin-2 (*Prdx2*)	P35704	21.8	100%	0.0%	7	4	4	22.0%		
	KEGGLGPLNIPLLADVTK									43.5	2064.2
	NDEGIAYR									31.2	937.4
	QITVNDLPVGR									58.7	1211.7
	SVDEALR									41.8	789.4
42	1433T_RAT 14-3-3 protein theta (*Ywhaq*)	P68255	27.8	100%	0.0%	5	4	4	21.0%		
	AVTEQGAELSNEER									88.1	1532.7
	EKVESELR									22	1218.7
	KQTIENSQGAYQEAFDISK									86.4	2386.2
	YLAEVACGDDR									61.3	1268.6
43	EF1A1_RAT Elongation factor 1-alpha 1 (*Eef1a1*)	P62630	50.1	100%	0.0%	4	3	4	8.4%		
	AAGAGKVTK									22.2	1031.6
	VETGVLKPGMVVTFAPVNVTTEVK									51.3	2760.5
	YEEIVK									22.8	780.4

#	Protein description (gene name)	UniProt entry	Mass (kDa)[483]	Protein ID probability	% of total spectra	Assigned spectra	Unique peptides	Unique spectra	Coverage	Best Mascot ion score	Calculated +1H peptide mass (AMU)
44	UBB_RAT Polyubiquitin-B (*Ubb*) RS27A_RAT Ubiquitin-40S ribosomal protein S27a (*Rps27a*) RL40_RAT Ubiquitin-60S ribosomal protein L40 (*Uba52*) UBC_RAT Polyubiquitin-C (*Ubc*)	P0CG51 P62982 P62986 Q63429	34.4 18 14.7 91.1	100%	0.0%	5	2	2	9.2%		
	LIFAGKQLEDGR									25.2	1575.9
	TITLEVEPSDTIENVK									55.7	1787.9
45	UBXN4_RAT UBX domain-containing protein 4 (*Ubxn4*)	Q5HZY0	56.4	99%	0.0%	2	1	1	1.0%		
	IYRLR									26.8	720.5
46	VDAC1_RAT Voltage-dependent anion-selective channel protein 1 (*Vdac1*)	Q9Z2L0	30.8	100%	0.0%	6	5	5	16.0%		
	FGIAAKYQVDPDACFSAK									25.5	2217.1
	LTFDSSFSPNTGK									45.2	1400.7
	LTLSALLDGK									91.4	1030.6
	VNNSSLIGLGYTQTLKPGIK									60.5	2103.2
	YQVDPDACFSAK									32.3	1400.6
47	FBX3_RAT F-box only protein 3 (*Fbxo3*)	D4ABP9	55.4	100%	0.0%	6	6	6	17.0%		
	EEDLDAVEAQIGCK									75	1576.7
	EEDLDAVEAQIGCKLPDDYR									33.9	2565.2
	EGAREEDLDAVEAQIGCK									43.8	1989.9
	ITNAKGDVEEVQGPGVVGEFPIISPGR									25.1	2994.6
	LSQLSTHDPLWR									45.2	1452.8
	SEDLLDVDTAAGGFQQR									96	1821.9
48	NFL_RAT Neurofilament light polypeptide (*Nefl*)	P19527	61.3	100%	0.0%	5	5	5	11.0%		
	AAKDEVSESR									34.7	1320.7
	FTVLTESAAKNTDAVR									33.9	1952.1
	KGADEAALAR									25.3	1230.7

#	Protein description (gene name)	UniProt entry	Mass (kDa)[483]	Protein ID probability	% of total spectra	Assigned spectra	Unique peptides	Unique spectra	Coverage	Best Mascot ion score	Calculated +1H peptide mass (AMU)
	LAAEDATNEKQALQGER									38.5	2073.1
	QKHSEPSR									20.9	1180.6
49	RS18_RAT 40S ribosomal protein S18 (*Rps18*)	P62271	17.7	100%	0.0%	5	5	5	25.0%		
	AGELTEDEVER									71.3	1247.6
	IPDWFLNR									45.4	1060.6
	LREDLER									22.2	930.5
	QYKIPDWFLNR									28.3	1708.9
	VLNTNIDGR									67.8	1001.5
50	ACON_RAT Aconitate hydratase, mitochondrial (*Aco2*)	Q9ER34	85.4	85%	0.0%	5	1	1	1.2%		
	VDVSPTSQR									56.7	988.5
51	AKT3_RAT RAC-gamma serine/threonine-protein kinase (*Akt3*)	Q63484	55.8	86%	0.0%	1	1	1	2.7%		
	SDVTIVKEDWVQK									19.8	1546.8
52	MCPT4_RAT Mast cell protease 4 (*Mcpt4*)	P97592	27.0	89%	0.0%	3	1	2	2.4%		
	DIMLLK									25.5	748.4
53	EF2_RAT Elongation factor 2 (*Eef2*)	P05197	95.3	100%	0.0%	3	3	3	5.4%		
	ALLELQLEPEELYQTFQR									49	2220.2
	ETVSEESNVLCLSK									75.6	1594.8
	YLAEKYEWDVAEAR									27.6	1972.0
54	RSSA_RAT 40S ribosomal protein SA (*Rpsa*)	P38983	32.8	100%	0.0%	2	2	2	8.5%		
	AVLKFAAATGATPIAGR									30.9	1844.1
	LLVVTDPR									30.8	912.6
55	RS20_RAT 40S ribosomal protein S20 (*Rps20*)	P60868	13.4	100%	0.0%	5	5	5	34.0%		
	DTGKTPVEPEVAIHR									45.2	1878.0
	LIDLHSPSEIVK									34.1	1350.8

#	Protein description (gene name)	UniProt entry	Mass (kDa)[483]	Protein ID probability	% of total spectra	Assigned spectra	Unique peptides	Unique spectra	Coverage	Best Mascot ion score	Calculated +1H peptide mass (AMU)
	NVKSLEK									23.3	1046.6
	SLEKVCADLIR									23.4	1532.9
	VCADLIR									31.9	846.5
56	RS12_RAT 40S ribosomal protein S12 (*Rps12*)	P63324	14.5	100%	0.0%	5	5	5	27.0%		
	DVIEEYFK									29.6	1042.5
	ESQAKDVIEEYFK									26.3	1814.9
	LGEWVGLCK									35.3	1061.5
	LGEWVGLCKIDR									28.4	1674.9
	TALIHDGLAR									33.5	1066.6
57	RS29_RAT 40S ribosomal protein S29 (Rps29)	P62275	6.7	100%	0.0%	2	2	2	41.0%		
	GHQQLYWSHPR									31.6	1637.8
	QYAKDIGFIKLD									21.6	1622.9
58	H2B1_RAT Histone H2B type 1 H2B1A_RAT Histone H2B type 1-A (*Hist1h2ba*)	Q00715 Q00729	14 14.2	89%	0.0%	4	1	1	7.2%		
	LLLPGELAK									37.9	953.6
59	PI51C_RAT Phosphatidylinositol-4-phosphate 5-kinase type-1 gamma (*Pip5k1c*)	Q5I6B8	75.6	79%	0.0%	3	1	1	1.2%		
	KTTSSTLK									25.8	865.5
60	VAPB_RAT Vesicle-associated membrane protein-associated protein B (*Vapb*)	Q9Z269	26.9	100%	0.0%	4	3	3	12.0%		
	QLKEEDGLR									23.4	1299.7
	RLQGEVQR									32.2	985.6
	TEAPVAAKPLTSPLDDAEVK									34.8	2281.2
61	ALDOA_RAT Fructose-bisphosphate aldolase A (*Aldoa*)	P05065	39.4	100%	0.0%	2	2	2	9.1%		
	IVAPGKGILAADESTGSIAK									27.4	2127.2
	LQSIGTENTEENR									41.6	1490.7

#	Protein description (gene name)	UniProt entry	Mass (kDa)[483]	Protein ID probability	% of total spectra	Assigned spectra	Unique peptides	Unique spectra	Coverage	Best Mascot ion score	Calculated +1H peptide mass (AMU)
62	TBB4B_RAT Tubulin beta-4B chain (*Tubb4b*)	Q6P9T8	49.8	100%	0.0%	3	2	2	7.0%		
	AVLVDLEPGTMDSVR									78.8	1601.8
	INVYYNEATGGKYVPR									41.5	2073.1
63	KPYM_RAT Pyruvate kinase isozymes M1/M2 (*Pkm2*)	P11980	57.8	100%	0.0%	4	4	4	6.0%		
	APIIAVTR									46.4	840.5
	LDIDSAPITAR									62.4	1171.6
	NTGIICTIGPASR									62.6	1359.7
	RFDEILEASDGIMVAR									20.9	1821.9
64	SKP1_RAT S-phase kinase-associated protein 1 (*Skp1*)	Q6PEC4	18.7	100%	0.0%	3	2	2	11.0%		
	KTFNIKNDFTEEEEAQVR									59.5	2656.4
	NDFTEEEEAQVR									55.7	1466.6
65	UCHL1_RAT Ubiquitin carboxyl-terminal hydrolase isozyme L1 (*Uchl1*)	Q00981	24.8	100%	0.0%	4	3	3	15.0%		
	FSAVALCKAA									52.3	1266.7
	MPFPVNHGASSEDSLLQDAAK									86.9	2230.0
	MPFPVNHGASSEDSLLQDAAKVCR									49.3	2874.4
66	MGST1_RAT Microsomal glutathione S-transferase 1 (*Mgst1*)	P08011	17.5	100%	0.0%	2	2	2	12.0%		
	VFANPEDCAGFGK									46.6	1411.6
	VFANPEDCAGFGKGENAK									44.6	2140.0
67	PPIA_RAT Peptidyl-prolyl cis-trans isomerase A (*Ppia*)	P10111	17.9	100%	0.0%	3	2	3	20.0%		
	IIPGFMCQGGDFTR									73.4	1614.7
	VNPTVFFDITADGEPLGR									57.4	1948.0
68	TBA4A_RAT Tubulin alpha-4A chain (*Tuba4a*)	Q5XIF6	49.9	100%	0.0%	1	1	1	3.3%		
	AVFVDLEPTVIDEIR									121	1715.9
69	PYGB_RAT Glycogen phosphorylase, brain form (Fragment) (*Pygb*)	P53534	96.2	85%	0.0%	3	2	2	2.3%		

#	Protein description (gene name)	UniProt entry	Mass (kDa)[483]	Protein ID probability	% of total spectra	Assigned spectra	Unique peptides	Unique spectra	Coverage	Best Mascot ion score	Calculated +1H peptide mass (AMU)
	IYYLSLEFYMGR									31	1554.8
	VAIQLNDTHPALSIPELMR									23.2	2134.1
70	GRM1_RAT Metabotropic glutamate receptor 1 (*Grm1*)	P23385	133.2	85%	0.0%	3	1	1	0.7%		
	KICTRKPR									31.6	1001.6
71	MPCP_RAT Phosphate carrier protein, mitochondrial (*Slc25a3*)	P16036	39.4	100%	0.0%	3	2	2	6.2%		
	GSTASQVLQR									50.3	1046.6
	IQTQPGYANTLR									63.3	1361.7
72	ECHB_RAT Trifunctional enzyme subunit beta, mitochondrial (*Hadhb*)	Q60587	51.4	100%	0.0%	3	2	2	4.6%		
	AALSGLLYR									58.6	963.6
	DQLLLGPTYATPK									38.3	1416.8
73	RS14_RAT 40S ribosomal protein S14 (*Rps14*)	P13471	16.3	100%	0.0%	3	2	2	17.0%		
	IEDVTPIPSDSTR									95.5	1429.7
	TKTPGPGAQSALR									55.9	1512.9
74	KCAB1_RAT Voltage-gated potassium channel subunit beta-1 (*Kcnab1*)	P63144	44.7	89%	0.0%	2	1	1	1.5%		
	QQNKLK									28.9	758.5
75	SCN4B_RAT Sodium channel subunit beta-4 (*Scn4b*)	Q7M730	25.2	89%	0.0%	2	1	1	2.6%		
	SDPKVR									33.9	701.4
76	PRAF3_RAT PRA1 family protein 3 (*Arl6ip5*)	Q9ES40	21.5	98%	0.0%	2	2	2	5.9%		
	AWDDFFPGSDR									36.4	1312.6
	FADYISK									21.1	843.4
77	FAS_RAT Fatty acid synthase (*Fasn*)	P12785	272.7	76%	0.0%	1	1	1	0.4%		
	QEGVFAKEVR									19	1162.6
78	PGAP1_RAT GPI inositol-deacylase (*Pgap1*)	Q765A7	104.4	79%	0.0%	1	1	1	1.2%		
	VNVVSKCTGGK									21.5	1148.6

#	Protein description (gene name)	UniProt entry	Mass (kDa)[483]	Protein ID probability	% of total spectra	Assigned spectra	Unique peptides	Unique spectra	Coverage	Best Mascot ion score	Calculated +1H peptide mass (AMU)
79	NUCB2_RAT Nucleobindin-2 (*Nucb2*)	Q9JI85	50.1	89%	0.0%	1	1	1	1.7%		
	DLDMLIK									23.4	847.5
80	HEPS_RAT Serine protease hepsin (*Hpn*)	Q05511	44.9	89%	0.0%	1	1	1	1.7%		
	KPGVYTK									31.2	792.5
81	KTU_RAT Protein kintoun (*Ktu*)	Q5FVL7	89.3	100%	0.0%	3	3	3	4.9%		
	ESSTAYSAEEK									28.5	1201.5
	EWYWGLNKDSLEER									24.7	2054.0
	LQECSDPDGLQGKEK									31.3	1933.0
82	MAP4_RAT Microtubule-associated protein 4 (*Map4*)	Q5M7W5	110.3	100%	0.0%	1	1	1	1.1%		
	TEFIPLLDGDEK									30.9	1376.7
83	RPN1_RAT Dolichyl-diphosphooligosaccharide-protein glycosyltransferase subunit 1 (*Rpn1*)	P07153	68.3	100%	0.0%	2	2	2	4.0%		
	AVTSEIAVLQSR									60.4	1273.7
	NIQVDSPYDISR									70.8	1406.7
84	ANXA1_RAT Annexin A1 (*Anxa1*)	P07150	38.8	100%	0.0%	2	2	2	5.5%		
	ALYEAGER									33.5	908.4
	DITSDTSGDFR									53.8	1213.5
85	RS21_RAT 40S ribosomal protein S21 (*Rps21*)	P05765	9.1	100%	0.0%	2	2	2	14.0%		
	LAKADGIVSK									25.7	1230.8
	LAKADGIVSKNF									20.6	1721.0
86	NDKB_RAT Nucleoside diphosphate kinase B (*Nme2*) NDKA_RAT Nucleoside diphosphate kinase A (*Nme1*)	P19804 Q05982	17.3 17.2	100%	0.0%	2	2	2	14.0%		
	GDFCIQVGR									43.9	1051.5
	TFIAIKPDGVQR									30	1573.9
87	CH60_RAT 60 kDa heat shock protein, mitochondrial (*Hspd1*)	P63039	61.0	90%	0.0%	2	2	2	2.1%		
	VGGTSDVEVNEK									22	1233.6

#	Protein description (gene name)	UniProt entry	Mass (kDa)[483]	Protein ID probability	% of total spectra	Assigned spectra	Unique peptides	Unique spectra	Coverage	Best Mascot ion score	Calculated +1H peptide mass (AMU)
	VTDALNATR									44.9	960.5
88	CP4F6_RAT Cytochrome P450 4F6 (*Cyp4f6*)	P51871	61.5	86%	0.0%	2	1	1	1.5%		
	MLQLSLSR									44.7	963.5
89	H2AJ_RAT Histone H2A.J (*H2afj*) H2A1_RAT Histone H2A type 1 H2AZ_RAT Histone H2A.Z (*H2afz*) H2A1C_RAT Histone H2A type 1-C H2A1E_RAT Histone H2A type 1-E H2A2A_RAT Histone H2A type 2-A (*Hist2h2aa3*) H2A4_RAT Histone H2A type 4 H2A3_RAT Histone H2A type 3 H2A1F_RAT Histone H2A type 1-F	A9UMV8 P02262 P0C0S7 P0C169 P0C170 P0CC09 Q00728 Q4FZT6 Q64598	14.0 14.1 13.6 14.1 14.4 14.4 14.3 14.1 14.2	85%	0.0%	2	1	1	7.0%		
	AGLQFPVGR									63.2	944.5
90	DCXR_RAT L-xylulose reductase (*Dcxr*)	Q920P0	25.7	86%	0.0%	1	1	1	2.9%		
	DLGLAGR									33.4	701.4
91	LDHA_RAT L-lactate dehydrogenase A chain (*Ldha*) LDHB_RAT L-lactate dehydrogenase B chain (*Ldhb*)	P04642 P42123	36.5 36.6	84%	0.0%	2	1	1	3.6%		
	VIGSGCNLDSAR									60.4	1248.6
92	RS25_RAT 40S ribosomal protein S25 (*Rps25*)	P62853	13.7	83%	0.0%	2	1	1	11.0%		
	NTKGGDAPAAGEDA									49.2	1502.7
93	UBA1_RAT Ubiquitin-like modifier-activating enzyme 1 (*Uba1*)	Q5U300	117.8	83%	0.0%	2	1	1	1.5%		
	SPPAVQQDNVDEDLIR									111	1795.9
94	GDF8_RAT Growth/differentiation factor 8 (*Mstn*)	O35312	42.8	77%	0.0%	2	1	1	1.6%		
	LIKPMK									31.2	745.5
95	PGRC2_RAT Membrane-associated progesterone receptor component 2 (*Pgrmc2*)	Q5XIU9	23.4	77%	0.0%	2	1	1	6.9%		
	GGDGSPGGAGATAAR									58.2	1201.6
96	STRN3_RAT Striatin-3 (*Strn3*)	P58405	87.1	89%	0.0%	1	1	1	0.9%		
	QKGQEIK									21.5	830.5

#	Protein description (gene name)	UniProt entry	Mass (kDa)[483]	Protein ID probability	% of total spectra	Assigned spectra	Unique peptides	Unique spectra	Coverage	Best Mascot ion score	Calculated +1H peptide mass (AMU)
97	ENOA_RAT Alpha-enolase (*Eno1*)	P04764	47.1	84%	0.0%	1	1	1	4.1%		
	AAVPSGASTGIYEALELR									77.2	1804.9
98	STS_RAT Steryl-sulfatase (*Sts*)	P15589	62.7	85%	0.0%	1	1	1	1.2%		
	LALEGVK									20.4	729.5
99	RN114_RAT RING finger protein 114 (*Rnf114*)	Q6J2U6	25.7	83%	0.0%	1	1	1	3.1%		
	KDFVLSK									25.1	836.5
100	REEP5_RAT Receptor expression-enhancing protein 5 (*Reep5*)	B2RZ37	21.4	100%	0.0%	2	2	2	11.0%		
	ATVNLLGDEKK									32.5	1416.8
	HESQVDSVVK									22.5	1127.6
101	GLNA_RAT Glutamine synthetase (*Glul*)	P09606	42.3	100%	0.0%	2	2	2	9.9%		
	LTGFHETSNINDFSAGVANR									68.9	2150.0
	RPSANCDPYAVTEAIVR									43.8	1918.9
102	DHSB_RAT Succinate dehydrogenase [ubiquinone] iron-sulfur subunit, mitochondrial (*Sdhb*)	P21913	31.8	100%	0.0%	2	2	2	7.1%		
	IKTFAIYR									30	1240.8
	LAKLQDPFSLYR									22.8	1680.0
103	CNBP_RAT Cellular nucleic acid-binding protein (*Cnbp*)	P62634	19.5	100%	0.0%	2	2	2	17.0%		
	EQCCYNCGKPGHLAR									17.1	2079.0
	GFQFVSSSLPDICYR									72.6	1775.8
104	1433Z_RAT 14-3-3 protein zeta/delta (*Ywhaz*)	P63102	27.8	100%	0.0%	2	2	2	11.0%		
	NLLSVAYKNVVGAR									28.5	1733.0
	SVTEQGAELSNEER									92.2	1548.7
105	TBB2A_RAT Tubulin beta-2A chain (*Tubb2a*)	P85108	49.9	100%	0.0%	1	1	1	3.6%		
	INVYYNEAAGNKYVPR									38.7	2100.1
106	ADT1_RAT ADP/ATP translocase 1 (*Slc25a4*)	Q05962	33.0	100%	0.0%	2	2	2	6.4%		

#	Protein description (gene name)	UniProt entry	Mass (kDa)[483]	Protein ID probability	% of total spectra	Assigned spectra	Unique peptides	Unique spectra	Coverage	Best Mascot ion score	Calculated +1H peptide mass (AMU)
	EFNGLGDCLTK									45.1	1253.6
	TAVAPIER									44	856.5
107	TPM3_RAT Tropomyosin alpha-3 chain (*Tpm3*)	Q63610	29.0	100%	0.0%	2	2	2	10.0%		
	IQLVEEELDR									54.2	1243.7
	KIQVLQQQADDAEER									20.1	2000.1
108	OST48_RAT Dolichyl-diphosphooligosaccharide--protein glycosyltransferase 48 kDa subunit (*Ddost*)	Q641Y0	48.9	100%	0.0%	2	2	2	4.5%		
	SSLNPILFR									65	1046.6
	TLVLLDNLNVR									47.5	1269.8
109	TM109_RAT Transmembrane protein 109 (*Tmem109*)	Q6AYQ4	26.2	100%	0.0%	2	2	2	7.4%		
	ESSADILTEIGR									76.2	1290.7
	QIEELR									32.7	787.4
110	DDB1_RAT DNA damage-binding protein 1 (*Ddb1*)	Q9ESW0	126.9	100%	0.0%	2	2	2	2.2%		
	IGRPSETGIIGIIDPECR									48.8	1983.0
	VVEELTR									42.2	845.5
111	INSRR_RAT Insulin receptor-related protein (Fragments) (*Insrr*)	Q64716	144.8	99%	0.0%	1	1	1	1.2%		
	SEVTELR									30.8	833.4
112	ATP5I_RAT ATP synthase subunit e, mitochondrial (*Atp5i*)	P29419	8.3	89%	0.0%	1	1	1	17.0%		
	ELAEAEDVSIFK									68.4	1579.8
113	ODBB_RAT 2-oxoisovalerate dehydrogenase subunit beta, mitochondrial (*Bckdhb*)	P35738	42.8	85%	0.0%	1	1	1	2.8%		
	LGVSCEVIDLR									21.2	1203.6
114	CNCG_RAT Retinal cone rhodopsin-sensitive cGMP 3',5'-cyclic phosphodiesterase subunit gamma (*Pde6h*)	P61250	9.0	90%	0.0%	1	1	1	7.2%		
	QTRQFK									23.6	807.4
115	CLAP2_RAT CLIP-associating protein 2 (*Clasp2*)	Q99JD4	140.6	90%	0.0%	1	1	1	0.6%		

#	Protein description (gene name)	UniProt entry	Mass (kDa)[483]	Protein ID probability	% of total spectra	Assigned spectra	Unique peptides	Unique spectra	Coverage	Best Mascot ion score	Calculated +1H peptide mass (AMU)
	MQTKVIER									24.8	1004.6
116	RL38_RAT 60S ribosomal protein L38 (*Rpl38*)	P63174	8.2	89%	0.0%	1	1	1	19.0%		
	KIEEIKDFLLTAR									33.8	1575.9
117	CRIP1_RAT Cysteine-rich protein 1 (*Crip1*)	P63255	8.6	89%	0.0%	1	1	1	12.0%		
	GGAESHTFK									37.4	1162.6
118	HBB1_RAT Haemoglobin subunit beta-1 (*Hbb*) HBB2_RAT Haemoglobin subunit beta-2	P02091 P11517	16.0 16.0	84%	0.0%	1	1	1	6.8%		
	LLVVYPWTQR									42.5	1274.7
119	HS90A_RAT Heat shock protein HSP 90-alpha (*Hsp90aa1*)	P82995	84.8	83%	0.0%	1	1	1	1.0%		
	ALLFVPR									44.4	815.5
120	MACOI_RAT Macoilin (*Tmem57*)	Q4V7D3	76.1	83%	0.0%	1	1	1	1.4%		
	QNISQLEKR									19.5	1115.6
121	FUBP2_RAT Far upstream element-binding protein 2 (*Khsrp*)	Q99PF5	74.2	83%	0.0%	1	1	1	1.4%		
	KDAFADAVQR									32.9	1349.7
122	CXCR4_RAT C-X-C chemokine receptor type 4 (*Cxcr4*)	O08565	39.3	83%	0.0%	1	1	1	1.7%		
	KLLAEK									23.4	930.6
123	CYB5B_RAT Cytochrome b5 type B (*Cyb5b*)	P04166	16.3	83%	0.0%	1	1	1	23.0%		
	FLSEHPGGEEVLLEQAGADATESFEDVGHSPDAR									54.6	3596.6
124	SODC_RAT Superoxide dismutase [Cu-Zn] (*Sod1*)	P07632	15.9	83%	0.0%	1	1	1	9.7%		
	GGNEESTKTGNAGSR									33.2	1693.8
125	ATPD_RAT ATP synthase subunit delta, mitochondrial (*Atp5d*)	P35434	17.6	83%	0.0%	1	1	1	11.0%		
	ANLEKAQSELSGAADEAAR									80.8	2160.1
126	AN32A_RAT Acidic leucine-rich nuclear phosphoprotein 32 family member A (*Anp32a*)	P49911	28.6	79%	0.0%	1	1	1	2.4%		
	IYLELR									33.8	806.5
127	PHB_RAT Prohibitin (*Phb*)	P67779	29.8	79%	0.0%	1	1	1	4.4%		

#	Protein description (gene name)	UniProt entry	Mass (kDa)[483]	Protein ID probability	% of total spectra	Assigned spectra	Unique peptides	Unique spectra	Coverage	Best Mascot ion score	Calculated +1H peptide mass (AMU)
	ILFRPVASQLPR									32.8	1396.8
128	DEFI8_RAT Differentially expressed in FDCP 8 homolog (*Def8*)	Q4V8I4	52.7	79%	0.0%	1	1	1	1.1%		
	QTCDK									25.9	823.4
129	SNX20_RAT Sorting nexin-20 (*Snx20*)	Q5BK61	35.7	79%	0.0%	1	1	1	3.2%		
	GATLKELTVR									20.4	1087.6
130	EMD_RAT Emerin (*Emd*)	Q63190	29.7	79%	0.0%	1	1	1	6.9%		
	RPGTSLVDADDTFHHQVR									32.9	2051.0
131	PSME1_RAT Proteasome activator complex subunit 1 (*Psme1*)	Q63797	28.6	79%	0.0%	1	1	1	2.8%		
	IVVLLQR									45.3	840.6
132	CC127_RAT Coiled-coil domain-containing protein 127 (*Ccdc127*)	Q6PEB9	30.5	79%	0.0%	1	1	1	4.2%		
	QNIYCSLILPR									35.3	1376.7
133	SRA1_RAT Steroid receptor RNA activator 1 (*Sra1*)	Q6QGW5	25.3	79%	0.0%	1	1	1	4.3%		
	VAAPQDGSPR									48.8	997.5
134	PBIP1_RAT Pre-B-cell leukaemia transcription factor-interacting protein 1 (*Pbxip1*)	A2VD12	80.3	78%	0.0%	1	1	1	1.1%		
	EKWRGGQR									23.7	1016.5
135	HA11_RAT Class I histocompatibility antigen, Non-RT1.A alpha-1 chain (*RT1-Aw2*)	P15978	36.6	78%	0.0%	1	1	1	2.8%		
	YDSDAENPR									30.9	1066.4
136	GNAS2_RAT Guanine nucleotide-binding protein G(s) subunit alpha isoforms short (*Gnas*) GNAS1_RAT Guanine nucleotide-binding protein G(s) subunit alpha isoforms XLas (*Gnas*)	P63095 Q63803	45.7 122.9	78%	0.0%	1	1	1	2.5%		
	IEDYFPEFAR									23.4	1286.6
137	ARFP2_RAT Arfaptin-2 (*Arfip2*)	Q6AY65	37.8	78%	0.0%	1	1	1	5.0%		
	HPSHSTSPSGPGDEVAR									55.1	1717.8
138	RS5_RAT 40S ribosomal protein S5 (*Rps5*)	P24050	22.9	77%	0.0%	1	1	1	6.4%		

#	Protein description (gene name)	UniProt entry	Mass (kDa)[483]	Protein ID probability	% of total spectra	Assigned spectra	Unique peptides	Unique spectra	Coverage	Best Mascot ion score	Calculated +1H peptide mass (AMU)
	VNQAIWLLCTGAR									37.5	1501.8
139	H4_RAT Histone H4 (*Hist1h4b*)	P62804	11.4	77%	0.0%	1	1	1	7.8%		
	VFLENVIR									30.1	989.6
140	CH082_RAT UPF0598 protein C8orf82 homolog	Q642A4	24.4	77%	0.0%	1	1	1	5.5%		
	VSYTQGQSPEPR									64.9	1348.6
141	DEST_RAT Destrin (*Dstn*)	Q7M0E3	18.5	77%	0.0%	1	1	1	8.5%		
	YALYDASFETKESR									20.4	1909.0
142	OSTC_RAT Oligosaccharyltransferase complex subunit OSTC (*Ostc*)	B0K025	16.8	76%	0.0%	1	1	1	8.1%		
	VPFLVLECPNLK									49.6	1428.8
143	MDHM_RAT Malate dehydrogenase, mitochondrial (*Mdh2*)	P04636	35.7	76%	0.0%	1	1	1	6.5%		
	LTLYDIAHTPGVAADLSHIETR									56.2	2393.2
144	AINX_RAT Alpha-internexin (*Ina*)	P23565	56.1	76%	0.0%	1	1	1	1.6%		
	TIEIEGLR									40.1	930.5
145	RPN2_RAT Dolichyl-diphosphooligosaccharide--protein glycosyltransferase subunit 2 (*Rpn2*)	P25235	69.1	76%	0.0%	1	1	1	3.6%		
	YHVPVVVVPEGSASDTQEQAILR									69.9	2494.3
146	C1TC_RAT C-1-tetrahydrofolate synthase, cytoplasmic (*Mthfd1*)	P27653	101.0	76%	0.0%	1	1	1	1.4%		
	TDPAALTDDEINR									63.9	1430.7
147	DPYL2_RAT Dihydropyrimidinase-related protein 2 (*Dpysl2*)	P47942	62.3	76%	0.0%	1	1	1	4.7%		
	ILDLGITGPEGHVLSRPEEVEAEAVNR									28.7	2900.5
148	PUR6_RAT Multifunctional protein ADE2 (*Paics*)	P51583	47.1	76%	0.0%	1	1	1	4.7%		
	IKAEYEGDGIPTVFVAVAGR									24.5	2092.1
149	TBB5_RAT Tubulin beta-5 chain (*Tubb5*)	P69897	49.7	76%	0.0%	1	1	1	3.6%		
	ISVYYNEATGGKYVPR									30.3	2046.1
150	VDAC2_RAT Voltage-dependent anion-selective channel protein	P81155	31.7,	76%	0.0%	1	1	1	3.4%		

#	Protein description (gene name)	UniProt entry	Mass (kDa)[483]	Protein ID probability	% of total spectra	Assigned spectra	Unique peptides	Unique spectra	Coverage	Best Mascot ion score	Calculated +1H peptide mass (AMU)
	2 (*Vdac2*) VDAC3_RAT Voltage-dependent anion-selective channel protein 3 (*Vdac3*)	Q9R1Z0	30.8								
	LTLSALVDGK									69.8	1016.6
151	LIPL_RAT Lipoprotein lipase (*Lpl*)	Q06000	53.1	76%	0.0%	1	1	1	3.6%		
	LSPDDADFVDVLHTFTR									57.2	1947.9
152	SSRG_RAT Translocon-associated protein subunit gamma (*Ssr3*)	Q08013	21.1	76%	0.0%	1	1	1	11.0%		
	APKGGSKQQSEEDLLLQDFSR									29.2	2791.5
153	LSAMP_RAT Limbic system-associated membrane protein (*Lsamp)*	Q62813	37.3	76%	0.0%	1	1	1	4.7%		
	EFEGEEEYLEILGITR									52.2	1926.9
154	LYAG_RAT Lysosomal alpha-glucosidase (*Gaa*)	Q6P7A9	106.2	76%	0.0%	1	1	1	1.9%		
	THFPLDVQWNDLDYMDAR									57.2	2236.0
155	VKOR1_RAT Vitamin K epoxide reductase complex subunit 1 (*Vkorc1*)	Q6TEK4	17.8	76%	0.0%	1	1	1	8.1%		
	ALCDVGTAISCSR									55.8	1409.7

Appendix 2: Experimental protocols

Protocol 1: Routine PCR and agarose DNA electrophoresis

Buffers

6X Orange G gel loading buffer

100mg Orange G

30% (v/v) Glycerol

Adjust with double distilled water (ddH_2O) to a final volume of 50 ml. Dispense in 5 ml aliquots and store at RT.

Sterile ddH_2O

Sterilise 100 ml by autoclaving, dispense in 5 ml aliquots and store at RT.

50X Tris-Acetate EDTA (TAE) buffer (Severn Biotech Ltd 20-6001-10)

Dilute 1:50 with ddH_2O to obtain a 1X working solution.

Agarose (SIGMA A9539)

Reagents

5000 U/ml *Taq* DNA Polymerase with 10X Standard *Taq* Buffer 1.5 mM $MgCl_2$ (New England Biolabs M0273)

Dispense Taq in 20 µl aliquots and buffer in 100 µl aliquots, store at -20°C.

100 mM Deoxynucleotide (dNTP) Solution Set (New England Biolabs N0446)

To obtain a 10 mM dNTPs working solution, dilute 1:10 each deoxynucleotide in sterile ddH_2O to a final volume of 100 µl. Dispense in 20 µl aliquots and store at -20°C.

10 µM PCR primers (forward and reverse)

Dilute 1:10 from 100 µM in sterile ddH_2O or TE buffer, store at -20°C.

GelRed Nucleic Acid Gel Stain, 10000X in water (Biotium 41003)

GeneRuler 100 bp DNA Ladder (Life Technologies SM0241)

Dilute ladder and included loading dye 1:6 in ddH_2O to obtain a 1X working solution, store working solution at RT.

1 kb DNA ladder (New England Biolabs N3232S)

Samples

DNA samples to be amplified

Materials

0.2 ml (individual tubes or strips) or 0.5 ml and 1.5 ml polypropylene tubes

Pipettes and tips

Conical flask

Tray, comb and dams for agarose gels

Parafilm and Saran wrap

Equipment

PCR hood

GS1 Thermal Cycler (G-Storm)

Eppendorf 5424 microcentrifuge (Eppendorf)

Microwave oven

MultiSUB Mini horizontal electrophoresis tank (Cleaver Scientific Ltd)

Consort E835 electrophoresis power supply (Cleaver Scientific Ltd)

UVP Ultraviolet Transilluminator

UVIDOC Gel documentation system

Method

Defrost all the reagents and samples on ice before starting. Work in the PCR hood, keeping all the reagents on ice.

1. Place the racks, pipettes, tips, tubes, ddH_2O and PCR buffer to be used in the PCR hood and expose them to UV light for 5-10 min.
2. Working in the PCR hood, set up the following master mix in a 1.5 µl tube (adjust according to the number of samples to be processed, considering a 10% excess):

Final concentration:	Reagent:
1X	10X Standard *Taq* Buffer
0.2 mM	10 mM dNTPs
0.5 µM	10 µM Forward PCR primer
0.5 µM	10 µM Reverse PCR primer
1.25 U per 50 µl	5 U/µl *Taq* DNA Polymerase

   Adjust with sterile ddH_2O to the desired final volume (usually 25-50 µl)

   Mix well by pipetting or vortexing and spin down to remove any drops from the tube's lid.
3. Dispense the master mix in the PCR tubes (0.2 or 0.5 ml), placing it in the bottom of each tube.
4. Add the appropriate sample to each tube and ddH_2O to the negative control.
5. Close the tubes tightly, mix by vortexing, spin down and place them on the thermal cycler.
6. Run the appropriate PCR program, based on the following example:

   One cycle:

   95°C 2 min

   35 cycles:

95°C 15 sec

(Variable) 15 sec

68°C 1 min per each 1000 bp of PCR product size

One cycle:

68°C 5 min

10°C Hold

7. In the meantime, prepare an agarose gel as follows:
    - Mix an appropriate amount of agarose with 40 ml of 1X TAE buffer in a conical flask, cover with Saran wrap (make a hole at the centre to allow partial evaporation).
    - Heat up in the microwave oven until the agarose is completely dissolved (approximately 1:30 min).
    - Add Gel Red to a final concentration of 1X and pour on the gel tray with the rubber dams on both sides. Ensure no bubbles are left and place a comb on the gel. Let it sit at RT.
8. Fill the electrophoresis tank with 1X TAE and place the tray with the gel inside, making sure that the buffer covers the gel.
9. Place an appropriate volume of loading dye for each sample in separate drops (1X final concentration) on the Parafilm and mix with the desired volume of each PCR product.
10. Load 5 µl of DNA ladder in the first well of the gel and the samples in the rest of the wells.
11. Run the gel at 110 V until the loading dye reaches the bottom of the gel.
12. Place the gel on the transilluminator and obtain an image using the gel documentation system.

Note:

- *To determine the optimum annealing temperature for the primers, carry out a gradient PCR starting from 5°C below the lowest predicted annealing temperature according to the primer designing software (usually 5-6 samples spanning 10°C is enough). Choose the temperature rendering the strongest specific bands and no non-specific bands in the agarose gel.*

Protocol 2. DNA extraction from paraffin-embedded tissues mounted on slides

Solutions and reagents

100% Histo-Clear (National Diagnostics HS-200), or xylene

100% Ethanol

Proteinase K (QIAGEN 19131)

DNeasy Blood & Tissue Kit (QIAGEN 69504)

Samples

Unstained histological slides containing the samples to be extracted, and one H&E-stained slide obtained from the same block.

Materials

Plastic or glass containers
Slide rack (optional)
1.5ml polypropylene tubes
Pipettes and tips

Equipment

Fume hood (if working with xylene)
Hybridisation oven
Hot block
Eppendorf 5424 microcentrifuge (Eppendorf)
Vortex
NanoDrop 1000 spectrophotometer (Thermo Scientific)

Method

1. Place slides for extraction into a metal/plastic slide rack and place them in the oven at 60°C for 5 min.
2. Verify that the wax is melted and transfer the rack to a container with enough xylene to cover the slides. Gently agitate the rack for a few moments, let it to sit for 5 min.
3. Transfer the rack to a container with enough ethanol to cover the slides. Gently agitate the rack for a few moments, then transfer it to another container with ethanol and let it to sit for 5 min.

4. Transfer the rack to a container with enough ddH_2O to cover the slides and thoroughly rinse the slides to remove excess ethanol. Transfer the rack to another container with ddH_2O and let it to sit for 5 min.
5. Label 1.5 ml according to the identity of the slides and add to each tube 150 µl of buffer ATL (from QIAGEN kit) and 30 µl of Proteinase K.
6. Identify the area of interest on each slide to be extracted (use a marked H&E-stained slide as a guide) and, using a pipette tip or a scalpel, scrape from the slide the relevant tissue and transfer it to the corresponding tube with ATL buffer/proteinase K. If necessary, pipette a little amount of the ATL buffer/proteinase K on the surface of the slide to facilitate the removal of the tissue.
7. Incubate the tubes at 56°C overnight.
8. Incubate at 90°C for 1 h. If using only one heating block, keep the sample at RT until the heating block has reached 90°C.
9. Briefly centrifuge the tube to remove drops from the inside of the lid.
10. Add 200 µl buffer AL and mix thoroughly by vortexing. Then add 200 µl ethanol (96-100%) and mix thoroughly again by vortexing or pipetting.
    It is essential that the sample, buffer AL and ethanol are mixed immediately and thoroughly by vortexing or pipetting to yield a homogeneous solution. Buffer AL and ethanol can be premixed and added together in one step to save time when processing multiple samples. A white precipitate may form on addition of buffer AL and ethanol. This precipitate does not interfere with the procedure.
11. Transfer the entire sample to a QIAamp MinElute spin column placed in a 2 ml collection tube. Close the lid gently and centrifuge for 1 min at 16000 g to wash the spin column membrane. Discard the flow-through. If the sample has not completely passed through the membrane after centrifugation, centrifuge again until the spin column is empty.
12. Place the spin column in a new 2 ml collection tube. Add 500 µl of buffer AW1 to the spin column. Close the lid gently and centrifuge for 1 min at 16000 g to wash the spin column membrane. Discard the flow-through. Reuse the collection tube in the next step.
13. Add 500 µl of buffer AW2 to the spin column. Close the lid gently and centrifuge for 1 min at 16000 g to wash the spin column membrane. Discard the flow-through. Reuse the collection tube in the next step.
14. Place the spin column in a new 2 ml collection tube. Centrifuge at 16000 g for 3 min. Discard the collection tube with the flow-through.
15. Place the spin column in a new 1.5 ml tube and add 55 µl of buffer ATE. Close the lid and incubate for 1 min at 16000 g. Add 50 µl of buffer ATE and centrifuge again.
16. Verify DNA concentration using a NanoDrop spectrophotometer and store at -20°C.

Notes:

- *If a precipitate is noted in buffer ATL, mix well and incubate at 56°C for a few min before use.*
- *If using xylene, incubations and washes should be done in the fume hood.*
- *Buffers AW1 and AW2 are supplied as concentrates. Ensure that ethanol is added before use, as indicated by the manufacturer.*

Protocol 3: Preparation of calcium competent *E. coli*

Solutions and media

1X LB broth

20 g LB broth powder (SIGMA L3022)

Adjust with ddH_2O to a final volume of 1 l

Dilute the powder in the water and dispense in 250 ml aliquots. Sterilise by autoclaving, store at RT.

1X LB agar

20 g LB broth powder (SIGMA L3022)

12 g Bacteriological agar powder (SIGMA A5306)

Adjust with ddH_2O to a final volume of 1 l

Dilute the powder in the water and dispense in 250 ml aliquots. Sterilise by autoclaving and store at RT. To prepare agar plates, heat up the agar in the microwave until melted (approximately 4min at high power), cool down in water to approximately 40°C, add the appropriate antibiotic and pour in Petri dishes (25-30 ml per dish) under sterile conditions (use Bunsen's burner). Leave open until the agar has solidified, close and seal with Parafilm, label appropriately and store upside down at 4°C.

0.1M $CaCl_2$

Adjust with ddH_2O to a final volume of 1 l

Autoclave and store in the fridge or keep at RT and chill on ice before use.

0.1M $CaCl_2$ + 15% (v/v) glycerol

Prepare 500 ml, using sterile 0.1M $CaCl_2$ and glycerol. Store in the fridge or keep at RT and chill on ice before use.

Bacterial strain

Glycerol stock (LB broth + 15% [v/v] glycerol) of *E. coli* strain of preference, stored at -80°C.

Materials

Sterile cryotubes or 1.5ml polypropylene tubes

15 ml polypropylene

Petri dishes

500 ml conical flask, sterile

Pipettes and tips

Pipette controller and disposable serological pipettes

Glass loops

Equipment

Bunsen's burner

Incubator for bacterial plates

Shaking incubator

NanoDrop 1000 spectrophotometer (Thermo Scientific) or cuvette spectrophotometer

Heraeus Multifuge 3SR Plus (Thermo Scientific)

Method

1. Plate a small amount of bacteria from the glycerol stock (~5 µl or a drop taken with the loop) on an LB agar plate and incubate overnight at 37°C.
2. Inoculate one colony from the LB agar plate into 2-3 ml of LB broth in a 15 ml tube. Incubate overnight at 37°C/250 rpm.
3. Inoculate 1 ml of the overnight cell culture into a conical flask with 100 ml of LB broth. Read the OD600 in a spectrophotometer. Incubate for 1 h at 37°C/250 rpm.
4. Read the OD600 every 15-30 min until it reaches ~0.25-0.3 (it usually takes1.5-2 h).
5. Chill the culture on ice for 15 min.
6. Centrifuge the cells for 10 min at 3300 g/4°C.
7. Discard the medium and resuspend the cell pellet in 30-40 ml of cold 0.1M $CaCl_2$ (20 ml per 50 ml culture if using conical tubes). Resuspend using a serological pipette, do not vortex.
8. Incubate the cells on ice for 30 min. Centrifuge the cells as above.
9. Remove the supernatant, and resuspend the cell pellet in 6 ml 0.1M $CaCl_2$ + 15% glycerol.
    - 3 ml per 50 ml culture if using conical tubes.
    - If preparing using multiple Falcon tubes, once the 3 ml is added, pool all the samples together and mix well using the serological pipette, so that all the aliquots will have the same transformation efficiency when tested.
10. Label and chill cryotubes or 1.5 ml tubes at -80°C.
11. Pipette 400-500 µl of the cell suspension into the chilled tubes. Freeze these tubes on dry ice and then transfer them to -80°C freezer.
    - If using many tubes, take six out from the freezer at a time, keep them on ice and aliquot out. Once filled, immediately place them at -80°C, preferably on the ice to speed up the freezing, or alternatively use dry ice.

Notes:

- *Open tubes or plates with bacteria only under sterile conditions (Bunsen's burner).*
- *The agar plate with bacteria can be taken out from the incubator in the morning and kept in the fridge (sealed with Parafilm), so the colonies can be isolated in the afternoon and incubated overnight.*
- *Preferably, isolate two or more colonies, in case some of them do not grow.*

- *If using a NanoDrop for reading the OD600, it is important to note that Beer Lamberts law uses a light path length of 1cm, but the NanoDrop is 1mm.To account for this, an OD600 of ~0.025-0.03 should be used instead.*
- *All the steps after harvesting the cells should be done on ice (or at 4°C).*
- *The transformation efficiency is about 1-5x10^6/µl DNA when using the competent cells prepared with this method.*
- *The frozen competent cells are stable for 6 months, but once a tube is taken from the freezer and thawed, any unused portion should be discarded (it can be reused, but the transfection efficiency will be lower).*
- *After the competent cells are made, the transformation efficiency should be checked by transformation using plasmid DNA of known concentration, using the formula:*

$$\text{Transformation efficiency} = \frac{\text{total no. of colonies on plate}}{\text{Amount of DNA plated (µg/ml)}}$$

Reference:
Ausubel FM. Current protocols in Molecular Biology. John Wiley & Sons, 1998. Protocol 1.8.2.

Protocol 4: Transformation of calcium competent *E. coli*

Reagents, solutions and media

1X LB broth

20 g LB broth powder (SIGMA L3022)

Adjust with ddH_2O to a final volume of 1 l

Dilute the powder in the water and dispense in 250 ml aliquots. Sterilise by autoclaving and store at RT. Once antibiotic has been added, store at 4°C.

1X LB agar

20 g LB broth powder (SIGMA L3022)

12 g Bacteriological agar powder (SIGMA A5306)

Adjust with ddH_2O to a final volume of 1 l

Dilute the powder in the water and dispense in 250 ml aliquots. Sterilise by autoclaving and store at RT. To prepare agar plates, heat up the agar in the microwave until melted (approximately 4min at high power), cool down in water to approximately 40°C, add the appropriate antibiotic and pour in Petri dishes (25-30 ml per dish) under sterile conditions (use Bunsen's burner). Leave open until the agar has solidified, close and seal with Parafilm, label appropriately and store upside down at 4°C.

SOC medium

2%(w/v)	Tryptone
0.5%(w/v)	Yeast extract
10 mM	NaCl (dilute from 1 M stock)
2.5 mM	KCl (dilute from 250 mM stock)
10 mM	$MgCl_2$ (dilute from 2 M stock)
20 mM	Glucose (dilute from 1 M stock)

Adjust with ddH_2O to a final volume of 50 ml

Dissolve the first four reagents in water and sterilise by autoclaving, then add sterile $MgCl_2$ and glucose. Dispense in 1 ml aliquots and store at -20°C.

Antibiotics (stock solutions):

100 mg/ml ampicillin

1 g Ampicillin sodium salt (SIGMA A0166)

Adjust with ddH_2O to a final volume of 10 ml

50 mg/ml kanamycin

0.5 g Kanamycin B sulfate salt (SIGMA B5264)

Adjust with ddH_2O to a final volume of 10 ml

Dispense in 1 ml aliquots and store at 20°C or at 4°C for a short term. These solutions are to be used at a 1:1000 dilution in the media.

Bacterial strain

Calcium competent *E. coli* strain of preference, according to the experimental purpose.

Plasmids

10-500 ng of DNA of the plasmid of interest

Materials

1.5 ml polypropylene tubes

Pipettes and tips

Glass loops

Equipment

Bunsen's burner

Water bath

Shaking incubator

Incubator for bacterial plates

Method

Pre-heat one LB agar plate and one aliquot of SOC medium at 37°C before starting.

1. Defrost on ice an aliquot (400-500 µl) of calcium competent cells (stored at -80°C) and add 10-500 ng of DNA of the plasmid of interest (DNA should not surpass 10% of the volume of bacteria) and mix by swirling the tube gently for a few sec. Incubate for 30 min on ice.
2. Heat-shock the bacteria at 42°C for 45 sec in a water bath.
3. Incubate the bacteria for 2 min on ice.
4. Add 1 ml of SOC medium and incubate for 1 h at 37°C in agitation.
5. Centrifuge the bacteria for 2 min at 16000 g. Discard the supernatant, leaving approximately 50 µl plus the bacterial pellet.
6. Re-suspend the pellet in the remaining supernatant and plate on the LB agar plate, using the glass loop, under sterile conditions (Bunsen's burner).
7. Incubate overnight at 37°and select colonies by PCR or miniprep analysis.

Note:

- *Open tubes or plates with bacteria always under sterile conditions (Bunsen's burner).*

Protocol 5: Extraction of plasmid DNA from small-scale bacterial cultures (miniprep)

Reagents

QIAprep Spin Miniprep Kit (QIAGEN 27106)

Buffer P1 should be kept at 4°C, rest of the kit should be kept at RT.

Bacteria

5-10 ml bacterial cell culture

Materials

1.5 ml polypropylene tubes

Pipettes and tips

Equipment

Heraeus Multifuge 3SR Plus (Thermo Scientific)

Eppendorf 5424 microcentrifuge (Eppendorf)

NanoDrop 1000 spectrophotometer (Thermo Scientific)

Method

1. Centrifuge the bacterial cell culture for 10 min at 4000 g/RT, discard the supernatant.
2. Re-suspend the bacterial pellet in 250 µl of buffer P1 (resuspension buffer) *for each 5 ml of bacterial culture* and transfer to an Eppendorf tube *for each 5 ml of bacterial culture.*
3. Add 250 µl of buffer P2 (lysis buffer) to each tube and mix thoroughly by inverting the tube 4-6 times until the solution becomes clear. Do not allow the lysis reaction to proceed for more than 5 min. If LyseBlue reagent has been added to buffer P1, the solution will turn blue.
4. Add 350 µl of buffer N3 (neutralisation buffer) to each tube and mix immediately and thoroughly by inverting the tube 4-6 times. If LyseBlue reagent has been added to buffer P1, the solution will turn colourless.
5. Centrifuge for 10 min at 13000 g.
6. Apply the supernatant from one of the tubes from step 5 to the QIAprep spin column assembled into a collection tube by decanting or pipetting. Centrifuge for 1 min at 13000 rpm and discard the flow-through. If more than 5 ml of bacterial culture are being processed, apply the supernatant from the second Eppendorf tube to the column and repeat this step. Replace the collection tube.
7. Wash the QIAprep spin column by adding 750 µl of buffer PE, centrifuge for 1 min at 13000 rpm and discard the flow-through. Replace the collection tube.

8. Centrifuge for 3 min at 13000rpm to remove residual washing buffer. Discard the collection tube
9. Place the QIAprep column into a clean Eppendorf tube. To elute DNA, add 100 µl of buffer EB (elution buffer) to the centre of the QIAprep spin column, let stand for 1 min, and centrifuge for 1 min at 13000 rpm.
10. Optional: repeat the previous step (plasmid concentration can be verified before).
11. Verify plasmid DNA concentration using a NanoDrop spectrophotometer and store at -20°C.

References:

This is a modification of the protocol provided by the kit's manufacturer.

Protocol 6: Site-directed mutagenesis

Reagents and media

QuikChange II XL Site-Directed Mutagenesis Kit (Agilent Technologies 200521)

XL10-Gold Ultracompetent Cells should be kept at -80°C, rest of the kit should be kept at -20°C. Defrost on ice before use.

Sterile ddH_2O

1X LB broth

20 g LB broth powder (SIGMA L3022)

Adjust with ddH_2O to a final volume of 1 l

Dilute the powder in the water and dispense in 250 ml aliquots. Sterilise by autoclaving and store at RT. Once antibiotic has been added, store at 4°C.

1X LB agar

20 g LB broth powder (SIGMA L3022)

12 g Bacteriological agar powder (SIGMA A5306)

Adjust with ddH_2O to a final volume of 1 l

Dilute the powder in the water in dispense in 250 ml aliquots. Sterilise by autoclaving and store at RT. To prepare agar plates, heat up the agar in the microwave until melted (approximately 4 min at high power), cool down in water to approximately 40°C, add the appropriate antibiotic and pour in Petri dishes (25-30 ml per dish) under sterile conditions (use Bunsen's burner). Leave open until the agar has solidified, close and seal with Parafilm, label appropriately and store upside down at 4°C.

NZY$^+$ broth

1%(w/v)	NZ amine
0.5% (w/v)	Yeast extract
0.5% (w/v)	NaCl
12.5 mM	$MgCl_2$ (dilute from 2 M stock)
12.5 mM	$MgSO_4$ (dilute from 2 M stock)
20 mM	Glucose (dilute from 1 M stock)

Adjust with ddH_2O to a final volume of 50 ml

Dissolve the first four reagents in water, adjust the pH to 7.5 with NaOH and sterilise by autoclaving, then add sterile $MgCl_2$, $MgSO_4$ and glucose. Dispense in 1 ml aliquots and store at -20°C.

100 mg/ml ampicillin

1 g Ampicillin sodium salt (SIGMA A0166)

Adjust with ddH_2O to a final volume of 10 ml

Dispense in 1 ml aliquots and store at 20°C or at 4°C for a short term. Use at a 1:1000 dilution in the media.

Plasmids

10 ng of plasmid to be mutagenised

Materials

0.2 ml and 1.5 ml polypropylene tubes

Pipettes and tips

Glass loops

Equipment

PCR hood

GS1 Thermal Cycler (G-Storm)

Eppendorf 5424 microcentrifuge (Eppendorf)

Bunsen's burner

Water bath

Shaking incubator

Incubator for bacterial plates

Method:

Defrost all the reagents and samples on ice before starting.

1. Place the racks, pipettes, tips, tubes ddH_2O and PCR buffer to be used in the PCR hood and expose them to UV light for 5-10 min.
2. Working in the PCR hood, set up the following reaction:

5 µl	10X reaction buffer
10 ng	Plasmid to be mutagenised
125 ng	Forward primer
125 ng	Reverse primer
1 µl	dNTP mix
3 µl	QuikSolution reagent

   Adjust with sterile ddH_2O to a final volume of 50 µl

   Then add 1 µl of 2.5U/µl *PfuUltra* HF DNA polymerase
3. Place the tube into the thermal cycler and cycle using the following program:

   One cycle:

95°C	1 min

   18 cycles:

95°C	30 sec
60°C	50 sec
68°C	1 min/kb of plasmid length

One cycle:

68°C 7 min

4. Add 1 µl of *DpnI* restriction enzyme (10 U/µl). Gently and thoroughly mix the reaction, spin down in a microcentrifuge for 1 min, immediately place the tube back in the thermal cycler and incubate at 37°C for 1 h.
5. Thaw the XL10-Gold Ultracompetent Cells on ice and transfer a 45 µl aliquot to a pre-chilled 1.5 ml Eppendorf tube.
6. Add 2 µl of the β-mercaptoethanol mix included in the kit, swirl the tube gently and incubate on ice for 10 min, swirling every 2 min.
7. Add 2 µl of the *DpnI*-treated DNA to the cells, swirl the tube gently and incubate on ice for 30 min.
8. Pre-heat NZY^+ broth at 42°C in a water bath.
9. Heat-pulse the reaction tube in a 42°C water bath for 30 sec.
10. Incubate on ice for 2 min.
11. Add 500 µl of pre-heated NZY^+ broth and incubate for 1 h at 37°C/250 rpm.
12. Centrifuge for 2 min at 13000 g, discard the supernatant, leaving approximately 50-100 µl.
13. Resuspend the pellet in the remaining supernatant and plate on a LB agar plate with 100 µg/ml ampicillin.
14. Incubate overnight at 37°C, select 1-3 colonies and grow them overnight at 37°C/250 rpm in LB broth with 100 µg/ml ampicillin.
15. Extract plasmid DNA (Protocol 5), and send for sequencing.

References:

This is a summarised version of the protocol provided by the kit's manufacturer.

Protocol 7: Extraction of plasmid DNA from large-scale bacterial cultures (maxiprep)

Reagents

GenElute™ HP Plasmid Maxiprep Kit (SIGMA NA0310-1KT)

Resuspension/RNase A and neutralization solutions should be kept at 4°C, rest of the kit should be kept at RT

Bacteria

200-250 ml bacterial cell culture

Materials

1.5 ml and 50 ml polypropylene tubes

Pipettes and tips

Pipette controller and disposable serological pipettes

Equipment

Heraeus Multifuge 3SR Plus (Thermo Scientific)

Eppendorf 5424 microcentrifuge (Eppendorf)

NanoDrop 1000 spectrophotometer (Thermo Scientific)

Method

1. Transfer the bacterial cell culture to 50 ml tubes and centrifuge for 10 min at 4000 g/RT, discard the supernatant. Frozen bacterial pellets (kept at -80°C) can be used instead.
2. Resuspend the bacterial pellet(s) in a total of 12 ml of resuspension/RNase A solution by vortexing or pipetting, pool all the resuspended pellets together in one 50 ml tube.
3. Add 12 ml of lysis solution and gently invert the tube 6-8 times. Let the mixture to sit 3-5 min.
4. In the meantime, prepare a filter syringe by removing the plunger and placing the barrel in a rack so that the syringe barrel is upright (a 1 l conical tube can be used if there is an appropriate rack is not available).
5. Add 12 ml of chilled neutralisation solution and gently invert the tube 4-6 times.
6. Add 9 ml of binding solution and invert 1-2 times. Immediately pour into the barrel of the filter syringe. Allow the lysate to sit for 5 min.
7. In the meantime, place a GenElute HP Maxiprep binding column into a 50 ml collection tube (included in the kit). Add 12 ml of the of the column preparation

solution to the column and centrifuge for 2 min at 3000 g/RT. Discard the flow-through.

8. Hold the filter syringe barrel over the binding column and gently apply pressure to the plunger to expel half of the cleared lysate into the column. Pull back slightly on the plunger to stop the flow of the remaining lysate. Centrifuge for 2 min at 3000 g/RT. Discard the flow-through. Add the rest of the cleared lysate to the column and centrifuge again.
9. Add 12 ml of wash solution 1 and centrifuge for 2 min at 3000 g/RT. Discard the flow-through.
10. Add 12 ml of wash solution 2 and centrifuge for 5 min at 3000 g/RT. Discard the flow-through.
11. Transfer the binding column to a clean 50 ml tube (included in the kit). Add 3 ml of elution solution and centrifuge for 3 min at 3000 g/RT.
12. Optional: apply the eluate from the previous step back into the column and centrifuge again (plasmid concentration can be verified before).
13. Verify plasmid DNA concentration using a NanoDrop spectrophotometer, dispense in 1 ml aliquots and store at -20°C.

References:

This is a summarised version of the protocol provided by the kit's manufacturer.

Protocol 8: Polyacrylamide gel electrophoresis

Buffers and solutions

20X 2-(N-Morpholino)ethanesulfonic acid (MES) electrophoresis buffer (stock solution)

1M MES hydrate (SIGMA M8250)

1M Tris base

69.3mM Sodium dodecyl sulfate (SDS, 2% w/v)

20.5mM EDTA free acid

Adjust with ddH_2O to a final volume of 1 l

SDS is easier to dissolve if using a hot plate. Sterilisation not needed, store at RT. Do not adjust pH: the final pH of this 20X stock will be 7.1, and 7.3 when diluted to 1X. Dilute accordingly with ddH_2O to obtain a 1X working solution.

6X SDS gel loading buffer

300 mM Tris-Cl pH 6.8 (dilute from 1M stock)

600 mM Dihidrothreitol (DTT)

12% w/v SDS

0.6% w/v Bromophenol blue

60% v/v Glycerol

Adjust with ddH_2O to a final volume of 50 ml

SDS is easier to dissolve if using a hot plate. Sterilise by filtration. Dispense in 1 ml aliquots and store at -20°C.

Reagents

Novex® Sharp Pre-stained Protein Standard (Life Technologies LC5800) or Kaleidoscope™ Prestained Standards (BIO-RAD 161-0324)

Materials

0.2 (strips) or 1.5 polypropylene tubes

Pipettes and tips, including long gel loading tips

NuPAGE® Novex® 4-12% Bis-Tris Protein Gels, 1.0 mm, 10-well (Life Technologies NP0321BOX) or 15-well (Life Technologies NP0323BOX)

Equipment

Vortex

Hot block (set at 95°C) or GS1 Thermal Cycler (G-Storm)

BR4i refrigerated centrifuge (Jouan) or Eppendorf 5424 microcentrifuge (Eppendorf)

XCell SureLock™ Mini-Cell Electrophoresis System (Life Technologies)

Consort E835 electrophoresis power supply (Cleaver Scientific Ltd)

Method

1. Combine the desired amount of protein with an appropriate volume of 6X gel loading buffer (to a final concentration of 1X) in 0.2 or 1.5 ml polypropylene tubes. Mix well by pipetting or vortexing.
2. Denature the samples at 95°C for 5 min on a hot block or thermal cycler and spin them down.
3. Assemble the electrophoresis tank. Remove the sealing tape from the bottom of one or two gels and place them into the buffer core of the tank with the printed side facing out and lock the gel tension wedge.
4. Fill both chambers of the tank with 1X MES and carefully remove the combs from the gels.
5. Using gel loading tips, load 6-10 µl of molecular weight marker in the first well and the samples in the next wells.
6. Connect the tanks to the power supply and run the gels at 120 V (for 15-well gels) or 150 V (for 10-well gels) until the blue loading buffer reaches the bottom of the gel (~1:15-1:35 h).

Protocol 9: Coomassie staining of polyacrylamide gels

Solutions

Staining solution

50% (v/v) Methanol

10% (v/v) Glacial acetic acid

0.25% (w/v) Coomassie brilliant blue R-250

Adjust with ddH_2O to a final volume of 1 l

Filter using a Whatman No.1 filter. Store at RT.

Destaining solution

40% (v/v) Methanol

10% (v/v) Glacial acetic acid

Adjust with ddH_2O to a final volume of 1 l

Store at RT

20% (v/v) glycerol in ddH_2O (optional)

Material

Spatula

Plastic or glass containers

Equipment

Shaking platform

Odyssey® Infrared Imaging System (LI-COR)

Method

1. After electrophoresis, take out the polyacrylamide gel from the tank and carefully remove it from the glass or plastic cassette.
2. Immerse the gel in a container with at least 5 volumes of destaining solution (or enough volume to completely cover the gel) and incubate for 10 min on a shaking platform at low speed at RT.
3. Remove the destaining solution and save it for future use. Add at least 5 volumes of staining solution (or enough volume to completely cover the gel) and place it back on the shaking platform. Incubate for at least 4 h at RT.
4. Remove the stain and save it for future use. Destain the gel by soaking it in destaining solution for 4-8 h, changing the destaining solution 3-4 times, until the protein bands are seen without background staining.
5. Scan the gel in an Odyssey infrared imager, using the “protein gel” option at 700 nm (place the stained gel directly on the surface of the scanner).

6. If desired, keep the gel in 20% (v/v) glycerol in ddH_2O at 4°C in a sealed bag.

Reference:

Sambrook J, Russell DV. *Molecular Cloning: A Laboratory Manual*. CSHL Press, 2001. Vol.3, A8.46-47.

Protocol 10: Production and purification of GST-tagged proteins

Buffers, solutions and media:

1X LB broth with 100 µg/ml ampicillin

20 g LB broth powder (SIGMA L3022)

Adjust with ddH_2O to a final volume of 1 l

Dilute the powder in the water and dispense in 250 ml aliquots. Sterilise by autoclaving and store at RT. Add 1 ml of 100 mg/ml ampicillin before use. Once antibiotic has been added, store at 4°C.

1X LB agar with 100 µg/ml ampicillin

20 g LB broth powder (SIGMA L3022)

12 g Bacteriological agar powder (SIGMA A5306)

Adjust with ddH_2O to a final volume of 1 l

Dilute the powder in the water in dispense in 250 ml aliquots. Sterilise by autoclaving and store at RT. To prepare agar plates, heat up the agar in the microwave until it is melted (approximately 4 min at high power), cool down in water to approximately 40°C, add 1 ml of 100 mg/ml ampicillin and pour in Petri dishes (25-30 ml per dish) in sterile conditions (use Bunsen's burner). Leave open until the agar has solidified, close and seal with Parafilm, label appropriately and store at 4°C.

1X SOC medium

2%(w/v)	Tryptone
0.5%(w/v)	Yeast extract
10 mM	NaCl (dilute from 1 M stock)
2.5 mM	KCl (dilute from 250 mM stock)
10 mM	$MgCl_2$ (dilute from 2 M stock)
20 mM	Glucose (dilute from 1 M stock)

Adjust with ddH_2O to a final volume of 50 ml

Dissolve the first four reagents in water and sterilise by autoclaving, then add sterile $MgCl_2$ and glucose. Dispense in 1 ml aliquots and store at -20°C.

Buffer A

100 mM	NaCl
20 mM	Tris-HCl pH 7.5

Adjust with ddH_2O to a final volume of 2 l

Sterilise by filtration, store at RT.

Buffer B

20 mM	Reduced glutathione in buffer A

Adjust with ddH_2O to a final volume of 50 ml

Adjust pH to 7.5 with NaOH. Prepare fresh before use.

6M Urea in ddH_2O

Adjust with ddH_2O to a final volume of 1 l

Sterilise by filtration, store at RT.

1M IPTG (Promega V3951) in ddH_2O

Adjust with ddH_2O to a final volume of 50 ml

Sterilise by filtration, dispense in 1 ml aliquots and store at -20°C.

100% glycerol

Reagents:

100 mg/ml Ampicillin

1 g Ampicillin sodium salt (SIGMA A0166)

Adjust with ddH_2O to a final volume of 10 ml

Complete® Protease Inhibitor Cocktail tablets (Roche 11836145001)

Glutathione Sepharose 4 Fast Flow (GE Healthcare 17-5132-02)

Bacterial strain

Calcium competent BL21-PLyss *E. coli*

Plasmids

pTHREE-E (A. Oliver, University of Sussex) containing CDS for WT AIP and variants (10-500 ng)

Materials

1.5, 15 and 50 ml polypropylene tubes

Cryotubes

Pipettes and tips

Pipette controller and disposable serological pipettes

Glass or plastic loops

Petri dishes

3 l glass conical flasks

1 l round bottom plastic centrifuge tubes

Econo-Column® Chromatography Column, 2.5 × 10 cm (BIO-RAD 737-2512)

Vivaspin 20 (50000 MWCO) (Sartorius VS2032) centrifugal concentrators

10 ml syringes and needles

96-well, 2.2 ml plastic fraction collection block

Equipment

Bunsen's burner

Water bath

Shaking incubator

Incubator for bacterial plates

Spectrophotometer

Centrifuge for 1 l tubes

Vortex

Sonicator

Refrigerated centrifuge for 15 and 50 ml tubes

Roller Mixer

HiPrep 26/60 Sephacryl S-200 HR gel filtration chromatography column (GE Healthcare 17-1195-01)

ÄKTA Prime chromatography equipment (GE Healthcare)

NanoDrop 1000 spectrophotometer (Thermo Scientific)

Method:

1. Prime the gel filtration chromatography equipment with buffer A, avoiding air to enter into the equipment.
2. Place the gravity flow column upright on a support in the cold room. Pour ~20 ml of GST agarose into the column and wash it several times with buffer A, until agarose becomes a compact material at the bottom (let the buffer flow through by gravity). Lock the bottom of the column and store at 4°C until use, properly hydrated with buffer A.

   Glutathione agarose is a 50% solution in ethanol. The final volume of agarose will be ~10 ml.
3. Transform one aliquot of BL21-PLyss cells with each of the plasmids carrying *AIP* mutations (see Protocol 4). Plate the total volume of the transformation reaction, divided in three LB agar plates with ampicillin. Incubate overnight at 37°C.
4. Prepare three conical flasks with 1 l LB broth with 100 µg/ml ampicillin per plasmid to be grown and incubate overnight at 37°C without agitation.
5. Harvest all the colonies by scraping the three plates and dissolving the bacteria in 15 ml of LB broth with 100 µg/ml ampicillin.
6. Verify that the flasks with medium remain clear and add fresh ampicillin (same amount than before).
7. Inoculate each flask with 5 ml of bacteria, incubate them at 37°C/250 rpm and measure OD_{600} until it reaches 0.6-0.8 (OD_{600} is expected to double approximately every 20 min). Add 1M IPTG to a final concentration of 1mM and incubate at 20°C/250 rpm overnight.

8. Transfer the cultures to 500 ml tubes and centrifuge at 4500 g for 12 min. Transfer bacterial pellets to 50 ml tubes containing one tablet of protease inhibitor cocktail, dissolved in 35 ml of buffer A and resuspend by vortexing.
   Pellets can be stored at -80°C if planned to be used later.
9. To sonicate the bacteria, place the tube in a glass with ice (to avoid overheating) and perform 5 sec pulses with 10 sec pauses, for 3 min total time (40% power, frequency 50 Hz) twice. Save a sample for PAGE.
10. Centrifuge the bacteria for 1 h at 20000 rpm/4°C. Transfer cleared lysates to new tubes and save a sample for PAGE.
11. Pour cleared lysate into the column with glutathione agarose and mix it on a roller for 30 min at 4°C.
12. Place the column upright on a support in the cold room and let the lysate flow through the column by gravity. Save a sample of the flow-through for PAGE.
    If the volume of cleared lysate surpasses the capacity of the column, once the flow-through has passed, close the end of the column, add the rest of the lysate and repeat steps 11 and 12.
13. Wash the glutathione sepharose with three volumes of buffer A by gravity, ensuring not to leave it dry in the cold room.
14. Elute the protein with 20 ml of buffer B by gravity, in the cold room.
    Glutathione sepharose can be regenerated by incubation with 6M urea.
15. Transfer the eluate into a concentrator and centrifuge at 4000 rpm/4°C until concentrated to a final volume of ~10 ml.
    Centrifuge the concentrator with ddH_2O to hydrate the membrane before use.
16. Recover the concentrated sample with a 10 ml syringe, avoiding bubble formation.
17. Load the sample in the gel filtration chromatography equipment using the following parameters: flow 3 ml/min, pressure <0.7 mPa.
18. Let the first 100 ml flow through (dead volume). Collect 1.8 ml samples following the chromatography curves, until no peaks are observed.
19. Analyse 10 µl of each fraction and 10 µl of each of the samples collected in previous steps by PAGE-Coomassie staining (see Protocol 8 and Protocol 9). Store the purified fractions in the fridge until the Coomassie-stained gel has been analysed.
20. Pool the fractions containing the expected protein into a concentrator and centrifuge as before, until a 1 mg/ml concentration is reached (measure the sample every 15-20 min using the protein A280 function in the NanoDrop).
    Centrifuge the concentrator with ddH_2O to hydrate the membrane before use.
21. Add glycerol to a final concentration of 5% and dispense the purified protein in 1 ml aliquots in 1.5 ml tubes or cryotubes, previously labelled, transfer immediately to dry ice for fast freezing and store at -80°C.

Reference:

Protocol provided by M. Morgan, Molecular Chaperones/Structural Biology Group, Genome Damage and Stability Centre, University of Sussex.

Protocol 11: Western blotting

Buffers

Transfer buffer

25mM Tris base

190 mM Glycine

20% (v/v) Methanol

Adjust with ddH_2O to a final volume of 1 l

Dissolve tris and glycine in ddH_2O, then add methanol. Store at RT.

Washing buffer

0.1% (v/v) Tween 20

Adjust with 1X sterile PBS to a final volume of 1 l

Store at RT.

Blocking buffer

5% (w/v) Semi-skimmed milk in washing buffer

Adjust with ddH_2O to a final volume of 50 ml

Preferably prepare fresh, but it can be stored at 4°C for a few days.

1X PBS

Adjust with ddH_2O to a final volume of 1 l

Sterilise by autoclaving and store at RT.

Reagents

Primary and secondary antibodies, according to the experimental conditions.

Materials

50 ml polypropylene tubes

Protran BA85 nitrocellulose membrane 0.45 µm (GE Healthcare 10402594)

BIO-RAD extra thick blot paper, 7.5X10 cm (BIO-RAD 170-3965)

Cut one 7.5X9 cm rectangle for each mini-gel to be transferred.

Plastic or glass containers

Roller

Spatula

Equipment

Semi-dry blotter SD10 (Cleaver Scientific Ltd)

Consort E835 electrophoresis power supply (Cleaver Scientific Ltd)

Roller Mixer SRT6 (Stuart)

Method

1. Cut the upper right corner of the membrane in diagonal and soak it in transfer buffer for at least 15 min (alternatively, leave it in a container with enough transfer buffer to cover it for the whole duration of the electrophoresis). Soak one pair of blotting papers just before use.
2. Place one blotting paper on the blotter and place the membrane on top of it. Manipulate the membrane touching only the edges with gloved hands or tweezers. Pour a small amount of transfer buffer on the membrane to keep it wet.
3. After electrophoresis, take out the polyacrylamide gel from the tank and carefully remove it from the glass or plastic cassette using a spatula.
4. Place the gel on top of the membrane. Pour a small amount of transfer buffer on top of the gel and gently press it against the membrane to eliminate any bubbles.
5. Place a second blotting paper on top of the membrane and pass the roller on its surface, to eliminate any bubbles in the WB sandwich.
6. Place the lid of the blotter on top of the sandwich and gently fix it with the screws. Be careful in this step, as too much pressure can break the gel.
7. Connect the blotter to the power pack (the positive electrode is on the bottom piece of the blotter and the negative one is on the lid).
8. Turn on the power pack and set up the transfer conditions (usually 15 V/500 mA for 30 min is enough for medium-sized proteins) and press start. Make sure that the power pack raises the desired voltage.
9. Once the transference is finished, open the blotter, remove the upper blotting paper and then carefully separate the gel from the membrane, making sure that no residues of gel are left.
10. If necessary, mark the location of the molecular weight markers with a pencil. Transfer the membrane to a 50 ml tube (appropriately labelled) with ~10 ml of washing buffer and place it on the roller at RT, making sure that the side of the membrane that was in contact with the gel (protein side) is facing the inside of the tube.
11. Wash the membrane for a total of three times for 2-5 min on the roller.
12. Add 15-20 ml of blocking buffer and incubate on the roller for 1 h or as specified in the protocol for the primary antibody(ies) to be used.
13. Remove the blocking buffer and add the primary antibody(ies) diluted in 5 ml of blocking buffer. Incubate overnight at 4°C on a roller.
14. Remove the primary antibody and store it at -20°C (keep track of the number of times the antibody has been used, five times is usually fine). Wash the membrane three times with ~10 ml of washing buffer on the roller at RT.
15. Add the secondary antibodies diluted in 5 ml of blocking buffer. Incubate for 40-60 min on the roller at RT.

16. Remove the secondary antibodies and wash the membrane three times with ~10 ml of washing buffer and then once with 1X PBS on the roller at RT.
17. Place the membrane on the Odyssey imager face down, making sure no bubbles are left. Open the Odyssey application and scan the membrane using “membrane” function (intensity and quality parameters can be adjusted if necessary).

Protocol 12: Pull-down assay for GST-AIP proteins

Buffers and solutions

Lysis buffer

20 mM Tris-Cl pH8 (dilute from 1 M stock)

200 mM NaCl (dilute from 1 M stock)

1 mM EDTA pH8 (dilute from 0.5 M stock)

0.5% (v/v) IGEPAL® CA-630 (SIGMA I3021)

Adjust with sterile ddH_2O to a final volume of 50 ml

Sterilisation not needed. Store at 4°C. Just before use, add 1 tablet of Complete® Protease Inhibitor Cocktail (Roche 11836145001). The fully prepared buffer can be aliquoted and stored at -80°C for several weeks.

Elution buffer

50 mM Tris-Cl pH8 500µl from 1M stock

20 mM Reduced glutathione

Adjust with sterile ddH_2O to a final volume of 10 ml

Mix Tris-HCl with 9 ml ddH_2O, add glutathione and mix well. Adjust pH to 8 with NaOH (~35 µl of 3 M solution) and adjust volume to 10 ml with ddH_2O. Prepare fresh before use.

1X PBS, pH 7.4

To obtain a 5X stock, dissolve 25 tablets of PBS (SIGMA P4417) in ddH_2O and sterilise by autoclaving. Store at RT. Dilute accordingly with ddH_2O to obtain a 1X working solution.

PAGE buffers

See Protocol 8

WB buffers

See Protocol 11.

Reagents:

Purified GST-AIP proteins

Glutathione HiCap Matrix (QIAGEN 30900)

Protein™ Kaleidoscope™ Standard (BIO-RAD 161-0375)

Reagents for protein quantification (see Protocol 14)

Cell culture media:

See Protocol 13

Cell line

See Protocol 13

Materials:

T75 or T175 cell culture flasks

1.5 and 15 ml polypropylene tubes

Pipettes and tips

Pipette controller and disposable serological pipettes

5 ml syringes, 23G needles and insulin syringes and needles

1 l glass

Floating rack for 1.5 ml tubes

Slide-A-Lyzer MINI Dialysis Devices (2K MWCO) (Thermo Scientific 69580)

Magnetic stirrer

Materials for cell culture, protein quantification, PAGE and WB (see appropriate protocols).

Equipment

Water bath

Set at 37°C

Inverted microscope

Labofuge 400 centrifuge (Heraeus)

BR4i refrigerated centrifuge (Jouan)

GS1 Thermal Cycler (G-Storm)

Stuart tube rotator SB2 (Stuart)

Equipment for cell culture, protein quantification PAGE and WB (see appropriate protocols).

Protocol

For details on growth and maintenance of GH3 and HEK293 cells see Protocol 13 and Protocol 17.

Cell culture must be performed in aseptic conditions. From step 2 onwards, all the procedures must be done at 4ºC or on ice.

1. Grow GH3 cells in T175 flasks until ~80-90% confluent, trypsinise, count the cells and pellet (see Protocol 13), and wash the pellet with 10 ml PBS.
2. Resuspend the cell pellet in the appropriate amount of cold lysis buffer to obtain a solution with $12X10^6$ cells/ml.
3. Incubate for 20 min at 4°C on a rotator (alternatively, incubate on ice, vortexing occasionally). Collect the lysate in a syringe and pass it through a 23G needle six times.
4. Transfer to 1.5 ml tubes and centrifuge the lysates for 10 min at 17000 g/4°C and transfer the supernatants (cleared lysates) to new tubes.
5. Quantify the protein concentration in the lysates using the Bradford method (see Protocol 14). Separate ~60 µl of cleared lysate for PAGE analysis.

6. Homogenise glutathione beads, transfer 50 µl to 16X1.5 ml tubes, add 500 µl of lysis buffer and mix well by inverting the tube. Centrifuge for 2 min at 1000 g/4ºC. Discard supernatant and add 25 µl of lysis buffer.
7. Add to each of eight tubes with glutathione beads either 10 µg of one of the GST-AIP proteins, GST or 10µl ddH_2O and add 1 ml of cleared lysate to the rest of the tubes. Label appropriately.
8. Incubate all the tubes for 1 h at 4ºC on a rotator. Centrifuge for 2 min at 1000 g/4ºC. *Binding of purified GST-AIP proteins to the beads before the addition of lysate may improve pull-down efficiency. Exposing the lysate to the beads before the pull-down ("pre-cleaning" the lysate) reduces non-specific binding.*
9. Transfer the lysate to each tube with glutathione beads and GST-AIP protein (1 ml of lysate per reaction) and incubate for 4 h at 4ºC on a rotator. Centrifuge for 2 min at 1000 g/4ºC. Save supernatants in different tubes for PAGE analysis.
10. Add 1 ml of lysis buffer to each tube, mix well by inverting the tube and centrifuge for 2 min at 1000 g/4ºC. Discard the supernatant and repeat this step three more times. After the last wash, carefully eliminate any residue of lysis buffer with an insulin needle.
11. Add 30 µl of elution buffer to each tube, incubate 1 h at 4ºC on a rotator and centrifuge for 2 min at 1000 g/4ºC. Transfer the supernatant into a new tube and label appropriately. Repeat this step with 20 µl of elution buffer and pool this second eluate together with the first one. Store at -80°C.
12. Repeat the pull-down assay four times for each bait protein and pool together the eluates of the four experiments.
13. Transfer each pooled eluate to a dialysis tube, place them all on a floater and dialyse against 1 l PBS overnight at 4°C, in agitation on a magnetic stirrer.
14. Analyse the eluates and unbound fractions by PAGE (see Protocol 8) and Coomassie staining (see Protocol 9) or WB (see Protocol 11).

Reference:

Detection of protein-protein interactions using the GST fusion protein pull-down technique. *Nat Methods.* 2004;1(3):275-276.

Protocol 13: Initiation and maintenance of a stock culture of GH3 cells

Cell culture regents

Dulbecco´s Eagle Modified Medium (DMEM, SIGMA D5030)

FBS (Life Technologies 10270-106), filtered

1X Dulbecco's PBS (SIGMA D8537)

1X Trypsin-EDTA (TE) (SIGMA T3924)

Pre-heat all these reagents at 37°C before using.

Trypan blue solution (SIGMA T8154)

Cell line

GH3 (rat somatotropinoma) (ECACC 87012603)

Materials

1.5 and 15 ml polypropylene tubes

T75 or T175 cell culture flasks

Pipettes and tips

Pipette controller and disposable serological pipettes

Equipment

Water bath

Set at 37°C

Cell culture incubator and hood

Inverted microscope

Heraeus Labofuge 400 centrifuge

Haemocytometer

Manual cell counter

Calculator

Method

Work in cell culture hood under aseptic conditions. For initiating a stock culture:

1. Transfer 12 ml of complete medium (DMEM supplemented with 10% FBS) into a T75 flask or 18 ml into a T175 flask.
2. Take out a vial of frozen GH3 cells (stored in liquid nitrogen) and immerse it in the water bath for approximately 1 min or until the contents are completely thawed.
3. Transfer the contents of the vial to the flask with medium, label appropriately and incubate at 37°C/5% CO_2 for 24 h.
4. Change the medium and continue incubation until cells reach ~80-90% confluence.

For maintaining a stock culture:

1. When the cell culture reaches ~80-90% confluence, remove the medium the cells grew in and carefully wash the cells thrice with 10 ml of PBS.
2. Add 3 ml of 1X TE for a T75 or 4 ml for a T175, ensuring it covers the totality of the cells and incubate at 37°C for 3 (for a T75) to 4 min (for a T175). Verify cell detachment under the microscope.
3. Add complete medium, using double of the volume than for TE. Wash the surface where the cells grew thrice, mix well with the pipette to separate cell clumps and transfer to a 15 ml tube.
4. Take 20 µl of the cell suspension and mix with 20 µl of trypan blue in a 1.5 ml tube. Transfer 10 µl of this mixture to each of the chambers of a haemocytometer and count the cells under the microscope as follows:
    a. Count the cells on each of the four external squares of the haemocytometer (those with large squares), avoiding blue cells (not viable) and obtain the average of the four squares.
    b. Multiply X2 (dilution factor with trypan blue), then X10000 to obtain number of cells per ml. Finally, multiply for the volume of the cell suspension, to obtain the total cell number.
5. Centrifuge at 800 g for 3 min at RT.
6. Remove the supernatant and resuspend the pellet in an appropriate volume of complete medium with antibiotic to obtain a suspension with $1X10^6$ cells per ml.
7. Transfer 1 ml of this cell suspension ($1x10^6$ cells) into a T75 or 2 ml ($2X10^6$ cells) into a T175 and adjust to a final volume of 12 ml for a T75 or 18 ml for a T175 with complete medium.
8. Incubate at 37°C/5% CO_2 until ~80-90% confluence (approximately 6-7 days). Change the medium every 3-4 days.

Protocol 14. Protein quantification using the Bradford method

Reagents

Bio-Rad Protein Assay Dye Reagent Concentrate (BIO-RAD 500-0006)

Dilute 1:5 with ddH_2O before use (approximately 20 ml are enough for one 96-well plate)

10 mg/ml Bovine Serum Albumin (BSA, Promega R3961)

Material and equipment

Plates

0.2 µl PCR tubes

Multichannel pipette

Plate shaker

Wallac Victor plate reader

Method

1. Prepare concentration standards:
   - In a PCR tube, mix 12 µl of 10 mg/ml BSA + 18 µl of ddH_2O to obtain a 4000 µg/ml standard.
   - Take 15 µl of this solution and mix with 15 µl of ddH_2O to obtain a 2000 µg/ml standard, and continue diluting sequentially until obtaining a 125 µg/ml standard. For the standard 0 use ddH_2O only.
2. Add 196 µl of 1X Bradford reagent to each well of a 96-well plate using a multichannel pipette.
3. Add 4 µl of each standard or sample (diluted or undiluted, as appropriate) to three contiguous wells with Bradford reagent (for triplicate readings).
4. Mix for 1 min on a plate shaker.
5. Read absorbance at 595nm on a plate reader.
6. Export the results to an Excel file and copy the absorbance readings for the whole plate in “Absorbance” area of the “Bradford assay with microplate reader” Excel template (see printout below).
7. Enter a label for each sample in the “Template” area.
8. The program will plot the results for the standards and calculate and R value using a linear equation. The R value should be as close to 1 as possible. If necessary, delete one or more standards (usually the standard 4000 µg/ml) to improve the R value.
9. In the “Protein concentration” area, the program will calculate the protein concentration for each sample using the slope curve, based on the results obtained for the standards.

10. In the “Average concentration of samples” area, enter the dilution factor for each sample (if the samples were not diluted, enter 1). The concentration for each sample will be automatically calculated, considering an average of the triplicates.

Note:

- *If the concentration of a sample displayed in the “Protein concentration” area lies beyond the limit of the standard curve, the sample should be diluted and read again.*

	STD µg/ml	ABS 595
	4000	=AVERAGE(C27:E27)
	2000	=AVERAGE(C28:E28)
	1000	=AVERAGE(C29:E29)
	500	=AVERAGE(C30:E30)
	250	=AVERAGE(C31:E31)
	125	=AVERAGE(C32:E32)
	0	=AVERAGE(C33:E33)

X=Y-Intercept/Slope	
slope	=SLOPE(E3:E9,D3:D9)
intercept	=INTERCEPT(E3:E9,D3:D9)

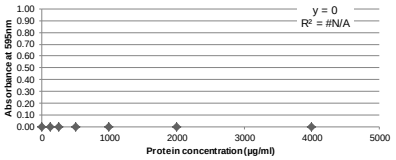

TEMPLATE

	1	2	3	4	5	6	7	8	9	10	11	12
A	STD 4000	STD 4000	STD 4000	SAMPLE 1	SAMPLE 1	SAMPLE 1	SAMPLE 9	SAMPLE 9	SAMPLE 9	SAMPLE 17	SAMPLE 17	SAMPLE 17
B	STD 2000	STD 2000	STD 2000	SAMPLE 2	SAMPLE 2	SAMPLE 2	SAMPLE 10	SAMPLE 10	SAMPLE 10	SAMPLE 18	SAMPLE 18	SAMPLE 18
C	STD 1000	STD 1000	STD 1000	SAMPLE 3	SAMPLE 3	SAMPLE 3	SAMPLE 11	SAMPLE 11	SAMPLE 11	SAMPLE 19	SAMPLE 19	SAMPLE 19
D	STD 500	STD 500	STD 500	SAMPLE 4	SAMPLE 4	SAMPLE 4	SAMPLE 12	SAMPLE 12	SAMPLE 12	SAMPLE 20	SAMPLE 20	SAMPLE 20
E	STD 250	STD 250	STD 250	SAMPLE 5	SAMPLE 5	SAMPLE 5	SAMPLE 13	SAMPLE 13	SAMPLE 13	SAMPLE 21	SAMPLE 21	SAMPLE 21
F	STD 125	STD 125	STD 125	SAMPLE 6	SAMPLE 6	SAMPLE 6	SAMPLE 14	SAMPLE 14	SAMPLE 14	SAMPLE 22	SAMPLE 22	SAMPLE 22
G	STD 0	STD 0	STD 0	SAMPLE 7	SAMPLE 7	SAMPLE 7	SAMPLE 15	SAMPLE 15	SAMPLE 15	SAMPLE 23	SAMPLE 23	SAMPLE 23
H	EMPTY	EMPTY	EMPTY	SAMPLE 8	SAMPLE 8	SAMPLE 8	SAMPLE 16	SAMPLE 16	SAMPLE 16	SAMPLE 24	SAMPLE 24	SAMPLE 24

ABSORBANCE

	1	2	3	4	5	6	7	8	9	10	11	12
A												
B												
C												
D												
E												
F												
G												
H												

PROTEIN CONCENTRATION IN µg/ml:

	1	2	3	4	5	6	7	8	9	10	11	12
A	=(C27-$H$5)/$H$4	=(D27-$H$5)/$H$4	=(E27-$H$5)/$H$4	=(F27-$H$5)/$H$4	=(G27-$H$5)/$H$4	=(H27-$H$5)/$H$4	=(I27-$H$5)/$H$4	=(J27-$H$5)/$H$4	=(K27-$H$5)/$H$4	=(L27-$H$5)/$H$4	=(M27-$H$5)/$H$4	=(N27-$H$5)/$H$4
B	=(C28-$H$5)/$H$4	=(D28-$H$5)/$H$4	=(E28-$H$5)/$H$4	=(F28-$H$5)/$H$4	=(G28-$H$5)/$H$4	=(H28-$H$5)/$H$4	=(I28-$H$5)/$H$4	=(J28-$H$5)/$H$4	=(K28-$H$5)/$H$4	=(L28-$H$5)/$H$4	=(M28-$H$5)/$H$4	=(N28-$H$5)/$H$4
C	=(C29-$H$5)/$H$4	=(D29-$H$5)/$H$4	=(E29-$H$5)/$H$4	=(F29-$H$5)/$H$4	=(G29-$H$5)/$H$4	=(H29-$H$5)/$H$4	=(I29-$H$5)/$H$4	=(J29-$H$5)/$H$4	=(K29-$H$5)/$H$4	=(L29-$H$5)/$H$4	=(M29-$H$5)/$H$4	=(N29-$H$5)/$H$4
D	=(C30-$H$5)/$H$4	=(D30-$H$5)/$H$4	=(E30-$H$5)/$H$4	=(F30-$H$5)/$H$4	=(G30-$H$5)/$H$4	=(H30-$H$5)/$H$4	=(I30-$H$5)/$H$4	=(J30-$H$5)/$H$4	=(K30-$H$5)/$H$4	=(L30-$H$5)/$H$4	=(M30-$H$5)/$H$4	=(N30-$H$5)/$H$4
E	=(C31-$H$5)/$H$4	=(D31-$H$5)/$H$4	=(E31-$H$5)/$H$4	=(F31-$H$5)/$H$4	=(G31-$H$5)/$H$4	=(H31-$H$5)/$H$4	=(I31-$H$5)/$H$4	=(J31-$H$5)/$H$4	=(K31-$H$5)/$H$4	=(L31-$H$5)/$H$4	=(M31-$H$5)/$H$4	=(N31-$H$5)/$H$4
F	=(C32-$H$5)/$H$4	=(D32-$H$5)/$H$4	=(E32-$H$5)/$H$4	=(F32-$H$5)/$H$4	=(G32-$H$5)/$H$4	=(H32-$H$5)/$H$4	=(I32-$H$5)/$H$4	=(J32-$H$5)/$H$4	=(K32-$H$5)/$H$4	=(L32-$H$5)/$H$4	=(M32-$H$5)/$H$4	=(N32-$H$5)/$H$4
G	=(C33-$H$5)/$H$4	=(D33-$H$5)/$H$4	=(E33-$H$5)/$H$4	=(F33-$H$5)/$H$4	=(G33-$H$5)/$H$4	=(H33-$H$5)/$H$4	=(I33-$H$5)/$H$4	=(J33-$H$5)/$H$4	=(K33-$H$5)/$H$4	=(L33-$H$5)/$H$4	=(M33-$H$5)/$H$4	=(N33-$H$5)/$H$4
H	=(C34-$H$5)/$H$4	=(D34-$H$5)/$H$4	=(E34-$H$5)/$H$4	=(F34-$H$5)/$H$4	=(G34-$H$5)/$H$4	=(H34-$H$5)/$H$4	=(I34-$H$5)/$H$4	=(J34-$H$5)/$H$4	=(K34-$H$5)/$H$4	=(L34-$H$5)/$H$4	=(M34-$H$5)/$H$4	=(N34-$H$5)/$H$4

AVERAGE CONCENTRATION OF SAMPLES IN µg/ml:

SAMPLE	DIL FACTOR	µg/ml
=F16		=AVERAGE(F38:H38)*C49
=F17		=AVERAGE(F39:H39)*C50
=F18		=AVERAGE(F40:H40)*C51
=F19		=AVERAGE(F41:H41)*C52
=F20		=AVERAGE(F42:H42)*C53
=F21		=AVERAGE(F43:H43)*C54
=F22		=AVERAGE(F44:H44)*C55
=F23		=AVERAGE(F45:H45)*C56
=J16		=AVERAGE(I38:K38)*C57
=J17		=AVERAGE(I39:K39)*C58
=J18		=AVERAGE(I40:K40)*C59
=J19		=AVERAGE(I41:K41)*C60
=J20		=AVERAGE(I42:K42)*C61
=J21		=AVERAGE(I43:K43)*C62
=J22		=AVERAGE(I44:K44)*C63
=J23		=AVERAGE(I45:K45)*C64
=L16		=AVERAGE(L38:N38)*C65
=L17		=AVERAGE(L39:N39)*C66
=L18		=AVERAGE(L40:N40)*C67
=L19		=AVERAGE(L41:N41)*C68
=L20		=AVERAGE(L42:N42)*C69
=L21		=AVERAGE(L43:N43)*C70
=L22		=AVERAGE(L44:N44)*C71
=L23		=AVERAGE(L45:N45)*C72

Protocol 15. Tandem mass tagging and in-gel digestion of proteins separated by polyacrylamide gel electrophoresis for analysis by mass spectrometry

Buffers and solutions

1 M Triethylammonium bicarbonate (TEAB) buffer, pH 8.5 (SIGMA T7408)
Store at RT.

2% (w/v) SDS
Dilute in ddH_2O to a final volume of 10 ml.
Store at RT.

20 mM Tris(2-carboxyethyl)phosphine hydrochloride (TCEP)
Dilute in ddH_2O to a final volume of 1 ml.
Prepare fresh.

100 mM Ammonium bicarbonate (SIGMA A6141)
Dilute in ddH_2O to a final volume of 100 ml.
Store at RT.

50 mM Ammonium bicarbonate (SIGMA A6141)
Dilute in ddH_2O to a final volume of 80 ml.
Store at RT.

10 mM DTT, SIGMA D5545)
Dilute in 100 mM ammonium bicarbonate to a final volume of 1 ml.
Prepare fresh.

55mM Iodoacetamide (IAA, SIGMA I1149)
Dilute in 100 mM ammonium bicarbonate to a final volume of 1 ml.
Prepare fresh.

PAGE buffers
See Protocol 8

Coomassie staining solutions
Brilliant Blue G-colloidal concentrate (SIGMA B2025)
See Protocol 9 for the rest of the solutions.

Reagents

Trypsin, bovine sequencing grade (Roche 11418475001)

Dilute in trifluoroacetic acid (Merck 108178) to a final concentration of 0.1% (w/v) and final volume of 250 µl. Dispense in 30 µl aliquots and store at -20°C.

Acetonitrile (ACN, Fisher Scientific A998-212)

TMTsixplex™ Label Reagent Set, 1 x 0.8 mg (Thermo Scientific 90061)

Pull-down eluates

Reagents for protein quantification (Protocol 14) and PAGE.

Materials

1.5, 15 and 50 ml polypropylene tubes

Pipette controller and disposable serological pipettes

Materials for cell culture, protein quantification, PAGE and WB (see appropriate protocols).

Equipment

Savant™ SpeedVac concentrator (Thermo Scientific)

Eppendorf Thermomixer Compact (Eppendorf)

Equipment for cell culture, protein quantification PAGE and WB (see appropriate protocols).

Method

1. Mix 10 µg of the samples to be analysed with 2% SDS to a final concentration of 0.1% (w/v) and 1M TEAB buffer to a final concentration of 100 mM. Adjust with ddH_2O to a final volume of 50 µl.
2. Add 2.6 µl of the TCEP solution to each sample (to a final concentration of 1 mM TCEP) and incubate for 1 h at 55°C.
3. Add 18.5 µl of TMT label reagent stock to the respective sample (each eluate will be tagged with a different TMT, to a final concentration of 25 mM of TMT reagent) and incubate for 1 h at RT.
4. Add 3.9 µl of 5% hydroxylamide to each sample (to adjust to a final concentration of 15 mM TMT reagent) and incubate for 15 min at RT.
5. Combine all the samples in one tube and incubate the pooled sample for 15 min at RT.
6. Separate the samples by PAGE and stain the gel with Coomassie staining (see Protocol 8 and Protocol 9, but use Brilliant Blue G-colloidal concentrate from SIGMA instead of preparing the dye).
7. Excise bands cutting as close to the edge as possible. Chop into ~2 mm^2 pieces and transfer into a 1.5 ml tube.

   Gel pieces can be stored at 4°C until required.
8. Wash the gel cubes with 200 µl of 100 mM ammonium bicarbonate for 5 min (decant water first if gel pieces have been stored) and decant. Repeat two more times.

9. Add 200 µl of ACN, decant and add the same volume again to fully and quickly dehydrate the gel pieces, decant and dry in SpeedVac for 5 min.
10. Rehydrate the gel with 100 µl of 10 mM DTT and heat up at 56°C for 30 min.
11. Decant DTT, wash with ACN twice (as on step 9), decant and dry in SpeedVac for 5 min.
12. Add 100 µl of 55 mM IAA, incubate for 20 min at RT in the dark.
13. Discard the supernatant, wash briefly with 100 µl of 100 mM ammonium bicarbonate, then replace and wash for a further 5 min and discard the buffer.
14. To destain the gel, wash with 200 µl of a 1:1 solution of 100 mM ammonium acetate and ACN. Incubate for 30 min at 37°C, shaking. Repeat this step until the gel is destained).
15. Decant the liquid, dehydrate once again with ACN (as in step 9) and dry off in a SpeedVac for 5 min.
16. Mix 30 µl of the trypsin solution and 200 µl of 50 mM ammonium bicarbonate to a final concentration of 13 ng/µl trypsin.
17. Rehydrate the gel pieces in a minimal volume of trypsin solution (i.e. just enough to cover and rehydrate the gel pieces) for 20 min at 4°C.
18. Remove unabsorbed trypsin and add a minimal volume of 50 mM ammonium bicarbonate (10-20 µl) to cover the gel pieces and keep them wet during enzyme cleavage.
19. Incubate at 37°C for 2 h and then overnight at RT.
20. Decant supernatant from gel pieces and collect it into a new tube.
21. Wash gel pieces with 50-100 µl of 50 mM ammonium bicarbonate for 5 min at 37°C, decant and pool into the tube from step 20.
22. Dehydrate gel pieces with 50-100 µl of ACN for 10 min at 37°C, decant and pool into the tube from step 20.
23. Repeat steps 21 and 22.
24. Freeze the peptide extract and dry down the pooled supernatants to completion, avoid over drying. Store at -80°C until required.

Reference:
Protocol provided by Steven Lynham, Centre of Excellence for Mass Spectrometry, King's College London.

Protocol 16. RNA extraction from HEK293 cells

Solutions and reagents

70% Ethanol

Dilute in ddH_2O to a final volume of 50 ml.

RNeasy Mini Kit (QIAGEN 74104)

RNase-Free DNase Set (QIAGEN 79254)

RNase AWAY (Thermo Scientific 7002)

Materials

1.5 and 15 ml polypropylene tubes

Pipettes and tips

Materials for cell culture (see Protocol 17).

Equipment

Hot block

Vortex

Eppendorf 5424 microcentrifuge (Eppendorf)

NanoDrop 1000 spectrophotometer (Thermo Scientific)

Equipment for cell culture (see Protocol 17).

Method

1. Clean the working surface and the pipettes to be used with RNase away.
2. Trypsinise and pellet one T75 flask of HEK293 cells (~80-90% confluent) as specified in Protocol 17. Wash the pellet once with PBS.
3. Resuspend the cells in 600 µl of Buffer RLT by vortexing or pipetting.
4. Pipet the lysate directly into a QIAshredder spin column placed in a 2 ml collection tube, and centrifuge for 2 min at 16000 g.
5. Add 1 volume of 70% ethanol to the homogenised lysate, and mix well by pipetting. Do not centrifuge.
6. Transfer up to 700 µl of the sample, including any precipitate that may have formed, to an RNeasy spin column placed in a 2 ml collection tube (supplied). Close the lid gently, and centrifuge for 15 sec at 16000 g. Discard the flow-through. Transfer the rest of the sample to the column and centrifuge again, reusing the same collection tube. Discard the flow-through and reuse the collection tube in the next step.
7. Add 350 µl of buffer RW1 to the RNeasy spin column. Close the lid gently, and centrifuge for 15 sec at 16000 g. Discard the flow-through and reuse the collection tube in the next steps.

8. Add 10 µl of DNase I stock solution to 70 µl of buffer RDD. Mix by gently inverting the tube and centrifuge briefly to collect residual liquid from the sides of the tube.
9. Add the DNase I incubation mix (80 µl) directly to the RNeasy spin column membrane, and incubate for 15 min at RT.
10. Add 350 µl of buffer RW1 to the RNeasy spin column. Close the lid gently, and centrifuge for 15 sec at 16000 g; discard the flow-through.
11. Add 500 µl of buffer RPE to the RNeasy spin column. Close the lid gently, and centrifuge for 15 sec at 16000 g to wash the spin column membrane. Discard the flow-through and reuse the collection tube in the next step.
12. Add 500 µl of buffer RPE to the RNeasy spin column. Close the lid gently, and centrifuge for 3 min at 16000 g.
13. Place the RNeasy spin column in a new 1.5 ml collection tube (included in the kit). Add 30–50 µl of RNase-free water directly to the spin column membrane. Close the lid gently and centrifuge for 1 min at 16000 g to elute the RNA. Add the same volume of RNase-free water and centrifuge again, collecting the eluate in the same tube.
14. Verify RNA concentration using a NanoDrop spectrophotometer, dispense in aliquots and store at -20°C.

Note:

- *Before using RPE for the first time, add 4 volumes of ethanol (96–100%) to obtain a working solution.*

Protocol 17: Initiation and maintenance of a stock of HEK293 cells

Cell culture regents

MEM, no glutamine (Life Technologies 21090-022)

1X Opti-MEM® Reduced Serum Medium, GlutaMAX™ Supplement (Life Technologies 51985-034)

100X MEM NEAA (Life Technologies 11140-050)

20 mM L-Glutamine (Life Technologies 25030-024)

FBS (Life Technologies 10270-106), filtered

1X Dulbecco's PBS (SIGMA D8537)

1X Trypsin-EDTA (TE) (SIGMA T3924)

Pre-heat all these reagents at 37°C before using.

Trypan blue solution (SIGMA T8154)

Cell line

HEK 293 (human embryo kidney) (ECACC 85120602)

Materials

1.5 and 15 ml polypropylene tubes

T75 or T175 cell culture flasks

Pipettes and tips

Pipette controller and disposable serological pipettes

Equipment

Water bath

Set at 37°C

Cell culture incubator and hood

Inverted microscope

Heraeus Labofuge 400 centrifuge

Haemocytometer

Manual cell counter

Calculator

Method

Work in cell culture hood under aseptic conditions. For initiating a stock culture:

1. Transfer 12 ml of complete medium (MEM supplemented with 10% FBS, 2 mM L-glutamine and 1% NEAA) into a T75 flask or 18 ml into a T175 flask.
2. Take out a vial of frozen HEK293 cells (stored in liquid nitrogen) and immerse it in the water bath for approximately 1 min or until the contents are completely thawed.

3. Transfer the contents of the vial to the flask with medium, label appropriately and incubate at 37°C/5% CO_2 for 24 h.
4. Change the medium and continue incubation until cells reach ~80-90% confluence.

For maintaining a stock culture:

1. When the cell culture reaches ~80-90% confluence, remove the medium the cells grew in and carefully wash the cells twice with 10 ml of PBS.
2. Add 3 ml of 1X TE for a T75 or 4ml for a T175, ensuring it covers the totality of the cells and incubate at 37°C for three (for a T75) to four min (for a T175). Verify cell detachment under the microscope.
3. Add complete medium, using double of the volume than for TE. Wash the surface where the cells grew thrice, mix well with the pipette to separate cell clumps and transfer to a 15 ml tube.
4. Take 20 µl of the cell suspension and mix with 20 µl of trypan blue in a 1.5 ml tube. Transfer 10 µl of this mixture to each of the chambers of a haemocytometer and count the cells under the microscope as follows:
    a. Count the cells on each of the four external squares of the haemocytometer (those with large squares), avoiding blue cells (not viable) and obtain the average of the four squares.
    b. Multiply X2 (dilution factor with trypan blue), then X10000 to obtain number of cells per ml. Finally, multiply for the volume of the cell suspension, to obtain the total cell number.
5. Centrifuge at 800 g for 3 min at RT.
6. Remove the supernatant and resuspend the pellet in an appropriate volume of complete medium with antibiotic to obtain a suspension with $1X10^6$ cells per ml.
7. Transfer 1 ml of this cell suspension ($1x10^6$ cells) into a T75 or 2 ml ($2X10^6$ cells) into a T175 and adjust to a final volume of 12 ml for a T75 or 18 ml for a T175 with complete medium.
8. Incubate at 37°C/5% CO_2 until ~80-90% confluence (approximately 6-7 days). Change the medium every 3-4 days.

Protocol 18. RNA reverse transcription

Reagents

50-100 U/µl M-MLV Reverse Transcriptase, RNase H Minus, Point Mutant and 5X Reaction Buffer (Promega M3681)

500 ng/µl Random Primers (Promega C1181)

100 mM Deoxynucleotide (dNTP) Solution Set (New England Biolabs N0446)

To obtain a 10 mM dNTPs working solution, dilute 1:10 each dNTP in sterile ddH_2O to a final volume of 100 µl. Dispense in 20 µl aliquots and store at -20°C.

10 µM PCR primers (forward and reverse)

Sterile ddH_2O

Sterilise 100 ml by autoclaving, dispense in 5 ml aliquots and store at RT.

Samples

RNA samples to be reverse transcribed

Materials

0.2 ml (individual tubes or strips) or 0.5 ml and 1.5 ml polypropylene tubes

Pipettes and tips

Equipment

PCR hood

GS1 Thermal Cycler (G-Storm)

Eppendorf 5424 microcentrifuge (Eppendorf)

Method

Defrost all the reagents and samples on ice before starting. Work in the PCR hood, keeping all the reagents on ice.

1. Place the racks, pipettes, tips, tubes, ddH_2O and PCR buffer to be used in the PCR hood and expose them to UV light for 5-10 min.
2. In a 0.2 µl tube, mix 1 µg of RNA and 250 ng of random primers. Adjust with ddH_2O to a final volume of 17.75 µl.
3. Place the tube in the thermal cycler and incubate for 5 min at 70°C and then for 5 min on ice
4. Add the following reagents (a master mix can be prepared if working with many samples):

Final concentration:	Reagent:
1X	5X M-MLV RT 5X Reaction Buffer
0.2 mM	10 mM dNTPs

50-100 U (1 µl) M-MLV RT (H-) Point Mutant

The final reaction volume is 25 µl.

Mix well by pipetting or vortexing and spin down.

5. Transfer the samples to the thermal cycler and run the following program:

One cycle:

25°C 10 min

55°C 50 min

70°C 15 min

10°C Hold

6. Store the samples at -20°C.

References:

This is a modification of the protocol provided by the kit's manufacturer.

Protocol 19. High-fidelity PCR for cloning, addition of 3'A overhangs and agarose gel electrophoresis

Buffers

6X Orange G gel loading buffer

100mg Orange G

30% (v/v) Glycerol

Adjust with ddH_2O to a final volume of 50 ml. Dispense in 5 ml aliquots and store at RT.

Sterile ddH_2O

Sterilise 100 ml by autoclaving, dispense in 5 ml aliquots and store at RT.

50X TAE buffer (Severn Biotech Ltd 20-6001-10)

Dilute 1:50 with ddH_2O to obtain a 1X working solution.

Agarose (SIGMA A9539)

Reagents

2 U/µl Q5 High-Fidelity DNA Polymerase and 5X Q5 Reaction Buffer (2 mM $MgCl_2$) (New England Biolabs M0491S)

Dispense Q5 in 20 µl aliquots and buffer in 100 µl aliquots, store at -20°C.

100 mM Deoxynucleotide (dNTP) Solution Set (New England Biolabs N0446)

To obtain a 10 mM dNTPs working solution, dilute 1:10 each dNTP in sterile ddH_2O to a final volume of 100 µl. Dispense in 20 µl aliquots and store at -20°C. To obtain a 10 mM dATP solution, dilute the dATP stock 1:10 in sterile ddH_2O to a final volume of 50 µl.

10 µM PCR primers (forward and reverse)

Dilute 1:10 from 100 µM in sterile ddH_2O or TE buffer, store at -20°C.

5000 U/ml *Taq* DNA Polymerase with 10X Standard *Taq* Buffer 1.5 mM $MgCl_2$ (New England Biolabs M0273)

Dispense Taq in 20 µl aliquots and buffer in 100 µl aliquots, store at -20°C.

GelRed Nucleic Acid Gel Stain, 10,000X in water (Biotium 41003)

GeneRuler 100 bp DNA Ladder (Life Technologies SM0241)

Dilute ladder and included loading dye 1:6 in ddH_2O to obtain a 1X working solution, store working solution at RT.

1 kb DNA ladder (New England Biolabs N3232S)

Samples

DNA samples to be amplified

Materials

0.2 ml (individual tubes or strips) or 0.5 ml and 1.5 ml polypropylene tubes

Pipettes and tips

Conical flask

Tray, comb and dams to prepare agarose gels

Parafilm and Saran wrap

Equipment

PCR hood

GS1 Thermal Cycler (G-Storm)

Eppendorf 5424 microcentrifuge (Eppendorf)

Microwave oven

MultiSUB Mini horizontal electrophoresis tank (Cleaver Scientific Ltd)

Consort E835 electrophoresis power supply (Cleaver Scientific Ltd)

UVP Ultraviolet Transilluminator

UVIDOC Gel documentation system

Method

Defrost all the reagents and samples on ice before starting. Work in the PCR hood, keeping all the reagents on ice.

1. Place the racks, pipettes, tips, tubes ddH_2O and PCR buffer to be used in the PCR hood and expose them to UV light for 5-10 min.
2. Working in the PCR hood, set up the following master mix in a 1.5 µl tube (adjust according to the number of samples to be processed, considering a 10% excess):

Final concentration:	Reagent:
1X	5X Q5 Reaction Buffer
0.2 mM	10 mM dNTPs
0.5 µM	10 µM Forward PCR primer
0.5 µM	10 µM Reverse PCR primer
1 U per 50 µl	2U/µl Q5 High-Fidelity DNA Polymerase

   Adjust with sterile ddH_2O to the desired final volume (usually 50 µl)

   Mix well by pipetting or vortexing and spin down to remove any drops from the tube's lid.
3. Dispense the master mix in the PCR tubes (0.2 or 0.5 ml), trying to place it in the bottom of each tube.
4. Add the appropriate sample to each tube and ddH_2O to the negative control.

5. Close the tubes tightly, mix by vortexing, spin down and place them on the thermal cycler.
6. Run the appropriate PCR program, based on the following example:

   One cycle:

   95°C 2 min

   35 cycles:

   95°C 15 sec

   (Variable) 15 sec

   72°C 30 sec per each 1000 bp of PCR product size

   One cycle:

   72°C 5 min

   10°C Hold
7. Optional: add 3' A-overhangs if the PCR product is intended to be cloned into a PCR cloning vector, as follows:
   - Place the PCR products on ice and add 10 mM dATP to a final concentration of 0.2 mM and 5U/µl Taq DNA Polymerase to a final concentration of 1.25 U per 50 µl.
   - Transfer the tubes back to the thermal cycler and incubate for 15 min at 68°C.
8. Prepare an agarose gel as follows:
   - Mix an appropriate amount of agarose with 40 ml of 1X TAE buffer in a conical flask, cover with Saran wrap (make a hole at the centre to allow partial evaporation).
   - Heat up in the microwave oven until the agarose is completely dissolved (approximately 1:30 min).
   - Add Gel Red to a final concentration of 1X and pour on the gel tray with the rubber dams on both sides. Ensure no bubbles are left and place a comb on the gel. Let it sit at RT.
9. Fill the electrophoresis tank with 1X TAE and place the tray with the gel inside, making sure that the buffer covers the gel.
10. Place an appropriate volume of loading dye for each sample in a separate drop (1X final concentration) on the Parafilm and mix with the desired volume of each PCR product.
11. Load 5 µl of DNA ladder in the first well of the gel and the samples in the rest of the wells.
12. Run the gel at 110 V until the loading dye reaches the bottom of the gel.
13. Place the gel on the transilluminator and obtain an image using the gel documentation system.

Note:

- *To determine the optimum annealing temperature for the primers, carry out a gradient PCR starting from 5°C below the lowest predicted annealing temperature for the primers according to the primer designing software (usually 5-6 samples*

spanning 10°C is enough). Choose the temperature rendering the strongest specific bands and no non-specific bands in the agarose gel.

Protocol 20. DNA extraction from agarose gels

Reagents

QIAquick Gel Extraction Kit (QIAGEN 28704)

Samples

Agarose gel containing bands of interest

Materials

1.5 ml polypropylene tubes

Pipettes and tips

Scalpel blade

Equipment

Precision scale

UVP Ultraviolet Transilluminator

Anti-UV protective mask and goggles

Hot block

Eppendorf 5424 microcentrifuge (Eppendorf)

Method

1. Wearing appropriate anti-UV protection, place the gel on the transilluminator and excise the DNA band of interest from the agarose gel with a clean scalpel blade. Minimise the size of the gel slice by removing extra agarose and work as fast as possible, to reduce UV exposure. Transfer the band to a 1.5 ml tube.
2. Weigh the band and add three volumes of buffer QG to one volume of gel (100 mg ~100 µl).
3. Incubate for 10 min at 50°C, or until the gel slice has completely dissolved. To help dissolve the gel, mix by vortexing the tube every 2–3 min during the incubation.
4. Place a QIAquick spin column in a provided 2 ml collection tube and apply the sample to the column. Centrifuge for 1 min at 16000 g. Discard the flow-through and place the column back in the same collection tube.
   The maximum volume of the column reservoir is 800 µl. For sample volumes of more than 800 µl, load and spin again.
5. Add 750 µl of buffer PE and centrifuge for 1 min at 16000 g. Discard the flow-through and place the column back in the same collection tube.
6. Centrifuge the column for 3 min at 16000 g.
7. Place the column into a clean 1.5 ml microcentrifuge tube and apply 50 µl of Buffer EB on the centre of the membrane. Incubate for 1 min at RT and centrifuge for 1 min at 16000 g.

8. Place the eluate into the column and centrifuge again, using the same collection tube.
9. Verify DNA concentration using a NanoDrop spectrophotometer and store at -20°C.

References:

This is a modification of the protocol provided by the kit's manufacturer.

Protocol 21. TA cloning

Media

1X LB agar plates for blue-white screening

20 g LB broth powder (SIGMA L3022)

12 g Bacteriological agar powder (SIGMA A5306)

Adjust with ddH_2O to a final volume of 250 ml

Dilute the powder in the water, sterilise by autoclaving and store at RT. To prepare agar plates, heat up the agar in the microwave until melted (approximately 4 min at high power), cool down in water to approximately 40°C, and add the following reagents:

100 µg/ml Ampicillin (dilute from 100 mg/ml stock) (SIGMA A0166)

0.1 mM IPTG (dilute from 1M stock) (Promega V3951)

20 µg/ml X-Gal (dilute from 20 mg/ml [in DMSO] stock) (SIGMA B4252)

Mix well and pour in Petri dishes (25-30 ml per dish) under sterile conditions (use Bunsen's burner). Leave open until the agar has solidified, close and seal with Parafilm, label appropriately and store upside down at 4°C.

SOC medium

2% (w/v) Tryptone

0.5% (w/v) Yeast extract

10 mM NaCl (dilute from 1 M stock)

2.5 mM KCl (dilute from 250 mM stock)

10 mM MgCl2 (dilute from 2 M stock)

20 mM Glucose (dilute from 1 M stock)

Adjust with ddH_2O to a final volume of 50 ml

Dissolve the first four reagents in water and sterilise by autoclaving, then add sterile MgCl2 and glucose. Dispense in 1 ml aliquots and store at -20°C.

Reagents

TA cloning kit with pCR2.1 vector (Life Technologies K2020-20)

Samples

Purified DNA band to be ligated

Materials and equipment

0.5 ml polypropylene tubes

Pipettes and tips

Materials and equipment for transformation of calcium competent E. coli (see Protocol 4).

Method

Defrost all the reagents and samples on ice before starting.

1. Calculate the amount of insert to be ligated, using the following formula:

$$\text{ng of insert} = \frac{(50 \text{ ng of pCR2.1})\,(\text{size of the insert in bp})}{3900 \text{ bp}} \times 3$$

2. Set up the ligation reaction as follows:

Final concentration:	Reagent:
1X	5X T4 DNA Ligase Reaction Buffer
(As calculated) ng	Insert
50 ng	25 µg/µl pCR2.1
5 U	5 U/µl ExpressLink T4 DNA Ligase

   Adjust with sterile ddH_2O to a final volume of 10 µl

   Mix well by pipetting.

3. Incubate for 2 h at RT.
4. Use the whole ligation volume for transformation of DH5α cells, according to Protocol 4.
5. Plate the transformed cells in agarose plates with IPTG and X-Gal.
6. Incubate overnight at 37°C and select white colonies only for screening by colony PCR.

Note:

- *The proportion of plasmid: insert (3:1) suggested can be adjusted if necessary.*

Reference:

This is a modification of the protocol provided by the reagents' supplier.

Protocol 22. Colony PCR

Buffers

6X Orange G gel loading buffer

100 mg Orange G

30% (v/v) Glycerol

Adjust with ddH_2O to a final volume of 50 ml. Dispense in 5 ml aliquots and store at RT.

Sterile ddH_2O

Sterilise 100 ml by autoclaving, dispense in 5 ml aliquots and store at RT.

50X TAE buffer (Severn Biotech Ltd 20-6001-10)

Dilute 1:50 with ddH_2O to obtain a 1X working solution.

Agarose (SIGMA A9539)

Reagents

5000 U/ml *Taq* DNA Polymerase with 10X Standard *Taq* Buffer 1.5 mM $MgCl_2$ (New England Biolabs M0273)

Dispense Taq in 20 µl aliquots and buffer in 100 µl aliquots, store at -20°C.

100 mM Deoxynucleotide (dNTP) Solution Set (New England Biolabs N0446)

To obtain a 10 mM dNTPs working solution, dilute 1:10 each dNTP in sterile ddH_2O to a final volume of 100 µl. Dispense in 20 µl aliquots and store at -20°C.

10 µM PCR primers (forward and reverse)

Dilute 1:10 from 100 µM in sterile ddH_2O or TE buffer, store at -20°C.

GelRed Nucleic Acid Gel Stain, 10,000X in water (Biotium 41003)

GeneRuler 100 bp DNA Ladder (Life Technologies SM0241)

Dilute ladder and included loading dye 1:6 in ddH_2O to obtain a 1X working solution, store working solution at RT.

1 kb DNA ladder (New England Biolabs N3232S)

Samples

Agar plate with colonies to be screened

Materials

0.2 ml (individual tubes or strips) or 0.5 ml and 1.5 ml polypropylene tubes

Pipettes and tips

Conical flask

Tray, comb and dams to prepare agarose gels

Parafilm and Saran wrap

Equipment

PCR hood

GS1 Thermal Cycler (G-Storm)

Eppendorf 5424 microcentrifuge (Eppendorf)

Microwave oven

MultiSUB Midi horizontal electrophoresis tank (Cleaver Scientific Ltd)

Consort E835 electrophoresis power supply (Cleaver Scientific Ltd)

UVP Ultraviolet Transilluminator

UVIDOC Gel documentation system

Method

Defrost all the reagents and samples on ice before starting. Prepare PCR reactions in the PCR hood, keeping all the reagents on ice.

1. Under sterile conditions, transfer 20 µl of ddH_2O to 0.2 ml tubes and 1 ml of LB broth with the appropriate antibiotic to 1.5 ml tubes; prepare one tube with water and one with LB broth for each colony to be screened (usually 10 colonies per plate).
2. Using a pipette and a sterile tip, pick one colony and dissolve it in the 20 µl of ddH_2O. Take 15 µl of this mixture and use them to inoculate the tubes with medium. Label each PCR tube and each 1.5 ml tube accordingly.
3. Incubate the 1.5 ml tubes at 37°C/250rpm.
4. Prepare the following PCR master mix (adjust volume according to the number of samples to be processed, considering a 10% excess):

Final concentration:	Reagent:
1X	10x Standard *Taq* Buffer
0.2 mM	10 mM dNTPs
0.5 µM	10 µM Forward PCR primer
0.5 µM	10 µM Reverse PCR primer
1.25 U per 50 µl	5U/µl *Taq* DNA Polymerase

   Adjust with sterile ddH_2O to a final volume of 12.5 µl)

   Mix well by pipetting or vortexing and spin down to remove any drops from the tube's lid.
5. Add 7.5 µl of master mix to each PCR tube with ~5 µl of dissolved bacteria, mix well. Prepare negative (5 µl ddH_2O) and positive (1 ng of a control plasmid, adjust to 5 µl with ddH_2O) controls in the same way. Close the tubes tightly.
6. Place the samples in the thermal cycler and run the following program:

One cycle:

95°C 10 min

25 cycles:

95°C 15 sec

(Variable)* 15 sec

68°C 1 min per each 1000 bp of PCR product size

One cycle:

68°C 5 min

10°C Hold

* 58°C for CMV_F and R3 primers, 55°C for pUC/mM13_F and R primers

7. In the meantime, prepare an agarose gel as follows:
    - Mix an appropriate amount of agarose with 80 ml of 1X TAE buffer in a conical flask, cover with Saran wrap (make a hole at the centre to allow partial evaporation).
    - Heat up in the microwave oven until the agarose is completely dissolved (approximately 1:30 min).
    - Add Gel Red to a final concentration of 1X and pour on the gel tray with the rubber dams on both sides. Ensure no bubbles are left and place a comb (20 wells) on the gel. Let it sit at RT.
8. Fill the electrophoresis tank with 1X TAE and place the tray with the gel inside, making sure that the buffer covers the gel.
9. Add 2.5 µl of 6X gel-loading dye to each sample and load 10 µl of this mixture in each of the wells of the agarose gel. Load an appropriate DNA ladder as a reference.
10. Run the gel at 110 V until the loading dye reaches the bottom of the gel.
11. Place the gel on the transilluminator and use the gel documentation system to obtain a representative image. Choose positive colonies.
12. Transfer the inoculated medium for each of the positive colonies to a tube with 10 ml of LB broth with an appropriate antibiotic and incubate overnight at 37°C/250 rpm. Use these cultures for minipreps and for inoculating a large-scale culture.

Protocol 23. DNA digestion with restriction enzymes and dephosphorylation of digested plasmids

Buffers

6X Orange G gel loading buffer

100mg Orange G

30% (v/v) Glycerol

Adjust with ddH_2O to a final volume of 50 ml. Dispense in 5 ml aliquots and store at RT.

50X TAE buffer (Severn Biotech Ltd 20-6001-10)

Dilute 1:50 with ddH_2O to obtain a 1X working solution.

Agarose (SIGMA A9539)

Reagents

Restriction enzymes and 10X reaction buffer, as indicated (New England Biolabs or Promega)

Optional: 10 mg/ml Bovine serum albumin (BSA) (if using Promega's enzymes or old New England Biolabs buffers)

Shrimp Alkaline Phosphatase and 10X Cut Smart buffer (NEB M0371)

GelRed Nucleic Acid Gel Stain, 10,000X in water (Biotium 41003)

GeneRuler 100 bp DNA Ladder (Life Technologies SM0241)

Dilute ladder and included loading dye 1:6 in ddH_2O to obtain a 1X working solution, store working solution at RT.

1 kb DNA ladder (New England Biolabs N3232S)

Samples

pSF-CMV-NH2-HA-EKT-NcoI plasmid

Plasmid or PCR product containing the insert of interest

Materials

0.2 ml (individual tubes or strips) or 0.5 ml and 1.5 ml polypropylene tubes

Pipettes and tips

Conical flask

Tray, comb and dams to prepare agarose gels

Saran wrap

Equipment

Water bath

Eppendorf 5424 microcentrifuge (Eppendorf)

Microwave oven

MultiSUB Mini horizontal electrophoresis tank (Cleaver Scientific Ltd)

Consort E835 electrophoresis power supply (Cleaver Scientific Ltd)

UVP Ultraviolet Transilluminator

UVIDOC Gel documentation system

Method

Defrost reagents and samples on ice before starting and keep all the reagents on ice while setting up the reaction.

1. Set up the following reaction in a 1.5 ml tube:

Final concentration:	Reagent:
1X	10X Reaction buffer
10 U	Restriction enzyme 1
10 U	Restriction enzyme 2
0.1 mg/ml	BSA (only if using Promega's enzymes or old New England Biolabs buffers)

   Add the whole volume of the purified insert or 3 µg of plasmid

   Adjust with ddH_2O to a final volume of 50 µl

   Mix well by pipetting or and spin down
2. Incubate in a water bath at 37°C for 1 h.
3. Transfer to ice. If phosphorylation is not required, continue with step 5.
4. Add 1 µl of shrimp alkaline phosphatase and 5 µl of Cut Smart buffer (if the digestion was done in a different buffer). Incubate at 37°C for 30 min and then at 65°C for 5 min.
5. Prepare an agarose gel as follows:
   - Mix an appropriate amount of agarose with 60 ml of 1X TAE buffer in a conical flask, cover with Saran wrap (make a hole at the centre to allow partial evaporation).
   - Heat up in the microwave oven until the agarose is completely dissolved (approximately 1:30 min).
   - Add Gel Red to a final concentration of 1X and pour on the gel tray with the rubber dams on both sides. Ensure no bubbles are left and place a comb on the gel (6 deep and wide wells). Let it sit at RT.
6. Fill the electrophoresis tank with 1X TAE and place the tray with the gel inside, making sure that the buffer covers the gel.
7. Add 10 µl of loading to each digestion reaction and mix by pipetting.
8. Load 5 µl of DNA ladder in the first well of the gel and carefully load the whole volume of each digestion reaction in one well.
9. Run the gel at 110 V until the loading dye reaches the bottom of the gel.

10. Place the gel on the transilluminator and print an image using the gel documentation system.
11. Cut the bands of interest and extract DNA as specified in Protocol 20.

Protocol 24. Ligation with T4 DNA ligase

Reagents

T4 DNA Ligase (400000 cohesive end units/ml and 2000000 cohesive end units/ml) and 10X T4 DNA Ligase Buffer (New England Biolabs M0202)

Dispense the buffer in 20 µl aliquots and store at -20°C.

Samples

Insert and plasmid to be ligated, digested and gel-extracted

Materials

0.5 ml polypropylene tubes

Pipettes and tips

Method

Defrost reagents and samples on ice before starting and keep all the reagents on ice while setting up the reaction.

1. Calculate the amount of insert to be ligated, using the following formula:

$$\text{ng of insert} = \frac{(100 \text{ ng of plasmid}) \, (\text{size of the insert in bp})}{\text{size of plasmid in bp}} \times 3$$

2. Set up the following reaction:

Final concentration:	Reagent:
2 µl	10X T4 DNA Ligase Buffer
100 ng	Plasmid
(As calculated) ng	Insert
1 µl	T4 DNA Ligase

   Adjust with ddH_2O to a final volume of 20 µl

3. Incubate at RT for 4 h.
4. Transform bacteria with the whole reaction volume according to Protocol 4.

Note:

- *The proportion of plasmid: insert (3:1) suggested can be adjusted if necessary.*

Reference:

This is a modification of the protocol provided by the reagents' supplier.

Protocol 25: Co-immunoprecipitation of AIP and AIP candidate partners

Buffers and solutions

Lysis buffer

150 mM NaCl (dilute from 1 M stock)

10 mM Tris-Cl pH 7.5 (dilute from 1 M stock)

10% (v/v) Glycerol

1% (v/v) IGEPAL® CA-630 (SIGMA I8896)

Adjust with ddH_2O to a final volume of 1 l

Sterilisation not needed, store at 4°C. Just before use, dispense in 50 ml aliquots and add 1 tablet of Complete® Protease Inhibitor Cocktail (Roche 11836145001) to each aliquot. The fully prepared buffer can be stored at -20°C for several weeks.

1X PBS, pH 7.4

To obtain a 5X stock, dissolve 25 tablets of PBS (SIGMA P4417) in ddH_2O and sterilise by autoclaving. Store at RT. Dilute accordingly with ddH_2O to obtain 1X working solution.

PAGE buffers

See Protocol 8

WB buffers

See Protocol 11

Cell culture media

See Protocol 17

1X Opti-MEM® Reduced Serum Medium, GlutaMAX™ Supplement (Life Technologies 51985-034)

Reagents and antibodies

Lipofectamine 2000 (Life Technologies 11668027)

Protein G Sepharose 4 Fast Flow (GE Healthcare 17-0618-01)

Monoclonal anti-Myc from mouse (SIGMA M4439)

Monoclonal anti-HA antibody from mouse (SIGMA H3663)

Polyclonal anti-HA antibody from rabbit (SIGMA H6908)

Mouse IgG (SIGMA I5381)

IRDye® 680 RD Goat anti-Mouse IgM (µ chain specific) (LI-COR 926-68180)

IRDye® 800CW Goat anti-Rabbit IgG (H + L) (LI-COR 926-32211)

Reagents for cell culture and protein quantification (see Protocol 14).

Cell line

See Protocol 17

Nucleic acids and oligonucleotides

100 ng/µl pcDNA3.0-Myc-WT_AIP and 100 ng/µl pCI-neo-WT_AIP or psF-CMV-NH2-HA-EKT-NcoI plasmid containing the candidate AIP partner to be studied.

Materials

0.2 (strips), 1.5, 2, 15 and 50 ml polypropylene tubes

T75 or T175 cell culture flasks

Pipette controller and disposable serological pipettes

5 ml syringes, 23G needles and insulin syringes and needles

Materials for cell culture, protein quantification, PAGE and WB (see appropriate protocols).

Equipment

Water bath

Set at 37°C

Inverted microscope

Labofuge 400 centrifuge (Heraeus)

Vortex

BR4i refrigerated centrifuge (Jouan)

Hot block

Stuart tube rotator SB2 (Stuart)

Equipment for cell culture, protein quantification PAGE and WB (see appropriate protocols).

Method

For details on growth and maintenance of HEK293 cells see Protocol 17. Cell culture must be performed in aseptic conditions. From step 11 onwards, all the procedures must be done at 4ºC or on ice.

1. Plate $10X10^6$ HEK 293 cells in a T175 flask in 18 ml of complete medium and incubate for 24 h at 37ºC/5% CO_2.
2. In a 1.5 ml tube, mix equimolar amounts of pcDNA3.0-Myc-AIP (Myc-AIP CDS=1026 bp) and of pCI-neo-WT_AIP or pSF-CMV-NH2-HA-EKT-NcoI containing the candidate AIP partner to be studied, calculated according to the size of their inserts (CDS for the tagged proteins), to obtain final amount of 20 µg of total plasmid. Add Opti-MEM to a final volume of 500 µl (TUBE 1).
3. In a different 1.5 ml tube, mix 480 µl (490 µl for a T75) of Opti-MEM and 20 µl of Lipofectamine 2000 (TUBE 2). Incubate for 5 min at RT, shaking occasionally.
4. Mix the contents of TUBES 1 and 2 to obtain a final volume of 1 ml of cotransfection mixture. Incubate for 20 min at RT, shaking occasionally.
5. Discard the medium the cells grew in. Add 1 ml of cotransfection mixture and 17 ml of complete medium and incubate for 8-12 h at 37ºC/5% CO_2.

6. Replace the medium with complete medium and continue incubation for 24 h more.
7. Discard the medium, wash the cells with 10 ml PBS and discard the PBS.
8. Add 4 ml of 1X TE and incubate for 3 min at 37°C. Verify cell detachment under the microscope.
9. Add 8 ml of complete medium, transfer to a 15 ml tube and centrifuge for 3 min at 800 g. Discard the supernatant.
10. Wash the pellet with 10 ml of PBS and centrifuge for 3 min at 800 g. Discard the supernatant.
11. Re-suspend the pellet in 1.5 ml of lysis buffer and transfer to a 2 ml tube. Incubate for 20 min at 4°C on a rotator (alternatively, incubate on ice, vortexing occasionally). Collect the lysate in a syringe and pass it through a 23G needle six times.
12. Centrifuge the lysate for 10 min at 17000 g/4°C
13. In the meantime, transfer 50 µl of Protein G Sepharose (80% slurry) to 1X2 ml and 3X1.5 ml tubes, and add 1 ml of lysis buffer to each tube. Shake well and centrifuge for 30 sec at 17000 g/4°C. Discard the supernatant and repeat this step two more times. Add 50 µl of lysis buffer to obtain a ~50% slurry.
14. Transfer the cleared lysate to a 2 ml tube with equilibrated slurry. Incubate for 1 h at 4ºC on a rotator.
15. Centrifuge for 30 sec at 17000 g/4°C. Reserve ~60 µl of this pre-cleaned lysate in a different tube, for protein quantification and PAGE analysis.
16. Label 3X1.5 ml tubes as “Myc”, “HA” and “IgG”, indicating the immunoprecipitation to be done in each tube, and transfer ~500 µl of the pre-cleaned lysate to each tube.
17. Add 5 µg of anti-Myc, anti-HA or mouse IgG (approximately 2.5 µl of anti-Myc and 5 µl of the other two antibodies) to each tube, according to the labelling.
18. Incubate for 1 h at 4ºC on a rotator. In the meantime, quantify the total protein content of the lysates (see appropriate protocol). Reserve 20-50 µg (~20 µl) for loading in gel.
19. Transfer the content of each tube to a 1.5 ml tube with equilibrated slurry, label appropriately. Incubate overnight at 4ºC on a rotator.
20. Centrifuge for 30 sec at 17000 g/4°C.
21. Wash the pellet thrice with 1 ml lysis buffer and once with PBS, centrifuging at for 30 sec at 17000 g/4°C between washes. After the last wash, eliminate carefully any remnants of the supernatant using an insulin needle.
22. Re-suspend the final pellet in 30 µl of 2XSDS gel-loading buffer. Heat to 95ºC for 3 min, shake, rotate or vortex for 5 min (to ensure the release of most of the immunoprecipitated proteins), heat again and finally centrifuge for 30 sec at 16000 g/RT to separate the beads. The final volume of the supernatant will be ~25 µl.
23. Load the supernatants in a 4-12% 10-well NuPAGE Bis-Tris gel as follows:

Lane	Sample	Volume
1	Novex® Sharp Pre-stained Protein Standard	6 µl
2	Input (cleared lysate)	~20 µl + 4 µl 6X SD gel-loading buffer

3	IP Myc	~25 µl
4	IP HA	~25 µl
5	IP IgG	~25 µl

24. Run the gel in 1X MES at 150 V for ~1:15 h.
25. Use this gel for WB (refer to appropriate protocol), applying the following conditions:
    - Transference for 30 min at 15V.
    - Blocking for 2 h at RT with 5% semi-skimmed milk in washing buffer.
    - Overnight incubation at 4°C with 1:3000 (v/v) mouse anti-Myc and rabbit anti-HA primary antibodies in blocking buffer.
    - Incubation for 1 h at RT with 1:20000 (v/v) secondary antibodies in blocking buffer.
26. Obtain image at 700 and 800nm using Odyssey imager.

Notes:

- *To calculate amount of plasmids to be used: [(1 µg pcDNA3.0-Myc-AIP)(size of 2nd CDS)]/(size of pcDNA3.0-Myc-AIP CDS). The result of this equation added to 1 is equal to 100%, calculate the corresponding % of each plasmid and transform to µg considering a final amount of 6 µg as 100%.*
- *Centrifugation steps for 30 sec can be carried out at RT, but care should be taken not to leave the samples at RT for longer periods of time.*
- *Each 10-well gel can be used for 2 different experiments.*
- *The transferring conditions are optimal for AIP, but time can be adjusted, if required, according to the AIP candidate partners to be tested.*
- *This experiment can be done in a T75, using 1X10^{5} cells and adjusting the rest of the reagents proportionally.*

References:

Moreno-Mateos MA, Espina AG, Torres B et al. PTTG1/securin modulates microtubule nucleation and cell migration. Mol Biol Cell 2011; 22(22):4302-4311.

Lee C. Coimmunoprecipitation assay. Methods Mol Biol 2007; 362:401-406.

http://www.gelifesciences.co.jp/tech_support/manual/pdf/71501754.pdf

Protocol 26: Co-immunoprecipitation of Myc-AIP and AIP-FLAG with TOMM20 10mer as a crosslinker

Buffers and solutions

Lysis buffer

150 mM NaCl (dilute from 1 M stock)

10 mM Tris-Cl pH 7.5 (dilute from 1 M stock)

10% (v/v) Glycerol

1% (v/v) IGEPAL® CA-630 (SIGMA I8896)

Adjust with ddH_2O to a final volume of 1 l

Sterilisation not needed, store at 4°C. Just before use, dispense in 50 ml aliquots and add 1 tablet of Complete® Protease Inhibitor Cocktail (Roche 11836145001) to each aliquot. The fully prepared buffer can be stored at -20°C for several weeks.

1X PBS, pH 7.4

To obtain a 5X stock, dissolve 25 tablets of PBS (SIGMA P4417) in ddH_2O and sterilise by autoclaving. Store at RT. Dilute accordingly with ddH_2O to obtain 1X working solution.

PAGE buffers

See Protocol 8

WB buffers

See Protocol 11

Cell culture media

See Protocol 13

1X Opti-MEM® Reduced Serum Medium, GlutaMAX™ Supplement (Life Technologies 51985-034)

Reagents and antibodies

Lipofectamine 2000 (Life Technologies 11668027)

Protein G Sepharose 4 Fast Flow (GE Healthcare 17-0618-01)

Monoclonal anti-Myc from mouse (SIGMA M4439)

Monoclonal anti-Flag antibody from mouse (SIGMA F3165)

Mouse IgG (SIGMA I5381)

TOMM20 10mer peptide (C. Prodromou's laboratory)

IRDye® 680 RD Goat anti-Mouse IgM (μ chain specific) (LI-COR 926-68180)

Reagents for cell culture and protein quantification (see Protocol 14).

Cell line

See Protocol 17

Nucleic acids and oligonucleotides

100 ng/µl pcDNA3.0-Myc-WT_AIP and 100 ng/µl pCI-neo-WT_AIP

Materials

0.2 (strips), 1.5, 2, 15 and 50 ml polypropylene tubes

T75 or T175 cell culture flasks

Pipette controller and disposable serological pipettes

5 ml syringes, 23G needles and insulin syringes and needles

Materials for cell culture, protein quantification, PAGE and WB (see appropriate protocols).

Equipment

Water bath

Set at 37°C

Inverted microscope

Labofuge 400 centrifuge (Heraeus)

Vortex

BR4i refrigerated centrifuge (Jouan)

Hot block

Stuart tube rotator SB2 (Stuart)

Equipment for cell culture, protein quantification PAGE and WB (see appropriate protocols).

Method

For details on growth and maintenance of HEK293 cells see Protocol 17. Cell culture must be performed in aseptic conditions. From step 8 onwards, all the procedures must be done at 4ºC or on ice.

1. Plate $2X10^6$ GH3 cells in a T25 flask with 5 ml of complete medium and incubate for 24 h at 37ºC/5% CO_2.
2. In a 1.5 ml tube, mix 450 µl Opti-MEM and 2.5 µg of each vector (~25 µl each one) to obtain a final volume of 500 µl (TUBE 1).
3. In a different 1.5 ml tube, mix 490 µl of Opti-MEM and 10 µl of Lipofectamine 2000 (TUBE 2). Incubate for 5 min at RT, shaking occasionally.
4. Mix the contents of TUBES 1 and 2 to obtain a final volume of 1 ml of cotransfection mixture. Incubate for 20 min at RT, shaking occasionally.
5. Discard the medium the cells grew in. Add 1 ml of cotransfection mixture and 4 ml of complete medium and incubate overnight at 37ºC/5% CO_2.
6. Replace the medium with complete medium and continue incubation for 24 h more.
7. Discard the medium, wash the cells with 5 ml of ice-cold PBS and discard the PBS.
8. Add 1 ml of lysis buffer, scrape the cells and transfer the content of the flask to a 1.5 ml tube (label appropriately). Incubate for 20 min at 4°C on a rotator (alternatively,

incubate on ice, vortexing occasionally). Collect the lysate in a syringe and pass it through a 23G needle six times.

9. Centrifuge the lysate for 10 min at 17000 g/4°C
10. In the meantime, transfer 50 µl of Protein G Sepharose (80% slurry) to 1X2 ml and 3X1.5 ml tubes, and add 1 ml of lysis buffer to each tube. Shake well and centrifuge for 30 sec at 17000 g/4°C. Discard the supernatant and repeat this step two more times. Add 50 µl of lysis buffer to obtain a ~50% slurry.
11. Transfer the cleared lysate to a 2 ml tube with equilibrated slurry. Incubate for 1 h at 4ºC on a rotator.
12. Centrifuge for 30 sec at 17000 g/4°C. Reserve ~60 µl of this pre-cleaned lysate in a different tube, for protein quantification and PAGE analysis.
13. Centrifuge at 12000 g for 20 sec at 4ºC. For each lysate (A to E), label 3X1.5 ml tubes as “Myc”, “Flag” and “IgG” (indicating the immunoprecipitation [IP] to be performed in each tube), respectively, and transfer 1/3 of the pre-cleaned lysate to each tube.
14. Add 2 µg (approximately 1 µl of anti-Myc and anti-Flag and 2 µl of IgG) of anti-Myc, anti-Flag or mouse IgG to each tube, according to the labelling. Add 1 µg of TOMM20 10mer peptide (~50 µl) to each tube.
15. Incubate for 1 h at 4ºC on a rotator. In the meantime, quantify the total protein content of the lysates (see appropriate protocol). Reserve ~50 µl for loading in gel.
16. Transfer the content of each tube to a 1.5 ml tube with equilibrated slurry, label appropriately. Incubate overnight at 4ºC on a rotator.
17. Centrifuge for 30 sec at 17000 g/4°C.
18. Wash the pellet thrice with 1 ml lysis buffer and once with PBS, centrifuging at for 30 sec at 17000 g/4°C between washes. After the last wash, eliminate carefully any remnants of the supernatant using an insulin needle.
19. Re-suspend the final pellet in 40 µl of 2XSDS gel-loading buffer. Heat to 95ºC for 3 min, shake, rotate or vortex for 5 min (to ensure the release of most of the immunoprecipitated proteins), heat again and finally centrifuge for 30 sec at 16000 g/RT to separate the beads. The final volume of the supernatant will be ~25 µl.
20. Load the supernatants in a 4-12% 10-well NuPAGE Bis-Tris gel as follows:

Lane	Sample	Volume
1	Kaleidoscope pre-stained protein standard	6 µl
2	Input (cleared lysate)	20 µl + 4 µl 6X SD gel-loading buffer
3	IP Myc	20 µl
4	IP Flag	20 µl
5	IP IgG	20 µl
6	Kaleidoscope pre-stained protein standard	6 µl
7	Input (cleared lysate)	20 µl + 4 µl 6X SD gel-loading buffer
8	IP Myc	25 µl
9	IP Flag	25 µl

10	IP IgG	25 µl

21. Run the gel in 1X MES at 150 V for ~1:15 h.
22. Use this gel for WB (refer to appropriate protocol), applying the following conditions:
    - Transference for 30 min at 15 V.
    - Blocking for 2 h at RT with 5% semi-skimmed milk in washing buffer.
    - Cut by the half and incubate overnight at 4°C in blocking buffer, one half with 1:3000 (v/v) mouse anti-Myc and the other half with 1:3000 (v/v) mouse anti-Flag.
    - Incubation for 1 h at RT with 1:20000 (v/v) secondary antibody in blocking buffer.
23. Obtain image at 700 using Odyssey imager.

Note:

- *Centrifugation steps for 30 sec can be carried out at RT, but care should be taken not to leave the samples at RT for longer periods of time.*

References:

Moreno-Mateos MA, Espina AG, Torres B et al. PTTG1/securin modulates microtubule nucleation and cell migration. Mol Biol Cell 2011; 22(22):4302-4311.

Lee C. Coimmunoprecipitation assay. Methods Mol Biol 2007; 362:401-406.

http://www.gelifesciences.co.jp/tech_support/manual/pdf/71501754.pdf

Protocol 27: Co-immunoprecipitation of Myc-AIP and AIP-Flag with formaldehyde as a crosslinker

Buffers and solutions

Lysis buffer

150 mM NaCl (dilute from 1M stock)

10 mM Tris-Cl pH 7.5 (dilute from 1M stock)

10% (v/v) Glycerol

1% (v/v) IGEPAL® CA-630 (SIGMA I8896)

Adjust with ddH_2O to a final volume of 1 l

Sterilisation not needed, store at 4°C. Just before use, dispense in 50 ml aliquots and add 1 tablet of Complete® Protease Inhibitor Cocktail (Roche 11836145001) to each aliquot. The fully prepared buffer can be stored at -20°C for several weeks.

1X PBS, pH 7.4

To obtain a 5X stock, dissolve 25 tablets of PBS (SIGMA P4417) in ddH_2O and sterilise by autoclaving. Store at RT. Dilute accordingly with ddH_2O to obtain 1X working solution.

0.8% (w/v) Formaldehyde

Adjust with 1X PBS to a final volume of 50 ml

Sterilisation not needed. Dispense in 5 ml aliquots and store at -20ºC, protected from light.

1.25 M Glycine

Adjust with 1X PBS to a final volume of 100 ml

Sterilisation not needed. Store at 4°C.

PAGE buffers

See Protocol 8

WB buffers

See Protocol 11

Cell culture media

See Protocol 13

1X Opti-MEM® Reduced Serum Medium, GlutaMAX™ Supplement (Life Technologies 51985-034)

Reagents and antibodies

Lipofectamine 2000 (Life Technologies 11668027)

Protein G Sepharose 4 Fast Flow (GE Healthcare 17-0618-01)

Monoclonal anti-Myc from mouse (SIGMA M4439)

Monoclonal anti-Flag antibody from mouse (SIGMA F3165)

Mouse IgG (SIGMA I5381)

IRDye® 680 RD Goat anti-Mouse IgM (µ chain specific) (LI-COR 926-68180)

Reagents for cell culture and protein quantification (see Protocol 14).

Cell line

See Protocol 17

Nucleic acids and oligonucleotides

100 ng/µl pcDNA3.0-Myc-WT_AIP and 100 ng/µl pCI-neo-WT_AIP

Materials

0.2 (strips), 1.5, 2, 15 and 50 ml polypropylene tubes

T75 or T175 cell culture flasks

Pipette controller and disposable serological pipettes

5 ml syringes, 23G needles and insulin syringes and needles

Materials for cell culture, protein quantification, PAGE and WB (see appropriate protocols).

Equipment

Water bath

Set at 37°C

Inverted microscope

Labofuge 400 centrifuge (Heraeus)

Vortex

BR4i refrigerated centrifuge (Jouan)

Hot block

Stuart tube rotator SB2 (Stuart)

Equipment for cell culture, protein quantification PAGE and WB (see appropriate protocols).

Method

For details on growth and maintenance of HEK293 cells see Protocol 17. Cell culture must be performed in aseptic conditions. From step 10 onwards, all the procedures must be done at 4ºC or on ice.

1. Plate $3.6X10^6$ GH3 cells in a T75 flask with 12 ml of complete medium and incubate for 24 h at 37ºC/5% CO_2.
2. In a 1.5 ml tube, mix 400 µl Opti-MEM and 5 µg of each vector to obtain a final volume of 500 µl (TUBE 1).
3. In a different 1.5 ml tube, mix 480 µl of Opti-MEM and 20 µl of Lipofectamine 2000 (TUBE 2). Incubate for 5 min at RT, shaking occasionally.

4. Mix the contents of TUBES 1 and 2 to obtain a final volume of 1 ml of cotransfection mixture. Incubate for 20 min at RT, shaking occasionally.
5. Discard the medium the cells grew in. Add 1 ml of cotransfection mixture and 11 ml of complete medium and incubate overnight at 37ºC/5% CO_2.
6. Replace the medium with complete medium and continue incubation for 24 h more.
7. Discard the medium, wash the cells with 10 ml of warm PBS and discard the PBS.
8. Add 2 ml of 0.8% formaldehyde solution and incubate for 10 min at 37ºC (this step can also be done at RT).
9. Discard formaldehyde and add 2 ml of ice-cold 1.25 M glycine solution. Incubate for 5 min at RT.
10. Discard glycine. Add 1 ml of lysis buffer, scrape the cells and transfer the content of the flask to a 1.5 ml tube (label appropriately). Incubate for 20 min at 4°C on a rotator (alternatively, incubate on ice, vortexing occasionally). Collect the lysate in a syringe and pass it through a 23G needle six times.
11. Centrifuge the lysate for 10 min at 17000 g/4°C.
12. In the meantime, transfer 50 µl of Protein G Sepharose (80% slurry) to 1X2 ml and 3X1.5 ml tubes, and add 1 ml of lysis buffer to each tube. Shake well and centrifuge for 30 sec at 17000 g/4°C. Discard the supernatant and repeat this step two more times. Add 50 µl of lysis buffer to obtain a ~50% slurry.
13. Transfer the cleared lysate to a 2 ml tube with equilibrated slurry. Incubate for 1 h at 4ºC on a rotator.
14. Centrifuge for 30 sec at 17000 g/4°C. Reserve ~60 µl of this pre-cleaned lysate in a different tube, for protein quantification and PAGE analysis.
15. Centrifuge for 30 sec at 17000 g/4ºC. For each lysate (A to E), label 3X1.5 ml tubes as “Myc”, “Flag” and “IgG” (indicating the immunoprecipitation [IP] to be performed in each tube), respectively, and transfer 1/3 of the pre-cleaned lysate to each tube.
16. Add 2 µg (approximately 1 µl of anti-Myc and anti-Flag and 2 µl of IgG) of anti-Myc, anti-Flag or mouse IgG to each tube, according to the labelling. Add 1 µg of TOMM20 10mer peptide (~50 µl) to each tube.
17. Incubate for 1 h at 4ºC on a rotator. In the meantime, quantify the total protein content of the lysates (see appropriate protocol). Reserve ~50 µl for loading in gel.
18. Transfer the content of each tube to a 1.5 ml tube with equilibrated slurry, label appropriately. Incubate overnight at 4ºC on a rotator.
19. Centrifuge for 30 sec at 17000 g/4°C.
20. Wash the pellet thrice with 1 ml lysis buffer and once with PBS, centrifuging at for 30 sec at 17000 g/4°C between washes. After the last wash, eliminate carefully any remnants of the supernatant using an insulin needle.
21. Re-suspend the final pellet in 40 µl of 2XSDS gel-loading buffer. Heat to 95ºC for 3 min, shake, rotate or vortex for 5 min (to ensure the release of most of the immunoprecipitated proteins), heat again and finally centrifuge for 30 sec at 16000 g/RT to separate the beads. The final volume of the supernatant will be ~25 µl.

22. Load the supernatants in a 4-12% 10-well NuPAGE Bis-Tris gel as follows:

Lane	Sample	Volume
1	Kaleidoscope pre-stained protein standard	6 µl
2	Input (cleared lysate)	20 µl+4 µl 6X SD gel-loading buffer
3	IP Myc	20 µl
4	IP Flag	20 µl
5	IP IgG	20 µl
6	Kaleidoscope pre-stained protein standard	6 µl
7	Input (cleared lysate)	20 µl+4 µl 6X SD gel-loading buffer
8	IP Myc	25 µl
9	IP Flag	25 µl
10	IP IgG	25 µl

23. Run the gel in 1X MES at 150 V for ~1:15 h.
24. Use this gel for WB (refer to appropriate protocol), applying the following conditions:
    - Transference for 30 min at 15 V.
    - Blocking for 2 h at RT with 5% semi-skimmed milk in washing buffer.
    - Cut by the half and incubate overnight at 4°C in blocking buffer, one half with 1:3000 (v/v) mouse anti-Myc and the other half with 1:3000 (v/v) mouse anti-Flag.
    - Incubation for 1 h at RT with 1:20000 (v/v) secondary antibody in blocking buffer.
25. Obtain image at 700 using Odyssey imager.

Note:

- *Centrifugation steps for 30 sec can be carried out at RT, but care should be taken not to leave the samples at RT for longer periods of time.*

References:

Moreno-Mateos MA, Espina AG, Torres B et al. PTTG1/securin modulates microtubule nucleation and cell migration. Mol Biol Cell 2011; 22(22):4302-4311.

Lee C. Coimmunoprecipitation assay. Methods Mol Biol 2007; 362:401-406.

http://www.gelifesciences.co.jp/tech_support/manual/pdf/71501754.pdf

Protocol 28. Co-localisation of AIP and its candidate interacting partners in HEK293 cells by immunocytofluorescence

Buffers and solutions

Fixation buffer

4% (w/v) Formaldehyde

Adjust with 1X PBS to a final volume of 40 ml

Dispense in 5 ml aliquots and store at -20°C, protected from light, and pre-heat at 37°C before use.

1X PBS

Store at RT and pre-heat at 37°C before use.

Permeabilisation buffer

0.1% (v/v) Triton X-100

Adjust with 1X PBS to a final volume of 50 ml

Store at RT

Blocking buffer

10% (v/v) Normal Goat Serum Blocking Solution (VECTOR Laboratories S-1000)

Adjust with permeabilisation buffer to a final volume of 5 ml

Store at 4°C.

Cell culture media

See Protocol 17

Reagents and antibodies

UltraCruz Hard-set Mounting Medium (Santa Cruz Biotechnology sc-359850)

Store at 4°C, protected from light.

Primary antibodies according to experimental purpose

Alexa Fluor® 488 Goat Anti-Mouse IgG (H+L) Antibody (green) (Life Technologies A-11029)

Alexa Fluor® 568 Goat Anti-Rabbit IgG (H+L) Antibody (orange) (Life Technologies A-11036)

Reagents for cell culture (see appropriate protocols).

Cell lines

See Protocol 17

Materials

0.5,1.5, and 15 ml polypropylene tubes

Pipette controller and disposable serological pipettes

8 wells 25X75 mm Nunc™ Lab-Tek™ II Chamber Slides (Thermo Scientific 154534)

Disposable Pasteur pipettes

24x50 mm #1.5 Menzel-Gläser cover slips (Thermo Scientific)

Nail polish

Materials for cell culture (see appropriate protocols)

Equipment

Water bath

Set at 37°C

Inverted microscope

Labofuge 400 centrifuge (Heraeus)

Cell culture incubator and hood

Zeiss LSM 510 (Mark 4) Laser Scanning Confocal Microscope

Humidity chamber (alternatively, use a Petri dish with a wet paper towel)

Equipment for cell culture (see appropriate protocols)

Method

1. Plate $5X10^4$ cells/well in 400 µl of complete medium in a chamber slide and incubate for 48 h at 37°C/5% CO_2.
2. Take the slide to the lab bench, add 200 µl of fixation buffer and incubate for 2 min at RT (pre-fixation).
3. Remove the medium with a Pasteur pipette, add 200 µl of fixation buffer and incubate for 10 min at RT (fixation).
4. Remove the buffer with a Pasteur pipette or by inverting the slide and wash the cells thrice with 400 µl of PBS.
5. Incubate the cells with 400 µl of permeabilisation buffer for 20 min at RT.
6. Remove the permeabilisation buffer with a Pasteur pipette or by inverting the slide and incubate the cells with 200 µl of blocking buffer for 1 h at RT.
7. Remove the blocking buffer and add the appropriate primary antibodies (adjust dilution in each case) diluted in 100 µl of blocking buffer. Incubate overnight at 4°C in a humidity chamber.
8. Wash the chambers with 400 µl of permeabilisation buffer for 5 min three times.
9. Add the appropriate secondary antibodies, diluted 1:500 in 100µl of blocking buffer, and incubate for 1 h at RT protected from light.
10. Wash the chambers with 400 µl of permeabilisation buffer for 5 min three times.
11. Remove the chamber walls and make sure that the surface of the slide is even (remove any residues of plastic or glue).
12. Add a few drops of mounting medium, cover with a cover slip, ensuring no bubbles are left, seal the edges with nail polish (optional) and store at 4°C overnight,

protected from light (to allow mounting medium to harden completely). Keep at 4°C, protected from light, until analysis.

Protocol 29: Initiation and maintenance of a stock of EBV-immortalised lymphoblastoid cells

Cell culture regents

Roswell Park Memorial Institute (RPMI)-1640 medium (SIGMA R8758)

20 mM L-Glutamine (Life Technologies 25030-024)

FBS (Life Technologies 10270-106), filtered

1X Dulbecco's PBS (SIGMA D8537)

Pre-heat all these reagents at 37°C before use.

Trypan blue solution (SIGMA T8154)

Cell lines

EBV-transformed LC (ECACC CO137 for WT AIP or F70M38 for AIP p.R304* mutation carrier)

Materials

1.5, 15 and 50 ml polypropylene tubes

T175 cell culture flasks

Pipettes and tips

Pipette controller and disposable serological pipettes

Equipment

Water bath

Set at 37°C

Cell culture incubator and hood

Inverted microscope

Heraeus Labofuge 400 centrifuge

Haemocytometer

Manual cell counter

Calculator

Method

Work in cell culture hood under aseptic conditions. For initiating a stock culture:

1. Transfer 5 ml of complete medium (RPMI-1640 supplemented with 10% FBS, and 2mM L-glutamine) into a 15 ml tube.
2. Take out a vial of frozen cells (stored in liquid nitrogen) and immerse it in the water bath for approximately 1 min or until the contents are completely thawed.
3. Take 20 µl of the cell suspension and mix with 20 µl of trypan blue in a 1.5 ml tube. Transfer 10 µl of this mixture to each of the chambers of a haemocytometer and count the cells under the microscope as follows:

a. Count the cells on each of the four external squares of the haemocytometer (those with large squares), avoiding blue cells (not viable) and obtain the average of the four squares.
b. Multiply X2 (dilution factor with trypan blue), then X10000 to obtain number of cells per ml. Finally, multiply for the volume of the cell suspension, to obtain the total cell number.

4. Transfer the cells to a T175 flask and adjust the cell confluence with complete medium to $5X10^5$ cells/ml in 15 ml, label appropriately and incubate at 37°C/5% CO_2.
5. Check the cell confluence twice per week, maintaining it between $3X10^5$ and $2X10^6$ cells/ml by adding complete medium to a maximum of 60 ml.

For maintaining a stock culture:

1. When the cell culture reaches maximum confluence and volume, transfer the cells to 50 ml tubes, mix well and take 20 µl of the cell suspension to quantify, as described before.
2. Centrifuge the rest of the cells at 800 g for 3 min at RT.
3. Resuspend the cells in complete medium to a concentration of $1X10^6$ cells per ml.
4. Transfer 4.5 ml of this cell suspension ($4.5x10^6$ cells) into a T175 and adjust to a final volume of 15 ml with complete medium.
5. Check the cell confluence twice per week, maintaining it between $3X10^5$ and $2X10^6$ cells/ml by adding complete medium to a maximum of 60 ml.

Protocol 30: Determining the half-life of endogenous AIP in HEK293 cells

Buffers and solutions

Lysis buffer

150 mM NaCl (dilute from 1M stock)

10 mM Tris-Cl pH 7.5 (dilute from 1M stock)

10% (v/v) Glycerol

1% (v/v) IGEPAL® CA-630 (SIGMA I8896)

Adjust with ddH_2O to a final volume of 1 l

Sterilisation not needed, store at 4°C. Just before use, dispense in 50 ml aliquots and add 1 tablet of Complete® Protease Inhibitor Cocktail (Roche 11836145001) to each aliquot. The fully prepared buffer can be stored at -20°C for several weeks.

PAGE buffers

See Protocol 8

WB buffers

See Protocol 11

Cell culture media

See Protocol 17

Reagents and antibodies

100 mg/ml CHX solution in DMSO (SIGMA C4859-1ML)

DMSO (SIGMA W387509)

Novex® Sharp Pre-stained Protein Standard (Life Technologies LC5800)

Monoclonal anti-AIP antibody from mouse (Novus NB100-127)

Polyclonal anti-ACTB antibody from rabbit (Abcam ab8227)

IRDye® 680 RD Goat anti-Mouse IgM (µ chain specific) (LI-COR 926-68180)

IRDye® 800CW Goat anti-Rabbit IgG (H + L) (LI-COR 926-32211)

Reagents for cell culture and protein quantification (see Protocol 14).

Cell line

See Protocol 17*.*

Materials

0.2 (strips), 1.5, 2, 15 and 50 ml polypropylene tubes

12-well cell culture plates

Pipette controller and disposable serological pipettes

Cell scrapers

Materials for cell culture, protein quantification, PAGE and WB (see appropriate protocols)

Equipment

Water bath

Set at 37°C

Inverted microscope

Labofuge 400 centrifuge (Heraeus)

BR4i refrigerated centrifuge (Jouan)

GS1 Thermal Cycler (G-Storm)

Stuart tube rotator SB2 (Stuart)

Equipment for cell culture, protein quantification PAGE and WB (see appropriate protocols)

Method

For details on growth and maintenance of HEK293 cells see Protocol 17. Cell culture must be performed in aseptic conditions. From step 4c onwards, all the procedures must be done at 4ºC or on ice.

1. Plate 5X10^5 cells per well in 1 ml of complete medium in one column of three wells (repeats A, B, and C) of 4X12-well plates for each experimental condition (a total of 12 wells divided in four plates for CHX treatment and the same for DMSO treatment). Incubate for 48 h at 37ºC/5% CO_2.
2. Prepare the following dilutions of CHX and DMSO:

Experimental condition	CHX solution	DMSO	Complete medium
100 µg/ml CHX	10 µl	-	10 ml
DMSO control	-	10 µl	10 ml

3. Label the plates with the experimental condition and the appropriate time point. Remove the medium where the cells grew and add 1 ml of CHX or DMSO dilution to each well, except for the first plate with 3 wells. Consider the moment when CHX or DMSO was added as time 0.
4. Harvest the first plate with three wells for each experimental condition at time 0, the second one after 6 h of treatment, the third one at 12 h and the fourth one at 24 h, as follows:
    a. Take the plate to the lab bench.
    b. Wash each well with 1 ml of RT PBS and remove it carefully.
    c. Add 75 µl of lysis buffer and scrape the cells.
    d. Incubate the plate on ice for 5 min.
    e. Collect the lysate in a 1.5 ml tube, label appropriately, and incubate for at least 20 min at 4°C on a rotator.
    f. Centrifuge the lysates for 10 min at 17000 g/4°C and transfer the supernatants (cleared lysates) to new tubes.

g. The lysates for the 0, 12 and 24 h should be stored at -80°C until the all the samples are ready for protein quantification and WB.
h. Quantify the protein concentration in the lysates using the Bradford method (see *Protocol 14*).

5. Transfer 10-20 µg of each sample to a 0.2 ml tube with an appropriate amount of 6X SDS gel loading buffer and denature for 5 min at 95-100°C on a thermal cycler (Protocol 8).
6. Load the samples in a 15-well PAGE gel (one gel per plate). Preferably load the repeat "A" for 0, 12, 24 and 48 h sequentially, then samples for repeat "B" and finally samples for repeat "C".
7. Run the gel in 1X MES at 120 V for ~1:35 h.
8. Use this gel for WB (refer to Protocol 11), applying the following conditions:
    a. Transference at 15VX30 min using a nitrocellulose membrane.
    b. Blocking for 1 h at RT in PBS with 1% Tween 20 and 5% w/v non-fat dry milk.
    c. Overnight incubation at 4°C with 1:1000 v/v mouse anti-AIP and rabbit anti-ACTB primary antibodies in blocking buffer.
    d. Incubation for 1 h at RT with 1:20000 v/v secondary antibodies in blocking buffer.
9. Obtain images at 700 and 800nm using the Odyssey imager.
10. Quantify the integrated density of the bands using the Odyssey software or ImageJ and use these values to calculate the AIP/ACTB ratios.
11. Calculate the protein half-life under the different treatments.

Protocol 31: Determining the half-life of endogenous AIP in EBV-LC cells

Buffers and solutions

Lysis buffer

150 mM NaCl (dilute from 1M stock)

10 mM Tris-Cl pH 7.5 (dilute from 1M stock)

10% (v/v) Glycerol

1% (v/v) IGEPAL® CA-630 (SIGMA I8896)

Adjust with ddH_2O to a final volume of 1 l

Sterilisation not needed, store at 4°C. Just before use, dispense in 50 ml aliquots and add 1 tablet of Complete® Protease Inhibitor Cocktail (Roche 11836145001) to each aliquot. The fully prepared buffer can be stored at -20°C for several weeks.

PAGE buffers

See Protocol 8

WB buffers

See Protocol 11

Cell culture media

See Protocol 29

Reagents and antibodies

100 mg/ml CHX solution in DMSO (SIGMA C4859-1ML)

DMSO (SIGMA W387509)

Novex® Sharp Pre-stained Protein Standard (Life Technologies LC5800)

Monoclonal anti-AIP antibody from mouse (Novus NB100-127)

Polyclonal anti-ACTB antibody from rabbit (Abcam ab8227)

IRDye® 680 RD Goat anti-Mouse IgM (µ chain specific) (LI-COR 926-68180)

IRDye® 800CW Goat anti-Rabbit IgG (H + L) (LI-COR 926-32211)

Reagents for cell culture and protein quantification (see Protocol 14*)*

Cell lines

See Protocol 29

Materials

0.2 (strips), 1.5, 2, 15 and 50 ml polypropylene tubes

6-well cell culture plates

Pipette controller and disposable serological pipettes

5 ml syringes and 23G needles

Materials for cell culture, protein quantification, PAGE and WB (see appropriate protocols)

Equipment

Water bath

Set at 37°C

Inverted microscope

Labofuge 400 centrifuge (Heraeus)

BR4i refrigerated centrifuge (Jouan)

GS1 Thermal Cycler (G-Storm)

Stuart tube rotator SB2 (Stuart)

Equipment for cell culture, protein quantification PAGE and WB (see appropriate protocols)

Method

For details on growth and maintenance of EBV-LC cells see Protocol 29.

Cell culture must be performed in aseptic conditions. From step 2e onwards, all the procedures must be done at 4ºC or on ice.

1. Plate $3X10^6$ cells per well in 2 ml of complete medium in one column of three wells (repeats 1, 2, and 3) of 4X6-well plates for each experimental condition (a total of 12 wells divided in four plates for CHX treatment and the same for DMSO treatment). Incubate for 48 h at 37ºC/5% CO_2. The wells for time 0 hours should contain complete medium with nothing added. For the rest of the wells, prepare the following dilutions of CHX and DMSO:

Experimental condition	CHX solution	DMSO	Complete medium
100 µg/ml CHX	20 µl	-	20 ml
DMSO control	-	20 µl	20 ml

2. Considering the moment when the cells were plated as time 0, harvest the first row of three wells at time 0 hours, the second column after 6 h, the third one at 12 h and the fourth one at 24 hours, as follows:
    a. Take the plate to the lab bench.
    b. Transfer the contents of each well to a 2 ml tube, appropriately labelled.
    c. Centrifuge at 1200 g for 5 min and discard the supernatant.
    d. Wash the pelled with 1 ml of RT PBS and remove it carefully and centrifuge again.
    e. Discard the supernatant and resuspend the pellet in 75 µl of lysis buffer by vortexing.
    f. Pass the lysates through a 23G needle six times.
    g. Incubate the lysates for at least 20 min at 4°C on a rotator.
    h. Centrifuge the lysates for 10 min at 17000 g/4°C and transfer the supernatants (cleared lysates) to new tubes.

i. The lysates for the 0, 6 and 12 h should be stored at -80°C until the all the samples are ready for protein quantification and WB.
j. Quantify the protein concentration in the lysates using the Bradford method (see Protocol 14).

3. Transfer 20-25 µg of each sample to a 0.2 ml tube with an appropriate amount of 6X SDS gel loading buffer and denature for 5 min at 95-100°C on a thermal cycler (Protocol 8).
4. Load the samples in a 15-well PAGE gel (one gel per plate). Preferably load the repeat "1" for 0, 6, 12 and 24 h sequentially, then samples for repeat "2" and finally samples for repeat "3".
5. Run the gel in 1X MES at 120 V for ~1:35 h.
6. Use this gel for WB (refer to Protocol 11), applying the following conditions:
    a. Transference at 15VX30 min using a nitrocellulose membrane.
    b. Blocking for 1 h at RT in PBS with 1% Tween 20 and 5% w/v non-fat dry milk.
    c. Overnight incubation at 4°C with 1:1000 v/v mouse anti-AIP and rabbit anti-ACTB primary antibodies in blocking buffer.
    d. Incubation for 1 h at RT with 1:20000 v/v secondary antibodies in blocking buffer.
7. Obtain images at 700 and 800nm using the Odyssey imager.
8. Quantify the integrated density of the bands using the Odyssey software or ImageJ and use these values to calculate the AIP/ACTB ratios.
9. Calculate the protein half-life under the different treatments.

Protocol 32: Determining the half-life of overexpressed AIP in HEK293 cells

Buffers and solutions

Lysis buffer

150 mM NaCl (dilute from 1 M stock)

10 mM Tris-Cl pH 7.5 (dilute from 1 M stock)

10% (v/v) Glycerol

1% (v/v) IGEPAL® CA-630 (SIGMA I8896)

Adjust with ddH_2O to a final volume of 1 l

Sterilisation not needed, store at 4°C. Just before use, dispense in 50 ml aliquots and add 1 tablet of Complete® Protease Inhibitor Cocktail (Roche 11836145001) to each aliquot. The fully prepared buffer can be stored at -20°C for several weeks.

PAGE buffers

See Protocol 8

WB buffers

See Protocol 11

Cell culture media

See Protocol 17

1X Opti-MEM® Reduced Serum Medium, GlutaMAX™ Supplement (Life Technologies 51985-034)

Reagents and antibodies

Lipofectamine 2000 (Life Technologies 11668027)

100 mg/ml CHX solution in DMSO (SIGMA C4859-1ML)

DMSO (SIGMA W387509)

Novex® Sharp Pre-stained Protein Standard (Life Technologies LC5800)

Monoclonal anti-Myc from mouse (SIGMA MM4439-100UL)

Polyclonal anti-ACTB antibody from rabbit (Abcam ab8227)

IRDye® 680 RD Goat anti-Mouse IgM (µ chain specific) (LI-COR 926-68180)

IRDye® 800CW Goat anti-Rabbit IgG (H + L) (LI-COR 926-32211)

Reagents for cell culture and protein quantification (see Protocol 14)

Cell line

See Protocol 17

Nucleic acids and oligonucleotides

100 ng/µl pcDNA3.0-Myc-AIP, WT or mutant

Materials

0.2 (strips), 1.5, 15 and 50 ml polypropylene tubes

12-well cell culture plates

Pipette controller and disposable serological pipettes

Cell scrapers

Materials for cell culture, protein quantification, PAGE and WB (see appropriate protocols)

Equipment

Water bath

Set at 37°C

Inverted microscope

Labofuge 400 centrifuge (Heraeus)

Vortex

BR4i refrigerated centrifuge (Jouan)

GS1 Thermal Cycler (G-Storm)

Stuart tube rotator SB2 (Stuart)

Equipment for cell culture, protein quantification PAGE and WB (see appropriate protocols)

Method

For details on growth and maintenance of HEK293 cells see Protocol 17. Cell culture must be performed in aseptic conditions. From step 9c onwards, all the procedures must be done at 4ºC or on ice.

1. Plate 2.5X10^5 HEK293 cells/well in 1 ml of complete medium in one column of three wells (repeats A, B, and C) of 4X12-well plates for each experimental condition. Incubate for 24 h at 37ºC/5% CO_2.
2. In a 15 ml tube mix 520µl (40µl/well*13) of Opti-MEM+ GlutaMAX medium and 130µl (13 µg=1µg/well*13) of plasmid DNA (TUBE 1).
3. In a different 15ml tube mix 637µl (49µl/well*13) of Opti-MEM+GlutaMAX medium and 13µl (1 µl/well*13) of Lipofectamine 2000 (TUBE 2). Incubate for 5 min at RT, shaking occasionally.
4. Mix the contents of TUBES 1 and 2 by vortexing and incubate for 30 min at RT, vortexing occasionally.
5. Remove the medium where the cells grew and add 100µl of the transfection mix and 900µl of complete medium to each well. Incubate for 24 h at 37ºC/5% CO_2.
6. Prepare the following dilution of CHX or DMSO (vehicle control):

Experimental condition	CHX solution	DMSO	Complete medium
20 µg/ml CHX	2 µl	-	10 ml
DMSO control	-	2 µl	10 ml

7. Remove the medium the cells grew in and add 1 ml of the CHX or DMSO dilution to each well, except for the first three wells. Consider the moment when the CHX or DMSO was added as time 0.
8. Label the plates with the appropriate experimental condition and the time point. Remove the medium the cells grew in and add 1 ml of CHX or DMSO dilution to each well, except for the first three wells. Consider the moment when CHX or DMSO was added as time 0.
9. Harvest the first column of three wells for each experimental condition at time 0, the second one after 6 h of treatment, the third one at 12 h and the fourth one at 24 h, as follows:
    a. Take the plate to the lab bench.
    b. Wash each well with 1 ml of RT PBS and remove it carefully.
    c. Add 50 µl of lysis buffer and scrape the cells.
    d. Incubate the plate on ice for 5 min.
    e. Collect the lysate in a 1.5 ml tube, label appropriately, and incubate for at least 20 min at 4°C on a rotator.
    f. Centrifuge the lysates for 10 min at 17000 g/4°C and transfer the supernatants (cleared lysate) to new tubes.
    g. The lysates for the 0, 6 and 12 h should be stored at -80°C until the all the samples are ready for protein quantification and WB.
    h. Quantify the protein concentration in the lysates using the Bradford method (see Protocol 14).
10. Transfer 10-20 µg of each sample to a 0.2 ml tube with an appropriate amount of 6X SDS gel loading buffer and denature for 5 min at 95-100°C on a thermal cycler (Protocol 8).
11. Load the samples in a 15-well PAGE gel (one gel per plate). Preferably load the repeat “A” for 0, 6, 12 and 24 h sequentially, then samples for repeat “B” and finally samples for repeat “C”.
12. Run the gel in 1X MES at 120 V for ~1:35 h.
13. Use this gel for WB (refer to Protocol 11), applying the following conditions:
    a. Transference at 15VX30 min using a nitrocellulose membrane.
    b. Blocking for 1 h at RT in PBS with 1% Tween 20 and 5% w/v non-fat dry milk.
    c. Overnight incubation at 4°C with 1:1000 v/v mouse anti-AIP and rabbit anti-ACTB primary antibodies in blocking buffer.
    d. Incubation for 1 h at RT with 1:20000 v/v secondary antibodies in blocking buffer.
14. Obtain images at 700 and 800nm using the Odyssey imager.
15. Quantify the integrated density of the bands using the Odyssey software or ImageJ and use these values to calculate the AIP/ACTB ratios.
16. Calculate the protein half-life under the different treatments.

Protocol 33: Rescuing overexpressed short half-life AIP variants with the proteasome inhibitor MG-132 in HEK293 cells

Buffers and solutions

Lysis buffer

150 mM NaCl (dilute from 1 M stock)

10 mM Tris-Cl pH 7.5 (dilute from 1 M stock)

10% (v/v) Glycerol

1% (v/v) IGEPAL® CA-630 (SIGMA I8896)

Adjust with ddH_2O to a final volume of 1 l

Sterilisation not needed, store at 4°C. Just before use, dispense in 50 ml aliquots and add 1 tablet of Complete® Protease Inhibitor Cocktail (Roche 11836145001) to each aliquot. The fully prepared buffer can be stored at -20°C for several weeks.

PAGE buffers

See Protocol 8

WB buffers

See Protocol 11

Cell culture media

See Protocol 17

1X Opti-MEM® Reduced Serum Medium, GlutaMAX™ Supplement (Life Technologies 51985-034)

Reagents and antibodies

Lipofectamine 2000 (Life Technologies 11668027)

100 mg/ml CHX solution in DMSO (SIGMA C4859-1ML)

100 mM MG-132 (Enzo Life Sciences BML-PI102-0005), diluted in DMSO

DMSO (SIGMA W387509)

Novex® Sharp Pre-stained Protein Standard (Life Technologies LC5800)

Monoclonal anti-Myc from mouse (SIGMA MM4439-100UL)

Polyclonal anti-ACTB antibody from rabbit (Abcam ab8227)

IRDye® 680 RD Goat anti-Mouse IgM (µ chain specific) (LI-COR 926-68180)

IRDye® 800CW Goat anti-Rabbit IgG (H + L) (LI-COR 926-32211)

Reagents for cell culture and protein quantification (see Protocol 14).

Cell line

See Protocol 17

Nucleic acids and oligonucleotides

100 ng/µl pcDNA3.0-Myc-AIP, WT or mutant

Materials

0.2 (strips), 1.5, 15 and 50 ml polypropylene tubes

12-well cell culture plates

Pipette controller and disposable serological pipettes

Cell scrapers

Materials for cell culture, protein quantification, PAGE and WB (see appropriate protocols)

Equipment

Water bath

Set at 37°C

Inverted microscope

Labofuge 400 centrifuge (Heraeus)

Vortex

BR4i refrigerated centrifuge (Jouan)

GS1 Thermal Cycler (G-Storm)

Stuart tube rotator SB2 (Stuart)

Equipment for cell culture, protein quantification PAGE and WB (see appropriate protocols)

Method

For details on growth and maintenance of HEK293 cells see Protocol 17.

Cell culture must be performed in aseptic conditions. From step 8c onwards, all the procedures must be done at 4ºC or on ice.

1. Plate 2.5X10^5 HEK293 cells/well in 1 ml of complete medium in one column of three wells (repeats A, B, and C) of 4X12-well plates for each experimental condition. Incubate for 24 h at 37ºC/5% CO_2.
2. In a 15 ml tube mix 520 µl (40 µl/well*13) of Opti-MEM+ GlutaMAX medium and 130 µl (13 µg=1µg/well*13) of plasmid DNA (TUBE 1).
3. In a different 15ml tube mix 637µl (49µl/well*13) of Opti-MEM+GlutaMAX medium and 13µl (1 µl/well*13) of Lipofectamine 2000 (TUBE 2). Incubate for 5 min at RT, shaking occasionally.
4. Mix the contents of TUBES 1 and 2 by vortexing and incubate for 30 min at RT, vortexing occasionally.
5. Remove the medium the cells grew in and add 100µl of the transfection mix and 900µl of complete medium to each well. Incubate for 24 h at 37ºC/5% CO_2.
6. Prepare 15 ml of 20 µg/ml CHX in complete medium. Remove the medium the cells grew in and replace it for 1 ml of this dilution. Incubate for 6 h at 37ºC/5% CO_2
7. Label the plates with the appropriate time point. Prepare 10 ml of 20 µg/ml CHX plus 20µM MG-132 in complete medium. Replace the medium in the wells for 1 ml of this

dilution, except for the first three wells. Consider the moment when the MG-132 was added as time 0.

8. Harvest the first column of three wells at time 0 (untreated), the second one after 6 h of treatment, the third one at 12 h and the fourth one at 24 h, as follows:
    a. Take the plate to the lab bench.
    b. Wash each well with 1 ml of RT PBS and remove it carefully.
    c. Add 50 µl of lysis buffer and scrape the cells.
    d. Incubate the plate on ice for 5 min.
    e. Collect the lysate in a 1.5 ml tube, label appropriately, and incubate for at least 20 min at 4°C on a rotator.
    f. Centrifuge the lysates for 10 min at 17000 g/4°C and transfer the supernatants (cleared lysate) to new tubes.
    g. The lysates for the 0, 6 and 12 h should be stored at -80°C until the all the samples are ready for protein quantification and WB.
    h. Quantify the protein concentration in the lysates using the Bradford method (see Protocol 14).
9. Transfer 10-20 µg of each sample to a 0.2 ml tube with an appropriate amount of 6X SDS gel loading buffer and denature for 5 min at 95-100°C on a thermal cycler (Protocol 8).
10. Load the samples in a 15-well PAGE gel (one gel per plate). Preferably load the repeat “A” for 0, 6, 12 and 24 h sequentially, then samples for repeat “B” and finally samples for repeat “C”.
11. Run the gel in 1X MES at 120 V for ~1:35 h.
12. Use this gel for WB (refer to Protocol 11), applying the following conditions:
    a. Transference at 15VX30 min using a nitrocellulose membrane.
    b. Blocking for 1 h at RT in PBS with 1% Tween 20 and 5% w/v non-fat dry milk.
    c. Overnight incubation at 4°C with 1:1000 v/v mouse anti-AIP and rabbit anti-ACTB primary antibodies in blocking buffer.
    d. Incubation for 1 h at RT with 1:20000 v/v secondary antibodies in blocking buffer.
13. Obtain images at 700 and 800nm using the Odyssey imager.
14. Quantify the integrated density of the bands using the Odyssey software or ImageJ and use these values to calculate the AIP/ACTB ratios.
15. Calculate the protein half-life under the different treatments.

Appendix 3: Abstracts presented in scientific meetings

2015: Hernández-Ramírez LC, Martucci F, Ferraù F, Morgan RM, Trivellin G, Begum F, Tilley D, Ramos-Guajardo N, Iacovazzo D, Prodromou C, and Korbonits M. **The enhanced proteasomal degradation of AIP mutant proteins is a mechanism for AIP deficiency in *AIP* mutation-associated pituitary adenomas.** OR35-2.
Oral presentation at the The Endocrine Society Annual Meeting ENDO 2015, San Diego, USA, March 5-8, 2015.

Schernthaner-Reiter MH, Trivellin G, Hernández-Ramírez LC, Korbonits M, and Stratakis C. **Interaction between AIP and the cAMP-dependent protein kinase (PKA) pathway in pituitary tumor formation.** SAT-427.
Poster presentation by M.H. Schernthaner-Reiter at the The Endocrine Society Annual Meeting ENDO 2015, San Diego, USA, March 5-8, 2015.

Hernández-Ramírez LC, Morgan RML, Prodromou C, and Korbonits M. **A proteomic approach for explaining AIP mutation-associated pituitary tumorigenesis**.
Oral presentation at the New Year Celebration, *William Harvey Research Institute, Barts and The London School of Medicine, Queen Mary University of London, London, UK, February 13th, 2014.*

2014: Hernández-Ramírez LC, Gabrovska P, Dénes J, Trivellin G, Radian S, Tilley D, Ferraù F, Akker SA, Grossman AB, Gadelha MR, Korbonits M, and The International FIPA Consortium. **Pituitary adenomas in *AIP* mutation positive individuals: genotype-phenotype associations and role of the germline *FGFR4* G388R variant and the somatic *GNAS1* mutations.**
Poster presented at the William Harvey Day, *William Harvey Research Institute, Barts and The London School of Medicine, Queen Mary University of London, London, UK, October 21st, 2014.*

Hernández Ramírez LC, Ferraù F, Miljic D, Kastelan D, Drake W, Musat M, Mercado-Atri M, Musolino N, Karavitaki N, Korbonits M, and The International FIPA Consortium. **Absence of *GNAS1* mutations in somatotropinomas from *AIP*mut positive patients: possible implications for phenotype.**
Oral presentation by M. Korbonits at the 14th International Workshop on Multiple Endocrine Neoplasia and other rare endocrine tumors, World MEN 2014, Vienna, Austria, September 25-27, 2014.

Hernández-Ramírez LC, Gabrovska P, Hunter S, Howell S, Salvatori R, Dzeranova L, Grossman AB., Roncaroli F, Korbonits M, and The International FIPA Consortium. **Extra-pituitary neoplasms in AIP mutation positive individuals: Findings in a large cohort of familial isolated pituitary adenoma (FIPA) and young-onset sporadic pituitary adenoma patients.**
Oral presentation at the 16º Meeting of the European Neuroendocrine Association, Sofia, Bulgaria, September 10-13, 2014.

Hernández-Ramírez LC, Gabrovska P, Dénes J, Trivellin G, Radian S, Tilley D, Ferraù F, Akker SA, Grossman AB, Gadelha MR, Korbonits M, and The International FIPA Consortium. **Pituitary adenomas harboring *AIP* mutations exhibit phenotype-genotype correlation, but no association with the germline *FGFR4* G388R variant or somatic *GNAS1* mutations**. *Endocr.Rev.*2014;35 (03_MeetingAbstracts): OR09-3.
Oral presentation at the 15th International Congress of Endocrinology, International Society of Endocrinology/The Endocrine Society ENDO 2014, Chicago, USA, June 21-24, 2014.

Radian S, Gabrovska P, Holland B, Wallace H, Ryan AW, McGurren K, Stals K, Bussell AM, Thomas MG, Holland A, Aflorei ED, Barry S, Stiles CE, Pernicova I, Trivellin G, Dénes J, Hérincs M, Hernández-Ramírez LC, Samuels J, McCloskey R, Azjensztejn M, Abid N, Kumar AV, Atkinson BA, Ellard S, McManus R, Thompson CJ, Linden GJ, Bradley L, Agha A, Hunter SJ, Morrison PJ, and Korbonits M. **Population screening for the Irish founder *AIP* mutation R304* reveals a prevalence of 1/500 in the Local population, while high mutation frequency is present among Irish familial and sporadic somatotropinoma patients.** *Endocr Rev* 2014;35,OR17-1.
Oral presentation by S. Radian at the 15th International Congress of Endocrinology, International Society of Endocrinology/The Endocrine Society ENDO 2014, Chicago, USA, June 21-24, 2014.

Schernthaner-Reiter MH, Trivellin G, Nesterova MV, Hernández-Ramírez LC, Aflorei ED, Sierra ML, Stratakis C, and Korbonits M. **Interaction of AIP with the cAMP-dependent protein kinase (PKA) pathway and its role in pituitary tumor formation.** *Endocr Rev* 2014;35,PP09-4.
Poster presentation by M.H. Schernthaner-Reiter at the 15th International Congress of Endocrinology, International Society of Endocrinology/The Endocrine Society ENDO 2014, Chicago, USA, June 21-24, 2014.

2013: Hernández-Ramírez LC, Gabrovska P, Dénes J, Trivellin G, Akker SA, Grossman AB, Gadelha MR, Korbonits M, and The International FIPA Consortium. **Pituitary adenomas due to aryl hydrocarbon receptor interacting protein (*AIP*) gene mutations: genotypic-phenotypic characteristics, screening and prospective diagnosis**. *Endocr.Rev.*2013;34 (03_MeetingAbstracts): OR42-5.
Oral presentation at The Endocrine Society Annual Meeting ENDO 2013, San Francisco, USA, June 15-18, 2013.

Ramírez C, Hernández-Ramírez LC, Gabrovska P, Portocarrero L, Korbonits M, and Mercado M. **Prevalence of *AIP* mutations in young mexican patients with acromegaly.** *Endocr Rev.* 2013;34 (05_MeetingAbstracts):SUN-152.
Poster presentation by C. Ramírez at The Endocrine Society Annual Meeting ENDO 2013, San Francisco, USA, June 15-18, 2013.

2012: Hernández-Ramírez, LC, and Korbonits M. **Evaluation of a *FGFR4* polymorphism as a posible predictor of disease penetrance in *AIP* mutation-carrier FIPA patients.** *Austrian Journal of Clinical Endocrinology and Metabolism* 2012;5(Special Issue 3):57.
Poster presentation at the 15º Meeting of the European Neuroendocrine Association, Vienna, Austria, September 12-15, 2012.

Appendix 4: Manuscripts

OPEN ACCESS Freely available online

PLOS ONE

Structure of the TPR Domain of AIP: Lack of Client Protein Interaction with the C-Terminal α-7 Helix of the TPR Domain of AIP Is Sufficient for Pituitary Adenoma Predisposition

Rhodri M. L. Morgan[1], Laura C. Hernández-Ramírez[2], Giampaolo Trivellin[2], Lihong Zhou[1], S. Mark Roe[3], Márta Korbonits[2], Chrisostomos Prodromou[1]*

1 Genome Damage and Stability Centre, University of Sussex, Brighton, United Kingdom, **2** Department of Endocrinology, Barts and the London School of Medicine, Queen Mary University of London, London, United Kingdom, **3** Biochemistry and Molecular Biology, Chichester 2, University of Sussex, Brighton, United Kingdom

Abstract

Mutations of the *aryl hydrocarbon receptor interacting protein* (*AIP*) have been associated with familial isolated pituitary adenomas predisposing to young-onset acromegaly and gigantism. The precise tumorigenic mechanism is not well understood as AIP interacts with a large number of independent proteins as well as three chaperone systems, HSP90, HSP70 and TOMM20. We have determined the structure of the TPR domain of AIP at high resolution, which has allowed a detailed analysis of how disease-associated mutations impact on the structural integrity of the TPR domain. A subset of C-terminal α-7 helix (Cα-7h) mutations, R304* (nonsense mutation), R304Q, Q307* and R325Q, a known site for AhR and PDE4A5 client-protein interaction, occur beyond those that interact with the conserved MEEVD and EDDVE sequences of HSP90 and TOMM20. These C-terminal AIP mutations appear to only disrupt client-protein binding to the Cα-7h, while chaperone binding remains unaffected, suggesting that failure of client-protein interaction with the Cα-7h is sufficient to predispose to pituitary adenoma. We have also identified a molecular switch in the AIP TPR-domain that allows recognition of both the conserved HSP90 motif, MEEVD, and the equivalent sequence (EDDVE) of TOMM20.

Citation: Morgan RML, Hernández-Ramírez LC, Trivellin G, Zhou L, Roe SM, et al. (2012) Structure of the TPR Domain of AIP: Lack of Client Protein Interaction with the C-Terminal α-7 Helix of the TPR Domain of AIP Is Sufficient for Pituitary Adenoma Predisposition. PLoS ONE 7(12): e53339. doi:10.1371/journal.pone.0053339

Editor: Giorgio Colombo, Consiglio Nazionale delle Ricerche, Italy

Received October 2, 2012; **Accepted** November 27, 2012; **Published** December 31, 2012

Funding: The authors acknowledge support from the Diamond Light Source and the Wellcome Trust senior investigator award (LHP), 095605/Z11/Z. LCH-R is supported by the National Council of Science and Technology of Mexico and by the Barts and The London Charity. The funders had no role in study design, data collection and analysis, decision to publish, or preparation of the manuscript.

Competing Interests: The authors have declared that no competing interests exist.

* E-mail: chris.prodromou@sussex.ac.uk

Introduction

Recently, mutations in aryl hydrocarbon receptor interacting protein (AIP) [1,2] have been linked to familial isolated pituitary adenomas (FIPA) [3–5], a condition most often characterized by young-onset growth hormone and prolactin-secreting pituitary tumors (reviewed by [6]), which leads to acromegaly and gigantism. The human *AIP* gene encodes a 37 kDa protein of 330 amino acids that, based on similarities to other proteins, is predicted to have an N-terminal immunophilin-like domain [7] and a C-terminal tetratricopeptide repeat (TPR) domain. Typically, TPR domains consist of three sets of a highly degenerate consensus sequence of 34 amino acids, often arranged in tandem repeats, formed by two alpha-helices forming an antiparallel amphipathic structure and a final C-terminal α-7 helix (Cα-7h; Fig. 1A). The TPR domain of AIP appears to be similar to the corresponding domains of HOP, CHIP, CYP40, PP5, FKBP51 and FKBP52 and the aryl hydrocarbon receptor-interacting protein like 1 (AIPL1) (Fig. 1A). Although the immunophilin domain of AIP shows significant homology to equivalent domains of FKBP12 and FKBP52, AIP does not bind immunosuppressant drugs such as FK506 and rapamycin [2] and displays no PPIase activity [8,9].

AIP has been reported to interact with a number of different proteins: chaperones (HSP90, HSP70, TOMM20), and client proteins including nuclear receptors (AhR, ERα), phosphodiesterase 4A5 (rat isoform of human PDE4A4) and PDE2A3, survivin, G proteins, RET and EBNA3 amongst others (see recent review by [10]). Interestingly, HSP90, HSP70 and TOMM20 share a common conserved C-terminal motif, EEVD (HSP90 and HSP70) and DDVE (TOMM20) that potentially act as the binding sites for the AIP TPR-domain [11,12]. A similar motif, EELD, has been identified in PDE4A5 [13]. HSP90 is a molecular chaperone that is involved in the maturation of many signal transduction proteins ([14–16]), while HSP70 is a more generalised protein-folding chaperone [17,18]. In contrast, TOMM20 acts as a receptor for unfolded proteins destined for translocation across the outer mitochondrial membrane [19]. Together, these chaperones are responsible for the activation and maturation of a vast array of other proteins.

AhR, a client protein of the HSP90-AIP complex, may function as a tumor suppressor that becomes silenced. [4,5,20–25], but its precise role in predisposition to pituitary adenoma is not well understood. AhR binds environmental dioxins, such as the non-metabolizable agonist 2,3,7,8 tetra-chlorodibenzo-ρ-dioxin

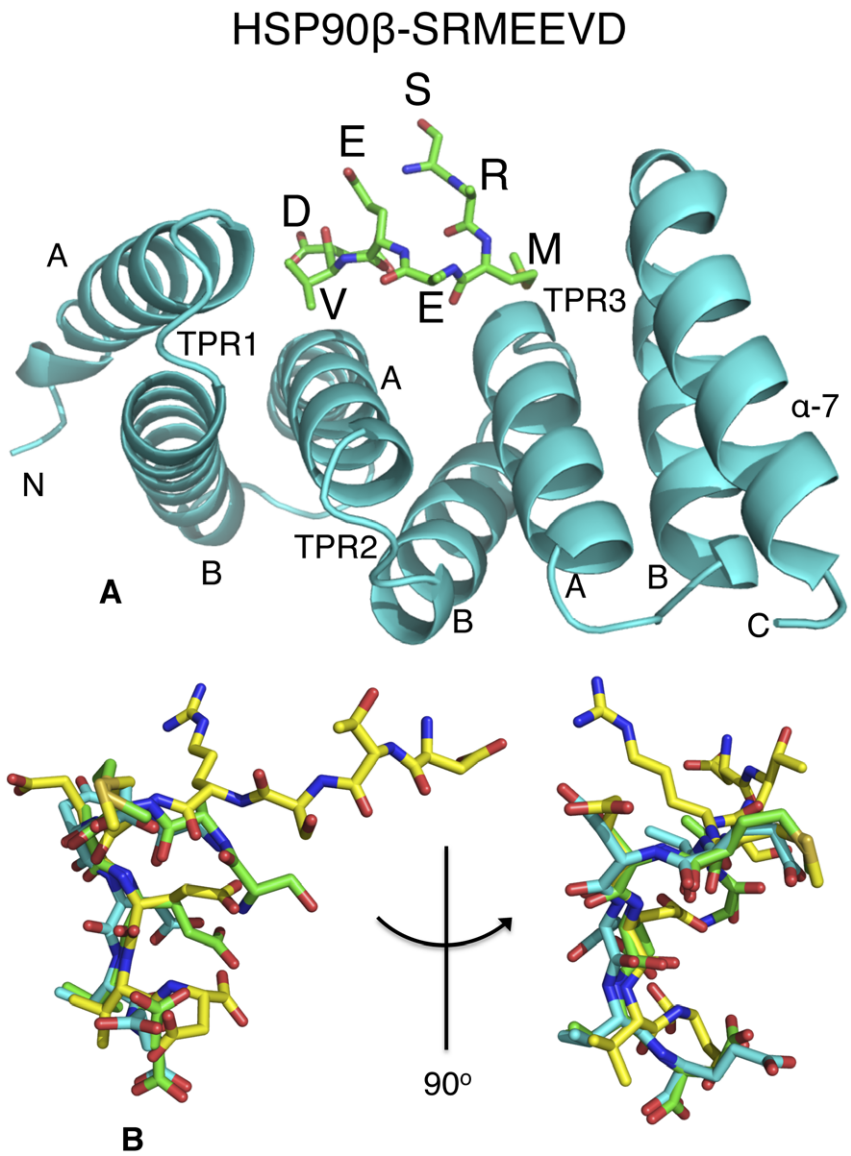

Figure 1. PyMol cartoon of the structure of human AIP. (A), PyMol cartoon of the HSP90β EDASRMEEVD-peptide (green) bound to the TPR domain of AIP (cyan). Only SRMEEVD of the peptide was visible. The structure was obtained at 2.0 Å (PDB, 4AIF) while that with the TOMM20 AQSLAEDDVE-peptide was obtained at 1.9 Å (PDB, 4APO, not shown). The A and B helices of each TPR motif (TPR1 to 3) and the C-terminal alpha helix (α-7) are indicated. (B), Superimposition of peptide conformations of HSP90β EDASRMEEVD (green), TOMM20 AQSLAEDDVE (cyan) bound to AIP (only SRMEEVD and AEDDVE of the peptides is shown), and HSP90α DTSRMEEVD (yellow) peptide bound to CHIP, showing that the peptide backbone conformation is essentially the same.
doi:10.1371/journal.pone.0053339.g001

(TCDD), which is known to promote tumorigenesis, but it is unclear whether this has a role in AIP-related tumorigenesis.

The cAMP pathway is important for somatotroph cell function and proliferation. As AIP interacts with phosphodiesterases (PDE4A5 and PDE2A), enzymes which degrade cAMP, this interaction may have an important role in AIP-related pituitary tumorigenesis. AIP has an opposite effect on PDE4A5 and PDE2A function [13,26,27] and very little data exist on the possible interaction with other PDEs. As there are over 52 different PDEs known, this aspect remains an important field of study.

Recently, AIP was shown to inhibit ERα transcriptional activity and AIP mutations lead to enhanced ERα transcriptional activity. Prolonged and a high-level exposure to estrogen is a known risk factor for developing a variety of tumors [28–31] including pituitary tumors [32,33]. Furthermore, AIP has also been shown to upregulate PLAGL1 (also known as ZAC1), a zinc finger protein with apoptotic and cell cycle arrest activity [34,35].

Around 75% of AIP mutations completely disrupt the C-terminal TPR domain and/or the Cα-7h [36]. The vast majority of the missense variants affect the two final TPR-motifs and the Cα-7h, both of which are involved in protein interactions. The client proteins AhR and PDE4A5 have been shown to bind to the Cα-7h part of the AIP molecule. How the lack of AIP or its dysfunction leads to tumorigenesis and how interactions are disrupted that predispose cells to tumorigenesis are poorly understood and difficult to predict as AIP interacts directly with a number of proteins and indirectly, via the three chaperone systems, with a bewildering number of proteins [10].

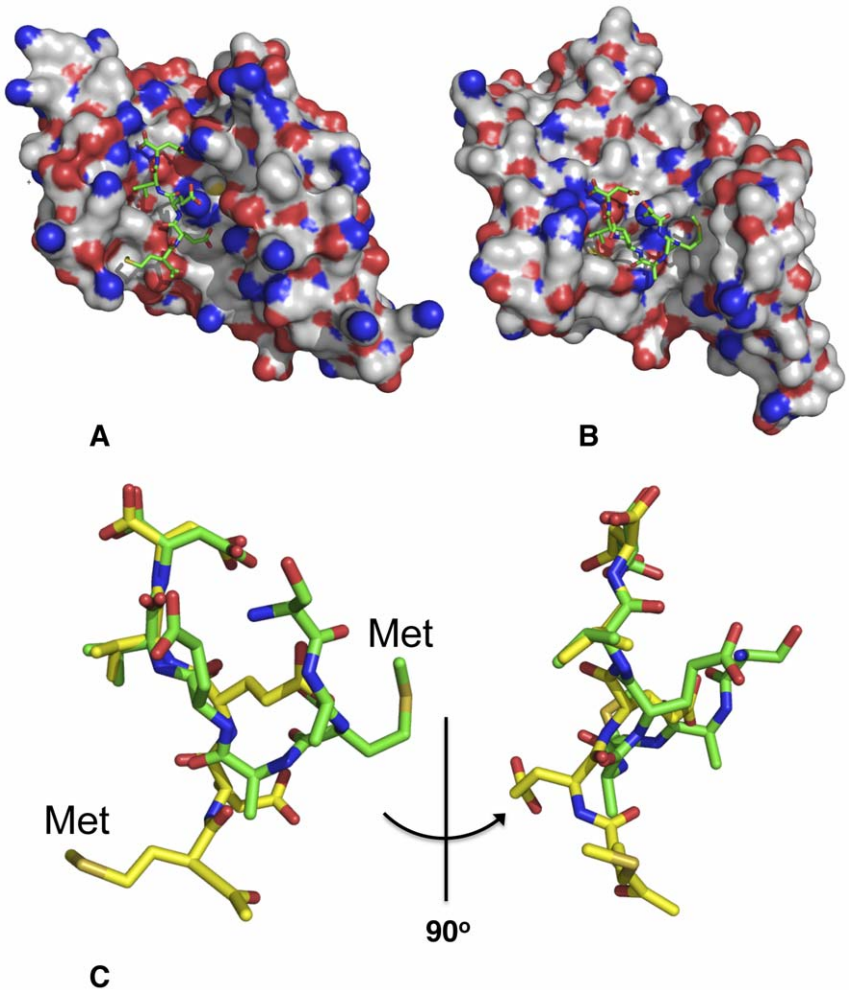

Figure 2. Binding of peptide to the TPR domains of Hop and AIP. (A), PyMol Space-filling model showing the binding of the MEEVD peptide of HSP90 to the TPR domain of Hop TPR2A and (B), the EDASRMEEVD peptide of HSP90β bound to the TPR domain of AIP (only SRMEEVD of the peptide is shown). (C), Superimposition of the peptides bound to the TPR domains of HOP2A (yellow) and AIP (green).
doi:10.1371/journal.pone.0053339.g002

Here we aim to classify the effect of a variety of FIPA associated mutations on the structural integrity of AIP. We present the structure showing the molecular interactions of the TPR domain of AIP in complex with the peptide-binding motifs of HSP90 and TOMM20. Our results show that no known disease-associated mutation causes loss of binding of chaperones alone. However, a subset of mutations affects binding of client proteins to the Cα-7h of AIP. Consequently, loss of client protein interaction with the Cα-7h of AIP is sufficient for pituitary adenoma predisposition.

Materials and Methods

Protein Purification

The TPR domain (residues 166–330) of human AIP was expressed as a PreScission cleavable His-tagged protein from pTWO-E (pET-17b derived; personal communication, A. W. Oliver, Sussex University). The TPR domain was purified by talon-affinity chromatography (Clontech, Oxford, UK), then concentrated and desalted on a HIPrep 26/10 desalting column equilibrated in 20 mM Tris pH 7.5 containing 1 mM EDTA. The sample was then cleaved overnight with GST-tagged PreScision protease. The cleaved protein was subsequently passed through a GST column equilibrated in 20 mM Tris pH 7.5, 1 mM EDTA and 150 mM NaCl and then through a second Talon column to remove any remaining uncleaved protein. The flow through was then concentrated and subjected to superdex 75HR gel-filtration chromatography equilibrated in 20 mM Tris pH 7.5, 1 mM EDTA, 1 mM DTT and 500 mM NaCl. Pure TPR domain were concentrated and then desalted on a HIPrep 26/10 column equilibrated in 20 mM Tris pH 7.5 containing 1 mM EDTA. The protein was stored frozen at 2 mg ml^{-1}.

Structure Determination and Analysis

Human AIP TPR-domain was mixed with EDASRMEEVD (HSP90β) or AQSLAEDDVE (TOMM20) peptide at a 1:20 molar ratio and concentrated to 15 mg ml^{-1}. Crystals of AIP TPR-domain in complex with peptide were obtained at 7.5 mg ml^{-1} from sitting well drops equilibrated against 1 M ammonium sulphate, 1% PEG 3350, 0.1 M Bis-Tris pH5.5. Crystals appeared at 14°C and were harvested by successive transfer to crystallization buffer with increasing glycerol to 30%. Crystals were flash frozen in liquid nitrogen. Diffraction data were collected from crystals frozen at 100 K on Station I03 at the Diamond Light Source (Didcot, UK). Refinement was carried out using Phenix Refine [37,38], and manual rebuilding was

Table 1. Crystallography statistics.

Data collection	**HSP90 (SRMEEVD)***	**TOMM20 (AEDDVE)***
Space group	C2	C2
Unit cell a, b, c (Å) α β, γ (°)	63.82, 104.49, 69.27 90, 97.41, 90	60.2, 106.82, 68.47 90, 100.85, 90
Maximal resolution (Å)	2.01	1.9
Highest resolution bin	2.06−2.01	2−1.9
Observations	98171	92304
Unique reflections	29974	28523
Completeness (%)	99.4(98.5)	84.8 (68.1)
Rmerge	0.061(0.588)	0.049 (0.246)
Mean I/σI	10.9(2.4)	13.6 (4.2)
Multiplicity	3.3(3.2)	3.2 (3.1)
Refinement	**HSP90 (SRMEEVD)***	**TOMM20 (AEDDVE)***
Total atoms	2732	3007
Protein atoms	2402	2486
Ligand atoms	100	94
Residues modeled	D/1-7;E1-7	D/1-6; E/1-6
Non-protein residues modeled	327 waters, $1SO_4$	484 waters, 1 SO_4, 1 PEG
Resolution range (Å)	40.4−2.01	28.46−1.9
Rconv	0.1879	0.1809
Rfree	0.236	0.2344
Residues in most favored regions (%)	98	100
Residues in allowed regions (%)	99.7	100
Residues in outlier regions (%)	0.3	0
RMSD bond (Å)	0.006	0.006
RMSD angle	0.960	0.906
Mean B-factor ($Å^2$)	Protein 36.03 Solvent 50.34	Protein 29.98 Solvent 45.1

*10-mer peptides were used in the crystallization, but only 6–7 resides were visible.

doi:10.1371/journal.pone.0053339.t001

performed in Coot [39]. All other programs used were part of the CCP4 suite [40]. Evolutionary conservation was calculated using the ConSurf server [41–43] and conservation, as well as other PDB files, displayed using PyMol (The PyMOL Molecular Graphics System, Version 1.2r3pre, Schrödinger, LLC, USA).

Isothermal Titration Calorimetry and HSP90 ATPase Assays

The heat of interaction was measured on an ITC_{200} microcalorimeter (Microcal), with a cell volume of 200 μL, under the same buffer conditions (20 mM Tris, pH 7.5, containing 5 mM NaCl) at 30°C. Twenty 1.9 μL aliquots of AIP TPR-domain at 350 μM were injected into 30 μM of human HSP90β. For peptide interactions twenty 1.9 μL aliquots of peptide ranging from 350 to 600 μM were injected into 30 μM of AIP TPR-domain. Heats of dilution were determined in a separate experiment by diluting protein or peptide into buffer, and the corrected data were fitted using a non-linear least-squares curve-fitting algorithm (Microcal Origin) with three floating variables: stoichiometry, binding constant and change in enthalpy of interaction. ATPase assays were previously described [44–46].

Co-immunoprecipitation

The vectors used were pCI-neo-AIP-Flag and pcDNA 3.0-Myc-AIP, containing wild-type AIP cDNA with the Flag tag located downstream AIP and the Myc tag placed upstream, respectively. GH3 cells (3.6×10^6) were cultured in Dulbeccos Modified Eagles Medium (SIGMA) containing 10% fetal bovine serum and 1% penicillin/streptomycin (SIGMA) for 24 hours before transfection with 2.5 μg of each vector, using Lipofectamine 2000 (Life Technologies). The cells were then lysed (20 mM Tris-Cl pH 8.0, 200 mM NaCl, 1 mM EDTA pH 8.0, 0.5% Igepal and Complete Protease Inhibitor Cocktail [Roche]) and ~150 μg of total protein was used for immunoprecipitation with 1 μg of TOMM20 peptide and 2 μg of either anti-Myc (SIGMA), anti-Flag (SIGMA) or mouse IgG (SIGMA) antibodies, respectively. Co-immunoprecipitation was carried out with Protein G Sepharose 4 Fast Flow (GE Healthcare) according to the protocol suggested by the manufacturer. Finally, the proteins were eluted by incubation for 5 minutes at 95°C with 40 μl of 1× Laemmli buffer, fractionated by SDS-PAGE and then transferred to a nitrocellulose membrane. Proteins were detected with 1:3000 of either anti-Myc or anti-Flag antibodies. The bands were visualized on an Odyssey infrared scanner after incubation with of 1:20000 goat anti-mouse 680 IRDye secondary antibody (Licor). As controls, we performed the

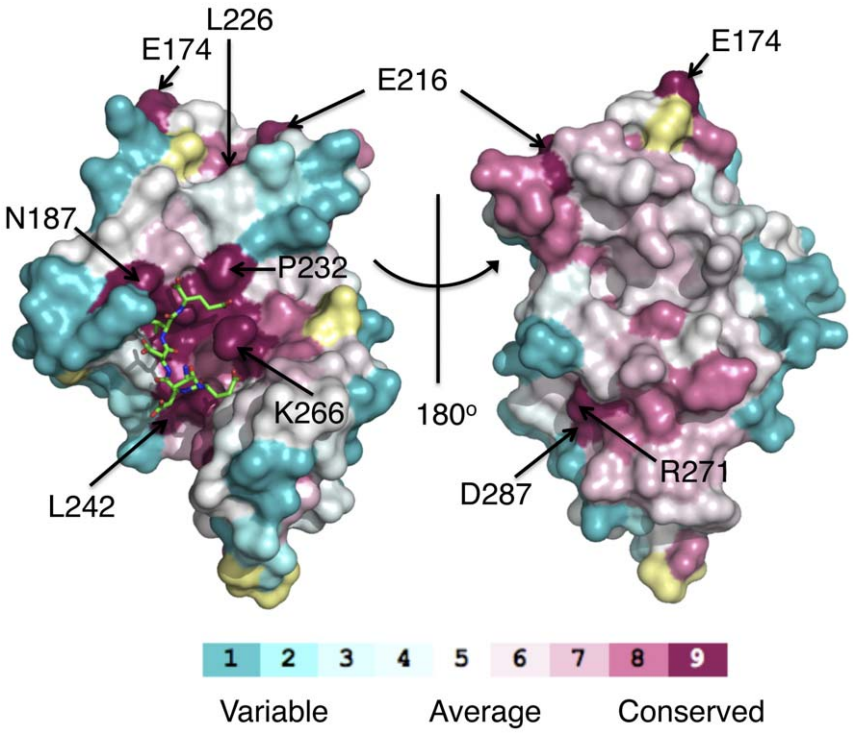

Figure 3. PyMol diagram showing the conservation of residues on the surface of AIP TPR-domain. The most highly conserved residues line the cavity of the TPR domain in which the TPR-motif containing peptides bind to.
doi:10.1371/journal.pone.0053339.g003

same experiments using the following combinations of vectors: pCI-neo-Flag+pcDNA 3.0-Myc, pCI-neo-AIP-Flag+pcDNA 3.0-Myc, pCI-neo-Flag+pcDNA 3.0-Myc-AIP and no co-transfection.

Results

The Structural Features of the TPR Domain of AIP in Complex with HSP90 and TOMM20 Peptide

TPR domains that bind HSP90, HSP70 and TOMM20 are known to bind a specific short conserved motif at the C-terminal end of these chaperones (HSP90, MEEVD; HSP70, IEEVD; and TOMM20, EDDVE) [11,12,47]. The structures of the AIP TPR-domain in complex with peptide fragments from human HSP90β and TOMM20 were solved at 2.0 (PDB 4AIF) and 1.9 Å (PDB 4APO) resolution, respectively (Table 1). The TPR domain of AIP is similar to other TPR-domain proteins consisting of three pairs of anti-parallel helices and a Cα-7h (Fig. 1A). We found that the EDASRMEEVD (HSP90) and AQSLAEDDVE (TOMM20) peptides bind within the TPR-domain cleft and adopt a similar backbone conformation (Fig. 1). The mode of interaction of these peptides resembles that of the HSP90 and HSP70 C-terminal peptides binding to the TPR-domain of CHIP rather than that of HOP [11,12] (Fig. 1 and 2).

The residues lining the TPR-binding site are highly conserved (Fig. 3). The structures show that the C-terminal carboxylate group and the C-terminal aspartate (HSP90) or glutamate (TOMM20) side-chain are involved in a series of hydrogen bonds that is reminiscent of the carboxylate clamp seen in the MEEVD-HOP complex [11] (Fig. 4). In the AIP-EDASRMEEVD (HSP90) structure the C-terminal carboxylic acid makes direct hydrogen bonds to one of the ring nitrogens of His 183 and to the amine nitrogen of Asn 187 and Asn 236. The aspartate group makes water-mediated interactions to the main-chain carbonyl of Pro 232, to the carboxylic-acid oxygen of Asn 236, to the amine-group nitrogen of Lys 266 as well as an intramolecular interaction to the main-chain carbonyl of the serine of the EDASRMEEVD peptide. The C-terminal aspartic acid side-chain carboxyl-group also forms a direct interaction with the amine group of Lys 266.

For the peptide valine the main-chain carbonyl is hydrogen bonded to the secondary amine of Arg 191 via a water molecule, and via this same water molecule but also directly, to the carboxylic-acid oxygens of the second glutamate residue of the HSP90 peptide (EDASRMEEVD). The other carboxyl-group oxygen of this glutamate (EDASRMEEVD) is hydrogen-bonded to the secondary amine of Arg 191, while the other oxygen forms an intramolecular interaction with the main-chain amide of serine of the HSP90 peptide. The main-chain amide group of the peptide valine is also hydrogen bonded to one of the oxygens of the second glutamate of the peptide. The valine side-chain is itself packed into a hydrophobic pocket formed by the side chains of Asn 187, Tyr 190, Arg 191 and Asn 236.

The carbonyl of the second glutamate of the HSP90 peptide (EDASRMEEVD) forms a direct interaction with the side-chain amine of Lys 266, and via a water molecule to the side-chain amine group of Lys 270. The side-chain hydroxyl of Tyr 190 forms a direct interaction with the main-chain carbonyl of the second glutamate in the HSP90 peptide.

The methionine of the HSP90 peptide is itself packed into a hydrophobic pocket formed by the side chains of Val 265, Lys 266, Phe 269, Lys 270 and Leu 298. Interestingly, Lys 266 was predicted to be a ligand-binding residue [48]. However, the main-chain amine of the peptide methionine also forms both a direct interaction and a water-mediated hydrogen bond with the side-chain amine of Lys 270. The main-chain carbonyl of the peptide arginine directly interacts with the side-chain amine of Lys 266, while the main-chain carbonyl of the peptide serine forms

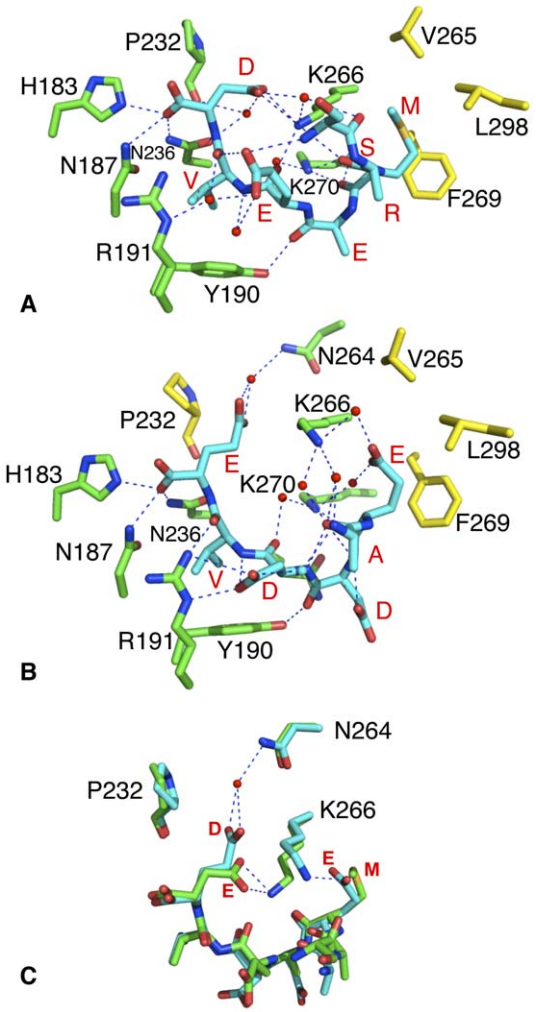

Figure 4. PyMOL diagram showing binding interactions. (A) Interactions with HSP90β EDASRMEEVD peptide and (B), with TOMM20 AQSLAEDDVE peptide bound to the TPR domain of AIP. Peptide residues that where visible (SRMEEVD and AEDDVE) are shown in red as single letter code. Dotted blue lines represent hydrogen bonds and green, the amino acid residues involved; red-colored spheres, water molecules and yellow residues, residues solely in van der Waals contact. The structures were obtained at 2.0 (PDB, 4AIF) and 1.9 Å (PDB, 4APO), respectively. (C), Molecular switching in the TPR domain of AIP. The alternative conformations of Lys 266 allow selection of the Hsp90 MEEVD- (green) or TOMM20 EDDVE-motif (cyan). Dotted blue lines represent hydrogen bonds while red-colored spheres represent water molecules.
doi:10.1371/journal.pone.0053339.g004

hydrogen bonds via a water molecule to the side-chain amine of Lys 266.

Interactions between the TOMM20 peptide and the TPR domain of AIP are similar but not identical. The main differences result due to the need to pack the first glutamate side-chain of the TOMM20 peptide (AQSLAEDDVE) into the hydrophobic pocket that accepts the methionine residue in the case of HSP90 peptide (MEEVD) (Fig. 4). While the side chain of this glutamate enters the hydrophobic pocket the carboxylate oxygens point back towards and interacts with the side-chain amine of Lys 266. Consequently, Lys 266 adopts an alternative conformation to that seen with the HSP90 bound peptide. The conformational change in Lys 266 acts like a switch that not only allows the binding of the TOMM20 glutamate in the methionine pocket, but also allows the longer C-terminal glutamate side-chain of TOMM20 (Asp in HSP90), to pack between the side chain of Pro 232 and Lys 266; and consequently form a hydrogen bond via a water molecule with the side-chain amine of Asn 264 (Fig. 4C).

Although attempts to obtain the structure of an equivalent HSP70 peptide bound to the TPR domain of AIP failed, we assume that the isoleucine (IEEVD) binds to the same hydrophobic pocket as the methionine of HSP90.

Dimerization of the AIP TPR-domain and the Role of Arg 304

The crystal structure of the TPR domain of AIP in complex with peptide revealed the possibility that the TPR domain might form a biological dimer (Fig. 5A and B). Significantly, Arg 304, whose missense mutation is linked to disease, was found to form interactions with the aspartates of the TOMM20 peptide (AQSLAEDDVE) bound in the neighbouring TPR domain. In contrast, in the HSP90 peptide bound structure Arg 304 is disordered and no significant interactions are made. The question therefore arises as to whether Arg 304 is naturally involved in intermolecular or intramolecular interactions with bound peptide (or intact chaperone) and whether the TPR AIP-domain forms a biological dimer. It has been previously reported that two molecules of AIP can be found in some HSP90 complexes, but whether AIP was a biological dimer in these complexes was not established [49].

We conducted reciprocal co-immunoprecipitations experiments (Fig. 5C) in which cells were transfected with Flag- and Myc-tagged AIP in the presence of the TOMM20 peptide. We found that using either anti-Flag or anti-Myc antibodies failed to co-immunoprecipitate the tagged proteins suggesting that AIP dimerization is not biologically relevant. Furthermore, using isothermal titration calorimetry (ITC) the stoichiometry of the interaction between the TPR domain of AIP and HSP90β was found to be 0.3:1, showing that one molecule of AIP interacts with a dimer of HSP90 (Table 2). In addition, the E192R AIP mutant, where Glu 192 forms the core of the interaction interface of the AIP dimer (Fig. 5D), did not alter the stoichiometry or thermodynamics of the interaction with HSP90β (0.47:1, AIP-TPR-E192R: HSP90β, Table 2). We next tested the effect of mutating Arg 304, which directly interacts with TOMM20 peptide bound in the neighbouring AIP molecule. The binding of HSP90β, HSP70 and TOMM20 peptides to the R304A and R304Q mutants was unaltered relative to the wild type interaction (Table 2). Failure to form stable dimerization of AIP, caused by these mutations, would significantly change the thermodynamic properties of the interaction. We therefore conclude that the dimerization interface seen in the crystals is not a true biological interface, but a crystallographic one.

Selectivity in the Binding of Proteins to the TPR Domain of AIP

We next wanted to understand the selectivity for the different chaperones that bind to AIP and utilised ITC to measure the affinity for these interactions. The TPR domain of AIP bound full-length HSP90β with a $K_d = 13.3 \pm 1.8$ μM and showed a favourable entropic contribution (Table 2). The peptides representing the extreme C-terminus of HSP90 (MEEVD), HSP90β (EDASRMEEVD), HSP90α (DDTSRMEEVD) and TOMM20 (AQSLAEDDVE) also bound with similar affinities ($K_d = 12.6 \pm 1.6$; 14.4 ± 1.0; 9.5 ± 0.6 and 12.3 ± 0.5 μM, respectively; Table 2), suggesting that the core interaction between these

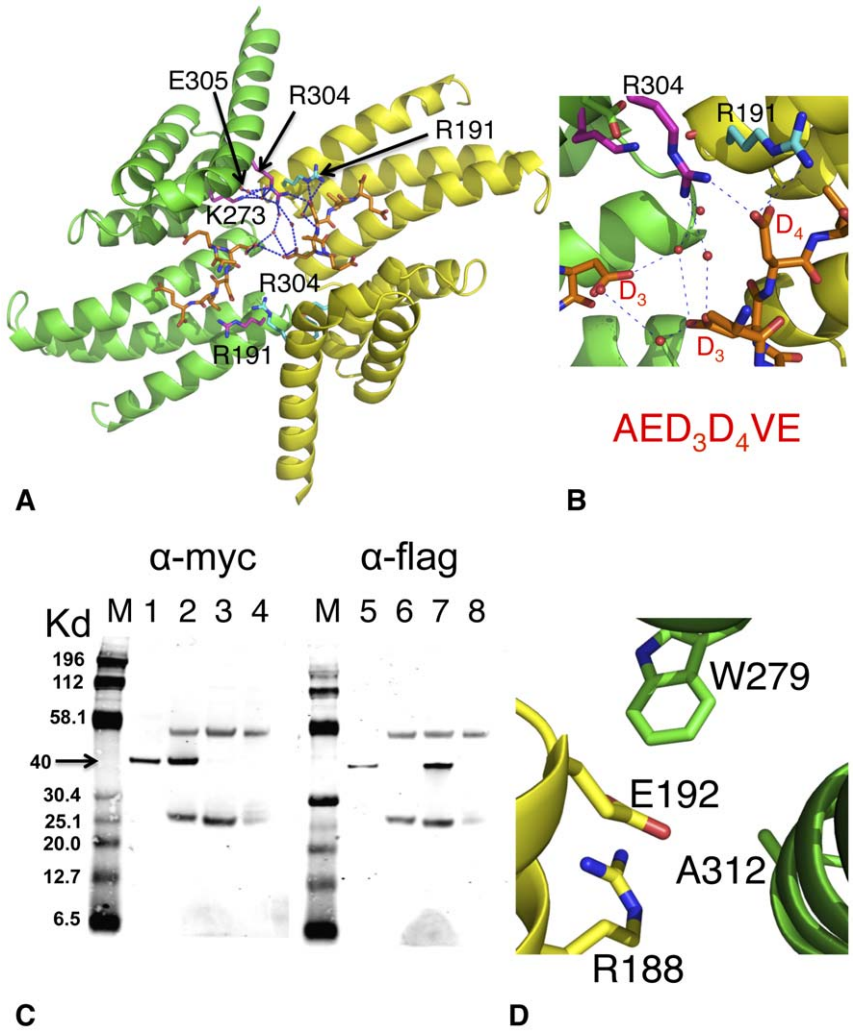

Figure 5. PyMol cartoon showing dimerization of AIP TPR-domain through crystal lattice contacts. (A), The AIP domains are in green and yellow. Amino acid residues are in magenta or cyan, hydrogen bonds as blue dotted lines, water molecules as red spheres and bound TOMM20 AQSLAEDDVE-peptide used in the crystallization in gold. However, only residues AEDDVE are visible in the structure. The TPR domains are symmetrically related and hydrogen bonding is shown in only one half of the figure. The cartoon shows that Arg 304 is hydrogen bounded directly to the neighboring TOMM20 bound peptide (gold). (B), PyMol cartoon showing a close up of the main interactions between Arg 304 and bound peptide used in the crystallization (AQLSLAED$_3$D$_4$VE) in panel A. However, only residues AED$_3$D$_4$VE are visible in the structure. (C), Co-immunoprecipitation of Flag-AIP and Myc-AIP in the presence of TOMM20 peptide (AQSLAEDDVE). The results show that Flag-AIP and Myc-AIP do not co-immunoprecipitate. M, molecular mass markers, with molecular mass indicated to the left of the panel; lane 1 and 5 AIP input (cleared lysate) protein; lane 2 and 6 are anti-Myc co-immunoprecipitation, lanes 3 and 7 are anti-Flag co-immunoprecipitations, while lanes 4 and 8 are IgG control. Lanes 1–4 (first gel) was blotted for Myc tag and lanes 5–8 (second gel) for Flag tag. The arrow indicates the position where the flag- and myc-tagged AIP runs (40 Kd). (D), The core interaction of the AIP dimerization interface shows that E192 is buried and shielded from solvent by Ala 312, Arg 188 and Trp 279.
doi:10.1371/journal.pone.0053339.g005

chaperones and the TPR domain of AIP involves the terminal five amino acids of these proteins.

Although we were unable to test the binding of intact PDE4A5 to AIP, we instead measured the affinity for the interaction of the peptide TLEELDW, which contains the core binding sequence LEELD (identified in PDE2A as LYDLD). The LEELD motif of PDE4A5 is not a C-terminal sequence and its ability to bind to the TPR domain is questionable. The binding affinity of the PDE4A5 peptide (TLEELDW; $K_d = 64.5 \pm 3.2$ μM) was found to be significantly weaker than the equivalent peptides form HSP90α, HSP90β and TOMM20 ($K_d = 9.5$, 14.4–18.6; and 12.3 μM, respectively; Table 2). Furthermore, a structural analysis of the PDE2A homologue indicates that the homologous LYDLD sequence is unlikely to be accessible for binding to the TPR domain of AIP as it is involved in folding of the protein. Consequently, the interaction of AIP with PDE4A5 is not mediated by binding to the LEELD peptide sequence.

AIP does not Affect the HSP90 ATPase Activity

The first TPR-domain protein shown to influence the ATPase activity of HSP90 was Sti1p [45]. We wanted to see if AIP could similarly affect HSP90 ATPase activity. A 20-fold molar excess of full-length AIP did not influence the ATPase activity of HSP90 (Link to Supporting information).

Disease Associated Mutations of AIP

Nonsense, splice variant and frameshift mutations (Table 3) clearly disrupt the TPR-domain of AIP and lead to a dysfunctional

Table 2. Isothermal titration calorimetry binding of AIP and target.

TPR-domain	Ligand	Kd (μM)	N	ΔH (cal/mol)	ΔS (Cal/mol/deg)
WT	FL-hHSP90β	13.3±1.8	0.30	−4554	7.29
E192R	FL-hHSP90β	11.1±1.3	0.47	−4114	9.11
WT	MEEVD (HSP90)	12.6±1.6	1.0	−4140	8.75
WT	EDASRMEEVD (hHSP90β)	18.6±2.0 14.4±1.0	1.2 1.1	−5041 −3921	5.02 9.22
R304A	EDASRMEEVD (hHSP90β)	15.6±0.85	0.96	−6435	0.76
R304Q	EDASRMEEVD (hHSP90β)	16.2±1.1	0.98	−6417	0.76
WT	DDTSRMEEVD (hHSP90α)	9.5±0.6	1.2	−3529	11.3
WT	GSGPTIEEVD (hHSP70)	18.1±1.9	0.63	−6348	0.76
R304A	GSGPTIEEVD (hHSP70)	22.8±1.6	0.66	−5456	3.24
R304Q	GSGPTIEEVD (hHSP70)	31.1±2.6	0.84	−5498	2.48
WT	AQSLAEDDVE (hTomm20)	12.3±0.5	0.87	−6765	0.16
R304A	AQSLAEDDVE (hTomm20)	16.6±0.5	0.69	−4508	7.0
R304Q	AQSLAEDDVE (hTomm20)	22.5±2.2	0.66	−6073	1.23
WT	TLEELDW (hPDE4A5)	64.5±3.2	0.89	−4418	4.6

doi:10.1371/journal.pone.0053339.t002

protein. However, the effect of missense mutations is difficult to predict. We have used our structure to define mutations associated with disease to understand how they might affect the function of this domain. Many of the missense mutations are involved in the folding and stability of the TPR AIP-domain. C238Y, K241E, I257V, R271W, and possibly A299V all disrupt either hydrophobic or polar interactions that impact on the folding of the domain (Table 3). In fact, attempts to purify C238Y and A299V resulted in much of the protein aggregating suggesting that the proteins were at least partly unfolded. In contrast, R304* (nonsense mutation), R304Q, Q307* and R325Q were identified as 'disease-associated' mutations that, *in vitro* at least, do not disrupt chaperone binding. Our ITC results show that for R304A and R304Q the HSP90, HSP70 and TOMM20 peptides bind normally (Table 2). Structural analysis showed that the Gln 307 and Arg 325 amino acid residues (all clearly visible in the TOMM20-AIP structure), are further away from the TPR domain-binding site than Arg 304, and are not involved in packing interactions or in binding of the bound conserved peptide motifs. Thus, at least *in vitro*, these residues do not disrupt chaperone binding although they have been strongly implicated in causing FIPA [4,6,50–52]. Furthermore, the extreme C-terminus of AIP has been shown to represent the binding site for the client proteins AhR and PDE4A5 [48,52]. These results suggest that disruption of client-protein binding alone is sufficient for pituitary tumor predisposition.

Further analyses of the extreme C-terminus of the Cα-7h shows that there are a number of conserved charged and hydrophobic residues (Fig. 6). These residues are predicted to be part of a helical structure (PSIPRED, UCL Department of Computer Science, Bioinformatics Group), and form two conserved regions on either side of the helix (Fig. 6C). Hydrophobic residues beyond Ile 313, the last residue in the structure that is involved in packing with the main fold of the domain, would not be buried if the Cα-7h continues as such into solvent. The conservation of these residues suggests that they represent a binding site for specific client proteins; especially for AhR and PDE4A5, which are client proteins known to interact with this helix (Fig. 6D).

Discussion

The structure of the TPR domain of AIP in complex with peptide representing the TPR-domain binding motif from HSP90 and TOMM20 were determined to high resolution. The structure with TOMM20 peptide showed that electron density for residues Asp 172 to Arg 325 of the TPR domain was visible. We show that HSP90, HSP70 and TOMM20, but not the PDE4A5 TLEELDW-peptide, can interact with the TPR domain of AIP with similar affinity. Using ITC we show that the stoichiometry of the interaction between AIP and intact HSP90 was 0.5:1 (AIP:HSP90).

AIP binding of these conserved peptide sequences is similar to that observed for CHIP, rather than that seen with HOP. Unlike HOP-bound peptides, for AIP and CHIP the upstream sequence of the peptides is directed up and out of the binding cleft to avoid interaction with these upstream sequences, which differ between HSP70 and HSP90 [11,12]. HOP is a co-chaperone of HSP90 that not only acts as scaffold between HSP70 and HSP90, but also silences the ATPase activity of HSP90 [45]. It thus stalls the ATPase-coupled conformational cycle of HSP90 and allows client protein loading from HSP70 to HSP90 [11,44,45]. HOP binds HSP70 and HSP90 using separate TPR-domain modules [11], and therefore can associate with both chaperone systems simultaneously. CHIP on the other hand is a U box E3 ubiquitin ligase that binds either HSP70 or HSP90 using a single TPR-domain module and appears to ubiquitinate client proteins of these chaperone systems [12,53,54]. The conformation that the bound peptides adopt with HOP and CHIP/AIP is largely dependent on the position of the hydrophobic pockets that accept the methionine and valine amino acid residues of the conserved binding motif MEEVD, in the case for HSP90. Thus, the TPR domains can be reclassified depending on the relative position of these hydrophobic pockets. When both pockets are on the same side of the TPR-binding cleft we observe the HOP-type mediated binding (*cis*-mode). When the methionine pocket is on the other side we see the CHIP/AIP (*trans*-mode) of binding. The *trans*-mode of binding appears to be used where numerous similarly related peptides are binding to the same TPR domain.

Another interesting feature by which AIP accommodates these different TPR-binding sequences is by way of a specific side chain rearrangement (Fig. 4C). The methionine side-chain of the conserved MEEVD motif being hydrophobic in nature can enter the appropriate hydrophobic pocket, while for the TOMM20 glutamate its side chain enters the hydrophobic pocket but the carboxylic acid group points back out and interacts with the side-chain amine group of Lys 266. The 'switched' conformation of Lys 266 then allows the side-chain of the C-terminal glutamate to pack between Lys 266 and Pro 232 and to form a water-mediated interaction to the side-chain amine of Asn 264. In contrast, for the HSP90 peptide, Lys 266 forms direct hydrogen bonds with the carboxyl group of the shorter C-terminal aspartic acid side-chain as part of the carboxylate clamp. Thus, the rearrangement that allows the glutamate residue of TOMM20 (EDDVE) to bind the

Table 3. Classification of the effect TPR-AIP mutations on its structure.

Mutation	Mutation type	AIP domain	Probable effect of the mutation
Q184*	Nonsense	TPR domain	Non-functional
K201*	Nonsense	TPR domain	Non-functional
E216*	Nonsense	TPR domain	Non-functional
Q217*	Nonsense	TPR domain	Non-functional
E222*	Nonsense	TPR domain	Non-functional
C238Y	Missense	TPR domain	Disrupts packing of hydrophobic core
Q239*	Nonsense	TPR domain	Non-functional
C240R	Missense	TPR domain	Disrupts packing of hydrophobic core
K241E	Missense	TPR domain	Disrupts hydrogen bonding to Glu246
K241*	Nonsense	TPR domain	Non-functional
I257V	Missense	TPR domain	Disrupts packing of hydrophobic core
Y261*	Nonsense	TPR domain	Ligand binding
K266A	Missense	TPR domain	Ligand binding
Y268C	Missense	TPR domain	Disrupts packing of hydrophobic core
Y268*	Nonsense	TPR domain	Non-functional
R271W	Missense	TPR domain	Disrupts hydrogen bonding to Asp287 and Ser255
A277P	Missense	TPR domain	Disrupts hydrophobic packing against Tyr 247
A291M/E	Missense	TPR domain	Disrupts packing of hydrophobic core. (Forms base of hydrophobic pocket interacting with bound peptide)
A299V	Missense	TPR domain	At start of Cα-7h and may disrupt some small degree of packing with Leu292
R304*	Nonsense	TPR domain	Weakens PDE4A5 binding (see E304Q and [52]) and would disrupt AhR binding
R304Q	Missense	TPR domain	Weakens PDE4A5 binding (see [52])
Q307*	Nonsense	TPR domain	Would disrupt AhR binding
R325Q	Missense	TPR domain	Potentially client-protein binding. One residue short of the 5-residue deletion that disrupts AhR binding

doi:10.1371/journal.pone.0053339.t003

hydrophobic pocket also allows the longer C-terminal glutamate side-chain of TOMM20 to be accommodated.

Analysis of the mutations that occur in AIP in the context of the structure (residues visible were Asp 172 to Arg 325) has allowed us to define their effects on the structural integrity of the AIP protein. Most mutations affect the structural integrity of the TPR domain (Table 3). However, no single mutation of the TPR domain prevents chaperone binding alone. In contrast, a subset of disease-associated mutations of conserved residues of the Cα-7h that affect client-protein binding alone was identified. Our structures and ITC data show that for the R304A/Q mutations chaperone binding is unaffected. For Gln 307 and Arg 325 these residues are further away from the TPR domain binding-site and are not involved in domain packing interactions. Consequently, they are not part of the chaperone-binding site of the TPR-domain. Interestingly, the R325Q mutation is one residue short of the 5-residue deletion that disrupts AhR binding [5,48,52]. Of these five residues only two are conserved, Ile 327 and Phe 328 (Fig. 6), which alone are unlikely to represent the complete interaction site of AhR as this would be very weak. Consequently, the extensive conservation of the Cα-7h is likely to represent an interaction site for at least AhR. However, the R304Q mutation is also known to slightly destabilize the PDE4A5 interaction [52], providing clear evidence that the conservation in the Cα-7h represents a binding site for client proteins (Fig. 6D). Our results therefore suggest that the primary change in a subset of AIP mutant of the Cα-7h is loss of association with, at least some, client proteins. Whether *in vivo* this also leads to a breakdown in the association of HSP90 and AIP is currently unknown and warrants further investigation. However, it appears that AIP acts as a co-chaperone that delivers client protein to HSP90, in common with other co-chaperones of HSP90 such as HOP and CDC37 [14].

The destabilization of AhR would naturally imbalance assembly of AhR/ARNT complex and it has been shown that levels of either ARNT or ARNT2, but not both, are devoid in AIP-deficient mouse pituitary tumors [55]. Furthermore, PDE2A, which is AIP dependent, inhibits nuclear translocation of AhR by lowering cAMP levels. Consequently, elevated and aberrant cAMP signalling, often seen in pituitary tumors, may imbalance AhR/ARNT and ARNT/Hif-1e signalling. Disruption of AhR binding to AIP might also have profound effects on ERα-dependent transcription. Loss of AIP binding to AhR causes degradation of AhR [56]. Thus, a model can be proposed (Fig. 7), which results in the destabilization of AhR, which could then upregulate expression from ERα dependant promoters by affecting several different mechanisms. Thus, AhR would not compete for ERα cofactors and transcription factors, would fail to promote the proteasomal degradation of ERα and would not be available for binding to inhibitory xenobiotic response elements (iXRE), that downregulate specific ERα-directed expression [57]. However, the exact effects on ERα levels and ERα-directed transcription are currently unknown. Certainly work by Cai *et al.*, [58] shows that AIP acts as a negative regular of ERα. Although, the same authors show that ERα is still able to associate with AIP

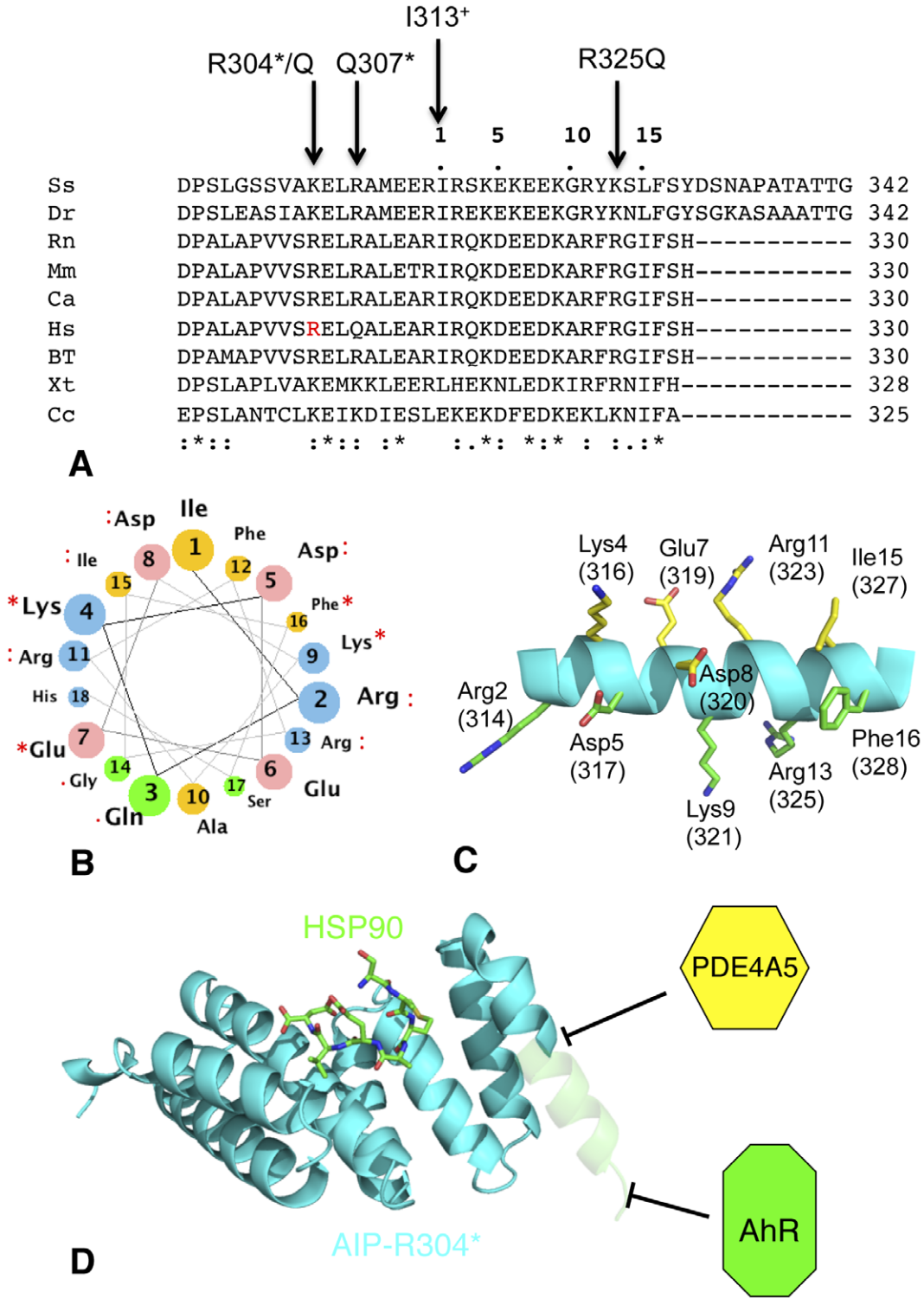

Figure 6. Sequence conservation of the Cα-7h of AIP. (A), sequence alignment showing conservation of amino acid residues. Ss, Salmo salar (NM_001140060.1); Dr, Danio rerio (NM_214712.1); Rn, Rattus norvegicus (NM_172327.2); Mm, Macaca mulatta (NM_001194313); Ca, Chlorocebus aethiops (O97628); Hs, Homo sapiens (FJ514478.1); Bt, Bos taurus (NM_183082.1), Xt, Xenopus (Silurana) tropicalis (NM_001102749.1) and Cc, Caligus clemensi (BT080130.1). ($I313^{+}$), Ile 313 represents the last residue in the sequence that is involved in packing interactions of the TPR domain. Mutations associated with disease are indicated above the sequence. (* below the sequence), Amino acids at these positions are identical; (:), highly conserved (.) or conserved. Arg 304 of Human AIP is shown in red type face. Numbers above the sequence (positions 1 to 15) represent residue numbers of the helical wheel shown in panel B. (B), Helical wheel showing the position of identical and conserved residues form the alignment in panel A for the Cα-7h of AIP. Orange, non-polar; green, polar uncharged; pink, acidic and blue, basic amino-acid residues. (C), PyMol cartoon showing a hypothetical helix (residues beyond Arg 325) with the identical and highly conserved amino acid residues shown in panels A and B. Conserved residues on one side of the helix are shown in green and on the other in yellow. Residue numbers shown are those in panel B, while those in brackets

are actual residue numbers in panel A. (D), The TPR-domain of the R304* mutant of AIP. Deletion of the terminal region of AIP (transparent helical region) allows chaperone binding but disrupts association with PDE4A5 and AhR.
doi:10.1371/journal.pone.0053339.g006

R304* mutant. Furthermore, these experiments used overexpressed AIP mutant and therefore do not address whether the mutation fails to provide the normal negative regulatory effect on ERα under normal AIP levels. Interestingly, other mutations, such as Q217*, that disrupt the TPR domain were seen to activate ERα directed transcriptional activity. Furthermore, it is also known that tumor suppressor levels of PLAGL1 decline in the absence of functional AIP, but the mechanism leading to this is poorly understood. None-the-less the loss of an important tumor suppressor is likely to have some role in the formation of pituitary adenomas. However, it is evident that because of AIP's promiscuity a variety of biochemical changes in pituitary cells occur under conditions when AIP is non functional. Consequently, pituitary tumor predisposition is likely to be a result of these biochemical changes that may all contribute to a varying degree in the process.

In conclusion, our results show that Arg 304 does not play any significant role in mediating AIP binding to HSP90, HSP70 or

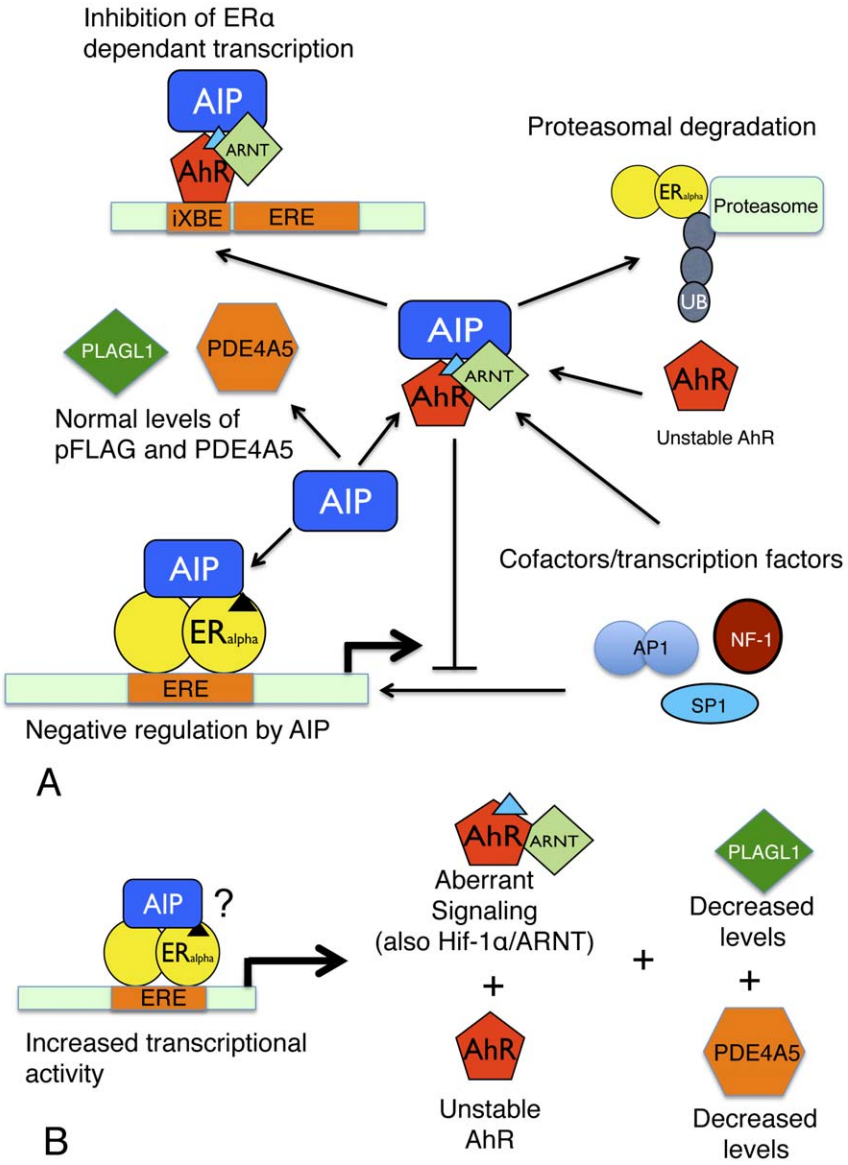

Figure 7. Model showing the affect of mutant AIP on cellular signaling pathways. (A), Wild type AIP stabilizes AhR, which in turn downregulates ERα dependent transcription by promoting the ubiquitination and proteasomal destruction of ERα, by competing for specific cofactors required for ERα dependent transcription and by binding to iXRE sites that block ERα dependent transcription. AIP downregulates transcription by ERα at ERE sites. AIP is also known to maintain cellular levels of PLAGL1 and PDE4A5. Small triangles represent ligand bound to their appropriate receptor. (B), Mutant AIP fails to bind AhR, PDE4A5 and possibly ERα, resulting in unstable AhR and PDE4A5 and perhaps upregulation of transcription at ERE sites. A decline in levels of PLAGL1 and changes in cAMP concentration also result. The question mark emphasizes that AIP may or may not interact with ERα at ERE sites, but if it does it may fail to provide appropriate negative regulation.
doi:10.1371/journal.pone.0053339.g007

TOMM20. Taken together with the highly conserved C-terminus of AIP, and specific mutations that occur on the Cα-7h, our results support the idea that this helix is involved in client protein interactions, at least with AhR and PDE4A5, and that loss of such interactions leads to a variety of biochemical changes in pituitary cells that predisposes to pituitary adenoma. Consequently, understanding the role AIP plays in maintaining and activating Cα-7h interacting client proteins will help towards understanding the cellular events that lead to pituitary tumor predisposition. This study forms the springboard for more detailed investigations in isolating AIP client-proteins that when deregulated predispose to pituitary tumors.

Supporting Information

Figure S1
(TIF)

Author Contributions

Conceived and designed the experiments: RMLM MK CP. Performed the experiments: RMLM LCHR LZ SMR CP. Analyzed the data: GT MK CP. Contributed reagents/materials/analysis tools: LCHR GT MK. Wrote the paper: CP. Commented on the manuscript: RMLM LCHR GT MK. Supplied the AIP cDNA: LCHR GT MK. Expressed and purified the proteins: RMLM CP. Did the biochemistry: RMLM LCHR LZ CP. Carried out the crystallography: RMLM SMR CP.

References

1. Kuzhandaivelu N, Cong YS, Inouye C, Yang WM, Seto E (1996) XAP2, a novel hepatitis B virus X-associated protein that inhibits X transactivation. Nucleic Acids Res 24: 4741–4750.
2. Carver LA, Bradfield CA (1997) Ligand-dependent interaction of the aryl hydrocarbon receptor with a novel immunophilin homolog in vivo. J Biol Chem 272: 11452–11456.
3. Daly AF, Vanbellinghen JF, Khoo SK, Jaffrain-Rea ML, Naves LA, et al. (2007) Aryl hydrocarbon receptor-interacting protein gene mutations in familial isolated pituitary adenomas: analysis in 73 families. J Clin Endocrinol Metab 92: 1891–1896.
4. Vierimaa O, Georgitsi M, Lehtonen R, Vahteristo P, Kokko A, et al. (2006) Pituitary adenoma predisposition caused by germline mutations in the AIP gene. Science 312: 1228–1230.
5. Leontiou CA, Gueorguiev M, van der Spuy J, Quinton R, Lolli F, et al. (2008) The role of the aryl hydrocarbon receptor-interacting protein gene in familial and sporadic pituitary adenomas. J Clin Endocrinol Metab 93: 2390–2401.
6. Chahal HS, Chapple JP, Frohman LA, Grossman AB, Korbonits M (2010) Clinical, genetic and molecular characterization of patients with familial isolated pituitary adenomas (FIPA). Trends Endocrinol Metab 21: 419–427.
7. Linnert M, Haupt K, Lin YJ, Kissing S, Paschke AK, et al. (2012) NMR assignments of the FKBP-type PPIase domain of the human aryl-hydrocarbon receptor-interacting protein (AIP). Biomolecular NMR assignments 6: 209–212.
8. Carver LA, LaPres JJ, Jain S, Dunham EE, Bradfield CA (1998) Characterization of the Ah receptor-associated protein, ARA9. J Biol Chem 273: 33580–33587.
9. Laenger A, Lang-Rollin I, Kozany C, Zschocke J, Zimmermann N, et al. (2009) XAP2 inhibits glucocorticoid receptor activity in mammalian cells. FEBS lett 583: 1493–1498.
10. Trivellin G, Korbonits M (2011) AIP and its interacting partners. J Endocrinol 210: 137–155.
11. Scheufler C, Brinker A, Bourenkov G, Pegoraro S, Moroder L, et al. (2000) Structure of TPR domain-peptide complexes: critical elements in the assembly of the Hsp70-Hsp90 multichaperone machine. Cell 101: 199–210.
12. Zhang M, Windheim M, Roe SM, Peggie M, Cohen P, et al. (2005) Chaperoned ubiquitylation–crystal structures of the CHIP U box E3 ubiquitin ligase and a CHIP-Ubc13-Uev1a complex. Mol cell 20: 525–538.
13. Bolger GB, Peden AH, Steele MR, MacKenzie C, McEwan DG, et al. (2003) Attenuation of the activity of the cAMP-specific phosphodiesterase PDE4A5 by interaction with the immunophilin XAP2. J Biol Chem 278: 33351–33363.
14. Pearl LH, Prodromou C, Workman P (2008) The Hsp90 molecular chaperone: an open and shut case for treatment. Biochem J 410: 439–453.
15. Prodromou C (2012) The 'active life' of Hsp90 complexes. Biochim Biophys Acta 1823: 614–623.
16. Jackson SE (2012) Hsp90: Structure and Function. Topics in current chemistry.
17. Bukau B, Weissman J, Horwich A (2006) Molecular chaperones and protein quality control. Cell 125: 443–451.
18. Mayer MP, Bukau B (2005) Hsp70 chaperones: cellular functions and molecular mechanism. Cellular and molecular life sciences : CMLS 62: 670–684.
19. Perry AJ, Rimmer KA, Mertens HD, Waller RF, Mulhern TD, et al. (2008) Structure, topology and function of the translocase of the outer membrane of mitochondria. Plant physiology and biochemistry : PPB/Societe francaise de physiologie vegetale 46: 265–274.
20. Huang G, Elferink CJ (2005) Multiple mechanisms are involved in Ah receptor-mediated cell cycle arrest. Mol Pharmacol 67: 88–96.
21. Marlowe JL, Knudsen ES, Schwemberger S, Puga A (2004) The aryl hydrocarbon receptor displaces p300 from E2F-dependent promoters and represses S phase-specific gene expression. J Biol Chem 279: 29013–29022.
22. Puga A, Barnes SJ, Dalton TP, Chang C, Knudsen ES, et al. (2000) Aromatic hydrocarbon receptor interaction with the retinoblastoma protein potentiates repression of E2F-dependent transcription and cell cycle arrest. J Biol Chem 275: 2943–2950.
23. Kolluri SK, Weiss C, Koff A, Gottlicher M (1999) p27(Kip1) induction and inhibition of proliferation by the intracellular Ah receptor in developing thymus and hepatoma cells. Genes Dev 13: 1742–1753.
24. Pang PH, Lin YH, Lee YH, Hou HH, Hsu SP, et al. (2008) Molecular mechanisms of p21 and p27 induction by 3-methylcholanthrene, an aryl-hydrocarbon receptor agonist, involved in antiproliferation of human umbilical vascular endothelial cells. J Cell Physiol 215: 161–171.
25. Heliovaara E, Raitila A, Launonen V, Paetau A, Arola J, et al. (2009) The expression of AIP-related molecules in elucidation of cellular pathways in pituitary adenomas. Am J Pathol 175: 2501–2507.
26. de Oliveira SK, Smolenski A (2009) Phosphodiesterases link the aryl hydrocarbon receptor complex to cyclic nucleotide signaling. Biochem Pharmacol 77: 723–733.
27. de Oliveira SK, Hoffmeister M, Gambaryan S, Muller-Esterl W, Guimaraes JA, et al. (2007) Phosphodiesterase 2A forms a complex with the co-chaperone XAP2 and regulates nuclear translocation of the aryl hydrocarbon receptor. J Biol Chem 282: 13656–13663.
28. Feigelson HS, Henderson BE (1996) Estrogens and breast cancer. Carcinogenesis 17: 2279–2284.
29. Persson I, Weiderpass E, Bergkvist L, Bergstrom R, Schairer C (1999) Risks of breast and endometrial cancer after estrogen and estrogen-progestin replacement. Cancer Causes Control 10: 253–260.
30. Greiser CM, Greiser EM, Doren M (2007) Menopausal hormone therapy and risk of ovarian cancer: systematic review and meta-analysis. Hum Reprod Update 13: 453–463.
31. Zeng Q, Chen G, Vlantis A, Tse G, van Hasselt C (2008) The contributions of oestrogen receptor isoforms to the development of papillary and anaplastic thyroid carcinomas. J Pathol 214: 425–433.
32. Fujimoto M, Yoshino E, Hirakawa K, Chihara K, Ibata Y (1987) Studies on estrogen induced pituitary tumor in the rat with special reference to the relationship of the tuberoinfundibular dopamine neuron system. J Neurooncol 5: 151–159.
33. Heaney AP, Horwitz GA, Wang Z, Singson R, Melmed S (1999) Early involvement of estrogen-induced pituitary tumor transforming gene and fibroblast growth factor expression in prolactinoma pathogenesis. Nat Med 5: 1317–1321.
34. Spengler D, Villalba M, Hoffmann A, Pantaloni C, Houssami S, et al. (1997) Regulation of apoptosis and cell cycle arrest by Zac1, a novel zinc finger protein expressed in the pituitary gland and the brain. EMBO J 16: 2814–2825.
35. Chahal HS, Trivellin G, Leontiou CA, Alband N, Fowkes RC, et al. (2012) Somatostatin Analogs Modulate AIP in Somatotroph Adenomas: The Role of the ZAC1 Pathway. J Clin Endocrinol Metab 97: E1411–1420.
36. Ozfirat Z, Korbonits M (2010) AIP gene and familial isolated pituitary adenomas. Mol Cell Endocrinol 326: 71–79.
37. Afonine PV, Grosse-Kunstleve RW, Echols N, Headd JJ, Moriarty NW, et al. (2012) Towards automated crystallographic structure refinement with phenix.refine. Acta Crystallogr D Biol Crystallogr 68: 352–367.
38. Davis IW, Leaver-Fay A, Chen VB, Block JN, Kapral GJ, et al. (2007) MolProbity: all-atom contacts and structure validation for proteins and nucleic acids. Nucleic Acids Res 35: W375–383.
39. Emsley P, Cowtan K (2004) Coot: model-building tools for molecular graphics. Acta Crystallogr D Biol Crystallogr 60: 2126–2132.
40. Krissinel EB, Winn MD, Ballard CC, Ashton AW, Patel P, et al. (2004) The new CCP4 Coordinate Library as a toolkit for the design of coordinate-related applications in protein crystallography. Acta Crystallogr D Biol Crystallogr 60: 2250–2255.
41. Ashkenazy H, Erez E, Martz E, Pupko T, Ben-Tal N (2010) ConSurf 2010: calculating evolutionary conservation in sequence and structure of proteins and nucleic acids. Nucleic Acids Res 38: W529–533.
42. Landau M, Mayrose I, Rosenberg Y, Glaser F, Martz E, et al. (2005) ConSurf 2005: the projection of evolutionary conservation scores of residues on protein structures. Nucleic Acids Res 33: W299–302.
43. Glaser F, Pupko T, Paz I, Bell RE, Bechor-Shental D, et al. (2003) ConSurf: identification of functional regions in proteins by surface-mapping of phylogenetic information. Bioinformatics 19: 163–164.

44. Siligardi G, Hu B, Panaretou B, Piper PW, Pearl LH, et al. (2004) Co-chaperone regulation of conformational switching in the Hsp90 ATPase cycle. J Biol Chem 279: 51989–51998.
45. Prodromou C, Siligardi G, O'Brien R, Woolfson DN, Regan L, et al. (1999) Regulation of Hsp90 ATPase activity by tetratricopeptide repeat (TPR)-domain co-chaperones. EMBO J 18: 754–762.
46. Panaretou B, Siligardi G, Meyer P, Maloney A, Sullivan JK, et al. (2002) Activation of the ATPase activity of hsp90 by the stress-regulated cochaperone aha1. Mol Cell 10: 1307–1318.
47. Yano M, Terada K, Mori M (2003) AIP is a mitochondrial import mediator that binds to both import receptor Tom20 and preproteins. The Journal of cell biology 163: 45–56.
48. Bell DR, Poland A (2000) Binding of aryl hydrocarbon receptor (AhR) to AhR-interacting protein. The role of hsp90. J Biol Chem 275: 36407–36414.
49. Hollingshead BD, Petrulis JR, Perdew GH (2004) The aryl hydrocarbon (Ah) receptor transcriptional regulator hepatitis B virus X-associated protein 2 antagonizes p23 binding to Ah receptor-Hsp90 complexes and is dispensable for receptor function. J Biol Chem 279: 45652–45661.
50. Chahal HS, Stals K, Unterlander M, Balding DJ, Thomas MG, et al. (2011) AIP mutation in pituitary adenomas in the 18th century and today. N Engl J Med 364: 43–50.
51. Daly AF, Tichomirowa MA, Petrossians P, Heliovaara E, Jaffrain-Rea ML, et al. (2010) Clinical characteristics and therapeutic responses in patients with germline AIP mutations and pituitary adenomas: an international collaborative study. J Clin Endocrinol Metab 95: E373–383.
52. Igreja S, Chahal HS, King P, Bolger GB, Srirangalingam U, et al. (2010) Characterization of aryl hydrocarbon receptor interacting protein (AIP) mutations in familial isolated pituitary adenoma families. Hum Mutat 31: 950–960.
53. Muller P, Ruckova E, Halada P, Coates PJ, Hrstka R, et al. (2012) C-terminal phosphorylation of Hsp70 and Hsp90 regulates alternate binding to co-chaperones CHIP and HOP to determine cellular protein folding/degradation balances. Oncogene.
54. Cook C, Petrucelli L (2012) Tau Triage Decisions Mediated by the Chaperone Network. Journal of Alzheimer's disease : JAD.
55. Raitila A, Lehtonen HJ, Arola J, Heliovaara E, Ahlsten M, et al. (2010) Mice with inactivation of aryl hydrocarbon receptor-interacting protein (Aip) display complete penetrance of pituitary adenomas with aberrant ARNT expression. Am J Pathol 177: 1969–1976.
56. Pocar P, Fischer B, Klonisch T, Hombach-Klonisch S (2005) Molecular interactions of the aryl hydrocarbon receptor and its biological and toxicological relevance for reproduction. Reproduction 129: 379–389.
57. Safe S, Wormke M, Samudio I (2000) Mechanisms of inhibitory aryl hydrocarbon receptor-estrogen receptor crosstalk in human breast cancer cells. J Mammary Gland Biol Neoplasia 5: 295–306.
58. Cai W, Kramarova TV, Berg P, Korbonits M, Pongratz I (2011) The immunophilin-like protein XAP2 is a negative regulator of estrogen signaling through interaction with estrogen receptor alpha. PLoS One 6: e25201.

Pituitary Disorders

Diagnosis and Management

EDITED BY

Edward R. Laws Jr.
MD FACS

Professor of Surgery
Harvard Medical School;
Department of Neurosurgery
Brigham and Women's Hospital
Boston, MA, USA

Shereen Ezzat
MD FRCP(C) FACP

Head, Endocrine Oncology Site Group
Princess Margaret Hospital;
Senior Scientist, Ontario Cancer Institute
University Health Network;
Professor, Department of Medicine
University of Toronto
Toronto, ON, Canada

Sylvia L. Asa MD PhD

Medical Director, Laboratory Medicine Program
Senior Scientist, Ontario Cancer Institute
University Health Network;
Professor
Department of Laboratory Medicine and Pathobiology
University of Toronto
Toronto, ON, Canada

Linda M. Rio MA MFT

Director of Professional and Public Education
Pituitary Network Association
Newbury Park, CA;
Marriage & Family Therapist
New Beginnings Counseling Center
Camarillo, CA, USA

Lorin Michel BA

Medical Writer
Associate
Pituitary Network Association
Oak Park, CA, USA

Robert Knutzen MBA

Chairman and CEO
Pituitary Network Association
Newbury Park, CA, USA

WILEY-BLACKWELL

A John Wiley & Sons, Ltd., Publication

Wiley-Blackwell is an imprint of John Wiley & Sons, formed by the merger of Wiley's global Scientific, Technical and Medical business with Blackwell Publishing.

Registered office: John Wiley & Sons, Ltd, The Atrium, Southern Gate, Chichester, West Sussex, PO19 8SQ, UK

Editorial offices: 9600 Garsington Road, Oxford, OX4 2DQ, UK
The Atrium, Southern Gate, Chichester, West Sussex, PO19 8SQ, UK
111 River Street, Hoboken, NJ 07030-5774, USA

For details of our global editorial offices, for customer services and for information about how to apply for permission to reuse the copyright material in this book please see our website at www.wiley.com/wiley-blackwell

Library of Congress Cataloging-in-Publication Data
Pituitary disorders : diagnosis and management / edited by Edward R. Laws Jr. . . . [et al.].
p. ; cm.
Includes bibliographical references and index.
ISBN 978-0-470-67201-3 (pbk. : alk. paper)
I. Laws, Edward R.
[DNLM: 1. Pituitary Diseases. WK 550]
616.4'7–dc23

A catalogue record for this book is available from the British Library.

Wiley also publishes its books in a variety of electronic formats. Some content that appears in print may not be available in electronic books.

Cover images: from left to right – Shutterstock file number #71338543 © vetpathologist, iStock file number #4606038 theasis, fotolia pituitary tumor © Dr Cano file number #1559123, iStock file number #20015759 asiseeit. Main image iStock file number #17548218, Janulla.
Cover design by Steve Thompson

Set in 9/12 pt Meridien by Toppan Best-set Premedia Limited

1 2013

Contents

Section 8: Research and Clinical Trials

Section 9: Resources

CHAPTER 10
Familial Pituitary Adenomas

Laura C. Hernández-Ramírez and Márta Korbonits
Barts and the London School of Medicine, Queen Mary University of London, London, UK

Introduction

Despite their relative rarity, familial pituitary tumors represent a very interesting group of conditions, with a heterogeneous genetic background and a widely variable phenotype within affected families (Figure 10.1). Previously, around 4–5% of the cases were suggested to occur in a family setting, either isolated or as part of an endocrine tumor syndrome [1], but current data suggest a higher proportion of familial cases [2], and the recent establishment of familial isolated pituitary adenoma (FIPA) as a separate clinical entity is expected to increase this prevalence [2]. There is a higher proportion of genetic forms of pituitary adenomas within young patients (both hereditary and nonhereditary) [3]. In fact, up to 20% of children with a hormone-secreting pituitary adenoma have a germline mutation in a known predisposing gene [4,5]. A better understanding of the causative genes and the pathogenic mechanisms of this particular group of tumors is needed to improve the diagnosis and management of these patients, which, hopefully, will lead to a better prognosis.

The inherited conditions that, to date, are known to predispose to pituitary adenomas are multiple endocrine neoplasia type 1 (MEN1), multiple endocrine neoplasia type 4 (MEN4), Carney complex (CNC), FIPA and, possibly, mutations in DICER1 [6] and succinate dehydrogenase (SDH) genes [7–9]. Previous data suggest that approximately 2.7% of all pituitary tumors occur in the context of MEN1 [10] and that FIPA accounts for another 2.5% [11]. CNC explains a few hundred cases worldwide [11], while MEN4 and SDH-related familial pituitary adenomas have only been described in a few individuals [7,12–18]. Nevertheless, the genetic basis for these conditions has not been identified for all cases: in 5–10% of MEN1 patients [19], 27% of CNC patients [20], and 70–85% of FIPA patients [21] the causative gene or genes have not been identified as yet.

An important aspect of the study of these rare genetic syndromes is the potential role of the causative genes in the more common sporadic pituitary adenomas. Therefore, somatic mutations have been studied in sporadic pituitary adenomas: *MEN1* mutations have very rarely been identified [19], but no mutations have been described in other genes associated with familial pituitary adenomas (*PRKAR1A* and *AIP*) [22–25].

Multiple Endocrine Neoplasia Type 1

In 1954, Wermer reported the first clinical description of a family with an association of pituitary tumors, hypercalcemia and pancreatic adenomas [26]. MEN1 (OMIM #131100) is a syndrome characterized by the development of tumors mainly in endocrine but also nonendocrine organs. The three main components of the syndrome are hyperparathyroidism, enteropancreatic endocrine

Pituitary Disorders: Diagnosis and Management, First Edition. Edited by Edward R. Laws, Shereen Ezzat, Sylvia L. Asa, Linda M. Rio, Lorin Michel and Robert Knutzen.

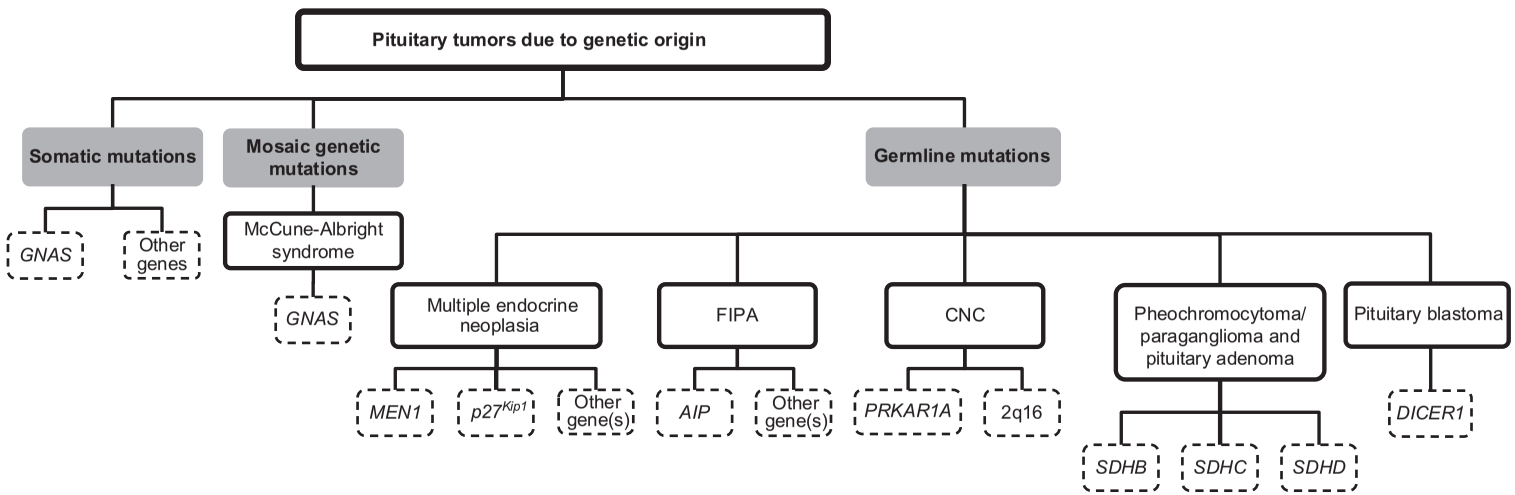

Figure 10.1. Pituitary tumors of genetic origin. Though the genetic abnormalities that lead to pituitary tumorigenesis are diverse and incompletely described so far, mutations in a variety of genes are known causes of pituitary adenomas or blastomas, either isolated or as part of a syndrome. Germline mutations originate familial (e.g., inherited) pituitary adenomas.

tumors, and pituitary adenomas [26]. The diagnosis of MEN1 is established when two of these features are present or when one feature is present together with a first-degree relative with established MEN1 [27]. Other endocrine components of the syndrome are foregut carcinoids, adrenal cortex nonfunctioning tumors, and, rarely, pheochromocytomas, while lipomas, facial angiofibromas, collagenomas, and ependymomas are nonendocrine tumors associated with MEN1 [27].

The observation of loss of heterozygosity (LOH) of chromosome 11q13 in tumors from MEN1 patients led to the mapping, in 1988 [28], and later cloning, in 1997 [29,30], of MEN1. This gene spans 7.2 kb of genomic sequence, contains a 1830-bp coding region with 10 exons (the first is not translated) and encodes a 610-amino-acid protein, menin [29]. MEN1 mutations are detected in 90–95% of MEN1 patients [19].

To date, more than 1300 MEN1 mutations are known, distributed through the whole gene, although there are mutational 'hot spots' in exons 2, 3, 9, and 10 and intron 4 [19,31]. Until 2008, 1133 germline and 203 somatic mutations had been described: 23% were nonsense, 9% splice-site, 41% frameshift deletions or insertions, 6% in-frame deletions or insertions, 20% missense, and 1% whole or partial gene deletions [19].

LOH in 11q13 occurs in around 90% of tumors from MEN1 patients but LOH can also be found at this region in 5–50% of sporadic endocrine tumors [19]. Somatic MEN1 mutations are common in sporadic parathyroid (9.5–21% of cases) and pancreatic islet cell tumors (19–44%), but they occur only very rarely (0–3.67%, only 10 mutations described) in sporadic pituitary tumors [19]. Nonsense, frameshift, splice-site, and missense mutations have been identified and characterized by several excellent publications.

Menin

MEN1 is considered a tumor suppressor gene because heterozygous inactivating mutations predispose to neoplasia, MEN1 knockout mice reproduce the human phenotype, and the majority of MEN1-related tumors show LOH at 11q13 [28, 32–35]. In tumors without LOH, it is speculated that other mechanisms of gene inactivation (hypermethylation, mutations of the promoter or noncoding regions microRNA regulation) may occur [32]. By transcriptional regulation, MEN1 produces two transcripts: a ubiquitously expressed 2.9-kb transcript with several alternatively spliced isoforms, and a 4.2-kb transcript, present in the pancreas and thymus [30]. Menin is a 67-kDa protein without homology to any other protein [29,36] (Figure 10.2). It is highly conserved within species: murine menin shows 97% identity/98% similarity to human menin [37].

Menin controls the promoter activity of various genes involved in transcriptional regulation, genome stability, cell division, and proliferation. It interacts with numerous partners:

- Menin activates the transcription of CDKN1B (encoding the cyclin-dependent kinase inhibitor $p27^{Kip1}$) and CDKN2C (encoding the cyclin-dependent kinase inhibitor 2C, also known as $p18^{Ink4c}$) by recruiting the histone methyltransferase mixed lineage leukemia protein (MLL) to the promoters and coding regions of these genes, where MLL catalyzes histone H3 lysine 4 (H3K4) methylation. Although menin expression does not differ between endocrine and nonendocrine organs, MLL, $p27^{Kip1}$, and $p18^{Ink4c}$ are predominantly expressed in endocrine organs and this expression profile could partially explain the selectivity of tumorigenesis in patients with MEN1 [38]. Through interaction with MLL, menin also regulates the transcription of homeobox (HOX) genes (particularly Hoxa9), important for cell proliferation, differentiation and morphogenesis [39]. In a similar way, menin recruits polycomb group (PcG) proteins to enhance H3K27 methylation at the pleiotropin (PTN) gene, silencing the expression of this pro-proliferative gene.
- In the normal pituitary, menin interacts with activin, negatively regulating cell proliferation and the secretion of prolactin (PRL), growth hormone (GH), and adrenocorticotropin (ACTH), through inhibition of POU1F1.
- The transforming growth factor-β (TGF-β) signaling pathway exerts inhibition of proliferation and transcriptional activity through Smad2 and Smad3

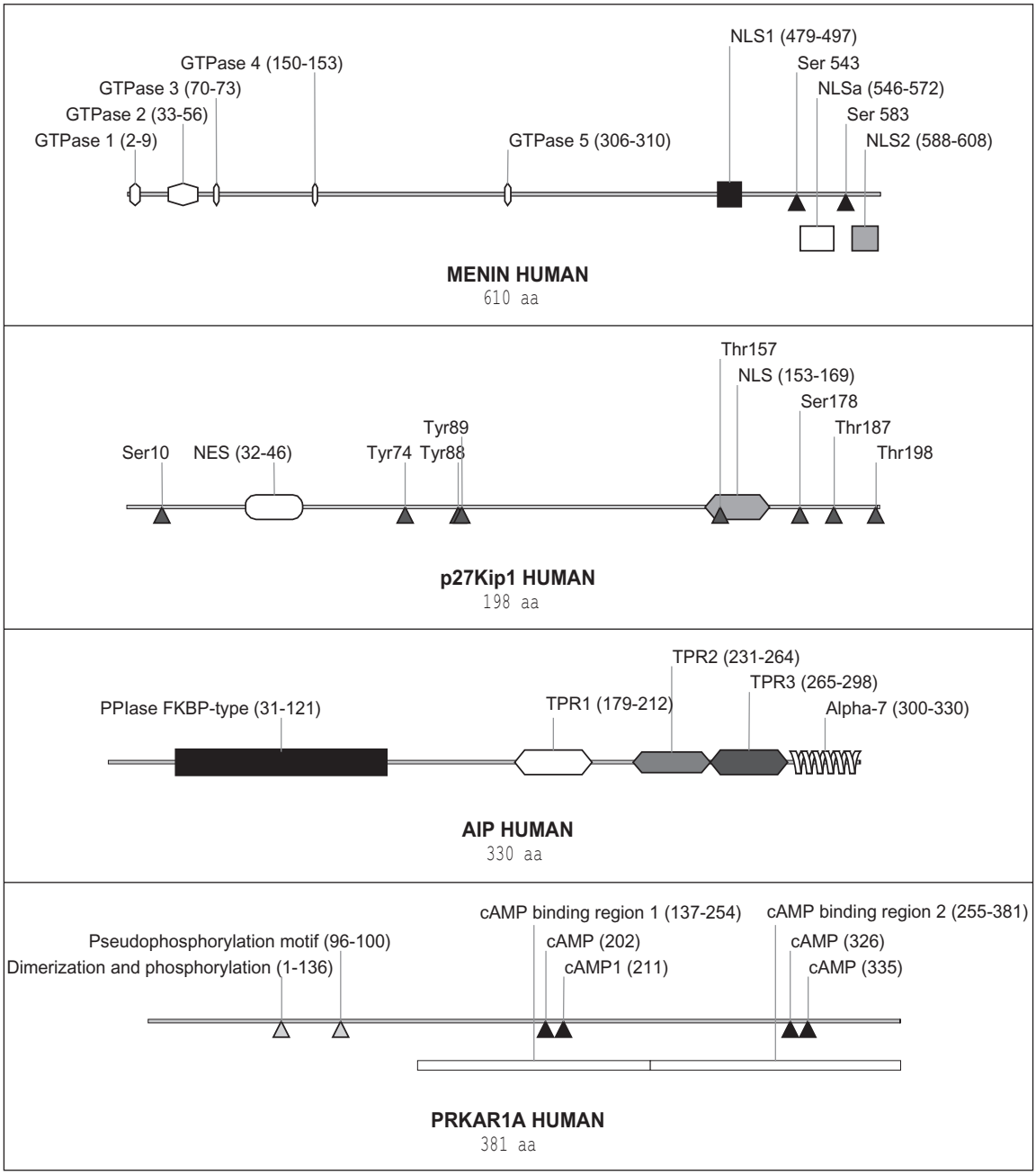

Figure 10.2. Functional domains of the main proteins implicated in familial pituitary adenomas: menin, $p27^{Kip1}$, AIP, and PRKAR1A. Menin has three nuclear localization signals (NLS) at its C-terminal domain, two phosphorylation sites at Ser 543 and 583, and five putative guanosine triphosphatase (GTPase) motifs [19,142]. $p27^{Kip1}$ has a nuclear export signal (NES) and a NLS, as well as multiple phosphorylable residues, important for its regulation by other proteins [73,143]. The N-terminal half of AIP contains the so-called immunophilin-like domain (PPIase, FKBP-type), while its C-terminal region has three TPR domains and an α-7 helix [85,144,145]. The most important regions of PRKAR1A are those necessary for cAMP binding, in its C-terminal half [146].

proteins [39]. Menin interacts with Smad3 and the loss of this function prevents Smad3 to bind DNA, blocking TGF-β effects [40].

- Other menin effects over transcriptional activity are the inhibition of JunD-mediated and enhancement of c-Jun-mediated transactivation of the activating protein-1 (AP-1) [41], as well as its interaction with members of the nuclear factor-kappa B (NF-κB) family, modulating their transcriptional activity [42].
- Menin interacts with the nuclear receptors peroxisome proliferator-activated receptor γ (PPAR-γ) and the vitamin D receptor (VDR), enhancing the expression of their target genes [43].
- The expression of insulin-like growth factor binding protein 2 (IGFBP-2) [44], insulin-like growth factor 2 (IGF-2) and parathyroid hormone-related protein (PTHrp) [45], important proliferative factors in endocrine tumors, is negatively modulated by menin.
- Menin directly interacts with β-catenin and carries it out of the nucleus, thus inhibiting transcriptional activity and cell proliferation by the wingless-type MMTV integration site family (WNT)/β-catenin signaling pathway [46].
- Menin interacts with the 32 kDa subunit of replication protein A (RPA2) [47] as well as with FANCD2 [48]; both are proteins involved in DNA repair. Through its interaction with the promoter of the human telomerase reverse transcriptase (hTERT), menin apparently acts as a repressor of telomerase activity [49].
- Other menin interactors are proteins involved in cell division, such as non-muscle myosin II-A heavy chain (NMHC II-A) [50], glial fibrillary acidic protein (GFAP) and vimentin [51].

In mice, homozygous deletion of MEN1 is lethal in utero due to multiple developmental delay and craniofacial, cardiac, neural, and hepatic abnormalities [19,33,52]. Heterozygous mice for partial deletions of MEN1 develop a syndrome similar to human MEN1 [33,52]. In another model, the same deletion, conditionally restricted to the pancreas, showed that heterozygous loss of menin expression caused hyperplasia, but LOH was necessary for progression to a tumor [34].

Clinical Features

MEN1 has an autosomal dominant pattern of inheritance. Eighty-five percent of the cases are familial and 15% are sporadic, but the frequency of MEN1 mutations is apparently not different between these two groups. Penetrance is variable and age and organ-specific [27]. Female gender slightly predominates (52–57% of patients) [53]. Within MEN1 patients, pituitary tumors are more common in females, while gastrinomas and thymic carcinomas are more common in males [53]. There is no clear genotype–phenotype correlation [54].

Hyperparathyroidism is the most constant feature of the syndrome: it is present in 90–100% of the patients by the age of 50 years [27]. Parathyroid adenomas are usually the first manifestation of the syndrome (72–87% of patients). These tumors are usually multiple, and require extensive surgical treatment [27].

Thirty to 80% of MEN1 patients develop enteropancreatic islet cell tumors [27]. In the setting of MEN1, these tumors are multicentric and hormone-secreting, and may become invasive or metastasic (especially gastrinomas and glucagonomas) [27, 55]. They are the first manifestation of the disease in around 25% of patients [56]. Tumors arise in any part of the pancreas or the duodenal mucosa. The most common subtype is gastrinoma (in 40–63% of patients), causing the Zollinger–Ellison syndrome (ZES) [57,58]. Surgery is usually curative only for insulinoma, but other enteropancreatic islet cell tumors respond well to medical treatment with proton pump inhibitors (gastrinomas) or somatostatin analogs (SA) [27]. Carcinoids related to MEN1 arise in thymus and gastric mucosa and rarely hypersecrete hormones [27], but they may cause the ectopic ACTH syndrome or increased GH-releasing hormone (GHRH) secretion and acromegaly [59]. Metastasic neuroendocrine tumors represent the main MEN1-related cause of death [60].

Adrenal cortical tumors are present in 20–40% of MEN1 patients, and most often are bilateral, hyperplastic, and nonfunctional lesions; adrenal carcinomas are rare [27]. Up to one-third of the

patients develop lipomas, both cutaneous and visceral [27]. Multiple facial angiofibromas are found in 40–80% of cases [27].

Approximately 40% of MEN1 patients develop pituitary adenomas [61]. A pituitary adenoma is the first manifestation of MEN1 in around 17% of patients [61] (ranging from 10 to 25% [27]). Pituitary adenomas in the context of MEN1 arise at a younger age (35.1 ± 14.8 years) than in patients with sporadic pituitary adenomas [61]. The earliest age of presentation reported is 5 years [62]. Prolactinomas predominate (62%), but nonfunctioning pituitary adenomas (NFPAs) (15%), somatotropinomas (9%), corticotropinomas (4%), and rarely thyrotropinomas can also arise [61,63]. One case of gonadotroph cells carcinoma in a MEN1 patient has been reported [63]. Ten to 39% of tumors secrete more than one hormone, usually PRL/GH [61,64]. The majority of these tumors are macroadenomas (76–85%) and around half of them are invasive [61,64]. Four percent of patients present multiple adenomas [64].

Pituitary adenomas in MEN1 patients are significantly larger and more invasive than in sporadic patients, but the Ki-67 index and the mitotic activity are not different [64]. Hyperplasia of somatotroph or mammosomatotroph cells has been described, but it is not common and in some cases it is due to an ectopic GHRH-secreting tumor [64,65]. In an invasive tumor from a very young MEN1 patient, overexpression of genes related to tumorigenesis (*TPD52*, *FOS*, and *SHC1*), and cell growth (*GNAS*, *FOSB*, and *SRF*) as well as loss of E-cadherin function were detected [62].

In general, the response of secretory pituitary adenomas to medical and/or surgical treatment is suboptimal; normalization of hormone secretion is achieved in only 42% of patients [61]. Medical treatment of prolactinomas in MEN1 patients is complicated because they show a poor response to dopamine agonists [61].

Sequence analysis of MEN1 in index cases and their relatives is important in order to determine which individuals require follow-up, as well as to identify phenocopies (they are present in ~5% of families). MEN1 mutation carriers and MEN1 patients should have long-term follow-up, because new components of the syndrome can arise at any age [27]. An annual biochemical screening, including calcium, parathyroid hormone, gastrin, fasting glucose, insulin, chromogranin-A, glucagon, proinsulin, PRL, and IGF-1 is recommended [27]. Imaging studies (CT, MRI, and, rarely, ^{111}In-DTPA octreotide scan) should be done at regular intervals [27].

Multiple Endocrine Neoplasia Type 4

The absence of MEN1 mutations in a minority (5–10%) of patients with MEN1 clinical features drove a search for additional loci implicated in this phenotype. Spontaneous mutations were found in Cdkn1b in association with a multiple endocrine neoplasia syndrome (called MENX) showing features of both human MEN1 and MEN2 syndromes, occurring spontaneously in a laboratory rat strain [12]. Following this discovery, mutations in CDKN1B were identified in a small group of human patients with multiple endocrine tumors typical of MEN1 but not MEN2 or other clinical features, but without germline mutations in MEN1 or RET (the gene associated with MEN2 syndrome) [66]. This infrequent MEN1-like syndrome was named MEN4 (OMIM #610755) [67].

CDKN1B, a gene located at 12p13.1, encodes the cyclin-dependent kinase inhibitor (CDKI) $p27^{Kip1}$. Since the first report, mutations in CDKN1B have been sought in many patients with MEN1 features, negative for MEN1 mutations, but they have rarely been found [68–71]. These patients might have a different genetic background, not yet identified. A large screening study of MEN1-like patients identified mutations in genes encoding *CDKN1B* as well as other CDKIs, p15, p18, and p21; however, these mutations appear to be uncommon [14].

$p27^{Kip1}$

$p27^{Kip1}$ is a highly conserved 27-kDa protein (Figure 10.2). CDKN1B is a tumor suppressor gene. Subcellular localization of $p27^{Kip1}$ determines its functions. In G0 and early G1, $p27^{Kip1}$ expression is maximal

and is localized in the nucleus, where it binds and inhibits the cyclin E-CDK2 complex. In proliferating cells, $p27^{Kip1}$ is sequestered in the cytoplasm, with a substantial proportion bound to cyclin D-CDK4. As cells progress through phase G1, $p27^{Kip1}$ expression decreases, allowing cyclin E-CDK2 and cyclin A-CDK2 to activate the transcription of genes necessary for G1-S transition and the initiation of DNA replication. On the other hand, $p27^{Kip1}$ can act as a substrate for the cyclin E–CDK2 complex, resulting in tyrosine phosphorylation which triggers ubiquination and proteasomal degradation of $p27^{Kip1}$ [72]. Many other proteins and also microRNAs modulate $p27^{Kip1}$ transcription and proteolysis [73]. Regarding cyclin D-CDK4 and cyclin D-CDK6 complexes, $p27^{Kip1}$ exerts a dual role. Under adverse conditions for replication, $p27^{Kip1}$ inhibits type D cyclins, while in early G1 to mid-G1 phase it promotes cyclin D-CDK4 assembly and nuclear import [73].

In tumoral cells, cytoplasmic sequestration of $p27^{Kip1}$ (via AKT-dependent phosphorylation on residue Thr157) inhibits its activity, leading to enhanced tumor invasiveness. $p27^{Kip1}$ activity can also be reduced via SKP2, the E3 ubiquitin ligase of $p27^{Kip1}$, which promotes its degradation [66,67]. $p27^{Kip}$ is a downstream element of the tumor suppressor gene MEN1 signaling pathway. Menin, through its interaction with histone methyltransferases, enhances the activity of the CDKN1B promoter [66]. Paradoxically, $p27^{Kip1}$ can display oncogenic activity through a CDK-independent mechanism in experiments using knock-in mice with a mutated $p27^{Kip1}$ unable to bind CDKs [74].

Homozygous knockout mice for $p27^{Kip1}$ have increased body size and develop multiorgan hyperplasia, retinal dysplasia, ovulatory defects, female sterility and, in 100% of cases, hyperplasia or adenomas of the pituitary pars intermedia, secreting ACTH [75]. $p27^{Kip1}$ somatic mutations or LOH at its locus have only rarely been described in human tumors [12,66,76]. Decreased $p27^{Kip1}$ expression, either due to heterozygous mutation or because of changes in extragenic pathways that regulate protein levels, is enough for tumor development in $p27^{Kip1+/-}$ mice [77]. Furthermore, an important reduction in CDKN1B expression has been described in multiple human cancers, correlating with aggressive behavior [73], as well as in some endocrine malignant and benign tumors (pheochromocytomas, parathyroid adenomas and pancreatic and digestive endocrine tumors) [66,78].

Germline mutations in CDKN1B are extremely rare: they explain only 1.5–2.8% of MEN1 phenotype/MEN1-mutation negative cases [13,14], therefore, only ~0.1–0.2% of all MEN1 cases. The first CDKN1B germline mutation identified in a MEN4 patient was a nonsense mutation that had been previously identified as a somatic change in an adult patient with leukemia [12,66]. To date, eight CDKN1B germline mutations have been described in MEN4 patients, including a frameshift, a nonsense mutation, a nonstop mutation, a deletion in the 5′ untranslated region (UTR), a mutation in the Kozak sequence, and three missense mutations [12,14–17]. The functional effect of these mutations is the production of a low-expressing and/or unstable and nonfunctional protein [12,14–16,66,71]. To better define the role of CDKN1B mutations as a cause of pituitary adenomas, 124 affected subjects from 88 FIPA families, negative for AIP mutations, were recently studied [18]. None of the identified variants was found to be causing the disease; thus, systematic screening for these mutations in FIPA patients is currently unjustified [18].

Pituitary Adenomas

Under physiologic conditions, $p27^{Kip1}$ is especially highly expressed in the human pituitary [38] in all types of cells except normal corticotroph cells, which show a lower expression [79]. Expression of $p27^{Kip1}$ is significantly reduced in all pituitary adenoma types, but the protein is practically absent in corticotropinomas and pituitary carcinomas [79], however, no somatic *CDKN1B* mutations, nor LOH of 12p13, have been found in corticotropinomas [76,80]. Out of the eight cases with germline *CDKN1B* mutations reported to date, only three pituitary adenomas have been reported among MEN4 patients (somatotropinoma, corticotropinoma, and NFPA) [71]. Because of the scarcity of cases, data about the specific histological features of pituitary adenomas in MEN4 cases are lacking.

Clinical Features

As only a few MEN4 patients have been reported, penetrance of the syndrome, frequency of familial and sporadic cases, and possible phenotype–genotype correlations cannot be determined at this moment. Nevertheless, as in MEN1, the most common component of the syndrome is parathyroid involvement. Three CDKN1B mutations have been described in familial and five in sporadic MEN4 patients. In two of the familial cases not only CDKN1B mutation carriers but also clinically affected relatives were identified [12,14]. The patients described to date have presented 1–4 endocrine tumors concomitantly. Apart from parathyroid and pituitary adenomas, other benign and malignant tumors described as part of MEN4 are renal angiomyolipoma, an adrenal nonfunctional tumor, uterine fibroids, and a gastrinoma, as well as a neuroendocrine cervical carcinoma, bronchial carcinoid, papillary thyroid carcinoma, and gastric carcinoma [12–17].

Due to the lack of a specific MEN4 phenotype, it is not possible to establish this diagnosis only by clinical data [71]. Because of the low prevalence of MEN4, screening for CDKN1B mutations in patients with MEN1 diagnosis and negative MEN1 mutations is currently not done routinely in the United Kingdom; however, patients previously considered as MEN1 phenocopies could be tested for CDKN1B mutations in a research setting [71].

Familial Isolated Pituitary Adenoma

FIPA (OMIM #102200) is characterized by the presence of pituitary adenomas in two or more members of a family without associated clinical or genetic abnormalities of the classic syndromes (e.g., related to MEN1, CNC, or pheochromocytomas/paragangliomas). FIPA includes families previously identified as isolated familial somatotropinoma and also the subgroup of FIPA patients with pituitary adenoma predisposition (PAP) due to mutations in the aryl-hydrocarbon receptor interacting protein gene (*AIP*) [21,81].

Since the late 1990s, linkage analysis and LOH for 11q13 has been demonstrated in tumors from patients with a familial history of isolated pituitary adenomas. In 2006, linkage analysis identified a truncating germline mutation in AIP as the cause of multiple cases of pituitary adenomas (somatotropinomas and prolactinomas) in one large Finnish family [81]. Further studies identified many other novel mutations in AIP in individuals from familial acromegaly and prolactinoma families and also in patients with apparently sporadic pituitary adenomas [24,81,82]. Germline AIP mutations have been identified in only 20–25% of FIPA families (40% when only somatotrophinoma families are considered) [21], while the causative gene(s) in the rest of the families remain unknown.

The prevalence of FIPA is currently unknown, but is probably similar to or higher than MEN1. AIP mutations have been found only in 2–3.6% of patients with apparently sporadic pituitary adenomas [21,83]. On the other hand, in patients younger than 30 years with apparently sporadic pituitary macroadenomas, AIP mutations are present in 11.7% of the whole group and in 20.5% of pediatric patients [5], and thus many of these patients represent previously unsuspected FIPA cases.

AIP

Also known as X-associated protein 2 (XAP2), Ah receptor-activated 9 (ARA9), and FK506-binding protein 37 (FKBP37), AIP was first described in 1996 as an inhibitor of hepatitis B virus X protein-mediated transactivation. It shows homology with members of the FK506-binding protein family (FKBP). AIP is ubiquitously expressed in human and murine tissues, and present in lower organisms such as Drosophila rerio, D. melanogaster and Caenorhabditis elegans, but its tissue-specific functions remain elusive.

The AIP locus is on chromosomal region 11q13.2, just 2.6 Mb downstream from MEN1 [84]. AIP has six exons, coding for a 37-kDa protein, AIP. AIP is a co-chaperone protein, made up of 330 amino acids, and is member of the tetratricopeptide repeat (TPR) domain-containing protein family that includes proteins important for cell cycle control

[21,85,86]. AIP contains three TPR motifs, and a final α-helix, located in its C-terminal half, essential for interactions with other proteins [85] (Figure 10.2). Since the identification of AIP as the gene related with FIPA, around 60 mutations have been described.

AIP mutations in FIPA patients include deletions, insertions, segmental duplications, nonsense, missense, splice-site, and promoter mutations, as well as large deletions of whole exons or the entire gene [21]. A de-novo mutation has been described in a single patient [4]. There are three mutational hotspots in AIP, corresponding to CpG islands: mutation of both members of the c.910–911 CpG site have been described (c.910C > T, p.R304X and c.911G > A, p.R304Q), c.811C > T (p.R271W), and c.241C > T (p.R81X) [87]. The c.40C > T, p.Q14X mutation has been described only in Finnish families, suggesting a founder effect. Loss of the C-terminal end of AIP occurs in 78% of the mutants, due to stop codons or frameshifts resulting in stop codons. The missense variants and the in-frame segmental duplication mostly affect the TPR domains or the C-terminal α-helix. It is important that a technique able to analyze a large segment of DNA, such as multiplex ligation-dependent probe amplification (MLPA), should be used in AIP mutation screening, because approximately 10% of families that are negative for AIP mutations by conventional methods do indeed have large AIP deletions [21].

The role of AIP as a tumor suppressor is supported by the association of multiple loss-of-function mutations in this gene with the development of pituitary adenomas and the presence of LOH in 11q13 in pituitary adenomas from AIP mutation-positive FIPA patients [24,84,88,89]. Mutations in AIP lead to loss of function of the protein. Furthermore, AIP, like most tumor suppressor genes, is evolutionarily conserved among species [85], and its overexpression slows down cell proliferation in vitro [24] while AIP knockdown leads to increased proliferation [90]. As often occurs with other tumor suppressor genes, AIP plays a role in early development: AIP-null mice die during embryonic development due to congenital cardiovascular abnormalities [91,92].

Despite the ubiquitous expression of AIP, no other tumor types have been consistently associated with AIP mutations. Screening in a large series of samples from different types of endocrine and nonendocrine cancer (colorectal, breast, and prostate), revealed that neither germline nor somatic AIP mutations are associated with these neoplasms [93]. Somatic mutations have not been found in pituitary adenomas either [23,24].

AIP Partners

Direct and indirect associations of AIP with a number of proteins, such as aryl-hydrocarbon receptor (AhR), heat shock protein 90 (Hsp90), phosphodiesterases 4A5 (PDE4A5) [94] and 2A (PDE2A), heat shock cognate 70 (Hsc70), survivin, PPAR-α, thyroid hormone receptor β-1 (TRβ1), estrogen receptor (ER)-α, Epstein–Barr virus-encoded nuclear protein 3 (EBNA-3), hepatitis B virus X protein, translocase of the outer membrane of mitochondria 20 (TOMM20), rearranged during transfection tyrosine-kinase receptor (RET), and G-protein α-13 ($G_{\alpha 13}$) have been described (see review [85]). The most studied associations are with AhR, but these may not be the ones involved in the pituitary tumorigenesis pathway.

AhR is a transcription factor whose best known function is as a mediator in the toxic effects (immune, hepatic, cardiac, dermal, teratogenic, endocrine, and carcinogenic) of the environmental toxin 2,3,7,8-tetrachloro-*p*-dioxin (TCDD, dioxin) [95]. Endogenous ligands have been described, such as indigo, indirubin, equilenin, 2-(1′-H-indole-3′-carbonyl)-thiazole-4-carboxylic acid methyl ester, lipoxin 4A, prostaglandin G2, tryptamine, indole acetic acid, 6-formylindolo-[7] carbazole, bilirubin [96], and, most recently, kynurenine [97]. The physiological role of AhR is, apparently, ligand, tissue, and species-specific and includes a wide variety of effects, such as regulation of the activity of nuclear receptors, transcription factors and protein kinases, and modulation of cell cycle, cell adhesion, and migration as well as alteration of multiple intracellular signaling pathways [95]. AhR-dependent transcription is regulated by interactions with multiple partners, thus AhR integrates

signals from diverse ligands and molecular pathways [98]. Although there are some earlier controversial data, more recent studies suggest that AIP inhibits the transcriptional effects of AhR in humans. Some data indicate that AIP modulates AhR levels; this effect is also apparently tissue-specific [85] and potentially relevant for pituitary tumorigenesis.

Ligand-free AhR is localized in the cytoplasm, attached to a heterotetramer composed of a dimer of the chaperone Hsp90 and one unit of each of the co-chaperone proteins p23 [99] and AIP. AIP binds to both Hsp90 and AhR, but Hsp90 is required to model AhR to a ligand-binding configuration. The co-chaperone p23 binds to Hsp90, stabilizing the complex and favoring its nuclear import. After binding dioxin or other exogenous or endogenous ligands, AhR undergoes a conformational change, allowing protein complex translocation to nucleus. In the nucleus, aryl-hydrocarbon receptor nuclear translocator 1 (ARNT, also known as HIF-1β) binds to ligand-bound AhR [100], dissociating it from the rest of the complex. Thus, the ligand:AhR:ARNT complex is able to bind a dioxin-responsive element (DRE), also known as xenobiotic or Ah-responsive element (XRE or AhRE), leading to the activation of AhR-responsive genes [95].

Disruptions in the cyclic adenosine monophosphate (cAMP) molecular pathway are important in pituitary tumorigenesis, and therefore phosphodiesterases, which degrade cAMP, are potentially important AIP interactors. AIP interacts with PDE4A5, causing reversible inhibition of the enzymatic activity of PDE4A5, and attenuation of the ability of cAMP-dependent protein kinase to phosphorylate PDE4A5 [94]. PDE2A is another phosphodiesterase that binds to AIP. This interaction inhibits dioxin and cAMP-induced nuclear translocation of AhR, attenuating AhR-dependent gene transcription [101].

Survivin, a protein involved in cell survival, interacts with AIP. AIP mediates the import of survivin to mitochondria (via TOMM20), thus enabling its anti-apoptotic function [102].

As AIP has numerous partners, it is not clear which one is relevant for pituitary tumorigenesis. The most promising candidates are phosphodiesterases and AhR, as both are involved in the cAMP pathway. The cAMP pathway is known to be important for somatotroph function, as it is the second-messenger pathway for GHRH receptor and also as disruption of this pathway via mutations in GNAS (somatic *GNAS* mutations, so-called 'gsp' mutations, and mosaic mutations in McCune–Albright syndrome) result in pituitary adenomas. Loss of the AIP–PDE4A5 interaction has been demonstrated in vitro with multiple missense and nonsense mutations [24,84]. More functional studies are needed to explain the role of *AIP* mutations in pituitary tumorigenesis, determining if it involves only an absence of tumor suppression activity or if, additionally, mutant proteins acquire oncogenic abilities.

AIP in the Pituitary

AIP is expressed in the normal pituitary, predominantly in somatotroph and lactotroph cells [24,103]. Interestingly, AIP is associated with GH- and PRL-containing vesicles in normal somatotroph and lactotroph cells [24]. Unexpectedly, AIP has been detected in corticotropinomas and it is especially increased in NFPAs (usually of gonadotroph cell origin), while it is absent in normal corticotroph and gonadotroph cells. In addition, in these adenomas AIP is not located in the secretory vesicles but is free in the cytoplasm [24].

In somatotropinomas from FIPA patients, sparsely granulated tumors are more frequent than in sporadic patients; this histological characteristic is associated with increased invasive potential and a poor response to SA [24]. In AIP mutation-positive patients, *AIP* expression is reduced at the level of both mRNA and protein, correlating with invasiveness [103].

The role of AIP in patients with no germline mutations has been studied. Although no somatic *AIP* mutations have been found in pituitary adenomas to date, there is reduced expression of AIP in aggressive somatotroph adenomas compared to less aggressive ones [103,104].

Clinical Features

More than 400 FIPA families have been identified to date. FIPA appears to be more common than

initially thought, but exact prevalence data are not currently available.

FIPA shows an autosomal dominant pattern of inheritance, with incomplete penetrance, around 15–30%, but with a wide variation among families [81,103,105]. The observed earlier diagnosis in the consequent generations is due to patient education regarding the symptoms in other family members [21,106]. Two-thirds of AIP mutation-positive patients are male, but the reason for this remains unclear [106].

Most of FIPA families are composed of 2–5 affected members. Somatotropinomas, prolactinomas, and somatomammotropinomas are the most common tumors [84,106], but NFPA, corticotropinomas, gonadotropinomas, and a thyrotropinoma have also been diagnosed. Families can be categorized as homogeneous, when patients within the same family exhibit the same pituitary tumor type, or heterogeneous, when two or more different tumor types are found within a family [11]. Patients from FIPA kindreds are on average 13–16 years younger at diagnosis than patients with sporadic pituitary adenomas, with a mean age of 33 years [107], but this large difference is due to AIP mutation-positive families.

The phenotype is better defined in AIP mutation-positive patients: most tumors (93.3%) are macroadenomas, commonly invasive [106]. Symptoms start during childhood or young adulthood and the diagnosis is established at a mean age of 18–24 years [106,107]. In more than one-half of patients, the tumors are aggressive [58]. Gigantism is diagnosed in one-third of AIP mutation-positive patients with somatotropinomas, while this condition is rare in sporadic cases [106]. Around 76–78% of *AIP* mutation-positive patients present with somatotropinomas, almost always macroadenomas [106,107]. Nevertheless, in AIP-mutation-positive patients detected as apparent sporadic cases, somatotropinomas account for only 37.5% of tumors [83]. More than one-half cosecrete PRL, while macroprolactinomas arise in 11–13% of patients [106]. The majority of AIP mutation-positive patients require more than one surgical intervention for their treatment and, usually, require a combination of multiple modalities of treatment [106].

Tumors in AIP mutation-positive patients show a considerably reduced response to the treatment with SA and dopamine agonists, regarding both tumor size and hormone secretion [5]. Recent data suggest that AIP is a mediator of the response of somatotropinomas to treatment with SA. AIP is upregulated in sporadic somatotropinomas with preoperative SA treatment, compared to patients with no pretreatment [108]. Similar AIP upregulation was shown in vitro in GH3 cells treated with SA. In addition, AIP overexpression upregulated ZAC1 [108], an antiproliferative target of somatostatin [109]. Another set of data suggest that AIP expression in somatotropinomas is a positive predictor of responsiveness to treatment with SA [110]. These data need to be confirmed in larger studies.

Though AIP mutation-negative patients represent the wide majority of FIPA cases, their clinical features have been less accurately described, perhaps because they represent a genetically heterogeneous population [24]. These patients are 12–16 years older at diagnosis than AIP mutation-positive patients and their tumors are smaller [107,111]. Somatotropinomas predominate (55%), but less markedly than in AIP mutation-positive patients [107]. Although their response to treatment is poor, it is not as bad as in AIP mutation-positive patients [111]. Childhood-onset disease is present in 11% of *AIP* mutation-negative families, while it is demonstrated in 80% of AIP mutation-positive families [107].

Genetic screening is now available for selected patients with pituitary adenomas (Figure 10.3). Follow-up of AIP mutation-positive FIPA families includes genetic testing for all at-risk subjects. For children we suggest genetic screening and, if positive, then follow-up from 4 years of age. Yearly measurement of height and weight, surveillance of height velocity and puberty development with biochemical tests as necessary, and baseline MRI around the age of 10 years are suggested. For adults, follow-up includes baseline clinical assessment, pituitary function tests, and pituitary MRI, followed by yearly pituitary function tests. The likelihood of the development of a pituitary adenoma after the age of 50 years is low.

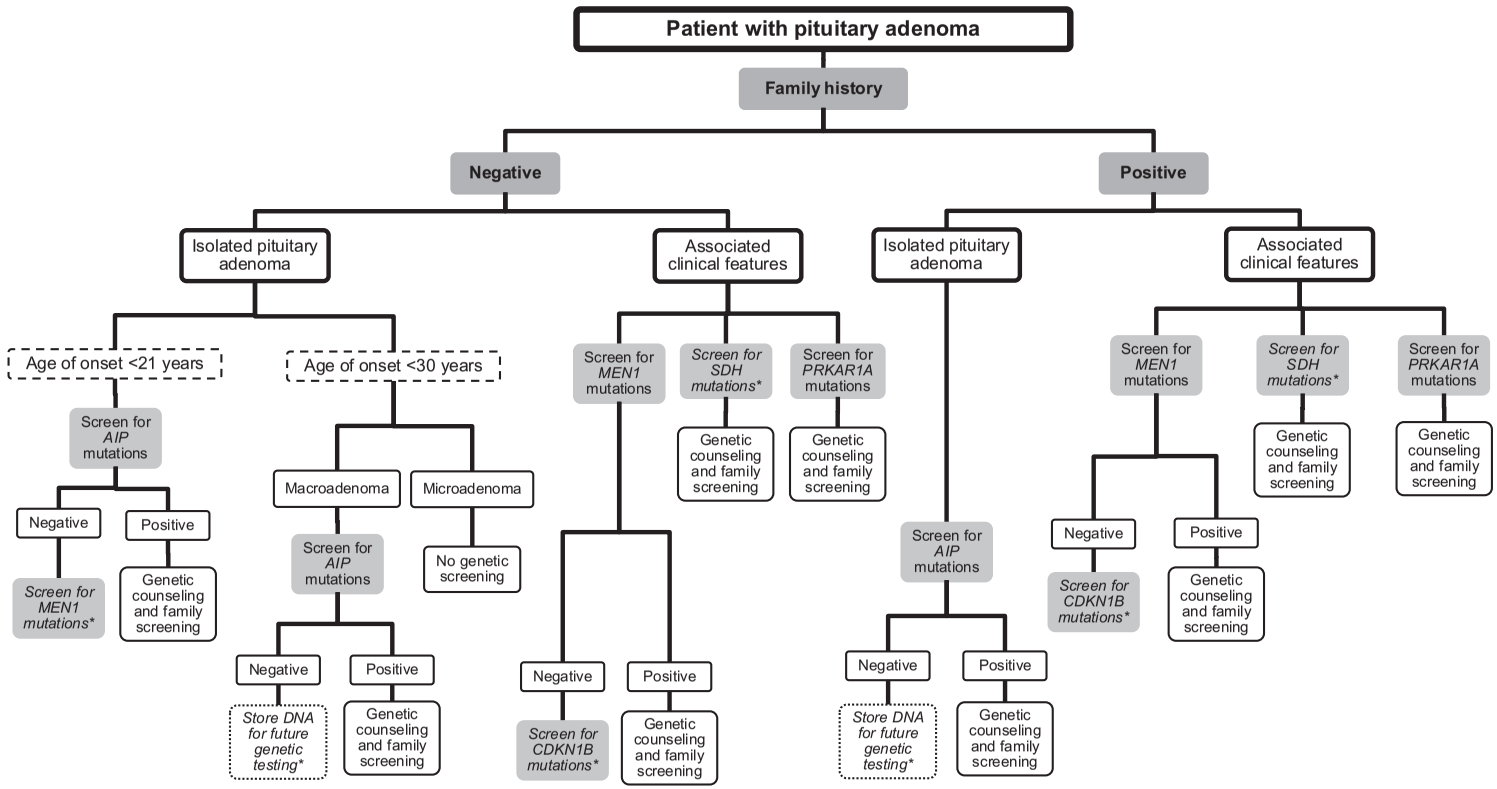

Figure 10.3. Suggested approach for genetic testing in patients with pituitary adenomas. See text. The asterisk (*) indicates there is weak evidence for these suggestions.

Screening of AIP mutation-negative patients is more problematic, as carrier status cannot be established and the penetrance is lower. We suggest education regarding symptoms for all potential carrier subjects and we offer yearly screening for family members who wish to undergo these tests.

Carney Complex

In 1985, Carney and collaborators described the clinical features and reported the first series of patients with myxomas, spotty skin pigmentation and endocrine overactivity [112]. CNC (OMIM #160980 and %605244) is a syndrome characterized by the association of multiple endocrine neoplasia and cardiocutaneous manifestations [113]. A few patients with some components of the complex have previously been described as NAME (nevi, atrial myxomas, and ephelides, i.e., light-brown dermal maculas) or LAMB (lentigines, atrial myxomas, and blue nevi); currently all these cases are grouped as CNC [113,114].

CNC is an infrequent clinical entity: until 2006, around 500 cases had been registered [113]. Patients are from diverse ethnicity and are distributed worldwide [115]. Diagnostic criteria are [114]:

- Spotty skin pigmentation with a typical distribution
- Myxoma (cutaneous and mucosal)
- Cardiac myxoma
- Breast myxomatosis or MRI suggestive image
- Paradoxical positive response of urinary glucocorticoids to dexamethasone (PPNAD)
- Acromegaly
- Large-cell calcifying Sertoli cell tumors (LCCSCT) or characteristic calcification on testicular ultrasonography
- Thyroid carcinoma or multiple hypoechoic thyroid nodules in a young patient
- Psammomatous melanotic schwannoma
- Blue nevus or epithelioid blue nevus (multiple)
- Breast ductal adenoma (multiple)
- Osteochondromyxoma

The diagnosis is established if two major criteria are present or in the presence of one major criterion plus an inactivating PRKAR1A mutation or a first-degree relative with CNC [114,115]. Other clinical manifestations have been associated to CNC, though with a lower frequency: intense freckling, multiple blue nevi, café-au-lait spots, elevated IGF-1 levels, paradoxical GH response to thyrotropin releasing hormone (TRH) or oral glucose tolerance test (OGTT), cardiomyopathy, pilonidal sinus, a history of Cushing's syndrome, acromegaly or sudden death in extended family, multiple skin tags or other lesions, lipomas, colonic polyps, hyperprolactinemia, a single benign thyroid nodule in a young patient or multiple nodules in older patients, and a family history of carcinoma or other benign or malignant tumors [115].

The genetic basis of CNC is heterogeneous, involving at least two loci, as demonstrated by linkage analysis [116]. The *CNC1* gene is located at 17q24.2 and encodes the regulatory subunit 1-α of the protein kinase A (PRKAR1A) [113,117]. *PRKAR1A* is 21 kb in length, contains 11 exons and has a coding region of 1143 bp [54]. Seventy-three percent of patients with CNC present germline mutations in this gene [20]. The CNC2 gene, located at 2p16, is still unknown [118]. This locus frequently presents amplification in tumors of CNC patients, including some with known mutations in PRKAR1A, and thus it is suspected that an oncogene may be implicated [119].

PRKAR1A

Protein kinase A (PKA) acts as a main mediator of cAMP signaling. PKA is a tetramer composed of a regulatory subunit dimer and two catalytic subunits. When four molecules of cAMP bind to the regulatory subunit dimer, catalytic subunits are released to phosphorylate serine or threonine residues in the target protein. The regulatory subunit has four isoforms: Iα, Iβ, IIα, and IIβ, which can pair up as homodimers or type I or type II heterodimers, composing holoenzyme complexes of PKA with a number of combinatorial configurations, including RIα2C2, RIβ2C2, RIIα2C2, RIIβ2C2, and RIαRIβC2 (Figure 10.2).

Experimental downregulation of PRKAR1A with antisense oligonucleotides inhibits growth in human cancer cell lines, while overexpression of type I PKA stimulates cell growth and proliferation, via

interactions with the epidermal growth factor receptor (EGF-R) [120]. Tumors in CNC often present LOH at 17q22–24, supporting the role or PRKAR1A as a tumor suppressor gene [117].

Mutations in PRKAR1A are distributed throughout the gene, with higher frequency in exons 2, 3, 5, 7, and 8 [20]. Almost 80% of PRKAR1A mutations originate in a premature stop codon, but truncated proteins are not expressed [20,121]. The abnormal mRNA transcribed from the affected allele is destroyed by a mechanism called nonsense mediated decay (NMD), in which the cells degrade mRNA containing a deleterious premature stop codon mutation prior to its translation [120]. This loss of expression of PRKAR1A in CNC tumors leads to a reduced regulatory activity over PKA, but also to compensatory increases in the other PKA subunits [117]. These alterations derive in an increased response of PKA to cAMP, with upregulation of this important signaling pathway [120].

There is no clear genotype–phenotype correlation for most of the mutations in CNC [122], although the intronic deletion exon7 IVS del(−7→−2) is related to isolated PPNAD [123]. Differences in presentation of molecular defects and clinical features may be due to disease-modifying genes located at other loci [116,122]. In a cohort of CNC patients, variants of the phosphodiesterase type 11A gene (PDE11A) showed association with a higher incidence of PPNAD and LCCSCT, suggesting that PDE11A can modify the phenotype [124]. No association was found with other components of the complex.

PRKAR1A$^{-/-}$ mice are not viable. Lethality occurs during embryogenesis, due to a failure in mesoderm-derived structures [25]. Pituitary-conditional PRKAR1A$^{-/-}$ mice develop pituitary adenomas with a higher frequency than their littermates. These tumors are sometimes multiple and immunohistochemistry is positive for GH, PRL, and thyroid-stimulating hormone (TSH) [25]. PRKAR1A$^{+/-}$ mice are prone to develop tumors in some cAMP-responsive tissues, such as bone, Schwann cells, and thyroid, but not myxomas or pituitary adenomas [125,126]. E2f, a downstream effector of Rb, mediates the proliferative effects of defective PRKAR1A, and E2f activity is regulated by p53, providing a link between these tumor suppressor genes [125,127]. PRKAR1A haploinsufficiency causes an increase in cAMP levels, leading to increased MAPK activity, while complete PRKAR1A deficiency causes constitutive activation of PKA and immortalization of mouse embryonic fibroblasts (MEF) through upregulation of cyclin D1 in vitro [125]. Multiple elements of the Wnt signaling pathway are overexpressed in different tumors from PRKAR1A$^{+/-}$, PRKAR1A$^{+/-}$/Trp53$^{+/-}$, PRKAR1A$^{+/-}$/Rb1$^{+/-}$ and PRKAR1A$^{+/-}$/Prkaca$^{+/-}$ mice, suggesting its implication in PRKAR1A-derived tumorigenesis [125,126,128]. A microarray analysis of tumors from 3 mouse models of PRKAR1A haploinsufficiency (PRKAR1A$^{+/-}$, PRKAR1A$^{+/-}$/Trp53$^{+/-}$ and PRKAR1A$^{+/-}$/Rb1$^{+/-}$) identified Wnt signaling as the main pathway activated by abnormal cAMP signaling, along with the mentioned cell cycle abnormalities [125]. In human tissue from PPNAD, PKA activates the expression of WISP2, a component of the WNT signaling pathway, via microRNA regulation [129].

Twenty percent of patients present PRKAR1A mutations in intronic sequences that affect splicing [20]. At least some of these mutations escape from NMD, leading to expression of the truncated protein [130]. LOH is not a universal finding in CNC tumors [20], and in vitro the expression of an abnormal PRKAR1A without concomitant loss of the normal allele causes increased PKA activity [130]. The contribution of possible PKA-independent effects due to different protein interactions cannot be discounted [20].

Clinical Features

CNC is inherited as an autosomal dominant trait [114]. Penetrance for CNC due to PRKAR1A is almost complete for some of the manifestations [20,131]. Clinical manifestations are variable, even within members of the same family. Thirty-two percent of cases present as simplex (sporadic) disease [20]. More than 85% of simplex cases with a PRKAR1A mutation have a de-novo mutation [20].

Lentiginosis is the most common feature of CNC (70% of patients) [20] and is present in half of patients before other components of the complex arise [120]. It consists of 2–10 mm brown to black

macules, distributed on the lips, eyelids, ears, and genital area [113]. Lesions can be present at birth, but do not acquire their clinical characteristics until puberty [114]. Half of patients present others skin lesions, such as blue, Spitz, and compound nevi and café-au-lait spots [20]. Skin myxomas are found in 20% of patients in eyelids, external ear canal, nipple, oropharynx, female genital tract, and female pelvis [20,114]. Twenty percent of female patients present breast myxomas [20], and a few cases of breast ductal adenoma have also been reported [114].

Cardiac myxomas are detected in 32% of cases [20]. In the setting of CNC, these tumors occur at any age, are multicentric, can be present in any cardiac chamber, tend to recur, and can grow aggressively [113]. Surgical resection is necessary to avoid complications such as embolism, strokes, and cardiac failure.

ACTH-independent Cushing's syndrome due to PPNAD is the main endocrine manifestation of CNC (60% of patients) [20,114]. PPNAD almost always occurs in the context of CNC, but a very infrequent sporadic form also exists [127]. It has a bimodal age distribution: most cases are diagnosed during the second and third decades of life but a minority present at 2–3 years of age [114]. Adrenal histology in PPNAD is characterized by small pigmented micronodules, with minimal atrophy or hyperplastic perinodular cortex, positive for synaptophysin and multiple steroidogenic enzymes by immunohistochemistry [120]. The disease is usually bilateral [113]. The adrenal glands do not always show an obvious enlargement on imaging studies as nodules can be very small [113]. Hypercortisolism generally progresses subtly over years or follows a cyclic pattern, but the circadian cycle of cortisol is completely abolished, sometimes even in periods of inactive disease [115,132]. Pseudoprecocious puberty or hirsutism can appear [132]. Diagnosis is better established with the 6-day Liddle test, showing a paradoxical increase in the 24-hour urinary free cortisol and/or 17-hydroxysteroids [132,133]. This test is performed as follows: after 2 days of baseline measurements of urinary steroid excretion, 0.5 mg of dexamethasone are administered orally every 6 hours for 2 days, starting at 06:00 hours; then the dosage is increased to 2 mg every 6 hours for 2 days more. The 6-day Liddle test is considered positive if there is an increase of 50% or more in urinary free cortisol levels on day 6 (sensitivity 69.2%) [133]. Bilateral adrenalectomy is the treatment of choice for PPNAD; however, some patients respond to ketoconazole or mitotane [115,132].

LCCSCT is a common (41% of male patients) [20] and almost always benign tumor in CNC; it usually appears in the first decade of life, most often detected by ultrasonography as microcalcifications [115]. This tumor can rarely lead to gynecomastia and precocious puberty, but impairment of fertility (due to obstruction of seminiferous tubules or inappropriate hormone production or aromatization) is common. Adrenal rests and Leydig cell tumors can exist concomitantly with LCCSCT. Ovarian cysts and cystadenoma have been found in some patients [115].

Thyroid nodules are present in 25% of patients and usually correspond to nontoxic adenomas of follicular type [20,113,114]. Thyroid cancer (follicular or papillary) develop in up to 10% of CNC patients with previous thyroid nodules [115].

Psammomatous melanotic schwannoma (PMS) is a very rare tumor that can arise in any peripheral nerve, usually in the gastrointestinal tract and paraspinal sympathetic chain; it is pigmented, multicentric, and frequently calcified [114]. It is found in 8% of CNC patients [20] and in 10% of cases is malignant and metastasizes to lungs, liver, or brain [115].

The possible association between CNC and pancreatic neoplasms has recently been proposed. There is an unexpectedly high prevalence (2.5%) of pancreatic neoplasms within CNC patients, some of them of a very uncommon histological type (acinar cell carcinoma) [134]. Most of the analyzed cases presented LOH at chromosome 17 and loss of PRKAR1A immunostaining [134]. The main CNC-related cause of death is metastasic cancer (56% of deaths) and pancreatic cancer accounts for one-third of cancer-related deaths in CNC patients [20].

Osteochondromyxomas of the bone and tetralogy of Fallot have been found in some CNC patients

and are possible components of the syndrome [114].

Pituitary Adenomas

In the pituitary, GHRH requires the cAMP/PKA pathway to stimulate GH synthesis and release [25]. Other hormones are mainly regulated by different pathways, thus they are not affected by PRKAR1A mutations. Pituitary tumorigenesis in the context of CNC is a slow-developing process that requires mutation accumulation ("multiple hits") [135]. Apparently, in CNC patients, germline mutations cause a predisposition, but other molecular events are necessary for pituitary adenoma development [135].

Histologically, pituitaries of CNC patients show zones of mammosomatotroph hyperplasia, that only occasionally progress to adenomatous tissue [135]. This "pro-acromegalic state" is a common characteristic shared by CNC and McCune–Albright syndrome, in which the same molecular pathway is disturbed, but at a different level [136]. By immunohistochemistry, almost all somatotropinomas also stain for PRL and most tumors stain for multiple hormones, but, although staining for glycoprotein α-subunit, TSH-β, luteinizing hormone (LH)-β and occasionally follicle-stimulating hormone (FSH)-β has been described, staining for ACTH has not been reported [25,136]. Microadenomas are much more common than macroadenomas; they are frequently multiple, sometimes microscopic, and commonly grow surrounded by hyperplastic tissue [135,136]. Electron microscopy features are highly variable: from mammosomatotroph cells with abundant rough endoplasmic reticulum, immature secretory granules, and a small percentage (1%) of densely granulated cells, to sparsely granulated cells with poorly developed endoplasmic reticulum, and fibrous bodies, or a mixture of both types of cells [136]. Aggressive pituitary adenomas in CNC show genetic instability, whereas cytogenetic abnormalities are absent in hyperplasia or microadenomas [135]. Though LOH of 17q is expected in pituitary adenomas of CNC patients with PRKAR1A mutations, it is not always detected [25]. PRKAR1A mutations have not been found in sporadic pituitary tumors [22], but low levels of PRKAR1A have been detected in sporadic functioning and nonfunctioning pituitary adenomas, despite adequate mRNA [137].

Clinically evident acromegaly is a relatively infrequent manifestation of CNC; the incidence of GH-producing pituitary tumors in CNC is 12% [20]. Nevertheless, paradoxical GH responses to TRH or nonsuppressible GH during a glucose challenge and/or IGF-1 elevation are present in up to 80% of patients, even in the absence of detectable tumors [114]. Acromegaly in CNC patients shows a slow progressive course [135]. In some patients it only becomes apparent after the patient undergoes bilateral adrenalectomy for Cushing's syndrome [67]. Pituitary tumors in CNC are almost exclusively GH or GH/PRL-secreting tumors. Around two-thirds of CNC patients have a mild hyperprolactinemia (generally <100 ng/mL), but there are few cases of frank prolactinomas [25].

Regular screening for the manifestations of the disease is recommended for patients with CNC and known carriers of PRKAR1A mutations. Screening for cardiac myxomas by echocardiography must start at diagnosis or during the first 6 months of life, and be done yearly thereafter [114]. If a cardiac myxoma was excised in the past, echocardiography is necessary every 6 months [115]. During childhood, screening for the other manifestations should be performed only by clinical examination, because, although possible, it is rare to detect endocrine tumors in CNC before the second decade of life [115]. Pubertal staging and growth rate must be monitored [113]. Additionally, for postpubertal patients the following annual studies are recommended: urinary free cortisol determination (plus diurnal cortisol or overnight 1 mg dexamethasone test), serum IGF-1 and testicular ultrasonography in male patients [114]. Brain and spine MRI should be obtained at diagnosis and repeated only if clinical signs suggest the possibility of a schwannoma [115]. Pelvic ultrasonography in women is recommended at diagnosis and then as needed [114]. Thyroid ultrasonography is indicated at diagnosis and then as clinically indicated [114]. There are no specific recommendations regarding pancreatic cancer.

Other Possible Familial Pituitary Adenoma Syndromes

Pituitary Blastoma

Pituitary blastoma is a very rare and aggressive, apparently congenital, pituitary tumor. Only two cases have been reported to date, both in infants with Cushing's disease [6,138]. Nevertheless, a recent review considered the possibility of this diagnosis in three further cases (two corticotropinomas and one nonsecretory tumor), reported in the literature as adenomas [139]. The most recent case was reported by Wildi-Runge and colleagues in a 9-month-old boy with Cushing's syndrome and a familial history of pleuropulmonary blastoma in a second cousin and renal cysts and an ovarian tumor in a grandmother [6]. Genetic analysis showed a mutation in the RNase endonuclease gene DICER1 as the possible cause [6]. The genetic cause was not assessed in the remaining cases.

CDKIs

A mutation in the gene encoding the CDKI p21 (CDKN1A) was described in two sisters with a MEN1-like syndrome of primary hyperparathyroidism and macroprolactinoma [14]. Mutations in the genes encoding the CDKIs p15 and p18 (CDKN2B and CDKN2C, respectively) have also been detected in the context of multiple endocrine neoplasia, but these cases have not included pituitary tumors as part of the syndrome [14].

Pheochromocytoma/Paraganglioma and Pituitary Adenoma

Although it was not considered as a syndrome until recently, coexistence of pheochromocytoma/paraganglioma and a pituitary adenoma (usually a somatotropinoma) has been previously reported in the literature [140]. Mutations in the genes encoding subunits A, B, C, and D of the SDH mitochondrial complex II are known to be associated with the development of pheochromocytomas, paragangliomas, gastrointestinal stromal tumors, renal and papillary thyroid cancer, neuroblastoma, adrenal medullary hyperplasia, and testicular seminoma [7,141]. A germline missense mutation in *SDHB* has been described in association with familial paragangliomas, together with a prolactinoma in one individual [9]. A germline frameshift mutation in SDHD was related to multiple paragangliomas and bilateral pheocromocytomas together with a somatotropinoma in a member of a kindred with familial paragangliomas [7]. A germline missense mutation in SDHC was described in a family with paragangliomas and prolactinomas. In the families with the SDHB and SDHD mutation, LOH at the respective loci was demonstrated in a prolactinoma and a somatotropinoma, respectively, in the index cases. Though still scarce, these data support the possibility of a new association between paraganglioma and pituitary adenoma.

Recommendations for Genetic Screening of Patients with Pituitary Adenomas

With the technical advancement of DNA sequencing, block screening of several or all of the candidate genes might overtake gene-by-gene screening in the future. However, careful assessment of clinical features of the patient and family history remains crucially important and should be able to distinguish most, although not all, cases of MEN1, MEN4, FIPA, CNC, SDH-related or pituitary blastoma phenotypes, allowing for targeted gene screening (Figure 10.3):

- If clinical features of MEN1 are present, then MEN1 screening is recommended. Screening for CDKNB1 mutations can be performed on special request.
- In patients with pituitary adenomas and clinical findings compatible with CNC, PRKAR1A mutations can be searched for.
- In patients with pituitary adenomas and pheochromocytoma/paraganglioma, SDH mutations could be looked for.
- Patients with a family history of pituitary adenoma and no other syndromic features should be screened for AIP mutations.
- Screening for AIP mutations is suggested in isolated cases of macro or microadenoma, without

syndromic features, diagnosed before the age of 21 years [67].

• Data supports the recommendation for patients with pituitary macroadenomas diagnosed before the age of 30 years to be screened for AIP mutations, even in the absence of relevant family history [5].

• For young patients with prolactinomas and somatotropinomas and no AIP mutation, genetic testing for MEN1 mutations can be considered [4].

• Cushing's disease diagnosed during infancy might be an indication for DICER1 mutation screening, though the scarcity of data precludes the establishment of a firm recommendation.

Genetic counseling is essential for these patients and their relatives. Follow-up of mutation carriers, by clinical, biochemical, and imaging studies, can lead to earlier pituitary tumor detection, allowing more efficient treatment [21]. For family studies, the high prevalence of pituitary incidentalomas must be kept in mind. FIPA patients, with or without AIP mutations, and their families should be informed about the low penetrance of the disease in order to avoid unnecessary concern.

References

1. Melmed S. Acromegaly pathogenesis and treatment. *J Clin Invest* 2009; **119**: 3189–3202.
2. Couldwell WT, Cannon-Albright L. A heritable predisposition to pituitary tumors. *Pituitary* 2010; **13**: 130–137.
3. Nozieres C, Berlier P, Dupuis C, et al. Sporadic and genetic forms of paediatric somatotropinoma: a retrospective analysis of seven cases and a review of the literature. *Orphanet J Rare Dis* 2011; **6**: 67.
4. Stratakis CA, Tichomirowa MA, Boikos S, et al. The role of germline AIP, MEN1, PRKAR1A, CDKN1B and CDKN2C mutations in causing pituitary adenomas in a large cohort of children, adolescents, and patients with genetic syndromes. *Clin Genet* 2010; **78**: 457–463.
5. Tichomirowa MA, Barlier A, Daly AF, et al. High prevalence of AIP gene mutations following focused screening in young patients with sporadic pituitary macroadenomas. *Eur J Endocrinol* 2011; **165**: 509–515.
6. Wildi-Runge S, Bahubeshi A, Carret A, et al. New phenotype in the familial DICER1 tumor syndrome: pituitary blastoma presenting at age 9 months (abstract). *Endocr Rev* 2011; **32**: P1–777.
7. Xekouki P, Pacak K, Almeida M, et al. Succinate dehydrogenase (SDH) D subunit (SDHD) inactivation in a growth-hormone-producing pituitary tumor: a new association for SDH? *J Clin Endocrinol Metab* 2012; **97**: E357–366.
8. Denes J, Swords FM, Xekouki P, et al. Familial pituitary adenoma and paraganglioma syndrome – a novel type of multiple endocrine neoplasia. *Endocr Rev* 2012; **33**(04_MeetingAbstracts): OR41–2.
9. Brahma A, Heyburn P, Swords F. Familial prolactinoma occuring in association with SDHB mutation positive paraganglioma. *Endocr Abstrs* Spring 2009; **19**: 239.
10. Scheithauer BW, Laws ER Jr., Kovacs K, et al. Pituitary adenomas of the multiple endocrine neoplasia type I syndrome. *Semin Diagn Pathol* 1987; **4**: 205–211.
11. Daly AF, Jaffrain-Rea ML, Ciccarelli A, et al. Clinical characterization of familial isolated pituitary adenomas. *J Clin Endocrinol Metab* 2006; **91**: 3316–3323.
12. Pellegata NS, Quintanilla-Martinez L, Siggelkow H, et al. Germ-line mutations in p27Kip1 cause a multiple endocrine neoplasia syndrome in rats and humans. *Proc Natl Acad Sci U S A* 2006; **103**: 15558–15563.
13. Georgitsi M, Raitila A, Karhu A, et al. Germline CDKN1B/p27Kip1 mutation in multiple endocrine neoplasia. *J Clin Endocrinol Metab* 2007; **92**: 3321–3325.
14. Agarwal SK, Mateo CM, Marx SJ. Rare germline mutations in cyclin-dependent kinase inhibitor genes in multiple endocrine neoplasia type 1 and related states. *J Clin Endocrinol Metab* 2009; **94**: 1826–1834.
15. Molatore S, Marinoni I, Lee M, et al. A novel germline CDKN1B mutation causing multiple endocrine tumors: clinical, genetic and functional characterization. *Hum Mutat* 2010; **31**: E1825–1835.
16. Malanga D, De GS, Riccardi M, et al. Functional characterization of a rare germline mutation in the gene encoding the cyclin-dependent kinase inhibitor p27Kip1 (CDKN1B) in a Spanish patient with multiple endocrine neoplasia (MEN)-like phenotype. *Eur J Endocrinol* 2012; **166**: 551–560.
17. Belar O, De la Hoz C, Perez-Nanclares G, Castano L, Gaztambide S. Novel mutations in Men1, CDKN1b

and AIP genes in patients with multiple endocrine neoplasia type 1 syndrome in Spain. *Clin Endocrinol (Oxf)* 2012; **76**: 719–724.

18. Tichomirowa MA, Lee M, Barlier A, et al. Cyclin dependent kinase inhibitor 1B (CDKN1B) gene variants in AIP mutation-negative familial isolated pituitary adenomas (FIPA) kindreds. *Endocr Relat Cancer* 2012; **19**: 233–241.
19. Lemos MC, Thakker RV. Multiple endocrine neoplasia type 1 (MEN1): analysis of 1336 mutations reported in the first decade following identification of the gene. *Hum Mutat* 2008; **29**: 22–32.
20. Bertherat J, Horvath A, Groussin L, et al. Mutations in regulatory subunit type 1A of cyclic adenosine 5′-monophosphate-dependent protein kinase (PRKAR1A): phenotype analysis in 353 patients and 80 different genotypes. *J Clin Endocrinol Metab* 2009; **94**: 2085–2091.
21. Chahal HS, Chapple JP, Frohman LA, Grossman AB, Korbonits M. Clinical, genetic and molecular characterization of patients with familial isolated pituitary adenomas (FIPA). *Trends Endocrinol Metab* 2010; **21**: 419–427.
22. Kaltsas GA, Kola B, Borboli N, et al. Sequence analysis of the PRKAR1A gene in sporadic somatotroph and other pituitary tumours. *Clin Endocrinol (Oxf)* 2002; **57**: 443–448.
23. Barlier A, Vanbellinghen JF, Daly AF, et al. Mutations in the aryl hydrocarbon receptor interacting protein gene are not highly prevalent among subjects with sporadic pituitary adenomas. *J Clin Endocrinol Metab* 2007; **92**: 1952–1955.
24. Leontiou CA, Gueorguiev M, van der Spuy J, et al. The role of the aryl hydrocarbon receptor-interacting protein gene in familial and sporadic pituitary adenomas. *J Clin Endocrinol Metab* 2008; **93**: 2390–2401.
25. Kirschner LS. PRKAR1A and the evolution of pituitary tumors. *Mol Cell Endocrinol* 2010; **326**: 3–7.
26. Wermer P. Genetic aspects of adenomatosis of endocrine glands. *Am J Med* 1954; **16**: 363–371.
27. Brandi ML, Gagel RF, Angeli A, et al. Guidelines for diagnosis and therapy of MEN type 1 and type 2. *J Clin Endocrinol Metab* 2001; **86**: 5658–5671.
28. Larsson C, Skogseid B, Oberg K, Nakamura Y, Nordenskjold M. Multiple endocrine neoplasia type 1 gene maps to chromosome 11 and is lost in insulinoma. *Nature* 1988; **332**: 85–87.
29. Chandrasekharappa SC, Guru SC, Manickam P, et al. Positional cloning of the gene for multiple endocrine neoplasia-type 1. *Science* 1997; **276**: 404–407.
30. Lemmens I, Van de Ven WJ, Kas K, et al. Identification of the multiple endocrine neoplasia type 1 (MEN1) gene. The European Consortium on MEN1. *Hum Mol Genet* 1997; **6**: 1177–1183.
31. Bassett JH, Forbes SA, Pannett AA, et al. Characterization of mutations in patients with multiple endocrine neoplasia type 1. *Am J Hum Genet* 1998; **62**: 232–244.
32. Pannett AA, Thakker RV. Somatic mutations in MEN type 1 tumors, consistent with the Knudson "two-hit" hypothesis. *J Clin Endocrinol Metab* 2001; **86**: 4371–4374.
33. Crabtree JS, Scacheri PC, Ward JM, et al. A mouse model of multiple endocrine neoplasia, type 1, develops multiple endocrine tumors. *Proc Natl Acad Sci U S A* 2001; **98**: 1118–1123.
34. Crabtree JS, Scacheri PC, Ward JM, et al. Of mice and MEN1: Insulinomas in a conditional mouse knockout. *Mol Cell Biol* 2003; **23**: 6075–6085.
35. Bertolino P, Tong WM, Galendo D, Wang ZQ, Zhang CX. Heterozygous Men1 mutant mice develop a range of endocrine tumors mimicking multiple endocrine neoplasia type 1. *Mol Endocrinol* 2003; **17**: 1880–1892.
36. Guru SC, Goldsmith PK, Burns AL, et al. Menin, the product of the MEN1 gene, is a nuclear protein. *Proc Natl Acad Sci U S A* 1998; **95**: 1630–1634.
37. Guru SC, Crabtree JS, Brown KD, et al. Isolation, genomic organization, and expression analysis of Men1, the murine homolog of the MEN1 gene. *Mamm Genome* 1999; **10**: 592–596.
38. Taguchi R, Yamada M, Horiguchi K, et al. Haploinsufficient and predominant expression of multiple endocrine neoplasia type 1 (MEN1)-related genes, MLL, p27(Kip1] and p18(Ink4C) in endocrine organs. *Biochem Biophys Res Commun* 2011.
39. Wu T, Hua X. Menin represses tumorigenesis via repressing cell proliferation. *Am J Cancer Res* 2011; **1**: 726–739.
40. Kaji H, Canaff L, Lebrun JJ, Goltzman D, Hendy GN. Inactivation of menin, a Smad3-interacting protein, blocks transforming growth factor type beta signaling. *Proc Natl Acad Sci U S A* 2001; **98**: 3837–3842.
41. Ikeo Y, Yumita W, Sakurai A, Hashizume K. JunD-menin interaction regulates c-Jun-mediated AP-1 transactivation. *Endocr J* 2004; **51**: 333–342.
42. Heppner C, Bilimoria KY, Agarwal SK, et al. The tumor suppressor protein menin interacts with NF-kappaB proteins and inhibits NF-kappaB-mediated transactivation. *Oncogene* 2001; **20**: 4917–4925.

43. Dreijerink KM, Varier RA, van Nuland R, et al. Regulation of vitamin D receptor function in MEN1-related parathyroid adenomas. *Mol Cell Endocrinol* 2009; **313**: 1–8.
44. La P, Schnepp RW, Petersen D, Silva C, Hua X. Tumor suppressor menin regulates expression of insulin-like growth factor binding protein 2. *Endocrinology* 2004; **145**: 3443–3450.
45. Fontaniere S, Tost J, Wierinckx A, et al. Gene expression profiling in insulinomas of Men1 beta-cell mutant mice reveals early genetic and epigenetic events involved in pancreatic beta-cell tumorigenesis. *Endocr Relat Cancer* 2006; **13**: 1223–1236.
46. Cao Y, Liu R, Jiang X, et al. Nuclear-cytoplasmic shuttling of menin regulates nuclear translocation of {beta}-catenin. *Mol Cell Biol* 2009; **29**: 5477–5487.
47. Sukhodolets KE, Hickman AB, Agarwal SK, et al. The 32-kilodalton subunit of replication protein A interacts with menin, the product of the MEN1 tumor suppressor gene. *Mol Cell Biol* 2003; **23**: 493–509.
48. Jin S, Mao H, Schnepp RW, et al. Menin associates with FANCD2, a protein involved in repair of DNA damage. *Cancer Res* 2003; **63**: 4204–4210.
49. Hashimoto M, Kyo S, Hua X, et al. Role of menin in the regulation of telomerase activity in normal and cancer cells. *Int J Oncol* 2008; **33**: 333–340.
50. Obungu VH, Lee BA, Agarwal SK, et al. Menin, a tumor suppressor, associates with nonmuscle myosin II-A heavy chain. *Oncogene* 2003; **22**: 6347–6358.
51. Lopez-Egido J, Cunningham J, Berg M, et al. Menin's interaction with glial fibrillary acidic protein and vimentin suggests a role for the intermediate filament network in regulating menin activity. *Exp Cell Res* 2002; **278**: 175–183.
52. Bertolino P, Radovanovic I, Casse H, et al. Genetic ablation of the tumor suppressor menin causes lethality at mid-gestation with defects in multiple organs. *Mech Dev* 2003; **120**: 549–560.
53. Goudet P, Bonithon-Kopp C, Murat A, et al. Gender-related differences in MEN1 lesion occurrence and diagnosis: a cohort study of 734 cases from the Groupe d'Etude des Tumeurs Endocrines. *Eur J Endocrinol* 2011; **165**: 97–105.
54. Horvath A, Stratakis CA. Clinical and molecular genetics of acromegaly: MEN1, Carney complex, McCune-Albright syndrome, familial acromegaly and genetic defects in sporadic tumors. *Rev Endocr Metab Disord* 2008; **9**: 1–11.
55. Marini F, Falchetti A, Del MF, et al. Multiple endocrine neoplasia type 1. *Orphanet J Rare Dis* 2006; **1**: 38.
56. Pieterman CR, Schreinemakers JM, Koppeschaar HP, et al. Multiple endocrine neoplasia type 1 (MEN1): its manifestations and effect of genetic screening on clinical outcome. *Clin Endocrinol (Oxf)* 2009; **70**: 575–581.
57. Trump D, Farren B, Wooding C, et al. Clinical studies of multiple endocrine neoplasia type 1 (MEN1). *QJM* 1996; **89**: 653–669.
58. Vasilev V, Daly AF, Petrossians P, Zacharieva S, Beckers A. Familial pituitary tumor syndromes. *Endocr Pract* 2011; **17 Suppl 3**: 41–46.
59. Ghazi AA, Dezfooli AA, Mohamadi F, et al. Cushing syndrome secondary to a thymic carcinoid tumor due to multiple endocrine neoplasia type 1. *Endocr Pract* 2011; **17**: e92–96.
60. Machens A, Schaaf L, Karges W, et al. Age-related penetrance of endocrine tumours in multiple endocrine neoplasia type 1 (MEN1): a multicentre study of 258 gene carriers. *Clin Endocrinol (Oxf)* 2007; **67**: 613–622.
61. Verges B, Boureille F, Goudet P, et al. Pituitary disease in MEN type 1 (MEN1): data from the France-Belgium MEN1 multicenter study. *J Clin Endocrinol Metab* 2002; **87**: 457–465.
62. Farrell WE, Azevedo MF, Batista DL, et al. Unique gene expression profile associated with an early-onset multiple endocrine neoplasia (MEN1)-associated pituitary adenoma. *J Clin Endocrinol Metab* 2011; **96**: E1905–1914.
63. Benito M, Asa SL, Livolsi VA, West VA, Snyder PJ. Gonadotroph tumor associated with multiple endocrine neoplasia type 1. *J Clin Endocrinol Metab* 2005; **90**: 570–574.
64. Trouillas J, Labat-Moleur F, Sturm N, et al. Pituitary tumors and hyperplasia in multiple endocrine neoplasia type 1 syndrome (MEN1): a case-control study in a series of 77 patients versus 2509 non-MEN1 patients. *Am J Surg Pathol* 2008; **32**: 534–543.
65. Capella C, Riva C, Leutner M, La RS. Pituitary lesions in multiple endocrine neoplasia syndrome (MENS) type 1. *Pathol Res Pract* 1995; **191**: 345–347.
66. Marinoni I, Pellegata NS. p27kip1: a new multiple endocrine neoplasia gene? *Neuroendocrinology* 2011; **93**: 19–28.

67. Xekouki P, Azevedo M, Stratakis CA. Anterior pituitary adenomas: inherited syndromes, novel genes and molecular pathways. *Expert Rev Endocrinol Metab* 2010; **5**: 697–709.
68. Ozawa A, Agarwal SK, Mateo CM, et al. The parathyroid/pituitary variant of multiple endocrine neoplasia type 1 usually has causes other than p27Kip1 mutations. *J Clin Endocrinol Metab* 2007; **92**: 1948–1951.
69. Igreja S, Chahal HS, Akker SA, et al. Assessment of p27 (cyclin-dependent kinase inhibitor 1B) and aryl hydrocarbon receptor-interacting protein (AIP) genes in multiple endocrine neoplasia (MEN1) syndrome patients without any detectable MEN1 gene mutations. *Clin Endocrinol (Oxf)* 2009; **70**: 259–264.
70. Owens M, Stals K, Ellard S, Vaidya B. Germline mutations in the CDKN1B gene encoding p27 Kip1 are a rare cause of multiple endocrine neoplasia type 1. *Clin Endocrinol (Oxf)* 2009; **70**: 499–500.
71. Georgitsi M. MEN-4 and other multiple endocrine neoplasias due to cyclin-dependent kinase inhibitors (p27(Kip1] and p18(INK4C)) mutations. *Best Pract Res Clin Endocrinol Metab* 2010; **24**: 425–437.
72. Sgambato A, Cittadini A, Faraglia B, Weinstein IB. Multiple functions of p27(Kip1] and its alterations in tumor cells: a review. *J Cell Physiol* 2000; **183**: 18–27.
73. Chu IM, Hengst L, Slingerland JM. The Cdk inhibitor p27 in human cancer: prognostic potential and relevance to anticancer therapy. *Nat Rev Cancer* 2008; **8**: 253–267.
74. Besson A, Hwang HC, Cicero S, et al. Discovery of an oncogenic activity in p27Kip1 that causes stem cell expansion and a multiple tumor phenotype. *Genes Dev* 2007; **21**: 1731–1746.
75. Fero ML, Rivkin M, Tasch M, et al. A syndrome of multiorgan hyperplasia with features of gigantism, tumorigenesis, and female sterility in p27(Kip1]-deficient mice. *Cell* 1996; **85**: 733–744.
76. Dahia PL, Aguiar RC, Honegger J, et al. Mutation and expression analysis of the p27/kip1 gene in corticotrophin-secreting tumours. *Oncogene* 1998; **16**: 69–76.
77. Fero ML, Randel E, Gurley KE, Roberts JM, Kemp CJ. The murine gene p27Kip1 is haploinsufficient for tumour suppression. *Nature* 1998; **396**: 177–180.
78. Pellegata NS, Quintanilla-Martinez L, Keller G, et al. Human pheochromocytomas show reduced p27Kip1 expression that is not associated with somatic gene mutations and rarely with deletions. *Virchows Arch* 2007; **451**: 37–46.
79. Lidhar K, Korbonits M, Jordan S, et al. Low expression of the cell cycle inhibitor p27Kip1 in normal corticotroph cells, corticotroph tumors, and malignant pituitary tumors. *J Clin Endocrinol Metab* 1999; **84**: 3823–3830.
80. Bamberger CM, Fehn M, Bamberger AM, et al. Reduced expression levels of the cell-cycle inhibitor p27Kip1 in human pituitary adenomas. *Eur J Endocrinol* 1999; **140**: 250–255.
81. Vierimaa O, Georgitsi M, Lehtonen R, et al. Pituitary adenoma predisposition caused by germline mutations in the AIP gene. *Science* 2006; **312**: 1228–1230.
82. Daly AF, Vanbellinghen JF, Khoo SK, et al. Aryl hydrocarbon receptor-interacting protein gene mutations in familial isolated pituitary adenomas: analysis in 73 families. *J Clin Endocrinol Metab* 2007; **92**: 1891–1896.
83. Cazabat L, Bouligand J, Salenave S, et al. Germline AIP mutations in apparently sporadic pituitary adenomas: prevalence in a prospective single-center cohort of 443 patients. *J Clin Endocrinol Metab* 2012; **97**: E663–670.
84. Igreja S, Chahal HS, King P, et al. Characterization of aryl hydrocarbon receptor interacting protein (AIP) mutations in familial isolated pituitary adenoma families. *Hum Mutat* 2010; **31**: 950–960.
85. Trivellin G, Korbonits M. AIP and its interacting partners. *J Endocrinol* 2011; **210**: 137–155.
86. Allan RK, Ratajczak T. Versatile TPR domains accommodate different modes of target protein recognition and function. *Cell Stress Chaperones* 2011; **16**: 353–367.
87. Ozfirat Z, Korbonits M. AIP gene and familial isolated pituitary adenomas. *Mol Cell Endocrinol* 2010; **326**: 71–79.
88. Gadelha MR, Une KN, Rohde K, et al. Isolated familial somatotropinomas: establishment of linkage to chromosome 11q13.1–11q13.3 and evidence for a potential second locus at chromosome 2p16–12. *J Clin Endocrinol Metab* 2000; **85**: 707–714.
89. Soares BS, Eguchi K, Frohman LA. Tumor deletion mapping on chromosome 11q13 in eight families with isolated familial somatotropinoma and in 15 sporadic somatotropinomas. *J Clin Endocrinol Metab* 2005; **90**: 6580–6587.
90. Heliovaara E, Raitila A, Launonen V, et al. The expression of AIP-related molecules in elucidation

of cellular pathways in pituitary adenomas. *Am J Pathol* 2009; **175**: 2501–2507.

91. Lin BC, Sullivan R, Lee Y, et al. Deletion of the aryl hydrocarbon receptor-associated protein 9 leads to cardiac malformation and embryonic lethality. *J Biol Chem* 2007; **282**: 35924–35932.
92. Lin BC, Nguyen LP, Walisser JA, Bradfield CA. A hypomorphic allele of aryl hydrocarbon receptor-associated protein-9 produces a phenocopy of the AHR-null mouse. *Mol Pharmacol* 2008; **74**: 1367–1371.
93. Georgitsi M, Karhu A, Winqvist R, et al. Mutation analysis of aryl hydrocarbon receptor interacting protein (AIP) gene in colorectal, breast, and prostate cancers. *Br J Cancer* 2007; **96**: 352–356.
94. Bolger GB, Peden AH, Steele MR, et al. Attenuation of the activity of the cAMP-specific phosphodiesterase PDE4A5 by interaction with the immunophilin XAP2. *J Biol Chem* 2003; **278**: 33351–33363.
95. Denison MS, Soshilov AA, He G, DeGroot DE, Zhao B. Exactly the same but different: promiscuity and diversity in the molecular mechanisms of action of the aryl hydrocarbon (dioxin) receptor. *Toxicol Sci* 2011; **124**: 1–22.
96. Nguyen LP, Bradfield CA. The search for endogenous activators of the aryl hydrocarbon receptor. *Chem Res Toxicol* 2008; **21**: 102–116.
97. Opitz CA, Litzenburger UM, Sahm F, et al. An endogenous tumour-promoting ligand of the human aryl hydrocarbon receptor. *Nature* 2011; **478**: 197–203.
98. de Oliveira SK, Smolenski A. Phosphodiesterases link the aryl hydrocarbon receptor complex to cyclic nucleotide signaling. *Biochem Pharmacol* 2009; **77**: 723–733.
99. Nair SC, Toran EJ, Rimerman RA, et al. A pathway of multi-chaperone interactions common to diverse regulatory proteins: estrogen receptor, Fes tyrosine kinase, heat shock transcription factor Hsf1, and the aryl hydrocarbon receptor. *Cell Stress Chaperones* 1996; **1**: 237–250.
100. Whitlock JP, Jr. Mechanistic aspects of dioxin action. *Chem Res Toxicol* 1993; **6**: 754–763.
101. de Oliveira SK, Hoffmeister M, Gambaryan S, et al. Phosphodiesterase 2A forms a complex with the co-chaperone XAP2 and regulates nuclear translocation of the aryl hydrocarbon receptor. *J Biol Chem* 2007; **282**: 13656–13663.
102. Kang BH, Xia F, Pop R, et al. Developmental control of apoptosis by the immunophilin aryl hydrocarbon receptor-interacting protein (AIP) involves mitochondrial import of the survivin protein. *J Biol Chem* 2011; **286**: 16758–16767.
103. Jaffrain-Rea ML, Angelini M, Gargano D, et al. Expression of aryl hydrocarbon receptor (AHR) and AHR-interacting protein in pituitary adenomas: pathological and clinical implications. *Endocr Relat Cancer* 2009; **16**: 1029–1043.
104. Kasuki Jomori de PL, Vieira NL, Armondi Wildemberg LE, et al. Low aryl hydrocarbon receptor-interacting protein expression is a better marker of invasiveness in somatotropinomas than Ki-67 and p53. *Neuroendocrinology* 2011; **94**: 39–48.
105. Naves LA, Daly AF, Vanbellinghen JF, et al. Variable pathological and clinical features of a large Brazilian family harboring a mutation in the aryl hydrocarbon receptor-interacting protein gene. *Eur J Endocrinol* 2007; **157**: 383–391.
106. Daly AF, Tichomirowa MA, Petrossians P, et al. Clinical characteristics and therapeutic responses in patients with germ-line AIP mutations and pituitary adenomas: an international collaborative study. *J Clin Endocrinol Metab* 2010; **95**: E373–383.
107. Cain J, Miljic D, Popovic V, Korbonits M. Role of the aryl hydrocarbon receptor-interacting protein in familial isolated pituitary adenoma. *Expert Rev Endocrinol Metab* 2010; **5**: 681–695.
108. Chahal HS, Trivellin G, Leontiou CA, et al. Somatostatin analogs modulate AIP in somatotroph adenomas: the role of the ZAC1 pathway. *J Clin Endocrinol Metab* 2012, **97**: E1411–E1420.
109. Theodoropoulou M, Zhang J, Laupheimer S, et al. Octreotide, a somatostatin analogue, mediates its antiproliferative action in pituitary tumor cells by altering phosphatidylinositol 3-kinase signaling and inducing Zac1 expression. *Cancer Res* 2006; **66**: 1576–1582.
110. Kasuki L, Vieira NL, Wildemberg LE, et al. AIP expression in sporadic somatotropinomas is a predictor of the response to octreotide LAR therapy independent of SSTR2 expression. *Endocr Relat Cancer* 2012; **19**: L25–29.
111. Beckers A, Daly AF. The clinical, pathological, and genetic features of familial isolated pituitary adenomas. *Eur J Endocrinol* 2007; **157**: 371–382.
112. Carney JA, Gordon H, Carpenter PC, Shenoy BV, Go VL. The complex of myxomas, spotty pigmentation, and endocrine overactivity. *Medicine (Baltimore)* 1985; **64**: 270–283.
113. Bertherat J. Carney complex (CNC). *Orphanet J Rare Dis* 2006; **1**: 21–26.

114. Stratakis CA, Kirschner LS, Carney JA. Clinical and molecular features of the Carney complex: diagnostic criteria and recommendations for patient evaluation. *J Clin Endocrinol Metab* 2001; **86**: 4041–4046.
115. Rothenbuhler A, Stratakis CA. Clinical and molecular genetics of Carney complex. *Best Pract Res Clin Endocrinol Metab* 2010; **24**: 389–399.
116. Kirschner LS, Sandrini F, Monbo J, et al. Genetic heterogeneity and spectrum of mutations of the PRKAR1A gene in patients with the Carney complex. *Hum Mol Genet* 2000; **9**: 3037–3046.
117. Kirschner LS, Carney JA, Pack SD, et al. Mutations of the gene encoding the protein kinase A type I-alpha regulatory subunit in patients with the Carney complex. *Nat Genet* 2000; **26**: 89–92.
118. Toledo RA, Sekiya T, Horvath A, et al. Assessing the emerging oncogene protein kinase C epsilon as a candidate gene in families with Carney complex-2. *Clin Endocrinol (Oxf)* 2011.
119. Matyakhina L, Pack S, Kirschner LS, et al. Chromosome 2 [2p16] abnormalities in Carney complex tumours. *J Med Genet* 2003; **40**: 268–277.
120. Sandrini F, Stratakis C. Clinical and molecular genetics of Carney complex. *Mol Genet Metab* 2003; **78**: 83–92.
121. Cazabat L, Guillaud-Bataille M, Bertherat J, Raffin-Sanson ML. Mutations of the gene for the aryl hydrocarbon receptor-interacting protein in pituitary adenomas. *Horm Res* 2009; **71**: 132–141.
122. Stratakis CA. Mutations of the gene encoding the protein kinase A type I-alpha regulatory subunit (PRKAR1A) in patients with the "complex of spotty skin pigmentation, myxomas, endocrine overactivity, and schwannomas" (Carney complex). *Ann N Y Acad Sci* 2002; **968**: 3–21.
123. Groussin L, Horvath A, Jullian E, et al. A PRKAR1A mutation associated with primary pigmented nodular adrenocortical disease in 12 kindreds. *J Clin Endocrinol Metab* 2006; **91**: 1943–1949.
124. Libe R, Horvath A, Vezzosi D, et al. Frequent phosphodiesterase 11A gene (PDE11A) defects in patients with Carney complex (CNC) caused by PRKAR1A mutations: PDE11A may contribute to adrenal and testicular tumors in CNC as a modifier of the phenotype. *J Clin Endocrinol Metab* 2011; **96**: E208–214.
125. Almeida MQ, Muchow M, Boikos S, et al. Mouse Prkar1a haploinsufficiency leads to an increase in tumors in the Trp53+/- or Rb1+/- backgrounds and chemically induced skin papillomas by dysregulation of the cell cycle and Wnt signaling. *Hum Mol Genet* 2010; **19**: 1387–1398.
126. Tsang KM, Starost MF, Nesterova M, et al. Alternate protein kinase A activity identifies a unique population of stromal cells in adult bone. *Proc Natl Acad Sci U S A* 2010; **107**: 8683–8688.
127. Almeida MQ, Stratakis CA. How does cAMP/protein kinase A signaling lead to tumors in the adrenal cortex and other tissues? *Mol Cell Endocrinol* 2011; **336**: 162–168.
128. Azevedo MF, Stratakis CA. The transcriptome that mediates increased cyclic adenosine monophosphate signaling in PRKAR1A defects and other settings. *Endocr Pract* 2011; **17 Suppl 3**: 2–7.
129. Iliopoulos D, Bimpaki EI, Nesterova M, Stratakis CA. MicroRNA signature of primary pigmented nodular adrenocortical disease: clinical correlations and regulation of Wnt signaling. *Cancer Res* 2009; **69**: 3278–3282.
130. Groussin L, Kirschner LS, Vincent-Dejean C, et al. Molecular analysis of the cyclic AMP-dependent protein kinase A (PKA) regulatory subunit 1A (PRKAR1A) gene in patients with Carney complex and primary pigmented nodular adrenocortical disease (PPNAD) reveals novel mutations and clues for pathophysiology: augmented PKA signaling is associated with adrenal tumorigenesis in PPNAD. *Am J Hum Genet* 2002; **71**: 1433–1442.
131. Stratakis CA. Clinical genetics of multiple endocrine neoplasias, Carney complex and related syndromes. *J Endocrinol Invest* 2001; **24**: 370–383.
132. Cazabat L, Ragazzon B, Groussin L, Bertherat J. PRKAR1A mutations in primary pigmented nodular adrenocortical disease. *Pituitary* 2006; **9**: 211–219.
133. Stratakis CA, Sarlis N, Kirschner LS, et al. Paradoxical response to dexamethasone in the diagnosis of primary pigmented nodular adrenocortical disease. *Ann Intern Med* 1999; **131**: 585–591.
134. Gaujoux S, Tissier F, Ragazzon B, et al. Pancreatic ductal and acinar cell neoplasms in Carney complex: a possible new association. *J Clin Endocrinol Metab* 2011; **96**: E1888–1895.
135. Pack SD, Kirschner LS, Pak E, et al. Genetic and histologic studies of somatomammotropic pituitary tumors in patients with the "complex of spotty skin pigmentation, myxomas, endocrine overactivity and schwannomas" (Carney complex). *J Clin Endocrinol Metab* 2000; **85**: 3860–3865.
136. Stergiopoulos SG, Abu-Asab MS, Tsokos M, Stratakis CA. Pituitary pathology in Carney complex patients. *Pituitary* 2004; **7**: 73–82.

137. Lania AG, Mantovani G, Ferrero S, et al. Proliferation of transformed somatotroph cells related to low or absent expression of protein kinase a regulatory subunit 1A protein. *Cancer Res* 2004; **64**: 9193–9198.
138. Scheithauer BW, Kovacs K, Horvath E, et al. Pituitary blastoma. *Acta Neuropathol* 2008; **116**: 657–666.
139. Scheithauer BW, Horvath E, Abel TW, et al. Pituitary blastoma: a unique embryonal tumor. *Pituitary* 2012; **15**: 365–367.
140. Breckenridge SM, Hamrahian AH, Faiman C, et al. Coexistence of a pituitary macroadenoma and pheochromocytoma – a case report and review of the literature. *Pituitary* 2003; **6**: 221–225.
141. Pasini B, Stratakis CA. SDH mutations in tumorigenesis and inherited endocrine tumours: lesson from the phaeochromocytoma-paraganglioma syndromes. *J Intern Med* 2009; **266**: 19–42.
142. Balogh K, Racz K, Patocs A, Hunyady L. Menin and its interacting proteins: elucidation of menin function. *Trends Endocrinol Metab* 2006; **17**: 357–364.
143. Borriello A, Cucciolla V, Oliva A, Zappia V, Della RF. p27Kip1 metabolism: a fascinating labyrinth. *Cell Cycle* 2007; **6**: 1053–1061.
144. Carver LA, Bradfield CA. Ligand-dependent interaction of the aryl hydrocarbon receptor with a novel immunophilin homolog in vivo. *J Biol Chem* 1997; **272**: 11452–11456.
145. Bell DR, Poland A. Binding of aryl hydrocarbon receptor (AhR) to AhR-interacting protein. The role of hsp90. *J Biol Chem* 2000; **275**: 36407–36414.
146. The Uniprot Consortium. Reorganizing the protein space at the Universal Protein Resource (UniProt). *Nucleic Acids Res* 2012; **40**: D71–75.

Stratakis CA (ed): Endocrine Tumor Syndromes and Their Genetics.
Front Horm Res. Basel, Karger, 2013, vol 41, pp 111–140 (DOI: 10.1159/000345673)

Genetics of Pituitary Adenomas

Monica R. Gadelha[a] · Giampaolo Trivellin[b] ·
Laura Cristina Hernández-Ramírez[b] · Márta Korbonits[b]

[a]Division of Endocrinology, Clementino Fraga Filho University Hospital, Federal University of Rio de Janeiro, Rio de Janeiro, Brazil; [b]Centre for Endocrinology, Barts and London School of Medicine, Queen Mary University of London, London, UK

Abstract

Pituitary adenomas are common tumors of the adenohypophysis which can cause considerable morbidity, due to excessive hormonal secretion or compression and local invasion of surrounding structures. The vast majority of pituitary adenomas occur sporadically. Altered gene expression is commonly detected but somatic mutations, epigenetic changes and abnormal microRNAs have also been described. Occurrence of *GNAS* mutations at a postzygotic stage lead to McCune-Albright syndrome (MAS), a disease causing endocrine hyperfunction and tumors in several organs, including the pituitary. Familial pituitary adenomas occur as part of a syndrome affecting other organs, such as in MEN1 or Carney complex, or occur with pituitary adenomas only as in familial isolated pituitary adenoma (FIPA). FIPA, an autosomal-dominant disease with variable penetrance, is explained in 20% of patients by germline mutations in the tumor suppressor *aryl hydrocarbon receptor interacting protein (AIP)*, while no gene abnormality has been identified to date in the majority of the FIPA families. AIP mutation-positive patients have a characteristic clinical phenotype with usually young- or childhood-onset growth hormone (GH) and/or prolactin (PRL)-secreting adenomas and can be seen in cases with no apparent family history as well. Understanding the tumorigenic process in *AIP*-positive and *AIP*-negative FIPA patients could result in better diagnostic and treatment options for both familial and sporadic cases.

Pituitary adenomas are common tumors of the adenohypophysis. They can cause considerable morbidity due to excessive hormonal secretion or lack of appropriate hormone release and due to compression and local invasion of important surrounding structures. The prevalence of pituitary adenomas is high (14–22%) in autopsy and MRI studies [1], but many of these lesions remain clinically silent and represent incidentalomas. Clinically relevant adenomas diagnosed due to symptoms are significantly less common, ~1:1,100 patients have been identified with pituitary adenomas in the general population in population-based studies [2, 3].

The vast majority of pituitary adenomas are sporadic tumors. Genetic alterations are commonly seen in the tumor tissue, such as *GNAS* gene mutations in 40% of somatotroph adenomas. On the other hand, increasing proportion of familial cases have been reported [4], and the recent establishment of a novel clinical entity, familial isolated pituitary adenoma (FIPA), is expected to increase awareness and lead to an improved recognition of familial cases.

Despite their relative rarity, familial pituitary tumors represent an important group of conditions as often they have a more aggressive course and show younger age of onset, such as in patients with mutations in the *multiple endocrine neoplasia 1 (MEN1*, MIM*613733*)* or *aryl hydrocarbon receptor interacting protein (AIP*, MIM*605555*)* genes. The genetic background of familial pituitary tumors is heterogeneous and the phenotype of the families varies quite widely. A better understanding of the causative genes and the pathogenic mechanisms of this particular group of tumors is needed to improve the diagnosis and management of these patients, which, hopefully, will lead to a better prognosis, and may help to understand the pathogenesis of sporadic adenomas as well.

The inherited conditions that, to date, are known to predispose to pituitary adenomas are multiple endocrine neoplasia type 1 (MEN1, MIM#131100, see chapter by Agarwal, this vol.) and type 4 (MEN4, MIM#610755, see chapter by Lee and Pellegata, this vol.), Carney complex (MIM#160980, see chapter by Espiard and Bertherat, this vol.) and FIPA (MIM#102200, this chapter). More recently case reports raised the possibility that mutations in the *DICER1* [5] and *succinate dehydrogenase (SDH)* genes [6–9] can also predispose to pituitary tumors. Genetic conditions associated with pituitary neoplasms have been summarized on figure 1. In the current chapter, we will discuss experimental and clinical data regarding FIPA and McCune-Albright syndrome. In addition, genes and microRNAs implicated in sporadic adenoma development will be discussed.

Familial Isolated Pituitary Adenomas

Clinical Characteristics

Approximately 5% of the pituitary adenomas occur with familial aggregation (MEN1, MEN4, Carney complex and FIPA). FIPA syndrome is defined as the occurrence of at least two cases of pituitary adenomas in a family that does not exhibit any other syndromic features, such as MEN1, MEN4 or Carney complex. Somatotroph, lactotroph and somatolactotroph adenomas are the most common subtypes, but other subtypes have also been reported. FIPA is an autosomal dominant disease with a variable penetrance. Germline *AIP* mutations are identified in 20% (range 15–40%) of patients with FIPA syndrome, while the causative gene in the majority of the families is unknown. The penetrance in *AIP*-positive FIPA families is usually 15–30% (range 10–80%) [12–14], while it is somewhat lower in *AIP*-negative families [13].

Stratakis CA (ed): Endocrine Tumor Syndromes and Their Genetics.
Front Horm Res. Basel, Karger, 2013, vol 41, pp 111–140 (DOI: 10.1159/000345673)

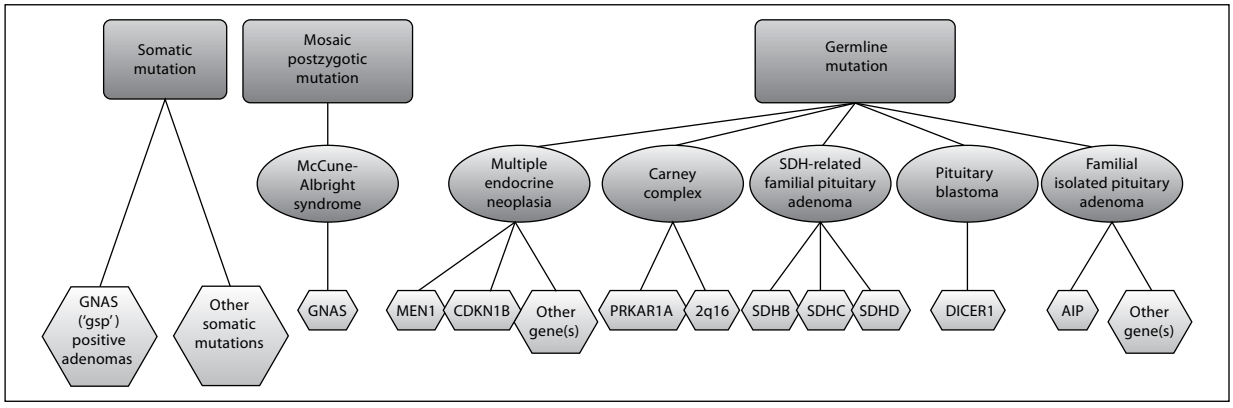

Fig. 1. Pituitary tumors due to genetic origin. A somatic activating mutation in the *GNAS* gene can be found in 30–40% of sporadic somatotroph adenomas. Theoretically, somatic mutations in other genes could also lead to pituitary adenoma development. Mosaic post-zygotic activating mutation of the *GNAS* gene leads to the McCune-Albright syndrome; some of these patients develop somatotroph hyperplasia or adenoma. Germline mutation in the *MEN1* gene or rarely in the *CDKN1B* (coding for cell cycle regulator protein p27) gene cause MEN1 or MEN4; in a small proportion other cell cycle regulators have been implicated (p18 (*CDKN2C*) and p21 (*CDKN1A*)) [11] or no gene abnormality can be found. A mutation in the type 1A regulatory subunit of the cAMP-dependent protein kinase A *(PRKAR1A)* is found in the majority (60%) of patients with Carney complex; in the remainder patients, data suggest a putative causative gene in the 2q16 chromosome region. Patients have been described with *SDH* mutation-related familial paraganglioma/pheochromocytoma and familial pituitary adenomas [6–9]. A mutation in the *DICER1* gene, a gene which regulates microRNAs, may cause an ACTH-secreting pituitary blastoma of infant onset [5]. A fifth of FIPA cases show a mutation in the *AIP* gene; in the majority of families the causative gene has not yet been identified. Adapted from Korbonits et al. [10].

There is a phenotypic difference between *AIP*-positive and *AIP*-negative families. The mean age at diagnosis (24 years) in *AIP*-positive families is approximately 13 years lower than in *AIP*-negative families and the majority of *AIP*-positive families harbor a childhood-onset case [15]. Two-thirds of *AIP*-positive patients are males, while there is no gender predominance in *AIP*-negative familial cases and in sporadic pituitary adenomas [16]. In addition, families with members harboring *AIP* mutations are mainly composed of patients with either pure somatotroph adenomas or with mixed somatotroph and lactotroph adenomas [12, 15]. Actually, *AIP* mutations are found in 50% of homogeneous somatotroph FIPA families [15, 17]. *AIP*-positive cases that presented clinically as nonfunctioning pituitary adenomas (NFPAs) can also exhibit positive growth hormone (GH)/prolactin (PRL) staining [15]. Rarely, ACTH-, LH/FSH- and TSH-secreting adenomas or true null cell adenomas were also identified. The *AIP*-negative families can have a more varied phenotype, with families composed of homologous prolactinoma, NFPA or rarely Cushing's disease or comprising heterogeneous families. *AIP*-positive acromegalic patients often exhibit sparsely granulated somatotroph adenomas [18]. Consistent with this, the tumors of *AIP*-positive patients usually have an aggressive clinical behavior, being large, with frequent invasion of nearby structures and, as a con-

Stratakis CA (ed): Endocrine Tumor Syndromes and Their Genetics.
Front Horm Res. Basel, Karger, 2013, vol 41, pp 111–140 (DOI: 10.1159/000345673)

sequence, these patients are submitted to more surgical interventions [16]. Regarding the response to medical therapy, Leontiou et al. [18] observed that *AIP*-positive patients showed a poorer response to somatostatin analogues (SSAs). Indeed, Daly et al. [16] compared 38 *AIP*-positive acromegaly patients and 160 matched acromegaly controls (without *AIP* mutations). They observed that patients harboring *AIP* mutations presented less GH and insulin-like growth factor type 1 (IGF-1) reductions than controls with SSAs therapy (40.0 and 75.0% for GH and 47.4 and 56.0% for IGF-1, respectively). They also observed that the median magnitude of tumor shrinkage achieved with SSAs was significantly higher in the control group (median 41.1 vs. 0.0% in the *AIP*-mutated patients; $p < 0.001$). This poor response to SSAs therapy is not due to a different expression profile of somatostatin receptor (SSTR) in these tumors, as there is no significant reduction of the SSTR subtypes in *AIP*-positive samples compared to sporadic somatotroph adenomas; actually, SSTR5 staining was shown to be slightly higher in *AIP*-positive FIPA samples compared to sporadic adenoma samples [19].

Interestingly, AIP protein expression is reduced in a subset of acromegalic patients with sporadic disease without *AIP* mutation, especially in more invasive cases [20]. Indeed, low AIP expression has been shown to be a better predictor of tumor invasion in somatotrophinomas than Ki-67 or p53 [20]. The mechanism involved in this low AIP expression is currently under investigation. Kasuki et al. [21] reported that sporadic patients with acromegaly harboring somatotrophinomas with low AIP expression are more prone to exhibit resistance to SSAs therapy. The authors compared the AIP protein expression in somatotroph tumors from 35 sporadic patients with acromegaly treated with octreotide LAR after surgery. Of the 18 patients whose tumors exhibited low AIP expression, only 4 (22%) achieved disease control with octreotide therapy, in contrast with 11 of 17 patients (65%) whose tumors presented high AIP expression ($p = 0.013$). In the same study, the authors evaluated SSTR2 expression and observed that there was no difference in SSTR2 expression between patients with low or high AIP expression, in agreement with data on *AIP* mutant tissues [19, 21].

Assessment for FIPA

If a patient with pituitary adenoma has a relative presenting also with pituitary adenoma and no other known associated syndromes then we consider the diagnosis of FIPA. Genetic testing can be offered for *AIP*. According to our current practice, we screen all FIPA cases, all childhood-onset pituitary adenomas and all young-onset (<30 years) macroadenomas even without known family history. We summarized our current strategy in figure 2 [22].

If an *AIP* mutation is identified, genetic screening can be offered to family members. Based on the youngest known affected *AIP*-positive case, we currently suggest screening at age 4 years or earlier [12]. Unaffected carrier family members should undergo regular clinical assessment. For pediatric cases yearly measurements of height and weight with calculation of height velocity and documentation of development of puberty together with pituitary function tests are recommended. Baseline pituitary MRI is advised

Stratakis CA (ed): Endocrine Tumor Syndromes and Their Genetics.
Front Horm Res. Basel, Karger, 2013, vol 41, pp 111–140 (DOI: 10.1159/000345673)

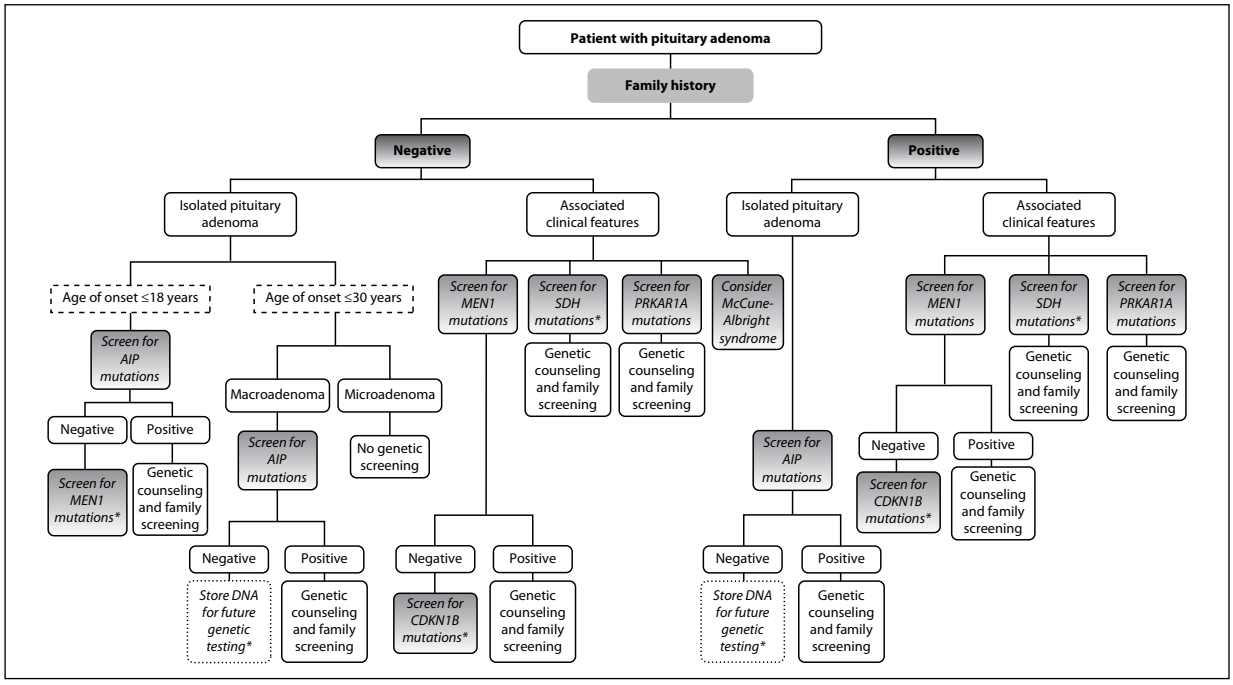

Fig. 2. Suggested approach for genetic testing in patients with pituitary adenomas. * Weak evidence for these suggestions. Adapted from Hernández-Ramírez and Korbonits [22].

around the age of 10 years and repeat MRI scanning of the pituitary every 5 years can be considered if clinical and pituitary function tests remain normal. Adult patients are suggested to have a baseline clinical assessment with pituitary function tests and MRI followed by yearly pituitary function tests. Although there is no long-term experience, repeat MRI of the pituitary every 5 years could be considered until the age of 30 years if clinical and pituitary function tests remain normal. Currently, we follow-up all patients, but in the future monitoring frequency may be reduced above the age of 30–50 years. Surveillance data from *AIP* mutation-positive families in the last few years have revealed a number of *AIP* mutation carrier patients with abnormal biochemical and MRI findings who either underwent treatment or are followed closely [12, 17, 23]. Clinical, laboratory and MRI screening for family members of *AIP*-negative FIPA patients could be performed upon patients request and/or under a research protocol.

AIP Function, Mutations and Animal Models

The human *AIP* gene is located at the 11q13 chromosome region, 2.7 Mb downstream of the *MEN1* gene. *AIP* consists of 6 exons, encoding a 330 amino acid (37 kDa) cytoplasmic co-chaperone phosphoprotein [24], also known as X-associated

Stratakis CA (ed): Endocrine Tumor Syndromes and Their Genetics.
Front Horm Res. Basel, Karger, 2013, vol 41, pp 111–140 (DOI: 10.1159/000345673)

protein-2 (XAP2), Ah receptor-activated 9 (ARA9) or FK506-binding protein 37 (FKBP37). *AIP* is located on a conserved synthenic block in human, mouse and rat and the AIP protein sequence is evolutionarily conserved among species. The N-terminal AIP protein consists of a peptidyl-prolyl cis-trans isomerase (PPIase)-like domain, whose 3D structure has now been resolved [25]. The C-terminal protein consists of three tetratricopeptide repeat (TPR) motifs and a final α-7 helix and its structure has also been resolved [Prodromou and Korbonits, unpubl. data]. TPR domains are 34 amino acid sequences, often arranged in tandem repeats, formed by two α-helices forming an antiparallel structure that mediates intra- and intermolecular interactions [26]. Other TPR protein family members are aryl hydrocarbon receptor-interacting protein-like 1 (AIPL1), protein phosphatase 5 (PP5), FKBP51, FKBP52, cyclophilin 40 (Cyp40), carboxyl-terminus of hsc70-interacting protein (CHIP), and heat shock protein 70 (hsp70)/hsp90 organizing protein (Hop) [26].

Numerous proteins have been identified to interact with AIP directly (viral proteins (HBV X and EBNA-3), chaperone proteins (hsp90 and hsc70), phosphodiesterases (PDE4A5 and PDE2A3), nuclear receptors (AhR, PPARα and TRβ1), transmembrane receptors (RET and possibly EGFR), G proteins (Gα13 and Gαq), an inhibitor of apoptosis protein (survivin) and a mitochondrial import receptor (TOMM20)) or indirectly (glucocorticoid receptor and the co-chaperone protein p23) [26]. The potential for AIP to interact with several other steroid hormone receptors, such as the androgen and progesterone receptors, has recently been reported [27]. The multiplicity of AIP interactions suggests that AIP is involved in various cellular pathways; however, at the moment it is uncertain which of them play a role in pituitary tumorigenesis. The AhR-cAMP-PDE pathway seems to be a very attractive candidate as AhR activation has well-known tumorigenic effects and phosphodiesterases are involved in the tight control of cellular cAMP levels, which are known to be involved in Gsα mutation-related as well as Carney complex-related somatotroph tumorigenesis [26].

AIP is widely expressed in the human body, but its expression levels vary considerably among tissues. For instance, high expression levels have been observed in spleen and thymus, whereas low AIP expression was detected in liver, kidney and lung [28].

In the normal pituitary gland AIP is expressed only in somatotroph and lactotroph cells, where it associates with secretory vesicles, whereas in sporadic pituitary tumors AIP is expressed in all cell types and shows lack of colocalization with secretory vesicles in prolactinomas, corticotrophinomas and NFPAs [18]. High AIP expression levels are usually observed in NFPAs [18, 29], whereas a low expression was described in invasive GH-secreting adenomas [20]. These observations suggest that the regulation of AIP is different in somatotroph compared to other pituitary cell types.

Although AIP was originally identified in 1996, its clinical relevance was only established 10 years later when heterozygous germline mutations were found in pituitary adenomas [30]. No genotype-phenotype correlation for age of onset, tumor type or level of penetrance has been established to date.

Stratakis CA (ed): Endocrine Tumor Syndromes and Their Genetics.
Front Horm Res. Basel, Karger, 2013, vol 41, pp 111–140 (DOI: 10.1159/000345673)

The presence of somatic *AIP* mutations has been studied in both endocrine and nonendocrine tumors, but no mutations have been reported so far [10].

To date, 112 different *AIP* variants have been reported in the literature. In addition to single nucleotide polymorphisms, various missense, nonsense, splice-site and promoter mutations, as well as small deletions and insertions (in-frame or leading to frame-shift), and large genomic deletions have been described. The latter constitutes about 10% of mutations in *AIP*-positive FIPA families and can only be detected with specific techniques, such as MLPA (multiplex ligation-dependent probe amplification). About 65% of *AIP* mutations result in a truncated/lost protein, while missense variants and the in-frame changes mostly affect the TPR domain or the C-terminal α-helix. All known mutations are predicted to lead to loss of function of the protein. There are a few hotspot mutations described in *AIP*, mostly affecting CpG sites, such as codons 81, 271 and 304. Founder mutations have also been described in Finland, Northern Ireland and Italy [12, 14, 30].

The loss-of-function mutations, together with LOH and functional data, suggest that *AIP* functions as a tumor suppressor gene in the pituitary gland [13, 18, 30, 31]. Homozygous *Aip* loss in mice was shown to cause embryonic lethality due to congenital defects in heart development and inability to maintain productive erythropoiesis [32, 33], whereas heterozygous *Aip* (*Aip*+/–) mice were shown to be prone to develop pituitary adenomas, especially somatotrophinomas [34]. Interestingly, unlike in humans, Aip+/– mice display complete penetrance of pituitary tumors [34] possibly due to homogenous genetic background.

GNAS Mutations and McCune-Albright Syndrome

Definition and Epidemiology

Originally described in the 1930s (first by McCune [35] and then by Albright et al. [36]) as the triad of polyostotic fibrous dysplasia, *café-au-lait* spots and precocious puberty. McCune-Albright syndrome (MAS, MIM#174800) is a complex genetic syndrome encompassing other diseases due to endocrine hyperfunction. According to the current definition of MAS, this diagnosis is established in the presence of (1) monostotic or polyostotic fibrous dysplasia, and (2) at least one manifestation of endocrine hyperfunction and/or café-au-lait spots [37]. The original clinical triad is known as classic MAS, while the presence of only 2 manifestations is known as nonclassic MAS. Even though the presence of only one manifestation is not included in this definition, Lumbroso et al. [38] found that there is a subgroup of girls with isolated precocious puberty bearing GNAS mutations. This manifestation can appear isolated and remain like that, but it could also be the first manifestation in patients who will develop other components of the disease in the future. Café-au-lait spots are the commonest component of the syndrome (53–95% of patients) [39]. In the largest available series (113 patients with MAS-related abnormalities), the classic triad was

Stratakis CA (ed): Endocrine Tumor Syndromes and Their Genetics.
Front Horm Res. Basel, Karger, 2013, vol 41, pp 111–140 (DOI: 10.1159/000345673)

present in only 24% of patients, one third had 2 components of the triad and the rest of them had only one (usually precocious puberty) [38].

MAS is a very rare disease with a prevalence around 1/100,000–1/1,000,000 in the general population, but fibrous dysplasia (especially the monostotic variant) is much more common [37]. There is a gender imbalance with a predominance of female patients [38]; the reason for this is unknown.

Genetic Issues

The genetic basis of MAS is a postzygotic (i.e. somatic) mutation in the *GNAS* (also known as *GNAS1*) gene; the patients are somatic mosaics for *GNAS* mutations [40]. The clinical manifestations are widely variable due to the variable mutation status of the various tissues [40, 41]. Germline *GNAS* mutations are never inherited, they are probably embryonically lethal [41, 42]. Theoretically, severe MAS cases are related to a mutational event at an early developmental stage [42]. In agreement with this hypothesis, in MAS patients with involvement of several tissues, the same *GNAS* mutation is found in all the tissues analyzed [38]. Apparently, somatic mosaicism is a sine qua non condition for the development of MAS: cells bearing the mutation can only survive if they are interspersed with normal cells in the affected tissues [41], as has been proved for fibrous dysplasia lesions [43].

The *GNAS* locus displays complex genomic imprinting, generating multiple alternative products from the paternal and maternal alleles, driven by the activation of alternative promoters (4 sense and 1 antisense), differently imprinted [44, 45].

Gsα is the best known product coded by *GNAS*. Gsα is transcribed from the exons 1–13, resulting in four alternatively spliced products (two long, Gsα-1 and Gsα-2, and two short, Gsα-3 and Gsα-4), that might have variable biological roles [46]. Exons 2–13 are common to the other *GNAS* gene products: NESP55 and XLαs.

Gsα constitutive activation at multiple tissues is the accepted pathogenic basis of MAS, whereas there is not a clear contribution of the other *GNAS* locus products to the clinical features [40]. A tissue-specific imprinting pattern in some organs has been proposed [47] and supported by data from inactivating *GNAS* mutations.

In humans, tissue-specific imprinting has been demonstrated in the pituitary, where Gsα is exclusively expressed from the maternal allele [48]. Somatotrophinomas (both those with and without *GNAS* mutations) often show a relaxation of Gsα monoallelic expression, but retain the normal imprinting of NESP55 and XLαs, implying a possible role for loss of Gsα imprinting in somatotroph cells tumorigenesis [48]. In *GNAS* mutation-positive somatotrophinomas, both sporadic and MAS-related, mutations are almost always located in the maternal allele, in agreement with the pituitary-specific imprinting of this gene [49]. In thyroid and gonads, the expression of Gsα is mainly dependent on the maternal allele, but the paternal contribution is not negligible, indicating that genetic imprinting is not necessarily an all-or-nothing phenomenon [50]. Therefore, acromegaly occurs only in those MAS patients with an affected maternal allele, but there is not an apparent relationship between the origin of

Stratakis CA (ed): Endocrine Tumor Syndromes and Their Genetics.
Front Horm Res. Basel, Karger, 2013, vol 41, pp 111–140 (DOI: 10.1159/000345673)

the mutated allele and the rest of MAS components [49], each individual showing a particular distribution of abnormal cells in the affected tissues.

GNAS mutations in MAS patients always occur at codon 201 and usually result in the substitution of the residue arginine by a histidine or cysteine [46], or, infrequently, by a serine, glycine or leucine. On the other hand, in isolated endocrine tumors *GNAS* mutations can occur both at the 201 or 227 positions [51]. Indeed, 40% of sporadic somatotrophinomas bear a heterozygous activating *GNAS* mutation either at the position 201 or 227 (*gsp* oncogene) [52, 53]. Detection of *GNAS* mutations in affected tissues is high (90%), while peripheral blood lymphocytes show 21–27% positivity in MAS patients [38]. MAS is a clinical diagnosis but detection of *GNAS* mutations in affected tissues could be important in certain non-classical cases [38].

Pituitary Involvement

Pituitary disease in MAS is characterized by elevated GH and often (92%) accompanying high prolactin levels [54]. Excessive GH production is part of MAS in 21% of patients [54], but only 33–65% of these bear a pituitary adenoma detectable by imaging studies [54, 55]. The current concept is that pituitary involvement in MAS is widespread and diffuse, including areas of normal gland, somatotroph hyperplasia (most common), somatotroph neoplasia, lactotroph neoplasia and mammosomatotroph neoplasia [55]. Interestingly, *GNAS* mutation-related acromegaly patients (both MAS (100%) and sporadic acromegaly (78%)) respond positively to a TRH test while gsp negative cases only in 50% [54].

Surgical treatment in MAS-related acromegaly can be difficult due to the presence of craniofacial bone lesions, complicating surgical approaches [54, 55]. Visual and/or auditive compromise due to cranial nerve compression is more severe in patients with high GH and IGF-1 levels [54]. Medical treatment with cabergoline and octreotide can lead to disease control, although often partial. Combined treatment with pegvisomant and radiotherapy achieved total disease control in a series of 5 out of 6 acromegalic SSA-resistant MAS patients [56].

Other features of MAS include peripheral (primary) precocious puberty in girls (30–50% [57]), hyperthyroidism (50%), Cushing's syndrome (7%), renal phosphate wasting (50%) (explained by the production of the phosphaturic factor fibroblast growth factor 23 (FGF-23) by the fibrous dysplasia lesions [58]). Nonendocrine manifestations include fibrous dysplasia, irregular café-au-lait spots ('cost of Maine' pattern), rarely gastrointestinal reflux, gastrointestinal polyps, pancreatitis, neonatal cholestasis, sudden death, tachycardia, aortic root dilatation and platelet dysfunction [37, 38, 59]. Hyperparathyroidism in MAS is secondary to the abnormalities in mineral metabolism and not caused by *GNAS* mutations [37]. A few cases of thyroid and breast cancer have been reported in association with MAS; nevertheless, a causative association has not been established [59].

Stratakis CA (ed): Endocrine Tumor Syndromes and Their Genetics.
Front Horm Res. Basel, Karger, 2013, vol 41, pp 111–140 (DOI: 10.1159/000345673)

Table 1 . Genes potentially involved in the pathogenesis of sporadic pituitary adenomas

Gene name	MIM number	Location (Chr)	Function	TSG/ oncogene	Defect
AIP	605555	11q13.2	Co-chaperone protein	Tumor suppressor gene (TSG)	Decreased expression in invasive somatotrophinomas
AKT1	164730	14q32.33	Regulates many processes including metabolism, proliferation, cell survival, growth and angiogenesis	Oncogene	Increased expression, especially in NFPAs
AKT2	164731	19q13.2	Regulates many processes including metabolism, proliferation, cell survival, growth and angiogenesis	Oncogene	Increased expression, especially in NFPAs
BAG1	601497	9p13.3	Inhibits the chaperone activity of HSP70/HSC70 and the pro-apoptotic function of PPP1R15A	–	Increased expression
BMI1 (BMI-1)	164831	10p12.2	Component of the polycomb repressive complex 1, which is required to maintain the transcriptionally repressive state of many genes	Oncogene	Increased expression, genetic amplification in one adenoma
BMP4	112262	14q22.2	Plays a crucial role in the control of the differentiation and proliferation of the different cell types in the anterior pituitary	TSG	Increased expression
CCNA1 (cyclin A1)	604036	13q13.3	Involved in the control of the G1/S and G2/M phases of the cell cycle	Oncogene	Increased expression, especially in recurrent adenomas
CCNB1 (cyclin B1)	123836	5q13.2	Involved in G2-M transition	Oncogene	Increased expression
CCNB2 (cyclin B2)	602755	15q22.2	Involved in G2-M transition	Oncogene	Increased expression that correlates with HMGA1 and HMGA2 expression
CCND1 (cyclin D1)	168461	11q13.3	Promotes progression through the G1-S phase of the cell cycle	Oncogene	Increased expression, allelic imbalance
CCNE1 (cyclin E1)	123837	19q12	Promotes progression through the G1-S phase of the cell cycle	Oncogene	Increased expression
CDKN1A ($p21^{CIP1}$)	116899	6p21.2	Regulator of cell cycle progression at G1	TSG	Decreased expression in NFPAs, increased expression in hormone producing adenomas, especially somatotrophinomas
CDKN1B ($p27^{KIP1}$)	600778	12p13.1	Blocks the cell cycle in the G0/G1 phase. Also involved in cell migration, proliferation, neuronal differentiation and apoptosis	TSG or oncogene depending on cellular context	Decreased expression, especially in recurrent adenomas
CDKN2A ($p16^{INK4}$)	600160	9p21.3	Induces cell cycle arrest in G1 and G2 phases	TSG	Decreased expression mostly by promoter methylation

Stratakis CA (ed): Endocrine Tumor Syndromes and Their Genetics.
Front Horm Res. Basel, Karger, 2013, vol 41, pp 111–140 (DOI: 10.1159/000345673)

Tumor types	Animal models	References
Invasive somatotrophinomas	*Aip* +/– mice develop pituitary tumors with complete penetrance	Kasuki et al. [20], 2011; Kasuki et al. [21], 2012
Various tumor types	No pituitary tumors	Musat et al. [75], 2005
Various tumor types	No pituitary tumors	Musat et al. [75], 2005
Somatotrophinomas, prolactinomas, NFPAs	No pituitary tumors	Morris et al. [76], 2005
Various tumor types	Conditional, neural and glial-specific transgenic expression of *Bmi1* in mice lead to development of intermediate and anterior lobe ACTH-secreting pituitary adenomas	Sanchez-Beato et al. [77], 2006; Palumbo et al. [74], 2012; Westerman et al. [78], 2012
Prolactinomas	No pituitary tumors	Paez-Pereda et al. [79], 2003
Various tumor types	No pituitary tumors	Turner et al. [80] 2000; Nakabayashi et al. [81], 2001
Various tumor types	Homozygous *Ccnb1* KO is embryonic lethal in mice	Turner et al. [80], 2000; Wierinckx et al. [82], 2007
All tumor types	*Ccnb2*-KO mice, although develop normally, are smaller than normal mice and have reduced litter sizes	De Martino et al. [83], 2009
Aggressive and nonfunctioning adenomas, somatotrophinomas	No pituitary tumors	Hibberts et al. [84], 1999; Jordan et al. [85], 2000; Turner et al. [80] 2000; Simpson et al. [86], 2001; Elston et al. [87], 2008
Mainly corticotropinomas	No pituitary tumors	Jordan et al. [85], 2000; Turner et al. [80] 2000
All tumor types	*Cdkn1a* KO mice do not develop pituitary adenomas, but both double *Cdkn1a* and *Rb1*, and *Cdkn1a* and *Cdkn2c* KO mice develop pituitary adenomas with a shorter latency than single *Rb1* and *Cdkn2c* mutants, respectively. Double *Cdkn1a* and *Cdkn1b* KO mice show higher incidence of pituitary adenomas than *Cdkn1b* mutants	Neto et al. [88], 2005
All tumor types, especially corticotropinomas and pituitary carcinomas	*Cdkn1b* KO mice develop intermediate lobe hyperplasia leading to corticotropinomas	Qian et al. [89], 1996; Lloyd et al. [90], 1997; Bamberger et al. [91], 1999; Jin et al. [92], 1997; Lidhar et al. [93], 1999; Komatsubara et al. [94], 2001; Nakabayashi et al. [81], 2001; Korbonits et al. [95], 2002; Musat et al. [75], 2005
All tumor types, but especially NFPAs	*Cdkn2a* KO mice do not show pituitary adenomas, but double *Cdkn2a* and *Cdkn2c* KO mice develop intermediate lobe tumors with a shorter latency than single *Cdkn2c* mutants	Woloschak et al. [96], 1996; Jaffrain-Rea et al. [97], 1999; Simpson et al. [98], 1999; Ruebel et al. [99], 2001; Seemann et al. [100], 2001; Ogino et al. [101], 2005; Yoshino et al. [102], 2006; Machiavelli et al. [103], 2008; Kirsch et al. [104], 2009

Stratakis CA (ed): Endocrine Tumor Syndromes and Their Genetics.
Front Horm Res. Basel, Karger, 2013, vol 41, pp 111–140 (DOI: 10.1159/000345673)

Table 1 . Continued

Gene name	MIM number	Location (Chr)	Function	TSG/ oncogene	Defect
CDKN2B ($p15^{INK4B}$)	600431	9p21.3	Inhibits progression of cell cycle at G1	TSG	Decreased expression partly by promoter methylation, homozygous deletion
CDKN2C ($p18^{INK4C}$)	603369	1p32.3	Regulator of cell cycle progression at G1	TSG	Decreased expression mostly by promoter methylation
COPS5 (JAB1)	604850	8q13.1	Probable protease subunit of the COP9 signalosome complex, which is involved in various cellular and developmental processes	–	Increased expression
CREB1 (CREB)	123810	2q33.3	Phosphorylation-dependent transcriptional activator of cAMP response elements (CREs), that regulates mitogenesis, metabolism, differentiation, and proliferation	Oncogene	Constitutive activation by phosphorylation
DAPK1	600831	9q21.33	Positive mediator of the programmed cell death induced by gamma-interferon	TSG	Decreased expression either by promoter methylation or by homozygous deletion of the promoter CpG island
DKC1	300126	Xq28	Pseudouridine synthase that modifies rRNA and regulates telomerase activity	TSG	Loss-of-function somatic mutation
DRD2 (D2R)	126450	11q23.2	G protein-coupled receptor for dopamine	–	Decreased expression
EGFR	131550	7p11.2	Transmembrane glycoprotein required for normal cellular proliferation, survival, adhesion, migration and differentiation	Oncogene	Increased expression
FGF2 (bFGF)	134920	4q27-28	Plays an important role in the regulation of cell survival, cell division, angiogenesis, cell differentiation and cell migration	–	Increased expression, decreased mRNA expression in TSH-secreting adenomas
FGFR1	136350	8p11.23-p11.22	Receptor for fibroblast growth factor	Oncogene	Increased expression especially in NFPAs, decreased mRNA expression in TSH-secreting adenomas
FGFR2	176943	10q26.13	Receptor for fibroblast growth factor	Oncogene	Decreased expression by promoter methylation
FGFR4	134935	5q35.2	Membrane-anchored receptor for fibroblast growth factor (preferentially binds acidic fibroblast growth factors)	Oncogene	Increased expression of a N-terminally truncated cytoplasmic isoform (ptd-FGFR4) by alternative transcription initiation
FOLR1 (FR)	136430	11q13.4	Binds to folate and reduces folic acid derivatives and mediates delivery of 5-methyltetrahydrofolate to the interior of cells	Oncogene?	Increased expression in NFPAs, decreased expression in PRL- and GH-secreting adenomas
GADD45B (GADD45-β)	604948	19p13.3	Regulation of growth and apoptosis	TSG	Decreased expression

Stratakis CA (ed): Endocrine Tumor Syndromes and Their Genetics.
Front Horm Res. Basel, Karger, 2013, vol 41, pp 111–140 (DOI: 10.1159/000345673)

Tumor types	Animal models	References
Various tumor types	No pituitary tumors	Ogino et al. [101], 2005; Yoshino et al. [102], 2006
All tumor types	*Cdkn2c* KO mice display intermediated lobe and anterior pituitary adenomas	Morris et al. [76], 2005; Hossain et al. [105], 2009; Kirsch et al. [104], 2009
Pituitary carcinomas	No pituitary tumors	Korbonits et al. [95], 2002
Somatotrophinomas	A transcriptionally inactive *Creb* transgene in somatotrophs leads to dwarfism and somatotroph hypoplasia in mice	Bertherat et al. [106], 1995
Various tumor types, preferentially invasive adenomas	No pituitary tumors	Simpson et al. [107], 2002
1 NFPA	No pituitary tumors	Bellodi et al. [108], 2010
Resistant prolactinomas compared to non-resistant tumors	*Drd2* KO mice develop lactotroph hyperplasia which leads to PRL-secreting adenomas	Caccavelli et al. [109], 1994
NFPAs	No pituitary tumors	Chaidarun et al. [110], 1994
All tumor types	Transgenic *Fgfr2* mice show lactotroph hyperplasia	McCabe et al. [111], 2003
All tumor types	No pituitary tumors	McCabe et al. [111], 2003
Various tumor types	Transgenic *Fgfr2* mice die shortly after birth (no pituitary abnormalities)	Zhu et al. [112], 2007
ptd-FGFR4 in all tumor types	Transgenic *Fgfr4* mice develop lactotroph adenomas	Ezzat et al. [113], 2002
NFPAs, PRL- and GH-secreting adenomas	No pituitary tumors	Evans et al. [114], 2001
Gonadotroph adenomas	No pituitary tumors	Michaelis et al. [115], 2011

Stratakis CA (ed): Endocrine Tumor Syndromes and Their Genetics.
Front Horm Res. Basel, Karger, 2013, vol 41, pp 111–140 (DOI: 10.1159/000345673)

Table 1 . Continued

Gene name	MIM number	Location (Chr)	Function	TSG/ oncogene	Defect
GADD45G (GADD45-γ)	604949	9q22.2	Growth suppression and apoptosis	TSG	Decreased expression mainly due to promoter methylation
GHR	600946	5p13-p12	Transmembrane receptor that mediates GH action	–	Loss-of-function somatic mutation
GHRH	139190	20q11.23	Stimulates growth hormone secretion	–	Increased expression
GHRHR	139191	7p14.3	Transmembrane receptor that mediates GHRH action	–	Truncated alternatively spliced nonfunctioning receptor
GNAI2 (Gi2α)	139360	3p21.31	Inhibition of adenylate cyclase and calcium influx	Oncogene	Gain-of-function somatic mutations
GNAS (GNAS1)	139320	20q13.32	Alpha subunit of the stimulatory G protein that activates adenylate cyclase	Oncogene	Gain-of-function somatic mutations, loss of imprinting, increased expression in some somatotrophinomas
HDAC2	605164	6q21	Enzyme that deacetylates of lysine residues on the N-terminal region of the core histones	Oncogene	Decreased expression
HMGA1	600701	6p21.31	Variety of biological functions. Key role in growth and development	Oncogene	Overexpression
HMGA2	600698	12q14.3	Variety of biological functions. Key role in growth and development	Oncogene	Amplification and overexpression
HRAS (Ras)	190020	11p15.5	GDP/GTP binding protein that regulates cell division in response to growth factor stimulation	Oncogene	Gain-of-function somatic mutations
IKZF1	603023	7p12.2	DNA-binding protein with crucial functions in the hematopoietic system and in the development of the immune system	Oncogene	Dominant-negative truncated isoform (Ik6)
LAPTM4B	8q22.1	613296	Required for lysosome homeostasis, acidification and function	Oncogene	Increased expression
MAGEA3	300174	Xq28	Unknown function, but may play a role in embryonal development and tumor transformation or progression	Oncogene	Increased expression by promoter hypomethylation and histone acetylation in association with FGFR2 down-regulation
MEG3	605636	14q32.3	long non-coding RNA. Induces apoptosis and inhibits proliferation of tumor cells	TSG	Decreased expression
MEN1	613733	11q13.1	Transcriptional regulator	TSG	Loss-of-function somatic mutations and deletions, decreased expression

Stratakis CA (ed): Endocrine Tumor Syndromes and Their Genetics.
Front Horm Res. Basel, Karger, 2013, vol 41, pp 111–140 (DOI: 10.1159/000345673)

Tumor types	Animal models	References
NFPAs, somatotrophinomas, prolactinomas	No pituitary tumors	Zhang et al. [116], 2002; Bahar et al. [117], 2004
Somatotrophinomas	Homozygous *Ghr* KO mice exhibit retarded postnatal growth, proportionate dwarfism, decreased IGF1 levels, small pituitaries	Asa et al. [118], 2007
Somatotrophinomas	Transgenic *Ghrh*–expressing mice develop somatotroph hyperplasia which leads to GH-secreting adenomas	Thapar et al. [119], 1997
Somatotrophinomas	Homozygous mice for a spontaneous null mutation exhibit reduced growth, impaired GH synthesis and release	Hashimoto et al. [120], 1995
NFPAs, 1 corticotropinoma	*Gnai2* KO mice display growth retardation and die prematurely	Williamson et al. [121], 1994; Williamson et al. [122], 1995
Mainly somatotrophinomas (about 40%), some NFPAs, corticotropinomas	Cholera toxin-transgenic mice develop somatotroph hyperplasia	Vallar et al. [123], 1987; Landis et al. [52],1989; Tordjman et al. [124], 1993; Williamson et al. [121], 1994; Williamson et al. [122], 1995; Hamacher et al. [125], 1998; Hayward et al. [48], 2001; Riminucci et al. [126], 2002; Picard et al. [127], 2007
Corticotropinomas	*Hdac2* –/– mice show partially penetrant embryonic lethality	Bilodeau et al. [128], 2006
All tumor types	*Hmga1* transgenic mice develop pituitary adenomas secreting PRL and GH	De Martino et al. [83], 2009
Prolactinomas, NFPAs	*Hmga2* transgenic mice develop GH- and PRL-secreting adenomas	Finelli et al. [129], 2002; Pierantoni et al. [130], 2005
Pituitary carcinomas metastases, 1 aggressive prolactinoma, invasive adenomas	No pituitary tumors	Karga et al. [131], 1992; Cai et al. [132], 1994; Pei et al. [133], 1994; Lin et al. [134], 2009
Subset of adenomas	*Ikaros*-null mice had contraction of the pituitary corticomelanotroph population, reduced circulating adrenocorticotrophic hormone levels, and adrenal glucocorticoid insufficiency	Ezzat et al. [135], 2003
NFPAs and corticotropinomas	No animal models available	Morris et al. [76], 2005
Various tumor types	No animal models available	Zhu et al. [136], 2008
NFPAs	2 *Meg3* KO mouse models available. *Meg3* deletion results in perinatal death	Zhang et al. [116], 2002; Zhang et al. [137], 2003; Zhao et al. [138], 2005; Gejman et al. [139], 2008; Cheunsuchon et al. [140], 2011; Mezzomo et al. [141], 2012
All tumor types	Heterozygous *Men1* KO mice develop, among others, pituitary tumors	Zhuang et al. [142], 1997; Tanaka et al. [143], 1998; Wenbin et al. [144], 1999; Schmidt et al. [145],1999; McCabe et al. [146],1999

Stratakis CA (ed): Endocrine Tumor Syndromes and Their Genetics.
Front Horm Res. Basel, Karger, 2013, vol 41, pp 111–140 (DOI: 10.1159/000345673)

Table 1 . Continued

Gene name	MIM number	Location (Chr)	Function	TSG/ oncogene	Defect
MERTK (CMP-tk)	604705	2q13	Receptor tyrosine kinase that transduces signals from the extracellular matrix into the cytoplasm by binding to several ligands	Oncogene	Increased expression in corticotropinomas, decreased expression in prolactinomas
NR3C1 (GR, GCR)	138040	5q31.3	Nuclear receptor for glucocorticoids	–	Loss-of-function somatic mutation, LOH
ODC1 (ODC)	165640	2p25.1	Catalyzes the decarboxylation of ornithine to form putrescine	Oncogene	Increased expression in somatotrophinomas, decreased expression in corticotropinomas
PIK3CA	171834	3q26.32	Catalytic subunit of phosphatidylinositol 3-kinase, which coordinates a diverse range of cell functions such as proliferation, cell survival, degranulation, vesicular trafficking and cell migration	Oncogene	Gain-of-function somatic mutations and genetic amplification
PITX2	601542	4q25	Member of the bicoid-like homeobox transcription factor family, which is involved in the Wnt/ Dvl/β-catenin pathway	–	Increased expression
PLAGL1 (ZAC1)	603044	6q24.2	Zinc finger transcription factor that plays a role in pituitary development, differentiation, maturation and tumorigenesis	TSG	Decreased expression
POU1F1 (PIT1)	173110	3p11.2	Transcription factor with a key role in specification, expansion and survival of different pituitary cell types during anterior pituitary development	–	Increased expression
PRKCA (PKC α)	176960	17q24.2	Kinase that participates in growth factor- and hormone-mediated transmembrane signaling and cell proliferation	Oncogene	Increased expression, gain-of-function somatic mutations in invasive tumors
PTTG1 (PTTG, Securin)	604147	5q33.3	Cell cycle regulation and cell senescence	Oncogene	Increased expression, especially in corticotropinomas
PTTG1IP (PBF)	603784	21q22.3	Facilitates the nuclear translocation of PTTG1 and potentiates the transcriptional activation of FGF2 by PTTG1	Oncogene	Increased expression, especially in NFPAs
RB1 (pRB)	614041	13q14.2	Key regulator of entry into cell division	TSG	Decreased expression partly by promoter methylation
RHBDD3 (PTAG)	–	22q12.2	Pro-apoptotic mediator	TSG	Decreased expression partly due to promoter methylation
SMARCA4 (Brg1)	603254	19p13.2	Member of the SWI/SNF protein family with helicase and ATPase activities. Regulates gene transcription by altering chromatin structure	TSG	Decreased expression, altered subcellular localization
SSTR2	182452	17q25.1	G protein-coupled receptor for somatostatin	–	Decreased expression

Stratakis CA (ed): Endocrine Tumor Syndromes and Their Genetics.
Front Horm Res. Basel, Karger, 2013, vol 41, pp 111–140 (DOI: 10.1159/000345673)

Tumor types	Animal models	References
Corticotropinomas, prolactinomas	No pituitary tumors	Evans et al. [114], 2001
Corticotropinomas	Homozygous null mutants die at birth	Karl et al. [147], 1996; Huizenga et al. [148], 1998
Somatotrophinomas, corticotropinomas	Homozygous null embryos die prior to gastrulation	Evans et al. [114], 2001
Mutations in invasive corticotroph, lactotroph, plurihormonal and non-functioning adenomas, amplifications in all types of adenomas, both invasive and non-invasive	Homozygous KO or knock-in mutations of *Pik3ca* lead to embryonic death associated with growth retardation	Lin et al. [134], 2009
NFPAs	Transgenic overexpression of *Pitx2* in mouse pituitary increases gonadotroph population	Acunzo et al. [149], 2011
NFPAs	*Zac1* KO results in neonatal lethality in mice	Pagotto et al. [150], 2000; Noh et al. [151], 2009
GH-, PRL- and TSH-secreting adenomas	Homozygous *Pou1f1* KO mice for spontaneous mutations exhibit hypoplasia of the anterior pituitary cells resulting in deficiencies in GH, PRL, and TSH, dwarfism	Palmieri et al. [152], 2012
NFPAs	No pituitary tumors	Alvaro et al. [153], 1993
All tumor types	Targeted *Pttg* overexpression in mice results in focal pituitary hyperplasia with hormone hypersecretion; transgenic zebrafish overexpressing *zPttg* targeted to POMC cells show hypercortisolism and pituitary corticotroph expansion	Zhang et al. [154], 1999; McCabe et al. [111], 2003; Morris et al. [76], 2005; Salehi et al. [155], 2010
All tumor types	No animal models available	McCabe et al. [111], 2003
Aggressive adenomas	pRB+/- mice develop intermediate lobe hyperplasia which leads to ACTH-secreting adenomas	Simpson et al. [156], 2000; Ogino et al. [101], 2005; Yoshino et al. [102], 2006
Various tumor types	No animal models available	Bahar et al. [157], 2004
Corticotropinomas	*Brg1* -/- mice died during the periimplantation stage. Brg1 +/- mice are predisposed to exencephaly and various tumors (no pituitary)	Bilodeau et al. [128], 2006
Resistant somatotrophinomas compared to non-resistant tumors	No pituitary tumors	Corbetta et al. [158], 2001

Stratakis CA (ed): Endocrine Tumor Syndromes and Their Genetics.
Front Horm Res. Basel, Karger, 2013, vol 41, pp 111–140 (DOI: 10.1159/000345673)

Table 1 . Continued

Gene name	MIM number	Location (Chr)	Function	TSG/ oncogene	Defect
THRB (TRβ)	190160	3p24.2	Nuclear receptor that mediates gene regulation by thyroid hormone	TSG	Loss-of-function somatic mutation and aberrant alternatively spliced variant
TP53 (P53)	191170	17p13.1	Involved in cell cycle regulation as a trans-activator that acts to negatively regulate cell division by controlling a set of genes required for this process	TSG	Loss-of-function somatic mutations
WIF1	605186	12q14.3	Secreted protein that binds WNT proteins and inhibits their activities	TSG	Decreased expression by promoter methylation

White background = Abnormal gene expression; light grey background = genetic defects; dark grey background = both genetic defects and abnormal expression. Gene names are shown accordingly to the HGNC (HUGO Gene Nomenclature Committee) approved gene symbol. Commonly used alternative symbols are shown in brackets. Data from nonvalidated microarray experiments are not reported in the table. MIM = Mendelian inheritance in man database; Chr = chromosome; TSG = tumor suppressor gene; SNP = single nucleotide polymorphism; KO = knock-out; LOH = loss of heterozygosity; NFPAs = nonfunctioning pituitary adenomas.

Somatic Alterations in Pituitary Adenomas

Pituitary adenomas are monoclonal in origin, expanding from molecular abnormalities in a single somatic cell [60]. These alterations, which include activation of proto-oncogenes, inactivation of tumor suppressor genes, and epimutations, confer the cell a growth advantage. The resulting genomic instability facilitates subsequent mutation accumulation [61].

The majority (about 95%) of pituitary adenomas occur sporadically. The most common somatic mutation is in the *GNAS* gene (gsp mutation), which occurs in around 40% of GH-secreting adenomas. Alterations in classical tumor suppressor genes such as *TP53* and *RB1* or oncogenes such as *HRAS* and *MYC* are only rarely identified, and exclusively in aggressive tumors or pituitary carcinomas [62] (table 1).

Numerous genes show altered expression in pituitary tumors (table 1), but it is still unknown whether they initiate the tumorigenic process or if they represent a later event. A number of alterations have been found to alter the expression of genes implicated in the regulation of the cell cycle, apoptosis, growth factors and their receptors, signal transduction pathways (in particular, the cAMP, MAPK and PI3K/Akt pathways [63]), specific hormonal factors, or other molecules with still unclear

Stratakis CA (ed): Endocrine Tumor Syndromes and Their Genetics.
Front Horm Res. Basel, Karger, 2013, vol 41, pp 111–140 (DOI: 10.1159/000345673)

Tumor types	Animal models	References
Thyrotropinomas	No pituitary tumors	Ando et al. [159], 2001; Ando et al. [160], 2001
1 atypical ACTH-secreting adenoma, 1 aggressive ACTH-secreting adenoma after radiotherapy, 1 atypical PRL-secreting adenoma and 1 pituitary carcinoma from the same patient, 2 ACTH-secreting carcinomas	*Tp53* KO mice are predisposed to develop pituitary adenomas, double *Tp53* and *Rb1* KO mice develop pituitary adenomas with a shorter latency than single *Tp53* and *Rb1* mutants	Tanizaki et al. [161], 2007; Kawashima et al. [162], 2009; Pinto et al. [163], 2011; Murakami et al. [164], 2011
Reduction of mRNA common to all tumor subtypes, reduction of protein levels predominantly limited to NFPAs	No pituitary tumors	Elston et al. [87], 2008

functions. Different mechanisms leading to abnormal gene expression have been described, such as allelic loss, gene amplification, and epigenetic changes [64]. Several tumor suppressor genes, in particular the inhibitors of cyclin-dependent kinase complexes, were shown to be frequently downregulated in pituitary tumors without presenting somatic mutations but as a consequence of epigenetic alterations like promoter hypermethylation or histone modifications [65, 66]. Moreover, abnormal miRNA expression profiles have been reported in recent years in pituitary adenomas [67] (table 2). Several animal models have been generated, which usually confirmed the functional role of these genes in the pathogenesis of pituitary tumors [62, 66].

To explain the predominance of benign versus malignant pituitary tumors, the occurrence of cellular senescence has been proposed [68]. Cellular senescence is an antiproliferative response triggered by DNA damage, chromosomal instability and aneuploidy, loss of tumor-suppressive signaling or oncogene activation, which leads to irreversible cell cycle arrest via activation of inhibitors of cell cycle progression, such as $p16^{INK4}$, $p19^{ARF}$, and $p21^{CIP1}$. Pituitary adenoma cells may undergo premature senescence in order to escape from the deleterious consequences that proliferative pressure of oncogenes, hormones and transformation factors could exert on their crucial

Stratakis CA (ed): Endocrine Tumor Syndromes and Their Genetics.
Front Horm Res. Basel, Karger, 2013, vol 41, pp 111–140 (DOI: 10.1159/000345673)

physiological function on homeostasis control. More than 70% of GH-secreting adenomas overexpress the *PTTG* gene, which leads to aneuploidy and induction of senescence markers, including $p21^{CIP1}$ and senescence-associated β-galactosidase. In contrast, $p21^{CIP1}$ is weakly expressed in normal pituitary tissue and undetectable in pituitary carcinomas [69].

MicroRNAs in Pituitary Adenomas

MicroRNAs (miRNAs) are small (approximately 22 nucleotides) noncoding RNA molecules involved in posttranscriptional regulation of gene expression [70]. They regulate about 30% of human genes, constituting a major class of molecular regulators. The mature miRNA, as part of a complex called RNA-induced silencing complex (RISC), either binds to a perfectly complementary sequence in the mRNA strand resulting in degradation of the mRNA by RISC, or binds to a partially complementary mRNA sequence and this induces translational repression of the target mRNA [71].

miRNAs have been implicated in the regulation of many cellular processes, including cell proliferation, apoptosis, cell adhesion and metabolism. Thus, alterations in miRNA expression can potentially be involved in the development of many diseases, including human neoplasias. miRNAs can act either as activators or inhibitors of carcinogenesis, being called oncomiRs and tumor suppressor miRNAs, respectively.

miRNA expression has been associated with pituitary tumor type, characteristics (size, invasion) and response to therapy. miRNAs have also been involved in the regulation of some genes associated with the pathogenesis of pituitary adenomas (table 2) [67].

Several different miRNAs have been shown to be differently expressed in the various subtypes of pituitary adenomas in comparison with normal pituitary and also in adenomas in comparison with carcinomas (table 2) [67, 72]. Degli Uberti's group observed that miR-15a and miR-16–1 were downregulated in GH- and PRL-producing adenomas in comparison with normal pituitary and the expression of these miRNAs was inversely correlated with tumor size [72]. Moreover, some miRNAs targets were evaluated individually in different studies:

- miR-16–1 predicted target arginyl-tRNA synthetase (RARS) mRNA levels inversely correlated with miR-16-1 expression and tumor size in both somatotrophinomas and prolactinomas [67, 72].
- The expression of miR let-7 inversely correlated with mRNA levels of *high-mobility group A protein 2 (HMGA2)*, a gene known to cause pituitary adenomas in transgenic mice, suggesting that the reduction of this miRNA may be responsible for the higher expression of HMGA2 in more invasive tumors [67]. Moreover, functional studies showed that transfection of this miRNA reduced the proliferation of GH3 cells, indicating that it might act as a tumor suppressor miRNA.

Stratakis CA (ed): Endocrine Tumor Syndromes and Their Genetics.
Front Horm Res. Basel, Karger, 2013, vol 41, pp 111–140 (DOI: 10.1159/000345673)

Table 2. Studies addressing microRNAs expression in pituitary adenomas

Study	Tumor type	Aberrant microRNAs expression	Affected gene(s)	Clinical correlation
Bottoni et al. [165], 2005	10 GH and 10 PRL	Underexpression of miR-15a and miR-16-1 in adenomas × NP	*RARS*	Inverse correlation with tumor size
Bottoni et al. [166], 2007	17 NFPA, 5 PRL, 4 ACTH and 6 GH	30 miRNAs differently expressed between adenomas and NP. 29 miRNAs predict tumor type	–	6 miRNAs correlated with tumor size in NFPA. 3 miRNAs up- and 3 down-regulated in NFPA treated with DA in comparison with non-treated ones
Qian et al. [167], 2009	98 adenomas of all types	Let-7 overexpression in tumors with low HMGA2 expression	*HMGA2*	
Amaral et al. [168], 2009	14 ACTH	Underexpression of miR-145, miR-21, miR-141, miR-150, miR-15a, miR-16, miR-143 and let-7a in adenomas × NP	–	miR-141 levels directly correlated with chance of disease recurrence
Stilling et al. [169], 2010	8 ACTH 2 ACTH carcinomas	188 miRNAs over- and 160 under-expressed in ACTH × NP 98 miRNAs differently expressed in adenoma × carcinoma	–	–
Butz et al. [170], 2010*	27 NFPA and 15 GH	miR-20a, miR-128a and miR-516-3p overexpressed in NFPA. miR-93 and miR-155 overexpressed in GH and NFPA	*WEE1*	–
Mao et al. [171], 2010	21 GH	23 miRNAs over- and 29 under-expressed in GH × NP	–	9 miRNAs differently expressed in micro × macroadenomas 13 differently expressed in lanreotide treated × surgery alone 7 differently expressed in lanreotide responders × non responders
Butz et al. [172], 2011	8 NFPA	70 miRNAs over- and 92 under-expressed in NFPA × NP	–	18 miRNAs inversely correlated with tumor size
Palmieri et al. [173], 2011*	14 PRL, 9 GH and 18 NFPA	miR-15, miR-16, miR26a, miR-196ab and Let-7a underexpressed in adenomas × NP	*HMGA1* and *HMGA2*	–
D'Ángelo et al. [174], 2012*	18 GH	miR34b, miR-326, miR-374b, miR-432, miR-548c-3p, miR-570, miR-603 and miR-633 under-expressed, and miR-320 over-expressed in adenomas × NP	*HMGA1*, *HMGA2* and *E2F1*	–
Palumbo et al. [74], 2012*	12 GH	5 miRNAs over- and 12 underexpressed in GH × NP	*PTEN* and *BMI1*	–
Trivellin et al. [73], 2012*	10 GH and 7 NFPA	miR-107 overexpressed in tumors × NP AIP expression inhibited by miR-107	*AIP*	–

GH = Somatotrophinoma; PRL = prolactinoma; NFPA = nonfunctioning pituitary adenoma; ACTH = corticotropinoma; NP = normal pituitary tissue; DA = dopamine agonist; × = versus. * Studies where functional validation was done.

- Several miRNAs (miR-135a, miR-140–5p, miR-582–3p, miR-582–2p and miR-938), known to inhibit Smad3, a protein underexpressed in NFPAs, were shown to be significantly overexpressed in NFPAs [67].
- Another group of miRNAs were suggested to influence the expression of cell cycle inhibitor *Wee1*. miR-155, miR-20a, miR-93, miR-128a and miR-516–3p were significantly overexpressed in NFPAs and GH-secreting adenomas compared to NP.

Stratakis CA (ed): Endocrine Tumor Syndromes and Their Genetics.
Front Horm Res. Basel, Karger, 2013, vol 41, pp 111–140 (DOI: 10.1159/000345673)

Functional studies proved that overexpression of miR-128a, miR-516–3p and miR-155 was associated with the reduced expression of Wee1 kinase, thereby indicating a role of these miRNAs in pituitary tumorigenesis [67].

- miR-107 is an interesting miRNA as it has been shown to have both tumor suppressor miR and oncomiR properties, depending on the tissue type. In pituitary adenomas it is upregulated in comparison with normal pituitary [73], however, it inhibits cell proliferation in human neuroblastoma SH-SY5Y and rat pituitary GH3 cell lines. *AIP* is a functional target of miR-107 as miR-107 inhibits human AIP expression [73]; therefore, miR-107 unlikely exerts its tumor suppressor role via *AIP*.
- A recent study using somatotroph hyperplasia samples showed that miR-26b was overexpressed and miR-128 was underexpressed compared to normal pituitary [74]. Molecular analysis revealed that these miRNAs regulate the expression levels of *PTEN* and *BMI1,* genes known to be involved in the regulation of cell proliferation.

Conclusion

Tumorigenesis is influenced by inherited and acquired mutations as well as epigenetic changes. An important feature of pituitary adenomas is that they are relatively common but rarely cause clinically relevant disease and exceedingly rarely develop into a metastatic carcinoma. One of the suggested mechanisms of lack of malignant transformation is the development of cellular senescence. However, the regulating factors influencing these processes in the vast majority of sporadic adenoma cases are unknown. On the other hand, understanding the tumorigenic process in the rare familial adenomas could result in better diagnostic and treatment options for both familial and sporadic cases.

References

1 Ezzat S, Asa SL, Couldwell WT, Barr CE, Dodge WE, Vance ML, McCutcheon IE: The prevalence of pituitary adenomas: a systematic review. Cancer 2004;101:613–619.

2 Daly AF, Rixhon M, Adam C, Dempegioti A, Tichomirowa MA, Beckers A: High prevalence of pituitary adenomas: a cross-sectional study in the province of Liege, Belgium. J Clin Endocrinol Metab 2006;91:4769–4775.

3 Fernandez A, Karavitaki N, Wass JA: Prevalence of pituitary adenomas: a community-based, cross-sectional study in Banbury (Oxfordshire, UK). Clin Endocrinol (Oxf) 2010;72:377–382.

4 Couldwell WT, Cannon-Albright L: A heritable predisposition to pituitary tumors. Pituitary 2010; 13:130–137.

5 Wildi-Runge S, Bahubeshi A, Carret A, Crevier L, Robitaille Y, Kovacs K, Horvath E, Schenck S, Foulkes WD, Deal C: New phenotype in the familial DICER1 tumor syndrome: pituitary blastoma presenting at age 9 months. Endocrine Rev 2011;32:P1–P777.

6 Denes J, Swords FM, Xekouki P, Kumar AV, Maher ER, Erscht N, Grieve J, Baldeweg SE, Stratakis CA, Korbonits M: Familial pituitary adenoma and paraganglioma syndrome – a novel type of multiple endocrine neoplasia. Endocrine Rev 2012;33:OR41–OR42.

7 Brahma A, Heyburn P, Swords F: Familial prolactinoma occurring in association with SDHB mutation positive paraganglioma. Endocrine Abstr 2009;19:239.
8 Xekouki P, Pacak K, Almeida M, Wassif CA, Rustin P, Nesterova M, de la Luz SM, Matro J, Ball E, Azevedo M, Horvath A, Lyssikatos C, Quezado M, Patronas N, Ferrando B, Pasini B, Lytras A, Tolis G, Stratakis CA: Succinate dehydrogenase (SDH) D subunit (SDHD) inactivation in a growth-hormone-producing pituitary tumor: a new association for SDH? J Clin Endocrinol Metab 2012; 97:E357–E366.
9 Varsavsky M, Sebastian-Ochoa A, Torres VE: Coexistence of a pituitary macroadenoma and multicentric paraganglioma: a strange coincidence. Endocrinol Nutr 2012, epub ahead of print.
10 Korbonits M, Storr H, Kumar AV: Familial pituitary adenomas. Who should be tested for AIP mutations? Clin Endocrinol (Oxf) 2012;77:3513–3556.
11 Agarwal SK, Mateo CM, Marx SJ: Rare germline mutations in cyclin-dependent kinase inhibitor genes in multiple endocrine neoplasia type 1 and related states. J Clin Endocrinol Metab 2009;94: 1826–1834.
12 Chahal HS, Stals K, Unterlander M, Balding DJ, Thomas MG, Kumar AV, Besser GM, Atkinson AB, Morrison PJ, Howlett TA, Levy MJ, Orme SM, Akker SA, Abel RL, Grossman AB, Burger J, Ellard S, Korbonits M: AIP mutation in pituitary adenomas in the 18th century and today. N Eng J Med 2011; 364:43–50.
13 Igreja S, Chahal HS, King P, Bolger GB, Srirangalingam U, Guasti L, Chapple JP, Trivellin G, Gueorguiev M, Guegan K, Stals K, Khoo B, Kumar AV, Ellard S, Grossman AB, Korbonits M: Characterization of aryl hydrocarbon receptor interacting protein (AIP) mutations in familial isolated pituitary adenoma families. Hum Mutat 2010;31:950–960.
14 Occhi G, Jaffrain-Rea ML, Trivellin G, Albiger N, Ceccato F, De ME, Angelini M, Ferasin S, Beckers A, Mantero F, Scaroni C: The R304X mutation of the aryl hydrocarbon receptor interacting protein gene in familial isolated pituitary adenomas: mutational hot-spot or founder effect? J Endocrinol Invest 2010;33:800–805.
15 Chahal HS, Chapple JP, Frohman LA, Grossman AB, Korbonits M: Clinical, genetic and molecular characterization of patients with familial isolated pituitary adenomas (FIPA). Trends Endocrinol Metab 2010;21:419–427.
16 Daly AF, Tichomirowa MA, Petrossians P, et al: Clinical characteristics and therapeutic responses in patients with germ-line AIP mutations and pituitary adenomas: an international collaborative study. J Clin Endocrinol Metab 2010;95:E373–E383.
17 Tichomirowa MA, Barlier A, Daly AF, et al: High prevalence of AIP gene mutations following focused screening in young patients with sporadic pituitary macroadenomas. Eur J Endocrinol 2011; 165:509–515.
18 Leontiou CA, Gueorguiev M, van der SJ, et al: The role of the aryl hydrocarbon receptor-interacting protein gene in familial and sporadic pituitary adenomas. J Clin Endocrinol Metab 2008;93:2390–2401.
19 Chahal HS, Trivellin G, Leontiou CA, Alband N, Fowkes RC, Tahir A, Igreja SC, Chapple JP, Jordan S, Lupp A, Schulz S, Ansorge O, Karavitaki N, Carlsen E, Wass JAH, Grossman AB, Korbonits M: Somatostatin analogues modulate AIP in somatotroph adenomas – the role of the ZAC1 pathway. J Clin Endocrinol Metab 2012;97:E14111–E14420.
20 Kasuki Jomori de PL, Vieira NL, Armondi Wildemberg LE, Gasparetto EL, Marcondes J, de Almeida NB, Takiya CM, Gadelha MR: Low aryl hydrocarbon receptor-interacting protein expression is a better marker of invasiveness in somatotropinomas than ki-67 and p53. Neuroendocrinology 2011;94: 39–48.
21 Kasuki L, Vieira NL, Wildemberg LE, Colli LM, de CM, Takiya CM, Gadelha MR: AIP expression in sporadic somatotropinomas is a predictor of the response to octreotide LAR therapy independent of SSTR2 expression. Endocr Relat Cancer 2012; 19:L25–L29.
22 Hernández-Ramírez LC, Korbonits M: Familial pituitary adenomas; in Laws ER, Ezzat S, Asa SL, Rio LM, Michel L, Knutzen R: Pituitary Disorders: Diagnosis and Management. John Wiley & Sons, Ltd., 2013, pp 87–110.
23 Korbonits M: Tracing back a gene's influence. Endocrine Abstr 2012;29:S22.2.
24 Dull AB, Carlson DB, Petrulis JR, Perdew GH: Characterization of the phosphorylation status of the hepatitis B virus X-associated protein 2. Arch Biochem Biophys 2002;406:209–221.
25 Linnert M, Haupt K, Lin YJ, Kissing S, Paschke AK, Fischer G, Weiwad M, Lucke C: NMR assignments of the FKBP-type PPIase domain of the human aryl-hydrocarbon receptor-interacting protein (AIP). Biomol NMR Assign 2012;6:209–212.
26 Trivellin G, Korbonits M: AIP and its interacting partners. J Endocrinol 2011;210:137–155.

Stratakis CA (ed): Endocrine Tumor Syndromes and Their Genetics.
Front Horm Res. Basel, Karger, 2013, vol 41, pp 111–140 (DOI: 10.1159/000345673)

27 Schulke JP, Wochnik GM, Lang-Rollin I, Gassen NC, Knapp RT, Berning B, Yassouridis A, Rein T: Differential impact of tetratricopeptide repeat proteins on the steroid hormone receptors. PLoS One 2010;5:e11717.
28 Petrulis JR, Perdew GH: The role of chaperone proteins in the aryl hydrocarbon receptor core complex. Chem Biol Interact 2002;141:25–40.
29 Jaffrain-Rea ML, Angelini M, Gargano D, et al: Expression of aryl hydrocarbon receptor (AHR) and AHR-interacting protein in pituitary adenomas: pathological and clinical implications. Endocr Relat Cancer 2009;16:1029–1043.
30 Vierimaa O, Georgitsi M, Lehtonen R, Vahteristo P, Kokko A, Raitila A, Tuppurainen K, Ebeling TM, Salmela PI, Paschke R, Gundogdu S, De ME, Makinen MJ, Launonen V, Karhu A, Aaltonen LA: Pituitary adenoma predisposition caused by germline mutations in the AIP gene. Science 2006;312:1228–1230.
31 Heliovaara E, Raitila A, Launonen V, Paetau A, Arola J, Lehtonen H, Sane T, Weil RJ, Vierimaa O, Salmela P, Tuppurainen K, Makinen M, Aaltonen LA, Karhu A: The expression of AIP-related molecules in elucidation of cellular pathways in pituitary adenomas. Am J Pathol 2009;175:2501–2507.
32 Lin BC, Sullivan R, Lee Y, Moran S, Glover E, Bradfield CA: Deletion of the aryl hydrocarbon receptor-associated protein 9 leads to cardiac malformation and embryonic lethality. J Biol Chem 2007;282:35924–35932.
33 Kang BH, Xia F, Pop R, Dohi T, Socolovsky M, Altieri DC: Developmental control of apoptosis by the immunophilin aryl hydrocarbon receptor-interacting protein (AIP) involves mitochondrial import of survivin. J Biol Chem 2011;286:16758–16767.
34 Raitila A, Lehtonen HJ, Arola J, Heliovaara E, Ahlsten M, Georgitsi M, Jalanko A, Paetau A, Aaltonen LA, Karhu A: Mice with inactivation of aryl hydrocarbon receptor-interacting protein (AIP) display complete penetrance of pituitary adenomas with aberrant ARNT expression. Am J Pathol 2010;177:1969–1976.
35 McCune DJ: Osteitis fibrosa cystica: the case of a nine year old girl who also exhibits precocious puberty, multiple pigmentation of the skin and hyperthyroidism. Am J Dis Child 1936;52:743–744.
36 Albright F, Butler AM, Hampton AO, Smith P: Syndrome characterized by osteitis fibrosa disseminata, areas of pigmentation and endocrine dysfunction, with precocious puberty in females – report of five cases. N Eng J Med 1937;216:727–746.
37 Dumitrescu CE, Collins MT: McCune-Albright syndrome. Orphanet J Rare Dis 2008;3:12.
38 Lumbroso S, Paris F, Sultan C: Activating Gsalpha mutations: analysis of 113 patients with signs of McCune-Albright syndrome – a European Collaborative Study. J Clin Endocrinol Metab 2004;89:2107–2113.
39 Shah KN: The diagnostic and clinical significance of cafe-au-lait macules. Pediatr Clin N Am 2010;57:1131–1153.
40 Weinstein LS, Shenker A, Gejman PV, Merino MJ, Friedman E, Spiegel AM: Activating mutations of the stimulatory G protein in the McCune-Albright syndrome. N Eng J Med 1991;325:1688–1695.
41 Happle R: The McCune-Albright syndrome: a lethal gene surviving by mosaicism. Clin Genet 1986;29:321–324.
42 Weinstein LS, Liu J, Sakamoto A, Xie T, Chen M: GNAS: normal and abnormal functions. Endocrinology 2004;145:5459–5464.
43 Bianco P, Kuznetsov SA, Riminucci M, Fisher LW, Spiegel AM, Robey PG: Reproduction of human fibrous dysplasia of bone in immunocompromised mice by transplanted mosaics of normal and Gsalpha-mutated skeletal progenitor cells. J Clin Invest 1998;101:1737–1744.
44 Hayward BE, Moran V, Strain L, Bonthron DT: Bidirectional imprinting of a single gene: GNAS1 encodes maternally, paternally, and biallelically derived proteins. Proc Natl Acad Sci USA 1998;95:15475–15480.
45 Hayward BE, Bonthron DT: An imprinted antisense transcript at the human GNAS1 locus. Hum Mol Genet 2000;9:835–841.
46 Weinstein LS, Yu S, Warner DR, Liu J: Endocrine manifestations of stimulatory G protein alpha-subunit mutations and the role of genomic imprinting. Endocrine Rev 2001;22:675–705.
47 Weinstein LS: The stimulatory G protein alpha-subunit gene: mutations and imprinting lead to complex phenotypes. J Clin Endocrinol Metab 2001;86:4622–4626.
48 Hayward BE, Barlier A, Korbonits M, Grossman AB, Jacquet P, Enjalbert A, Bonthron DT: Imprinting of the G(s)alpha gene GNAS1 in the pathogenesis of acromegaly. J Clin Invest 2001;107:R31–R36.
49 Mantovani G, Bondioni S, Lania AG, Corbetta S, de SL, Cappa M, Di BE, Chanson P, Beck-Peccoz P, Spada A: Parental origin of Gsalpha mutations in the McCune-Albright syndrome and in isolated endocrine tumors. J Clin Endocrinol Metab 2004;89:3007–3009.
50 Mantovani G, Ballare E, Giammona E, Beck-Peccoz P, Spada A: The gsalpha gene: predominant maternal origin of transcription in human thyroid gland and gonads. J Clin Endocrinol Metab 2002;87:4736–4740.

Stratakis CA (ed): Endocrine Tumor Syndromes and Their Genetics.
Front Horm Res. Basel, Karger, 2013, vol 41, pp 111–140 (DOI: 10.1159/000345673)

51 Lyons J, Landis CA, Harsh G, Vallar L, Grunewald K, Feichtinger H, Duh QY, Clark OH, Kawasaki E, Bourne HR: Two G protein oncogenes in human endocrine tumors. Science 1990;249:655–659.
52 Landis CA, Masters SB, Spada A, Pace AM, Bourne HR, Vallar L: GTPase inhibiting mutations activate the alpha chain of Gs and stimulate adenylyl cyclase in human pituitary tumours. Nature 1989;340: 692–696.
53 Freda PU, Chung WK, Matsuoka N, Walsh JE, Kanibir MN, Kleinman G, Wang Y, Bruce JN, Post KD: Analysis of GNAS mutations in 60 growth hormone secreting pituitary tumors: correlation with clinical and pathological characteristics and surgical outcome based on highly sensitive GH and IGF-I criteria for remission. Pituitary 2007;10:275–282.
54 Akintoye SO, Chebli C, Booher S, Feuillan P, Kushner H, Leroith D, Cherman N, Bianco P, Wientroub S, Robey PG, Collins MT: Characterization of gsp-mediated growth hormone excess in the context of McCune-Albright syndrome. J Clin Endocrinol Metab 2002;87:5104–5112.
55 Vortmeyer AO, Glasker S, Mehta GU, Abu-Asab MS, Smith JH, Zhuang Z, Collins MT, Oldfield EH: Somatic GNAS mutation causes widespread and diffuse pituitary disease in acromegalic patients with McCune-Albright syndrome. J Clin Endocrinol Metab 2012;97:2404–2413.
56 Galland F, Kamenicky P, Affres H, Reznik Y, Pontvert D, Le BY, Young J, Chanson P: McCune-Albright syndrome and acromegaly: effects of hypothalamopituitary radiotherapy and/or pegvisomant in somatostatin analog-resistant patients. J Clin Endocrinol Metab 2006;91:4957–4961.
57 De SC, Lala R, Matarazzo P, Balsamo A, Bergamaschi R, Cappa M, Cisternino M, de SV, Lucci M, Franzese A, Ghizzoni L, Pasquino AM, Segni M, Rigon F, Saggese G, Bertelloni S, Buzi F: McCune-Albright syndrome: a longitudinal clinical study of 32 patients. J Pediatr Endocrinol Metab 1999;12: 817–826.
58 Riminucci M, Collins MT, Fedarko NS, Cherman N, Corsi A, White KE, Waguespack S, Gupta A, Hannon T, Econs MJ, Bianco P, Gehron RP: FGF-23 in fibrous dysplasia of bone and its relationship to renal phosphate wasting. J Clin Invest 2003;112: 683–692.
59 Collins MT, Singer FR, Eugster E: McCune-Albright syndrome and the extraskeletal manifestations of fibrous dysplasia. Orphanet J Rare Dis 2012;7(suppl 1):S4.
60 Herman V, Fagin J, Gonsky R, Kovacs K, Melmed S: Clonal origin of pituitary adenomas. J Clin Endocrinol Metab 1990;71:1427–1433.
61 Peltomaki P: Mutations and epimutations in the origin of cancer. Exp Cell Res 2012;318:299–310.
62 Lania A, Mantovani G, Spada A: Genetics of pituitary tumors: Focus on G-protein mutations. Exp Biol Med (Maywood) 2003;228:1004–1017.
63 Cuny T, Gerard C, Saveanu A, Barlier A, Enjalbert A: Physiopathology of somatolactotroph cells: from transduction mechanisms to cotargeting therapy. Ann NY Acad Sci 2011;1220:60–70.
64 Vandeva S, Jaffrain-Rea ML, Daly AF, Tichomirowa M, Zacharieva S, Beckers A: The genetics of pituitary adenomas. Best Pract Res Clin Endocrinol Metab 2010;24:461–476.
65 Musat M, Vax VV, Borboli N, Gueorguiev M, Bonner S, Korbonits M, Grossman AB: Cell cycle dysregulation in pituitary oncogenesis. Front Horm Res 2004;32:34–62.
66 Quereda V, Malumbres M: Cell cycle control of pituitary development and disease. J Mol Endocrinol 2009;42:75–86.
67 Sivapragasam M, Rotondo F, Lloyd RV, Scheithauer BW, Cusimano M, Syro LV, Kovacs K: MicroRNAs in the human pituitary. Endocr Pathol 2011;22:134–143.
68 Chesnokova V, Zonis S, Ben-Shlomo A, Wawrowsky K, Melmed S: Molecular mechanisms of pituitary adenoma senescence. Front Horm Res 2010; 38:7–14.
69 Chesnokova V, Melmed S: Pituitary senescence: the evolving role of PTTG. Mol Cell Endocrinol 2010; 326:55–59.
70 Taft RJ, Pang KC, Mercer TR, Dinger M, Mattick JS: Non-coding RNAs: regulators of disease. J Pathol 2010;220:126–139.
71 Lee RC, Feinbaum RL, Ambros V: The *C. elegans* heterochronic gene lin-4 encodes small RNAs with antisense complementarity to lin-14. Cell 1993;75: 843–854.
72 Zatelli MC, Degli Uberti EC: MicroRNAs and possible role in pituitary adenoma. Semin Reprod Med 2008;26:453–460.
73 Trivellin G, Butz H, Delhove J, Igreja S, Chahal HS, Zivkovic V, McKay TR, Patocs A, Grossman AB, Korbonits M: MicroRNA miR-107 is overexpressed in pituitary adenomas and in vitro inhibits the expression of aryl hydrocarbon receptor-interacting protein (AIP). Am J Physiol Endocrinol Metab 2012;303:E708–E719.
74 Palumbo T, Faucz FR, Azevedo M, Xekouki P, Iliopoulos D, Stratakis CA: Functional screen analysis reveals miR-26b and miR-128 as central regulators of pituitary somatomammotrophic tumor growth through activation of the PTEN-AKT pathway. Oncogene 2012, epub ahead of print.
75 Musat M, Korbonits M, Kola B, Borboli N, Hanson MR, Nanzer AM, Grigson J, Jordan S, Morris DG, Gueorguiev M, Coculescu M, Basu S, Grossman AB: Enhanced protein kinase B/Akt signalling in pituitary tumours. Endocr Relat Cancer 2005;12:423–433.

Stratakis CA (ed): Endocrine Tumor Syndromes and Their Genetics.
Front Horm Res. Basel, Karger, 2013, vol 41, pp 111–140 (DOI: 10.1159/000345673)

76 Morris DG, Musat M, Czirjak S, Hanzely Z, Lillington DM, Korbonits M, Grossman AB: Differential gene expression in pituitary adenomas by oligonucleotide array analysis. Eur J Endocrinol 2005;153:143–151.
77 Sanchez-Beato M, Sanchez E, Gonzalez-Carrero J, Morente M, Diez A, Sanchez-Verde L, Martin MC, Cigudosa JC, Vidal M, Piris MA: Variability in the expression of polycomb proteins in different normal and tumoral tissues. A pilot study using tissue microarrays. Mod Pathol 2006;19:684–694.
78 Westerman BA, Blom M, Tanger E, van DV, Song JY, van SM, Gadiot J, Cornelissen-Steijger P, Zevenhoven J, Prosser HM, Uren A, Aronica E, van LM: GFAP-Cre-mediated transgenic activation of Bmi1 results in pituitary tumors. PLoS One 2012;7:e35943.
79 Paez-Pereda M, Giacomini D, Refojo D, Nagashima AC, Hopfner U, Grubler Y, Chervin A, Goldberg V, Goya R, Hentges ST, Low MJ, Holsboer F, Stalla GK, Arzt E: Involvement of bone morphogenetic protein 4 (BMP-4) in pituitary prolactinoma pathogenesis through a Smad/estrogen receptor crosstalk. Proc Natl Acad Sci USA 2003;100:1034–1039.
80 Turner HE, Nagy Z, Sullivan N, Esiri MM, Wass JA: Expression analysis of cyclins in pituitary adenomas and the normal pituitary gland. Clin Endocrinol (Oxf) 2000;53:337–344.
81 Nakabayashi H, Sunada I, Hara M: Immunohistochemical analyses of cell cycle-related proteins, apoptosis, and proliferation in pituitary adenomas. J Histochem Cytochem 2001;49:1193–1194.
82 Wierinckx A, Auger C, Devauchelle P, Reynaud A, Chevallier P, Jan M, Perrin G, Fevre-Montange M, Rey C, Figarella-Branger D, Raverot G, Belin MF, Lachuer J, Trouillas J: A diagnostic marker set for invasion, proliferation, and aggressiveness of prolactin pituitary tumors. Endocr Relat Cancer 2007;14:887–900.
83 De MI, Visone R, Wierinckx A, Palmieri D, Ferraro A, Cappabianca P, Chiappetta G, Forzati F, Lombardi G, Colao A, Trouillas J, Fedele M, Fusco A: HMGA proteins up-regulate CCNB2 gene in mouse and human pituitary adenomas. Cancer Res 2009;69:1844–1850.
84 Hibberts NA, Simpson DJ, Bicknell JE, Broome JC, Hoban PR, Clayton RN, Farrell WE: Analysis of cyclin D1 (CCND1) allelic imbalance and overexpression in sporadic human pituitary tumors. Clin Cancer Res 1999;5:2133–2139.
85 Jordan S, Lidhar K, Korbonits M, Lowe DG, Grossman AB: Cyclin D and cyclin E expression in normal and adenomatous pituitary. Eur J Endocrinol 2000;143:R1–R6.
86 Simpson DJ, Frost SJ, Bicknell JE, Broome JC, McNicol AM, Clayton RN, Farrell WE: Aberrant expression of G(1)/S regulators is a frequent event in sporadic pituitary adenomas. Carcinogenesis 2001;22:1149–1154.
87 Elston MS, Gill AJ, Conaglen JV, Clarkson A, Shaw JM, Law AJ, Cook RJ, Little NS, Clifton-Bligh RJ, Robinson BG, McDonald KL: Wnt pathway inhibitors are strongly down-regulated in pituitary tumors. Endocrinology 2008;149:1235–1242.
88 Neto AG, McCutcheon IE, Vang R, Spencer ML, Zhang W, Fuller GN: Elevated expression of p21 (WAF1/Cip1) in hormonally active pituitary adenomas. Ann Diagn Pathol 2005;9:6–10.
89 Qian X, Jin L, Grande JP, Lloyd RV: Transforming growth factor-beta and p27 expression in pituitary cells. Endocrinology 1996;137:3051–3060.
90 Lloyd RV, Jin L, Qian X, Kulig E: Aberrant p27kip1 expression in endocrine and other tumors. Am J Pathol 1997;150:401–407.
91 Bamberger CM, Fehn M, Bamberger AM, Ludecke DK, Beil FU, Saeger W, Schulte HM: Reduced expression levels of the cell-cycle inhibitor p27Kip1 in human pituitary adenomas. Eur J Endocrinol 1999;140:250–255.
92 Jin L, Qian X, Kulig E, Sanno N, Scheithauer BW, Kovacs K, Young WF Jr, Lloyd RV: Transforming growth factor-beta, transforming growth factor-beta receptor II, and p27Kip1 expression in nontumorous and neoplastic human pituitaries. Am J Pathol 1997;151:509–519.
93 Lidhar K, Korbonits M, Jordan S, Khalimova Z, Kaltsas G, Lu X, Clayton RN, Jenkins PJ, Monson JP, Besser GM, Lowe DG, Grossman AB: Low expression of the cell cycle inhibitor p27Kip1 in normal corticotroph cells, corticotroph tumors, and malignant pituitary tumors. J Clin Endocrinol Metab 1999;84:3823–3830.
94 Komatsubara K, Tahara S, Umeoka K, Sanno N, Teramoto A, Osamura RY: Immunohistochemical analysis of p27 (Kip1) in human pituitary glands and in various types of pituitary adenomas. Endocr Pathol 2001;12:181–188.
95 Korbonits M, Chahal HS, Kaltsas G, Jordan S, Urmanova Y, Khalimova Z, Harris PE, Farrell WE, Claret FX, Grossman AB: Expression of phosphorylated p27(Kip1) protein and Jun activation domain-binding protein 1 in human pituitary tumors. J Clin Endocrinol Metab 2002;87:2635–2643.
96 Woloschak M, Yu A, Xiao J, Post KD: Frequent loss of the P16INK4a gene product in human pituitary tumors. Cancer Res 1996;56:2493–2496.

Stratakis CA (ed): Endocrine Tumor Syndromes and Their Genetics.
Front Horm Res. Basel, Karger, 2013, vol 41, pp 111–140 (DOI: 10.1159/000345673)

97 Jaffrain-Rea ML, Ferretti E, Toniato E, Cannita K, Santoro A, Di SD, Ricevuto E, Maroder M, Tamburrano G, Cantore G, Gulino A, Martinotti S: p16 (INK4a, MTS-1) gene polymorphism and methylation status in human pituitary tumours. Clin Endocrinol (Oxf) 1999;51:317–325.
98 Simpson DJ, Bicknell JE, McNicol AM, Clayton RN, Farrell WE: Hypermethylation of the p16/CDKN2A/MTSI gene and loss of protein expression is associated with nonfunctional pituitary adenomas but not somatotrophinomas. Genes Chromosomes Cancer 1999;24:328–336.
99 Ruebel KH, Jin L, Zhang S, Scheithauer BW, Lloyd RV: Inactivation of the p16 gene in human pituitary nonfunctioning tumors by hypermethylation is more common in null cell adenomas. Endocr Pathol 2001;12:281–289.
100 Seemann N, Kuhn D, Wrocklage C, Keyvani K, Hackl W, Buchfelder M, Fahlbusch R, Paulus W: CDKN2A/p16 inactivation is related to pituitary adenoma type and size. J Pathol 2001;193:491–497.
101 Ogino A, Yoshino A, Katayama Y, Watanabe T, Ota T, Komine C, Yokoyama T, Fukushima T: The p15(INK4b)/p16(INK4a)/RB1 pathway is frequently deregulated in human pituitary adenomas. J Neuropathol Exp Neurol 2005;64:398–403.
102 Yoshino A, Katayama Y, Ogino A, Watanabe T, Yachi K, Ohta T, Komine C, Yokoyama T, Fukushima T: Promoter hypermethylation profile of cell cycle regulator genes in pituitary adenomas. J Neurooncol 2007;83:153–162.
103 Machiavelli G, Cotignola J, Danilowicz K, Carbonara C, Paes de LA, Basso A, Bruno OD, Szijan I: Expression of p16(INK4A) gene in human pituitary tumours. Pituitary 2008;11:71–75.
104 Kirsch M, Morz M, Pinzer T, Schackert HK, Schackert G: Frequent loss of the CDKN2C (p18INK4c) gene product in pituitary adenomas. Genes Chromosomes Cancer 2009;48:143–154.
105 Hossain MG, Iwata T, Mizusawa N, Qian ZR, Shima SW, Okutsu T, Yamada S, Sano T, Yoshimoto K: Expression of p18(INK4C) is down-regulated in human pituitary adenomas. Endocr Pathol 2009; 20:114–121.
106 Bertherat J, Chanson P, Montminy M: The cyclic adenosine 3′,5′-monophosphate-responsive factor CREB is constitutively activated in human somatotroph adenomas. Mol Endocrinol 1995;9:777–783.
107 Simpson DJ, Clayton RN, Farrell WE: Preferential loss of death associated protein kinase expression in invasive pituitary tumours is associated with either CpG island methylation or homozygous deletion. Oncogene 2002;21:1217–1224.
108 Bellodi C, Krasnykh O, Haynes N, Theodoropoulou M, Peng G, Montanaro L, Ruggero D: Loss of function of the tumor suppressor DKC1 perturbs p27 translation control and contributes to pituitary tumorigenesis. Cancer Res 2010;70:6026–6035.
109 Caccavelli L, Feron F, Morange I, Rouer E, Benarous R, Dewailly D, Jaquet P, Kordon C, Enjalbert A: Decreased expression of the two D2 dopamine receptor isoforms in bromocriptine-resistant prolactinomas. Neuroendocrinology 1994;60:314–322.
110 Chaidarun SS, Eggo MC, Sheppard MC, Stewart PM: Expression of epidermal growth factor (EGF), its receptor, and related oncoprotein (erbB-2) in human pituitary tumors and response to EGF in vitro. Endocrinology 1994;135:2012–2021.
111 McCabe CJ, Khaira JS, Boelaert K, Heaney AP, Tannahill LA, Hussain S, Mitchell R, Olliff J, Sheppard MC, Franklyn JA, Gittoes NJ: Expression of pituitary tumour transforming gene (PTTG) and fibroblast growth factor-2 (FGF-2) in human pituitary adenomas: relationships to clinical tumour behaviour. Clin Endocrinol (Oxf) 2003;58:141–150.
112 Zhu X, Lee K, Asa SL, Ezzat S: Epigenetic silencing through DNA and histone methylation of fibroblast growth factor receptor 2 in neoplastic pituitary cells. Am J Pathol 2007;170:1618–1628.
113 Ezzat S, Zheng L, Zhu XF, Wu GE, Asa SL: Targeted expression of a human pituitary tumor-derived isoform of FGF receptor-4 recapitulates pituitary tumorigenesis. J Clin Invest 2002;109:69–78.
114 Evans CO, Young AN, Brown MR, Brat DJ, Parks JS, Neish AS, Oyesiku NM: Novel patterns of gene expression in pituitary adenomas identified by complementary deoxyribonucleic acid microarrays and quantitative reverse transcription-polymerase chain reaction. J Clin Endocrinol Metab 2001;86:3097–3107.
115 Michaelis KA, Knox AJ, Xu M, Kiseljak-Vassiliades K, Edwards MG, Geraci M, Kleinschmidt-DeMasters BK, Lillehei KO, Wierman ME: Identification of growth arrest and DNA-damage-inducible gene beta (GADD45beta) as a novel tumor suppressor in pituitary gonadotrope tumors. Endocrinology 2011;152:3603–3613.
116 Zhang X, Sun H, Danila DC, Johnson SR, Zhou Y, Swearingen B, Klibanski A: Loss of expression of GADD45 gamma, a growth inhibitory gene, in human pituitary adenomas: implications for tumorigenesis. J Clin Endocrinol Metab 2002;87:1262–1267.
117 Bahar A, Bicknell JE, Simpson DJ, Clayton RN, Farrell WE: Loss of expression of the growth inhibitory gene GADD45gamma, in human pituitary adenomas, is associated with CpG island methylation. Oncogene 2004;23:936–944.

Stratakis CA (ed): Endocrine Tumor Syndromes and Their Genetics.
Front Horm Res. Basel, Karger, 2013, vol 41, pp 111–140 (DOI: 10.1159/000345673)

118 Asa SL, DiGiovanni R, Jiang J, Ward ML, Loesch K, Yamada S, Sano T, Yoshimoto K, Frank SJ, Ezzat S: A growth hormone receptor mutation impairs growth hormone autofeedback signaling in pituitary tumors. Cancer Res 2007;67:7505–7511.
119 Thapar K, Kovacs K, Stefaneanu L, Scheithauer B, Killinger DW, Lioyd RV, Smyth HS, Barr A, Thorner MO, Gaylinn B, Laws ER Jr: Overexpression of the growth-hormone-releasing hormone gene in acromegaly-associated pituitary tumors. An event associated with neoplastic progression and aggressive behavior. Am J Pathol 1997;151:769–784.
120 Hashimoto K, Koga M, Motomura T, Kasayama S, Kouhara H, Ohnishi T, Arita N, Hayakawa T, Sato B, Kishimoto T: Identification of alternatively spliced messenger ribonucleic acid encoding truncated growth hormone-releasing hormone receptor in human pituitary adenomas. J Clin Endocrinol Metab 1995;80:2933–2939.
121 Williamson EA, Daniels M, Foster S, Kelly WF, Kendall-Taylor P, Harris PE: Gs alpha and Gi2 alpha mutations in clinically non-functioning pituitary tumours. Clin Endocrinol (Oxf) 1994;41:815–820.
122 Williamson EA, Ince PG, Harrison D, Kendall-Taylor P, Harris PE: G-protein mutations in human pituitary adrenocorticotrophic hormone-secreting adenomas. Eur J Clin Invest 1995;25:128–131.
123 Vallar L, Spada A, Giannattasio G: Altered Gs and adenylate cyclase activity in human GH-secreting pituitary adenomas. Nature 1987;330:566–568.
124 Tordjman K, Stern N, Ouaknine G, Yossiphov Y, Razon N, Nordenskjold M, Friedman E: Activating mutations of the Gs alpha-gene in nonfunctioning pituitary tumors. J Clin Endocrinol Metab 1993;77:765–769.
125 Hamacher C, Brocker M, Adams EF, Lei T, Fahlbusch R, Buchfelder M, Derwahl M: Overexpression of stimulatory G protein alpha-subunit is a hallmark of most human somatotrophic pituitary tumours and is associated with resistance to GH-releasing hormone. Pituitary 1998;1:13–23.
126 Riminucci M, Collins MT, Lala R, Corsi A, Matarazzo P, Gehron RP, Bianco P: An R201H activating mutation of the GNAS1 (Gsalpha) gene in a corticotroph pituitary adenoma. Mol Pathol 2002;55:58–60.
127 Picard C, Silvy M, Gerard C, Buffat C, Lavaque E, Figarella-Branger D, Dufour H, Gabert J, Beckers A, Brue T, Enjalbert A, Barlier A: Gs alpha overexpression and loss of Gs alpha imprinting in human somatotroph adenomas: association with tumor size and response to pharmacologic treatment. Int J Cancer 2007;121:1245–1252.
128 Bilodeau S, Vallette-Kasic S, Gauthier Y, Figarella-Branger D, Brue T, Berthelet F, LaCroix A, Batista D, Stratakis C, Hanson J, Meij B, Drouin J: Role of Brg1 and HDAC2 in GR trans-repression of the pituitary POMC gene and misexpression in Cushing disease. Genes Dev 2006;20:2871–2886.
129 Finelli P, Pierantoni GM, Giardino D, Losa M, Rodeschini O, Fedele M, Valtorta E, Mortini P, Croce CM, Larizza L, Fusco A: The High Mobility Group A2 gene is amplified and overexpressed in human prolactinomas. Cancer Res 2002;62:2398–2405.
130 Pierantoni GM, Finelli P, Valtorta E, Giardino D, Rodeschini O, Esposito F, Losa M, Fusco A, Larizza L: High-mobility group A2 gene expression is frequently induced in non-functioning pituitary adenomas (NFPAs), even in the absence of chromosome 12 polysomy. Endocr Relat Cancer 2005;12:867–874.
131 Karga HJ, Alexander JM, Hedley-Whyte ET, Klibanski A, Jameson JL: Ras mutations in human pituitary tumors. J Clin Endocrinol Metab 1992;74:914–919.
132 Cai WY, Alexander JM, Hedley-Whyte ET, Scheithauer BW, Jameson JL, Zervas NT, Klibanski A: ras mutations in human prolactinomas and pituitary carcinomas. J Clin Endocrinol Metab 1994;78:89–93.
133 Pei L, Melmed S, Scheithauer B, Kovacs K, Prager D: H-ras mutations in human pituitary carcinoma metastases. J Clin Endocrinol Metab 1994;78:842–846.
134 Lin Y, Jiang X, Shen Y, Li M, Ma H, Xing M, Lu Y: Frequent mutations and amplifications of the PIK-3CA gene in pituitary tumors. Endocr Relat Cancer 2009;16:301–310.
135 Ezzat S, Yu S, Asa SL: Ikaros isoforms in human pituitary tumors: distinct localization, histone acetylation, and activation of the 5′ fibroblast growth factor receptor-4 promoter. Am J Pathol 2003;163:1177–1184.
136 Zhu X, Asa SL, Ezzat S: Fibroblast growth factor 2 and estrogen control the balance of histone 3 modifications targeting MAGE-A3 in pituitary neoplasia. Clin Cancer Res 2008;14:1984–1996.
137 Zhang X, Zhou Y, Mehta KR, Danila DC, Scolavino S, Johnson SR, Klibanski A: A pituitary-derived MEG3 isoform functions as a growth suppressor in tumor cells. J Clin Endocrinol Metab 2003;88:5119–5126.
138 Zhao J, Dahle D, Zhou Y, Zhang X, Klibanski A: Hypermethylation of the promoter region is associated with the loss of MEG3 gene expression in human pituitary tumors. J Clin Endocrinol Metab 2005;90:2179–2186.

Stratakis CA (ed): Endocrine Tumor Syndromes and Their Genetics.
Front Horm Res. Basel, Karger, 2013, vol 41, pp 111–140 (DOI: 10.1159/000345673)

139 Gejman R, Batista DL, Zhong Y, Zhou Y, Zhang X, Swearingen B, Stratakis CA, Hedley-Whyte ET, Klibanski A: Selective loss of MEG3 expression and intergenic differentially methylated region hypermethylation in the MEG3/DLK1 locus in human clinically nonfunctioning pituitary adenomas. J Clin Endocrinol Metab 2008;93:4119–4125.
140 Cheunsuchon P, Zhou Y, Zhang X, Lee H, Chen W, Nakayama Y, Rice KA, Tessa Hedley-Whyte E, Swearingen B, Klibanski A: Silencing of the imprinted DLK1-MEG3 locus in human clinically nonfunctioning pituitary adenomas. Am J Pathol 2011;179:2120–2130.
141 Mezzomo LC, Gonzales PH, Pesce FG, Kretzmann FN, Ferreira NP, Oliveira MC, Kohek MB: Expression of cell growth negative regulators MEG3 and GADD45gamma is lost in most sporadic human pituitary adenomas. Pituitary 2012;15:420–427.
142 Zhuang Z, Ezzat SZ, Vortmeyer AO, Weil R, Oldfield EH, Park WS, Pack S, Huang S, Agarwal SK, Guru SC, Manickam P, Debelenko LV, Kester MB, Olufemi SE, Heppner C, Crabtree JS, Burns AL, Spiegel AM, Marx SJ, Chandrasekharappa SC, Collins FS, Emmert-Buck MR, Liotta LA, Asa SL, Lubensky IA: Mutations of the MEN1 tumor suppressor gene in pituitary tumors. Cancer Res 1997; 57:5446–5451.
143 Tanaka C, Yoshimoto K, Yamada S, Nishioka H, Ii S, Moritani M, Yamaoka T, Itakura M: Absence of germ-line mutations of the multiple endocrine neoplasia type 1 (MEN1) gene in familial pituitary adenoma in contrast to MEN1 in Japanese. J Clin Endocrinol Metab 1998;83:960–965.
144 Wenbin C, Asai A, Teramoto A, Sanno N, Kirino T: Mutations of the MEN1 tumor suppressor gene in sporadic pituitary tumors. Cancer Lett 1999;142: 43–47.
145 Schmidt MC, Henke RT, Stangl AP, Meyer-Puttlitz B, Stoffel-Wagner B, Schramm J, von DA: Analysis of the MEN1 gene in sporadic pituitary adenomas. J Pathol 1999;188:168–173.
146 McCabe CJ, Gittoes NJ, Sheppard MC, Franklyn JA: Increased MEN1 mRNA expression in sporadic pituitary tumours. Clin Endocrinol (Oxf) 1999;50: 727–733.
147 Karl M, Von WG, Kempter E, Katz DA, Reincke M, Monig H, Ali IU, Stratakis CA, Oldfield EH, Chrousos GP, Schulte HM: Nelson's syndrome associated with a somatic frame shift mutation in the glucocorticoid receptor gene. J Clin Endocrinol Metab 1996;81:124–129.
148 Huizenga NA, de LP, Koper JW, Clayton RN, Farrell WE, van der Lely AJ, Brinkmann AO, de Jong FH, Lamberts SW: Human adrenocorticotropin-secreting pituitary adenomas show frequent loss of heterozygosity at the glucocorticoid receptor gene locus. J Clin Endocrinol Metab 1998;83:917–921.
149 Acunzo J, Roche C, Defilles C, Thirion S, Quentien MH, Figarella-Branger D, Graillon T, Dufour H, Brue T, Pellegrini I, Enjalbert A, Barlier A: Inactivation of PITX2 transcription factor induced apoptosis of gonadotroph tumoral cells. Endocrinology 2011;152:3884–3892.
150 Pagotto U, Arzberger T, Theodoropoulou M, Grubler Y, Pantaloni C, Saeger W, Losa M, Journot L, Stalla GK, Spengler D: The expression of the antiproliferative gene ZAC is lost or highly reduced in nonfunctioning pituitary adenomas. Cancer Res 2000;60:6794–6799.
151 Noh TW, Jeong HJ, Lee MK, Kim TS, Kim SH, Lee EJ: Predicting recurrence of nonfunctioning pituitary adenomas. J Clin Endocrinol Metab 2009;94: 4406–4413.
152 Palmieri D, Valentino T, De MI, Esposito F, Cappabianca P, Wierinckx A, Vitiello M, Lombardi G, Colao A, Trouillas J, Pierantoni GM, Fusco A, Fedele M: PIT1 upregulation by HMGA proteins has a role in pituitary tumorigenesis. Endocr Relat Cancer 2012;19:123–135.
153 Alvaro V, Levy L, Dubray C, Roche A, Peillon F, Querat B, Joubert D: Invasive human pituitary tumors express a point-mutated alpha-protein kinase-C. J Clin Endocrinol Metab 1993;77:1125–1129.
154 Zhang X, Horwitz GA, Heaney AP, Nakashima M, Prezant TR, Bronstein MD, Melmed S: Pituitary tumor transforming gene (PTTG) expression in pituitary adenomas. J Clin Endocrinol Metab 1999;84: 761–767.
155 Salehi F, Kovacs K, Scheithauer BW, Cantelmi D, Horvath E, Lloyd RV, Cusimano M: Immunohistochemical expression of pituitary tumor transforming gene (PTTG) in pituitary adenomas: a correlative study of tumor subtypes. Int J Surg Pathol 2010; 18:5–13.
156 Simpson DJ, Hibberts NA, McNicol AM, Clayton RN, Farrell WE: Loss of pRb expression in pituitary adenomas is associated with methylation of the RB1 CpG island. Cancer Res 2000;60:1211–1216.
157 Bahar A, Simpson DJ, Cutty SJ, Bicknell JE, Hoban PR, Holley S, Mourtada-Maarabouni M, Williams GT, Clayton RN, Farrell WE: Isolation and characterization of a novel pituitary tumor apoptosis gene. Mol Endocrinol 2004;18:1827–1839.
158 Corbetta S, Ballare E, Mantovani G, Lania A, Losa M, Di Blasio AM, Spada A: Somatostatin receptor subtype 2 and 5 in human GH-secreting pituitary adenomas: analysis of gene sequence and mRNA expression. Eur J Clin Invest 2001;31:208–214.
159 Ando S, Sarlis NJ, Oldfield EH, Yen PM: Somatic mutation of TRbeta can cause a defect in negative regulation of TSH in a TSH-secreting pituitary tumor. J Clin Endocrinol Metab 2001;86:5572–5576.

Stratakis CA (ed): Endocrine Tumor Syndromes and Their Genetics.
Front Horm Res. Basel, Karger, 2013, vol 41, pp 111–140 (DOI: 10.1159/000345673)

160 Ando S, Sarlis NJ, Krishnan J, Feng X, Refetoff S, Zhang MQ, Oldfield EH, Yen PM: Aberrant alternative splicing of thyroid hormone receptor in a TSH-secreting pituitary tumor is a mechanism for hormone resistance. Mol Endocrinol 2001;15:1529–1538.
161 Tanizaki Y, Jin L, Scheithauer BW, Kovacs K, Roncaroli F, Lloyd RV: P53 gene mutations in pituitary carcinomas. Endocr Pathol 2007;18:217–222.
162 Kawashima ST, Usui T, Sano T, Iogawa H, Hagiwara H, Tamanaha T, Tagami T, Naruse M, Hojo M, Takahashi JA, Shimatsu A: P53 gene mutation in an atypical corticotroph adenoma with Cushing's disease. Clin Endocrinol (Oxf) 2009;70:656–657.
163 Pinto EM, Siqueira SA, Cukier P, Fragoso MC, Lin CJ, de Mendonca BB: Possible role of a radiation-induced p53 mutation in a Nelson's syndrome patient with a fatal outcome. Pituitary 2011;14:400–404.
164 Murakami M, Mizutani A, Asano S, Katakami H, Ozawa Y, Yamazaki K, Ishida Y, Takano K, Okinaga H, Matsuno A: A mechanism of acquiring temozolomide resistance during transformation of atypical prolactinoma into prolactin-producing pituitary carcinoma: case report. Neurosurgery 2011;68:E1761–E1767.
165 Bottoni A, Piccin D, Tagliati F, Luchin A, Zatelli MC, Degli Uberti EC: miR-15a and miR-16–1 down-regulation in pituitary adenomas. J Cell Physiol 2005;204:280–285.
166 Bottoni A, Zatelli MC, Ferracin M, Tagliati F, Piccin D, Vignali C, Calin GA, Negrini M, Croce CM, Degli Uberti EC: Identification of differentially expressed microRNAs by microarray: a possible role for microRNA genes in pituitary adenomas. J Cell Physiol 2007;210:370–377.
167 Qian ZR, Asa SL, Siomi H, Siomi MC, Yoshimoto K, Yamada S, Wang EL, Rahman MM, Inoue H, Itakura M, Kudo E, Sano T: Overexpression of HMGA2 relates to reduction of the let-7 and its relationship to clinicopathological features in pituitary adenomas. Mod Pathol 2009;22:431–441.
168 Amaral FC, Torres N, Saggioro F, Neder L, Machado HR, Silva WA Jr, Moreira AC, Castro M: MicroRNAs differentially expressed in ACTH-secreting pituitary tumors. J Clin Endocrinol Metab 2009;94:320–323.
169 Stilling G, Sun Z, Zhang S, Jin L, Righi A, Kovacs G, Korbonits M, Scheithauer BW, Kovacs K, Lloyd RV: MicroRNA expression in ACTH-producing pituitary tumors: up-regulation of microRNA-122 and -493 in pituitary carcinomas. Endocrine 2010;38:67–75.
170 Butz H, Liko I, Czirjak S, Igaz P, Munayem KM, Zivkovic V, Balint K, Korbonits M, Racz K, Patocs A: Down-regulation of Wee1 kinase by a specific subset of microRNA in human sporadic pituitary adenomas. J Clin Endocrinol Metab 2010;95:E181–E191.
171 Mao ZG, He DS, Zhou J, Yao B, Xiao WW, Chen CH, Zhu YH, Wang HJ: Differential expression of microRNAs in GH-secreting pituitary adenomas. Diagn Pathol 2010;5:79.
172 Butz H, Liko I, Czirjak S, Igaz P, Korbonits M, Racz K, Patocs A: MicroRNA profile indicates downregulation of the TGFbeta pathway in sporadic nonfunctioning pituitary adenomas. Pituitary 2011;14:112–124.
173 Palmieri D, D'Angelo D, Valentino T, De Martino I, Ferraro A, Wierinckx A, Fedele M, Trouillas J, Fusco A: Downregulation of HMGA-targeting microRNAs has a critical role in human pituitary tumorigenesis. Oncogene 2012;31:3857–3865.
174 D'Angelo D, Palmieri D, Mussnich P, Roche M, Wierinckx A, Raverot G, Fedele M, Maria CC, Trouillas J, Fusco A: Altered MicroRNA expression profile in human pituitary GH adenomas: down-regulation of miRNA targeting HMGA1, HMGA2, and E2F1. J Clin Endocrinol Metab 2012;97:E1128–E1138.

Márta Korbonits, MD, PhD
Department of Endocrinology, Barts and London
School of Medicine and Dentistry, Charterhouse Square
London EC1M 6BQ (UK)
E-Mail m.korbonits@qmul.ac.uk

Stratakis CA (ed): Endocrine Tumor Syndromes and Their Genetics.
Front Horm Res. Basel, Karger, 2013, vol 41, pp 111–140 (DOI: 10.1159/000345673)

Sequence analysis of the catalytic subunit of PKA in somatotroph adenomas

Sarah J Larkin, Francesco Ferraù[1], Niki Karavitaki[2], Laura C Hernández-Ramírez[1], Olaf Ansorge[†], Ashley B Grossman[2,†] and **Márta Korbonits[1,†]**

Nuffield Department of Clinical Neurosciences, Department of Neuropathology, Level 1 West Wing, John Radcliffe Hospital, Headley Way, Oxford OX3 9DU, UK, [1]Department of Endocrinology, Barts and London School of Medicine, Queen Mary University of London, London EC1A 6BQ, UK and [2]Department of Endocrinology, Oxford Centre for Diabetes, Endocrinology and Metabolism, Churchill Hospital, Old Road, Headington, Oxford OX3 7LE, UK
[†](O Ansorge, A B Grossman and M Korbonits considered as joint senior authors)

Correspondence should be addressed to S J Larkin
Email
sarah.larkin@ndcn.ox.ac.uk

Abstract

Objective: The pathogenetic mechanisms of sporadic somatotroph adenomas are not well understood, but derangements of the cAMP pathway have been implicated. Recent studies have identified L206R mutations in the alpha catalytic subunit of protein kinase A (*PRKACA*) in cortisol-producing adrenocortical adenomas and amplification of the beta catalytic subunit of protein kinase A *PRKACB* in acromegaly associated with Carney complex. Given that both adrenocortical adenomas and somatotroph adenomas are known to be reliant on the cAMP signalling pathway, we sought to determine the relevance of the L206R mutation in both *PRKACA* and *PRKACB* for the pathogenesis of sporadic somatotroph adenomas.
Design: Somatotroph adenoma specimens, both frozen and formalin-fixed, from patients who underwent surgery for their acromegaly between 1995 and 2012, were used in the study.
Methods: The DNA sequence at codon 206 of *PRKACA* and *PRKACB* was determined by PCR amplification and sequencing. The results were compared with patient characteristics, the mutational status of the *GNAS* complex locus and the tumour granulation pattern.
Results: No mutations at codon 206 of *PRKACA* or *PRKACB* were found in a total of 92 specimens, comprising both WT and mutant *GNAS* cases, and densely, sparsely and mixed granulation patterns.
Conclusions: It is unlikely that mutation at this locus is involved in the pathogenesis of sporadic somatotroph adenoma; however, gene amplification or mutations at other loci or in other components of the cAMP signalling pathway, while unlikely, cannot be ruled out.

European Journal of Endocrinology
(2014) **171**, 705–710

European Journal of Endocrinology

Introduction

Genetic studies of the pathogenesis of sporadic somatotroph adenomas have identified a role for the cAMP signalling pathway, and conversely syndromes that feature a germline mutation in the components of this pathway can be associated with the formation of somatotroph adenomas. Thus, sporadic somatotroph adenomas are often associated with mutations at the *GNAS* complex locus, encoding the *GSP* oncogene. These mutations implicate the cAMP pathway in the pathogenesis of sporadic somatotroph adenomas in 15–58% of cases (1, 2, 3), although the tumourigenic mechanism is unclear. The McCune–Albright syndrome results from post-zygotic germline mutations in *GNAS* and is often characterised by endocrine neoplasia: it is associated with somatotroph adenomas and acromegaly in 10–20% of cases (4). Carney complex is an autosomal dominant syndrome characterised by multiple, often endocrine tumours, including somatotroph adenomas, in ~10% of cases (5). In over 60% of cases of Carney complex, a mutation is found in the regulatory subunit 1A of protein

www.eje-online.org
DOI: 10.1530/EJE-14-0545

Published by Bioscientifica Ltd.

kinase A (*PRKAR1A*), an intrinsic part of cAMP signalling, although such mutations are not found in sporadic pituitary adenomas (6, 7, 8). Recently, whole-exome sequencing studies have identified a mutation in the active-site cleft of catalytic subunit A of PKA (*PRKACA*) in cortisol-producing adrenocortical adenomas, most commonly R206 (9, 10, 11). This mutation was observed in 37–66% of cases and resulted in constitutive activation of PKA that was neither suppressed by the PKA regulatory subunit nor increased by addition of cAMP (either directly or indirectly by forskolin treatment) (10, 11). A recent report of a patient with Carney complex with acromegaly, spotty pigmentation and myxomas, but without Cushing's syndrome, has shown the presence of a triplication of chromosome 1p31.1 (containing *PRKACB*), leading to increased expression of *PRKACB* (12). The authors propose that amplification of *PRKACB* may be responsible for non-adrenal manifestations of Carney complex. Given the involvement of the cAMP pathway in sporadic somatotroph adenoma pathogenesis, we sought to determine whether mutations in the catalytic subunit of PKA might also occur in these lesions and be involved in the pathogenesis of these tumours. We therefore amplified and sequenced the region of *PRKACA* and *PRKACB* containing codon 206 in a large series of sporadic somatotroph adenomas. The findings were compared with patient characteristics, the mutational status of *GNAS* in a sub-group and the granulation pattern of the specimens.

Subjects and methods

Patients ($n=92$) with a diagnosis of acromegaly were included. None of the patients had a clinical history of FIPA, MEN1 or SDH-associated acromegaly, but germline mutations in *MEN1* and *SDH* were not sought routinely in all individuals. The tumour samples, either formalin fixed and paraffin embedded (FFPE; $n=43$) or frozen ($n=49$), were retrieved from the surgical neuropathology archive of the Oxford Brain Bank and the Tissue Bank of the Department of Endocrinology at Barts and the London School of Medicine. The specimens were excluded if the samples were too small or the DNA was of insufficient quality to enable successful amplification of the regions containing codon 206 of *PRKACA* and *PRKACB*. The specimens were preferentially included if previous analysis had shown them to be *GNAS* WT. The findings of Sato *et al*. (11) demonstrate that mutations in *PRKACA* and *GNAS* are mutually exclusive in adrenocortical adenomas and so we speculated that any *PRKACA* mutations identified might only be present in *GNAS*-mutation negative specimens. All studies were conducted on linked-anonymised samples under multi-site and local Research Ethics Committee (REC) approval.

DNA was extracted from either 5×10 μm sections of FFPE tissue (QiaAmp FFPE DNA Kit, Qiagen) or from homogenised fresh-frozen specimens (QiaAmp DNA Mini Kit or DNeasy Blood and Tissue Kit (Qiagen)) according to manufacturer's instructions. PCR was carried out to generate amplicons including codon 206 of *PRKACA* and *PRKACB*. The primers were designed using Primer-Blast (www.ncbi.nlm.nih.gov/tools/primer-blast). For FFPE specimens primers were as follows: *PRKACA* sense (5′-GGTGACAGACTTCGGTTTCGC-3′) and antisense (5′-CCTTGTTGTAGCCCTGGAGCA-3′); *PRKACB* sense (5′-TGGTTTTATTTCTTTGCAGTGAGC-3′) and antisense (5′-CCTGGATATAGCCTTGATGGTCA-3′). The primers for gDNA from frozen specimens were as follows: *PRKACA* sense (5′-CAACTGCCTGTTCTTGTGCC-3′) and antisense (5′-AGTCCACGGCCTTGTTGTAG-3′); *PRKACB* sense (5′-AAACTTTCAACGTAGGTGCAAT-3′) and antisense (5′-CAAAAGTCCATAGGGATGCATGT-3′). The primers for cDNA from frozen specimens were as follows: *PRKACA* sense (5′-CTGCACTCGCTGGATCTCAT-3′) and antisense (5′-CAGAGCTGAAGTGGGAAGGG-3′) and *PRKACB* sense (5′-GCAGCTCAGATAGTGCTAACATTC-3′) and antisense (5′-GGTCTGCAAAGAATGGGGGATA-3′).

For FFPE specimens, DNA template (100 ng) was added to 10× PCR buffer solution (10% v/v; Qiagen), $MgCl_2$ (final concentration 4 mmol/l, for *PRKACB* only), dNTPs (200 μmol/l) (Promega), 0.5 U of Taq polymerase (HotStarTaq Plus, Qiagen) and 400 nmol/l each of forward and reverse primers. The cycling conditions were as follows: 95 °C for 5 min, followed by 35 cycles of 95 °C for 30 s; annealing temperature for 30 s (61 °C for *PRKACA* and 57 °C for *PRKACB*) and 72 °C for 40 s, followed by a single 1 min extension. Total reaction volume was 20 μl. For frozen specimens, gDNA template ((100 ng) was added to 10× Taq reaction buffer (10% v/v; (New England Biolabs (NEB), Hitchin, UK)), dNTPs (200 μmol/l) (New England Biolabs), 0.12 U of Taq polymerase (New England Biolabs) and 200 nmol/l each of forward and reverse primers. The cycling conditions were as follows: 95 °C for 2 min, followed by 35 cycles at 95 °C for 30 s, annealing temperature for 30 s (67.6 °C for *PRKACA* and 62.5 °C for *PRKACB*) and 68 °C for 30 s, followed by a single 5 min extension. Total reaction volume was 25 μl.

RNA was extracted from frozen specimens using the RNeasy Kit (Qiagen), according to manufacturer's instructions. RT was performed using 500 ng RNA, random hexamer primers (0.5 μg/l, Promega) and M-MLV reverse

Table 1 Cases included in the study. Cases 1–21 have previously been reported (13).

Case	Sex	Age	Material	Preservation	Size	Granulation	*GNAS*	*PRKACA*	*PRKACB*
1	F	39	gDNA	FFPE	Macro	S	WT	WT	WT
2	F	64	gDNA	FFPE	Micro	D	WT	WT	WT
3	F	54	gDNA	FFPE	Macro	D	WT	WT	WT
4	F	41	gDNA	FFPE	Micro	D	WT	WT	WT
5	F	57	gDNA	FFPE	Macro	D	WT	WT	WT
6	M	49	gDNA	FFPE	Macro	D	WT	WT	WT
7	F	56	gDNA	FFPE	Micro	M	WT	WT	WT
8	M	35	gDNA	FFPE	Macro	ND	R201C	WT	WT
9	F	66	gDNA	FFPE	Macro	S	ND	WT	WT
10	F	23	gDNA	FFPE	Macro	S	ND	WT	WT
11	F	47	gDNA	FFPE	Macro	S	WT	WT	WT
12	M	43	gDNA	FFPE	Micro	D	WT	WT	WT
13	F	44	gDNA	FFPE	Macro	S	WT	WT	WT
14	F	62	gDNA	FFPE	Macro	M	WT	WT	WT
15	M	52	gDNA	FFPE	Macro	S	R102C	WT	WT
16	F	54	gDNA	FFPE	Macro	M	WT	WT	WT
17	F	26	gDNA	FFPE	Macro	S	ND	WT	WT
18	F	33	gDNA	FFPE	Macro	ND	WT	WT	WT
19	F	53	gDNA	FFPE	Macro	ND	WT	WT	WT
20	F	59	gDNA	FFPE	Micro	D	WT	WT	WT
21	M	56	gDNA	Frozen	Macro	D	R201C	WT	WT
22	F	49	gDNA	FFPE	ND	S	ND	WT	WT
23	M	31	gDNA	FFPE	ND	S	ND	WT	WT
24	F	45	gDNA	FFPE	ND	ND	ND	WT	WT
25	F	49	gDNA	FFPE	ND	ND	ND	WT	WT
26	M	34	gDNA	FFPE	Micro	S	ND	WT	WT
27	M	55	gDNA	FFPE	Micro	S	ND	WT	WT
28	M	43	gDNA	FFPE	Micro	ND	ND	WT	WT
29	F	46	gDNA	FFPE	Macro	ND	ND	WT	WT
30	F	61	gDNA	FFPE	Macro	S	ND	WT	WT
31	F	19	gDNA	FFPE	Macro	ND	ND	WT	WT
32	F	41	gDNA	FFPE	Macro	D	ND	WT	WT
33	M	52	gDNA	FFPE	ND	ND	ND	WT	WT
34	F	29	gDNA	FFPE	Micro	ND	ND	WT	WT
35	M	40	gDNA	FFPE	ND	ND	ND	WT	WT
36	M	69	gDNA	FFPE	ND	ND	ND	WT	WT
37	M	18	gDNA	FFPE	Macro	ND	ND	WT	WT
38	F	41	gDNA	FFPE	Micro	D	ND	WT	WT
39	F	25	gDNA	FFPE	Macro	S	ND	WT	WT
40	F	29	gDNA	FFPE	Macro	S	ND	WT	WT
41	F	67	gDNA	FFPE	Macro	D	ND	WT	WT
42	M	53	gDNA	FFPE	Macro	ND	WT	WT	WT
43	F	30	gDNA	FFPE	Macro	S	WT	WT	WT
44	F	36	gDNA	FFPE	Macro	S	WT	WT	WT
45	F	57	gDNA	Frozen	Macro	ND	ND	WT	WT
46	M	48	gDNA	Frozen	Micro	ND	ND	WT	WT
47	F	42	gDNA	Frozen	Macro	ND	ND	WT	WT
48	M	50	gDNA	Frozen	Micro	ND	WT	WT	WT
49	M	80	gDNA	Frozen	Macro	ND	ND	WT	WT
50	F	66	gDNA	Frozen	Macro	ND	ND	WT	WT
51	F	37	gDNA	Frozen	Macro	ND	ND	WT	WT
52	M	32	gDNA	Frozen	Macro	ND	ND	WT	WT
53	M	71	gDNA	Frozen	Macro	ND	ND	WT	WT
54	F	53	gDNA	Frozen	ND	ND	ND	WT	WT
55	M	42	gDNA	Frozen	Macro	ND	ND	WT	WT
56	F	33	gDNA	Frozen	Macro	ND	ND	WT	WT
57	M	44	gDNA	Frozen	Macro	ND	ND	WT	WT
58	F	38	gDNA	Frozen	Macro	ND	ND	WT	WT
59	M	48	gDNA	Frozen	ND	ND	ND	WT	WT
60	F	28	gDNA	Frozen	Macro	ND	ND	WT	WT
61	M	40	gDNA	Frozen	ND	ND	ND	WT	WT

Table 1 *Continued*

Case	Sex	Age	Material	Preservation	Size	Granulation	*GNAS*	*PRKACA*	*PRKACB*
62	F	33	gDNA	Frozen	Micro	ND	ND	WT	WT
63	F	43	gDNA	Frozen	Macro	ND	ND	WT	WT
64	F	26	gDNA	Frozen	Micro	ND	ND	WT	WT
65	M	63	gDNA	Frozen	Macro	ND	ND	WT	WT
66	F	57	gDNA	Frozen	Macro	ND	ND	WT	WT
67	M	48	gDNA	Frozen	Micro	ND	ND	WT	WT
68	F	46	gDNA	Frozen	ND	ND	ND	WT	WT
69	F	32	gDNA	Frozen	Macro	ND	ND	WT	WT
70	F	25	gDNA	Frozen	Macro	ND	ND	WT	WT
71	M	25	gDNA	Frozen	Macro	ND	ND	WT	WT
72	M	10	gDNA	Frozen	Macro	ND	ND	WT	WT
73	F	14	gDNA	Frozen	Macro	ND	ND	WT	WT
74	M	62	gDNA	Frozen	Macro	ND	ND	WT	WT
75	F	48	gDNA	Frozen	Micro	ND	ND	WT	WT
76	F	63	gDNA	Frozen	Macro	ND	ND	WT	WT
77	F	57	gDNA	Frozen	ND	ND	ND	WT	WT
78	M	34	gDNA	Frozen	Macro	ND	ND	WT	WT
79	M	26	gDNA	Frozen	Macro	ND	ND	WT	WT
80	F	28	gDNA	Frozen	ND	ND	ND	WT	WT
81	F	40	gDNA	Frozen	Macro	ND	ND	WT	WT
82	F	78	gDNA	Frozen	Micro	ND	ND	WT	WT
83	M	39	gDNA	Frozen	Macro	ND	ND	WT	WT
84	M	53	gDNA	Frozen	Macro	ND	ND	WT	WT
85	M	53	cDNA	Frozen	Macro	ND	WT	WT	WT
86	M	ND	cDNA	Frozen	Macro	ND	WT	WT	WT
87	M	69	cDNA	Frozen	Macro	ND	WT	WT	WT
88	M	62	cDNA	Frozen	Micro	ND	R201C	WT	WT
89	M	40	cDNA	Frozen	Macro	ND	ND	WT	WT
90	M	52	cDNA	Frozen	Macro	ND	ND	WT	WT
91	F	41	cDNA	Frozen	Macro	ND	ND	WT	WT
92	F	64	cDNA	Frozen	Macro	ND	ND	WT	WT

ND, not determined; DG, densely granulated; MG, mixed granulation pattern; SG, sparsely granulated; FFPE, formalin fixed, paraffin embedded; macro, macroadenoma; micro, microadenoma.

transcriptase (100 U) (Life Technologies). For amplification of *PRKACA*, cDNA template (100 ng) was added to 5× Q5 reaction buffer (20% v/v; (New England Biolabs)), 0.25 μl DNA polymerase (Q5 High-Fidelity DNA polymerase, New England Biolabs) 5× Q5 High GC Enhancer (20% v/v, New England Biolabs) dNTPs (200 μmol/l) and 500 nmol/l each of forward and reverse primers. The cycling conditions were as follows: 98 °C, 30 s, followed by 35 cycles of 98 °C for 10 s, 60 °C for 20 s, 72 °C for 20 s followed by a single extension for 2 min. Total reaction volume was 25 μl. For amplification of *PRKACB*, reaction and cycling conditions were identical to those for gDNA except that 400 μmol/l dNTPs were added and the annealing temperature was 62 °C.

The products were examined by agarose gel separation and purified (MinElute PCR Purification Kit (Qiagen)). Bidirectional sequencing of amplicons was carried out using BigDye Terminator chemistry (v3.1) and an ABI-3730 capillary sequencer (Applied Biosystems). The sequences were compared with the WT sequence (RefSeq NM_002730.3 (*PRKACA*) and NM_182948.2 (*PRKACB*)).

The tumours were categorised as sparsely granulated (SG), densely granulated (DG) or of mixed granulation pattern (MG). A mixed phenotype was assigned when more than 30% of tumour cells deviated from the dominant Cam5.2 pattern. The immunohistochemical methods for determination of granulation pattern and the sequencing of *GNAS* have been previously described (13).

Results

In this study, a total of 92 sporadic somatotroph adenoma specimens (54 from females) were used. Age at diagnosis varied between 10 and 80 years, and 77% of samples were obtained from patients with macroadenomas (where tumour size was known; $n=77$). There were mutations at the *GNAS* complex locus, G-protein α subunit codon 201 (R201C), in four of 26 cases for which sequences

were available (20 from FFPE specimens and six from frozen specimens) (Table 1). In the remaining FFPE specimens ($n=23$), DNA quality was not sufficient to allow amplification of codons 201 and 227 of G-protein α subunit, so such data for these cases were not available.

We did not find a mutation at codon 206 of *PRKACA* or *PRKACB* in either the gDNA or cDNA of any of the sporadic somatotroph adenomas. Although information regarding the mutational status of *GNAS* and the granulation pattern was not available for all cases, we did not find a mutation in either *GNAS* mutant or WT cases (mutational status was established in 26 of 92 specimens) or in tumours with any type of granulation pattern.

Discussion

The lack of a mutation in either *PRKACA* or *PRKACB* in our series suggests that constitutive activation of *PRKACA* or *PRKACB* by mutation of codon 206 is unlikely to be involved in the pathogenesis of sporadic somatotroph adenomas. However, as we did not sequence all exons of *PRKACA* or *PRKACB*, we cannot rule out mutations at other loci, although this seems unlikely.

Both adrenal adenomas and pituitary somatotroph adenomas are known to contain mutations in components of the cAMP signalling pathway in a proportion of cases, and mutations in *PRKAR1A* can underlie the development of both of these lesions. However, while mutation of *PRKACA* appears to be important for the development of up to two-thirds of cortisol-producing adrenal adenomas (9, 10), it does not appear to be the case for somatotroph adenomas, even though mutation of the cAMP signalling pathway has been shown to be involved in the pathogenesis of this tumour type (1, 2, 13, 14, 15, 16, 17, 18, 19). We did not determine whether there was amplification of either the *PRKACA* or *PRKACB* gene in this series. Amplification of chromosome 19p (containing *PRKACA*) and 1p31.1 has been shown to underlie impaired inhibition of the catalytic subunit by the PKA regulatory subunit and increased basal PKA activity (9, 12). In the absence of a *PRKACA* or *PRKACB* mutation, amplification could lead to increased cAMP signalling that might result in somatotroph tumourigenesis.

In adrenocortical adenomas, mutations in *PRKACA* have been found to be mutually exclusive with mutations in *GNAS* (11). In this series, we found no mutation in codon 206 of *PRKACA* or *PRKACB* in 22 specimens which were *GNAS* WT and four specimens that had *GNAS* R201C mutations. Where *GNAS* status was known, we preferentially included WT specimens in this series. However, there is a lack of information concerning the mutational status of *GNAS* in the remaining cases ($n=66$). Given the reported prevalence of *GNAS* mutations in somatotroph adenomas (1, 2, 3), we could expect 15–58% of them (between ten and 38 specimens) to harbour a *GNAS* mutation; this suggests that although the majority would be negative for GNAS mutation, GNAS mutation in a subset may preclude the finding of a *PRKACA* or *PRKACB* mutation.

Previously, we and others have suggested that DG and SG somatotroph adenomas may have differing clinical characteristics and responses to treatment (1, 18, 20, 21, 22). The genetic basis for this difference has yet to be determined, and so a series containing representative samples from all granulation subtypes was chosen for this study.

The findings of several groups (9, 10, 11, 12) support a central role for the cAMP signalling pathway in the pathogenesis of adrenocortical adenomas and somatotroph adenomas. Although we did not demonstrate the presence of a recurring mutation in either *PRKACA* or *PRKACB*, mutations in other components of this pathway cannot be ruled out and warrant further investigation. At present, any mutational event pathogenetic in the majority of sporadic somatotroph tumours remains elusive.

Declaration of interest
The authors declare that there is no conflict of interest that could be perceived as prejudicing the impartiality of the research reported.

Funding
The research was funded by the National Institute for Health Research (NIHR) Oxford Biomedical Research Centre based at Oxford University Hospitals NHS Trust and University of Oxford and by NIHR and grant support from Pfizer to M Korbonits' laboratory. L C Hernández-Ramírez is supported by the National Council of Science and Technology of Mexico and by the Barts and The London Charity. The views expressed are those of the author(s) and not necessarily those of the NHS, the NIHR or the Department of Health.

Acknowledgements
The authors acknowledge the Oxford Brain Bank, supported by the Medical Research Council (MRC), Brains for Dementia Research (BDR) and the NIHR Oxford Biomedical Research Centre.

References

1 Bakhtiar Y, Hirano H, Arita K, Yunoue S, Fujio S, Tominaga A, Sakoguchi T, Sugiyama K, Kurisu K, Yasufuku-Takano J *et al.*

Relationship between cytokeratin staining patterns and clinicopathological features in somatotropinomae. *European Journal of Endocrinology* 2010 **163** 531–539. (doi:10.1530/EJE-10-0586)

2 Landis CA, Masters SB, Spada A, Pace AM, Bourne HR & Vallar L. GTPase inhibiting mutations activate the alpha chain of Gs and stimulate adenylyl cyclase in human pituitary tumours. *Nature* 1989 **340** 692–696. (doi:10.1038/340692a0)

3 Taboada GF, Luque RM, Neto LV, Machado Ede O, Sbaffi BC, Domingues RC, Marcondes JB, Chimelli LM, Fontes R, Niemeyer P *et al*. Quantitative analysis of somatostatin receptor subtypes (1–5) gene expression levels in somatotropinomas and correlation to *in vivo* hormonal and tumor volume responses to treatment with octreotide LAR. *European Journal of Endocrinology* 2008 **158** 295–303. (doi:10.1530/EJE-07-0562)

4 Salenave S, Boyce AM, Collins MT & Chanson P. Acromegaly and McCune–Albright syndrome. *Journal of Clinical Endocrinology and Metabolism* 2014 **99** 1955–1969. (doi:10.1210/jc.2013.3826)

5 Stratakis CA, Kirschner LS & Carney JA. Clinical and molecular features of the Carney complex: diagnostic criteria and recommendations for patient evaluation. *Journal of Clinical Endocrinology and Metabolism* 2001 **86** 4041–4046. (doi:10.1210/jcem.86.9.7903)

6 Kaltsas GA, Kola B, Borboli N, Morris DG, Gueorguiev M, Swords FM, Czirjak S, Kirschner LS, Stratakis CA, Korbonits M *et al*. Sequence analysis of the PRKAR1A gene in sporadic somatotroph and other pituitary tumours. *Clinical Endocrinology* 2002 **57** 443–448. (doi:10.1046/j.1365-2265.2002.01643.x)

7 Sandrini F, Kirschner LS, Bei T, Farmakidis C, Yasufuku-Takano J, Takano K, Prezant TR, Marx SJ, Farrell WE, Clayton RN *et al*. PRKAR1A, one of the Carney complex genes, and its locus (17q22–24) are rarely altered in pituitary tumours outside the Carney complex. *Journal of Medical Genetics* 2002 **39** e78. (doi:10.1136/jmg.39.12.e78)

8 Yamasaki H, Mizusawa N, Nagahiro S, Yamada S, Sano T, Itakura M & Yoshimoto K. GH-secreting pituitary adenomas infrequently contain inactivating mutations of PRKAR1A and LOH of 17q23–24. *Clinical Endocrinology* 2003 **58** 464–470. (doi:10.1046/j.1365-2265.2003.01740.x)

9 Beuschlein F, Fassnacht M, Assie G, Calebiro D, Stratakis CA, Osswald A, Ronchi CL, Wieland T, Sbiera S, Faucz FR *et al*. Constitutive activation of PKA catalytic subunit in adrenal Cushing's syndrome. *New England Journal of Medicine* 2014 **370** 1019–1028. (doi:10.1056/NEJMoa1310359)

10 Cao Y, He M, Gao Z, Peng Y, Li Y, Li L, Zhou W, Li X, Zhong X, Lei Y *et al*. Activating hotspot L205R mutation in PRKACA and adrenal Cushing's syndrome. *Science* 2014 **344** 913–917. (doi:10.1126/science.1249480)

11 Sato Y, Maekawa S, Ishii R, Sanada M, Morikawa T, Shiraishi Y, Yoshida K, Nagata Y, Sato-Otsubo A, Yoshizato T *et al*. Recurrent somatic mutations underlie corticotropin-independent Cushing's syndrome. *Science* 2014 **344** 917–920. (doi:10.1126/science.1252328)

12 Forlino A, Vetro A, Garavelli L, Ciccone R, London E, Stratakis CA & Zuffardi O. PRKACB and Carney complex. *New England Journal of Medicine* 2014 **370** 1065–1067. (doi:10.1056/NEJMc1309730)

13 Larkin S, Reddy R, Karavitaki N, Cudlip S, Wass J & Ansorge O. Granulation pattern, but not GSP or GHR mutation, is associated with clinical characteristics in somatostatin-naive patients with somatotroph adenomas. *European Journal of Endocrinology* 2013 **168** 491–499. (doi:10.1530/EJE-12-0864)

14 Adams EF, Brockmeier S, Friedmann E, Roth M, Buchfelder M & Fahlbusch R. Clinical and biochemical characteristics of acromegalic patients harboring gsp-positive and gsp-negative pituitary tumors. *Neurosurgery* 1993 **33** 198–203 (discussion 203). (doi:10.1227/00006123-199308000-00003)

15 Fougner SL, Casar-Borota O, Heck A, Berg JP & Bollerslev J. Adenoma granulation pattern correlates with clinical variables and effect of somatostatin analogue treatment in a large series of patients with acromegaly. *Clinical Endocrinology* 2012 **76** 96–102. (doi:10.1111/j.1365-2265.2011.04163.x)

16 Kola B, Korbonits M, Diaz-Cano S, Kaltsas G, Morris DG, Jordan S, Metherell L, Powell M, Czirjak S, Arnaldi G *et al*. Reduced expression of the growth hormone and type 1 insulin-like growth factor receptors in human somatotroph tumours and an analysis of possible mutations of the growth hormone receptor. *Clinical Endocrinology* 2003 **59** 328–338. (doi:10.1046/j.1365-2265.2003.01851.x)

17 Lyons J, Landis CA, Harsh G, Vallar L, Grunewald K, Feichtinger H, Duh QY, Clark OH, Kawasaki E, Bourne HR *et al*. Two G protein oncogenes in human endocrine tumors. *Science* 1990 **249** 655–659. (doi:10.1126/science.2116665)

18 Spada A, Arosio M, Bochicchio D, Bazzoni N, Vallar L, Bassetti M & Faglia G. Clinical, biochemical, and morphological correlates in patients bearing growth hormone-secreting pituitary tumors with or without constitutively active adenylyl cyclase. *Journal of Clinical Endocrinology and Metabolism* 1990 **71** 1421–1426. (doi:10.1210/jcem-71-6-1421)

19 Yang I, Park S, Ryu M, Woo J, Kim S, Kim J, Kim Y & Choi Y. Characteristics of gsp-positive growth hormone-secreting pituitary tumors in Korean acromegalic patients. *European Journal of Endocrinology* 1996 **134** 720–726. (doi:10.1530/eje.0.1340720)

20 Bhayana S, Booth GL, Asa SL, Kovacs K & Ezzat S. The implication of somatotroph adenoma phenotype to somatostatin analog responsiveness in acromegaly. *Journal of Clinical Endocrinology and Metabolism* 2005 **90** 6290–6295. (doi:10.1210/jc.2005-0998)

21 Mazal PR, Czech T, Sedivy R, Aichholzer M, Wanschitz J, Klupp N & Budka H. Prognostic relevance of intracytoplasmic cytokeratin pattern, hormone expression profile, and cell proliferation in pituitary adenomas of akromegalic patients. *Clinical Neuropathology* 2001 **20** 163–171.

22 Obari A, Sano T, Ohyama K, Kudo E, Qian ZR, Yoneda A, Rayhan N, Mustafizur Rahman M & Yamada S. Clinicopathological features of growth hormone-producing pituitary adenomas: difference among various types defined by cytokeratin distribution pattern including a transitional form. *Endocrine Pathology* 2008 **19** 82–91. (doi:10.1007/s12022-008-9029-z)

Received 1 July 2014
Revised 11 September 2014
Accepted 15 September 2014

Landscape of Familial Isolated and Young-Onset Pituitary Adenomas: Prospective Diagnosis in *AIP* Mutation Carriers

Laura C. Hernández-Ramírez, Plamena Gabrovska, Judit Dénes, Karen Stals, Giampaolo Trivellin, Daniel Tilley, Francesco Ferraù, Jane Evanson, Sian Ellard, Prof Ashley B. Grossman, Federico Roncaroli, Mônica R. Gadelha, and Márta Korbonits, (on behalf of The International FIPA Consortium)

Centre for Endocrinology (L.C.H.-R., P.G., J.D., G.T., D.T., F.F., J.E., M.K.), William Harvey Research Institute, Barts and The London School of Medicine, Queen Mary University of London, London EC1M 6BQ, United Kingdom; Department of Molecular Genetics (K.S., S.E.), Royal Devon and Exeter National Health Service Foundation Trust, Exeter EX2 5DW, United Kingdom; Program on Developmental Endocrinology and Genetics (G.T.), Section on Endocrinology and Genetics, *Eunice Kennedy Shriver* National Institute of Child Health and Human Development, National Institutes of Health, Bethesda, Maryland 20892; Department of Endocrinology (A.B.G.), Oxford Centre for Diabetes, Endocrinology, and Metabolism, Churchill Hospital. Headington, Oxford OX3 7LE, United Kingdom; Division of Brain Sciences (F.R.), Faculty of Medicine, Charing Cross Hospital, Imperial College, London W6 8RP, United Kingdom; and Endocrinology Unit (M.R.G.), Clementino Fraga Filho University Hospital, Federal University of Rio de Janeiro, Rua Professor Rodolpho Paulo Rocco, Ilha do Fundaõ, Rio de Janeiro 21941–913, Brazil

Context: Familial isolated pituitary adenoma (FIPA) due to aryl hydrocarbon receptor interacting protein (*AIP*) gene mutations is an autosomal dominant disease with incomplete penetrance. Clinical screening of apparently unaffected *AIP* mutation (*AIP*mut) carriers could identify previously unrecognized disease.

Objective: To determine the *AIP* mutational status of FIPA and young pituitary adenoma patients, analyzing their clinical characteristics, and to perform clinical screening of apparently unaffected *AIP*mut carrier family members.

Design: This was an observational, longitudinal study conducted in over 7 years.

Setting: International collaborative study conducted at referral centers for pituitary diseases.

Participants: FIPA families (n = 216) and sporadic young-onset (≤30 y) pituitary adenoma patients (n = 404) participated in the study.

Interventions: We performed genetic screening of patients for *AIP*muts, clinical assessment of their family members, and genetic screening for somatic *GNAS1* mutations and the germline *FGFR4* p.G388R variant.

Main Outcome Measure(s): We assessed clinical disease in mutation carriers, comparison of characteristics of *AIP*mut positive and negative patients, results of *GNAS1*, and *FGFR4* analysis.

Results: Thirty-seven FIPA families and 34 sporadic patients had *AIP*muts. Patients with truncating *AIP*muts had a younger age at disease onset and diagnosis, compared with patients with nontruncating *AIP*muts. Somatic *GNAS1* mutations were absent in tumors from *AIP*mut-positive patients, and the studied *FGFR4* variant did not modify the disease behavior or penetrance in *AIP*mut-positive individuals. A total of 164 *AIP*mut-positive unaffected family members were identified; pituitary disease was detected in 18 of those who underwent clinical screening.

Conclusions: A quarter of the *AIP*mut carriers screened were diagnosed with pituitary disease, justifying this screening and suggesting a variable clinical course for *AIP*mut-positive pituitary adenomas. **(*J Clin Endocrinol Metab* 100: 0000–0000, 2015)**

ISSN Print 0021-972X ISSN Online 1945-7197
Printed in USA

Received April 5, 2015. Accepted July 15, 2015.
First Published Online July 17, 2015

Abbreviations: AIP aryl-hydrocarbon receptor interacting protein; *AIP*mut, *AIP* mutation; CI, confidence interval; FIPA, familial isolated pituitary adenoma; IQR, interquartile range; MEN, multiple endocrine neoplasia; MRI, magnetic resonance imaging; NFPA, nonfunctioning pituitary adenoma; OR, odds ratio; PRL, prolactin; SNP, single-nucleotide polymorphism.

Familial isolated pituitary adenoma (FIPA) is characterized by the presence of pituitary adenomas in two or more members of the same family in the absence of other syndromic clinical features, such as those characteristic of multiple endocrine neoplasia (MEN) type 1 and MEN4, Carney complex or tumors related to mutations in the succinate dehydrogenase genes. FIPA is a heterogeneous condition, encompassing cases with unknown genetic cause and patients with mutations in the aryl-hydrocarbon receptor interacting protein gene (*AIP*), with distinctive clinical characteristics. Germline *AIP* mutations (*AIP*-muts) play a role not only in a subset of FIPA families (1–4) but also in sporadically diagnosed pituitary adenomas (5–9), and in the setting of somatostatin analog (SSA)-resistant acromegaly (10). Another form of FIPA, X-linked acrogigantism, due to microduplications in the Xq26.3 region, has been recently identified in patients with very young-onset gigantism and pituitary adenoma/hyperplasia (11).

The phenotype of *AIP*mut-associated pituitary adenomas has been described before (2–4, 12), but a systematic follow-up of cases and families is lacking due to the relative novelty of this pathogenic association (1), the variable disease penetrance (4, 12–14), and the rarity of this clinical entity. We present the clinical and genetic characteristics of a large cohort of FIPA and simplex (patients with germline mutation and no family history) *AIP*mut-positive patients, aiming for the following: 1) to perform a systematic follow-up of families to identify and characterize *AIP*mut-positive carriers, 2) to seek the role of disease-modifying genes on the variable phenotype and penetrance of the disease, and 3) to confirm and extend the description of the phenotype of *AIP*mut-positive patients, providing a comparison with *AIP*mut-negative cases. We establish that genetic screening followed by clinical assessment identifies a large percentage of family members with pituitary abnormalities, supporting the facilitation of genetic diagnosis and follow-up of these patients and their families.

Patients and Methods

Our study population (1725 subjects, Table 1) was recruited via the collaborative research network of the International FIPA Consortium (15). Pituitary adenoma patients were grouped into 11 clinical diagnostic categories (Supplemental Table 1). The diagnoses of acromegaly, acromegaly/prolactinoma, gigantism, gigantism/prolactinoma, and mild acromegaly (16) were grouped together under the category of GH excess for some analyses.

Between January 2007 and January 2014, we recruited patients from 35 countries from two different groups: either members of FIPA families, defined by the presence of pituitary adenomas in two or more members of a family without other associated clinical features (1–3, 17) (familial cohort), or sporadically diagnosed pituitary adenoma patients with disease onset at 30 years of age or younger (sporadic cohort). As an exception to these inclusion criteria, one *AIP*mut-positive sporadic patient older than 30 years was found thanks to *AIP* screening in

Table 1. Study Population: Demographics and General Description

	Familial Cohort	Sporadic Cohort	Combined
Total individuals, n, %	1231 (71.4)	494 (28.6)	1725 (100)
Females, n, %	668 (54.3)	250 (50.6)	918 (53.2)
Current age, median (range [IQR])	46.2 (2–97 [32–62])	35 (3–77 [26–42])	42.6 (2–97 [29–56])
Clinical status, n, %			
Affected	502 (40.8)	404 (81.8)	906 (52.5)
Unaffected	729 (59.2)	90 (18.2)	819 (47.5)
Affected males, n, %	219 (43.6)	203 (50.2)	422 (46.6)
Affected females, n, %	283 (56.4)	201 (49.8)	484 (53.4)
Diagnoses, n, %			
Acromegaly	170 (33.9)	203 (50.2)	373 (41.2)
Acromegaly/prolactinoma	17 (3.4)	12 (3)	29 (3.2)
Cushing's disease	24 (4.8)	21 (5.2)	45 (5)
FSHoma	2 (0.4)	1 (0.2)	3 (0.3)
Gigantism	44 (8.8)	65 (16.1)	109 (12)
Gigantism/prolactinoma	1 (0.2)	10 (2.5)	11 (1.2)
Mild acromegaly	2 (0.4)	–	2 (0.2)
NFPA	91 (18.1)	21 (5.2)	112 (12.4)
Pituitary tumor	17 (3.4)	2 (0.5)	19 (2.1)
Prolactinoma	134 (26.7)	67 (16.6)	201 (22.2)
TSHoma	—	2 (0.5)	2 (0.2)
GH excess patients, n, %	234 (46.6)	290 (71.8)	524 (57.8)

Abbreviations: FSHoma, FSH secreting adenoma. TSHoma, thyrotropinoma.

Dash indicates no patients in this category.

the setting of a research study, and the screening of his relatives detected a second *AIP*mut-positive pituitary adenoma case; this family was included in the familial cohort. The first patient reported in each FIPA family and all the sporadic patients were considered probands. All the patients received treatment and were followed up in accordance with the guidelines and clinical criteria of their respective centers. Relevant clinical and family structure data were received from clinicians and/or patients, and genetic screening was performed in the families of all the *AIP*mut-positive probands, selecting individuals according to their risk of inheriting the mutation, based on their position in the family tree, and extending the screening to as many generations as possible. In both familial and sporadic cases, other causes of familial pituitary adenomas, such as MEN1 and MEN4, Carney complex, pheochromocytoma/paraganglioma and pituitary adenoma syndrome, and X-linked acrogigantism were ruled out by clinical, biochemical and, in some cases, genetic tests, as appropriate.

The study population included a great majority of new cases but also previously diagnosed patients being followed up by the participating centers and a few historical cases, corresponding to deceased members of FIPA families (further details in Supplemental Results). Four *AIP*-mut-positive patients (two with diagnosis of acromegaly and two with gigantism) died in the postrecruitment period. Three of the deaths were due to cardiovascular causes (stroke, chronic heart failure, and acute coronary syndrome), whereas the exact cause of death is unknown in the fourth, a patient with long-standing untreated familial acromegaly.

All the patients and family members included agreed to take part by providing signed informed consent forms approved by the local ethics committee. Further details on the study population and the procedures for genetic/clinical screening and search for disease-modifying genes are described in the Supplemental Material.

Statistical analysis

The qualitative, categorical variables were expressed as percentages and compared using the χ^2 test or the Fisher's exact test, as appropriate. The normal distribution of the quantitative variables was verified using the Shapiro-Wilk and the Kolmogorov-Smirnov tests for normality. Means and SDs were used to report parametric data, and nonparametric data were expressed as median and interquartile ranges. Parametric data were analyzed with the unpaired *t* test, with a 95% confidence interval (CI), whereas the Mann-Whitney *U* test was used for the nonparametric data. Statistical significance was considered when the *P* value was $< .05$. All the statistical analyses were carried out using the GraphPad Prism 6 (GraphPad Software Inc) and Stata 12 (StataCorp LP) statistical software.

Results

Study population

The familial cohort was composed of 216 FIPA families, including 156 new families (989 subjects: 337 patients and 652 unaffected family members) and 60 previously described families (3, 12), in which 46 new subjects (15 patients and 31 unaffected family members) were added to the previously reported 196 individuals (150 patients and 46 unaffected family members). The sporadic cohort originally included 409 pituitary adenoma patients 30 years old or younger at disease onset, with no known family history of pituitary adenoma, but we excluded five patients from further analysis due to harboring an Xq26.3 microduplication. Of the remaining 404 sporadic patients, six were reported previously (3). In addition to the *AIP*mut screening, a subset of *AIP*mut-negative FIPA (n = 55) and sporadic (n = 45) patients underwent genetic screening for other endocrine neoplasia-associated genes (Supplemental Table 2). All of these tests were negative for pathogenic variants. After the genetic screening and follow-up of the patients and carriers, 60 individuals in the familial cohort and seven in the sporadic cohort were classified as not at risk of inheriting an *AIP*mut and were excluded from further analysis. Twenty-three individuals initially thought to be unaffected were identified with pituitary abnormalities (see details in *Prospective diagnosis*).

Genetic screening results

Thirty-seven of 216 FIPA families screened (17.1%) and 34 of 404 sporadic patients (8.4%) were positive for pathogenic or likely pathogenic *AIP*muts, accounting for a total of 71 *AIP*mut-positive kindreds and 144 *AIP*mut-positive patients (76.4% familial and 23.6% simplex, Table 2). We also identified 164 *AIP*mut-positive apparently unaffected family members (see *Follow-up and prospective diagnosis*). Samples were not available from family members of 25 *AIP*mut-positive simplex cases to establish the presence or lack of de novo mutations. We identified three pituitary adenoma patients (two with clinically nonfunctioning pituitary adenoma [NFPA] and one with a microprolactinoma) belonging to *AIP*mut-positive FIPA families and being at risk of inheriting but not carrying an *AIP*mut; therefore, they were considered as phenocopies.

Thirty-one different *AIP*muts (10 not previously reported) were identified in our study population: 12 exclusively in familial cases, 12 in simplex cases only, and seven in both settings (Table 3 and Supplemental Figure 1). Of the total mutations, 70.8% (22/31) predicted a truncated or missing protein and were termed as truncating *AIP*muts (Supplemental Figure 2). We also identified 11 apparently

Table 2. Screening for *AIP*muts

	Familial Cohort			Sporadic Cohort			Combined		
	***AIP*mut-Positive Familial**	***AIP*mut-Negative Familial**	**Total Familial**	***AIP*mut-Positive Simplex**	***AIP*mut-Negative Sporadic**	**Total Sporadic**	***AIP*mut-Positive Familial and Simplex**	***AIP*mut-Negative Familial and Sporadic**	**Total**
Total number of kindreds, n, %	37 (17.1% of familial)	179 (82.9% of familial)	216 (34.8% of total)	34 (8.4% of sporadic)	370 (91.6% of sporadic)	404 (65.2% of total)	71 (11.5% of total)	549 (88.5% of total)	620 (100)
Total individuals, n, %	475 (38.6% of familial)	756 (61.4% of familial)	1231 (71.4% of total)	82 (16.6% of sporadic)	412 (83.4% of sporadic)	494 (28.6% of total)	557 (32.3% of total)	1168 (67.7% of total)	1725 (100)
Genetic status, n, %									
*AIP*mut-negative patients	3 (0.6)	389 (51.5)[a]	392 (31.8)	—	370 (89.8)	370 (74.9)	3 (0.5)	759 (65)	762 (44.2)
*AIP*mut-positive tested patients	95 (20)	—	95 (7.7)	34 (41.5)	—	34 (6.9)	129 (23.2)	—	129 (7.5)
At risk but not tested	33 (6.9)	—	33 (2.7)	8 (9.8)	—	8 (1.6)	41 (7.4)	—	41 (2.4)
Not at risk	48 (10.1)	12 (1.6)	60 (4.9)	7 (8.5)	—	7 (1.4)	55 (9.9)	12 (1)	67 (3.9)
Obligate unaffected carriers, not tested	8 (1.7)	—	8 (0.6)	2 (2.4)	—	2 (0.4)	10 (1.8)	—	10 (0.6)
Predicted *AIP*mut-positive patients	15 (3.2)	—	15 (1.2)	—	—	-	15 (2.7)	—	15 (0.9)
Unaffected *AIP*mut tested carriers	120 (25.3)	—	120 (9.7)	16 (19.5)	—	16 (3.2)	136 (24.4)	—	136 (7.9)
Unaffected and *AIP*mut negative	153 (32.2)	—	153 (12.4)	15 (18.3)	—	15 (3)	168 (30.2)	—	168 (9.7)
Unaffected relatives of *AIP*mut-negative patients	—	355 (47)	355 (28.8)	—	42 (10.2)	42 (8.5)	—	397 (34)	397 (23)
Summary of *AIP*mut-positive individuals, n, %									
Total *AIP*mut-positive patients[b]	110 (23.2)	—	110 (8.9)	34 (41.5)	—	34 (6.9)	144 (25.9)	—	144 (8.3)
Total unaffected *AIP*mut carriers[c]	128 (26.9)	—	128 (10.4)	18 (22)	—	18 (3.6)	146 (26.2)	—	146 (8.5)

Dash indicates no individuals in this category.

[a] In *AIP*mut-negative FIPA families, 199 patients were tested for *AIP*muts; the rest (n = 190) were assumed to be negative.

[b] This is equal to the sum of tested *AIP*mut-positive patients plus the predicted *AIP*mut-positive patients.

[c] Sum of tested unaffected carriers plus obligate unaffected carriers.

nonpathogenic *AIP* variants (three of them novel) in our population (Supplemental Table 3).

A multiple regression analysis was performed to determine which clinical features could more accurately predict the likelihood of a patient to carry an *AIP*mut. An age at diagnosis of 10 years or older and younger than 20 years conferred an odds ratio (OR) of 5.8 (P = .000, 95% CI 3.1–10.8) of having an *AIP*mut, whereas the OR was 2.8 if the age at diagnosis was 20 years or older and younger than 30 years (P= .000, 95% CI 1.3–5.7); thus, an age at diagnosis between 10 and 30 years is the best predictor of *AIP*muts. Inversely, a diagnosis of prolactinoma resulted in an OR of 0.2 (P= .000, 95% CI 0.1–0.5).

Genotype-phenotype correlation within the *AIP*mut-positive cohort

Truncating mutations accounted for 78.9% of the *AIP*muts found in the familial cohort (15 of 19) and for 57.9% of those detected in the sporadic cohort (11 of 19). To study a possible difference in disease penetrance between truncating and nontruncating mutations, we compared the number of affected individuals with truncating *AIP*muts in the familial (85 of 110 [77.3%]) and simplex cohorts (21 of 34 [61.8%]), finding no significant difference, although a trend was observed (P = .0729, analysis included prospectively diagnosed patients). No significant differences were found regarding the proportion of GH excess cases, number of patients per family, maximum tumoral diameter, frequency of macroadenomas, extrasellar invasion, or number of treatments received between the patients with truncating and nontruncating mutations. However, patients with truncating mutations were significantly younger at disease onset (median 16 [interquartile range (IQR) 15–25] vs 22 [IQR 17.3–27.8] y, P = .0046, Figure 1A) and at diagnosis (median 21 [IQR 16–30] vs 27 [IQR 20.8–37] y, P = .0028, Figure 1B), and the occurrence of pediatric cases was more common in this group (60% [57 of 95], Figure 1C), compared with the patients with nontruncating *AIP*muts (33.3% [12 of 36], P = .0064). In concordance with these differences, gigantism accounted for a significantly higher proportion of the GH excess cases in the patients with truncating *AIP*muts (54.7% [47 of 86]), compared with those with nontruncating *AIP*muts (30% [9 of 30], P = .0200). Because p.R304* was the most common *AIP*mut in our study pop-

Table 3. *AIP* Pathogenic or Likely Pathogenic Mutations in the Familial and Sporadic Cohorts

Mutation (DNA Level [Protein Level])	Mutation Type	Pathogenic	Location in Protein	Familial Cohort (n = 238)[a]	Simplex Cohort (n = 52)[a]	Combined (n = 290)[a]	References/SR[b]
g.4856_4857CG>AA	Promoter	Yes[c]	Not in protein (5′ UTR)	3 (1.3)	—	3 (1)	(3, 12)/(SR30)
c.3G>A (p.?)	Start codon	Likely[c]	N terminus	2 (0.8)	—	2 (0.7)	This paper
c.40C>T (p.Q14*)	Nonsense	Yes[c]	N terminus	2 (0.8)	—	2 (0.7)	(1)/(SR31, 32)
c.70G>T (p.E24*)	Nonsense	Yes[c]	N terminus	9 (3.8)	—	9 (3.1)	(3)/(SR33)
c.74_81delins7 (p.L25Pfs*130)	Frameshift	Yes[c]	PPIase domain	10 (4.2)	—	10 (3.4)	(12)/(SR34)
c.100–1025_279 + 357del (ex2del) (p.A34_K93del)	Large genomic deletion	Yes[c]	PPIase domain	12 (5)	2 (4)	14 (4.8)	(SR35)
c.100–18C>T	Intronic	Likely	Not in protein (intron 1)	—	3 (6)	3 (1)	(3, 7, 10)/(SR31)
c.241C>T (p.R81*)	Nonsense	Yes[c]	PPIase domain	12 (5)	4 (8)	16 (5.5)	(3)/(SR30, 36–38)
c.249G>T (p.G83Afs*15)	Splice site (cryptic splice site)	Yes[c]	PPIase domain	4 (1.7)	—	4 (1.4)	(12)
c.338_341dup (p.L115Pfs*16)	Frameshift	Yes[c]	PPIase domain	—	2 (4)	2 (0.7)	(6)
c.427C>T (p.Q143*)	Nonsense	Yes[c]	Between PPIase and TPR1 domains	—	1 (2)	1 (0.3)	This paper
c.469–2A>G (p.E158_Q184del)	Splice site	Likely	TPR1 domain	—	1 (2)	1 (0.3)	(5)/(SR39, 40)
c.490C>T (p.Q164*)	Nonsense	Yes[c]	Between PPIase and TPR1 domains	3 (1.3)	—	3 (1)	(12)
c.570C>G (p.Y190*)	Nonsense	Yes[c]	TPR1 domain	9 (3.8)	—	9 (3.1)	This paper
c.662dupC (p.E222*)	Nonsense	Yes[c]	Between TPR1 and 2 domains	3 (1.3)	—	3 (1)	(12)
c.713G>A (p.C238Y)	Missense	Yes	TPR2 domain	4 (1.7)	—	4 (1.4)	(3)/(SR33)
c.783C>G (p.Y261*)	Nonsense	Yes[c]	TPR2 domain	4 (1.7)	—	4 (1.4)	(9)/(SR39, 41, 42)
c.787 + 9C>T	Intronic	Uncertain	Not in protein (intron 5)	—	1 (2)	1 (0.3)	This paper
c.804C>A (p.Y268*)	Nonsense	Yes[c]	TPR3 domain	19 (8)	3 (6)	22 (7.6)	(SR43, 44)
c.805_825dup (p.F269_H275dup)	In-frame insertion	Yes	TPR3 domain	16 (6.7)	2 (4)	18 (6.2)	(3)/(SR30, 39, 45)
c.807C>T (p.(=))	Splice site (reduced transcript level)	Yes	TPR3 domain	7 (2.9)	4 (8)	11 (3.8)	(3, 5, 7, 10, 12)/ (SR46, 47)
c.811C>T (p.R271W)	Missense	Yes	TPR3 domain	—	1 (2)	1 (0.3)	(2, 7, 12)/(SR48)
c.816delC (p.K273Rfs*30)	Frameshift	Yes[c]	TPR3 domain	—	1 (2)	1 (0.3)	This paper
c.868A>T (p.K290*)	Nonsense	Yes[c]	TPR3 domain	—	1 (2)	1 (0.3)	This paper
c.872_877delTGCTGG (p.V291_L292del)	In-frame deletion	Yes	TPR3 domain	—	1 (2)	1 (0.3)	This paper
c.910C>T (p.R304*)	Nonsense	Yes[c]	C-terminal α-helix	88 (37)	16 (31)	104 (35.9)	(1–3, 5, 7, 9, 12, 14)/ (SR39, 49–51)
c.911G>A (p.R304Q)	Missense	Yes	C-terminal α-helix	20 (8.4)	3 (6)	23 (7.9)	(3, 5, 7, 9, 12)/ (SR31, 39, 52, 53)
c.967delC (p.R323Gfs*39)	Frameshift	Yes[c]	C-terminal α-helix	—	4 (8)	4 (1.4)	This paper
c.976_977insC (p.G326Afs*?)	Frameshift	Yes[c]	C-terminal α-helix	—	1 (2)	1 (0.3)	This paper
c.978dupG (p.I327Dfs*?)	Frameshift	Yes[c]	C-terminal α-helix	—	1 (2)	1 (0.3)	This paper
c.1-?_993+?del− (whole gene deletion)	Large genomic deletion	Yes[c]	Absence of the whole protein	11 (4.6)	—	11 (3.8)	(12)

Abbreviations: PPIase, peptidylprolyl isomerase; SR, supplemental references; TPR, tetratricopeptide repeat; UTR, untranslated region.

Dash indicates no individuals in this category.

[a] Number of positive individuals for each mutation, considering the *AIP*mut-positive tested individuals, the obligate carriers, and the predicted *AIP*mut patients.

[b] For supplemental references, see Supplemental Material.

[c] Truncating mutation.

ulation (20 kindreds), we analyzed whether these patients behaved differently from other patients with truncating mutations. We found more affected individuals per family (median 4 [IQR 2.5–5]) among families carrying the p.R304* *AIP*mut, compared with families with other *AIP*muts (median 2 [IQR 2–3], $P = .0133$). When con-

Figure 1. Patients with truncating vs nontruncating *AIP*muts. Patients with truncating *AIP*muts present with a more aggressive phenotype, characterized by an earlier age at onset (A) (P = .005) and (B) at diagnosis (P = .003). C, This earlier disease onset results in a higher frequency of pediatric cases (n [total] = 131); in fact, most of the patients with truncating mutations present in childhood and adolescence. **, $P < .01$.

sidering all the *AIP*mut-positive patients together (familial and sporadic), we found a higher proportion of pediatric patients among those with the *AIP* p.R304* mutation (65.8% [25 of 38] vs 46.5% [40 of 86], P = .0475).

Clinical and histopathological features

Findings regarding gender distribution, age at onset/diagnosis, distribution of clinical diagnoses, tumor size/extension, pituitary apoplexy, histopathological features, extrapituitary tumors, and specific analyses of patients with GH excess and with gigantism are detailed in the Supplemental Material and depicted in Supplemental Tables 4 and 5 and Supplemental Figures 3–7.

Disease penetrance

To calculate the penetrance of pituitary adenomas among *AIP*mut positive families, complete data are needed both for phenotype and genotype. Therefore, we have selected three families (two with p.R304* and one with p.A34_K39del mutations) in which complete data were available in three or more generations for consenting at-risk individuals. The *AIP* genotype was known in 76.6% (range 68.4%–94.7%) of the individuals at risk; of them, 16.8% were patients and 83.2% were unaffected carriers. The gender distribution was similar between patients and unaffected carriers. The mean penetrance in these three families was 28.6% (19%–38.1%), and it decreased to 22.7% (18.2%–26.7%) when 50% of the individuals at risk with unknown genotype were considered as unaffected carriers. When the prospectively diagnosed patients were omitted from this calculation, the total penetrance of pituitary adenomas was 12.5%, highlighting the importance of the follow-up of apparently unaffected carriers for the correct calculation of the disease penetrance.

Because penetrance cannot be appropriately calculated for *AIP*mut-negative families, we assessed the number of affected family members. The *AIP*mut-positive families had more affected individuals per family than the *AIP*mut-negative families ($P < .0001$, Supplemental Figure 7E). Whereas 84.9% of the *AIP*mut-negative families (152 of 179) had only two affected members, 48.6% of the *AIP*mut-positive families (18 of 37) had three or more pituitary adenoma patients per family. The maximum number of affected individuals within the same family was eight (six of them prospectively diagnosed) in a family carrying the p.R304* *AIP*mut, and the maximum number of cases of gigantism in the same family was five, in a FIPA family with the p.E24* *AIP*mut.

Follow-up and prospective diagnosis

Of the 164 originally identified *AIP*mut carriers, 160 were available and advised to undergo biochemical and clinical screening. Prospective diagnosis of a pituitary adenoma was established in 11.3% (18 subjects, 11 males) of the individuals originally considered as unaffected *AIP*mut carriers.

Six of the prospectively diagnosed patients had acromegaly (one of them with prolactin [PRL] cosecretion), one patient had gigantism, two patients were diagnosed with mild acromegaly (16), and nine patients harbored NFPAs. Of the 142 individuals remaining as apparently unaffected *AIP*mut carriers, 79 (55.6%) underwent clinical assessment and one or more biochemical or imaging tests, whereas 63 subjects (44.4%) had only clinical evaluation.

The prospective cases were diagnosed at an older age than the rest of the patients (median 30 [IQR 22.8–39.5] vs 23 [IQR 16–33] y, $P = .025$). At diagnosis, seven of the prospectively diagnosed patients were symptomatic (headaches, arthralgias, acral growth, facial changes, weight gain, or hyperhidrosis). Five of the 18 prospectively diagnosed tumors were macroadenomas, in contrast with a predominance of macroadenomas (89.9%, 71 of 79) in the rest of the *AIP*mut-positive FIPA patients ($P < .0001$). The maximum diameter was significantly smaller for prospective cases (median 5.8 [IQR 4.7–14.4] vs 16.5 [IQR 10–29] mm, $P = .0002$). Four of the patients with macroadenomas had surgery, and the histopathological study confirmed GH- or GH/PRL-positive adenomas. The fifth macroadenoma was identified in a 68-year-old male patient with high IGF-1, well-controlled hypertension and diabetes mellitus and no other comorbidities or symptoms, who did not want to receive any treatment. In addition, one *AIP*mut-negative pituitary adenoma patient, harboring a 25-mm NFPA, was prospectively diagnosed as part of an *AIP*mut-positive family (brother of the *AIP*-mut positive proband).

A further seven subjects had abnormalities in their screening tests, but a pituitary disease was not confirmed: five individuals had slightly elevated IGF-1 levels for their age/gender, one patient displayed acromegaloid features but normal pituitary magnetic resonance imaging (MRI) and biochemistry, and a 17-year-old female had repeatedly borderline high IGF-1 and incompletely suppressed GH on oral glucose tolerance test, but her bulky pituitary gland (11 mm in height), normal at this age group, is not changing during follow-up and her biochemical results are now within the normal range, after 3 years of follow-up.

The global penetrance of pituitary adenomas among the individuals initially considered as unaffected *AIP*mut carriers was 11.3% (18 of 160). However, the penetrance was higher in the group of carriers who underwent biochemical and imaging investigations, varying between 18.6% and 28.1%, depending on the depth of screening (Figure 2). Overall, these data suggest that approximately 20%–25% of the apparently unaffected *AIP*mut carriers screened with biochemical or imaging tests will be identified with a pituitary adenoma at some point in their lives.

Clinical screening was not systematically performed in the *AIP*mut-negative FIPA unaffected family members. Nevertheless, due to the increased disease awareness given by the existence of previous pituitary adenoma cases within their families, four individuals (three females and one male) from three different *AIP*mut-negative FIPA families were prospectively diagnosed. Three of them harbored NFPAs, but we lack complete information about the fourth patient. The mean age at diagnosis in the three

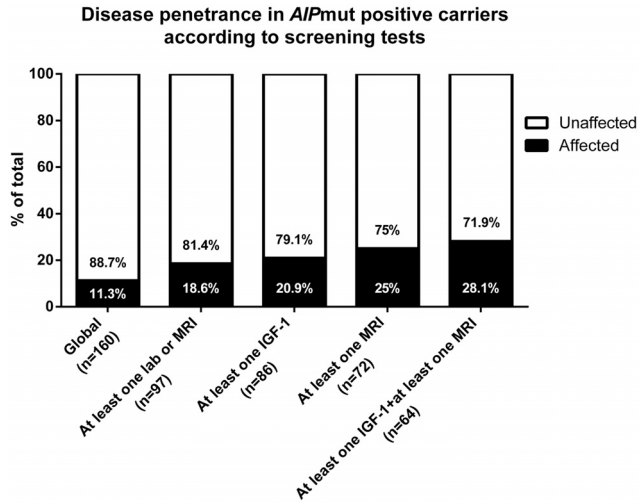

Figure 2. Penetrance in screened *AIP*mut-positive carriers (n [total] = 160). The probability of detecting new cases of pituitary adenomas within apparently unaffected *AIP*mut carriers depends on the clinical assessment and the type of complementary biochemical/imaging studies included in the screening protocol (see text).

NFPA cases was 37 years, and only one patient referred symptoms at diagnosis (galactorrhea, not clearly associated to stalk compression, and lethargy). All of them had microadenomas, with a mean diameter of 6.5 mm and did not require any therapeutic intervention other than hormonal replacement in one case. The characteristics of these cases resemble those of incidentalomas; however, the occurrence of two prospective cases in the same family supports an apparent inherited component.

Disease-modifying genes

We have studied the role of two possible disease-modifying genes: *GNAS1* (somatic) (18) and *FGFR4* (germline) (19). *GNAS1* mutations were absent in all the studied *AIP*mut-positive somatotropinomas (n = 23) but were detected in 50% of the *AIP*mut-negative familial somatotropinomas (5 of 10), 16.7% of the *AIP*mut-negative, young-onset cases (1 of 6), and 26.3% of the unselected acromegaly cases studied (5 of 19). The distribution of the *FGFR4* p.G388R single-nucleotide polymorphism (SNP) conserved the Hardy-Weinberg equilibrium (20), and the genotype distribution was similar between patients (n = 98) and *AIP*mut carriers (n = 108) ($P = .523$). The age at onset and at diagnosis, tumor size, and frequency of extrasellar invasion were not significantly different between the GG (wild type) and GR/RR patients.

Discussion

*AIP*muts are prevalent in young-onset, GH excess patients (24%) and FIPA (17.1%), with more than double frequency in patients with gigantism (46.7%) in our cohort,

in concordance with other studies (7, 9, 21, 22). However, in contrast to previous reports, in this large and extensively studied cohort, there was no predominance of male patients among the *AIP*mut-positive familial cases, and equal numbers of male and female unaffected carriers were identified. Earlier studies (3, 4, 12, 23) may have had an ascertainment bias for families with cases of gigantism, a disease that is more prevalent in males, at least partly due to the physiologically later puberty and therefore later cessation of growth in boys.

We have demonstrated that approximately a quarter of the individuals initially identified as unaffected *AIP*mut carriers who underwent clinical screening tests were diagnosed with pituitary abnormalities. Full clinical screening identified 28.1% of the carriers, with fewer tests understandably resulting in fewer positive cases. Our data suggest that not all the *AIP*mut-associated pituitary adenomas have a rapidly growing, aggressive phenotype. The follow-up of these patients allowed us to observe some probably very early cases of acromegaly, in which the current clinical scenario had not indicated intervention at data closure. We cannot rule out that some of the small NFPAs are indeed incidentalomas, similar to those frequently observed in *AIP*mut-negative subjects of the general population.

This frequency of prospective diagnosis may justify the clinical screening and, possibly, follow-up of all the *AIP*-mut-positive unaffected carriers. Our data would support the assessment of all the newly identified *AIP*mut carriers (clinical examination/history, PRL, and IGF-1, as a minimum, up to a full screening, also including an oral glucose tolerance test and contrast enhanced pituitary MRI). Follow-up of the younger family members should continue until at least 30 years of age, preferably annually, with clinical assessment and basal pituitary hormonal levels, leaving stimulation tests for cases with suspicion of pituitary disease and a follow-up MRI if necessary (24, 25). The cost-effectiveness and the possible psychological burden of this approach will need future study. Stopping the follow-up should be considered in older patients, given the low possibility of detecting new pituitary adenoma patients in these individuals after the fifth decade of life (24, 25). Once a case has been prospectively diagnosed, the treatment and follow-up should proceed as for the general population of pituitary adenoma patients because there are no data to suggest a different type of treatment in *AIP*mut-positive patients (26) although reduced SSA responsiveness has been described.

The genetic and clinical screening of *AIP*mut-negative FIPA families is uncertain at this point. Baseline screening and follow-up of obligate carriers could be considered, keeping in mind that the age of onset is considerably older in these families. Education on possible signs and symptoms of family members is a viable option in the routine setting. We expect that the identification of further genes implicated in the pathogenesis of FIPA in the next years will allow us to tailor these recommendations in accordance with the clinical behavior of each genetic entity.

Patients with GH excess starting before the age of 5 years should be tested for the recently identified Xq26.3 chromosomal microduplications (11). The genetic screening of other sporadic, young-onset pituitary adenoma patients with no evidence of other endocrine tumors should be focused on *AIP*muts in first instance in cases of GH excess (with or without PRL cosecretion) and on *MEN1* mutations, especially in cases of prolactinoma (9) because this can be the first manifestation of MEN1 (27). Whether it would be advisable to continue screening young patients with other diagnoses for *AIP*muts out of the setting of research studies needs longer follow-up.

To explain the variable clinical phenotype in our *AIP*-mut-positive patients, we evaluated the possible influence of two disease-modifying genes, *GNAS1* and *FGFR4*. Whereas somatic *GNAS1* mutations are common in unselected somatotropinomas (4.4%–59% of the cases) (28–35), we have not identified any in adenomas from *AIP*mut-positive patients, suggesting that germline *AIP*-muts and somatic *GNAS1* mutations are mutually exclusive in somatotropinomas. *GNAS1* mutations have rarely been studied in pediatric patients with acromegaly and gigantism, and they seem to be an extremely infrequent finding in this age group (36, 37). A recent study has shown no change in the AIP immunostaining in sporadic somatotropinomas in the presence of *GNAS1* mutations (38). The characteristic phenotype of adenomas containing the *GNAS1* mutations (small [32, 39], highly responsive to the treatment with SSAs, and more often densely granulated according to some [40], but not all studies [41]), seems to be in contrast with the typical *AIP*mut-positive tumor phenotype. On the other hand, in somatotroph adenomas of *AIP*mut-negative FIPA patients, half of the tested samples had *GNAS1* mutations. This suggests that in *AIP*mut-negative FIPA, the somatic *GNAS1* mutations could exist in a similar frequency as to in unselected somatotropinomas and possibly, in addition to a germline predisposing mutation, may play a role in their pathogenesis.

The *FGFR4* gene SNP rs351855 (c.1162G>A, p.G388R), with a minor allele frequency of 0.3, is a predictor of progression and poor prognosis in a variety of human neoplasms (42). A role for rs351855 as a facilitator of somatotroph cell tumorigenesis has been recently proposed (19), and we hypothesized that this variant could increase the penetrance and/or size and extension of *AIP*-

mut-positive pituitary adenomas. The screening for this SNP in our *AIP*mut-positive patients failed to show increase in size, extension, or apoplexy, even though this association had previously been suggested in sporadic acromegaly patients (19), and no earlier onset or higher penetrance was observed. The lack of association with these two potentially disease-modifying genes suggests that *AIP*mut-related pituitary adenomas are regulated by different pathogenic mechanisms than unselected somatotropinomas.

We recognize the numerous limitations of our study. We chose an arbitrary age cutoff (≤30 y), in concordance with previous *AIP*-related publications, but our data show that only 13.2% of the *AIP*mut-positive patients had disease onset after the age of 30 years. Our patients were recruited from different genetic backgrounds, and this could have influenced the disease penetrance and presentation. On the other hand, 19.7% of the *AIP*mut-positive kindreds (24.3% of the *AIP*mut positive patients) belong to a cohort with a founder *AIP*mut (p.R304*), originally from Northern Ireland (14). The larger number of subjects screened in these families provided a higher number of carriers and chance for detection of affected individuals. Additional genetic traits possibly cosegregating with this founder mutation could modify the phenotype and thus introduce a bias into our results. Full genotype and phenotype data were not available for all the families; therefore, we limited our penetrance calculations to three large, well-characterized families. A better assessment of the prevalence of pituitary apoplexy and extrapituitary adenomas in *AIP*mut-positive patients would require a large control group, screened ad hoc, which was beyond the scope of this study. Finally, the data about therapeutic modalities were limited, hampering the analysis of the response to different treatments.

Conclusions

The analysis of this large cohort of FIPA patients allowed us to establish a number of novel aspects of FIPA. A phenotype-genotype correlation was found with younger onset of disease in patients with truncating *AIP*muts. We identified a surprisingly high percentage of somatic *GNAS1* mutations in the *AIP*mut-negative somatotropinomas and their absence in *AIP*mut-positive tumors. The lack of influence of the germline *FGFR4* p.G388R variant on disease penetrance/severity suggests that currently unknown factors drive penetrance and variable phenotype in *AIP*mut-positive pituitary adenomas. The presence of milder, more indolent disease in some *AIP*mut-positive subjects has been established. Genetic and clinical screening leads to the prospective identification of an unexpectedly high proportion of affected patients in the originally apparently unaffected carrier group, resulting in earlier diagnosis and treatment and, possibly, better long-term outcome (25). The recruitment of a large study population with this uncommon disease has only been possible thanks to worldwide collaboration.

Acknowledgments

We are very grateful for patients and their family members and the numerous health care professionals supporting the study. We acknowledge Jonathan P. Bestwick (Wolfson Institute of Preventive Medicine, Barts and The London School of Medicine, Queen Mary University of London) for his valuable help with the statistical analysis and Dr Richard J. M. Ross (Department of Human Metabolism, School of Medicine and Biomedical Science, University of Sheffield, Sheffield, United Kingdom) for his collaboration in the recruitment of patients and collection of clinical data.

Address all correspondence and requests for reprints to: Márta Korbonits, MD, PhD, Professor of Endocrinology and Metabolism, Centre for Endocrinology, William Harvey Research Institute, Barts and The London School of Medicine, Queen Mary University of London, Charterhouse Square, London EC1M 6BQ, United Kingdom. E-mail: m.korbonits@qmul.ac.uk.

The International FIPA Consortium includes the following: Amar Agha, MD (Beaumont Hospital, Dublin, Republic of Ireland); Scott A. Akker, MD (St Bartholomew's Hospital, London, United Kingdom); Elena D. Aflorei, MD (Barts and The London School of Medicine, Queen Mary University of London, London, United Kingdom); Sándor Alföldi, MD (Szent Imre Egyeteni Oktatókórház, Budapest, Hungary); Professor Wiebke Arlt, MD (University of Birmingham, Birmingham, United Kingdom); Professor Brew Atkinson (Royal Victoria Hospital, Belfast, Northern Ireland, United Kingdom); Anna Aulinas-Masó, MD (Hospital de Sant Pau, Universitat Autònoma de Barcelona, Barcelona, Spain); Simon J. Aylwin, MD (Kings College Hospital National Health Service Foundation Trust, London, United Kingdom); Professor Philippe F. Backeljauw (Cincinnati Children's Hospital Medical Center, Cincinnati, Ohio); Corin Badiu, MD (Carol Davila University of Medicine and Pharmacy, Bucharest, Romania); Stephanie Baldeweg, MD (University College London Hospital, London, United Kingdom); Gul Bano, MD (St George's University of London, London, United Kingdom); Professor Ariel Barkan (University of Michigan Medical Center, Ann Arbor, Michigan); Julian Barwell, MD (Leicester Royal Infirmary, Leicester, United Kingdom); Carmen Bernal-González, MD (Hospital Universitario "12 de Octubre," Madrid, Spain); Professor G. Michael Besser (St Bartholomew's Hospital, London, United Kingdom); Professor John S. Bevan (Aberdeen Royal Infirmary, Foresterhill, Aberdeen, United Kingdom); Jo Blair, MD (Alder Hey Children's National Health Service Foundation Trust, Liverpool, United Kingdom); Pierre Bouloux, MD (Royal Free and University College School of Medicine, London, United Kingdom); Lisa Bradley, MD (St George's Healthcare National Health Service Trust, London, United Kingdom); Michael Buchfelder, MD (University of Erlangen, Erlangen, Germany); Professor Mehtap Cakir (Meram School of Medicine, Konya Nec-

mettin Erbakan University, Konya, Turkey); Natalie Canham, MD (North West Thames Regional Genetics Service, Northwick Park Hospital, London, United Kingdom); Paul Carroll, MD (Guy's and St Thomas' National Health Service Foundation Trust, London, United Kingdom); Harvinder S. Chahal, MD, PhD (Imperial College Healthcare National Health Service Trust, London, United Kingdom); Tim Cheetham, MD (University of Newcastle, Newcastle, United Kingdom); Farida Chentli, MD (Bab El Oued Teching Hospital, Algiers, Algeria); Richard N. Clayton, MD (University of Keele, Stoke-on-Trent, United Kingdom); Mark Cohen, MD (Royal Free National Health Service Foundation Trust, Barnet Hospital, Barnet, United Kingdom); Trevor Cole, MD (Birmingham Women's Hospital, Birmingham, United Kingdom); Hamish Courtney, MD (Royal Victoria Hospital, Belfast, Northern Ireland, United Kingdom); Elizabeth Crowne, MD (University Hospitals Bristol Foundation Trust, Bristol, United Kingdom); Daniel Cuthbertson, MD (University of Liverpool, Liverpool Merseyside, United Kingdom); Jacob Dal, MD (Aarhus University Hospital, Aarhus, Denmark); Nadezhda Dalantaeva, MD (Endocrinology Research Centre, Moscow, Russia); Christina Daousi, MD (University Hospital Aintree, Clinical Sciences Centre, University of Liverpool, Liverpool, United Kingdom); Ken Darzy, MD (Lister Hospital, Stevenage, United Kingdom); Professor Mehul Dattani, MD (University College London Institute of Child Health, London, United Kingdom); Justin H. Davies, MD (University Hospital Southampton, Southampton, United Kingdom); Professor Julian Davis, MD (Faculty of Medical and Human Sciences, University of Manchester and Central Manchester University Hospitals National Health Service Foundation Trust, Manchester, United Kingdom); Margaret De Castro, MD (Ribeirao Preto School of Medicine, University of Sao Paulo, Sao Paulo, Brazil); Laura De Marinis, MD (Università Cattolica del Sacro Cuore, Policlinico Universitario A. Gemelli, Rome, Italy); Professor William Drake, MD (St Bartholomew's Hospital, London, United Kingdom); Pinaki Dutta, MD (Postgraduate Institute of Medical Education and Research, Chandigarh, India); Larisa Dzeranova, MD (Endocrinology Research Centre, Moscow, Russia); Britt Edén-Engström, MD (Uppsala University Hospital, Uppsala, Sweden); Professor Rosalind Eeles, MD (Sutton Hospital, Sutton, United Kingdom); Maria Elfving, MD (Lund University Hospital, Lund, Sweden); Marianne Elston, MD (Waikato Hospital, Hamilton, New Zealand and Waikato Clinical School, University of Auckland, Hamilton, New Zealand); Louise Emmerson, MD (All Wales Medical Genetics Service, Glan Clwyd Hospital, Rhyl, United Kingdom); Naomi Fersht, MD (Department of Oncology, University College London Hospitals, London, United Kingdom); Professor Simona Fica, MD (Elias Hospital, Carol Davila University of Medicine and Pharmacy, Bucharest, Romania); Stefan Fischli, MD (Luzerner Kantonsspital, Luzern, Switzerland); Daniel Flanagan, MD (Derriford Hospital, Plymouth, United Kingdom); Maria Fleseriu, MD (Northwest Pituitary Center, Oregon Health and Science University, Portland, Oregon); Pamela U. Freda, MD (Columbia University College of Physicians and Surgeons, New York, New York); Professor Theodore Friedman, MD (Charles R. Drew University of Medicine and Science, Los Angeles, California); Professor Lawrence A. Frohman, MD (University of Illinois at Chicago, Chicago, Illinois); Patricia Gallego, MD (Western University, Children's Hospital, London Health Science Centre, London, Ontario, Canada); Evelien Gevers, MD (Barts and The London School of Medicine, Queen Mary University of London, London, United Kingdom); Edit Gláz, MD (Semmelweis University, Budapest, Hungary); James A. Goldman, MD (Harvard Vanguard Medical Associates, Boston Massachusetts); Anthony P. Goldstone (Imperial College Healthcare National Health Service Trust, Hammersmith Hospital, London, United Kingdom); Miklos Goth, MD (Health Center, Hungarian Defense Forces, Budapest, Hungary); Lynn Greenhalgh, MD (Alder Hey Children's Hospital Eaton Road, Liverpool, United Kingdom); Joan Grieve, MD (National Hospital for Neurology and Neurosurgery, Queen Square, London, United Kingdom); Mirtha Guitelman, MD (Hospital Durand, Buenos Aires, Argentina); Alper Gürlek, MD (Faculty of Medicine, Hacettepe University, Ankara, Sihhiye, Turkey); Mark Gurnell, MD (University of Cambridge and Cambridge Biomedical Research Centre, Addenbrooke's Hospital, Cambridge, United Kingdom); Katalin Horvath, MD (Gyor Hospital, Gyor, Hungary); Trevor A. Howlett, MD (University Hospitals of Leicester National Health Service Trust, Leicester Royal Infirmary, Leicester, United Kingdom); Charlotte Höybye, MD (Karolinska University Hospital, Stockholm, Sweden); Steven Hunter, MD (Royal Victoria Hospital, Belfast, Northern Ireland, United Kingdom); Donato Iacovazzo, MD (Barts and The London School of Medicine, Queen Mary University of London, London, United Kingdom, and Università Cattolica del Sacro Cuore, Policlinico Universitario A. Gemelli, Rome, Italy); Peter Igaz, MD (Faculty of Medicine, Semmelweis University, Budapest, Hungary); Warrick J. Inder, MD (School of Medicine, The University of Queensland, Brisbane, Queensland, Australia); Takeo Iwata, MD (Institute of Health Biosciences, The University of Tokushima Graduate School, Toskushima City, Japan); Louise Izatt (Guy's and St Thomas' Foundation Trust, Guy's Hospital, London, United Kingdom); Sujatha Jagadeesh, MD (Mediscan, Chennai, India); Gregory Kaltsas, MD (Laiko General Hospital, School of Medicine, National and Kapodistrian University of Athens, Athens, Greece); Felicity Kaplan, MD (Lister Hospital, Stevenage, United Kingdom); Niki Karavitaki, MD (Oxford Centre for Diabetes, Endocrinology, and Metabolism, Churchill Hospital, Oxford, United Kingdom); Darko Kastelan, MD (University Hospital Zagreb, and School of Medicine University of Zagreb, Zagreb, Croatia); Michelle Katz, MD (Massachusetts General Hospital and Harvard Medical School, Boston, Massachusetts); Tara Kearney, MD (Greater Manchester Neurosciences Centre, Salford Royal Foundation Trust, Manchester, United Kingdom); Bernard Khoo, MD (University College London, London, United Kingdom); Cathy Kiraly-Borri, MD (King Edward Memorial Hospital for Women, Subiaco, Australia); Robertas Knispelis, MD (Medical Academy, Lithuanian University of Health Sciences, Kaunas, Lithuania); Gábor László Kovács, MD (Flór Ferenc Hospital, Kistarcsa, Hungary); Ajith V. Kumar, MD (Great Ormond Street Hospital, London, United Kingdom); Edward R. Laws Jr, MD (Brigham and Women's Hospital, Boston, Massachusetts); Ronald M. Lechan, MD (Tupper Research Institute, Tufts Medical Center, Tufts University School of Medicine, Boston, Massachusetts); Miles J. Levy, MD (University Hospitals of Leicester National Health Service Trust, Leicester Royal Infirmary, Leicester, United Kingdom); Krzysztof Lewandowski, MD (Polish Mother's Memorial Hospital-Research Institute, and Medical University, Lodz, Poland); Janet Lo, MD (Harvard Medical School, Massachusetts General Hospital, Boston, Massachusetts); Niki Maartens, MD (University of Brisbaine, Brisbaine, Australia); Professor Akira Matsuno (Teikyo University, Tokyo, Japan); Barbara McGowan, MD (Guy's and St Thomas' Foundation Trust, St Thomas' Hospital,

London, United Kingdom); Siobhán E. McQuaid, MD (Mater Misericordiae University Hospital, Dublin, Republic of Ireland); Milica Medic-Stojanoska, MD (Clinical Center of Vojvodina and Medical Faculty, University of Novi Sad, Novi Sad, Serbia); Professor Moisés Mercado-Atri, MD (Hospital de Especialidades Centro Médico Nacional Siglo XXI, Instituto Mexicano del Seguro Social, Mexico City, Mexico); Emese Mezősi, MD (Faculty of Medicine, University of Pécs, Pécs, Hungary); Dragana Miljic, MD (Clinical Center of Serbia and Medical Faculty, University of Belgrade, Belgrade, Serbia); Karen K. Miller, MD (Massachusetts General Hospital, Harvard Medical School, Boston, Massachusetts); Silvia Modenesi, MD (Hospital das Clinicas, Minas Gerais Federal University, Belo Horizonte, Brazil); Mark E. Molitch, MD (Northwestern University Feinberg School of Medicine, Chicago, Illinois); Professor John Monson, MD (St Bartholomew's Hospital, London, United Kingdom); Damian G. Morris, MD (The Ipswich Hospital, Ipswich, United Kingdom); Patrick J. Morrison, MD (Belfast Health and Social Care Trust, Belfast, Northern Ireland, United Kingdom); Alia Munir, MD (Pinderfields Hospital, Yorkshire, United Kingdom, and Royal Hallamshire Hospital, Sheffield, United Kingdom); Professor Robert D. Murray, MD (Leeds Teaching Hospitals National Health Service Trust, St James's University Hospital, Leeds, United Kingdom); Madalina Musat, MD (Carol Davila University of Medicine and Pharmacy, Bucharest, Romania); Nina Musolino, MD (Universidade de São Paulo, São Paulo, Brazil); Lisa Nachtigall, MD (Harvard Medical School, Massachusetts General Hospital, Boston, Massachusetts); Professor John Newell-Price (School of Medicine and Biomedical Science, University of Sheffield, Sheffield, United Kingdom); Arla Ogilvie, MD (Watford Hospital, Watford, United Kingdom); Steve M. Orme, MD (Leeds General Infirmary, Leeds, United Kingdom); Ionela, Paşcanu MD (University of Medicine and Pharmacy, Tirgu-Mures, Romania); Attila Patócs, MD (Semmelweis University, Budapest, and Hungarian Academy of Sciences, Budapest, Hungary); Catherine Patterson, MD (Queen Margaret Hospital, Fife, United Kingdom); Simon H. Pearce, MD (Newcastle University, Newcastle-upon-Tyne, United Kingdom); Francesca Pecori Giraldi, MD (University of Milan, and Istituto Auxologico Italiano Istituto di Ricovero e Cura a Carattere Scientifico, Milan, Italy); Professor Marija Pfeifer, MD (University Medical Center Ljubljana, Ljubljana, Slovenia); Professor Vera Popovic (Clinical Center of Serbia and Medical Faculty, University of Belgrade, Belgrade, Serbia); Nicola Poplawski, MD (South Australia Pathology at the Women's and Children's Hospital, North Adelaide, South Australia, Australia); Michael Powell, MD (The National Hospital for Neurology and Neurosurgery, Queen Square, London, United Kingdom); Peter Pullan, MD (Sir Charles Gairdner Hospital, Nedlands, West Australia, Australia); Richard Quinton, MD (Institute of Genetic Medicine, University of Newcastle on Tyne, Royal Victoria Infirmary, Newcastle, United Kingdom); Serban Radian, MD, PhD (Barts and The London School of Medicine, Queen Mary University of London, London, United Kingdom); Harpal Randeva, MD (University of Warwick, Warwick, United Kingdom); Antônio Ribeiro-Oliveira Jr, MD (Hospital das Clinicas, Minas Gerais Federal University, Belo Horizonte, Brazil); Celia Rodd, MD (Wiinipeg University, Winnipeg, Canada); Fiona Ryan, MD (The John Radcliffe Hospital, Oxford, United Kingdom); Roberto Salvatori, MD (Johns Hopkins University School of Medicine, Baltimore, Maryland); Professor Christof Schöfl (Universitätsklinikum Erlangen, Friedrich-Alexander-Universität, Erlangen-Nürnberg, Germany); Debbie Shears, MD (Churchill Hospital, Oxford University Hospitals National Health Service Trust, Oxford, United Kingdom); Kevin Shotliff, MD (Chelsea and Westminster Hospital National Health Service Foundation Trust, London, United Kingdom); Beatriz S. Soares, MD (Hospital das Clinicas, Minas Gerais Federal University, Belo Horizonte, Brazil); Noel Somasundaram (National Hospital of Sri Lanka, Colombo, Sri Lanka); Professor Anna Spada, MD (Fondazione Cà Granda Istituto di Ricovero e Cura a Carattere Scientifico Ospedale Maggiore, University of Milan, Milan, Italy); James Sperber, MD (Endocrine Clinic, San Clemente, California); Helen A. Spoudeas, MD (The London Centre for Pediatric Endocrinology and Diabetes, Great Ormond Street Hospital for Children National Health Service Foundation Trust, London, United Kingdom); Susan Stewart, MD (University Hospital Birmingham, and Birmingham Women's Hospital, Birmingham, United Kingdom); Helen Storr, MD (Barts and The London School of Medicine, Queen Mary University of London, London, United Kingdom); Christian Strasburger, MD (Charite Campus Mitte, Berlin, Germany); Maria Elisabeth Street, MD (Santa Maria Nuova Hospital and Research Institute, Reggio-Emilia, Italy); Francesca Swords, MD (Norfolk and Norwich University Hospital, Norwich, United Kingdom); Professor Rajesh V. Thakker, MD (University of Oxford, Oxford Centre for Diabetes, Endocrinology, and Metabolism, Churchill Hospital, Oxford, United Kingdom); Elaine Tham, MD (Women's and Children's Hospital, Adelaide, Australia); Chris Thompson, MD (Beaumont Hospital, Dublin, Republic of Ireland); Dr Michael O. Thorner (University of Virginia, Charlottesville, Virginia); Miklós Tóth, MD (Faculty of Medicine, Semmelweis University, Budapest, Hungary); Professor Peter J. Trainer, MD (The Christie National Health Service Foundation Trust, Manchester, United Kingdom); Stylianos Tsagarakis, MD (Evangelismos Hospital, Athens, Greece); Marinella Tzanela, MD (Evangelismos Hospital, Athens, Greece); János Vadász, MD (Szolnok Hospital, Szolnok, Hungary); Vladimir Vaks, MD (Great Western Hospitals National Health Service Foundation Trust, Swindon, United Kingdom); Rasa Verkauskiene, MD (Institute of Endocrinology, Medical Academy, Lithuanian University of Health Sciences, Kaunas, Lithuania); Professor John A. Wass, MD (Oxford Centre for Diabetes, Endocrinology, and Metabolism, Churchill Hospital, Oxford, United Kingdom); Susan M. Webb, MD (Hospital Sant Pau, Centre for Biomedical Research on Rare Diseases (Centro de Investigación Biomédica en Red Enfermedades Raras Unit 747); Universitat Autònoma de Barcelona, Barcelona, Spain); Astrid Weber, MD (Liverpool Women's National Health Service Foundation Trust, Liverpool, United Kingdom); Shozo Yamada, MD (Toranomon Hospital, Tokyo, Japan); Sema Yarman, MD (Istanbul University, Istanbul Faculty of Medicine, Istanbul, Turkey); Philip Yeoh, MD (The London Clinic, London, United Kingdom); Katsuhiko Yoshimoto, MD (Institute of Health Biosciences, The University of Tokushima Graduate School, Tokushima City, Japan); and Nicola N. Zammitt, MD (Royal Infirmary of Edinburgh, Edinburgh, Scotland, United Kingdom).

Authors' contributions include the following: LC.H.-R. collected and entered the clinical and genetic data in the database, performed the statistical analysis and *GNAS1* and *FGFR4* genotyping, and prepared the manuscript; P.G. managed the ethics, recruited the patients, managed the samples and patient's data, extracted the DNA, collected and entered the clinical and genetic data in the database, and contacted the collaborators; J.D. re-

cruited the patients, managed the samples and patient's data, extracted the DNA, and collected and entered the clinical and genetic data in the database; K.S. performed the DNA sequencing and in silico analysis of *AIP*muts; G.T. collected the genetic data and performed the in silico analysis of *AIP*muts; D.T. performed the *FGFR4* genotyping; F.F. performed the DNA extraction and *FGFR4* genotyping; J.E. analyzed the MRI studies of the patients; S.E. supervised the DNA sequencing and in silico analysis of *AIP*muts; A.B.G. recruited the patients, collected the clinical and genetic data, and reviewed the manuscript; F.R. reviewed and completed the histopathological diagnoses; M.R.G. recruited the patients, collected the clinical and genetic data, and reviewed the manuscript; M.K. designed and coordinated the study, recruited the patients, collected and entered the clinical and genetic data in the database, reviewed the in silico analyses, and prepared and reviewed the manuscript; and The International FIPA Consortium members recruited the patients and provided the clinical data.

The trial of Genetics of Endocrine Tumors-Familial Isolated Pituitary Adenoma-FIPA is registered with clinicaltrials.gov with the identifier of NCT00461188.

This work was supported by the Medical Research Council of the United Kingdom (G0701307), the Wellcome Trust (097970/Z/11/Z), the National Institute of Health Research, the Barts and The London Charity, the Royal Society, and Pfizer. L.C.H.-R. is supported by grants from the National Council of Science and Technology and the Secretariat of Public Education from the Mexican Government.

The funding bodies had no role in the study design, collection, analysis, and interpretation of the data or in the manuscript preparation.

Disclosure Summary: M.G. serves on the Medical Advisory Board of Novartis. M.K. has received research grants from Pfizer and Novartis and serves on the Medical Advisory Board of Pfizer Inc. S.E. is a Wellcome Trust Senior Investigator. The other authors have nothing to disclose.

References

1. **Vierimaa O, Georgitsi M, Lehtonen R, et al.** Pituitary adenoma predisposition caused by germline mutations in the AIP gene. *Science*. 2006;312:1228–1230.
2. **Daly AF, Vanbellinghen JF, Khoo SK, et al.** Aryl hydrocarbon receptor-interacting protein gene mutations in familial isolated pituitary adenomas: analysis in 73 families. *J Clin Endocrinol Metab*. 2007;92:1891–1896.
3. **Leontiou CA, Gueorguiev M, van der Spuy J, et al.** The role of the aryl hydrocarbon receptor-interacting protein gene in familial and sporadic pituitary adenomas. *J Clin Endocrinol Metab*. 2008;93:2390–2401.
4. **Daly AF, Tichomirowa MA, Petrossians P, et al.** Clinical characteristics and therapeutic responses in patients with germ-line AIP mutations and pituitary adenomas: an international collaborative study. *J Clin Endocrinol Metab*. 2010;95:E373–E383.
5. **Cazabat L, Libe R, Perlemoine K, et al.** Germline inactivating mutations of the aryl hydrocarbon receptor-interacting protein gene in a large cohort of sporadic acromegaly: mutations are found in a subset of young patients with macroadenomas. *Eur J Endocrinol*. 2007;157:1–8.
6. **Stratakis CA, Tichomirowa MA, Boikos S, et al.** The role of germline AIP, *MEN1*, *PRKAR1A*, *CDKN1B* and *CDKN2C* mutations in causing pituitary adenomas in a large cohort of children, adolescents, and patients with genetic syndromes. *Clin Genet*. 2010;78:457–463.
7. **Tichomirowa MA, Barlier A, Daly AF, et al.** High prevalence of AIP gene mutations following focused screening in young patients with sporadic pituitary macroadenomas. *Eur J Endocrinol*. 2011;165:509–515.
8. **Cazabat L, Bouligand J, Salenave S, et al.** Germline AIP mutations in apparently sporadic pituitary adenomas: prevalence in a prospective single-center cohort of 443 patients. *J Clin Endocrinol Metab*. 2012;97:E663–E670.
9. **Cuny T, Pertuit M, Sahnoun-Fathallah M, et al.** Genetic analysis in young patients with sporadic pituitary macroadenomas: beside AIP don't forget MEN1 genetic analysis. *Eur J Endocrinol*. 2013;168:533–541.
10. **Oriola J, Lucas T, Halperin I, et al.** Germline mutations of AIP gene in somatotropinomas resistant to somatostatin analogues. *Eur J Endocrinol*. 2013;168:9–13.
11. **Trivellin G, Daly AF, Faucz FR, et al.** Gigantism and acromegaly due to Xq26 microduplications and GPR101 mutation. *N Engl J Med*. 2014;371:2363–2374.
12. **Igreja S, Chahal HS, King P, et al.** Characterization of aryl hydrocarbon receptor interacting protein (AIP) mutations in familial isolated pituitary adenoma families. *Hum Mutat*. 2010;31:950–960.
13. **Naves LA, Daly AF, Vanbellinghen JF, et al.** Variable pathological and clinical features of a large Brazilian family harboring a mutation in the aryl hydrocarbon receptor-interacting protein gene. *Eur J Endocrinol*. 2007;157:383–391.
14. **Chahal HS, Stals K, Unterlander M, et al.** AIP mutation in pituitary adenomas in the 18th century and today. *N Engl J Med*. 2011;364:43–50.
15. **The International FIPA Consortium.** http://www.fipapatients.org/fipaconsortium/. Accessed November 17, 2014.
16. **Dimaraki EV, Jaffe CA, DeMott-Friberg R, Chandler WF, Barkan AL.** Acromegaly with apparently normal GH secretion: implications for diagnosis and follow-up. *J Clin Endocrinol Metab*. 2002;87:3537–3542.
17. **Daly AF, Jaffrain-Rea ML, Ciccarelli A, et al.** Clinical characterization of familial isolated pituitary adenomas. *J Clin Endocrinol Metab*. 2006;91:3316–3323.
18. **Landis CA, Masters SB, Spada A, Pace AM, Bourne HR, Vallar L.** GTPase inhibiting mutations activate the alpha chain of Gs and stimulate adenylyl cyclase in human pituitary tumours. *Nature*. 1989;340:692–696.
19. **Tateno T, Asa SL, Zheng L, Mayr T, Ullrich A, Ezzat S.** The FGFR4–G388R polymorphism promotes mitochondrial STAT3 serine phosphorylation to facilitate pituitary growth hormone cell tumorigenesis. *PLoS Genet*. 2011;7:e1002400.
20. **Hardy-Weinberg Equilibrium Calculator.** http://www.koonec.com/k-blog/2010/06/20/hardy-weinberg-equilibrium-calculator/. Accessed January 3, 2014.
21. **Rostomyan, L, Daly AF, Lila A, et al.** Gigantism: results of an international clinical and genetic study. *Endocr Rev*. 2013;34(03_MeetingAbstracts):OR20–6.
22. **Schofl C, Honegger J, Droste M, et al.** Frequency of AIP gene mutations in young patients with acromegaly: a registry-based study. *J Clin Endocrinol Metab*. 2014;99(12):E2789–E2793.
23. **Beckers A, Daly AF.** The clinical, pathological, and genetic features of familial isolated pituitary adenomas. *Eur J Endocrinol*. 2007;157:371–382.
24. **Korbonits M, Storr H, Kumar AV.** Familial pituitary adenomas—who should be tested for AIP mutations? *Clin Endocrinol (Oxf)*. 2012;77:351–356.
25. **Williams F, Hunter S, Bradley L, et al.** Clinical experience in the screening and management of a large kindred with familial isolated pituitary adenoma due to an aryl hydrocarbon receptor interacting protein (AIP) mutation. *J Clin Endocrinol Metab*. 2014;99:1122–1131.
26. **Beckers A, Aaltonen LA, Daly AF, Karhu A.** Familial isolated pitu-

itary adenomas (FIPA) and the pituitary adenoma predisposition due to mutations in the aryl hydrocarbon receptor interacting protein (AIP) gene. *Endocr Rev*. 2013;34:239–277.
27. **Thakker RV, Newey PJ, Walls GV, et al.** Clinical practice guidelines for multiple endocrine neoplasia type 1 (MEN1). *J Clin Endocrinol Metab*. 2012;97:2990–3011.
28. **Landis CA, Harsh G, Lyons J, Davis RL, McCormick F, Bourne HR.** Clinical characteristics of acromegalic patients whose pituitary tumors contain mutant Gs protein. *J Clin Endocrinol Metab*. 1990; 71:1416–1420.
29. **Hosoi E, Yokogoshi Y, Hosoi E, et al.** Analysis of the Gsα gene in growth hormone-secreting pituitary adenomas by the polymerase chain reaction-direct sequencing method using paraffin-embedded tissues. *Acta Endocrinol (Copenh)*. 1993;129:301–306.
30. **Yoshimoto K, Iwahana H, Fukuda A, Sano T, Itakura M.** Rare mutations of the Gsα subunit gene in human endocrine tumors. Mutation detection by polymerase chain reaction-primer-introduced restriction analysis. *Cancer*. 1993;72:1386–1393.
31. **Shi Y, Tang D, Deng J, Su C.** Detection of gsp oncogene in growth hormone-secreting pituitary adenomas and the study of clinical characteristics of acromegalic patients with gsp-positive pituitary tumors. *Chin Med J (Engl)*. 1998;111:891–894.
32. **Buchfelder M, Fahlbusch R, Merz T, Symowski H, Adams EF.** Clinical correlates in acromegalic patients with pituitary tumors expressing GSP oncogenes. *Pituitary*. 1999;1:181–185.
33. **Park C, Yang I, Woo J, et al.** Somatostatin (SRIF) receptor subtype 2 and 5 gene expression in growth hormone-secreting pituitary adenomas: the relationship with endogenous srif activity and response to octreotide. *Endocr J*. 2004;51:227–236.
34. **Mendoza V, Sosa E, Espinosa-de-los-Monteros AL, et al.** GSPα mutations in Mexican patients with acromegaly: potential impact on long term prognosis. *Growth Horm IGF Res*. 2005;15:28–32.
35. **Freda PU, Chung WK, Matsuoka N, et al.** Analysis of GNAS mutations in 60 growth hormone secreting pituitary tumors: correlation with clinical and pathological characteristics and surgical outcome based on highly sensitive GH and IGF-I criteria for remission. *Pituitary*. 2007;10:275–282.
36. **Johnson MC, Codner E, Eggers M, Mosso L, Rodriguez JA, Cassorla F.** Gps mutations in Chilean patients harboring growth hormone-secreting pituitary tumors. *J Pediatr Endocrinol Metab*. 1999; 12:381–387.
37. **Metzler M, Luedecke DK, Saeger W, et al.** Low prevalence of Gsα mutations in somatotroph adenomas of children and adolescents. *Cancer Genet Cytogenet*. 2006;166:146–151.
38. **Jaffrain-Rea ML, Rotondi S, Turchi A, et al.** Somatostatin analogues increase AIP expression in somatotropinomas, irrespective of Gsp mutations. *Endocr Relat Cancer*. 2013;20:753–766.
39. **Larkin S, Reddy R, Karavitaki N, Cudlip S, Wass J, Ansorge O.** Granulation pattern, but not GSP or GHR mutation, is associated with clinical characteristics in somatostatin-naive patients with somatotroph adenomas. *Eur J Endocrinol*. 2013;168:491–499.
40. **Spada A, Arosio M, Bochicchio D, et al.** Clinical, biochemical, and morphological correlates in patients bearing growth hormone-secreting pituitary tumors with or without constitutively active adenylyl cyclase. *J Clin Endocrinol Metab*. 1990;71:1421–1426.
41. **Mayr B, Buslei R, Theodoropoulou M, Stalla GK, Buchfelder M, Schofl C.** Molecular and functional properties of densely and sparsely granulated GH-producing pituitary adenomas. *Eur J Endocrinol*. 2013;169:391–400.
42. **Frullanti E, Berking C, Harbeck N, et al.** Meta and pooled analyses of FGFR4 Gly388Arg polymorphism as a cancer prognostic factor. *Eur J Cancer Prev*. 2011;20:340–347.

SUPPLEMENTAL MATERIAL

SUPPLEMENTAL METHODS

Study population

At recruitment, relevant clinical and biochemical data were collected at each participating center using a standard datasheet designed for this study (available on request) and all the information was entered into our central database. Data about the follow-up, treatments and current status of the patients were prospectively requested and collected from the collaborating centers and directly from the patients. Data about the historical cases were collected from family members and from hospital archives, when available. With a few exceptions, genetic screening results were directly sent to our center and entered in the database. The available data did not allow a comprehensive analysis of the response to specific therapeutic modalities.

We identified subjects 'at risk' (those with the possibility of inheriting an *AIP*mut), 'obligate carriers' (based on their position in family tree, *AIP*muts were verified when possible) and 'unaffected carriers'. Therefore, in our analysis the term 'unaffected carrier' includes all the relatives of *AIP*mut-positive patients without clinical manifestations of a pituitary adenoma and with either a genetic screening positive for the *AIP*mut present in the proband or with a position in the family tree defining them as 'obligate carriers'. Additionally, the analysis of the family trees led to the identification of some affected individuals as 'predicted *AIP*mut-positive patients', defined as individuals with an established clinical diagnosis of pituitary adenoma in whom the genetic screening could not be carried out due to unavailability of a DNA sample, but in whom the presence of the mutation was assumed based on both the phenotype and the position in the family tree. Therefore, the term '*AIP*mut-positive patient' will refer to both 'predicted *AIP*mut-positive patients' and '*AIP*mut-positive patients' in whom the presence of the mutation was verified. Subjects 'not at risk' of inheriting an *AIP*mut were defined based on their position in the family tree. In the sporadic cohort, the *AIP*mut-positive patients

with no apparent familial history of pituitary disease were also referred as ‘simplex’ cases as they can be considered the first case of a potentially hereditary disease.

Genetic and clinical screening

Pituitary adenoma patients and their apparently unaffected relatives were screened for *AIP*muts using Sanger sequencing and multiplex ligation-dependent probe amplification (MLPA), as described in Supplemental Material. We have divided the *AIP* variants into five classes according to the likelihood of pathogenicity, as recommended by Plon *et al*. (SR1): definitely pathogenic, likely pathogenic, uncertain, unlikely pathogenic and not pathogenic. All the unaffected individuals with positive genetic screening for *AIP*muts were advised to undergo clinical, biochemical and image screening tests for the early diagnosis of possible pituitary disease, on an annual basis or as appropriate. The recommendations for screening were based on the published experience of our group (24) and others (26). Additional genetic tests were performed in subjects with no pituitary adenomas, but with other clinical features indicative of such tests (screening for mutations in *BRCA1* and *2* and *TP53* was performed in members of a family with breast cancer, osteosarcoma and a neuroendocrine tumor of the colon), as well as and in a randomly selected cohort of *AIP*mut-negative FIPA probands, searching for mutations in other genes via direct sequencing and MLPA (*BRCA1* and *2*, *CDKN1B, MEN1, TP53, PRKAR1A)* or via a next-generation sequencing panel *(MAX, RET, SDHA, SDHAF2, SDHB, SDHC, SDHD, TMEM127,* and *VHL*) (SR2).

Genomic DNA was obtained from blood (Ilustra DNA Extraction Kit BACC2, GE Healthcare, Little Chalfont, UK) or saliva (Oragene-DNA [collection] and prepIT-L2P [extraction] kits, DNA Genotek, Ontario, Canada) samples. The detection of the *AIP* gene variants and dosage was performed at the Molecular Genetics Laboratory, Royal Devon and Exeter, NHS Foundation Trust for the great majority of the samples, as previously described (3;12). Although the genetic tests were performed in one of the largest Genetics laboratories in the world, with appropriate quality controls, we cannot rule out that mutations were not identified in a small number of cases, due to either technical problems or due to location of mutations in areas not analyzed (such as intronic regions). The pathogenicity of the

detected variants was assessed using the Pathogenic Or Not-Pipeline (PON-P) and Alamut 2.2.1 *in silico* prediction programs, as well as considering the scientific literature concerning clinical and experimental data on the previously reported variants. Only those variants considered as definitely or likely pathogenic (SR1) were included in the study. Additionally, we included one novel intronic variant with no experimental data available, for which the prediction software could not exclude pathogenicity. The variants described in this paper are listed by their position in the DNA, with the corresponding change at the protein level in parentheses, according to the nomenclature guidelines of the Human Genome Variation Society (HGVS) version 1.0 (SR3) and the changes proposed for the version 2.0 (http://www.hgvs.org/mutnomen/). The nomenclature was verified using the Mutalyzer 2.0.beta-21 software (http://www.lovd.nl/mutalyzer/). The positions in the DNA are based on the GRCh37/hg19 assembly of the human genome and the human *AIP* reference sequence (Locus Reference Genomic code LRG_460 (SR4), based on NG_008969.1 and NM_003977.2). Array comparative genomic hybridization analysis was performed in a group of patients with gigantism, and patients positive for Xq26 microduplications (11) were excluded from further analysis.

Disease-modifying genes

Genomic DNA (gDNA) samples from 98 *AIP*mut-positive patients (55 males/43 females) and 108 unaffected *AIP*mut carriers (56 males/52 females) were subjected to PCR, using previously described primers (SR5) and screened for the *FGFR4* p.G388R (rs351855) single nucleotide polymorphism (SNP). Additionally, gDNA was extracted from paraffin-embedded somatotropinomas for 23 *AIP*mut-positive patients (familial and simplex), ten *AIP*mut-negative FIPA patients and six *AIP*mut-negative sporadic patients and cDNA was obtained from 19 frozen somatotropinomas from unselected acromegaly cases (control group, 13 males and six females, age at diagnosis 37-77 years). All these samples were screened for mutations in the *GNAS1* codons 201 and 227 using previously described primers for gDNA (SR6), and the primers 5'-CAAGCAGGCTGACTATGTGC-3' and 5'-ACCACGAAGATGATGGCAGT-3' for cDNA. The sequence analysis of the *FGFR4* and *GNAS1* PCR products was carried out by Sanger sequencing (BigDye Terminator v 3.1 kit in and ABI 3730 capillary sequencer, Applied Biosystems, Foster City, CA, USA).

SUPPLEMENTAL RESULTS AND DISCUSSION

Clinical and histopathological features

Gender distribution

Among the familial patients, there was a significantly different gender distribution of the affected individuals between the *AIP*mut-positive and negative subgroups (P=0.0015, Supplemental Figure 3a), showing a predominance of females in the *AIP*mut-negative families. This difference is unlikely to be due to a selection bias, as the gender distribution was not significantly different between affected and unaffected individuals in the whole study population (P=0.8581), or, in the familial cohort, between unaffected *AIP*mut-positive and negative individuals (P=0.4421, Supplemental Figure 3b), or between *AIP*mut-positive affected and unaffected individuals (P=0.1367). We did not see a difference in gender distribution between the *AIP*mut-positive and negative sporadic patients either (P=0.1605, Supplemental Figure 3c).

Age

Familial patients

FIPA *AIP*mut-positive patients were younger at disease onset (Supplemental Figure 4a) compared with *AIP*mut-negative FIPA patients. In the *AIP*mut-positive subgroup, the earliest age at onset was three years, while in the *AIP*mut-negative families a female patient with Cushing's disease had the earliest disease onset at seven years. Most of the *AIP*mut-positive FIPA patients (71.7% [71/99]) developed their pituitary adenomas during the second and third decades of life (10-29 years), whereas only 39.2% (121/309) of the *AIP*mut-negative FIPA patients had their first signs/symptoms of pituitary adenoma during the same stage of life (P<0.0001, Supplemental Figure 4a and b). The age at diagnosis was also significantly different (P<0.0001): 68.2% (75/110) of the *AIP*mut-positive FIPA patients were diagnosed at ≤30 years of age, whereas the diagnosis was established in only 36.7% (116/316) of the *AIP*mut-negative patients by that age. The earlier disease presentation was also reflected in a much higher frequency of pediatric cases (disease onset at ≤18 years of age,

Supplemental Figure 4c) in the *AIP*mut-positive FIPA families, compared with the *AIP*mut-negative FIPA families (44.1 vs. 11.8%, $P<0.0001$). These distributions were calculated taking into consideration the prospectively diagnosed *AIP*mut-positive patients; however, the statistical analysis results were not significantly different when those patients were excluded.

Sporadic patients

Even though our sporadic cohort included only young-onset pituitary adenoma patients, a significant younger age at onset was still found within this young group in the *AIP*mut-positive simplex patients in comparison with the *AIP*mut-negative ones (median 16 [IQR 14.8-22.3] vs. 22 [IQR 16-26] years, $P=0.0054$, Supplemental Figure 4d), and there was a higher proportion of pediatric cases within the *AIP*mut-positive subgroup (58.8% vs. 35.9%, $P=0.0085$). Nevertheless, while the youngest age at onset in the *AIP*mut-positive simplex patients was nine years, 3% (11/369) of the *AIP*mut-negative patients had disease onset before the nine years of age, with a minimum age of three years.

Clinical diagnoses

GH excess patients accounted for 57.8% (524/906) of the total affected individuals in the entire cohort: 46.6% (234/502) of the familial and 71.8% (290/404) of the sporadic cases. Patients with GH excess, prolactinomas and NFPAs were present in both *AIP*mut-positive and negative subgroups, but Cushing's disease, functioning gonadotropinomas and TSHomas were not found in patients bearing *AIP*muts.

Familial patients

We classified the FIPA families as 'homogeneous', when all the affected individuals within the family had the same diagnosis (GH excess was considered as a single category), or 'heterogeneous', when different diagnoses were found in the same family (17). Around one half of the families in our cohort were homogeneous FIPA families (families with only one pituitary adenoma type) in both the *AIP*mut-positive (48.6%) and negative (52.5%) subgroups (Supplemental Table 4). The most common family type in both subgroups (according to the diagnostic categories found in the affected members)

was the pure GH excess family, but it was significantly more frequent within the *AIP*mut-positive FIPA families (P=0.0249). The most common diagnoses in *AIP*mut-positive and negative families were the different categories of GH excess; nevertheless, these cases were significantly more frequent in the *AIP*mut-positive subgroup, with at least one case of GH excess in 91.9% (34/37) of the *AIP*mut-positive and in 53.1% (95/179) of the *AIP*mut-negative FIPA families (P<0.0001, Supplemental Figure 4e). There was a higher frequency of PRL co-secretion among the *AIP*mut-positive patients with acromegaly or gigantism, compared with the *AIP*mut-negative ones (P=0.0158, Supplemental Figure 4f). In the *AIP*mut-negative FIPA patients the most frequent diagnosis was acromegaly, in 35.3% (137/389) of the patients, with prolactinoma in the second place of frequency (30.9%, 120/389). In sharp contrast to *AIP*mut-positive families, where 31% (35/113) of the patients had gigantism, only 2.1% (8/389) of the *AIP*mut-negative FIPA patients had this diagnosis.

Sporadic patients

In the sporadic cohort, all the *AIP*mut-positive simplex patients harbored GH-secreting adenomas (vs. 69.2% of the *AIP*mut-negative cases), as proven by the clinical diagnosis and immunohistochemistry (IHC) report. The predominance of GH excess cases in both groups could be due to a selection bias, as the previously reported association between *AIP*muts and acromegaly/gigantism could have influenced the referral of these patients for the study.

Histopathology

Familial patients

The IHC analysis of the operated pituitary adenomas confirmed the clinical/biochemical picture in the vast majority of the cases, reporting a predominance of somatotropinomas and mammosomatotroph adenomas in FIPA patients, more evident in the *AIP*mut-positive subgroup (P= 0.0304, Supplemental Figure 5a and b). There was a unique case of a double adenoma (one tumor positive for GH and another one for PRL) and one unusual case of somatotroph hyperplasia in a patient with gigantism within the *AIP*mut-positive patients. None of the few *AIP*mut-positive clinically NFPA cases were

gonadotroph or null cell adenomas. In contrast, in the *AIP*mut-negative FIPA families, 48.3% of the NFPAs analyzed were reported as gonadotropinomas and 31% were null cell adenomas (based on negative immunostaining for GH, ACTH, PRL, TSH, LH and FSH). There was a similar prevalence of plurihormonal tumors in both subgroups (17.4% in the *AIP*mut-positive and 10.5% in the *AIP*mut-negative families, $P=0.2763$). Seventy five percent of all the plurihormonal tumors in both subgroups had positive GH staining. There was a significant difference among the *AIP*mut-positive and negative FIPA patients involving the granulation pattern in GH positive adenomas. All the *AIP*mut-positive FIPA patients for whom this parameter was available (22/22) had sparsely granulated adenomas, while 43.8% (7/16) of the *AIP*mut-negative patients harbored densely granulated adenomas ($P<0.0001$, Supplemental Figure 5c); this difference could correspond to the response to the treatment with SSA, as suggested by previous reports (SR7). We found no difference in the proportion of patients with Ki-67 index ≥3% between the two subgroups (global 28.1%, $P=1.0000$).

The presence of two different types of pituitary adenomas in the same gland is infrequent (2.3% of all the cases and 3.3% of the cases of Cushing's disease) (SR8). Multiple pituitary adenomas have been previously described in a few cases of MEN1 and FIPA (not screened for *AIP*muts) patients (SR9-13). Although somatotroph hyperplasia has been described before in the setting of *AIP*muts (10;SR14), this finding does not seem to be particularly frequent, as in our cohort it was found only in one patient with acromegaly and PRL co-secretion.

There was a marked predominance of sparsely granulated GH-secreting adenomas among the *AIP*mut-positive patients, compared with the *AIP*mut-negative ones. Patients with sparsely granulated tumors are usually younger at diagnosis than those with a densely granulated pattern (SR15;SR16), have increased invasiveness (SR7;SR15-17) and reduced response to the treatment with SSA (SR7;SR17), though the strength of these associations has been variable among different studies. The mechanism proposed for this effect in sporadic adenomas implies a reduced expression of the somatostatin receptor subtype 2 (SSTR2) (SR18;SR19). Since the expression of the SSTR2 and other somatostatin receptor subtypes is not reduced in somatotropinomas from *AIP*mut-positive patients,

other molecular mechanisms must be involved in the association of these mutations with decreased responsiveness to SSAs and a sparsely granulated pattern, such as ZAC1 activation (SR20;SR21) or an impaired inhibitory G protein subunit function in these tumors (SR22).

Sporadic patients

All the *AIP*mut-positive patients with available histopathology results (n=14) had GH positive pituitary adenomas by IHC, 28.6% of them (n=4) were mammosomatotroph adenomas (Supplemental Figure 5d). In contrast, the *AIP*mut-negative subgroup (n=89) included corticotropinomas (7.9%), null cell adenomas (3.4%), plurihormonal tumors (13.5%), prolactinomas (12.4%), somatotropinomas (32.6%), mammosomatotroph adenomas (29.2%), as well as a TSHoma (1.1%, Supplemental Figure 5e). In the *AIP*mut-positive subgroup, one third (2/6) of the somatotroph adenomas with available cytokeratin staining had a densely granulated pattern and the rest were sparsely granulated. The distribution was similar in the *AIP*mut-negative subgroup, where 31.6% of the GH adenomas presented a densely granulated pattern (6/19) and 68.4% were sparsely granulated. Additionally, one *AIP*mut-negative patient had a somatotropinoma with a mixed granulation pattern.

Pituitary adenoma size and extension

Familial patients

We compared size and extension of pituitary adenomas between *AIP*mut-positive and negative FIPA patients (Supplemental Figure 6), and for this purpose, the prospectively diagnosed *AIP*mut-positive patients were excluded from the analysis. Despite macroadenomas being predominant in both FIPA patient groups, the *AIP*mut-positive FIPA patients had larger tumors, demonstrated by a larger maximum diameter (P=0.0404, Supplemental Figure 6a) and a higher prevalence of macroadenomas (P<0.0001, Supplemental Figure 6b). The proportion of giant (maximum diameter ≥40mm) adenomas (6.3% in *AIP*mut-positive and 3% in *AIP*mut-negative patients) was not significantly different (P=0.1766). There was a higher frequency of extrasellar extension in *AIP*mut-positive FIPA patients with pituitary adenomas (P=0.004, Supplemental Figure 6c). Three of the *AIP*mut-negative, but none of the *AIP*mut-positive patients, harbored tumors with extensive invasion (defined as involvement of

intracranial areas beyond the perisellar region); two of them had somatotropinomas and the third one harbored a gonadotropinoma. None of the patients in our cohort had evidence of metastases to justify a diagnosis of pituitary carcinoma.

Sporadic patients

In the sporadic cohort, the maximum diameter of the tumors and the proportion of giant adenomas were similar between *AIP*mut-positive and negative sporadic cases (P=0.6965 and 0.7859, respectively). All the *AIP*mut-positive patients had macroadenomas (29/29) vs. 86.3% (283/328) of the *AIP*mut-negative subgroup, and the presence of extrasellar extension was more common in the former group (95% vs. 58.9%, P=0.0011).

Apoplexy of the pituitary adenoma

Excluding the prospectively diagnosed patients, symptomatic apoplexy of the pituitary adenoma occurred in 8.3% of the *AIP*mut-positive cases (9.1% of the familial cases, including three families with two cases per family, and 5.9% of the sporadic patients) and in only 1.3% of the patients in the *AIP*mut-negative subgroup (P<0.0001) and this difference remained significant when only the familial cases were analyzed (10.6% of the *AIP*mut-positive vs. 2.3% of the *AIP*mut-negative patients, P=0.0002, Supplemental Figure 6d). Eight (72.7%) of the *AIP*mut-positive patients with a history of pituitary apoplexy had a diagnosis of gigantism, and in three of them (27.2%) apoplexy was the manifestation that led to the diagnosis of pituitary disease (Supplemental Figure 6e). There were no significant differences in the age at onset/diagnosis or in the tumoral size between the *AIP*mut-positive patients that developed pituitary apoplexy and those who did not have this complication. Out of ten *AIP*mut-negative pituitary adenoma patients with a history of apoplexy, six had NFPA, two had acromegaly, one had gigantism and the specific diagnosis was unknown in the last patient.

The original description of multiple cases of pituitary adenoma apoplexy in *AIP*mut-positive patients (3) was later confirmed in other studies (4;12;25;SR14;SR23;SR24) as well as now in this larger cohort. Although the prevalence of 8.3% does not seem to be higher than the prevalence reported in

populations of unselected pituitary adenomas (7.9%) (SR25), in the latter study patients were older (mean age 60.5 years) and harbored NFPAs, while in our cohort the majority had gigantism and the rest, acromegaly or prolactinoma, with a mean age at diagnosis of 23.4 years. Our three familial apoplexy families, together with a recently reported family with three apoplexy cases (SR24) provide support for the phenotype of young-onset, familial apoplexy in *AIP*mut-positive patients. To our knowledge, there are no previously known genetic causes of familial pituitary adenoma apoplexy, and this remains an uncommon finding. The mechanism why *AIP*mut-positive cases are more prone to apoplexy needs further study.

GH excess patients

With the purpose of analyzing a relatively homogeneous population of patients, we compared the main clinical features of the *AIP*mut-positive and negative GH excess patients from both cohorts, excluding the prospectively diagnosed patients. Similar to the whole study population, the GH excess *AIP*mut-positive patients had an earlier disease onset and diagnosis, had significantly more apoplexy cases (8.4 vs. 1.2%, $P<0.0001$) and a higher frequency of sparsely granulated tumors (91.7 vs. 57.1%, $P=0.0073$). In the *AIP*mut-positive subgroup there is a preponderance of males (60.7% [65/107]), in contrast with the gender distribution found in patients with all the diagnostic categories. PRL co-secretion was more common in *AIP*mut-positive patients (14 vs. 5.9%, $P=0.0046$). There were no differences in tumor size, frequency of extrasellar extension, or giant tumors, though most of the tumors in both subgroups (89.5%) were macroadenomas. There was no significant difference in the number of therapeutic modalities employed between the two subgroups, but there were fewer patients cured or controlled in the *AIP*mut-negative subgroup (41/66 vs. 86/192, $P=0.0151$). Given that the *AIP*mut-positive patients had a significantly longer follow-up duration, we decided to evaluate the current status (i.e. effect of the therapies) only in patients with zero to five years of follow-up. In this subset of patients, there was no significant difference in the percentage of cured or controlled patients between the *AIP*mut-positive (57.1%) and the *AIP*mut-negative (41.7%) subgroups.

Gigantism

This study included 120 patients with gigantism, 45 of them, (37.5%) were part of FIPA families and 75 (62.5%) presented as sporadic patients. Overall, 46.7% (56/120) of the patients with gigantism were *AIP*mut-positive. Males were predominant among *AIP*mut-positive and negative patients (global 67.5%), as expected for gigantism cases. Childhood-onset GH excess resulting in gigantism was more prevalent among the *AIP*mut-positive patients (48.3% [56/116]) than GH excess with no pathological body height, while the opposite pattern was observed in the *AIP*mut-negative subgroup (only 16.7% [64/408] had gigantism, $P<0.0001$). Sixty percent of the *AIP*mut-positive families had at least one patient with gigantism. The frequency of *AIP*muts was much higher in the gigantism cases occurring in a familial setting (Supplemental Figure 7a), where 82.2% (37/45) of the patients were *AIP*mut-positive, in comparison with the sporadic cohort, where *AIP*mut-positive patients accounted for only 25.3% (19/75) of the patients ($P<0.0001$). Familial gigantism, defined as the occurrence of two or more gigantism cases due to pituitary adenoma in the same family, occurred only in *AIP*mut-positive FIPA families (9/37 families, 24.3%, Supplemental Figure 7b). Four of these families harbored the p.R304* *AIP*mut, and the *AIP*muts g.4856_4857CG>AA, p.Q164*, p.269_H275dup, p.E24* and a whole gene deletion accounted for one family each. *AIP*mut-positive gigantism patients were taller than their *AIP*mut-negative counterparts if we considered the criterion of height >3SD over percentile 50 but not when considering >2SD over midparental height (Supplemental Figure 7c and d).

There was no difference in the age at diagnosis (global median 18 [IQR 15-23]) between the *AIP*mut-positive and negative gigantism subgroups. Differences in the frequency of disease onset and diagnosis during the first decade of life did not reach statistical significance (onset: *AIP*mut-positive 9.1% vs. *AIP*mut-negative 9.5%; diagnosis: 3.6% vs. 1.6%). There were no significant differences in the parameters of tumor size and extension either (maximum diameter, frequency of giant adenomas and extrasellar invasion). However, it is worth noting that the vast majority of the tumors in both subgroups were macroadenomas (global 91.5%), and most of them displayed extrasellar invasion (77.6%). A small percentage of the patients had PRL co-secretion at diagnosis (9.2% global, not significantly different between *AIP*mut-positive and negative patients). There were no significant differences in the number of treatments received or the frequency of controlled patients between the

two subgroups. Overall, 43.2% of all the patients with gigantism have currently active or only partially controlled disease.

Extra-pituitary neoplasms in *AIP*mut-positive individuals

To explore the possibility of a syndromic presentation, we looked for additional neoplasms in the affected and unaffected *AIP*mut-positive individuals (n=290). We found a total of ten cases of eight different extra-pituitary neoplasms (osteosarcoma, breast cancer, neuroendocrine tumor of the colon, gastrointestinal stromal tumor [GIST], glioma, meningioma, non-Hodgkin's lymphoma and spinal ependymoma) in nine subjects (four patients and five unaffected *AIP*mut carriers, Supplemental Table 5), accounting for 3.1% of the *AIP*mut-positive individuals studied. *AIP*mut-positive GH excess patients accounted for 44.4% (4/9) of the individuals with extra-pituitary neoplasms, while the rest were unaffected *AIP*mut-positive carriers. We note that the association of these tumors with *AIP*muts could be coincidental.

An increased risk of malignancy among unselected pituitary adenoma patients has been previously reported (SR26;SR27). We have also found neoplasms within the *AIP*mut-positive individuals with no pituitary adenomas, where hormonal excess, especially GH, does not play a role. Further analyses are needed to establish whether there is a possible association between *AIP*muts and these neoplasms. Recently, germline *AIP*muts have been associated with three cases of parathyroid adenomas (two middle aged women in the setting of non-familial, isolated hyperparathyroidism and a young male with acromegaly) (SR28;SR29). An MEN-1 like phenotype was an exclusion criterion in our study, therefore, it was not possible to assess this novel pathogenic association, and none of our patients or carriers developed hyperparathyroidism during the follow-up.

SUPPLEMENTAL REFERENCE LIST (SR)

1. Plon SE, Eccles DM, Easton D, Foulkes WD, Genuardi M, Greenblatt MS, Hogervorst FB, Hoogerbrugge N, Spurdle AB, Tavtigian SV. Sequence variant classification and reporting: recommendations for improving the interpretation of cancer susceptibility genetic test results. Hum Mutat 2008; 29:1282-1291.

2. Rattenberry E, Vialard L, Yeung A, Bair H, McKay K, Jafri M, Canham N, Cole TR, Denes J, Hodgson SV, Irving R, Izatt L, Korbonits M, Kumar AV, Lalloo F, Morrison PJ, Woodward ER, Macdonald F, Wallis Y, Maher ER. A comprehensive next generation sequencing-based genetic testing strategy to improve diagnosis of inherited pheochromocytoma and paraganglioma. J Clin Endocrinol Metab 2013; 98:E1248-E1256.

3. den Dunnen JT, Antonarakis SE. Mutation nomenclature extensions and suggestions to describe complex mutations: a discussion. Hum Mutat 2000; 15:7-12.

4. Locus Reference Genomic LRG_460 - AIP. http://ftp.ebi.ac.uk/pub/databases/lrgex/LRG_460.xml. Accessed 21-8-2014.

5. Bange J, Prechtl D, Cheburkin Y, Specht K, Harbeck N, Schmitt M, Knyazeva T, Muller S, Gartner S, Sures I, Wang H, Imyanitov E, Haring HU, Knayzev P, Iacobelli S, Hofler H, Ullrich A. Cancer progression and tumor cell motility are associated with the FGFR4 Arg(388) allele. Cancer Res 2002; 62:840-847.

6. Lania A, Persani L, Ballare E, Mantovani S, Losa M, Spada A. Constitutively active Gs alpha is associated with an increased phosphodiesterase activity in human growth hormone-secreting adenomas. J Clin Endocrinol Metab 1998; 83:1624-1628.

7. Larkin S, Reddy R, Karavitaki N, Cudlip S, Wass J, Ansorge O. Granulation pattern, but not GSP or GHR mutation, is associated with clinical characteristics in somatostatin-naive patients with somatotroph adenomas. Eur J Endocrinol 2013; 168:491-499.

8. Iacovazzo D, Bianchi A, Lugli F, Milardi D, Giampietro A, Lucci-Cordisco E, Doglietto F, Lauriola L, De ML. Double pituitary adenomas. Endocrine 2013; 43:452-457.

9. Kannuki S, Matsumoto K, Sano T, Shintani Y, Bando H, Saito S. Double pituitary adenoma--two case reports. Neurol Med Chir (Tokyo) 1996; 36:818-821.

10. Ratliff JK, Oldfield EH. Multiple pituitary adenomas in Cushing's disease. J Neurosurg 2000; 93:753-761.

11. Sahdev A, Jager R. Bilateral pituitary adenomas occurring with multiple endocrine neoplasia type one. AJNR Am J Neuroradiol 2000; 21:1067-1069.

12. Kim K, Yamada S, Usui M, Sano T. Preoperative identification of clearly separated double pituitary adenomas. Clin Endocrinol (Oxf) 2004; 61:26-30.

13. Trouillas J, Labat-Moleur F, Sturm N, Kujas M, Heymann MF, Figarella-Branger D, Patey M, Mazucca M, Decullier E, Verges B, Chabre O, Calender A. Pituitary tumors and hyperplasia in multiple endocrine neoplasia type 1 syndrome (MEN1): a case-control study in a series of 77 patients versus 2509 non-MEN1 patients. Am J Surg Pathol 2008; 32:534-543.

14. Villa C, Lagonigro MS, Magri F, Koziak M, Jaffrain-Rea ML, Brauner R, Bouligand J, Junier MP, Di RF, Sainte-Rose C, Beckers A, Roux FX, Daly AF, Chiovato L. Hyperplasia-adenoma sequence in pituitary tumorigenesis related to aryl hydrocarbon receptor interacting protein gene mutation. Endocr Relat Cancer 2011; 18:347-356.

15. Mazal PR, Czech T, Sedivy R, Aichholzer M, Wanschitz J, Klupp N, Budka H. Prognostic relevance of intracytoplasmic cytokeratin pattern, hormone expression profile, and cell proliferation in pituitary adenomas of akromegalic patients. Clin Neuropathol 2001; 20:163-171.

16. Obari A, Sano T, Ohyama K, Kudo E, Qian ZR, Yoneda A, Rayhan N, Mustafizur RM, Yamada S. Clinicopathological features of growth hormone-producing pituitary adenomas:

difference among various types defined by cytokeratin distribution pattern including a transitional form. Endocr Pathol 2008; 19:82-91.

17. Bakhtiar Y, Hirano H, Arita K, Yunoue S, Fujio S, Tominaga A, Sakoguchi T, Sugiyama K, Kurisu K, Yasufuku-Takano J, Takano K. Relationship between cytokeratin staining patterns and clinico-pathological features in somatotropinomae. Eur J Endocrinol 2010; 163:531-539.

18. Kato M, Inoshita N, Sugiyama T, Tani Y, Shichiri M, Sano T, Yamada S, Hirata Y. Differential expression of genes related to drug responsiveness between sparsely and densely granulated somatotroph adenomas. Endocr J 2012; 59:221-228.

19. Brzana J, Yedinak CG, Gultekin SH, Delashaw JB, Fleseriu M. Growth hormone granulation pattern and somatostatin receptor subtype 2A correlate with postoperative somatostatin receptor ligand response in acromegaly: a large single center experience. Pituitary 2013; 16:490-498.

20. Chahal HS, Trivellin G, Leontiou CA, Alband N, Fowkes RC, Tahir A, Igreja SC, Chapple JP, Jordan S, Lupp A, Schulz S, Ansorge O, Karavitaki N, Carlsen E, Wass JA, Grossman AB, Korbonits M. Somatostatin analogs modulate AIP in somatotroph adenomas: the role of the ZAC1 pathway. J Clin Endocrinol Metab 2012; 97:E1411-E1420.

21. Gadelha MR, Kasuki L, Korbonits M. Novel pathway for somatostatin analogs in patients with acromegaly. Trends Endocrinol Metab 2013; 24:238-246.

22. Tuominen I, Heliovaara E, Raitila A, Rautiainen MR, Mehine M, Katainen R, Donner I, Aittomaki V, Lehtonen HJ, Ahlsten M, Kivipelto L, Schalin-Jantti C, Arola J, Hautaniemi S, Karhu A. AIP inactivation leads to pituitary tumorigenesis through defective Galpha-cAMP signaling. Oncogene 2014; 34:1174-1184.

23. Chahal HS, Chapple JP, Frohman LA, Grossman AB, Korbonits M. Clinical, genetic and molecular characterization of patients with familial isolated pituitary adenomas (FIPA). Trends Endocrinol Metab 2010; 21:419-427.

24. Xekouki P, Mastroyiannis SA, Avgeropoulos D, de la Luz SM, Trivellin G, Gourgari EA, Lyssikatos C, Quezado M, Patronas N, Kanaka-Gantenbein C, Chrousos GP, Stratakis CA. Familial pituitary apoplexy as the only presentation of a novel AIP mutation. Endocr Relat Cancer 2013; 20:L11-L14.

25. Fernandez A, Karavitaki N, Wass JA. Prevalence of pituitary adenomas: a community-based, cross-sectional study in Banbury (Oxfordshire, UK). Clin Endocrinol (Oxf) 2010; 72:377-382.

26. Popovic V, Damjanovic S, Micic D, Nesovic M, Djurovic M, Petakov M, Obradovic S, Zoric S, Simic M, Penezic Z, Marinkovic J. Increased incidence of neoplasia in patients with pituitary adenomas. The Pituitary Study Group. Clin Endocrinol (Oxf) 1998; 49:441-445.

27. Hemminki K, Forsti A, Ji J. Incidence and familial risks in pituitary adenoma and associated tumors. Endocr Relat Cancer 2007; 14:103-109.

28. Belar O, De la Hoz C, Perez-Nanclares G, Castano L, Gaztambide S. Novel mutations in MEN1, CDKN1B and AIP genes in patients with multiple endocrine neoplasia type 1 syndrome in Spain. Clin Endocrinol (Oxf) 2012; 76:719-724.

29. Pardi E, Marcocci C, Borsari S, Saponaro F, Torregrossa L, Tancredi M, Raspini B, Basolo F, Cetani F. Aryl hydrocarbon receptor-interacting protein (AIP) mutations occur rarely in sporadic parathyroid adenomas. J Clin Endocrinol Metab 2013; 98:2800-2810.

30. Soares BS, Eguchi K, Frohman LA. Tumor deletion mapping on chromosome 11q13 in eight families with isolated familial somatotropinoma and in 15 sporadic somatotropinomas. J Clin Endocrinol Metab 2005; 90:6580-6587.

31. Georgitsi M, Raitila A, Karhu A, Tuppurainen K, Makinen MJ, Vierimaa O, Paschke R, Saeger W, van der Luijt RB, Sane T, Robledo M, De ME, Weil RJ, Wasik A, Zielinski G, Lucewicz O, Lubinski J, Launonen V, Vahteristo P, Aaltonen LA. Molecular diagnosis of pituitary adenoma

predisposition caused by aryl hydrocarbon receptor-interacting protein gene mutations. Proc Natl Acad Sci U S A 2007; 104:4101-4105.

32. Raitila A, Georgitsi M, Karhu A, Tuppurainen K, Makinen MJ, Birkenkamp-Demtroder K, Salmenkivi K, Orntoft TF, Arola J, Launonen V, Vahteristo P, Aaltonen LA. No evidence of somatic aryl hydrocarbon receptor interacting protein mutations in sporadic endocrine neoplasia. Endocr Relat Cancer 2007; 14:901-906.

33. Gadelha MR, Prezant TR, Une KN, Glick RP, Moskal SF, Vaisman M, Melmed S, Kineman RD, Frohman LA. Loss of heterozygosity on chromosome 11q13 in two families with acromegaly/gigantism is independent of mutations of the multiple endocrine neoplasia type I gene. J Clin Endocrinol Metab 1999; 84:249-256.

34. Pestell RG, Alford FP, Best JD. Familial acromegaly. Acta Endocrinol (Copenh) 1989; 121:286-289.

35. Georgitsi M, Heliovaara E, Paschke R, Kumar AV, Tischkowitz M, Vierimaa O, Salmela P, Sane T, De ME, Cannavo S, Gundogdu S, Lucassen A, Izatt L, Aylwin S, Bano G, Hodgson S, Koch CA, Karhu A, Aaltonen LA. Large genomic deletions in AIP in pituitary adenoma predisposition. J Clin Endocrinol Metab 2008; 93:4146-4151.

36. Luccio-Camelo DC, Une KN, Ferreira RE, Khoo SK, Nickolov R, Bronstein MD, Vaisman M, Teh BT, Frohman LA, Mendonca BB, Gadelha MR. A meiotic recombination in a new isolated familial somatotropinoma kindred. Eur J Endocrinol 2004; 150:643-648.

37. Toledo RA, Mendonca BB, Fragoso MC, Soares IC, Almeida MQ, Moraes MB, Lourenco DM, Jr., Alves VA, Bronstein MD, Toledo SP. Isolated familial somatotropinoma: 11q13-loh and gene/protein expression analysis suggests a possible involvement of aip also in non-pituitary tumorigenesis. Clinics (Sao Paulo) 2010; 65:407-415.

38. Guaraldi F, Corazzini V, Gallia GL, Grottoli S, Stals K, Dalantaeva N, Frohman LA, Korbonits M, Salvatori R. Genetic analysis in a patient presenting with meningioma and familial isolated pituitary adenoma (FIPA) reveals selective involvement of the R81X mutation of the AIP gene in the pathogenesis of the pituitary tumor. Pituitary 2012; 15 Suppl 1:S61-S67.

39. Cazabat L, Bouligand J, Salenave S, Bernier M, Gaillard S, Parker F, Young J, Guiochon-Mantel A, Chanson P. Germline AIP mutations in apparently sporadic pituitary adenomas: prevalence in a prospective single-center cohort of 443 patients. J Clin Endocrinol Metab 2012; 97:E663-E670.

40. Martucci F, Trivellin G, Korbonits M. Familial isolated pituitary adenomas: an emerging clinical entity. J Endocrinol Invest 2012; 35:1003-1014.

41. Fukuoka, H., Iguchi G., Suda K., Yamamoto M., Nishizawa H., Takahashi, M., Seino S., Yamada, S., and Takahashi Y. A novel missense mutation of AIP gene in a patient with octreotide-resistant non-familial gigantism [abstract]. *Endocr Rev.* 2012;33(03_MeetingAbstracts):SUN-713.

42. Nishizawa H, Fukuoka H, Iguchi G, Inoshita N, Yamada S, Takahashi Y. AIP mutation identified in a patient with acromegaly caused by pituitary somatotroph adenoma with neuronal choristoma. Exp Clin Endocrinol Diabetes 2013; 121:295-299.

43. Jorge BH, Agarwal SK, Lando VS, Salvatori R, Barbero RR, Abelin N, Levine MA, Marx SJ, Toledo SP. Study of the multiple endocrine neoplasia type 1, growth hormone-releasing hormone receptor, Gs alpha, and Gi2 alpha genes in isolated familial acromegaly. J Clin Endocrinol Metab 2001; 86:542-544.

44. Toledo RA, Lourenco DM, Jr., Liberman B, Cunha-Neto MB, Cavalcanti MG, Moyses CB, Toledo SP, Dahia PL. Germline mutation in the aryl hydrocarbon receptor interacting protein gene in familial somatotropinoma. J Clin Endocrinol Metab 2007; 92:1934-1937.

45. Prescott RWG, Spruce BA, Kendall-Taylor P, Hall K, and Hall R. Acromegaly and gigantism presenting in two brothers [abstract]. *1st Joint Mtg Brit Endocr Soc* 1982;49.

46. McCarthy MI, Noonan K, Wass JA, Monson JP. Familial acromegaly: studies in three families. Clin Endocrinol (Oxf) 1990; 32:719-728.

47. Georgitsi M, De ME, Cannavo S, Makinen MJ, Tuppurainen K, Pauletto P, Curto L, Weil RJ, Paschke R, Zielinski G, Wasik A, Lubinski J, Vahteristo P, Karhu A, Aaltonen LA. Aryl hydrocarbon receptor interacting protein (AIP) gene mutation analysis in children and adolescents with sporadic pituitary adenomas. Clin Endocrinol (Oxf) 2008; 69:621-627.

48. Jennings JE, Georgitsi M, Holdaway I, Daly AF, Tichomirowa M, Beckers A, Aaltonen LA, Karhu A, Cameron FJ. Aggressive pituitary adenomas occurring in young patients in a large Polynesian kindred with a germline R271W mutation in the AIP gene. Eur J Endocrinol 2009; 161:799-804.

49. Occhi G, Jaffrain-Rea ML, Trivellin G, Albiger N, Ceccato F, De ME, Angelini M, Ferasin S, Beckers A, Mantero F, Scaroni C. The R304X mutation of the aryl hydrocarbon receptor interacting protein gene in familial isolated pituitary adenomas: Mutational hot-spot or founder effect? J Endocrinol Invest 2010; 33:800-805.

50. de Lima DS, Martins CS, Paixao BM, Amaral FC, Colli LM, Saggioro FP, Neder L, Machado HR, dos Santos AR, Pinheiro DG, Moreira AC, Silva WA, Jr., Castro M. SAGE analysis highlights the putative role of underexpression of ribosomal proteins in GH-secreting pituitary adenomas. Eur J Endocrinol 2012; 167:759-768.

51. Niyazoglu M, Sayitoglu M, Firtina S, Hatipoglu E, Gazioglu N, Kadioglu P. Familial acromegaly due to aryl hydrocarbon receptor-interacting protein (AIP) gene mutation in a Turkish cohort. Pituitary 2013; 17:220-226.

52. Vargiolu M, Fusco D, Kurelac I, Dirnberger D, Baumeister R, Morra I, Melcarne A, Rimondini R, Romeo G, Bonora E. The tyrosine kinase receptor RET interacts in vivo with aryl hydrocarbon receptor-interacting protein to alter survivin availability. J Clin Endocrinol Metab 2009; 94:2571-2578.

53. Occhi G, Trivellin G, Ceccato F, De LP, Giorgi G, Dematte S, Grimaldi F, Castello R, Davi MV, Arnaldi G, Salviati L, Opocher G, Mantero F, Scaroni C. Prevalence of AIP mutations in a large series of sporadic Italian acromegalic patients and evaluation of CDKN1B status in acromegalic patients with multiple endocrine neoplasia. Eur J Endocrinol 2010; 163:369-376.

54. Georgitsi M, Karhu A, Winqvist R, Visakorpi T, Waltering K, Vahteristo P, Launonen V, Aaltonen LA. Mutation analysis of aryl hydrocarbon receptor interacting protein (AIP) gene in colorectal, breast, and prostate cancers. Br J Cancer 2007; 96:352-356.

55. Raitila A, Georgitsi M, Bonora E, Vargiolu M, Tuppurainen K, Makinen MJ, Vierimaa O, Salmela PI, Launonen V, Vahteristo P, Aaltonen LA, Romeo G, Karhu A. Aryl hydrocarbon receptor interacting protein mutations seem not to associate with familial non-medullary thyroid cancer. J Endocrinol Invest 2009; 32:426-429.

56. Buchbinder S, Bierhaus A, Zorn M, Nawroth PP, Humpert P, Schilling T. Aryl hydrocarbon receptor interacting protein gene (AIP) mutations are rare in patients with hormone secreting or non-secreting pituitary adenomas. Exp Clin Endocrinol Diabetes 2008; 116:625-628.

57. Guaraldi F, Salvatori R. Familial isolated pituitary adenomas: from genetics to therapy. Clin Transl Sci 2011; 4:55-62.

58. Zatelli MC, Torre ML, Rossi R, Ragonese M, Trimarchi F, degli UE, Cannavo S. Should aip gene screening be recommended in family members of FIPA patients with R16H variant? Pituitary 2013; 16:238-244.

59. Rowlands JC, Urban JD, Wikoff DS, Budinsky RA. An evaluation of single nucleotide polymorphisms in the human aryl hydrocarbon receptor-interacting protein (AIP) gene. Drug Metab Pharmacokinet 2011; 26:431-439.

60. Ceccato F, Occhi G, Albiger NM, Rizzati S, Ferasin S, Trivellin G, Mantero F, Scaroni C. Adrenal lesions in acromegaly: do metabolic aspects and aryl hydrocarbon receptor interacting protein gene have a role? Evaluation at baseline and after long-term follow-up. J Endocrinol Invest 2011; 34:353-360.

61. Cai F, Zhang YD, Zhao X, Yang YK, Ma SH, Dai CX, Liu XH, Yao Y, Feng M, Wei JJ, Xing B, Jiao YH, Wei ZQ, Yin ZM, Zhang B, Gu F, Wang RZ. Screening for AIP gene mutations in a Han Chinese pituitary adenoma cohort followed by LOH analysis. Eur J Endocrinol 2013; 169:867-884.

62. Iwata T, Yamada S, Mizusawa N, Golam HM, Sano T, Yoshimoto K. The aryl hydrocarbon receptor-interacting protein gene is rarely mutated in sporadic GH-secreting adenomas. Clin Endocrinol (Oxf) 2007; 66:499-502.

63. Barlier A, Vanbellinghen JF, Daly AF, Silvy M, Jaffrain-Rea ML, Trouillas J, Tamagno G, Cazabat L, Bours V, Brue T, Enjalbert A, Beckers A. Mutations in the aryl hydrocarbon receptor interacting protein gene are not highly prevalent among subjects with sporadic pituitary adenomas. J Clin Endocrinol Metab 2007; 92:1952-1955.

64. Stals K, Trivellin G, Korbonits M. AIP mutation in pituitary adenomas. N Engl J Med 2011; 364:1974-1975.

SUPPLEMENTAL FIGURES AND TABLES

Supplemental Table 1. Definition of the clinical diagnostic categories used in our study.

Diagnosis		Criteria
Cushing's disease		Evidence of ACTH-depending hypercortisolemia with proven pituitary adenoma, in accordance to the diagnostic protocol of each institution
Clinically functioning FSH-secreting pituitary adenoma (FSHoma)		Raised serum FSH levels for age and gender and evidence of gonadal stimulation in a patient with a pituitary adenoma
GH excess	Acromegaly	Raised IGF-1 levels and unsuppressed GH during an oral glucose tolerance test (OGTT), with cut-offs according to the protocol of each institution
	Acromegaly/prolactinoma	Diagnosis of acromegaly with concurrent hyperprolactinemia
	Mild acromegaly*	Mild clinical features attributed to acromegaly, fulfilling the criterion of raised IGF-1 levels but not the lack of suppression of GH during an OGTT, or normal IGF-1 but lack of suppression of GH during an OGTT (16)
	Gigantism	Any of the following categories in a patient with a pituitary adenoma: (i) abnormally high growth velocity in children or teenagers with abnormal IGF-1 and OGTT, (ii) height >3SD above the mean height for age, (iii) >2SD over the calculated midparental height, using country-specific growth charts when possible
	Gigantism/prolactinoma	Diagnosis of gigantism with concurrent hyperprolactinemia
Clinically nonfunctioning pituitary adenoma (NFPA)		Pituitary adenoma in the absence of clinical or biochemical evidence of pituitary hypersecretion
Pituitary tumor		Cases of pituitary tumor where the diagnosis could not be specified, due to unavailability of histopathological specimens, clinical and/or biochemical data
Prolactinoma		Hyperprolactinemia in the presence of a pituitary adenoma and unlikely to be purely due to a stalk effect, based on either histopathology results or the relation between PRL levels and tumor size
Thyrotropinoma (TSHoma)		Hyperthyrotropinemia in a patient with a pituitary adenoma, with clinical and/or biochemical hyperthyroidism and no other demonstrable causes of raised TSH
* This category is important in our study, as we detected acromegaly via biochemical screening of *AIP*mut-positive carriers, often not presented (yet) clinically.		

Supplemental Table 2. Other genes tested.

	Familial cohort			Sporadic cohort			Combined, no. (%)
	***AIP*mut-positive, no. (%)**	***AIP*mut-negative, no. (%)**	**Total familial, no. (%)**	***AIP*mut-positive, no. (%)**	***AIP*mut-negative, no. (%)**	**Total sporadic, no. (%)**	
BRCA1	1 (14.3)	2 (0.7)	3 (1)	-	-	-	3 (0.8)
BRCA2	1 (14.3)	2 (0.7)	3 (1)	-	-	-	3 (0.8)
CDKN1B	-	20 (6.5)	20 (6.4)	-	1 (2.4)	1 (2.4)	21 (5.9)
GPR101	-	-	-	-	8 (19)	8 (19)	8 (2.2)
MAX	-	23 (7.5)	23 (7.3)	-	-	-	23 (6.5)
MEN1	3 (42.9)	51 (16.6)	54 (17.2)	-	33 (78.6)	33 (78.6)	87 (24.4)
PRKAR1A	-	23 (7.5)	23 (7.3)	-	-	-	23 (6.5)
RET	-	23 (7.5)	23 (7.3)	-	-	-	23 (6.5)
SDHA	-	23 (7.5)	23 (7.3)	-	-	-	23 (6.5)
SDHAF2	-	23 (7.5)	23 (7.3)	-	-	-	23 (6.5)
SDHB	-	23 (7.5)	23 (7.3)	-	-	-	23 (6.5)
SDHC	-	23 (7.5)	23 (7.3)	-	-	-	23 (6.5)
SDHD	-	25 (8.1)	25 (8)	-	-	-	25 (7)
TMEM127	-	23 (7.5)	23 (7.3)	-	-	-	23 (6.5)
TP53	2 (28.6)	-	2 (0.6)	-	-	-	2 (0.6)
VHL	-	23 (7.5)	23 (7.3)	-	-	-	23 (6.5)
Total	7	307	314	0	42	42	712
-, no individuals in this category.							

Supplemental Table 3. *AIP* nonpathogenic mutations in the familial and sporadic cohorts.

Variant (DNA level [protein level])	Variant type	Pathogenic	Location in protein	Familial cohort* (N=19)	Sporadic cohort* (N=37)	Combined* (N=56)	References/ SR‡
c.47G>A (p.R16H)	Missense	No	N-terminus	0	2	2	(2;5;7)/ (SR31;39;54-58)
c.132C>T (p.(=))	Synonymous	No	PPIase domain	0	3	3	(5)/(SR59)
c.144C>T (p.(=))	Synonymous	No	PPIase domain	0	1	1	(SR53;59-61)
c.516C>T (p.(=))	Synonymous	No	Between PPIase and TPR1 domains	8	13	21	(5;12)/(SR56;58; 59;61-63)
c.573C>T (p.(=))	Synonymous	No	TPR1 domain	0	0	0	This paper
c.579G>T (p.(=))	Synonymous	No	TPR1 domain	1	0	1	This paper
c.682A>C (p.K228Q) †	Missense	No	Between TPR1 and 2 domains	2	16	18	(5)/(SR58;59;63)
c.831C>T (p.(=))	Synonymous	Unlikely	TPR3 domain	1	0	1	This paper
c.891C>A (p.(=))	Synonymous	No	TPR3 domain	0	2	2	(5)/(SR59)
C.896C>T (p.A299V)	Missense	Unlikely	TPR3 domain	5	0	5	(12)/(SR31)
c.906G>A (p.(=))	Synonymous	No	C-terminal α-helix	2	0	2	(SR31;59)

* Number of positive individuals for each mutation, considering the *AIP*mut-positive tested individuals, the obligate carriers and the predicted *AIP*mut patients.
†There is a Q at this position in the *AIP* reference sequence, but we consider K as the wild type amino acid, due to its higher prevalence in the population screened so far (Stals K., unpublished data).
PPIase, peptidylprolyl isomerase, TPR, tetratricopeptide repeat.

Supplemental Table 4. Classification of FIPA families by diagnoses

	***AIP*mut-positive**	***AIP*mut-negative**	**Total**
Total families, no.:	37	179	216
Diagnoses:			
Cushing's disease only, no. (%)	-	3 (1.7)	3 (1.4)
Cushing's disease + FSHoma, no. (%)	-	1 (0.6)	1 (0.5)
Cushing's disease + NFPA, no. (%)	-	1 (0.6)	1 (0.5)
Cushing's disease + NFPA + pituitary tumor, no. (%)	-	1 (0.6)	1 (0.5)
Cushing's disease + prolactinoma, no. (%)	-	5 (2.8)	5 (2.3)
FSHoma + prolactinoma, no. (%)	-	1 (0.6)	1 (0.5)
Cushing's disease+ GH excess, no. (%)	-	7 (3.9)	7 (3.2)
GH excess only, no. (%)	16 (43.2)	44 (24.6)	60 (27.8)
GH excess + NFPA, no. (%)	8 (21.6)	12 (6.7)	20 (9.3)
GH excess + NFPA + prolactinoma, no. (%)	1 (2.7%)	3 (1.7)	4 (1.9)
GH excess + pituitary tumor, no. (%)	-	5 (2.8)	5 (2.3)
GH excess + pituitary tumor + prolactinoma, no. (%)	-	1 (0.6)	1 (0.5)
GH excess + prolactinoma, no. (%)	9 (24.3)	30 (16.8)	39 (18.1)
NFPA only, no. (%)	2 (5.4)	17 (9.5)	19 (8.8)
NFPA + pituitary tumor, no. (%)	-	7 (3.9)	7 (3.2)
NFPA + prolactinoma, no. (%)	1 (2.7)	10 (5.6)	11 (5.1)
Pituitary tumor + prolactinoma, no. (%)	-	1 (0.6)	1 (0.5)
Prolactinoma, no. (%)	-	30 (16.8)	30 (13.9)

* The category "GH excess" includes the following diagnoses: acromegaly, acromegaly/ prolactinoma, gigantism, gigantism/ prolactinoma and mild acromegaly.
-, no families in this category.
FSHoma, FSH secreting adenoma. NFPA, nonfunctioning pituitary adenoma.

Supplemental Table 5. Extrapituitary neoplasms in *AIP*mut-positive individuals.

Pituitary diagnosis	Cohort	Gender	*AIP*mut	Extrapituitary neoplasm
Unaffected	Familial	Male	c.910C>T (p.R304*)	Osteosarcoma and neuroendocrine tumor of the colon †
Unaffected	Familial	Female	c.910C>T (p.R304*)	Breast cancer†
Unaffected	Familial	Female	c.910C>T (p.R304*)	Breast cancer†
Acromegaly	Familial	Male	c.805_825dup (p.F269_H275dup)	GIST
Acromegaly	Familial	Male	c.241C>T (p.R81*)	GIST*
Unaffected	Sporadic	Male	c.910C>T (p.R304*)	Glioma
Acromegaly	Familial	Female	c.241C>T (p.R81*)	Meningioma*
Gigantism	Familial	Male	c.74_81delins7 (p.L25Pfs*130)	Non-Hodgkin's lymphoma
Unaffected	Familial	Female	c.100-1025_279+357del (ex2del) (p.A34_K93del)	Spinal ependymoma

* Brother and sister. † Brother and 2 sisters.
GIST, gastrointestinal stromal tumor.

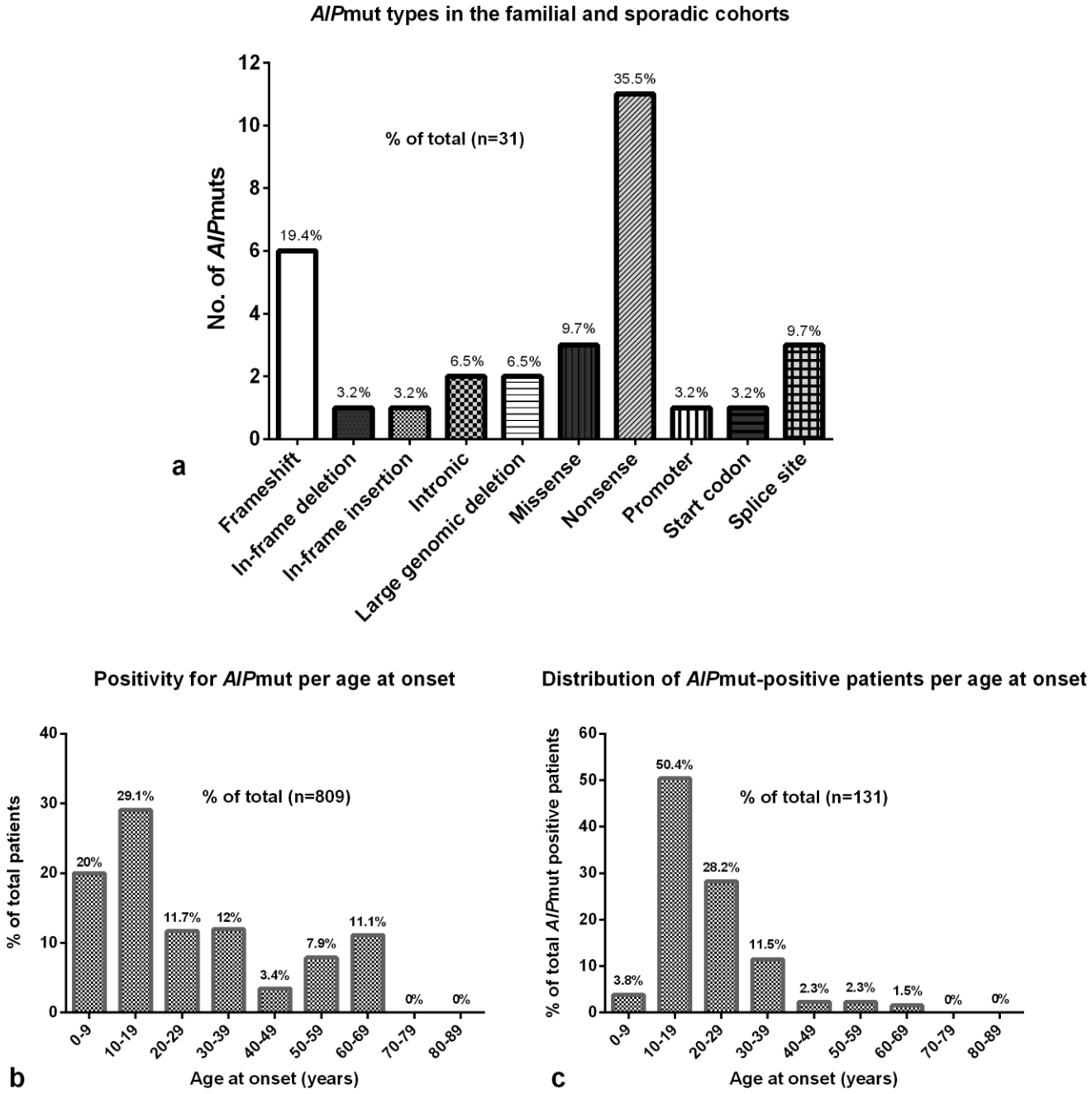

Supplemental Figure 1. *AIP*mut types and frequency according to age at disease onset in the familial and sporadic cohorts (whole study population). a) Number of *AIP*muts per mutation type, note the predominance of nonsense mutations. b) The probability of finding an *AIP*mut was higher when testing patients with disease onset during the second decade of life; c) in concordance, three quarters of all the *AIP*mut-positive patients had disease onset during the second and third decades of life.

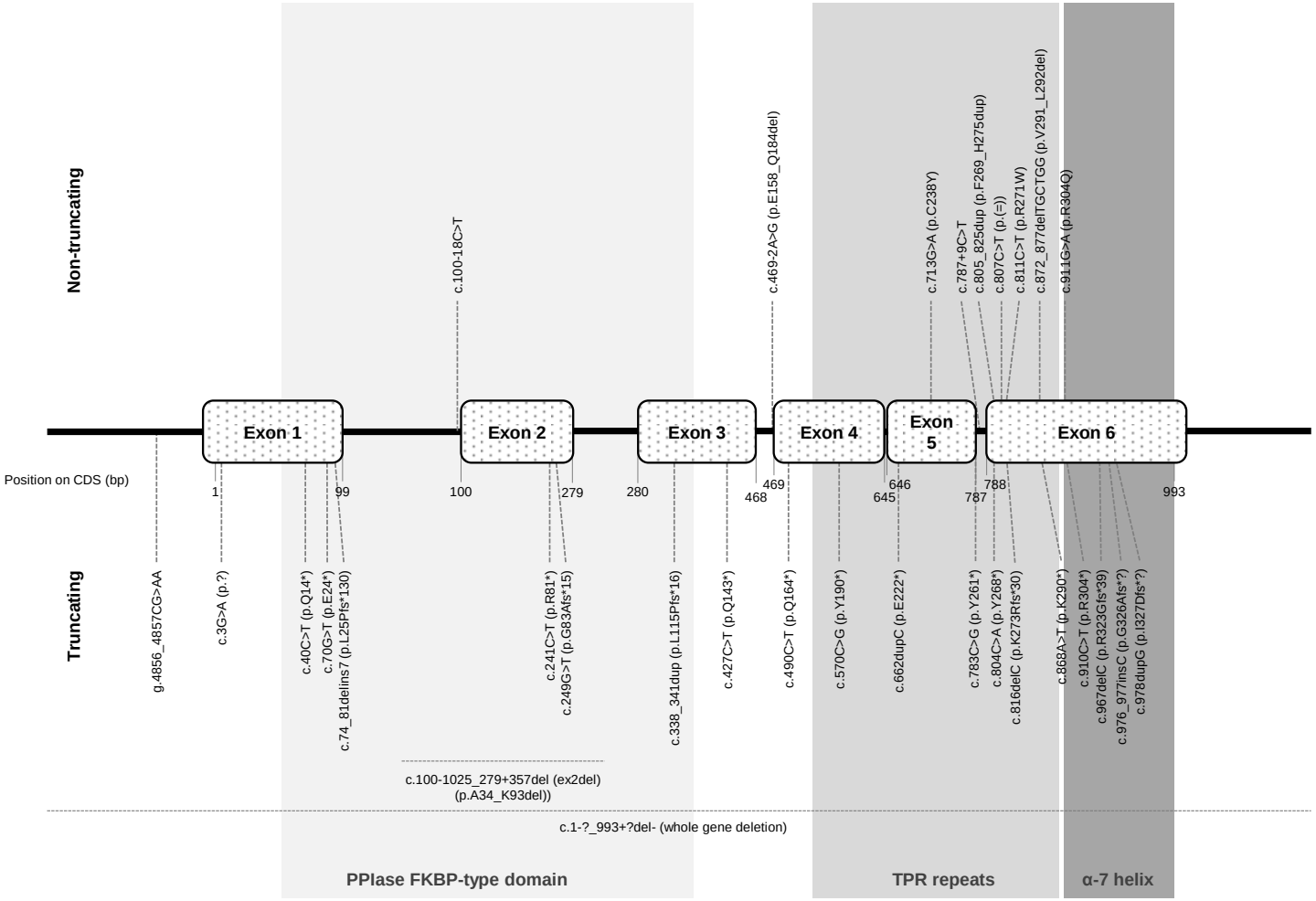

Supplemental Figure 2. *AIP*muts detected in the study population and their position in the *AIP* gene. Shadowed areas indicate the protein domains codified by each region of the gene. Mutations producing a truncated or missing protein are shown at the bottom of the scheme, and nontruncating mutations are at the top. Even though we identified variants throughout the whole *AIP* gene, mutations tended to cluster in the genomic regions encoding the tetratricopeptide repeat (TPR) domains and the C-terminal α-helix of the protein. Furthermore, the mutations located at the N-terminal extreme and inside the peptidylprolyl isomerase (PPIase) domain were essentially truncating mutations, resulting in short and unstable proteins, lacking the TPR domains. As expected based on previous data (26;SR64), the commonest mutation in both cohorts was c.910C>T (p.R304*), found in 33.3% of the *AIP*mut patients and in 35.9% of all the *AIP*mut-positive individuals (affected plus unaffected carriers). There were no exclusive associations of specific *AIP*muts with particular diagnoses. However, 77.4% of all the mutations (24/31) were found in cases of gigantism (with or without prolactin (PRL) co-secretion), being this the diagnosis with the highest number of associated *AIP*muts. Furthermore, all the mutations were found in at least one patient with GH excess, supporting this diagnostic category as the most frequent *AIP*mut pathogenic association. Patients with diagnosis of NFPA harbored 29% (9/31) of the *AIP*muts found in the study, and 22.6% of them (7/31) were detected in prolactinoma cases.

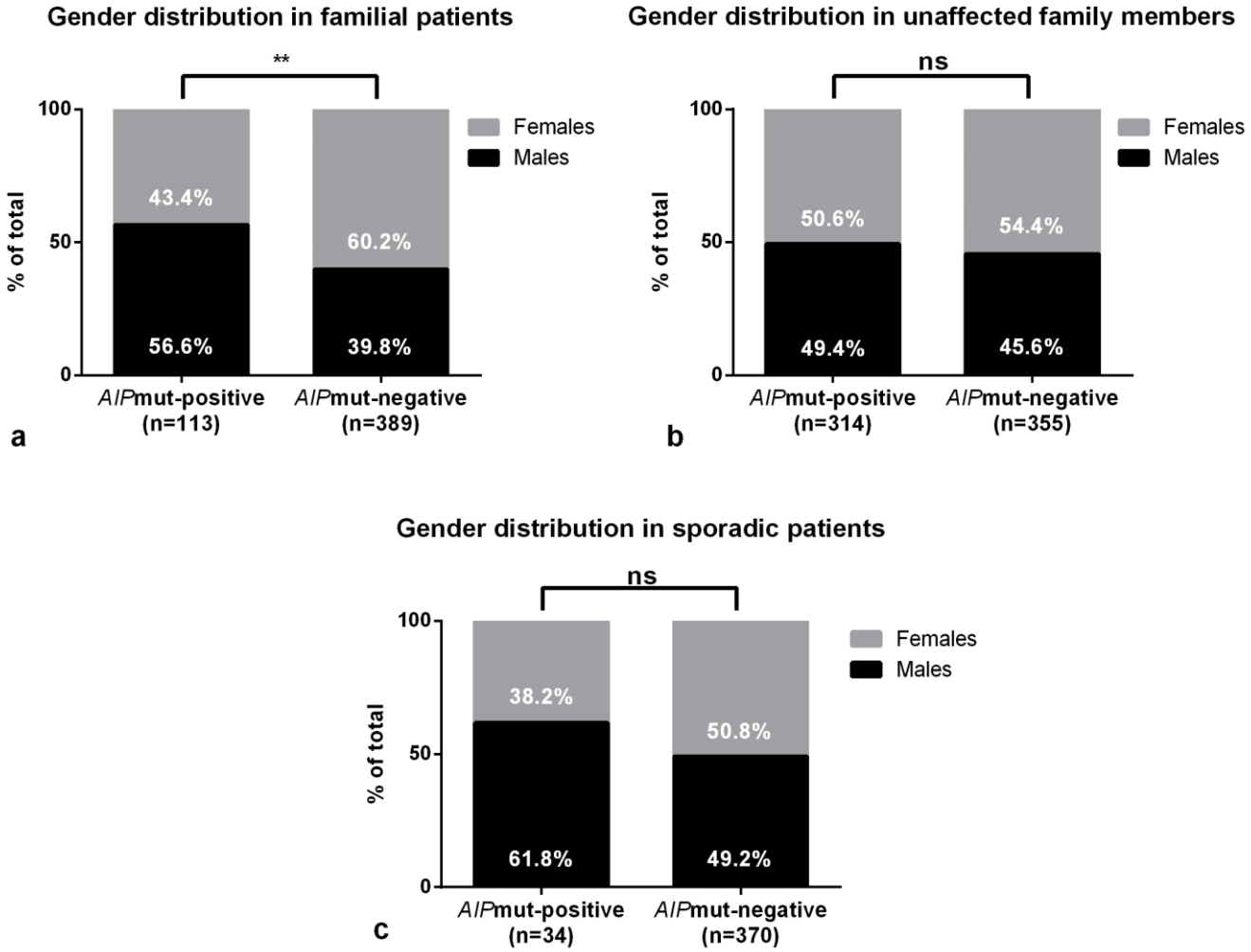

Supplemental Figure 3. Gender distribution in FIPA families and sporadic patients: a) Gender distribution was different between the *AIP*mut-positive and negative FIPA patients, due to a predominance of female patients within the *AIP*mut-negative families. b) This difference cannot be explained by a selection bias towards one specific gender, as there were similar numbers of males and females within the unaffected family members (excluding 'not at risk' individuals) of *AIP*mut-positive and negative FIPA families. c) The gender distribution was not significantly different between *AIP*mut-positive and negative patients, despite a slight prevalence of males in the *AIP*mut-positive subgroup. ns, not significant, **, $P<0.01$.

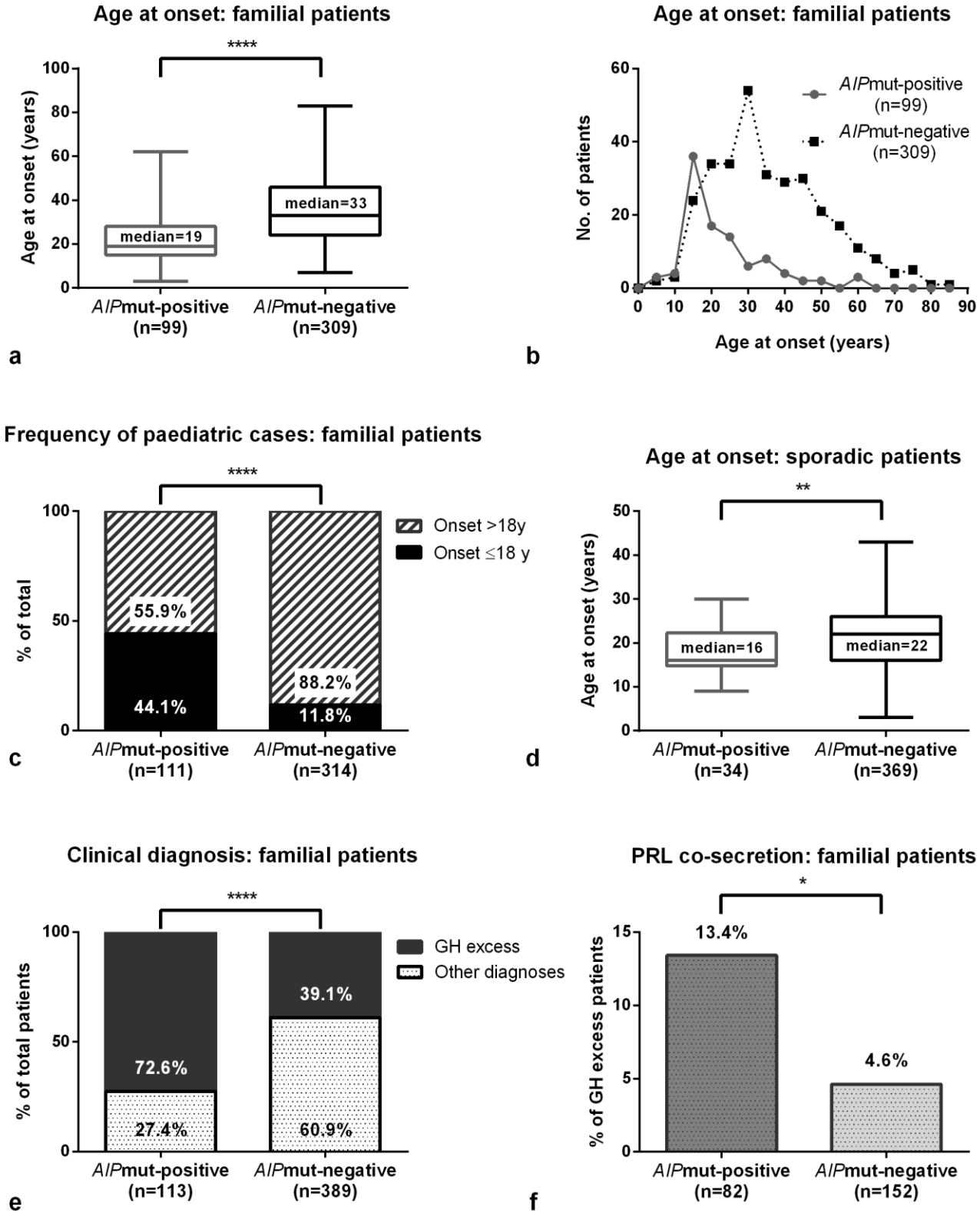

Supplemental Figure 4. Clinical features in FIPA families and sporadic patients: a) *AIP*mut-positive familial patients were younger at disease onset (P<0.0001), b) as most of them developed symptoms after the age of 10 and before the age of 40. c) There was a higher frequency of pediatric cases (n [total]=425) in the *AIP*mut-positive FIPA families, compared with the *AIP*mut-negative FIPA families. d) In the sporadic group, although all these patients were ≤30 years at disease onset, *AIP*mut-positive individuals were significantly younger at disease onset than the *AIP*mut-negative ones. e) GH excess and f) presence of GH and PRL co-secretion were significantly more frequent in *AIP*mut-positive familial patients. *, P<0.05, **, P<0.01, ****, P<0.0001.

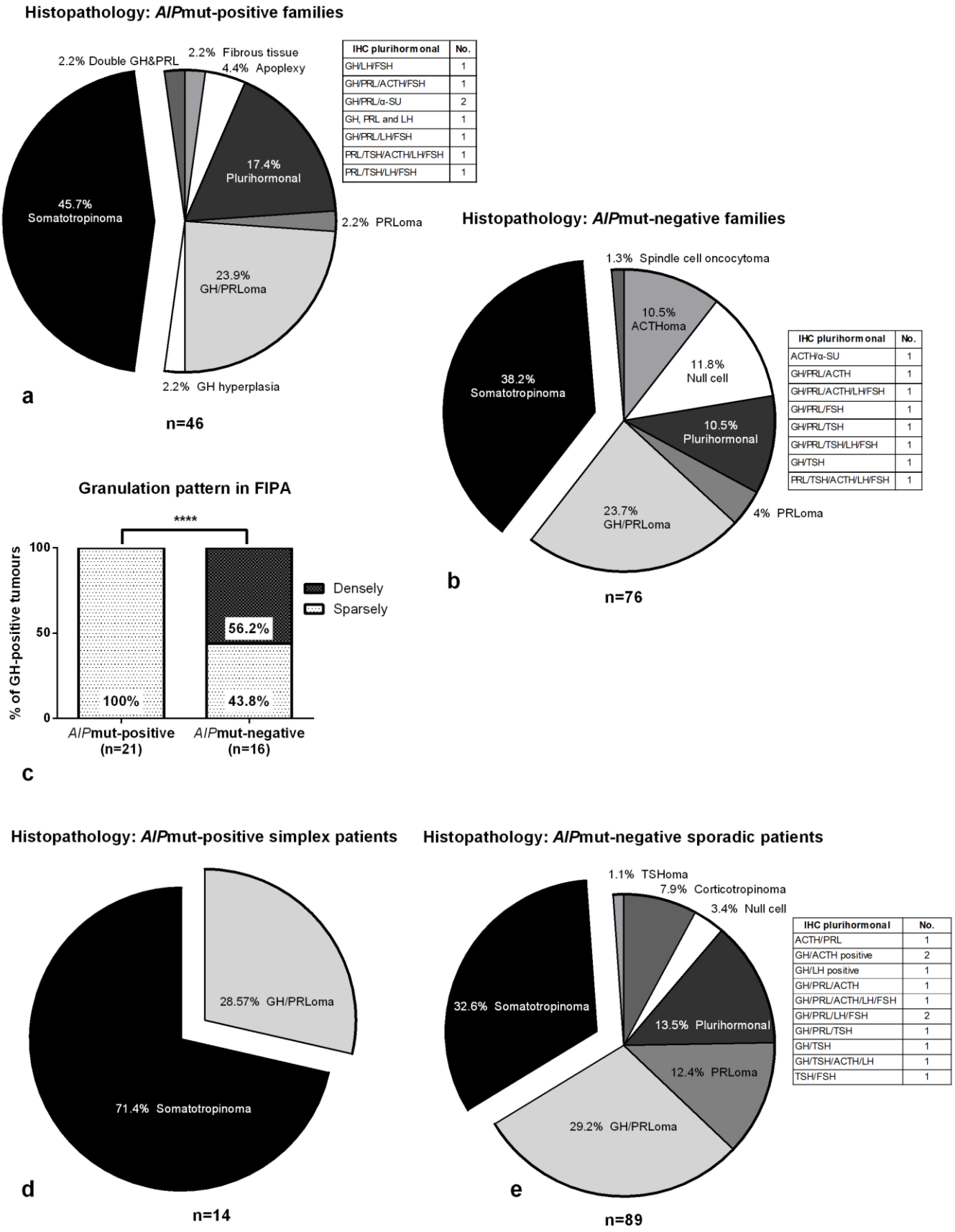

Supplemental Figure 5. Histopathological diagnoses in FIPA families and sporadic patients. The distribution of the IHC diagnoses was different between *AIP*mut-positive (a) and negative (b) familial patients, though GH positive tumors predominated in both subgroups. c) The analysis of the granulation pattern reported sparsely granulated tumors in all the *AIP*mut-positive and in 43.8% of the *AIP*mut-negative familial adenomas ($P<0.0001$). d) *AIP*mut simplex patients had GH positive adenomas (with or without positive PRL staining), while e) the *AIP*mut-negative sporadic patients had a variety of other tumor types. PRLoma, prolactinoma; GH/PRLoma, mammosomatotroph adenoma; ns, not significant; ****, $P<0.0001$.

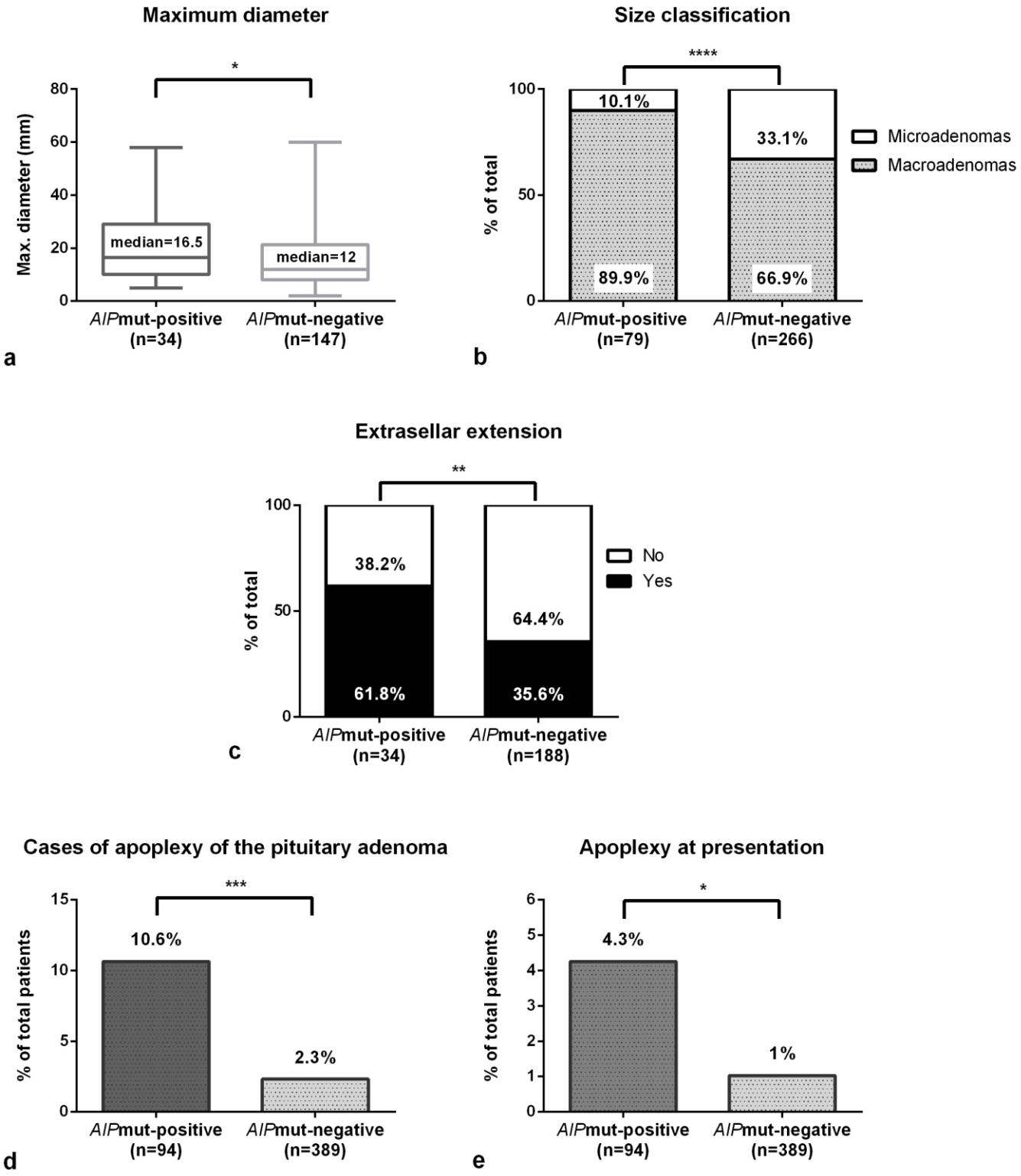

Supplemental Figure 6. Tumor size and and pituitary apoplexy in FIPA families (excluding prospectively diagnosed *AIP*mut-positive patients): *AIP*mut-positive vs. *AIP*mut-negative patients. a) Pituitary adenomas were larger in *AIP*mut-positive familial patients (P=0.040), b) what was reflected in a higher frequency of macroadenomas (P=0.0001). c) In concordance with this, there was a higher frequency of extrasellar extension within *AIP*mut-positive patients (P=0.004). d) The occurrence of symptomatic apoplexy of the pituitary adenoma was significantly more common among the *AIP*mut-positive families, occurring in 10.6% of these patients (vs. 2.3% of the *AIP*mut-negative FIPA patients, (P=0.0002), including one phenocopy NFPA patient. e) Apoplexy was the first sign of pituitary disease in 4.3% of the *AIP*mut-positive familial patients, but only in 1% of the *AIP*mut-negative ones. * P<0.05, **, P<0.01, ***, P<0.001, ****, P<0.0001.

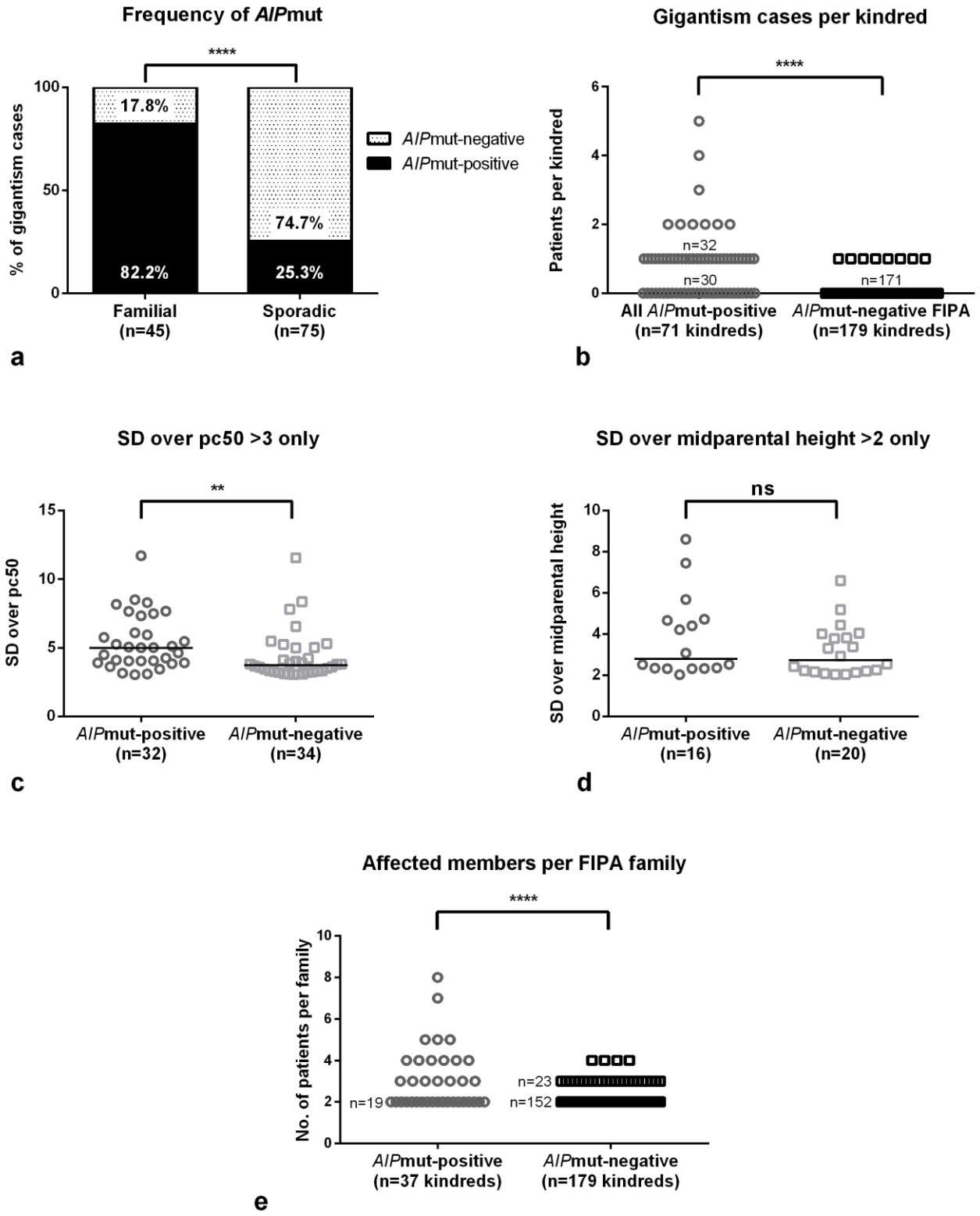

Supplemental Figure 7. Characteristics of gigantism cases (familial n=45, sporadic n=75) and penetrance. a) The great majority of the gigantism cases occurring in a familial setting were *AIP*mut-positive vs. only one quarter of those cases presenting sporadically ($P<0.0001$). b) In our study population, all the kindreds including more than one case of gigantism carried *AIP*muts (this graph includes all the *AIP*mut-positive kindreds, FIPA and simplex patients, and the *AIP*mut-negative FIPA families). c) Considering only those patients fulfilling the criterion of height >3SD over percentile 50, *AIP*mut-positive patients were taller at diagnosis than the *AIP*mut-negative ones ($P=0.0164$); however, d) there was no significant difference in height when the comparison was done among patients fulfilling the criterion of >2SD over midparental height. e) In average, there were more affected individuals per family in the *AIP*mut-positive families ($P<0.0001$). ns, not significant, * $P<0.05$, ** $P<0.01$, ****, $P<0.0001$.